Membrane Science and Technology Series, 5

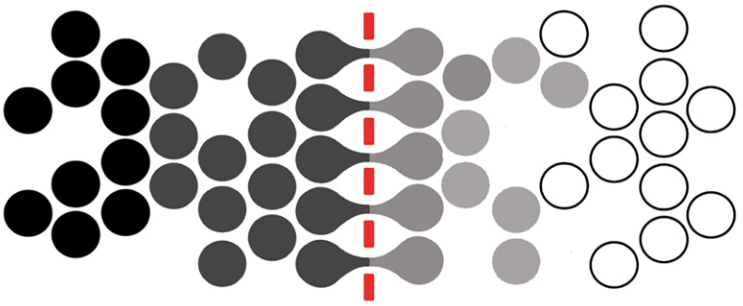

MEMBRANE BIOPHYSICS

AS VIEWED FROM EXPERIMENTAL BILAYER LIPID MEMBRANES

(Planar Lipid Bilayers and Spherical Liposomes)

H. Ti Tien
Angelica Ottova-Leitmannova

ELSEVIER

MEMBRANE BIOPHYSICS

AS VIEWED FROM EXPERIMENTAL BILAYER LIPID MEMBRANES

This Page Intentionally Left Blank

Membrane Science and Technology Series, 5

MEMBRANE BIOPHYSICS

AS VIEWED FROM EXPERIMENTAL BILAYER LIPID MEMBRANES

(Planar Lipid Bilayers and Spherical Liposomes)

H. Ti Tien

and

Angelica Ottova-Leitmannova

Department of Physiology, Michigan State University
East Lansing, MI 48824,USA

2000

ELSEVIER
Amsterdam - Lausanne - New York - Oxford - Shannon - Singapore - Tokyo

ELSEVIER SCIENCE B.V.
Sara Burgerhartstraat 25
P.O. Box 211, 1000 AE Amsterdam, The Netherlands

First edition 2000

Library of Congress Cataloging in Publication Data
A catalog record from the Library of Congress has been applied for.

ISBN: 0-444-82930-X

♾ The paper used in this publication meets the requirements of ANSI/NISO Z39.48-1992 (Permanence of Paper).
Printed in The Netherlands.

To see the world in a grain of sand,
eternity in an hour,
and hold the world in the palm of your hand,
heaven in a wild flower. – William Blake

Beholding life in a soap bubble,
Self-assembly is the key.
To make a BLM in vitro,
Shows the biomembrane's living complexity!
-- SST

To

Nick, Jesse,

James, Daniel,

Caroline, Mark,

Christopher, Julian,

Patrick, Veronika,

etc.

This Page Intentionally Left Blank

PREFACE

This collection of chapters is a textbook intended for undergraduate and graduate students interested in membrane biophysics. The book, a general introductory course is also aimed at students majoring in any fields of biological and physical sciences, including physiology, chemistry, physics, mathematics, engineering or applied sciences and technologies, who would like to be conversant with historical as well as the latest development in molecular self-assemblies, in particular, the lipid bilayer structure of the cell membrane.

The area of membrane biophysics is perused from the origin of the lipid bilayer concept to membrane transport, electrochemistry, physiology, bioenergetics, and to membrane photobiology. Emphasis is placed on theoretical and experimental model systems, as related to the structure and function of biomembranes. The connecting thread, among these topics, is experimental bilayer lipid membrane (mainly planar BLMs, supported BLMs, and spherical liposomes). The basic principles of thermodynamics, kinetics, the Nernst-Planck equation, colloid and surface chemistry are applied to the above-mentioned topics of membrane biophysics. Some practical applications of self-assembled lipid bilayers, for example. as biosensors are also presented. This is due to the fact that recent advances in the development of supported planar lipid bilayers (s-BLMs) for biosensing applications. Such s-BLMs have a unique role to play in interfacing conventional metal and semiconductor devices to the biological world. The biomimetic nature of such systems coupled with membrane research of the past decades has come of age, and is poised for biotechnological exploitation.

ACKNOWLEDGEMENT

Although the present work is not a sequel to the earlier book on 'Bilayer Lipid Membranes (BLM): Theory and Practice', published in 1974, the authors are grateful to their co-workers and colleagues since that time. We thank (listed chronologically in order of association) W. Stillwell, J. M. Mountz, J. D. Mountz, J. Higgins, J. Lopez, F. A. Siddiqi, Q. Y. Liu, N. B. Joshi, K. O'Boyle, X. R. Xiao, J. Kutnik, P. M. Vassilev, M. P. Kanazirska, Z. C. Bi, X. C. Shen, Z. K. Lojewska, J.-Y. Yu, P. Krysinski, G. Xu, B. Shi, S. Mureramanzi, C. Bender, K. Jackowska, J. Zon, R. Bhardwaj, T. Janas, Z. Salamon, J. Kotowski, J.-W. Chen, V. Kochev, K. T. L. De Silva, C. Bhardwaj, A. Wardak, T. Martynski, M. Zviman, D. L. Guo, A. Tripathy, W. Liu, W. Ziegler, V. Tvarozek, J. Sabo, T. Hianik, XianDao Lu, and K. Asaka.

TABLE OF CONTENTS

This Page Intentionally Left Blank

Chapter 1

Membrane Biophysics: An Overview

"... the lipid bilayer of cell membranes is the gateway and port as well as the window to the external world."

General References (cited by name in parenthesis in the text)
Specific References (cited by number in superscript in the text)

1.1 What is biophysics?

Because of its interdisciplinary focus, biophysics transcends the traditional boundaries between disciplines such as *Chemistry, Physics, Biology, and Engineering*. In Biophysics, researchers are interested in applying concepts, ideas, and techniques from the physical and applied sciences, and mathematics to problems in molecular cell biology and biomedical sciences. As stated by the American Biophysical Society, 'the range of interests referred to as *biophysics* is very broad, as biophysicists use experimental and theoretical approaches and develop new physical and chemical methods to address the mechanisms of biological processes at every level.' Biophysics is composed of subfields including cell

biology, genetics and physiology. Training in biophysics prepared students and post-doctoral fellows to acquire the skills necessary for careers in a world that increasingly values interdisciplinary and integrative outlook. There are many research areas in biophysics such as bioenergetics, electrophysiology, supramolecular assemblies, and membranes. In this book we will focus our attention exclusively on the physical, physiological and biochemical aspects of membranes using experimental lipid bilayers.

1.2 What is life and its Origin?

.. "*Life is nothing but a movement of electrons* !", so said Albert Szent-Gyorgyi, the discoverer of ascorbic acid (vitamin C) in connection with *'Life and Light'* in 1960. We will come back to this theme later (Chapters 6, and 8-10). Meanwhile, the simplest definition of life is that any living thing must possess the following attributes: metabolism, growth, and replication. In other words, a living system is defined by its ability to self-assemble, to use energy to produce order by decreasing local entropy at the expense of increasing entropy in its surroundings. The fundamental unit of all living systems is the cell. The cell theory of life, put forth in the middle of the 19th century, states that a cell is the simplest unit capable of independent existence, and all living things are made of cells. How about viruses ? Viruses are only alive while infecting a cell. Thus, the theory still holds true today. As to the origin of life, known theories are constrained by the laws of physics and chemistry. In terms of cells, prokaryotic bacteria (e.g. *Streptococcus pyogenes)* appeared on earth around 3.5×10^9 years ago. About some 2 billion years later, eukaryotic cells (e.g. yeast) appeared. How old is the Earth ? It was formed some 4.5 to 6 billion years ago. Both prokaryotic and eukaryotic cells have DNA (deoxyribonucleic acid -- the chemical structure that stores the cell's hereditary information) and ribosomes (the protein-synthesizing structures of the cell). Both types of cells have similar basic metabolism; they are membrane-bound. Eukaryotes differ from prokaryotes in that the former has a nucleus containing the DNA and membrane-bound organelles. Other major differences are that eukaryotes are about ten times bigger than prokaryotic cells which have a cell wall composed of peptidoglycan, a single large polymer of amino acids and carbohydrates. Since life on earth

is incredibly extensive and heterogeneous, and there is a need to make it easier to study, bioscientists have divided living systems up into several hierarchical levels:

I. molecules → organelles → cells
II. tissues → organs → organisms
III. populations → communities → ecosystems

The focus of this book is on the biophysical aspects of the cell membrane, that is the properties that are held in common among all living things. We will concentrate mainly on the systems of the first level, namely, molecular through the cellular level.

1.3 What are the relative sizes of biological molecules and cells?

Speaking about the relative sizes of cells, it is informative to remember the various systems we will be discussing throughout this book. Table 1.1 provides such a list. Note all the values given are approximations.

1.4 What is a biomembrane?

A biomembrane consists of a fluid phospholipid bilayer intercalated with proteins, carbohydrates, and their complexes. A biomembrane is a selective permeability barrier, which is capable of material transport. The process may be accomplished by either passive, simple or facilitated diffusion or by active transport. Biomembranes are described by the so-called *'dynamic membrane hypothesis'*; which is invoked to explain the membrane function. The self-assembled lipid bilayer is in a dynamic and liquid-crystalline state. A functional biomembrane should be considered in electronic and molecular terms; it can support ion or/and electron transport, and is the site of cellular activities in that it functions as a 'device' for either energy conversion or signal transduction. Such a system, as we know it intuitively, must act as some sort of a transducer capable of gathering information, processing it, and then delivering a response based on this information.

Table 1.1

Relative sizes of biological objects compared with other known systems

(Scale: Micron, 1 μm = 10^{-6} meter. 1 μm = 40 millionths of an inch)

Frog Egg	2 mm in diameter
Squid Giant Nerve Cell	1 mm in diameter
Resolution of the Human Eye	**100 microns**
Human Egg	100 μm
	10 microns
Human Red Blood Cell	8 μm
Chloroplast	5 μm in length
Mitochondrion	3 μm (1960 integrated circuits)
Bacterium *E.coli*	2 μm
	1 micron (μm)
Resolution of Optical Microscope	
	0.1 micron
Large Virus	100 nm
Nuclear Pore	50-80 nm
Soap films and 'black' soap films	5-100 nm
	10 nm
	10 nm to 0.1 μm - transistors)
Cell Membrane Thickness	6 nm
Liposomes	a few nm to a few cm (diameter)
Bilayer Lipid Membrane **(BLM)**	~ 5 nm
Globular Protein	4 nm
DNA α-helix	2 nm in diameter
	1 nm (10 Å)
Amino Acid	0.8 nm
Fullerene C_{60}	~ 0.5 nm
	(smallest artificial structure)
Resolution of Electron Microscope	
Diameter of a Hydrogen Atom	**0.1 nm** (1 Å)
Resolution of Scanning Tunneling Microscope	**0.01 nm**

1.5 What topics are covered in this book?

The area chosen is ***membrane biophysics***; it is motivated by the desire to understand as well as to interpret living organisms in physical and biochemical terms at the membrane level. This presupposes that a basic understanding of the physics and chemistry of the universe will result in an understanding of biological processes. Thus, the proper study of living cell is membrane. Since the plasma membrane of erythrocytes, one of the simplest membranes, is still too complex to be characterized in simple physico-chemical terms, we have resorted to study reconstituted model membrane systems. At the membrane level, most cellular activities involve some kind of lipid bilayer-based receptor-ligand contact interactions. Outstanding examples among these are ion-sensing, molecular recognition (e.g. antigen-antibody binding and enzyme-substrate interaction), light conversion and detection, gated channels, and active transport. Our approach to study these physiological happenings is facilitated by *in vitro* lipid bilayers. The development of self-assembled bilayer lipid membranes (BLMs and liposomes) have made it possible to investigate directly the electrical properties and transport phenomena across a 5 nm (nanometer) thick cell membrane element separating two aqueous phases. A modified or reconstituted BLM is viewed as a dynamic structure that changes in response to environmental stimuli and changes as a function of time, as described by the dynamic membrane hypothesis. In the past, we were limited by our lack of sophistication in manipulating and monitoring biomembranes and their experimental analogs. Today, membrane biophysics is a matured field of research as a result of applications of many elegant techniques including spectroscopy, membrane bioelectrochemistry, patch-clamp, and membrane reconstitution. In the chapters that follow, the area of membrane biophysics will be perused, from the origin of the lipid bilayer concept to membrane transport, electrochemistry, membrane reconstitution, bioenergetics, and to membrane photobiology. Fig. 1.1 gives an overview of the various topics covered in this book. It also illustrates the central role played by the cell membrane and its methods of investigation. Functionally, biomembranes may be broadly classified into five basic types, as also indicated in Fig. 1.1. Several investigators have proposed ways by which lipid bilayers (BLMs and vesicles) could form in nature [Tien, 1974]. For example,

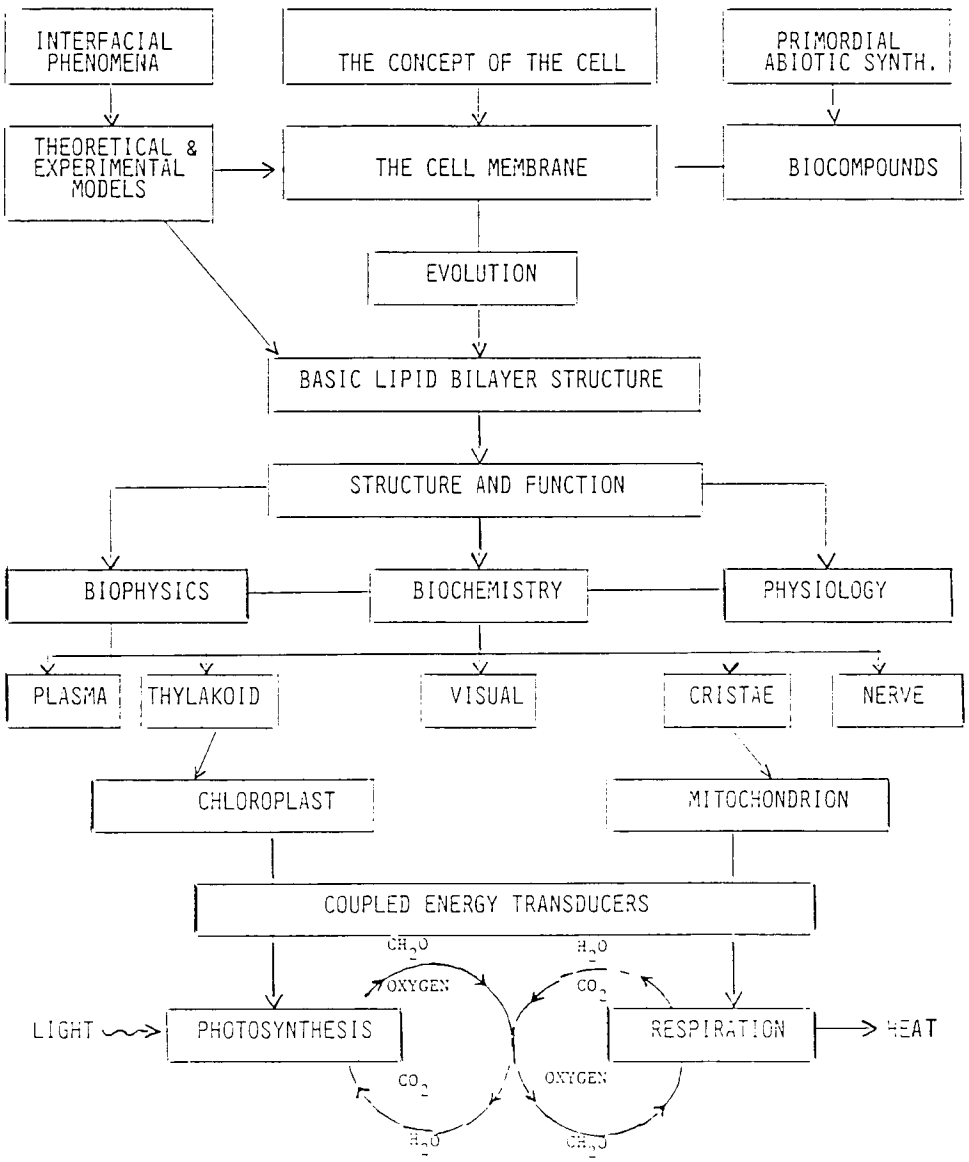

Fig. 1.1 The life cycle, biomembranes, their interrelationship and methods of inquiry. The pivotal idea of biomembranes is the lipid bilayer. An infinity sign shown at the bottom of the figure represents the life cycle, driven by solar energy. The two-coupled circles depict a steady-state energy transducing system of life.

by a process of selective absorption of photoactive pigments such as chlorophyll, these vesicles could be transformed into primitive quantum cells. Conversion of light by experimental pigmented lipid bilayers into electrical and/or chemical energy lends credence to these speculations [Volkov et al, 1998]. The life cycle, as we know it, is driven by the electromagnetic radiation of the Sun, which is depicted by an infinity sign at the lower portion of Fig. 1.1. The two basic processes of life are *photosynthesis* and *respiration*, which are carried out respectively by the thylakoid membrane of the chloroplast and by the cristae membrane of the mitochondrion. The two-coupled circles delineate a steady-state energy transducing system of life. The essential feature of this system is that it represents a steady state brought about by the flow of energy from a high potential source (the Sun) to a low potential sink (the Earth). It should be noted that it is not the energy itself that makes life possible, but the flow of energy through the energy-transducing membranes of the system. Thus, our task is to understand how energy in the form of sunlight is transformed into the electrical and/or chemical energy that fuels the life cycle (Chapters 8 & 9). In the final chapter potential applications of self-assembled lipid bilayers as biosensors will be presented. Recent advances in microelectronics coupled with membrane research of past decades have come of age and are poised for technological exploitation. The connecting thread among these topics is experimental lipid bilayers (planar BLMs and spherical liposomes). The basic principles of thermodynamics, kinetics, the Nernst-Planck equation, and physical chemistry will be applied to the above areas of membrane biophysics.

1.6 An idealized living cell

Perhaps, the best starting point of discussion on the biomembrane is to begin with an overview of the cell. Fig.1.2 shows schematically the plasma membrane of a highly idealized eukaryotic cell, together with its organelle membrane systems. It may be seen that, even in this greatly simplified drawing, the plasma membrane is an extremely complex and elaborate supramolecular structure. The most important feature is that the plasma membrane of cells is consisting of a two-dimensional liquid-crystalline lipid bilayer in which various functional entities (e.g. enzymes,

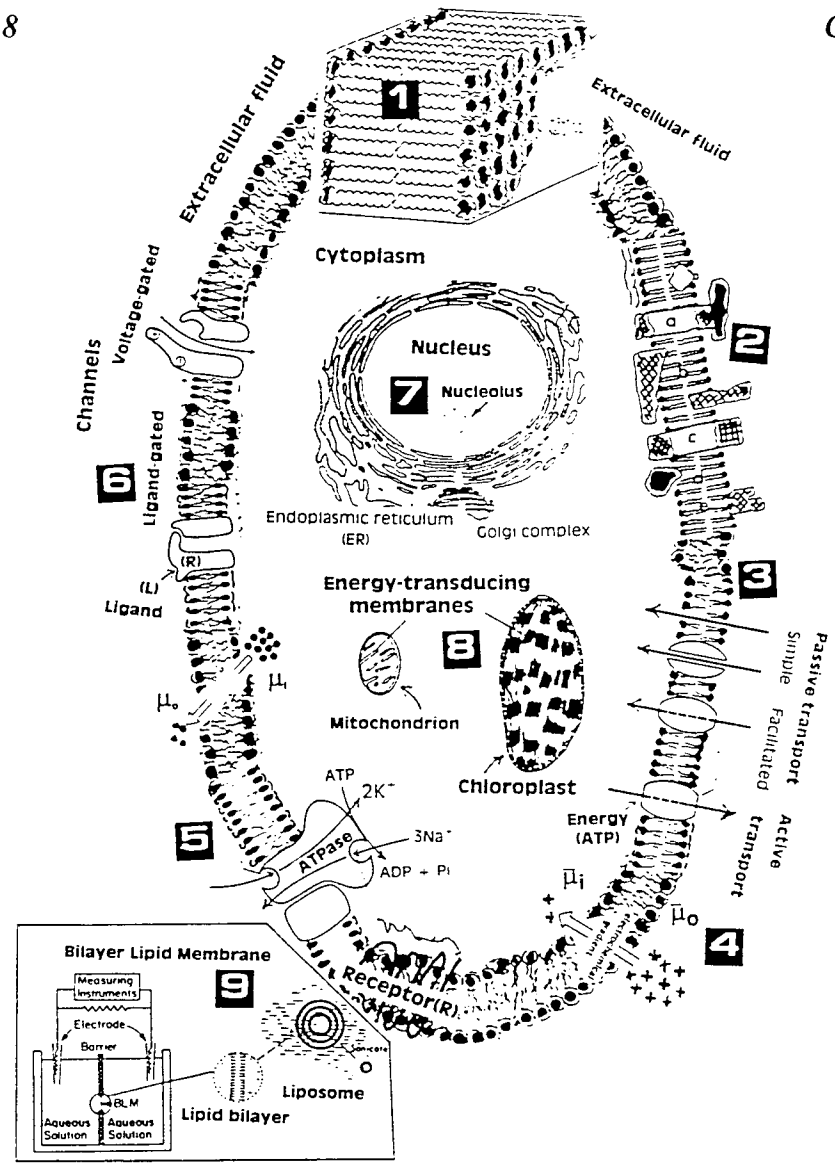

Fig. 1.2 An idealized plasma membrane of the cell possesses; an elaborate array of transmembrane entities are, either embedded in, or associated with, the lipid bilayer. Also shown are its organelle membrane systems. Figure captions are given on the facing page.

(1) **The Lipid Bilayer**: A universal element of all cell membranes.
(2) **Membrane Proteins**: Manners by which they are associated with the lipid bilayer: (a) span the bilayer, (b) partially immerse in the bilayer, (c) held by non-covalent interactions with other proteins, and (d) attach to fatty acid chains by anchoring the protein in one surface of the bilayer.
(3) **Permeability and Transport**: Passive transport occurs either by simple diffusion or by facilitated diffusion. Active transport needs an input of the metabolic energy.
(4) **The Electrochemical Potential**: $\underline{\mu}$, The driving force for membrane transport, oxidative- and photo-phosphorylation.
(5) **The Na^+ - K^+ Pump**: Virtually all animal cells contain a Na^+/K^+ pump that operates as an antiport, actively pumping K^+ into the cell and Na^+ out against their electrochemical gradients.
(6) **Ion Channels**: There are ligand-gated and voltage-gated channels made of proteins, which open in response to ligand interaction and voltage change. For example, a Ca^{2+} channel may be depicted as a port with negatively charged sites, to act as a 'selectivity filter' to distinguish among different cations, with voltage-sensors conferring voltage dependence on channel opening and closing.
(7) **The Nucleus**: Where genetic material (DNA) is located. Its nuclear membrane has numerous pores (up to ~ 80 nm in diameter) which probably transport large particles selectively.
(8) **Energy-transducing Organelle Membranes**: The mitochondrion converts foods into usable energy (ATP), whereas the chloroplast, in plants and other photosynthesizing organisms, transduces electromagnetic radiation (solar energy) into other forms of energy.
(9) **Experimental Bilayer Lipid Membranes**: Since their inception in the early 1960s, such lipid bilayer systems, either in the form of a planar BLM or of a vesicular liposome, have been used extensively as models of biomembranes(Chapter 4). The advantage of the planar lipid bilayer (BLM) system is that both sides of the membrane can be easily altered and probed by electrodes. For long-term investigations and practical applications, planar BLMs can also be formed on either gel or metallic supports (Chapter 10, *Applications*).

receptors, channels, pigments, etc.) are embedded. Structurally, the lipid bilayer is a very complex system, but it is predominantly composed of various phospholipids. Some small molecules such as ethanol, chloroform, and ether are known to interact with a lipid bilayer with dramatic results. For example, anesthetics interact with nerve cell membranes, which results in the anesthetic effect. Further, many cell functions are mediated by interactions of various molecules with the lipid bilayer and its associated receptor sites. Fortunately, many of these interactions are quite well understood at the molecular level, as a result of extensive investigations of past decades using experimental lipid bilayers (Chapter 4, *BLMs and Liposomes*). The rationale is that, in order to comprehend as well as to explain the structure and function of natural cell membranes in physical and biochemical terms, resorting to model systems has a long tradition in natural sciences. Thus, insofar as experimental model cell membranes are concerned, there are planar bilayer lipid membranes (BLMs) and spherical liposomes, both of which are also depicted in Fig. 1.2 and will be discussed in detail in the subsequent chapters. It should be pointed out that, however, planar BLMs and liposomes are more than mimetic biomembrane models; they are self-assembled lipid bilayers *in vitro*, which constitute the fundamental structure of all biomembranes.

As already stated above, the cell is the smallest functional unit of organelles and tissues. Thermodynamically speaking, a living cell is an open system capable of energy transformation and material transport. Both the cell and its organelles (e.g. mitochondria and chloroplasts) are separated from their environment by membranes that are believed to be crucial in the evolution of life. Structurally, the cell membrane is a lipid bilayer matrix modified by functional proteins, carbohydrates and their complexes. Compositionwise, cells are about 90% water. The rest, on the dry weight basis is approximately: 50% protein, 15% each for carbohydrate and nucleic acid, 10% lipid, and 10% miscellaneous compounds. In terms of the chemical elements, a typical cell consists of about 60% hydrogen (H), 25% oxygen (O), 12% carbon (C), and about 5% nitrogen (N). It should be noted that certain other elements that are significant constituents of living organisms are phosphorus (P), and sulphur (S). Additionally, trace amounts of sodium (Na), magnesium (Mg), chlorine (Cl), potassium (K), calcium (Ca), and iron (Fe), and even less quantities of certain other metals such as selenium (Se), silicon (Si),

and zinc (Zn) are also present. These trace elements are essential to some enzyme activities. In the case of selenium (Se), for example, there is a lot of interest in this element as a potential substance to prevent both heart disease and cancer; it is needed for human health. People and animals that eat them absorb Se in the soil by plants and subsequently. Natural Se levels in the soil are highly variable throughout the world. Selenium is naturally found in foods high in protein, such as meat, poultry, fish, cereals and other grains. It can also be found in vegetables like mushrooms and asparagus. Se is an antioxidant that can help to prevent the degradation of fats and cell membranes and block the action of cancer-causing chemicals. According to one recent report, people that naturally ingest about 60 to 120 micrograms per day or take the selenium supplements have the lowest levels of esophagus, lung, breast, pancreas, bladder, ovary, colon and rectum cancer.

Returning to the physicochemical aspect of the cell membranes, the formation of a lipid bilayer in water is a self-assembling, 'downhill' process involving rearrangements of water and lipid molecules such that the overall free energy change for the reaction is at an optimum. For the reactants involved, they must attain a state of minimum energy and maximum entropy. In order to accomplish this, the hydrocarbon chains of the lipids are sequestered *away* from water whereas the polar groups are in contact with water to attain maximal interactions. In other words, the chemist's rule of 'like dissolves like' is obeyed (Chapter 3). Here, one of the most important properties of the lipid bilayer, to keep in mind, is that it can exist in a *liquid* crystalline state. Functionally, the cell membrane plays a pivotal role in energy conversion, material translocation, signal transduction and information processing. Most biomembranes are semi-permeable, meaning they are permeable to water but selectively to solutes (e.g. glucose, ions, etc. *See* Chapter 5). Passive transport occurs either by simple diffusion or by facilitated diffusion and requires no energy input; the species involved moves down hill. For the process to take place at significant rates, the transfer of species requires either carriers or protein channels. When the movement of one permeant is dependent on the simultaneous movement of different permeant either in the same direction (symport) or in the opposite direction (antiport), this is termed as a co-transport system. The best-known antiport system is the Na^+/K^+-ATPase 'pump' that is present virtually in the plasma membrane of all animal

cells. This so-called pump moves Na^+ and K^+ through the lipid bilayer, and operates as an antiport, actively drawing K^+ into, and Na^+ out the cell against their electrochemical gradients. Active transport therefore needs an input of metabolic energy. For every ATP hydrolyzed, 3 Na^+ are pumped out and 2 K^+ are pumped in. Note that ouabain (an ATPase inhibitor) and K^+ compete for the same site on the external side of the ATPase pump. Transmembrane activities are thermodynamically driven by gradients of chemical, μ and/or electrochemical potentials, $\underline{\mu}$ (Chapter 6, *Membrane Electrochemistry*). To counter these spontaneous activities or processes, metabolic energy must be spent in order to make the living state of the cell viable. For example, in mitochondria, μ across the inner (cristae) membrane is responsible for pumping Ca^{2+} out of the cytosol (where concentration $[Ca^{2+}] < 10^{-7}$ M). The cristae membrane contains a transport protein that efficiently moves Ca^{2+} into the matrix where they are stored as calcium phosphate. The matrix is negatively charged owing to the efflux of H^+ ions.

Before considering signal transduction in Section 1.7, brief descriptions should be given regarding other items, such as the nucleus and its associated entities, and vacuoles shown in Fig. 1.2. The vacuole is unique in plant cells; it is a storage place for inorganic compounds, and is similar to lysosomes in function. There are many types of lysosomes in vesicular form containing acidic hydrolytic enzymes; they are sometimes referred to as 'microbodies'. The structures vary in size from 0.2 to 2 μm in diameter. The staining reveals a crystal like matrix in spherical vesicles. The crystalloid matrix is urate oxidase. These are small organelles containing around 40 enzymes for intercellular digestion. The lysosome membrane helps to protect the enzymes as much as it helps to protect the cell. This is because the optimal pH for these enzymes is around a pH of 5. The membrane of the lysosome is again a lipid bilayer and has an ATPase pump to draw protons (H_3O^+) into the lysosome to maintain the pH. The pump is operated by ATP hydrolysis. Other small molecules can pass through the lysosome lipid bilayer, but will then become charged by picking up a free proton, thereby making them difficult to leave the lysosome. Another organelle is the peroxisome, like the lysosome it is made of a lipid bilayer, encapsulating oxidative materials, but unlike lysosomes, it contains oxidative enzymes, such as D-amino acid oxidase, urate oxidase, and catalase. The peroxisome is self-replicating, like the

mitochondrion, and is a major site of oxygen utilization (along with the mitochondrion). One of the main functions of peroxisomes in liver cells is detoxification, where toxic byproducts are numerous (such as hydrogen peroxide, phenols or other metabolites). This is done by the oxidation of substances, for example, ethyl alcohol to acetaldehyde.

For the survival of the cell, there are other major structures spread randomly throughout the cytoplasm besides those already described. The cytoplasm, the site of many metabolic cycles and synthetic pathways, as well as the location of protein synthesis, is closely associated with the nucleus. The nucleus is where the genetic material (DNA) is located. Its nuclear membrane has numerous pores (up to ~ 80 nm in diameter) which probably transport large particles selectively. The nucleolus is usually visible as a dark spot in the nucleus, and is the site of ribosome formation. Other groups associated with the nucleus are the endoplasmic reticulum (ER) -- there are smooth ER, associated with many enzymes and rough ER, studded with ribosomes for protein synthesis; both types of ER's are usually attached to the nuclear envelope and extending into the cytoplasm. The Golgi complex -- similar to the smooth ER, is involved in pinocytosis (*see* Chapter 7, *Membrane Physiology*).

In closing this section, mention should be made concerning the cytoskeleton, which is transparent in standard light and electron microscope preparations, and is therefore 'invisible'. The cytoskeleton is an important complex and a dynamic cell component. It maintains the cell's shape, anchors organelles in place, and moves parts of the cell in processes of growth and mobility. The cytoskeleton is made of many types of protein filaments, the two most studied of which are the microtubules and actin. Microtubules are made of tubulin subunits; cells to change their shapes as well as restrain structures often use them. Experiments with tubulins with BLMs will be considered in Chapter 7 (*Membrane Physiology*).

1.7 Signal transduction

Information transfer across the cell membrane is paramount to the interaction of our bodies with the external world. The receipt of signals by a cell is a complex task. For example, a coordinated body activity such as walking requires integration of many systems such as respiratory, nerve, sensing, muscle, circulatory, etc. At the cellular level, communications via the membrane are essential, which may be termed generally as *signal transduction*, since proteins and peptide hormones, neurotransmitters, growth factors, and other bioactive molecules, known collectively as *ligands*, do not always exert their effects directly by entering cells. Instead, some of these chemical signaling agents interact with a specific receptor situated on/in the lipid bilayer of the membrane. It is called the ligand-receptor contact interaction. One outstanding example is the interaction between adrenaline and its receptor. Here, ligand L (i.e. adrenaline or epinephrine) interacts with its receptor R. This R is embedded in the lipid bilayer of the plasma membrane, made of a snake-like chain criss-crossing the lipid bilayer seven times. The epinephrine ligand (L) is not transported into the cell. Instead, while bound for a short period of time to its receptor (R), it causes the latter to release biochemical signals into the cell cytoplasm. When an animal such as a deer or a human being for that matter, is under stress, L is released from adrenal glands (associated with the kidneys) into the blood stream, which interacts with R situated on the plasma membrane surface (in the various parts of the body). The L-R contact interaction results in the so-called fight/flight primitive reaction, manifesting in an increased heart rate, a decreased blood flow to intestines, an increased blood flow to skeletal muscles, and an increased blood glucose. In general, each type of receptor (R) is said to bind specifically to its own ligand (L). For example, the so-called G-receptor is usually coupled to a guanosine nucleotide-binding protein (hence termed a G-protein), that in turn stimulates or inhibits an intracellular, lipid bilayer-bound enzyme. There are at least several hundred distinct ligand-receptor pairs in our body, each is devoted to the binding of a distinct extracellular ligand. Animal cells like our own have wide and diverse types of transmembrane G-protein receptors, for a number of vital signaling functions, including vision, smell, and taste. For vision, a carotenoid molecule related to vitamin A is bound in the ligand

position of rhodopsin in the rods and cones of our eyes. Rhodopsin, embedded in the lipid bilayer of the visual receptor membrane, serves to pick up photons, alters its conformation, and causes the photo-receptor to which it is bound to release signals into the rod/cone cytoplasm that results in our perception of light (Chapter 9, *Membrane Photobiology*). For smell, hundreds of distinct receptor species in the cells of our olfactory bulbs in the nose convey information about the presence of odorant ligands (odors). The subject will be further considered in Chapter 7 (*Membrane Physiology*). For taste, receptors on the cells lining of our tongue communicate sensation. This type of receptors is embedded in the membrane lipid bilayer, has a snake-like configuration, and does not depend upon L-R contact (such as antigen-antibody binding) in order to transduce signals across the plasma membrane. Instead, single receptor molecules will change their steric configuration in response to ligand binding. This three-dimensional shift affects the configuration of the cytoplasmic domains of the receptor that is the loops of a receptor protein that protrude into the cytoplasm. The process by which an extracellular signal (typically a hormone or a neurotransmitter) interacts with a receptor at the cell surface, causing a change in the level of a second messenger (e.g. Ca^{2+}, DAG -- diacylglycerol), is often called a signal cascade. Mobilization of intracellular Ca^{2+} can be triggered by a number signals including membrane potential change, cell-cell fusion, and hormone-binding to a specific surface receptor. These signals are linked to Ca^{2+}-release activators: inositol triphophate (IP_3), cyclic ADP, inositol triphosphate ribose (cADDPR) and sphingosine-1-phosphate. The subject of calcium signaling by cyclic ADP-Ribose and NAADP has been recently reviewed.[1,4] We will only describe the β-adrenergic receptor in more detail here. Mention should be made, however, that such processes can also be applied to the sensory signal transduction of light at photoreceptors, triggering the glucose uptake, or initiating cell division.

The β-adrenergic receptor communicates with the cytoplasm by stimulating a second G-protein (a guanosine nucleotide-binding protein), which normally resides near the receptor in a 'resting' state. When ligand binding activates the receptor, it will jolt the G protein in action. The G protein responds by switching itself on into an active state. Once in the active state, the G protein will send signals further into the cell. However, the G-protein will remain in the active state for only a short period of time,

after which it will shut itself off. In effect, the G protein acts like a timed on-off switch. This β-adrenergic receptor's on or off states are determined by the guanine nucleotide that it binds. When active, it binds GTP (guanine triphosphate) (on state), when it is inactive it binds GDP (guanine diphosphate) (off-state). While in the on state, it releases signals downstream. After a short period of time (a few seconds later), the G protein will then hydrolyze its own GTP down to GDP, thereby shutting itself off. This hydrolysis represents a negative feedback mechanism, which ensures that the G protein is only in the active, signal-emitting on mode for a short period of time. When the β-adrenergic receptor activates the G protein (it consists of α, β, and γ subunits), the α subunit releases GDP, binds GTP and falls away from the β and γ subunits. Once this happens, the GTP-bound subunit also loses affinity for the receptor, dissociates from it, and moves over and jolts yet another nearby enzyme, the enzyme adenylate cyclase, which until this time has been inactive. Once it is jolted by the active, GTP-binding G-protein, the adenylate cyclase enzyme gets activated and does its job, thereby generating cyclic or cAMP. The whole cycle has resulted in only a brief pulse of signaling, in this case the production of several hundred cAMP molecules made by the adenylate cyclase during its brief period of activity. The cAMP molecules acting as intracellular hormones are sometimes termed second messengers, in that they can diffuse throughout the cytoplasm and carry information to distant sites. There is enormous signal amplification in this cascade process.

Messengers, Signals and Membrane-bound Receptors

At the molecular level, there are at least four types of signals that are involved in signal transduction: nerve impulse, hormone release, muscle contraction, and growth stimulation. The chemical messengers mediate the process; they are small organic molecules, steroids, peptides, and proteins. The messenger molecule may interact with the cell in either of two ways: by diffusion through the cell membrane (e.g. lipid soluble steroids) or by binding to a receptor on the plasma membrane (forming a hormone-receptor complex, a type of L-R interaction). This is usually followed by a secondary event, formation of a second messenger, which is

then followed by the cellular response (some metabolic event). Removing the second messenger usually terminates the process.

Plasma membrane receptors

They bind specific messenger molecules on the exterior surface of the cell. Either of two types of response may occur: binding to the receptor directly causes the cellular response to the messenger, or binding to the receptor modifies it, leading to production of a second messenger, a molecule that causes the effect. In each case messenger binding brings about a conformational change in the receptor protein. In this sense, binding of the messenger resembles binding of a substrate to an enzyme in that there is a dissociation constant. Inhibition (by antagonists) which may be competitive, noncompetitive, etc. (*see* Chapter 3, *Basic Principles*). A variety of messengers can bind to various tissues. Either positive or negative responses may occur, even in the same tissue, depending on the type of receptor. Finally, the response of a cell to a messenger depends on the number of receptors occupied. In this connection, a typical cell may possess one thousand or more receptors, of which only a small fraction (~ 10%) of the receptors need to be occupied to get a significant response. This is because the very high formation constant involved between the ligand-receptor interaction, whose dissociation constant is on the order of 10^{-11}. Thus, very low concentrations of messengers may give a massive response. The subject will be further considered in Chapter 7, *Membrane Physiology*.

Messengers, Signals and Membrane-bound Receptors

At the molecular level, there are at least four types of signals that are involved in signal transduction: nerve impulse, hormone release, muscle contraction, and growth stimulation. The chemical messengers mediate the process; they are small organic molecules, steroids, peptides, and proteins. The messenger molecule may interact with the cell in either of two ways: by diffusion through the cell membrane (e.g. lipid soluble steroids) or by binding to a receptor on the plasma membrane (forming a hormone-receptor complex, a type of L-R interaction). This is usually followed by a secondary event, formation of a second messenger, which is

then followed by the cellular response (some metabolic event). Removing the second messenger usually terminates the process.

Plasma membrane receptors

They bind specific messenger molecules on the exterior surface of the cell. Either of two types of response may occur: binding to the receptor directly causes the cellular response to the messenger, or binding to the receptor modifies it, leading to production of a second messenger, a molecule that causes the effect. In each case messenger binding brings about a conformational change in the receptor protein. In this sense, binding of the messenger resembles binding of a substrate to an enzyme in that there is a dissociation constant. Inhibition (by antagonists) may be competitive, noncompetitive, etc. (*see* Chapter 3, *Basic Principles*). A variety of messengers can bind to various tissues. Either positive or negative responses may occur, even in the same tissue, depending on the type of receptor. Finally, the response of a cell to a messenger depends on the number of receptors occupied. In this connection, a typical cell may possess one thousand or more receptors, of which only a small fraction (~ 10%) of the receptors need to be occupied to get a significant response. This is because the very high formation constant involved between the ligand-receptor interaction, whose dissociation constant is on the order of 10^{-11}. Thus, very low concentrations of messengers may give a massive response.

The acetylcholine receptor (AchR)

The AchR of nervous tissue, for example, is a direct response class of receptor. Binding of acetylcholine, a small molecule, at the exterior surface of cell membrane causes the channel to open, allowing Na^+ and K^+ ions flow through the channel, depolarizing the membrane, initiating an action potential. Then, the choloineesterase activity of the receptor hydrolyses the acetylcholine, releasing acetate and choline, and terminating the effect. The receptor is ready for the next interaction and the process can now be repeated.

Receptors and second messengers

In some cases, the binding of an effector to a receptor leads to the formation of an intracellular molecule (mediator) which mediates the response of the effector (Fig. 1.3). This intracellular mediator is called a second messenger. Since a receptor usually forms many molecules of second messenger after being stimulated by one molecule of the original effector, second messenger formation is a means of amplifying the original signal. The formation and removal of the second messenger can be controlled and modulated. Specifically, cyclic AMP (cAMP = 3',5'-phosphodiester of adenylic acid) is a second messenger that mediates many cellular responses. The mechanism of action of cAMP is to activate an inactive protein kinase. This process is an amplification of the original signal. Another enzyme, adenyl cyclase is also part of the amplification system, which is controlled by two membrane G-protein complexes, Gs and Gi (so named because they stimulate and inhibit, respectively, adenyl cyclase). G-proteins are a class of proteins that they can react with GTP, causing the termination of the signal at several levels.

Other important second messengers are inositol triphosphate (IP_3) and diacylglycerol (DG), which are synthesized by the enzyme, phospholipase C. IP_3 releases Ca^{2+} from the endoplasmic reticulum. The Ca^{2+} then activates certain intracellular protein kinases. DG activates protein kinase c, a specific protein of the plasma membrane. This topic will be taken up again in Chapter 7 (*Membrane Physiology*).

In many cases the lipid bilayer-bound receptor is linked to an ion channel. There are Na^+, K^+, Ca^{2+}, Cl^-, and other channels. A signal, resulting from such a voltage-gated channel or lipid bilayer-specific interaction, is manifested in a change in the electrical properties of the membrane. Hence, an external message is transferred into the cell interior via an ever-present lipid bilayer. Additionally, there are so-called store-gated channels involving in particular Ca^{2+} ions, in which a direct protein-protein interaction is implicated. Fig. 1.3 illustrates a typical pattern of signal transduction steps. Both ligand-gated and voltage-gated ion channels have been embedded in experimental lipid bilayers (Chapter 7); they are useful in developing biosensors for technological applications,[2,3,5] as shown here and will be discussed in some details in Chapter 10 (*Applications*).

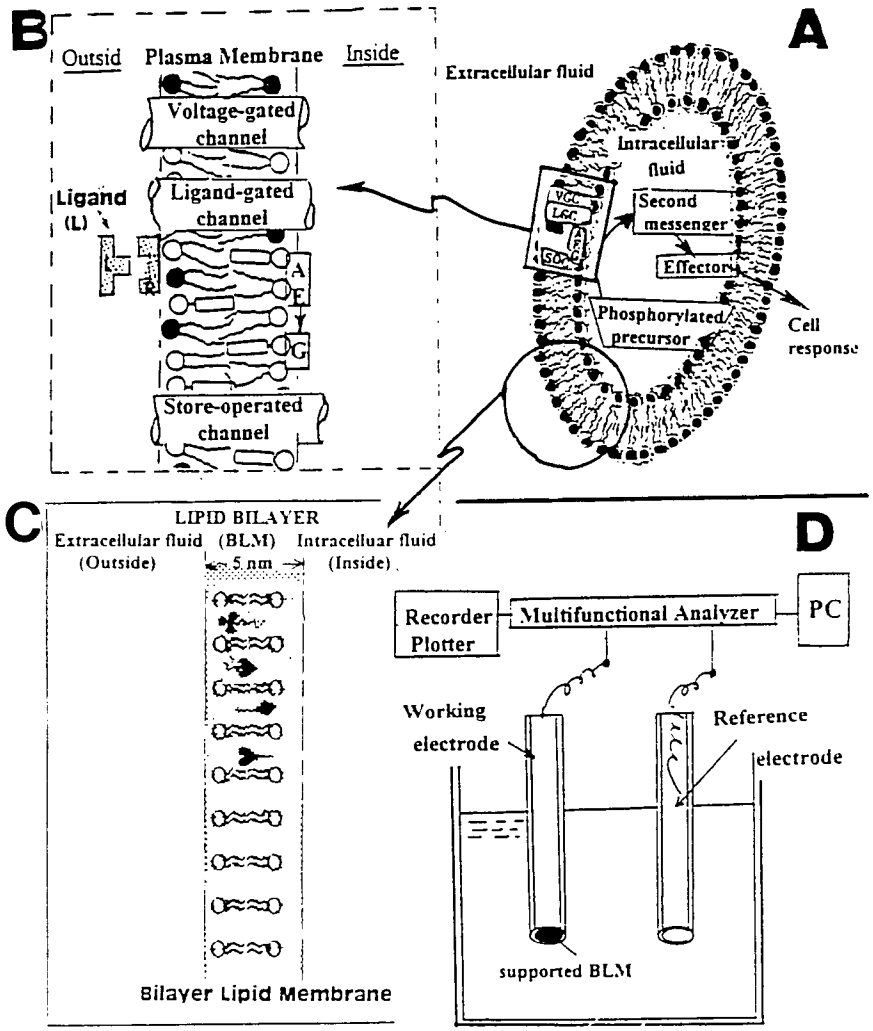

Fig. 1.3. Experimental bilayer lipid membrane (BLM) and signal transduction across the cell membrane. Also shown is a lipid bilayer-based sensor using electrical methods of detection. Figure descriptions are given on Page 21.

Figure descriptions for Fig. 1.3.

A A highly schematic diagram of a cell, illustrating one of the most common mechanisms of information transfer based on ligand-receptor interactions. Receptors are a special class of transmembrane lipid-protein-carbohydrate complexes that can be detected by their ligand. They have the reactive group projecting from the surface that binds a specific ligand. it shows in this figure the interaction between the ligand secreted by one cell (such as a hormone) and its receptor. The plasma membrane of the cell is depicted consisting of the following: a voltage-gated channel (VGC), a ligand-gated channel (LGC), a store-operated channel (SOC), G-proteins (G), amplifier enzyme (AE); all of these are lipid bilayer-bound. Upon receiving a signal (e.g. ligand, L) by the receptor (R), the resulting contact causes an enzyme to catalyze the production of second messengers from a phosphorylated precursor (cAMP, for example) which in turn triggers enzyme kinases through an intracellular effector leading ultimately to the cell response.

B An enlarged view of the above lipid bilayer-bound entities (R) and ligand (L) in the bathing solution.

C This diagram illustrates the molecular organization of a BLM separating two aqueous solutions. To mimic different biomembranes, a host of compounds (modifiers = ♣,♦,♥,♠) have been embedded in the BLM in order to impart unique functional characteristics.

D BLM-based biosensors. The schematic diagram illustrates an experimental arrangement used for the measurement of electrical properties of supported BLMs (*see* Chapter 10, *Applications*).

General References

H. T. Tien, *Bilayer Lipid Membranes (BLM): Theory and Practice*, Marcel Dekker, Inc. New York, 1974

B. Ivanov (ed.) *Thin Liquid Films: Fundamentals and Applications*, Marcel Dekker, Inc., NY. 1988. pp. 527-1057

G. Benga, ed., *Water Transport in Biological Membranes*, CRC Press, Boca Raton, Fl., 1988.

J. R. Harris and A.-H. Etemadi, eds *Subcellular Biochemistry*, Vol.., 14, Plenum Press, New York, 1989, Chapter 3.

J. R. Bourne (ed.) *Biomedical Engineering.*, 18(5), 323-340 (1991).

K. L. Mittal and D. O. Shah (eds.) *Surfactants in Solution*, Vols. **8** and **11**, Plenum, NY, 1990. 133-178; 1992. 61

R. F. Taylor and J. S. Schultz (eds.) *Handbook of Chemical and Biological Sensors* Institute of Physics Publishing, Philadelphia. 1996 .

M. Rosoff (ed.) *Vesicles*, Marcel Dekker, Inc., NY. 1996.

J. M. Kauffmann (ed.) 'Development and characterization of electrochemical biosensors based on organic molecular assemblies', *Bioelectrochemistry & Bioenergetics*, **42** (1997) 1-104

A. G. Volkov, D. W. Deamer, D. L. Tanelian and V. S. Markin, *Liquid Interfaces in Chemistry and Biology*, Wiley, Inc. New York, 1998

Y. Umezawa, S. Kihara, K. Suzuki, N. Teramae and H. Watarai (Eds.), Molecular recognition at liquid-liquid interfaces: fundamentals and analytical applications: *ANALYTIACAL SICENCES,* 14 (1998)

A. Brett and A. M. Oliverira Brett (eds.) Electroanalytical Chemistry, Special issue, *Electrochim, Acta*, 43: (23) 3587-3610 1998

Specific References

1. M. J. Berridge, *Biochem. J.*, **312** (1995) 1
2. A. Ottova, V. Tvarozek, J. Racek, J. Sabo, W. Ziegler, T. Hianik, and H. T. Tien, *Supramolecular Science*, **4** (1997) 101-112
3. H. C. Lee (Editor), *Cell Biochemistry and Biophysics*, **28** (1998) 1-73
4. H. T. Tien and A. L. Ottova, 'From self-assembled bilayer lipid membranes (BLMs) to supported BLMs on metal and gel substrates to practical applications, *Colloids and Surfaces A: Physicochemical and Engineering Aspects*, 149, 217-233 (1999)

Chapter 2

Fundamental Aspects Of Biological Membranes

"... the basic structure of all biomembranes is a lipid bilayer."

"Much of our knowledge of (soap) film behavior is of respectable antiquity. The color changes (to) ...'black film' studied by Newton...The most important contributor to our understanding ... is probably J. W. Gibbs, ...a theoretical investigator, his insight was based on personal observations and experiments."

----- from Soap Films by Mysels, Shinoda and Frankel (Pergamon, 1959. Page 3)

If I have seen further it is by standing on the shoulders of Giants."
Isaac Newton to Robert Hooke, February 5, 1675

2.1 Origins of the Lipid Bilayer Concept

2.2 Experimental Evidence for the Lipid Bilayer

2.3 Composition of Biomembranes

Interface Approach to Membrane Lipid Chemistry
Elements of Membrane Proteins
Elements of Membrane Carbohydrates
Lipid-protein-carbohydrate Complexes

2.4 The Ultrastructure of Biomembranes

The 'Chop Suey' Model

2.5 Functions of Biomembranes

The Lipid Bilayer: Structure and Function

General References (cited by name in brackets in the text)
Specific References (cited by number in superscript in the text)

2.1 Origins of the lipid bilayer concept

Since a plasma membrane exists in plant cells and in animal cells, it is therefore appropriate to use the term biological membranes or biomembranes for short. Having introduced the term biomembranes, the stage is set to present an overview of the evolution of the lipid bilayer concept, upon which our life, happiness and the pursuit of membrane biophysics depends!

Nowadays it is taken for granted that the fundamental structure of all biomembranes comprises a lipid bilayer as its principal element. The recognition of the lipid bilayer as a model for biomembranes dates back only about 75 years or so. The origin of the lipid bilayer concept, however, is much older; it may be traced back to more than three centuries! It all began with the physicist and inventor Robert Hooke of Hooke's Law fame, who in 1665 coined the term "cell" to describe the tiny array of a cork slice after observing it with a primitive microscope which he had constructed. By a happenstance, the same Robert Hooke also studied common soap bubbles under the microscope[1] and described his observation in 1672 as follows:

"*. . . the film of the soap bubble began to appear again white, and presently . . . there appear several (black) holes, which by degrees increase and grow bigger, and several of them break into one another, till at length they become very conspicuous and big . . . It is pretty hard to imagine, what curious net or invisible body it is, that should keep the form of the bubble . . .*". Some three decades later, Isaac Newton (see the cliche quoted under the chapter heading) estimated the thickness of 'blackest' soap films,[1] he wrote:

"*. . . I saw within it several smaller round spots, which appeared much blacker and darker than the rest . . .and by farther trial I found that I could see the images of the Sun very faintly reflected, not only from the great black spot but also from the little darker spots . . .I have composed the following Table wherein the thickness . . .at which each colour is most intense and specific is expressed in parts of an inch divided into ten*

hundred thousand equal parts . . . In this table very black is 3/8 of a part...".

Newton's value of 3/8 x 10^{-6} inch when converted into modern units is equal to 9.5 nm, which is in excellent agreement with modern measurements. As we shall discuss presently and in some later chapters, the early observation of "black holes" in soap films had a profound influence in the development of the lipid bilayer concept of biomembranes and subsequent realization in the experimental planar bilayer lipid membrane (BLM)[4a] and lipid vesicles or spherical liposomes[4b] (*see* Chapter 4).

Recently, there has been much discussion on the self-assemblies of molecules, meaning the aggregation of molecular moieties into thermodynamically stable and more ordered structures.[9] Without question, the inspiration for this exciting development comes from the biological world. For example, Nature uses self-assembly as a strategy to create complex, functional structures such as viral protein coatings, and DNA, besides the above-mentioned *lipid bilayer* of cell membranes. In this connection it should be stated that many researchers have reported self-assembling systems such as Langmuir-Blodgett monolayers and multi-layers.[3] A comprehensive list on man-made self-assembling systems is given in Table 2.1.

2.2 Experimental Evidence for the Lipid Bilayer

Osmotic properties (Pfeffer, 1877)

Question: Is there a plasma membrane?

Osmosis, a diffusion phenomenon, can be easily observed in a device called an osmometer in which a membrane permeable only to water separates two chambers. When solutions of different concentration are present, water will flow from the dilute chamber into the concentrated one until equilibrium is reached, at which the extra pressure known as the osmotic pressure is produced. Van't Hoff found empirically that the

osmotic pressure (π) is directly proportional to the concentration, C, of solute for dilute solutions and is given by

$$\pi = CRT \qquad (2.1)$$

where R = gas constant and T = absolute temperature. It should be remembered that the osmotic pressure of a solution depends on the number of particles in solution (a colligative property). If a solute dissociates into *i* number of particles (or ions), the right side of Eq. (2.1) should be multiplied by '*i*'. With Eq.(2.1) in mind, Pfeffer immersed plant cells of *Chara* in salt solutions of various concentrations and observed that the cells swelled in hypotonic (low salt) solutions and shrank in hypertonic (high

Table 2.1

Experimental self-assembling interfacial systems

System	Interfaces*
1. Soap films[1]	air | water | air
2. Monolayers[2]	air | molecular layer | water
3. Multilayers[3]	air | molecular layers | water
4. Bilayers[4] (BLMs and Liposomes)	water | lipid bilayer | water
5. Nuclepore supported BLMs[5]	water | lipid bilayer | water
6. Gold supported Monolayers[6]	air | molecular layers | gold
7. Metal supported BLMs[7] (s-BLMs)	water | lipid bilayer | metal
8. Salt-bridge supported BLMs[8] (sb-BLMs)	water | lipid bilayer | hydrogel

*where the vertical line | denotes an interface.

salt) solutions. To account for similarities in the osmotic behavior of plant cells and man-made osmometers, Pfeffer, recognizing that the boundary of discontinuity between the protoplasma and its environment must constitute an osmotically semipermeable membrane, postulated the existence of an invisible (under light microscope) plasma membrane in the plant cell. Later experiments with erythrocytes or red blood cells (RBC) fully supported the postulation of Pfeffer.

Penetration studies (Overton, 1890-1899)

Question*: What is the nature of the plasma membrane?*

Overton, over a ten-year period, carried out some 10,000 experiments with more than 500 different chemical compounds. Basically he measured the rate of entrance of compounds into cells and compared the rates with the partition coefficients (K) of these compounds between olive oil and aqueous solution. He found that fatty compounds such as diethyl ether with larger partition coefficients readily entered the cell. That is, following the chemists' rule of 'like-dissolves-like', the cell membrane must be oily or lipid-like. Overton concluded that there must be a lipoid film of lecithin and cholesterol in the cell membrane separating its cytoplasm from its surroundings. Overton's findings have since been confirmed and extended by Collander who found that these were compounds such as urea, glycerol, and ethylene glycol with small olive oil/water partition coefficients, but could still readily penetrat the cell. To explain this 'anomaly', water-filled pores in the plasma membrane were later proposed (*see* Chapter.7, *Membrane Physiology*).

Electric potential (Bernstein, 1902)

***Question*: What is the meaning of membrane potential?**

From the1900s on, the dominant theory for nerve cells was due to Bernstein, whose hypothesis postulated that a cell consists of a

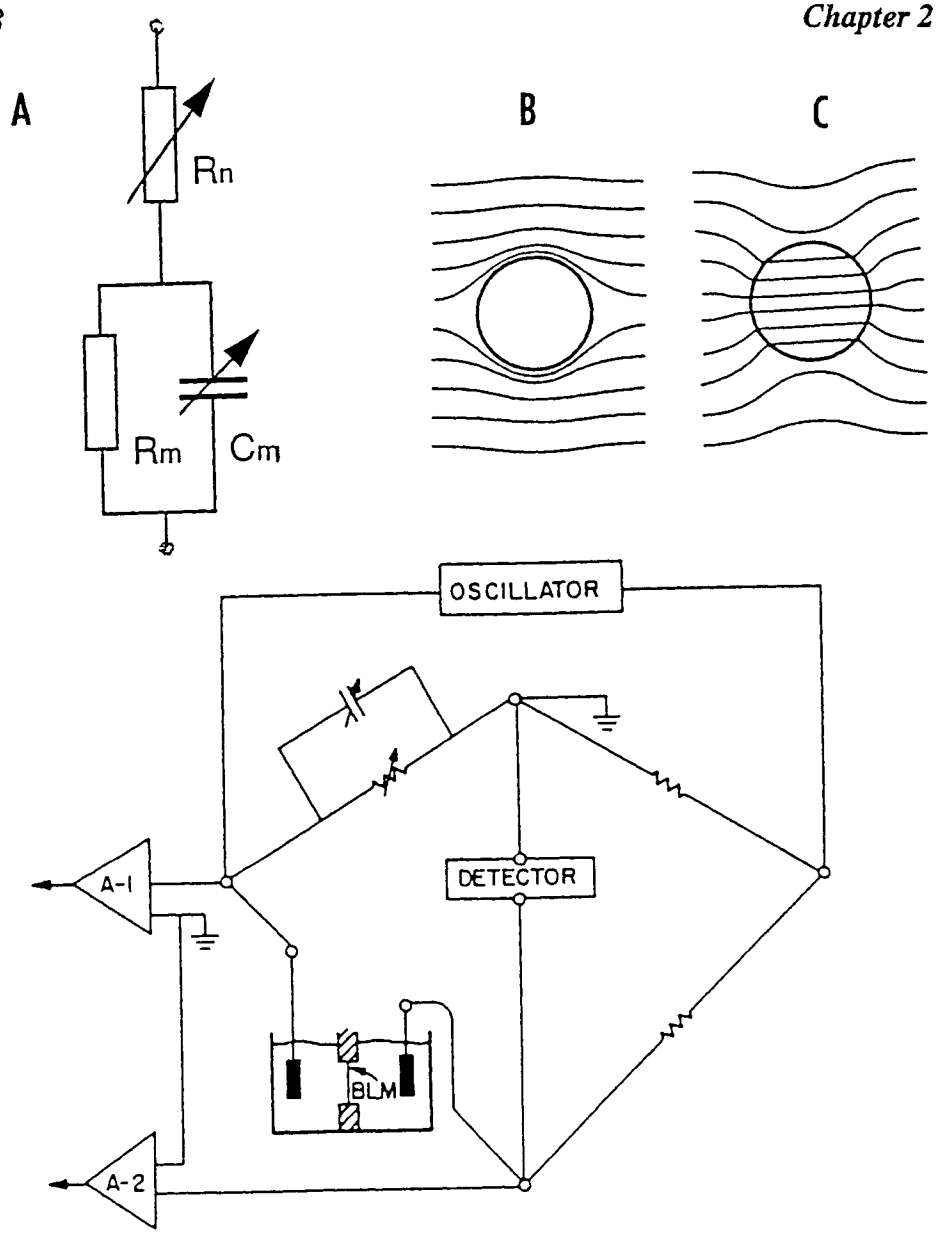

Fig. 2.1 Frequency dependence of red blood cell (RBC). *Upper.* A. Equivalent circuit. B. and C. show lines of current around a BRC. *Lower.* A setup used for BLM experiments.

semipermable membrane capable of electrical activities and recordable as an electric potential difference across the membrane. Changes in membrane permeability would result a change in this potential difference. At rest, the membrane was permeable to K^+ only. Although later shown to be not completely correct (Chapter 7, *Membrane Physiology*), the Bernstein hypothesis stimulated much discussion on the action potential among neuroscientists.

Electrical measurements (Fricke, 1923-25)

***Question*: How thick is the plasma membrane?**

Fricke, a physicist, carried out the following experiment shown in Fig. 2.1:

1. Red blood cells (RBC) were suspended in a saline (isotonic) solution,
2. Two Pt electrodes were placed in the suspension,
3. To one-arm of a Wheatstone bridge, the electrodes were connected, and
4. The conductivity and capacity of the RBC suspension were measured as a function of frequency.

At low frequencies the impedance of the suspension of RBC is very high, whereas at high frequencies the impedance decreases to a low value (Fig.2.1b). To explain his findings, Fricke proposed a model. RBC were surrounded by a thin layer of low dielectric material electrically equivalent to a resistor (R_m) and a capacitor (C_m) in parallel (Fig.2.1c). Thus, the lines of current flow around the RBC at low frequencies. At very high frequencies, the resistance becomes very low because all the current is shunted through the capacitor. It should be pointed out, however, that Hober in 1910 found that suspensions of intact RBC have a high electrical resistance, while the cytoplasm has a conductivity similar to that of physiological saline. From this fact, Hober concluded that the cell membrane has a high electrical resistance. Using the formula for a parallel

plate, Fricke determined the capacitance (C_m) of the RBC to be 0.81 μFcm^{-2}. For a parallel plate condenser, the capacitance is given by

$$C_m = \frac{\varepsilon}{4 \pi t_m} \qquad (2.2)$$

where C_m = membrane capacitance (μFcm^{-2}), ε = dielectric constant of the membrane and t_m = membrane thickness. Fricke calculated the thickness of RBC membrane, t_m, to be 3.3 nm and 11 nm, assuming $\varepsilon = 3$ and $\varepsilon = 10$, respectively. Indeed, modern measurements on artificial bilayer lipid membranes (BLMs) and biomembranes, fully confirmed Fricke's estimation of the thickness of the plasma membrane (*see* Chapter 4, *Experimental Models of Biomembranes*).

The monolayer experiment (Gorter and Grendel, 1925)

***Question*: What is the molecular organization of lipids in the plasma membrane ?**

In 1917 Langmuir demonstrated in a simple apparatus (now known as the Langmuir trough) that fatty materials including lipids in organic solvents spread in a monomolecular (monolayer) way when they are placed at an air/water interface.[2] From the known quantity of the material used and measured area covered, the dimensions of a molecule may be estimated. Less than a decade later using a Langmuir trough, E. Gorter, a pediatrician and F. Grendel, a chemist, determined the area occupied by lipid extracted from RBC ghosts and estimated that there was enough lipid to form a layer two molecules thick over the whole cell surface, that is

$$\frac{\textit{Surface area occupied} \text{ (from monolayer experiment)}}{\textit{Surface area of RBC} \text{ (from human, rat or pig source)}} \cong 2 \qquad (2.3)$$

On the basis of their results using simple but elegant experimental techniques, Gorter and Grendel made a historical suggestion that the plasma membrane of RBC may be thought of as a bimolecular lipid leaflet,[9] they wrote

"*...of which the polar groups are directed to the inside and to the outside, in much the same way as Bragg supposes the molecules to be oriented in a 'crystal' of fatty acid, and as the molecules of a soap bubble are according to Perrin.*"

Thus, the concept of a lipid bilayer as the fundamental structure of bio-membranes was born, and has ever since dominated our thinking about the molecular organization of all biomembranes.

From the 1930s on, research on biomembranes has gone in two major directions: (i) the further elaboration of the lipid bilayer concept using increasingly sophisticated physical chemical techniques, and (ii) the invention of model membrane systems so that physical, biochemical, and physiological processes may be isolated and analyzed in molecular terms. The former approach resulted in the unit membrane proposal, which led eventually to the so-called fluid mosaic model of biomembranes [Brown, 1971; Kerker, 1972; Robertson, 1981]. The other direction of research culminated in the reconstitution of lipid bilayers *in vitro*.[4] The use of experimental bilayer lipid membranes (BLMs and liposomes) will be discussed in details in Chapter 4 and in later chapters in the elucidation of biomembrane functions from a biophysics viewpoint.

For the time being, one needs to remember that all biomembranes possess a lipid bilayer of phospholipids as their foremost structural framework. However, in a real cell the membrane phospholipids create a spherical three-dimensional lipid bilayer sheath around the cell. Since the concept of the lipid bilayer is so crucial in our present understanding of membrane structure and function, therefore, the lipid bilayer can not be over-emphasized. Fig. 2.2 (upper) depicts a 3-dimensional structure of a bimolecular leaflet model. Nonetheless, the lipid bilayer is often represented two-dimensionally as an array of lipid molecules in an orderly fashion as illustrated in the lower part of Fig. 2.2. The circle, polar (head)

Table 2.2 The lipid bilayer concept: Origins and its Experimental Evolution

Year	Observer(s)	Experimental finding and insight
1665	R. Hooke	Microscopic observation of cork, Hooke coined the word "cell" which we use today
1672	R. Hooke	"Black holes" in soap bubbles[1a]
1704	I. Newton	Thickness of blackest soap films: 9.5 nm[1b]
1877	W. Pfeffer	Artificial osmometer and plasma membrane
1890s	E. Overton	Olive oil/water partition coefficient and lipoid nature of cell membrane
1917	I. Langmuir	The monolayer technique; orientation of "soapy" (amphipathic) molecules at interfaces[2]
1920s	H. Fricke	Electrical measurements of red blood cells; plasma membrane less than 10 nm thick
1925	E. Gorter & F. Grendel	Red blood cells covered by two lipid monolayers; the bilayer leaflet model was specifically put forth[9]
1940s	Davson & Danielli	A protein-lipid bilayer-protein sandwich model, a novel proposal [Robertson, 1981]
1950s	Robertson	Electron micrsoscopy – the unit membrane concept
1961	Rudin et al	The BLM technique for lipid bilayer reconstitution[4a]
1965	Bangham et al	Liposomes, vesicles with lipid bilayer structures[4b]

portion, is the negatively charged phosphate group and the two (tails) portion is the hydrophobic hydrocarbon chain of the phospholipids. The tails of the phospholipids orient towards each other creating a hydrophobic environment within the lipid bilayer. This leaves the charged phosphate groups reaching out into the aqueous environment. Fig. 2.2 further illustrates the organization of a lipid bilayer separating two aqueous solutions. The hydrophobic hydrocarbon chains (~ 5 nm) are in a fluid state and form the interior core of the bilayer, whereas the hydrophilic polar groups (~ 0.5 to 1.4 nm) are assembled in an orderly array as in a liquid crystal. The diameter of the area occupied per polar group is about 0.8 nm. The lipid bilayer is approximately 5 nm thick.

The major landmarks in the development of the lipid bilayer concept and its *in vitro* realization are chronologically listed in Table 2.2 [Kerker, 1972]. An examination of Table 2.2 reveals the diversity of techniques and approaches used in arriving the lipid bilayer, both theoretically and experimentally, as the central structural element of all biological membranes. It is instructive to summarize here that the origins of the lipid bilayer concept of the biomembrane structure and its experimental models, to be covered in the reminder of this book, are traceable to the early study of mundane soap bubbles and concomitant with the developments in cytology and in interfacial chemistry.[18] We will come back to this point later, after providing the chemical composition of biomembranes, which consist of lipids, proteins, carbohydrates and their complexes. The integral make-ups of these constituents are in close association with the current accepted bilayer leaflet model of membrane structure.

2.3 Composition of Biomembranes

The basic composition of biomembranes is a class of molecules called lipids. By virtue of their structures, lipids are amphiphilic (amphipathic); one portion of the molecule being hydrophilic (water-loving) and the other portion lipophilic (lipid-loving or hydrophobic). As a result of this unique water-oil solubility, lipids spontaneously form a bimolecular lipid leaflet (lipid bilayer) in aqueous solution. Embedded in the lipid

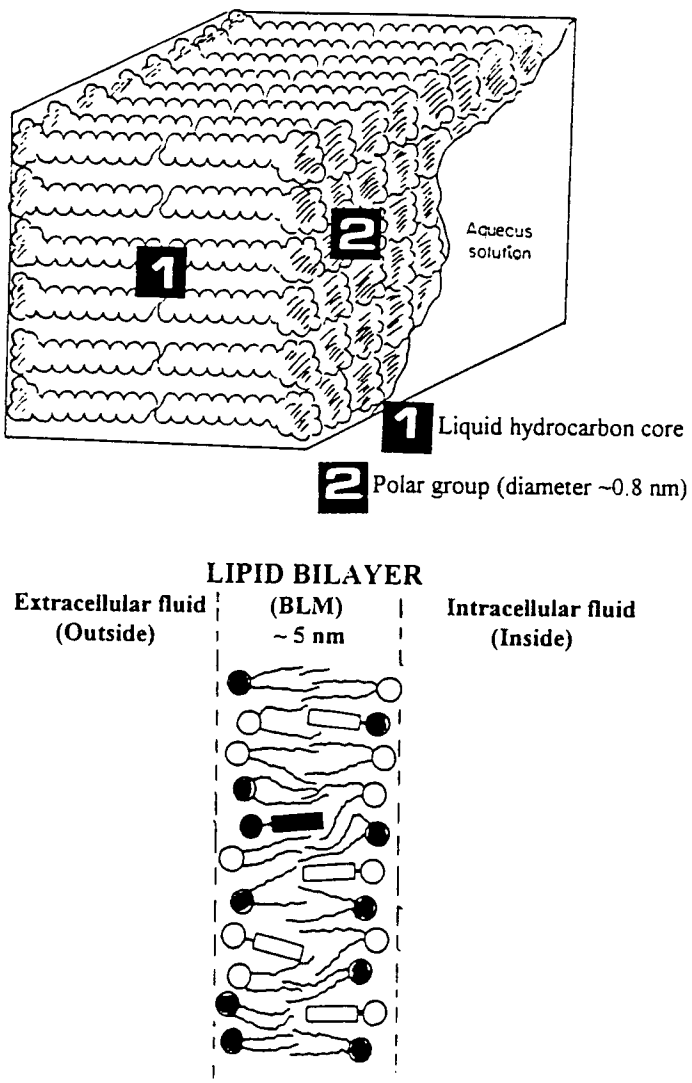

Fig. 2.2. *Upper.* The lipid bilayer of biomembranes. *Lower.* The lipid bilayer with fluid and self-sealing properties as an independent entity was reconstituted *in vitro* in the early 1960s.[4] (Reproduced with permission from *The Journal of Theoretical Biology.*[10])

bilayer are many different kinds of other lipids, proteins, carbohydrates, and their complexes, metallic ions and light-sensitive pigments, which give each type of biomembrane its distinctive identity and perform its specialized tasks. Generally speaking, all biomembranes are assemblies of lipid, protein, and carbohydrate molecules embedded in the *fluid* lipid bilayer, held together by non-covalent, hydrophobic interactions. The membrane is liquid-like, with individual lipid molecules able to diffuse freely within the bilayer. It may be therefore thought of as a '2-dimensional solvent' for other membrane constituents. For investigating purposes, biomembranes may be divided into two major groups: plant-cell membranes and animal-cell membranes, a brief summary of each is presented below.

Plant-Cell Membranes

Chloroplast membranes are the most unique among the important plant-cell membranes. The internal membranes of the chloroplast are the sites of photophysical and photochemical reactions. They are commonly known as *grana*, a stack of thylakoid membranes (*see* Chapter 9). Closely related to chloroplast membranes is the membrane of plastids which is simpler in structure and development. In addition to these, there are numerous other membraneous organelles that have been characterized. These are the plasma membrane, Golgi bodies, endoplasmic reticulum, nuclear membrane, and tonoplast. The familiar plasma membrane, often called plasmalemma, is the major diffusion barrier of cells. Golgi bodies (or apparatus) are usually made up of a stack of lamellar membranes. Nuclear membrane surrounding the nucleus is seen under the electron microscope to be perforated with channels (*see* Fig. 1.1, Chapter 1).

Animal-Cell Membranes

These membranes may be classified as external (plasma), internal (cytoplasmic), and organelle membranes. Plasma membranes of animal cells are frequently covered with a surface layer of mucopolysaccharide in addition to proteins. Endoplasmic reticulum and Golgi apparatus are types

of cytoplasmic membranes, which may have ribosomes attached. Membranes of mitochondria are complex, and they are further divided into the inner (cristae) membrane and the outer (plasma) membrane.

Morphologically, many types of membranes can be distinguished, such as plasma, nuclear, lysosomal, endoplasmic reticulum, cristae (or inner mitochondrial), Golgi membranes, and others. It is outside of the scope to consider them here. To facilitate our discussion, biological membranes are classified in terms of their functions and only five basic types will be considered in more details. These are the plasma membrane of cells (Chapter 5, *Membrane Transport*), the thylakoid membrane of chloroplasts (Chapter 9, Membrane *Photobiology*), the cristae membrane of mitochondria (Chapter 8, Membrane Bioenergetics), the nerve membrane of axon (Chapter 7, *Membrane Physiology*), and the visual receptor membrane of the eye (Chapter 9, *Membrane Photobiology*).

Methods for isolated membrane preparations

Essentially, one has to isolate the various components in a pure state and identify what they are. It should be pointed out that many procedures have been developed. Each group of investigators has their own particular ideas on the best method. Nonetheless, the basic procedure consists of the following steps:

1. *Rupture of cells.* There are various disruption procedures: mechanical rupture (homogenization) or sonication in hypotonic, isotonic or hypertonic medium. Ionic strength, pH, temperature are some important factors that can be varied to achieve the desired results.

2. *Separation of membranes.* Differential centrifugation (on the basis of size); density gradient centrifugation (a function of particle size and density); zonal separation (the particle's size and the viscosity of the medium affect the sedimentation rate).

3. *Purification of membrane fractions.* During the fractionation step, it is necessary to identify the desired final product. For this purpose, two techniques are available: (a) electron microscopy and (b) chemical and enzymic markers (e.g. Na^+ - K^+ ATPase activity).

4. *Identification by a variety of physicochemical analyses.* Spectroscopy (IR, UV, NMR, ESR, CD, ORD, DSC), x-ray diffraction, AFM, chromatography, electrophoresis, etc (*see* Section 2.4).

The above techniques are quite involved and are no easy task to apply to biomembranes. Some of the difficulties associated with isolated membrane preparations are:

- *Establishment of a method for disintegrating cells*
- *Isolation of the membrane component*
- *Determination of the origin of the isolated component*
- *Estimation of the purity of the preparation.*

Gross Chemical Composition

Table 2.3 summarizes the gross chemical composition of various types of membranes. The ubiquitous presence of water in membranes is often assumed but not explicitly stated. The role played by water, although obscure, must be crucial in maintaining the integrity of the membrane structure (see Drost-Hanson, in Chemistry of the Cell Interface, Part B. [Brown, 1971]). In most cells, membranous organelles constitute anywhere from 40 to 80% in terms of dry weight. The composition of biomembranes varies depending on function. The plasma membranes of mammalian cells are approximately 50% protein. The inner mitochondrial cristae membrane, which is involved in energy transduction, is about 75% protein, while the figure for myelin of the nerve axon, which functions as an electrical insulator, is roughly 80% lipid. The main membrane constituents in terms of lipids, proteins, and carbohydrates in variable proportions are given in Table 2.3, as well as further described below.

Plasma Membrane of Red Blood Cells (RBC)

This is by far the most extensively studied and best characterized of all biological membranes. Depending upon the species, the gross composition of the red blood cell plasma membrane is about 60 to 80% protein and 20 to 40% lipid. The major lipids are phospholipids and cholesterol. Phosphatidylcholine (PC), phosphatidylethanolamine (PE),

phosphatidylserine (PS), together with sphingomyelin (SM) account for about 50% of the phospholipids. Cholesterol content for different species varies from 22 to 32% of the total weight of the lipids. The protein of RBC plasma membranes has been very difficult to isolate and study. One method to separate the protein from the lipid is by sonication of ghosts in 15% butanol.

Table 2.3

Gross composition and function of some basic types of membranes*

	Lipids	Proteins	Carbohydrates	Function
	(expressed in % of dry weight)			
Plasma membrane	25-50	50-70	10	diffusion barrier active transport
(Gram + bacteria)	75	25	10	antigenic properties
Cristae (mitochondrion)	20-40	60-80	2-4	energy transduction ATP synthesis
Thylakoid (chloroplast)	40 8% pigments	35-65	6	sunlight conversion ATP synthesis
Visual (visual receptor)	40 4-10% pigments	50	4	Light detection signal transduction
Nerve (axon)	80	20	3	conduction of nervous impulse

*Data from [Brown, 1971; Datta, 1987]

Thylakoid Membrane of Chloroplasts

The gross composition of thylakoid membranes consists of 45% proteins and 55% lipids. Phospholipids and phosphatidyl glycerol make up 75% of the total lipids. The remaining 25% are chlorophylls, carotenoids, and other pigments. Sterols and glycerides are very minor constituents. The major lipids are digalactosyldiglyceride and monogalactosyldiglyceride. The structural proteins have been obtained with only one major peak, which was seen in the analytical ultracentrifuge. The molecular weight was 23,000.

Mitochondrial Membranes

Two types of mitochondria membranes are generally recognized - the outer membrane and inner (cristae) membrane. The outer membrane contains about 55% proteins and 45% lipids. Of the total lipids, a small portion is cholesterol. The inner membrane contains all the cytochromes and other enzymes and less lipid than the outer membrane. Note in Table 2.3 that the inner (cristae) mitochondrial membrane has a higher proportion of protein than the plasma membrane of the RBC. This is because the cristae membrane contains all of the protein carriers involved in oxidative phosphorylation (*see* catabolism in Chapter 8, *Membrane Bioenergetics*).

Nerve Membranes

Unlike other membranes, the nerve membrane as typified by myelin, contains the smallest percentage of protein. The myelin sheath in nerves is an insulating membrane composed of a high proportion of lipid. For example, human myelin consists of 80% lipid and only 20% protein.

Visual Receptor Membranes

The inner layers of the retina or double-membrane sacs of the outer segments of the retinal receptor cells are believed to have their origin in the plasma membrane. Chemically, the visual pigments, the integral part of the visual membrane structure, are well characterized. The gross

composition of the rod outer segments is about 40 to 60% protein, 20 to 40% lipids, and 4 to 10% retinenes. The visual pigment, rhodopsin, accounts for about 35% of the dry weight, the rest being mainly lipids. The protein moiety of the visual pigment, known as opsin, is less stable when isolated from rhodopsin, which has a molecular weight between 40,000 and 60,000. Of the retinenes, 11-cis plays the most crucial role in visual excitation.

Membrane lipids are amphiphilic and they are soluble in organic solvents and have limited solubility in water. The lipids of membranes form the key moiety, namely, the lipid bilayer. Proteins constitute the largest fraction by weight of most membranes. Interestingly, the lipid to protein ratio may be taken as an index of functional activity; the higher the ratio, the lower the activity (nerve axon acts as an excellent insulator, whereas the mitochondrial cristae with the lowest ratio exhibits the greatest activity) as may be seen in Table 2.3. Carbohydrates in membranes occur as complexes of lipids and proteins, known as glycolipids and glycoproteins, in which sugars are linked to lipids and proteins, respectively. Glycolipids and glycoproteins are interface-active in that they serve as receptor sites for the attachment of other physiologically active molecules. They are essential to membrane functions. The extracellular portion of the plasma membrane proteins are generally glycosylated (have carbohydrate groups attached). Likewise, the carbohydrate portions of glycolipids are exposed on the outer face of the plasma membrane.

2.3 Membrane lipid chemistry

The common membrane lipids belong to a category known as phospholipids, the most abundant and widely studied example of which is phosphatidylcholine (PC), popularly called lecithin. Fig. 2.3 shows the chemical formula of a major phospholipid and a few other membrane constituents at the oil-water interface.

The most unique property of membrane lipids that sets them apart from proteins and other membrane constituents is their amphiphilicity or dual water-oil solubility. They are interface-active and are capable of

bridging the two otherwise immicible worlds of water and oil. An outstanding practical example is lecithin (or PC, a major component of egg yolk) which stabilizes an oil-in-water emulsion as in mayonnaise.

Basic building blocks of lipids: An interface approach

As a result of the amphiphilic property, the two regions of a phospholipid molecule have opposite solubilities in oil (low dielectric medium) and in water (high dielectric medium). The phospholipid molecules, therefore, tend to organize themselves spontaneously in the form of a bilayer. Thus, to appreciate this unique property of phospholipids and other membrane lipid-like constituents, an interface approach is used to present the elements of membrane lipid chemistry. The basic building blocks for membrane lipids shown in Fig.2.4 are divided into oil-soluble and water-soluble moieties, a brief explanation of each part (**Groups A and B**) is given in the following paragraphs:

Group A—Shown on the left-hand side of the interface in Fig. 2.4 are those soluble in organic solvent (low dielectric medium, $\varepsilon = 2$ to10).

Fatty acids

They are usually straight chain molecules, but the fatty acids may also have branched chains. In mammalian membranes, fatty acids usually have an even number of carbon atoms from 12 to 26 (80% of which being 16 to 20 carbon atoms long). In phospholipids, usually one of the two fatty acids is saturated (e.g. palmitic, stearic, arachidic) and the other unsaturated (e.g. oleic, linoleic, linolenic, arachidonic). The double bonds can be present in either a '*cis*' configuration (most common) or in a '*trans*' configuration. Highly unsaturated fatty acids are present in polyunsaturated fatty acids (e.g. arachidonic acid with twenty carbon atoms, C20).

Long-chain unsaturated fatty alcohols

These alcohols, when present as in glycerophospholipids, possess an ether linkage instead of the acyl group at the C-1 position of glycerol, are known as plasmalogens, which have been isolated in relatively large quantity in the nerve myelin and in heart muscle membranes. A plasmalogen consists of a phosphoglyceride with a single fatty acid residue, containing an α,β unsaturated ether (R -H C = CH - OH) for one of the fatty acids, where R denotes a long-chain hydrocarbon. An example is ethanolamine plasmalogen.

Group B—Those that are soluble in aqueous solution (high dielectric medium, ε = 80) are grouped together on the right-hand side of the interface in Fig. 2.3.

Glycerol. Glycerol is an alcohol with three carbons, each with a hydroxyl group. It is a major fermentation product of glucose. Glycerol often acts as the central unit by combining in ester linkage with two fatty acids and a phosphate group (in phospholipids). When glycerol combines with three fatty acids, it is called triglyceride, commonly known as fat (see adipose tissues below).

Inorganic phosphate (700 g as P in human body) -- Of the three -OH's in a phosphate group, two of which are esterified as in phospholipids; one is linked to a glyceride and the other to an organic base (see below) or free as in phosphatidic acid (PA).

Organic bases : The first two bases are synthesized from serine, which is one of the essential amino acids.

Choline ($HOCH_2CH_2N^+(CH_3)_3Cl^-$) - when linked to a phosphoglyceride, it is called phosphatidylcholine (PC)

Ethanolamine ($HO\text{-}CH_2\text{-}CH_2\text{-}NH_2$) - when linked to a phosphoglyceride, it is called phosphatidylethanolamine (PE)

Serine ($HOCH_2\text{-}CNH_2$). When linked to a phosphoglyceride, it is called phosphatidylserine (PS).

Inositol (hexahydroxycyclohexane) a compound widely distributed in plants and animals, it has a molecular weight 180, capable of passing through gap junctions . When combined with phosphates, it forms a water-soluble inositol triphosphate (IP_3). When an inositol is linked to a phosphoglyceride, it is called phosphatidylinositol (PI). When an IP_3 is attached to a phophosglyceride, it is called phosphatidylinositol-4,5-bisphosphate (PIP_2). This compound is catalytically cleaved by phospholipase C into diacylglycerol (DAG) and IP_3.

Mention should be made here that all these phosphorylated derivatives of PI are the so-called 'second messengers' (meaning molecules that relay signals from the plasma membrane to the interior of the cell). Other important second messengers are Ca^{2+} and cyclic AMP -- 3',5' cyclic monophosphate. They are involved in signal transduction across the cell membrane (Chapter 1, Section 1.7).

Galactose, together with mannose, N-acetylglucosamine, and sialic acid (see below), they are the most common sugars involved in glycoproteins, membrane proteins with carbohydrate groups linked to amino acid side-chains.

N-acetyl-neuroaminic acid (sialic acid) -- an amino sugar, which is linked to the protein by attachment of the sugar to the free amino group of asparagine. The exposed hydrophilic sugar groups allow them to carry out crucial cell recognition functions.

Organic sulfates—as in sulfolipids, a kind of glycolipids exist in chloroplast thylakoid membranes. They are relatively simple structures containing one or two sugar units such as galactose. Glycolipids with two sugar units are found in the inner side of thylakoid membrane.

The Basics of Phospholipids (derivatives of phosphatidic acid, PA).

By combining basic building blocks from Groups A and B, the major membrane lipids can be made simple using the interface approach shown in Fig. 2.3. A phospholipid, for example, consists of two fatty acids, one glycerol, and one phosphoric acid. The structure of naturally occurring

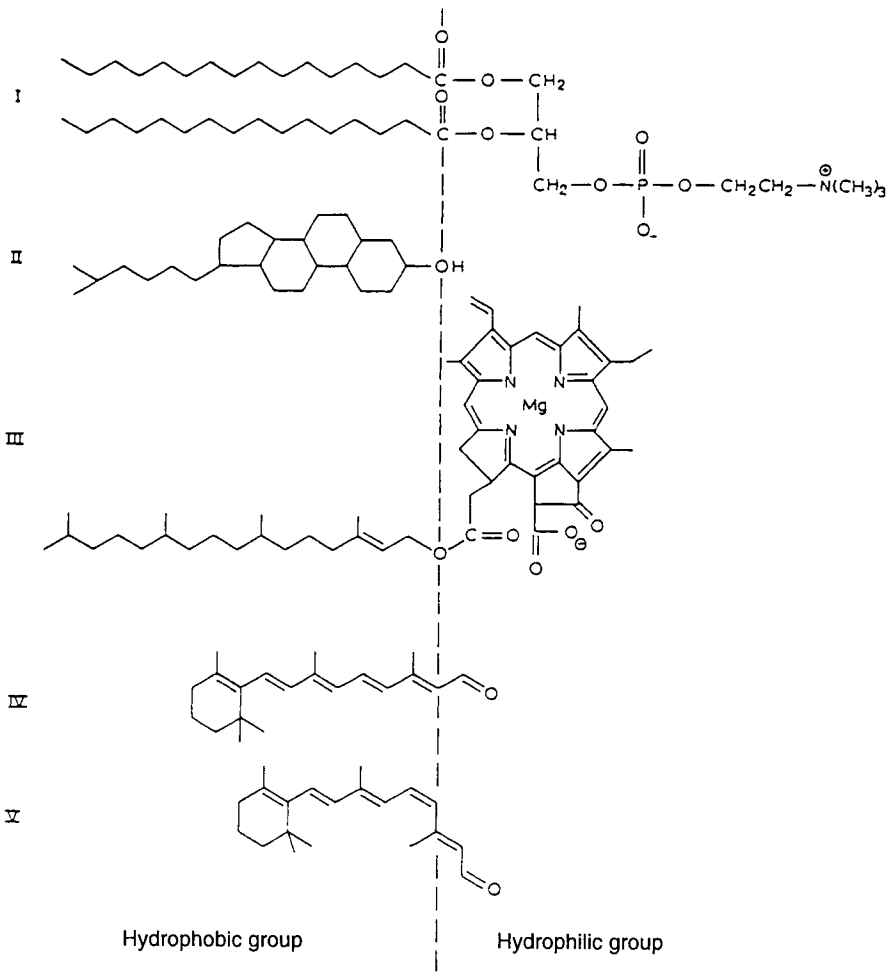

Fig. 2.3 An interface approach. *Upper*: the chemical formula of a major phospholipid and other membrane constituents at the oil-water interface. Lower: Basic building blocks of membrane lipids.

phospholipids comprises of a glycerol, which is esterified at positions 1 and 2 with fatty acids, and at position 3 with a phosphoric acid. The second -OH group in the acid group is, in turn, linked to a group that can be either H as in phosphatidic acid (PA), which is the basic phospholipid structure. A variety of groups can be esterified to the phosphate group to form the range of phospholipids required for membrane structure and function. The most common phospholipids include:

- *phosphatidylcholine (PC or lecithin),*
- *phosphatidylethanolamine (PE),*
- *phosphatidylserine (PS),*
- *phosphatidylinositol (PI),*
- *phosphatidylglycerol (PG), and*
- *diphosphatidylglycerol (cardiolipin).*

Of these, PC and PE are 2 of the most common constituents of biological membranes.

Other Membrane Lipids

Phosphosphingolipids

Sphingosine. (1,3-dihydroxy-2-amino-octadecene-4). Whose chemical formula is $H_3C\text{-}(CH_2)_{12}CH = CH\text{-}CH_2\text{-}C\text{-}CH_3$. The fatty acid may be of various acyl chain lengths and unsaturation. Polar lipids based on sphingosine and derivatives sphinganines) are the second major class of phospholipids. They are known collectively as phosphosphingolipids.

Sphingolipids. (sphingosine + phosphocholine). The backbone of these lipids is an 18-carbon amino alcohol, sphingosine (see above) rather than glycerol. Typically, a fatty acid is joined via an amide linkage to form a ceramide. Glycosphingolipids consist of ceramides with one or more sugars attached which are important components of nerve and muscle membranes. Gangliosides are more complex glycosphingolipids that consist of a ceramide backbone with 3 or more esterified, with one of them being a sialic acid (e.g. N- acetyl-neuraminic acid). Sphingomyelins represent a phosphorus containing subgroup of sphingolipids, which are abundant in nerve tissues.

Glycolipids. (a) Cerebrosides (mono-glycosylceramide): Cerebrosides (sphingosine + galactose) are monoglycosyl ceramides which contain a single monosaccharide unit. Monoglycosyl ceramide is an important lipid component of brain cells. Sphingosine forms a part of the compounds. More complex glycosphingolipids are also known. (b) Gangliosides are a class of compounds containing sialic acid (sialic acid + sphingosine + galactose).

Sulfolipids (galactosulfate) -- Organic sulfates (see Group B above).

Steroids. Steroids are a unique group of lipids characterized by a carbon skeleton consisting of four interconnected rings. Different steroids vary in the functional groups attached to this ensemble of rings. The most important steroid is cholesterol, a common constituent of the membranes of animal cells. It is also mildly interface-active (see Fig. 2.3).

Adipose tissues. A common name of these materials is fat. A significant number of fatty acids in animals exist as triacylglycerols. A fat is made of two kinds of smaller molecules: glycerol and fatty acids. The molecules consist of glycerol esterified to three fatty acids. All the fatty acids in a fat can be the same, or different. Fatty acids vary in hydrocarbon-chain length, and in the number as well as location of double bonds (unsaturation). If there are no double bonds between the carbon atoms composing the chain, then as many hydrogen atoms as possible are bonded to the carbon atom, creating a saturated fatty acid. An unsaturated fatty acid has one or more double bonds. Saturated and Unsaturated fats are terms derived from the structure of the hydrocarbon chains of the fatty acids. Most animal fats are saturated; they have fatty acids that lack double bonds. Saturated animal fats (e.g. lard) are waxy materials at room temperature. However, the fats of fish and plants are generally unsaturated, and usually liquid at room temperature; they are referred to as oils. Unsaturated fats can be converted to saturated fats, known as hydrogenated vegetable oils, by adding hydrogen atoms. In doing so, lipids in some food products are prevented from separating out in liquid form. It should be remembered that these fatty lipids are the major energy reserve and the principal neutral derivatives of glycerol found in the body. In terms of energetics, one gram of fat stores more than twice as much

energy as a gram of starch (a polysaccharide). So there is an advantage to having a more compact reservoir of adipose tissue for long-term food reserves and body insulation from cold.

Waxes. Waxes are esters of long-chain alcohols with long-chain fatty acids and are extremely insoluble in water. This property is used to impart water repellent character to animal skins. A well known example is lanolin, a component of wool wax, which is used as a substructure for pharmaceutical and cosmetic products because it is quickly absorbed by human skin.

2.3.2 Elements of Membrane Protein Chemistry

The basic structure of biomembranes is determined by the lipid bilayer; the functions, however, are mainly performed by membrane proteins, carbohydrates, their complexes and other constituents such as metallic ions and pigments. Since Danielli first depicted membrane proteins as globular (*see* Fishman, 1962), all conceivable arrangements of membrane proteins on or in as well as across the lipid bilayer have been proposed. Many proteins, like the lipids, are of amphiphilic nature: they have a domain where hydrophobic residues are in contact with the inner, hydrophobic part of the lipid bilayer.

Broadly speaking, membrane proteins may be classified into two main types: peripheral (or extrinsic) and integral (or intrinsic) on account of their interaction with the lipid bilayer. Extrinsic, or peripheral, membrane proteins can be readily detached from membranes by adjusting the pH or ionic strength of the bathing solution. Extrinsic membrane proteins are entirely outside of the membrane, but are bound to it by weak molecular attractions (ionic, hydrogen, and/or Van der Waals bonds). Examples of extrinsic membrane proteins are cytochrome *c* (MW:12,000) of cristae membrane and cytoskeleton of RBC. Intrinsic (integral or structural membrane) proteins are hydrophobically attached to the lipid bilayer; they can only be isolated by drastic means (e.g. detergent treatment). Intrinsic membrane proteins can be further classified into two categories: simple and complex, both of these are transmembrane proteins

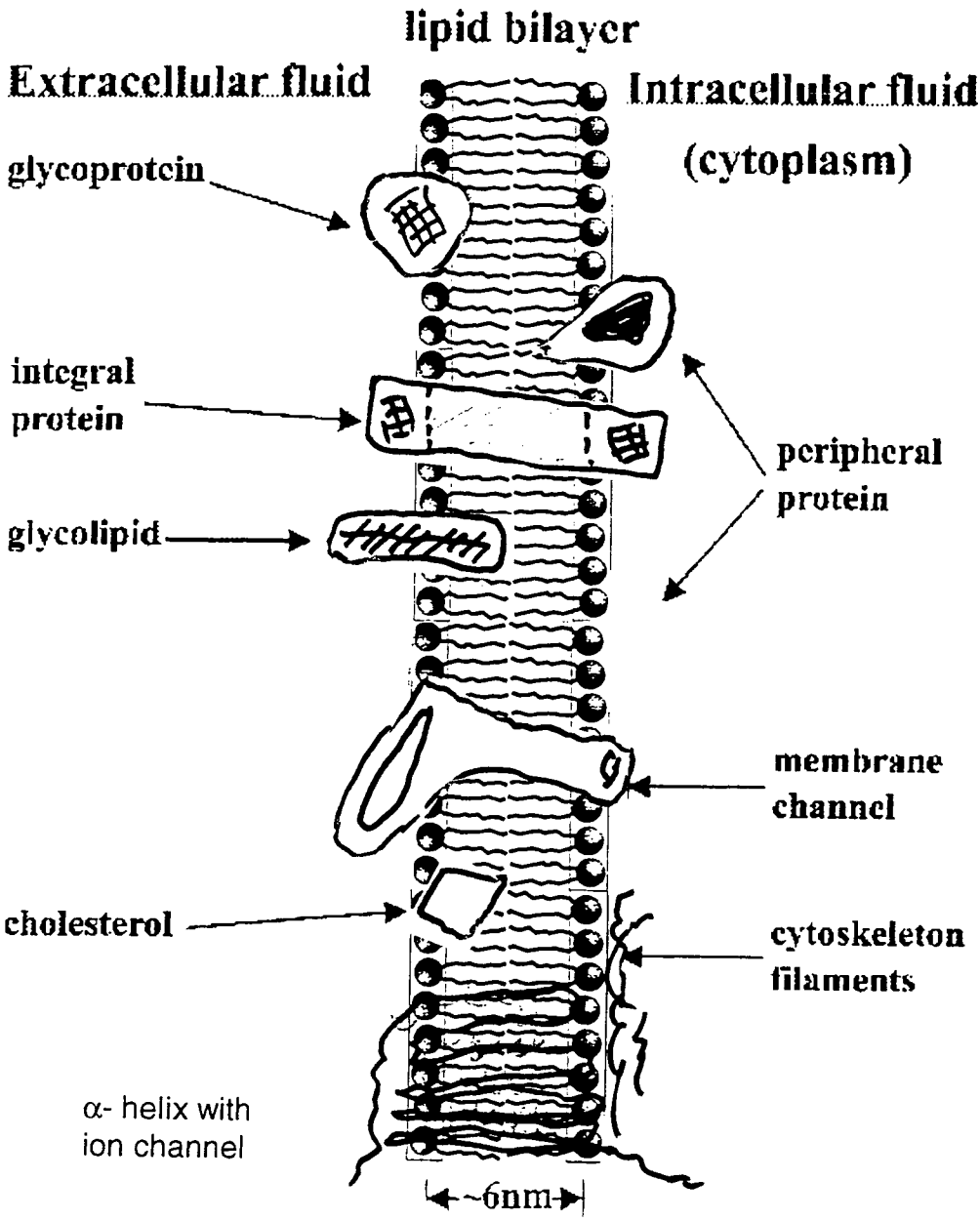

Fig. 2.4 Arrangements of some membrane proteins in a lipid bilayer.

since they span the lipid bilayer. Fig. 2.4 illustrates five different ways in which membrane proteins may be associated with the lipid bilayer. These are:

(1) A single hydrophobic domain spans the whole lipid bilayer. There is a hydrophilic domain at each end of this type of transmembrane proteins. Outstanding examples of simple transmembrane proteins are glycophorin of RBC (a sialoglycoprotein) and cytochrome b-5 of liver mitochondria. Transmembrane domains tend to consist of α-helices as in RBC, and many other lipid bilayer-bound receptors, including the receptor of platelet-derived growth factor, insulin, growth-hormone, and others.

(2) The protein is partially inserted into the lipid bilayer and a polar domain, which interacts with the polar heads of the lipids, and with the intracellular fluid. For example. some of the G-proteins, which bind guanyl nucleotides belong to this group. Interestingly to note that a few examples have been found in which such a protein occurs on the extracellular side of the lipid bilayer (a possible exception is the bee-venom toxin, *Mellitin*).

(3) Such membrane proteins have a particular orientation in the lipid bilayer; they are functionally asymmetrical. The polypeptide chain may traverse the membrane several times, usually seven. The protein may have a transmembrane channel running through it or act as ion pump. Examples of complex transmembrane proteins are gap junctions between cells, Ca^{2+}-ATPase of sarcoplasmic reticulum and bacteriorhodopsin (BR) of *Halobacterium halobium*. BR forms a crystalline array consisting of 7-helical rods embedded in the lipid bilayer. The gap junction structure at present is obscure but appears to consist of 6 rods across the lipid bilayer. As to Ca^{2+}-ATPase, it transverses the lipid bilayer several times, which may form an ion channel. The Ca^{2+}-ATPase may possess sites for phosphorylation on the cytoplasmic surface, the water-soluble peptides of which have been sequenced. Finally, mention should be made of the Na^{+}/K^{+}-ATPase, an important complex membrane protein which spans the lipid bilayer a number of times.

(4) These types of peripheral proteins are bound to the lipid bilayer principally by ionic interactions with the polar heads of the phospholipids, or with other membrane proteins. Examples are cytochrome *c* and the F1 subunit of the ATP-synthase.

(5) This is a third type of peripheral protein, located on the outside of the plasma membrane, but covalently linked to a glycolipid molecule that is situated within the lipid bilayer. An increasingly large number of bilayer-bound proteins have been found to be linked by a short oligosaccharide to a molecule of glycophosphatidylinositol that is embedded in the outer leaflet of the lipid bilayer. These proteins are released when membrane is treated with enzymes (e.g. phospholipases) that are specifically recognized and cleaved inositol-containing phospholipids.

For membrane lipid chemistry we have used an interface approach as pictured in Fig. 2.3. With membrane proteins an 'operational' approach may be used, that is based upon how an entity responds to a specified treatment (or operation), rather than upon the inherent nature of the stuff. On this basis there are two kinds of membrane proteins: (a) peripheral (extrinsic) proteins, which may be removed from the lipid bilayer, or solubilized, by mild treatment, such as shaking with a dilute salt solution. These proteins are often thought of as being loosely associated with the lipid bilayer surface, and (b) integral (intrinsic) membrane proteins that cannot be removed from the lipid bilayer without treatment that destroys the lipid bilayer structure, such as dissolving it with detergent. They are often depicted as being deeply embedded in the lipid bilayer or stick through it.

Peripheral membrane proteins are not embedded in the lipid bilayer but indirectly associated with the membrane through interactions with integral membrane proteins or by weak electrostatic interactions with the hydrophilic head groups of membrane lipids. They are located extracellular or associated with the cytoplasmic surface of the lipid bilayer. Peripheral proteins basically have no interaction with hydrophobic interior of lipid bilayer, water soluble proteins can be on either side of lipid bilayer. There are three possible ways for peripheral proteins to attach themselves to the lipid bilayer: (a) non-covalent attachment via an integral membrane protein, both sides of the lipid bilayer, (b) covalently

bound to a lipid molecule which anchors in the lipid bilayer, only on the cytoplasmic side, and (c) attached via a covalent link to a glycolipid, only on extracellular side of lipid bilayer.

Intrinsic membrane proteins are embedded in the lipid bilayer. Many of them extend from one side of the lipid bilayer to the other and are referred to as transmembrane proteins. It may be seen from the detailed structures of many transmembrane proteins that they often have three different domains, one hydrophobic and two hydrophilic. A hydrophilic domain, consisting of hydrophilic amino acids at the N-terminus, is poking out in the extracellular medium, a hydrophobic domain in the middle of the amino acid chain, often only 20-30 amino acids long, is threaded through the lipid bilayer, and a hydrophilic domain at the C-terminus protrudes into the cytoplasm. The transmembrane domain, because it is made of amino acids having hydrophobic side chains, exists cozily in the hydrophobic inner layers of the lipid bilayer. Because these transmembrane domains anchor many proteins in the lipid bilayer, they are not free-floating and cannot be isolated and purified biochemically without first dissolving away the lipid bilayer with interface-active agents (surfactants or detergents). Indeed, much of the preparation procedure used in isolating intrinsic proteins is necessitated by the need to solubilize those that are embedded in lipid membranes by using surfactants. As one browses along the amino acid sequence of these proteins, it becomes apparent that hydrophilic domains (hydrophilic amino acids) alternate with hydrophobic domains. The protein chain as a whole when embedded in the lipid bilayer actually weaves back and forth between the cytoplasmic and the extracellular side of the lipid bilayer. Since such proteins have snake-like configurations, some researchers name them serpentine membrane proteins. A commonly used type of structure seen in many hundreds of serpentine transmembrane proteins involves seven hydrophobic domains inserted into the lipid bilayer separated by hydrophilic regions that are alternatively looped in and out onto opposite sides of the membrane.

It should be mentioned that membrane constituents such as proteins are difficult to study by x-ray crystallography because they are usually not soluble in aqueous buffer solutions and denature easily in organic solvents. Methods such as Infrared spectroscopy, Raman spectroscopy, and circular dichroism are used to deduce membrane

proteins' secondary structures. The understanding of the properties of the lipids has benefited tremendously from such techniques as NMR and calorimetry. These and other physical methods are being applied to further clarify the physical chemistry of lipids and the biomembranes made from them [Datta, 1987].

2.3.3 Elements of Membrane Carbohydrate Chemistry

Membranes' carbohydrates are present either attached to the lipid or protein moiety. They are known, respectively, as glycolipids, and glycoproteins, which are of great importance. The glycolipids and glycoproteins are implicated in the specificity of the blood groupings and other immunological properties of membranes. Typical sugars in glycoproteins and glycolipids include glucose, galactose, mannose, fucose and the N-acetylated sugars like N-acetylglucosamine, N-acetylgalactosamine and N-acetylneuraminic acid (sialic acid). Here, membrane sugars seem to be involved in identification and recognition purposes. For example, ABO blood typing and various human diseases resulting from the genetic inability to degrade specific glycolipids (e.g. Tay-Sachs disease). Sugar containing glycolipids are generally only found on the extracellular half of the plasma lipid bilayer (asymmetrical distribution).

In plasma membranes, carbohydrate residues (monosaccharides) are N-acetyl glucosamine, galactose, neuraminic acid (sialic acid), and N-acetyl galactosamine. A typical mammalian cell may have several hundred distinct types of glycoproteins covering its plasma membrane. Each of these glycoproteins will have their extracellular domain glycosylated with a complex branching bush of sugar residues covalently linked to the asparagine side chains. Some glycoproteins may have 2 or 3 asparagine-linked sugar side chains, others may have dozens. Examples of glycoproteins in the RBC membrane are:

a) Glycophorin (60% carbohydrates and 40% proteins), also known as the major sialoglycoprotein - an integral (intrinsic) protein

spanning the entire lipid bilayer, amphipathic - polar amino acid residues on both sides.

b) Band - III (now known as the anion channel protein) glycoprotein which, like the major sialoglycoprotein, interacts with the extrinsic protein spectrin on the inner suface of the plasma membrane of the RBC.

The plasma membrane of the red blood cell (RBC) is an excellent model to illustrate the complexity of biomembranes, both structurally and functionally. In RBCs (erythrocytes) where the plasma membrane protein to lipid ratio is about 1, there are two major structural proteins: glycophorin and the anion channel protein. The former has a single translipid bilayer unit and is involved in cell recognition, whereas the latter channel protein spans the lipid bilayer at least six times and participates in CO_2/bicarbonate and Cl^- ion transport. Additionally, there is a peripheral protein known as ankyrin, which anchors the membrane to the cytoskeleton by linking the anion channel to the underlying α,β-spectrin. The free ends of spectrin tetramers are linked to actin and to an additional electrophoretic band 4.1 protein. Structurally, the biconcave discoidal shape of the erythrocyte (RBC) is due in part to the membrane protein. Functionally, a host of enzymes are present in the RBC lipid bilayer including Na^+-K^+ and Ca^{2+} pumps (ATPase-based), enzymes for carbohydrate metabolism, enzymes for nucleotide metabolism, and at least 10 other enzymes for membrane transport (*see* below on The Ultrastructure of Biomembranes, Section 2.4 and Chapter 5).

2.3.7 Membrane Components of Lipids, Proteins and Carbohydrates

The following diagram illustrates the membrane components from a combination of lipids, proteins and carbohydrates.

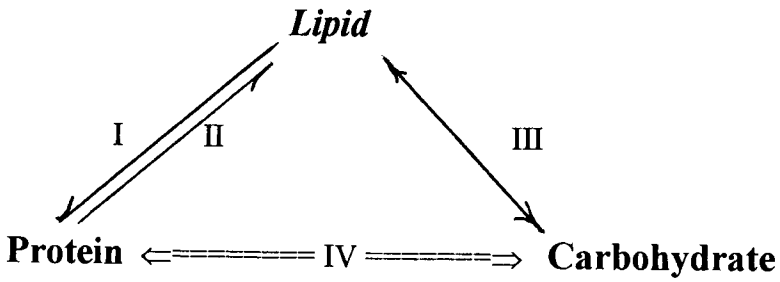

(I) *Lipoprotein*—It is formed from a lipid + a protein, which is usually soluble in aqueous solution.

(II) *Proteolipid*—It results from a protein + a lipid, which is usually soluble in ogranic solvent (e.g. 2:1 = $CHCl_3$: CH_3OH).

(III) *Glycolipid*—When a lipid combines with a carbohydrate. The sugar residues of glycolipids are located on the outer surface and most likely are involved in cell-cell communications.

(IV) *Glycoprotein*—It is produced from a carbohydrate + a protein. Like glycolipids, the sugar residues of glycoproteins are also attached on the non-cytoplasmic side of the membrane.

Glycoproteins have covalently bonded carbohydrate groups. In animal cells such chains are often attached to an asparagine's amide group. Carbohydrate chains of (III) and (IV) occur on the extracellular side of plasma membranes, and the luminal side of intracellular organelle membranes. At the present time, it is difficult to state to what extent those biological functions are the results of lipid-protein-carbohydrate interactions. On the other hand, we can state confidently the obvious, that no functional biological membranes can exist in the absence of lipid-lipid and lipid-protein-carbohydrate interactions.

2.4 The Ultrastructure of Biomembranes

Through the application of biophysical techniques, our insights of the ultrastructure of biomembranes have been attained. Here, the major physical chemical methods will be briefly remarked upon. For in-depth treatment of each topic mentioned, the references listed at the end of this chapter should be consulted [Robertson, 1981; Lipowsky, 1995].[16]

Electron Microscopy

Physical techniques such as NMR, ESR, etc. furnish only averaged information. The electron microscope makes it possible to observe specific sections within a specific membrane. The theory of the operations of the electron microscope is very similar to that of a light microscope. Owing to the electron wavelength used, the resolution of the electron microscope is less than 1 nm. Conventional electron microscopy provides information about the structure in a 4-6 nm thick section of a membrane, whereas the freeze-etch electron microscopy permits the examination of a 0.2 nm region of the membrane. A general procedure for electron microscopy is as follows: cellular material is fixed in buffered OsO_4, dehydrated, microtoned into thin sections and stained with a heavy metal salt (e.g. uranylacetate). For visualization of the interior of a membrane, the so-called freeze-etch electron microscopy technique is used. The technique involves essentially three steps: rapid freezing, etching (sublimation), and shadowing and replication. By freezing, fracturing and etching, the "inner" structures of a membrane may be seen. Indeed, the cleavage of the membrane systems by this technique, inner hydrophobic (hydrocarbon) interfaces are revealed, lending strong support to the concept of lipid bilayer.

X-ray Diffraction

The method is based on Bragg's law, $2d\sin\theta = n\lambda$, where d is lamellar spacing, θ is for radiation incident at an angle to the membrane plane, n is order of diffraction, λ is wavelength of x-rays. X-ray diffraction studies on membranes were mainly carried out on nerve myelin, retinal rod photoreceptors, and thylakoids, all of which possess a center of

symmetry and are treated as inhomogeneous smectic liquid crystals. The electron density profile indicates that a lipid bilayer is the principal structural element, with the protein moieties bound to it.

Electron Spin Resonance (ESR) Spectroscopy

The basis of spin-labelling technique is that a tagged molecule (spin label) on a molecule such as a lipid can be measured with an electron spin resonance (ESR) spectrometer. Except in detecting instrumentation, the use of a spin label is very much similar to introducing a dye into a biological material. The advantages of spin labels are sensitivity to the local environment, and ability to measure very rapid molecular motion. More specifically, the unpaired electron of the nitroxide radical (N-O) has both a negative moment and a spin angular momentum. It can adopt only two orientations when placed in a magnetic field. If a molecule containing this radical is incorporated into a lipid bilayer or membrane, it can "report" on the polarity of its environment, and also on the mobility of the probe in the membrane. Both "flip-flop" and lateral motion of phospholipids in bilayers have been obtained with this technique. To date, the spin label technique has been used to answer questions about membrane dynamics and fluidity. The technique has been applied to nerve membranes, bovine RBC ghosts, membrane proteins, and model systems. The conclusion drawn from these experiments is that biomembranes possess liquid-crystalline hydrophobic regions consistent with the bilayer leaflet model.

NMR Spectroscopy

Nuclear magnetic resonance (NMR) spectroscopy provides information about atoms and molecular fragments that is of interest to membranologists. The data can be interpreted in terms of structural features and dynamical phenomena. NMR experiments on membranes are interpreted by considering the membranes as solids or liquid crystals rather than liquids. The physical basis and chemical applications of nuclear spin interactions are based on the fact that the separation of the two energy levels or spin states, and transitions between the two levels can be induced by applied electromagnetic radiation frequency. The population of the energy levels is dictated by the Boltzmann distribution.

NMR spectra of ^{1}H, ^{2}H, ^{13}C, ^{31}P, and ^{19}F nuclei have been used to obtain information on the location and mobility of the relevant nuclei in lipid bilayers and membranes. The most useful conclusions have been reached by far via ^{2}H or ^{31}P NMR spectra.

Fluorescence Spectroscopy

The fluorescent properties of many polycyclic hydrocarbons are very sensitive to the environment of the molecule. These compounds have been used as 'fluorescent probes'. The best known example is ANS (1-anilino- napthalene-8-sulfonate). ANS is known to exhibit a strong fluorescence at 520 nm in non-polar solvents, but it fluoresces poorly in aqueous solution. Fluorescence spectroscopy has been used to obtain information on the polarity and viscosity of lipid bilayers and membranes. The orientation of the probe and the proximity of the probe in relation to other molecules which can act as excited-state energy donors or acceptors have provided valuable information on the structural and dynamic properties of membranes.

Differential Scanning Calorimetry

Differential scanning calorimetry (DSC) is a classic method, but application to biological systems is a recent event. The principle of DSC is to heat a sample in a reference compound of known melting point and measure the difference in power input. If a transition takes place, more heat must be supplied to the sample than to the known compound. The heat of transition is proportional to the area of recording. The phase transitions observed in the DSC can be correlated with changes in biological properties. DSC has been used to study phase transitions in lipid bilayers and membranes corroborating the results obtained with low-angle X-ray diffraction studies. The DSC should be ideally suited to investigate protein denaturation in membranes and intact cells.

Optical Rotatory Dispersion and Circular Dichroism

The variation of optical rotation with wavelength of incident light is called optical rotatory dispersion (ORD) whereas the variation of the

axial ratio of the ellipse with wavelength is known as circular dichroism (CD). These techniques are useful in establishing α-helical and random coil conformations of proteins in membranes.

Raman Spectroscopy

The classic Raman effect may be viewed as follows: a light wave with an electric vector oscillating at a frequency traverses a medium, the molecules of which have polarizability. An oscillating dipole is induced which, according to electromagnetic theory, radiates energy at the frequency of its oscillation. Biological applications of Raman spectroscopy require development of quantitative molecular interpretations of the spectra events in connection with conformation changes. For example, a portion of the Raman spectra of phospholipids is particularly sensitive to the conformational state of the hydrocarbon chains in the lipid bilayer. It has been claimed that such spectra simultaneously yield information about interchain (lateral) and intrachain (longitudinal) order.

Atomic Force Microscopy (AFM)

Fundamental mechanisms of the image formation are well-established. The application of AFM to organic samples ranging from thin films at molecular resolution to living cells became one of the most widely used near-field microscopes. For example, adsorbed fluid lipid bilayers, formed by rupture of phospholipid liposomes, have been imaged by AFM.[16]

The Plasma Membrane

As remarked by A. Mauro at the opening session of the Symposium on the Plasma Membrane, "*...although the existence of this entity (plasma membrane) has been firmly established, we should be reminded that we are a long way from having a clear understanding of the detailed molecular structure and the associated mechanisms operating in this region of the cell.*" [*see* Fishman, 1962].

In the intervening years, our knowledge about the ultrastructure of biomembranes has advanced considerably. The plasma membrane of a highly idealized cell, together with its organelle membrane systems, is depicted schematically in Fig.1.1 (Chapter 1, *Overview*). Also stated in the introductory chapter, the plasma membrane is the domain of the cell immediately surrounding the cytoplasm. Every living thing on Earth has some sort of a lipid bilayer, measuring 5-8 nm thick. The plasma membranes of cells are dynamic, constantly adapting to changing environmental conditions. Additionally, the plasma membrane, besides serving as a selective barrier to maintain concentration gradients of common ions, it is the site for signal transduction and information processing. The basic structure of the plasma membrane may be viewed as a phospholipid bilayer embedded with proteins, carbohydrates, and their complexes. The phospholipids on opposite sides of the membarne are not identical, and polar phospholipids at physiological pH are either in zwitterion form or negatively charged at physiological pH (~ 7.4). Hence, the surface of the plasma membrane is electrified in that an electrical field exists at the interfaces and/or across the lipid bilayer (Chapter 6, *Membrane Electrochemistry*). Here, we will use the plasma membrane of erythrocytes (red blood cells or RBC) as an example, whose structure is depicted in Fig. 2.5. There are differences in lipid composition on opposite sides of a membrane. The RBC membrane provides an example of such sidedness. Carbohydrate is mostly on the outer surface facing extracellular fluid. It is typically tacked on to the portion of membrane proteins that hang out. Some proteins such as spectrin and ankyrin are associated with the cytoplasmic surface of the lipid bilayer. Other proteins (e.g. glycophorin, and band 3 protein) either attach to the lipid bilayer, or loop back and forth through it from extracellular side to cytoplasmic side.

Evolution of Biomembrane Structure

Returning now to the broadly accepted bilayer leaflet model of membrane structure, discussed in Section 2.2 (Page 31), investigations of biomembrane ultrastructure can be conveniently divided into the following three periods:

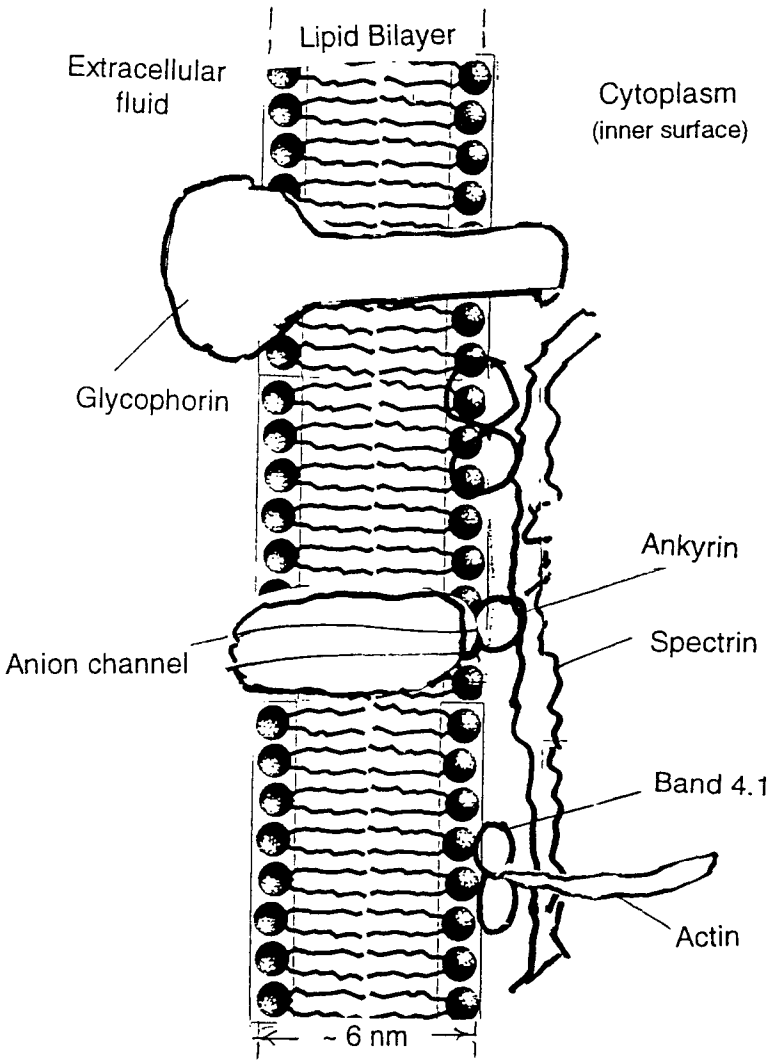

Fig. 2.5. BRC -- Examples of glycoproteins in the RBC membrane: a) Glycophorin (60% carbohydrates and 40% proteins), also known as the major sialoglycoprotein - an integral (intrinsic) protein spanning the entire lipid bilayer, amphipathic - polar amino acid residues on both sides b) Band - III (D) glycoprotein which, like the major sialoglycoprotein, interacts with the extrinsic protein spectrin on the inner surface of the RBC membrane.

- the classical period of Gorter-Grendel-Davson-Danielli,
- the unit-membrane period of the 1950s [Robertson, 1981], and
- the modern period from the early 1960s to the present time as popularized by the fluid mosaic model.

Following the seminal suggestion of E. Gorter and F. Grendel in 1925, the bilayer leaflet model of the plasma membrane has been used as a starting point for numerous models suggested in the 1960s. The development of these models to a large extent had its origin in surface and colloid chemistry. A succinct account of the role played by surface chemistry in biology was given by Lawrence in 1958 (for references *see* [Kerker, 1972]). The study of monomolecular layers (monolayers) at air/water interfaces introduced by Langmuir[2] had provided a physical picture of the organization and orientation of lipid molecules at interfaces. The bimolecular lipid layer with absorbed protein layers was put into pictorial form by Davson and Danielli in 1935 [Fishman, 1962], who deduced their model from the results of interfacial tension measurements on cells and model systems. The bilayer leaflet model for the structure of biomembranes may be simply stated as follows: The basic construct of all biological membranes consists of a bimolecular lipid leaflet (i.e. lipid bilayer for short) with adsorbed non-lipid layers (mostly proteins). The lipid molecules are oriented with their polar groups facing outward, and their hydrocarbon chains away from the interfaces, forming the interior of the membrane. In the interior of the bilayer, hydrocarbon chains are held together by London-van der Waals forces and are in a liquid-crystalline state.

At the electron microscope level, a biomembrane shares a common structure following routine preparative steps. It shows a typical 'Unit' membrane that resembles a railroad track with two dense lines separated by a clear space. The dense lines are formed by the reaction of Os_2O_4 (Osmium tetroxide), which is used both as a fixative (for lipids and some proteins) and as a heavy metal stain that allows one to visualize membranes with the electron microscope. In the 1950s, the bilayer leaflet model has been generalized by Robertson [1981] who, based upon his extensive electron microscope observations, has come to the conclusion that all biological membranes, irrespective of their origin, are lipid

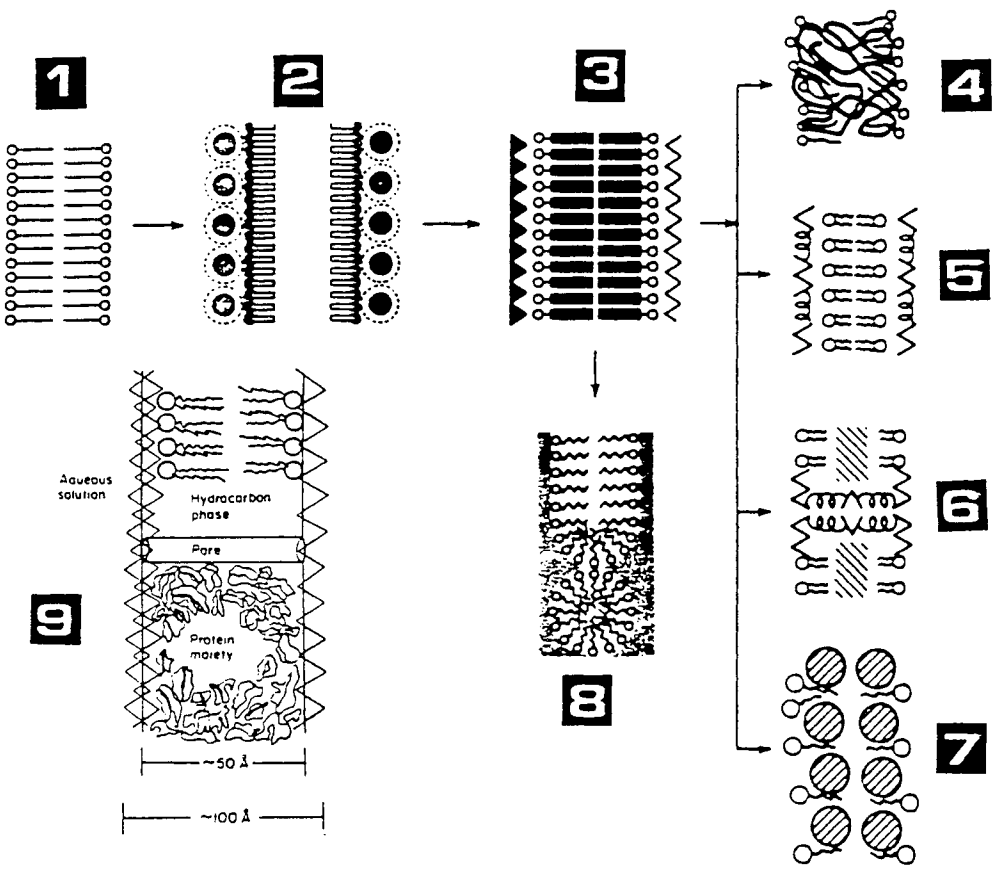

Fig. 2.6 Evolution of models of biomembranes.

bilayers or a modification thereof. Another line of evidence in support of the bimolecular leaflet model was the formation of a stable 'black' lipid membrane of planar configuration discovered by Rudin and his co-workers in 1960.[4a,18] Later investigations carried out by many groups have demonstrated that black or bilayer lipid membranes (BLMs) are excellent experimental models for biological membranes. This was soon followed by lipid vesicles of spherical configuration, namely liposomes, described by Bangham et al.[4b] With the availability of planar BLMs and spherical liposomes, it was then possible for the first time to investigate electrical properties and transport phenomena across an ultrathin (~ 6 nm) bilayer lipid membrane separating two aqueous solutions. The major historical landmarks in the development of biomembrane structure are given in Table 2.2. The modern period, beginning in the early 1960s, and continuing to the present time, is our main focus in this book, and therefore is reviewed in more detail in the following paragraphs.

Through the application of physicochemical methods, our current picture of biomembranes ultrastructure has evolved. The basic concept underlying our views was formulated by Gorter and Grendel in their classic paper published in 1925.[9] It can now be stated with confidence that the lipid bilayer is the *only* organizational feature universal to all biomembranes. However, the lipid compositions of the plasma membrane and the various organelle membranes of a given type of cell are all different. Further, there are two important properties of the lipid bilayer in the formation of a biomembrane: impermeability to ions and to most biocompounds, and fluidity. The latter exhibits the random motions characteristic of the liquid phase. The fluidity of the lipid bilayer is central to lipid-lipid, lipid-protein and lipid-protein-carbohydrate interactions. The heterogeneity of the lipids and proteins suggests that biomembranes are unlike other types of supramolecular aggregates whose constituents appear to be present in stoichiometric proportions.

Since the function and structure of biomembranes are the 'two sides' of the same lipid bilayer, the general ultrastructure of the biomembrane emerging from current work is that the lipids in the form of a bilayer provides the framework for proteins and other constituents. These membrane constituents are immersed to varying degrees in the lipid bilayer. The lipid bilayer of the membrane is actually fluid and has the

consistency of olive oil (viscosity ~ 1 centipoise). The lipids, proteins, and other constituents are thus perceived to be able to distribute freely within the confine of the lipid bilayer. However, the picture is a dynamic one, in that phospholipids and cholesterol form a hydrophobic, fluid bilayer in which functional entities such as receptors, ion channels, pigments, proteins can be embedded. That is that membrane constituents are able to exchange and/or be modified by compounds in contact with the cell membrane. At the molecular level, both lipids and proteins exhibit asymmetry; the composition of the inside of a membrane is different from the outside. This must be so in order to explain the active transport of species across the membrane. Also active sites of membrane-bound enzymes or immunlogical determinants are found on only one side of a lipid bilayer.

Thus, the above depiction of the biomembrane ultrastructure is able to account for the trilaminar (railroad track) appearance of biomembranes in electron micrographs. It is also able to account for the electron density profile across the biomembrane as determined by x-ray crystallography. Finally, mention should be made that this dynamic, liquid-crystalline, asymmetric lipid bilayer structure, modified by proteins and other membrane constituents, is also able to provide us with insights into the mechanism by which energies of various forms (electromagnetic, chemical, electrical, etc.) can be transduced in membrane systems (*see* Chapters 8, *Bioenergetics* and 9, *Photobiology*) as well as permitting inter- and intracellular exchange of solutes, information and signal transduction.

The 'Chop Suey' Model

Although in modern biology textbooks the pictures of biomembranes are getting fancier and fancier, our present understanding of biomembrane structure has not nevertheless departed from the basic construct of soap films and lipid bilayers (Table 2.2) that began nearly 4 centuries ago. Figure 2.6 illustrates schematically of various models that have been proposed since the bilayer leaflet model of Gorter and Grendel (**#1**). Concerning Fig. 2.6, some brief remarks deem appropriate. In the model of Harvey, Danielli and Davson (**#2**), a three-layered sandwich of protein-lipid bilayer-protein was then a novel concept. Experimental

support was shortly provided by Robertson and others (**#3**), on the basis of electron microscopy and x-ray diffraction. Except the spherical micelle model of Sjostrand and of Lucy (**#8**), the various other models proposed by Benson (**#4**), Lenard, Singer and Nicolson (**#5** & **#6**), and by Green (**#7**), shown in Fig. 2.6, are in essence an elaboration of the 'unit membrane' hypothesis of Robertson [Kerker, 1972; Robertson, 1981]. Finally, shown in (**#9**) is a composite model based on all previous proposals [Brown, 1971]. This historical panorama of the membrane structure in due time culminated in the so-called 'Chop Suey' model of biomembranes in the early 1970s, which is shown in Fig. 2.7. During that time it was said that, any bioscientist interested in biological membranes, and worthy of his or her 'salt', should have his/her own model! Perhaps, the 'Chop Suey' (or, if you are from Scandinavian countries, Smorgasbord) model is best described by one of its proponents, J. Koryta, a noted Czechoslovak electrochemist[14] associated with the Heyrovsky Institute, Prague, whose words are quoted below:

"... This is a difficult task when we consider the extreme complexity of the biological membrane...This cheerful picture (Fig. 2.6) was called the 'Chop Suey' model ..... The favorite Cantonese 'Chop Suey' type of dishes contain a mixture of various ingredients starting with noodles and bamboo shoots and ending up with fish and shrimps ... It would seem that the task of deciphering the intricacies of a system of such complexity indeed exceeds human powers. However, if we gave up we would lose the hope of elucidating basic processes in organisms. ..."

Frivolous remarks asides, it is worth stressing that phospholipids play a crucial role in the architecture of biomembranes as well as in many biochemical processes. This structural role of phospholipid molecules reflect their physical properties, which are determined by their extraordinary ability to self-assemble into a variety of supramolecular assemblies [Kerker, 1972]. These include the very essence of the lipid bilayer present in every living cell. Membranes are dynamic in that they are mobile; their components are continuously synthesized and degraded. The primary event in cell death (e.g. myocardial infarction) may be due to

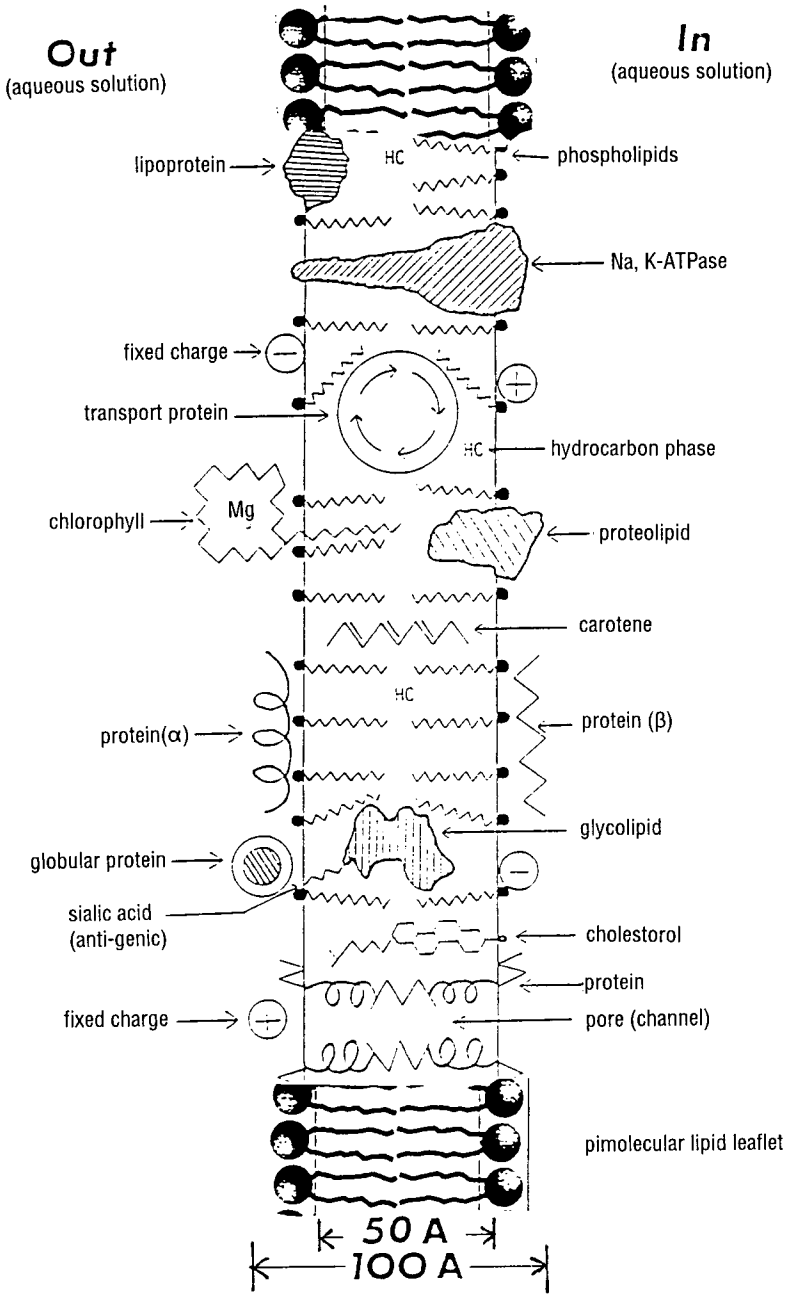

Fig. 2.7. The Chop-Suey Model

the damage to the plasma membrane, leading ultimately to cell death. In the 'Chop Suey' model of the biomembrane, the structure is fluid enough to permit the addition of various biomolecules such as transmembrane entities (e.g. porin, bacteriorhodopsin, photosynthetic reaction centers). As a first step toward biophysical and chemical investigation of biomembrane assemblies, it is helpful to sketch in broad strokes that the experimental lipid bilayer is a cogent approach to the understanding of the structure and function of biomembranes. As a general framework, the bilayer leaflet model is not only useful theoretically as in molecular simulations [Robertson, 1981; Lipowsky,1995; Mouritsen and Andersen, 1998],[11-13] but also suggests explicit experiments, as are being continuously carried out with BLMs and liposomes [Rosoff, 1996].[18]

2.5 Functions of Biomembranes

Two outstanding characteristics of the living cell are: (1) its ability to maintain many substances at an internal concentration different from those in the surrounding medium, and (2) the large difference in electrical potential existing between the inside of the cell and its external fluid. This second characteristic is closely associated with the first, which is maintained by the plasma membrane that bounds each cell. In order to sustain the life of the cell, nutrients must be supplied; to prevent poisoning, metabolic waste must be eliminated; and finally, to avoid rupture of the membrane, osmotic balance must be maintained. These rather perfunctory statements serve to illustrate that the membrane surrounding the cells is selectively permeable.

The selectivity properties of the cell or biomembrane are closely related to its structural components: phospholipids, proteins, and carbohydrates and their complexes. These components form a complicated structure which has been described as a bimolecular lipid leaflet (lipid bilayer) with sorbed proteins and other complexes. A membrane is not simply a physical barrier between the cell cytoplasm and its external environment, or between different compartments of a cell. Since the cell is separated from its environment and needs to get nutrients in and waste out, the membrane must be able to accommodate this. It acts as a selective

barrier. Some molecules can cross the membrane without assistance, but most cannot. Besides water, some small polar molecules and non-polar molecules can traverse the membrane, whereas non-polar molecules penetrate by actually dissolving into the lipid bilayer. Polar compounds such as amino acids, organic acids and inorganic salts are not allowed entry due to the energy barrier of the lipid bilayer, but instead must be specifically transported across the membrane by either proteins or polypeptide carriers. Membrane proteins play a pivotal role in many cellular and physiological processes. They are essential mediators of material and information transfer between cells and their environment, between compartments comprising the organelle systems. Membrane protein systems of particular interest to biophysicists include energy transducing membranes of mitochondria, chloroplasts, and bacteria, as well as cell membranes involved in transport of ions, electrons, and ATP synthesis (Chapter 8, *Membrane Energetics*). Functionally, normal membrane proteins are vital to health and specific defects are associated with many known disease states. Membrane proteins are the targets of a large number of pharmacologically and toxicologically active substances, and are responsible, in part for their uptake, metabolism, and clearance. Thus, the functions of membranes depend on the proteins and other constituents within them. Some of these proteins play largely a structural role, while other membrane proteins selectively transport specific molecules and ions into or out of the cell or organelle, and some others are receptors for chemical signals from outside the cell. Enzymes are proteins; they catalyze reactions in specialized biomembranes, such as the thylakoid membrane of the chloroplast that contains pigmented proteins for converting sunlight into electrical and chemical energy. Mitochondrial inner cristae membrane has high amounts of electron transport proteins that couple the flow of electrons to ATP synthesis, whereas the visual receptor membrane of the eye consists of lipids with *cis/trans* hydrocarbon chains for light signal transducton (Chapter 9, *Membrane Photobiology*). Generally speaking, biomembranes with similar function (i.e. from the same organelle) are similar across species lines, but membranes with different function (i.e. from different organelles) may differ strikingly within a species.

Due to complex structural and environmental factors associated with biomembranes, numerous investigators used different techniques and carried out studies on model systems in order to understand the fundamental life processes, such as ion accumulation or active transport, conduction of nerve impulses, energy transduction, protein synthesis, permeability barrier of ions and molecules, immunological reactions, phagocytosis and pinocytosis, etc., in physical and chemical terms. In view of what has been covered so far, a good experimental model should possess a lipid bilayer structure onto as well as into which functional entities can be embedded. To date, the two most widely used model membranes are bilayer lipid membranes of planar (BLM) and spherical (liposome) configuration. Planar lipid bilayers (BLMs) and spherical liposomes (also known as lipid microvesicles, LMV) are complementary to each other since both types are derived from common amphipathic lipids and related compounds. Both are excellent model membrane systems, and have been widely used for investigations into a variety of physical, chemical, and biological functions. We will discuss planar BLMs and liposomes in detail in Chapter 4, and in subsequent chapters throughout the book. Here, in the following sections, we will elaborate how some of these functions are related in terms of membrane constituents.

Principal Functions of Membrane Constituents

The main constituents of membranes are lipids, proteins and carbohydrates in variable proportions. Membrane lipids are amphipathic and they are soluble in organic solvents. The lipids of membranes form the key structural element, namely, the lipid bilayer of the membrane.

Lipids

Lipids can readily move laterally and can also undergo rotation. The degree of membrane liquidity (fluidity) is determined by temperature and lipid composition. Lipids with shorter hydrocarbon chains are less rigid and remain fluid at lower temperatures. This is because interactions between shorter chains is weaker than for longer chains. Lipids containing

unsaturated fatty acids increase lipid bilayer liquidity. The double bonds introduce kinks, preventing tight packing of the fatty acids. Generally speaking, the lipid bilayer is semipermeable, meaning that some molecules are allowed to pass freely (diffuse) through the structure. The lipid bilayer is virtually impermeable to large molecules, relatively impermeable to molecules as small as charged ions. All dissolved molecules, including those that can readily pass through lipid bilayers and those that transverse with difficulty (lipid bilayer-hampered substances), are capable of diffusion. For lipid bilayer-impeded substances, diffusion across cell membranes may nevertheless be highly probable but such diffusion must be facilitated by lipid bilayer spanning proteins. Such proteins and their polypeptides essentially form carriers or channels (pores). In this case they (a) accept specific lipid bilayer-hampered substances at one side (b) allow the substance to enter the lipid bilayer without dissolving in it, and (c) then deliver the substance to either side.

Both limiting the number of specific membrane proteins present and to specifically modify the function of those membrane proteins already present can control the rate of movement of lipid bilayer-hampered substances across cell membranes. A number of mechanisms by which lipid bilayer-hampered substances cross biomembranes via protein action will be discussed later (Chapter 5). These include:

- *diffusion through pores (channels)*
- *facilitated diffusion*
- *cotransport*
- *group translocation*
- *active transport*

Steroids

Cholesterol, one of the most important steroids, is a principal component of animal cell plasma membranes, and much smaller amounts are found in the membranes of intracellular organelles. Cholesterol is the precursor for all other animal steroids such as vitamins and the adrenal hormones. For instance, cholesterol is converted to vitamin D (if irradiated with ultra-violet light). Cholesterol is also the precursor from which most other steroids are synthesized. Steroids are essential hormones;

emulsifying agents for fat catabolism. Cholesterol is essential to keep membranes fluid. It can be synthesized in endoplasmic reticulum. The steroids derived from cholesterol in animals include several families of well known hormones such as androgens (testosterone) and oestrogens (oestradiol); both are involved in sexual characteristics and function, whereas progestins (progesterone, control of menstrual cycle and pregnancy), glucocortioids (cortisol, control of carbohydrate, protein and lipid metabolism), mineralocorticoids (regulate common ions Na^+, K^+ and Cl^-), bile acids (cholic and deoxycholic acids, secreted in bile from gall bladder that assist in digestion and absorption of dietary lipids in the intestine) are vital to healthy animal functions. At the membrane level, cholesterol with its hydrocarbon ring structure plays a distinct role in determining membrane fluidity.

Polar hydroxyl group positions close to the phosphate head group. Rigid rings of steroids interact with regions of fatty acid chain adjacent to phospholipid head groups. This interaction decreases the mobility of the outer portions of the fatty acid chains, making this region of the membrane more rigid, even at higher temperatures. On the other hand insertion of cholesterol interferes with interactions between fatty acids, thereby maintaining fluidity at lower temperatures. The difficulty with which flip-flop movement of membrane constituents occurs relates to the sidedness of membranes. Membrane surfaces have asymmetry—different characteristics on the two sides. However, cholesterol is able to flip-flop from one side of the lipid bilayer to the other side, owing to its small hydrophilic polar group. One of the important effects of cholesterol seems to be on the liquidity of the membrane; it increases the packing density of the phospholipids. Myelin, for example, is high in cholesterol but also high in saturated fatty acids, whereas mitochondria and bacteria have little or no cholesterol, but high in unsaturated fatty acids. Cholesterol is also a constituent of lipoprotein complexes in the blood and it is one of the components in the plaques that form on arterial walls in arteriosclerosis. At moderately high temperature (~ 100 °C), cholesterol is easily oxidized in air; the resulting products known as 'oxidized cholesterol' have been used in a bilayer lipid membrane (BLM) formation.[15]

Methods of isolation and characterization of membrane proteins

The basic structure of biomembranes is determined by the lipid bilayer; membrane proteins, carbohydrates and their lipid complexes, however, principally perform the functions. Since Danielli in the 1930s first depicted membrane proteins as globular, all conceivable arrangements of membrane proteins on or in as well as across the lipid bilayer have been proposed [see Fishman, 1962; Kerker, 1972; Robertson, 1981]. Fig.2.4 illustrates five ways in which membrane proteins may be associated with the lipid bilayer. As may be seen in Fig.2.4, membrane proteins are associated with the lipid bilayer by two types of interaction: ionic or electrostatic and hydrophobic. Hence, the methods for their detachment have been developed. The following is a summary of the essential steps:

a. *Concentrated salt solutions*. Salts such as KSCN, KBr, and Li iodosalicylate of high ionic strength (0.5 M) are used to disrupt the membrane/solution interface, thereby releasing weakly adsorbed peripheral membrane proteins.
b. *Organic solvent extraction*. Integral membrane proteins may be separated from the lipid bilayer using organic solvents such as chloroform-methanol mixture. Acetone is frequently used at low temperature (-20^{o}C) to precipitate membrane proteins as a first step in the purification procedure.
c. *Surfactant extraction*. Surfactants (or detergents) being lipid-like are used nowadays for solubilizing membrane proteins. A wide choice of surfactants are available; they can be either anionic, (Na dodecylsulfate, SDS) or non-ionic (polyoxyethylene octylphenol, Triton X-100). B-D-octyl-glucoside, also a non-ionic surfactant, is a popular one for solubilizing membrane proteins. The advantage of this detergent is that it can be readily removed by dialysis. Bile salts (sodium cholates), naturally occurring anionic detergents, are frequently used for they do not cause denaturation of membrane proteins.
d. *Using hypertonic buffered solutions* (including pH, and chelating agent) (proteins precipitated out)
e. *H_2O-butanol extraction*. Used for RBCs.

f. *Using proteolytic enzymes* (such as papain)
g. *Sonication* (cavitation - the rapid expansion and violent collapse of air bubbles trapped in the medium KCl).

Once the membrane proteins have been solubilized, the subsequent purification procedures are similar to those for soluble proteins. For example, they are purified by precipitation with $(NH_4)_2SO_4$. This step may be followed by a variety of techniques such as gel filtration, affinity chromatography, and ion-exchange chromatography. For a few intrinsic proteins that have been prepared in pure form, amino acid sequence data are now available.

In the previous section on lipids, a number of mechanisms by which lipid bilayer-hampered substances cross biomembranes via protein domain were mentioned. These include: diffusion through pores (channels), facilitated diffusion, cotransport, group translocation, and active transport. The unique mix of lipids and proteins gives each membrane its unique range of functions, these are:

- *Moving polar species across a biomembrane requires molecular support and energy input*
- *Facilitated diffusion (down an electrochemical potential gradient)*
- *Channels formed by protein (size/charge screening)*
- *Gates of channels formed by proteins (voltage/ligand requirements)*
- *Kinetics (rate vs. substrate concentration)--rate proportional to number of sites*
- *Active transport (up an electrochemical potential gradient)*
- *Use a second chemical potential gradient*
- *Metabolic energy requirements (e.g. ATP)*

Carbohydrates

They exist in biomembranes as complexes of lipids and proteins, known as glycolipids and glycoproteins, in which sugars are linked to lipids and proteins, respectively. Glycolipids and glycoproteins are

interface-active in that they serve as receptor sites for the attachment of other physiological and non-physiological molecules.

Glycolipids and glycoproteins

Some membrane lipids and proteins are covalently associated with carbohydrate residues. They are known, respectively, as glycolipids, and glycoproteins. The glycolipids and glycoproteins are implicated in the specificity of the blood groupings and other immunological properties of membranes. In plasma membranes, carbohydrate residues (monosaccharides) are N-acetyl glucosamine, galactose, neuraminic acid (sialic acid), and N-acetyl galactosamine.

Glycerol-based glycolipids are the primary form in plants and bacteria, whereas sphingolipid-based lipids depend on the addition of carbohydrate units to the sphingolipid nucleus. This type of glycolipid is the main form in animal cell membranes. Simple glycolipids formed by the addition of a single sugar unit are called cerebrosides. The addition of straight or branched sugar chains produces gangliosides. In gandliosides, remarkable differences exist in the fatty acids compositions of the plasma membranes. In general, there are about 40% polyunsaturated C_{18}-C_{22} fatty acids. The carbohydrates added can be have considerable variation in structure. Since glycolipids show such striking asymmetry in their distribution in the biomembrane, it is presumed that they mediate distinct functions on the cell surface, such as:

- self recognition, for example, blood group antigens, A, B, AB or O
- electrical effects
- cell recognition, for example, receptors for extracellular species.
- binding to the extracellular matrix
- protection of the cell exterior

One surprising fact is lipid bilayer's substantial permeability to water molecules, which is not well understood. Molecules that can diffuse through the lipid bilayer do so at differing rates depending upon their ability to enter the hydrophobic interior of the lipid bilayer. In Chapter 5

we will discuss the above topics of membrane transport in detail. Here, once more the essential aspects of the lipid bilayer are delineated in the following paragraphs.

The Lipid Bilayer: Structure and Function

All living systems are made of cells, and a cell's biomembrane comprises a lipid bilayer as its essential component. The cell membrane is the primary barrier between the intracellular and extracellular compartments. Assembled primarily of a lipid bilayer, the biomembrane comprises a variety of proteins that include carriers for certain nutrients, channels for ion transport, and receptors that mediate transmembrane signaling in growth, differentiation, and other cellular activities. The lipid bilayer is the universal basis for all biomembrane structure, whose paramount importance is thus self-evident. The lipid bilayer is made of lipids two molecules thick and can be seen under the electron microscope. This lipid bilayer is termed as a semipermeable membrane, meaning that some molecules are allowed to pass freely (diffuse) through the structure; it is virtually impermeable to charged ions and large molecules, and quite permeable to lipid soluble species. The lipid bilayer provides us with the key for understanding biomembrane functions.

First, all biomembrane lipids are amphiphilic (amphipathic), meaning they have a hydrophilic (water-loving) polar group and a hydrophobic (water-hating) hydrocarbon moiety. This dichotomy (or Ying-Yang property) in a single lipid molecule is the primary factor for lipid bilayer formation in aqueous solution. To appreciate this fact, one needs to take a closer look at the molecular composition of some typical lipids.

Second, there are three main types of lipids in biomembranes, namely, phospholipids, sterols and glycolipids. The most abundant and important lipid component in biomembranes are the phospholipids. For example, phospholipids of the phospphoglyceride variety consist of a phosphate group joined to a glycerol backbone which is esterified to two fatty acids. This complex is the phosphatidic acid (PA) nucleus of phospholipids. The common type of phospholipid in most biomembranes is phosphatidyl-

choline (commonly referred as lecithin), which has the phosphate as its hydrophilic head associated with choline. More precisely, the two hydrocarbon tails of the phospholipid molecules vary in length between 14 and 24 carbon atoms, 18-20 being most common. One of the two hydrocarbon chains of each phospholipid molecule has one or more double bonds between adjacent carbon atoms. Their unsaturation (that is, the number of double bonds they contain) together with the length of hydrocarbon chains greatly affects their packing in the bilayer. Each double bond makes it more difficult for the hydrocarbon chains to pack against one another, as a result of their stereo-configuration. Insofar as the chain length is concerned, a shorter one reduces the tendency of the hydrocarbon tails to interact with one another. Both of these properties increase the fluidity of the lipid bilayer. Membranes contain many types of phospholipids and their relative proportions differ among membranes. It is because of their cylindrical shape and amphipathic nature of these lipid molecules that these molecules form bilayers spontaneously in aqueous solutions.

Third, amphipathic phospholipids, like other amphiphilic molecules, are subject to two conflicting forces: the hydrophilic head is attracted to water, while the hydrophobic hydrocarbon moiety avoids water and seeks to aggregate with other hydrophobic molecules (chemists' rule – like-dissolves-like). This dichotomy is elegantly resolved by the formation of a lipid bilayer in an aqueous environment. The same forces that drive the amphipathic molecules to self-assemble to form a bilayer confer on that bilayer a self-sealing property (see below on mechanical probing). This self-sealing property is important in that, since any rip in the lipid bilayer will create a boundary with water, and because this is energetically unfavorable, the molecules of the bilayer will spontaneously self-assemble to eliminate this boundary. If the rip is small, this spontaneous rearrangement will lead to the repair of the bilayer, restoring a single continuous layer. If the rip is large, the layer may break up into separate vesicles, forming liposomes.[4b]

Fourth, the lipid bilayer, which is crucial for membrane function, is a two-dimensional fluid or solvent for other membrane constituents. As described here, it is hard to imagine how a cell could live, grow, and reproduce, if its lipid bilayer were not fluid. The aqueous environment

inside and outside a cell prevents membrane lipids from escaping from the bilayer, but being liquid which is dynamic allows these molecules from moving about, rotating rapidly around their axis and changing places with one another within the plane of the bilayer, due to thermal motions. It is estimated that this exchange leads to rapid diffusion in the plane of the membrane so that a lipid molecule in an experimental bilayer lipid membrane may diffuse within a second a length equal to that of a large bacterial cell.

Fifth, due to energetics, phospholipid molecules very rarely flip from one side of the bilayer to the other side. However, certain enzymes may facilitate the process. This so-called "flip-flop," occurs less than once a month for any individual lipid molecule.

Sixth, membrane fluidity is important to a cell for many reasons. It enables membrane proteins to diffuse rapidly in the plane of the bilayer and to interact with one another, as is crucial, for example, in signal transduction. It also provides a simple means of distributing membrane lipids and proteins, after their synthesis in other regions of the cell, by diffusion from sites where they are inserted into the bilayer. It allows membranes to fuse with one another and mix their molecules, and it ensures that membrane constituents are distributed evenly between cells when a cell divides.

Seventh, bilayers undergo a change in state; it is known as phase transition, in which they 'freeze' or 'melt' above or below certain temperatures. At low temperatures, hydrocarbon chains of lipids are tightly packed (gel state), whereas at temperatures above phase transition, the lipid bilayer is in a liquid-crystalline or fluid state.as illustrated below:

increasing temperature ⟶ ***(liquid state)***

lipid bilayer ⟵{ **phase transition** }⟶ lipid bilayer

(gel state) ⟵ *decreasing temperature*

In order to function properly, all membranes must operate at temperatures above phase transition. This phenomenon can be understood in the

following way: phase transition results from temperature-induced changes in packing and mobility of the membrane lipids. The temperature at which lipid phase transition occurs depends on two factors: length and degree of saturation of fatty acids in the lipids. Longer chains become fluid at *higher* temperatures and more unsaturated become more fluid at *lower* temperatures. An increase in membrane fluidity means that lipid molecules are capable of lateral diffusion in the plane of the membrane. Lateral diffusion is quite rapid and lipids can diffuse from one end of a cell to the other in seconds. However, flip-flop of membrane from one side of the lipid bilayer to the other side is normally very slow.

In bacterial and yeast cells, which have to adapt to varying temperatures, both the lengths and the unsaturation of the hydrocarbon chains in the bilayer are constantly adjusted to maintain the membrane at a relatively constant fluidity: at higher temperatures, for example, the cell makes membrane lipids with hydrocarbon tails that are longer and that contain fewer double bonds. In contrast, in animal cells, membrane fluidity is regulated by the presence of cholesterol, which is absent in bacteria, yeast, and plants. These short, rigid molecules are present in especially large amounts in the plasma membrane, where they fill the spaces between neighboring phospholipid molecules that are caused by the kinks in their unsaturated hydrocarbon chains. In this way cholesterol stiffens the bilayer and makes it less fluid and less permeable. In cold climate, for example, bears decrease the length of the fatty acid chains or increase the degree of unsaturation of these chains to maintain membrane fluidity at low temperatures.

The above descriptions are supported by a variety of experiments, as follows. Experiments, that have been performed, demonstrate the fluidity of the lipid bilayer including, mechanical probing, photobleaching, and cell fusion. As already mentioned above concerning the self-sealing property of the lipid bilayer. This was experimentally discovered in planar lipid bilayers (BLMs) many decades ago.[4a] It was found that a small glass pipette can be pushed through, moved around, and withdrawn without breaking the lipid bilayer, demonstrating the liquid character of the molecular assembly. In photobleaching experiments, fluorescent dyes are attached to membrane proteins or lipids. The dyes in a small region of the

lipid bilayer are then 'bleached' by exposure to a laser beam. The bleached spot gradually spreads and fades as the marked molecules diffuse, whereas in cell fusion experiments lateral movement of proteins in membranes, fused mouse and human cells, were demonstrated. Membrane proteins in each cell type were labeled with antibodies attached to different fluorescent dyes After fusion, labeled molecules were initially in different halves of the cell. However, after incubation at 37 ^{0}C, the labeled molecules were completely intermixed, indicating that proteins can diffuse laterally. In concluding this section on the properties and functions of the lipid bilayer, it is evident the pivotal role it plays in deciding the two sides of the cell. There is little doubt about the fluidity of the lipid bilayer, whose liquid-crystalline state is preeminent in performing the tasks essential to the living cell, hence to life itself as we know it.

Finally, a concluding remark of the present chapter, which can not be overstated, is that *the basic structure of all biomembranes is a lipid bilayer* (see Fig. 2.2). The evolution of the lipid bilayer concept and its experimental investigations of membrane-based life phenomena including signal transduction, transport, electrical properties, and energy conversion that began many years ago and continues to this day. Besides fundamental studies of experimental lipid bilayers, current research and development poised for biotechnological exploitation,[18] will be the main focus discussed in the remainder of this book.

General References

A. P. Fishman (ed.) *Symposium on the Plasma Membrane*, American Heart Association and New York Heart Association, New York City, December 8-9, 1961. *Circulation*, **26**(2), November 1962.

H. D. Brown (Ed), *Chemistry of Cell Interface*, Academic Press, NY, 1971. pp. 205-254

M. Kerker (ed.) MTP International Review of Science, **7**, Butterworths, London; University Park Press, Baltimore, 1972. pp. 25-78

H. T. Tien, *Bilayer Lipid Membranes (BLM): Theory and Practice*, Marcel Dekker, Inc. New York, 1974. 655 pp.

D. E. Metzler: *Biochemistry: The Reaction of Living Cells*, Academic Press, NY, 1977.

J. D. Robertson, *J. Cell Biol.*, 91 (1981) 189s-204s

T. E. Thompson and C. Huang, in 'Physiology of Membrane Disor ders', Plenum, NY, 1986. pp. 25-44

D. B. Datta, *Membrane Biochemistry*, Floral Publishing, Madison, 1987

R. Lipowsky, *The Morphology of Lipid Membranes*, Current Biology, Vol. 5, 1995. pp. 531-540

M. Rosoff (ed.) *Vesicles*, Marcel Dekker, Inc. New York, 1996

O. G. Mouritsen and O. S. Andersen (eds.) *In search of a New Biomem brane Model*, Bio. Skr. Dan. Vid. Selsik. Vol. 49, Munksgaard, Copenhagen, 1998, 224 pp.

Specific References*

1. (a) R. Hooke, in *The History of the Royal Society of London*, 3 (1672) 29; (b) I. Newton, *Opticks* (1704), reprinted edition, Dover, NY, 1952, pp. 215- 232
2. I. Langmuir, *J. Am. Chem. Soc.*, 39 (1917) 1848
3. K. B. Blodgett and I. Langmuir, *Phys. Rev.* 51 (1937) 964
5. (a) P. Mueller, D. O. Rudin, H. T.Tien & W. C.Wescott, *Nature,* 194 (1962) 979; *J. Phys. Chem.* 67 (1963) 534; (b) A. D. Bangham, Adv. Lipid Res., 1 (1963) 65; *in Progress in Biophysics and Molecular Biology*, (J. A. V. Butler and D. Noble, eds.) **18**, Pergamon Press, NY, 1968. pp. 29-95; *BioEssays*, 17 (1995) 1081
5. J. Mountz & H. T. Tien, *Photochem. Photobiol.*, 28 (1978) 395-400
6. (a) L. Taniguchi, K. Yoyosawa, H. Yamaguchi, *J. Electroanal. Chem.* 140 (1982) 187; (b) R. G. Nuzzo and D. L. Allara, *J. Am. Chem. Soc.*, 105 (1983) 4481; (c)L. Netzer and J. Sagiv, *J. Am. Chem. Soc.*, 105 (1983) 674
7. (a) H. T. Tien, *in Surfactants in Solution* (K. L. Mittal, ed.) Plenum Press, NY, 1989. pp. 133-178
   (b) A. Ottova et al., *in Molecular and Biomolecular Electronics*, R. Birge (ed.), ACS, Washington, DC, 1994. Chap. 17.
8. (a) Yuan et al., *Materials Sci. & Eng. C*: 4 (1996) 35-38
   (b) Lu et al., *Bioelectrochem. & Bioenergetics*, 39 (1996) 285-289
9. E. Gorter and F. Grendel, *J. Expt. Med.*, **41** (1925) 439-444
10. H. T. Tien, *Journal of Theoretical Biology*, 16 (1967) 97-110
11. B. A. Hill, *Medical Hypothesis*, **28** (1989) 85
12. Heller et al., *J. Phys. Chem.*, **97** (1993) 6358
13. D. Gallez et al., *J. Coll. Int. Sci.*, **160** (1993) 141
14. J. Koryta, *Ions, Electrodes and Membranes*, Wiley, New York, Toronto, Singapore, 1982. pp. 130-131
15. H. T. Tien et al. Nature, 212 (1966) 718
16. W. J. Parak, Domke, J., George M, Kardinal A, Radmacher M, Gaub HE, de Roos ADG, Theuvenet APR, Wiegand G, Sackmann E, Behrends JC, Biophys. J. 76: (3) 1659-1667 MAR 1999; Rotsch C, Jacobson K, Radmacher M. P NATL ACAD SCI USA 96: (3) 921 1999

17. R. F. Taylor and J. S. Schultz (eds) *Handbook of Chemical and Biological Sensors*, Institute of Physics Publishing, Philadelphia, 1996
18. H. T. Tien and A. l. Ottova, From self-assembled bilayer lipid mem branes (BLMs) to supported BLMs on metal and gel substrates to practical applications, *Colloids and Surfaces A: Physicochemical and Engineering Aspects*, 149, 217-233 (1999).

---

*For recent literature references, see web page at:
http://www.msu.edu/user/ottova/blm/biomembranes.html

Chapter 3

Membrane Biophysics—Basic Principles

'The wages of change is life!"

3.1 Thermodynamics

First of all, energy is required for the actions and processes of living things. For their growth and replication, living cells have to exchange and transduce energy for their various activities. Therefore, in order to appreciate energy exchange and transduction, one must have some knowledge of a branch of basic science, namely energetics or thermodynamics that is concerned with energy transduction in all kinds of systems including the living cell. Before considering the basic laws of thermodynamics, it is of some interest to state the increasing tendency to understand biological phenomena in physicochemical and molecular terms. The subject of thermodynamics used to be studied by students in theoretical physics more than a century ago, then in 1950s it became a must for a graduate student in chemistry; it is now introduced to students of sciences at elementary levels. Thus, for any student who is seriously interested in cellular phenomena, it is essential to be at least conversant

with the basic concepts of thermodynamics and other basic principles of energetics, which govern physiological changes.

The aim of thermodynamics or energetics (these two terms will be used interchangeably) is to establish the principles and laws, which govern transformation of all kinds, from black holes to living cells; i.e. it is aimed at universal applicability. The working philosophy and approaches are simple and logical, and require no special knowledge of chemistry or molecular theory. We need to become familiar with only a small portion of thermodynamic formalism in order to examine in a broad way the nature of biological energy transduction. Historically, thermodynamics was concerned with energy transformation of heat and steam engines. However, it is interesting to note that steam engines were developed without the benefit of thermodynamics. Rather, the science was developed as a result of steam engines. "Therm" means heat. Joule in the 1840s demonstrated that the mechanical work can be converted to the heat and that the heat generated is equal to the work done. As we shall see presently, the energetics is a better term than the thermodynamics, for we will be dealing with not just the heat. How much energy is absorbed or released during chemical/physiological reactions? How does the science of thermodynamics proceeds to analyze the energy transduction? To start, a few terms must be defined.

3.1.1 System and Surroundings

We must specify the ***system***. This system could be anything from a single cell, to one beaker of solution, a cockroach, all the way up to the whole universe that we wish to study. A system is a collection of matter. All the other matter in the universe apart from this system is called surroundings (or environment). A system can interact with its surroundings via a flow of heat, work or matter. Such a system (i.e. the cell) is called an ***open system***. If only heat and work, but no matter exchanges are involved, it is a ***closed system.*** A ***process*** is any change that is taking place in a system. Further, the system is constrained by a spatially defined place by the ***boundary*** that separates it from the rest of the surroundings. This boundary in our case is the cell membrane as shown in

Fig. 3.1. The system under consideration has a defined internal energy denoted *E*. This term represents all of the energy, from all forms, contained in the system, including the kinetic energy, the rotational and the vibrational energy, the energy stored in

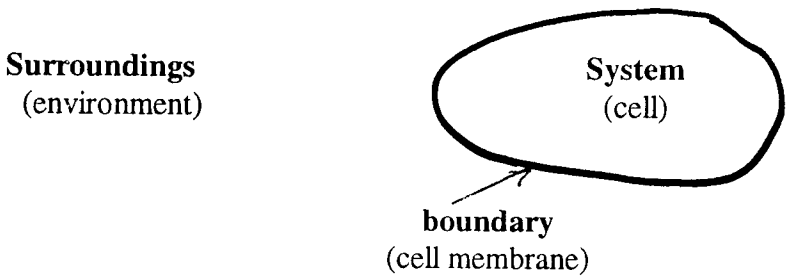

Fig. 3.1. The system under examination is the cell whose surroundings are its extracellular fluid and materials in it. The boundary is the cell membrane.

chemical bonds (e.g. ATP, a very important one for metabolic discussions). In experimental sciences, such as membrane biophysics, the properties of a system should be expressed in measurable quantities. For example, the energy is a function of the state of the system, meaning that it depends on the pressure, volume and temperature. There are two kinds of measurable properties of a system: ***intensive*** and ***extensive***. Intensive properties such as temperature (*T*), pressure (*P*), and specific gravity are independent of the size of a system. Extensive properties including mass (*m*), volume (*V*), and area (*A*) are size-dependent, which are also additive.

As the system proceeds from its ***initial state*** to the ***final state***, it may either absorb the energy from, or deliver to, the surroundings. The total energy of a system is very difficult to measure. Fortunately, we shall only be concerned with the change, or the difference (Δ) between the final and the initial state (known as a state function), and is given by

$$\Delta = final\ state - initial\ state \qquad (3.\ 1)$$

However, Δ is independent of the path chosen. In going from the initial to the final state, a certain amount of the 'free energy' may be available.

Thermodynamic laws are time-independent. It does not matter whether a given reaction (or a process, physical, chemical or physiological) takes place in picoseconds (10^{-12} sec) or tens of millennium to come to equilibrium. Further, the thermodynamics is statistical and macroscopic in approach; one does not have to know the atomic theory, the pathway or mechanisms of reactions (we shall deal with that later in the kinetics). There are two approaches to the study of energetics: (1) Phenomenological (macroscopic): based on common experience, and (2) Statistical (molecular): obeying the law of mechanics.

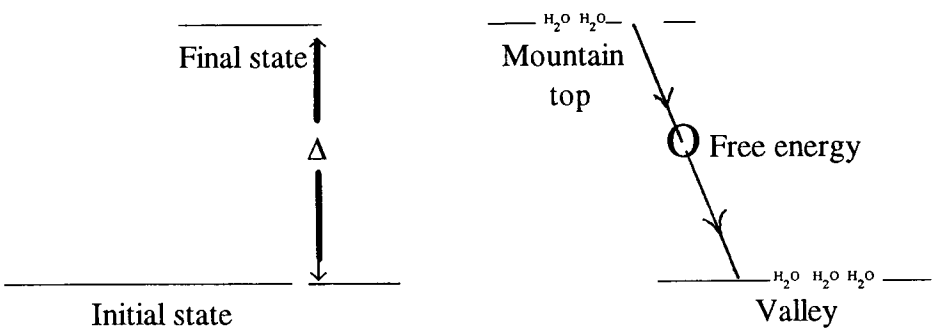

Fig. 3.2 The change of state functions and the free energy.

3.1.2. The first law of thermodynamics

This first law is generalized from the empirical experience and can not be derived from any other law or principle. It states that the energy, including the heat, is conserved. In other words, the total energy before

and after conversion is the same, as can be demonstrated for example in converting the electrical energy to the mechanical work. The first law, insofar as we know, governs the conversion and conservation of energy in every system known including the universe *without* exception.

Speaking about the heat and the work, we must have something concrete, for example, a material thing. From our common experience, the heat flows according to Eq. (3.2). This material thing is defined as a system (by convention). Empirical law of nature is that the heat flows from a hotter object (body *Y*) to a colder one (body *X*).

$$\underset{\textit{(cold)}}{\textbf{\textit{Body X}}} \xleftarrow{\textit{heat}\ Q} \underset{\textit{(hot)}}{\textbf{\textit{Body Y}}} \qquad (3.2)$$

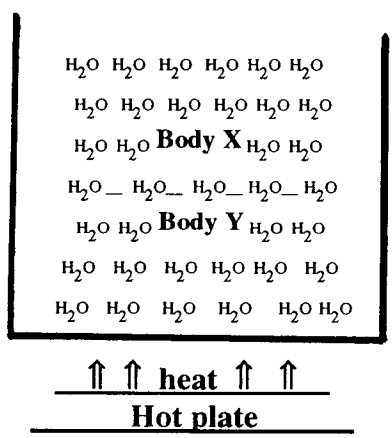

Fig. 3.3 The entropy: a system will always move in the direction that maximizes a choice.

The first law is a statement of the conservation of energy. Let the total energy of the system be designated as E, the change in E is given by

$$\Delta E = Q - W \qquad (3.3)$$

where Q is heat and W is work. By convention, the signs of these two terms are either positive or negative. $+Q$ or Q means that heat is absorbed by the system whereas $-Q$ is heat evolved by the system. W or $+W$ is work done on the system whereas -W is performed by the system. For a cyclic process,

$$\int E = 0 \qquad (3.4)$$

There could be many variables involved during an energy transduction process, such as:

Variable	**Convention**
Pressure, P	~ 1 atmosphere (atm)
Volume, V	a well-defined volume
Temperature, T	a fixed temperature
Concentration, C	a dilute solution
Electrical potential, ψ	< 0.1 volt (100 mV)

For most chemical and physiological reactions, we are interested in the conditions which has just been defined under convention by means of different variables. During a process all the above-mentioned variables remain practically constant. To a scientist, the importance of thermodynamics lies in its ability to predict the position of equilibrium in a system, i.e. whether a given reaction would proceed or not:

1st example:

$$ATP + H_2O \longrightarrow ADP + P_i \qquad (3.5)$$

$$\Delta E = -5 \text{ kcal/mol}$$

2nd example:

$$H_2O_{ice} \longrightarrow H_2O_{liquid} \qquad \Delta E = +1 \text{ kcal/mol} \qquad (3.6)$$

Under a specified set of conditions, we would like to know whether a particular biological reaction (or change) is feasible? Intuitively, if ΔE is negative, a process should be spontaneous. Unfortunately, as illustrated in the above examples, ΔE can be either >0 or <0. Obviously, a new criterion is needed. Here it is, where the second law of thermodynamics makes itself useful.

3.1.3. The second law of thermodynamics

In Nature, as we have observed, things as a rule go down hill. This is in accord with our empirical experiences as illustrated in Fig. 3.2. Before presenting the second law of thermodynamics, let us take a closer look of work. In Table 3.1, a variety of work are given. Quantitatively, the work is a product of an intensive factor multiplied by a capacitive factor; it is also a form of energy. However, one should be reminded that not all forms of energy are of the equal quality. For example, the visible light is an energy of high quality whereas the heat is an energy of poor-quality. This is owing to the simple fact that the high quality electrical energy, for instance, can be completely converted into heat, whereas vice versa it is not true on the basis of our experience

3.1.4. The concept of energy, work, and entropy

Energy manifests itself in various forms, and may be defined as the capacity to do work. Work is a scalar quantity, the product of two vectorial terms. Hence, one can write:

Work (energy) = intensity factor x capacity factor (units: ml^2time^{-2}).

Other forms of energy are:

- **Potential energy (PE) -- by virtue of its position**
- **Kinetic energy (KE) -- by virtue of its motion**

Heat (Q) is also a form of energy, measured in calories. Heat can be produced by work. However, no machine, a living cell or an organism, or for that matter natural and human-made devices of any kind, can do the work without an energy source. The unit for the work in physical, chemical, biochemical/physiological systems is ***calorie***. 1 calorie = the amount of heat required to raise the temperature of 1 gram of H_2O from 15 to 16 ^oC at 1 atm. The mechanical equivalent of heat is 1 calorie = 4.184 joules, 1 Kcal = 4.184 KJ, and 1 Joule = 10^7 ergs. (Note: one nutritional Calorie spelled with capital C differs from the small calorie as follows: 1 Calorie = 103 calories).

Table 3.1 Kinds of Work Defined

Work =	Intensity factor (Intensive property)	x	Capacity factor (Extensive property)
Gravitational	height, h		mass, m
Stretching	tension, t		length, l
Surface	surface tension, γ		area, A
Expansion	pressure, P		volume, V
Chemical	chemical potential, μ		moles, *mol*
Electrical	voltage, E or V		charge, q
Heat, Q(cal)	temperature, T (deg)		?

Question: **What is the capacity factor for heat in Table 3.1?**

From a dimensional analysis,

Energy = intensity factor x capacity factor;

$$Q(\text{cal}) = T(\text{deg}) \times \text{?}\ (\text{cal/deg}) \tag{3.7}$$

$$(Q/T)_{\text{system}} + (Q'/T)_{\text{surroundings}} = 0 \text{ or a positive number} = S_{\text{universe}} \tag{3.8}$$

$$\begin{array}{lll} & (Q/T) > 0 & \text{spontaneous} \\ \text{or} & (Q/T) = 0 & \text{at equilibrium} \\ & (Q/T) < 0 & \text{no reaction (N.R.)} \end{array} \tag{3.9}$$

Thus, $(Q/T) = S$, a special name is given; it is called ***entropy***.

***Question*: What is entropy?**

After an intellectual effort of more than 100 years, we can now say that the entropy is a measure of orderliness, and it is a property associated with a system. However, unlike other properties such as the mass and energy of a system, the entropy is not conserved; it tends to a maximal state. For example, take a glass of water and heat it briefly on a hot plate so that the water is cooler at the top half (roughly speaking) of the glass. Referring to Fig. 3.3, the portion of the water (Body Y) in the bottom of the glass possesses more thermal (kinetic) energy than the portion of the water (Body X) at the top. As time goes on, the entire glass of water would be at a certain temperature, T, since Body X and Body Y are in thermal contact. At the molecular level, there are about 10^{25} H_2O molecules in a glass of water. If the energy is exchanged freely and randomly among H_2O molecules, then there will be a greater quantity of energy to flow from the hot half to the cold half, simply because there are more quanta of energy in the bottom half of the H_2O molecules. In other words, the H_2O molecules in the lower half of the glass possess more energy and disorder than the H_2O molecules in the upper half. Thus, microscopically speaking, entropy is a measure of the number of ways in which the energy of a system (i.e. the H_2O molecules in the glass of water in our example) can be distributed among the available molecules such that *'a system will always move in the direction that maximizes choice'*. Perhaps, a more familiar

example will illustrate the point more clearly. As you know, the contents of your desk drawer will tend to get disordered with time unless you put a lot of work to keep it neat. In other words, the entropy is a state function that presents the degree of randomness or the lack of order in a system. The entropy of an ordered state is always lower than that of a disordered state. This state of affairs were recognized by Boltzmann who formulated an equation relating entropy (S) and the number of ways (W) as follows:

$$S = k \ln W \qquad (3.10)$$

where k is the Boltzmann's constant. Before discussing how one goes about to determine entropy experimentally, the statement attributed to **Clausius** (1865) is frequently quoted: *'The energy of the universe is constant, the entropy of the universe is increasing towards a maximum'*. If so, the universe must have started off in a highly ordered state at the beginning, in a tremendous explosion (the Big Bang theory)!

***Question*: Where have all the 'disorders' gone?**

***Question*: What happens when the entropy of the universe has reached its maximum ?**

These are the kind questions to be answered by cosmologists and theoretical physicists.[10] For us, a growing fertilized egg and other living systems represent the increasing orderliness rather than disorderliness. These apparent violations of the second law can be easily explained by remembering that living systems are ***open*** systems, they feed on high-energy and low-entropy stuff from their 'surroundings', The existence of life is not possible without the interchange of energy and matter with the surroundings, for *the wages of change is life*. Thus, the second law of thermodynamics provides us with a criterion for predicting the spontaneity of a reaction (a process, etc.). The entropy function as defined above, however, is hard to determine experimentally, for it involves both the system and its surroundings. Hence, a better function is required. This new function, due to J. Willard Gibbs designated as G, is known as the Gibbs'

free energy. Before discussing the concept of free energy, a brief mention should be made about the third law of thermodynamics. At absolute zero, the entropy of a pure substance is zero, when all motion ceases. What about life? A better question to ask is, perhaps, 'what is life? Insofar as we know, life is a state of high potential energy and low, or negative, entropy. At absolute zero, life as we know it, is not viable.

3.1.5 The free energy concept

For a system at equilibrium

$$\Delta S = (Q/T) = 0 \tag{3.11}$$

From the first law of thermodynamics

$$\Delta E = Q - W; \quad Q = \Delta E + W = \Delta E + PV \tag{3.12}$$

Since $dQ = TdS$

$$dQ = dE + PdV \tag{3.13}$$

or

$$T\Delta S = \Delta E + P\Delta V \tag{3.14}$$

From Eq. 3.8, we have

$$T\Delta S - \Delta E - P\Delta V \geq 0 \tag{3.15}$$

Thus, only processes that satisfy Eq. (3.15) will be spontaneous, which are now expressed in experimentally measurable quantities. W. Gibbs has defined a more useful function as follows: at constant pressure, P and constant temperature, T,

$$G = E + P\,V - T\,S \tag{3.16}$$

By combing Eq. 3.15 with Eq. 3.16, we have

$$(\Delta G)_{T,P} \leq 0$$

The Gibbs free energy, G function is then given by

$$G = H - T\,S \tag{3.17}$$

where H $(= E + P\,V)$ is known as the enthalpy function. Since ΔG is a state function, so is ΔH, Eq. (3.15) becomes

$$\Delta G = \Delta H - T\Delta S \tag{3.18}$$

ΔH is the heat evolved under constant pressure. If the PV term in Eq. (3.16) is negligible, therefore

$$F = E - TS$$

and from Eq. (3.15)

$$(\Delta F)_{T,V} = \Delta E - T\Delta S \leq 0 \tag{3.19}$$

where F is known as the Helmholtz free energy or function, where ΔF is at constant T and V. The important conclusions to be drawn are: for a system at equilibrium,

$$\Sigma_i\, \Delta S_i = 0;\ \ \Delta G = 0 \tag{3.20}$$

and for a spontaneous process,

$$\Sigma_i\, \Delta S_i > 0 \ \ and\ \Delta G < 0. \tag{3.21}$$

In words, when ΔG is negative the process is exergonic or energy-releasing A positive ΔG indicates an endogonic, or energy-consuming process, where in order for the process to occur, an input of energy is essential.

Standard states: ΔG, ΔG^o and $\Delta G^{o'}$

The change in the Gibbs free energy, ΔG, for the reaction of Eq. (3.5) at any concentration, is given by

$$\Delta G = \Delta G^o + \Sigma_i \, RT \ln a_i \qquad (3.22)$$

where ΔG^0 is defined as the change at the standard conditions (1 atm, all the reactants and products are at 1 M) and a_i are the activities of the reactants and products involved. At equilibrium, $\Delta G = 0$, therefore

$$\Delta G^0 = - RT \ln \frac{[ADP][P_i]}{[ATP][H_2O]} = - RT \ln K \qquad (3.23)$$

where K is the equilibrium constant for the reaction (Eq. 3.3). For biological standard state, $\Delta G^{0'}$ is defined by ΔG^0 as before whereas the hydrogen ion concentration is at pH = 7. Rigorously speaking, all the concentration terms (C's) in brackets should be expressed in activities (a), that is

$$a = \gamma C \qquad (3.24)$$

where γ is the activity coefficient that for an ideal dilute solution is taken as the unity. It is important to note that Eq. (3.23) makes it possible to measure the change in free energy for a given chemical reaction, if one can measure the equilibrium concentration of products and substrates. It is well to remember that a chemical or physiological reaction always goes in the direction that tends to decrease the free energy (the direction for which $\Delta G < 0$, as stated in Eq. 3.21).

3.1.6 The Chemical Potential, μ

The concept of chemical potential is important and has wide applications in biological systems (e.g. the material transport in addition to biochemical reactions). Again using the reaction given in Eq. (3.5) as a specific case, the change of free energy, dG, can be written with the aid of Eq. (3.14)

$$d\mu = dG = -SdT + VdP + \Sigma_i \mu_i dN_i \qquad (3.25)$$

where N_i denotes the number of moles of the chemical species i, Σ_i indicates summation for all the i chemical species that comprise the system. At constant P and T, Eq. (3.25) becomes

$$d\mu = \Sigma_i \mu_i dN_i = 0 \qquad (3.26)$$

which is related to Eq. (3.23).

How to evaluate ΔG°

- From equilibrium constants using Eq. (3.23)
- From enthalpy and entropy changes using Eq. (3.16).
- From free energies of formation (see data in biochemical handbooks)
- From reduction-oxidation (redox) potentials {see Eq. (3.28)}.

Example:

$$\underset{[G\text{-}1\text{-}P]}{\text{glucose 1-phosphate}} \longrightarrow \underset{[G\text{-}6\text{-}P]}{\text{glucose 6-phosphate}} \qquad (3.27)$$

$$K = \frac{[G\text{-}6\text{-}P]}{[G\text{-}1\text{-}P]}$$

- From Eq. (3.23), $\Delta G^0 = -RT \ln K$

$$= -1745 \text{ cal/mol (or } 1.745 \text{ kcal/mol)}$$

- From redox potentials

$$\Delta G^0 = -nFE^0 \qquad (3.28)$$

where E^0 = standard redox potential (for the half-cell reactions, see Tables in chemistry and biochemistry handbooks for biochemical standard redox potential. $E^{0'}$ (in volts) at pH 7.

- From enthalpy and entropy data

$$\Delta G^0 = \Delta H^0 - T\Delta S^0 \qquad (3.29)$$

(The heats of formation and absolute entropy values, see Tables in chemistry and biochemistry handbooks).

- From free energy of formation data

$$\text{ATP (1M)} + H_2O \text{ ----- ADP (1M)} + \text{Pi (1M)} \qquad (3.30)$$

$$\Delta G^0 = -7 \text{ kcal/mol}$$

Nonequilibrium (Irreversible) Thermodynamics[3]

Although it is outside the scope of the present course to consider the principles of irreversible thermodynamics, a brief reference should be made to the usefulness of such approach as applied to membrane processes, e.g. to the electrokinetic phenomena to be covered in Chapter 6 (*Membrane Electrochemistry).* For a detailed treatment of irreversible thermodynamics see the monograph "Nonequilibrium Thermodynamics in Biophysics" by Katchalsky and Curran and a recent comprehensive review.[3,4].

The importance of such approach is due to the fact, that metabolic processes of membranes are generally credited with being able to maintain steady nonequilibrium conditions across cell membranes by generating an active transport current of ions or electrons. For instance, in the case of excitable membranes this active transport of ions across cell membranes generates and maintains nonequilibrium electrolyte concentration gradients, and that electrical excitability is due to transient ion permeabilities allowing the membrane potential to shift back and forth between the equilibrium potentials of different ionic species.

It is empirically known that in a system characterized by only a single transport current or flow (e.g. flow of matter, charge, etc.), the flow is linearly related to its driving force X, if the system is not too far displaced from equilibrium. For such a general system we may write

$$J = L.X \qquad (3.31)$$

where L is a phenomenological coeffficient of proportionality independent of force X, which is often referred to as the "conjugate" force. Fick's first law of diffusion and Ohm's law are familiar examples of Eq.(3.31). If a system is characterized by more than one flow, it is experimentally confirmed that any 'single flow may be influenced by all the flows and thus, by all other conjugate forces present. This may be expressed by the following equations

$$J_i = L_{ii}X_i + L_{ij}X_j + \ldots + L_{in}X_n \qquad (3.32)$$

$$J_j = L_{ji}X_i + L_{jj}X_j + ... + L_{jn}X_n$$
$$J_n = L_{ni}X_i + L_{nj}X_j + ... + L_{nn}X_n$$

or

$$J_i = L_{ii}X_i + \quad L_{ik}X_k \qquad (3.34)$$

Here L_{ii} is the phenomenological coefficient relating J_i to its conjugate force X_i. The L_{ik}, where k = i are cross coefficients reflecting the influence of other forces in the system on flow "i". Let us now consider the case in which the flow of a given species depends only on its conjugate driving force and is not influenced by other flows. Eq.(3.34) then reads

$$J_i = L_{ii}X_i \qquad (3.35)$$

In such a case the responsible or conjugate force is the gradient of electrochemical potential of species "i", for instance across the membrane. At constant temperature and pressure we can write

$$J_i = -L_{ii} \text{ grad } \underline{\mu}_i \qquad (3.36)$$

Notice that driving force for the flow of matter is negative of the electrochemical potential gradient, as a positive flow takes place in the direction of decreasing electrochemical potential, $\underline{\mu}$.. It is also important to note that, although L_{ii} is not a function of grad $\underline{\mu}_i$, it is not a constant but a function of the state of the system, in particular of the concentration c_i of species "i". Thus, L_{ii} may be expressed as follows

$$L_{ii} = ku_ic_i \qquad (3.37)$$

where k is a constant to be evaluated and u_i = the mobility of species "i" ($m^2\ s^{-1}\ V^{-1}$). An example described below show the capability of the thermodynamics of irreversible processes.

Electrokinetic Phenomena[3,4]

The basic equation for electrokinetic effects, in the language of irrerversible thermodynamics, may be given by

$$\Phi = T\theta = J_v \Delta P + I \Delta\psi \qquad (3.38)$$

where Φ = dissipation function, J_v = volume flow, P = pressure, I = current, and ψ. In the case of water flow across a semipermeable membrane separatiang two electrolyte solutions, two electrokinetic phenomena may be demonstrated, namely, electro-osmosis and streaming potential. The former associated with J_v , volume flow, is driven by an electric current, I, (due to $\Delta\psi$), whereas the latter is owing to pressure difference (ΔP). From Eq. (3.38), we have

$$J_v = L_P \Delta P + L_{P\psi} \Delta\psi \qquad (3.39)$$

and

$$I = L_{\psi P} \Delta P + L_{\psi} \Delta\psi \qquad (3.40)$$

In other words, J_v and I are both dirven by ΔP and $\Delta\psi$, where $L_{\psi P} = L_{P\psi}$ (due to Onsager) is the so-called phenomenological (cross) coefficient. The most significant conclusion from the above equations is that the coefficients relate the volume flow and current in a given system. Thus, experimentally one needs only to measure one parameter or the other, which may not be directly determinable.[3,4]

3.2 Kinetics

Energetics (or thermodynamics), the most important function of which is the free energy, *G*. It provides us with the criteria for whether a given chemical reaction as written will proceed or not. For example,

$$\text{glucose 1-phosphate} \xrightarrow[\text{pH = 7}]{} \text{glucose 6-phosphate} \qquad (3.41)$$

$$\Delta G^{o\prime} = -1.7 \text{ kcal/mol}$$

Eq.(3.41) proceeds spontaneously, but it may take tens of thousands of seconds without the enzyme *phoshoglucomutase* being present. This is far too slow for most (physiological) reactions. For example, bacteria divide

about every 30 minutes. Thus, to obtain sufficient glucose 6-phosphate to complete one bacterial life cycle it would take tens of years! To make a "downhill" life process possible as we know it, the nature has invented a wonderful class of compounds, namely ***enzymes***. They are nature's catalysts. Catalysts are compounds that increase the rate of spontaneous reactions, widely used in industry. Most enzymes are proteins (e.g. an exception is the catalytic RNA). They speed up the chemical reactions in cells, but not the substrates or products of those reactions. A substrate is a substance upon which an enzyme acts to yield a product. Many enzymes include an inorganic ion or a non-protein group that contributes to their catalytic activity. Each enzyme is designed to carry out a specific task with a particular substrate. For instance, some enzymes are intimately involved in the transformation of different forms of energy. The biophysicist along with the physiologist wants to know, for examples, how fast a nerve can conduct an impulse? how quick different muscle types can contract? or how swift a cell can respond to a signal (e.g. a chemical agent).

Now, back to the question of how *fast* will a chemical or physiological reaction proceed. Such information comes from a branch of study called ***chemical kinetics***. When the principles are applied to enzyme systems, it is called enzyme kinetics. Generally, we speak of ***ligand-receptor contact interactions***, the 'lock and key' principle of Emil Fischer (1894). The range of rates of reactions from the viewpoint of time scales of interest here is from about 1 pico (10^{-12}) to 10^{2} seconds, with most physiological reactions fall in the upper end. It is worth noting that in order to obtain kinetic data over a wide time scale, appropriate techniques of perturbation are essential.

3.2.1 Ligand-receptor contact interactions

Almost all physiological activities involve some kind of contact interactions between participants. At the molecular level, several categories can be recognized: The first step is usually the formation of a ligand-receptor (L-R) complex. What we would like to know are : (1) how many ligands are bound to the receptor, (2) how strong are the L-R bonds, and (3) what is the molecular nature of forces of interaction. Thermodynamics

provides the framework for answering the first two questions. The last question may be answered with some additional molecular information such as through kinetics studies. It is worth noting that, in the study of the rates of reactions, exponential curves (either growing or decaying) appear frequently. To see why this is so, one is reminded of the ***law of mass action*** which states that '*the rate of reaction is directly proportional to the product of the concentrations of the reactants*'.

Table 3.2 Ligand-Receptor Contact Interactions

Category	Ligand (L)	Receptor (R)	Complex (L-R)
1) Protein catalysis	Substrate (S)	Enzyme (E)	S-E
2) Immunology	Antigen (Ag) (hapten)	Antibody (Ab) (IgG)	Ag-Ab
3) Neurofunction	Hormone (L) (neurotransmitters)	Synapse (R) (sites on membranes)	L-R
4) Ion transport	ion	carrier (C)	ion-C
	ion	channel (C)	

(Note: A ligand is usually smaller than a receptor)

3.2.2 Rate equations, reaction orders, and molecularity

Rate equations

The rate or reaction velocity (v) of a chemical, biochemical or physiological reaction is generally expressed as the change in concentration per unit time of either a reactant or a product. By convention, the rate constant is always a *positive* number even when it is stated as the decrease in concentration of a reactant. That is for the reaction

$$L + R \underset{k_b}{\overset{k_f}{<======>}} L\text{-}R \qquad (3.42)$$

$$\text{rate } (v) = d[R]/dt \propto [L][R],$$

or $$d[R]/dt = - k_f [L][R] \qquad (3.43)$$

or $$d[L\text{-}R]/dt = k_f [L][R] \qquad (3.44)$$

where L-R can be any one of the entities given in Table 3.2, and k_f is the proportionality constant, that is the forward rate constant (units per second) for the reaction in question. It is a measure of how fast a reaction occurs (or probability at the molecular level). The negative sign in front of k_f indicating the decreasing concentrations, since k's are always positive. Eq. (3.43) makes sense in that the larger the concentration the faster is the rate. At first, [L] and [R] will disappear very fast, but as their concentrations progressively decrease, the rate of reaction, in proportion, also decreases. When one plots the differences of a reactant concentrations between the initial concentration and its concentration at time, t, as a function of time, a straight line usually results. If one writes the concentration of [R] at time t as $[R]_t$, the rate of change is $d[R]_t/dt = - k[R]_t$, the solution of which is exponential in form. That is

$$[R]_t = [R]_0 \exp (- kt) \qquad (3.45)$$

where $[R]_0$ denotes the concentration of [R] at time t = 0. By taking natural logarithms of Eq. (3.45), we have

$$\ln [R]_t = \ln [R]_0 - kt \qquad (3.46)$$

Hence by plotting $\ln [R]_t$ vs. t, a straight line should result. From the plot, k and [R] at t = 0, will be, respectively, obtained from the slope and the intercept (Fig. 3.4)..

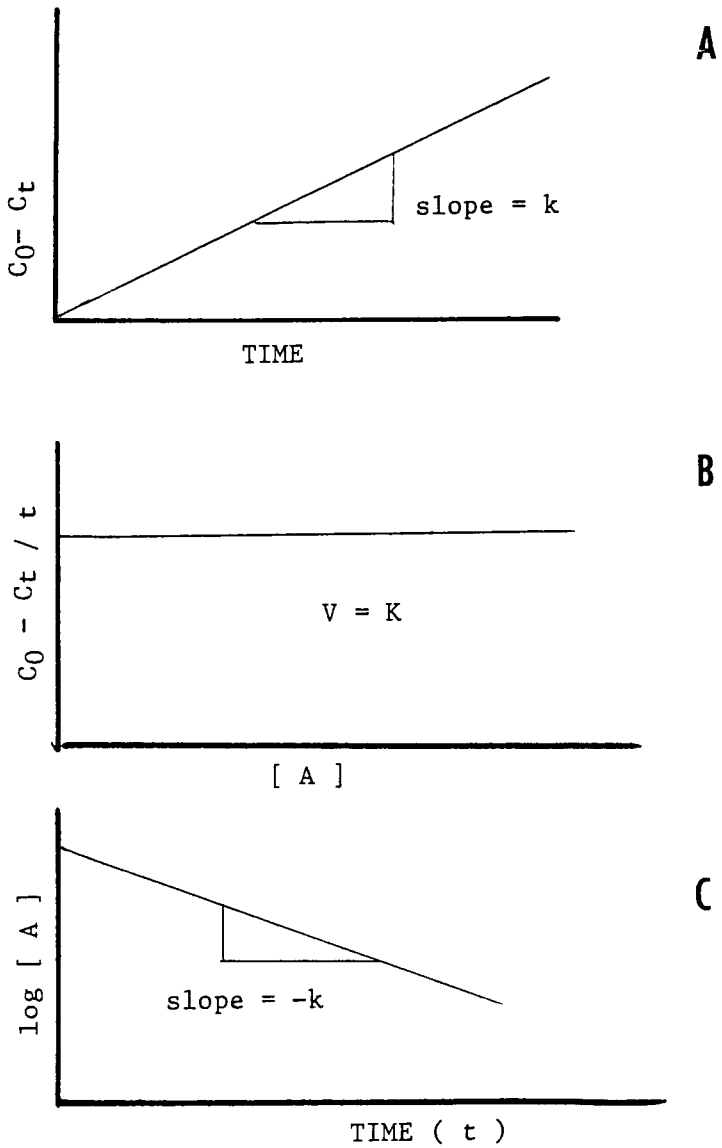

Fig. 3.4 Plotting experimental data. **A**. Concentration *vs.* time. **B**. Concentration difference / [A]. **C**. log. [A] *vs.* time.

3.2.3 Reaction orders

The order of a reaction is determined experimentally by measuring the concentration of a reactant or a product as a function of time, while the concentrations of the components of the reaction are varied. Thus, one takes the data and attempts by trial-and-error to fit the data to theoretical expressions for reactions of particular order and special characteristics. The order of a reaction is the sum of the exponents, namely a + b + ... in the rate equation. A general expression for the rate is $d[P]/dt = v = k [A]^a[B]^b$....., where P denotes the product, A and B are the reactants, v stands for velocity (rate). Specifically, in the following example

$$E + S \xrightarrow{k_f} ES \qquad (3.47)$$

$$d[ES]/dt = v = k_f [E]^1[S]^1 \qquad (3.48)$$

where [E-S] denotes the concentration of the enzyme-substrate complex. The order of the reaction, therefore, is equal to a + b = 2. This is a second order reaction. It is worth noting here that an enzyme is specific for a particular molecule or a molecular group, which is known as the substrate. Frequently, a non-protein or an inorganic group (mainly metallic ions such as K^+, Mg^{2+}, Mn^{2+}, Fe^{3+}, Co^{2+} , Cu^{2+}, Zn^{2+}, and Mo^{2+}), known as the cofactor, is associated with an enzyme via hydrogen, ionic or covalent bonds. When organic groups are associated with an enzyme, they are known as coenzymes or prosthetic groups. Coenzymes are all complex groups derived from vitamins (e.g. CoA = coenzyme A from pantothenic acid;FMN = flavin mononucleotide and FAD = flavin adenine dinucleotide, both from riboflavin; TPP = thiamin pyrophosphate from thiamin; NAD = nicotinamide adenine dinucleotide). Cofactors contribute to the lowering of the activation energy barrier, whereas coenzymes function as carriers of electrons, atoms or chemical groups removed from the substrates during reactions.

Zeroth order reaction. The rate of zeroth order depends only on a rate constant and *not* on any concentration term. In enzyme kinetics, it means that the enzyme combines with the substrate for reaction to take place, but

at high substrate concentrations, all available enzyme (*E*) is saturated with substrate (*S*). At this point, the rate of reaction is maximal and an additional substrate can have no further effect on the rate (i.e. v = k).

First order reaction. If you obtain data for the reaction that, when plotted, give a straight line:

$$A \longrightarrow Q + R \qquad (3.49)$$

$$d\,[A]/dt = k\,[A] \qquad (3.50)$$

in which k is the first order rate constant. Integration of Eq.(3.50) from $[A]_o$ at time 0 to $[A]_t$ at time t

$$\int d\,[A]/[A] = -\,k \int dt \qquad (3.51)$$

Since $[A]_t \propto t$, we have

$$\ln ([A]_t /[A]_0) = -\,k\,t \qquad (3.52)$$

A plot of $\ln ([A]_t /[A]_0)$ against t gives a straight line whose slope is –k. Note that if d[A]/dt is difficult to measure experimentally, whereas [Q] or [R] might be easier, k can be easily determined, for

$$d[A]/dt = d[Q]/dt = d[R]/dt = k[A] \qquad (3.53)$$

An important property of a first-order reaction can be seen by examining the half-life, $t_{1/2}$, of a reactant species, that is the time required for the concentration of a reactant to decrease to one-half of its initial value. From Eq.(3.52)

$$\ln ([A]_t /[A]_0) = -\,k\,t$$

the half-time is the time at which $[A] = \frac{1}{2}[A]_0$, so that

$$\ln (1/2[A]_0/[A]_0) = -\,k\,t$$

or

$$\ln 2 = k\,t; \quad t_{1/2} = \ln 2/k \tag{3.54}$$

Eq.(3.54) indicates that $t_{1/2}$ is independent of concentration and can be measured for any pairs of concentrations C_1 and C_2 such that $C_2 = ½\ C_1$. This fact is very valuable experimentally as we shall see in the so-called pseudo-first order enzyme kinetics. Now, let us consider the next three topics:

- The enzyme-substrate complex
- The effect of temperature on the reaction rate
- The absolute reaction rate theory.

3.2.4 The enzyme-substrate complex

Enzymes are cellular catalysts, made of proteins, whose function is to speed up reactions that otherwise would proceed too slowly to be of any use to cells. Other important facts to remember are: (1) enzymes *cannot* make thermodynamically impossible reactions to go, and (2) enzymes can not alter the equilibrium of a reaction; they can, however, cause the reaction to approach an equilibrium faster.

Since enzymes are proteins made of amino acid molecules, therefore, like all proteins, they are temperature and pH sensitive, which can change either their state of dissociation or their three-dimensional (3-D) conformation as a result of hydrogen bonds and van der Waals forces. Only a small portion of the amino acids that comprise an enzyme is involved in the catalytic reaction. That region of the protein that participates directly in the reaction is termed as the active site. For example, in their 3-D structure, the amino acid residues of proteins are greatly influenced by their local pH, whose activity of proton acceptors and donors acting as the active site. Enzymes are highly specific, both in the reaction catalyzed and in their choice of reactants, which are called ***substrates***. In order for any chemical reaction to take place, there must be collisions. That is, an enzyme (the ligand) must make contact and combine

with a reactant molecule, the substrate. Thus, the transition state and the active site of an enzyme are intimately involved towards the formation of products (P).

The first order of business in enzyme kinetics is the formation of an enzyme-substrate (ligand-receptor) complex. Pictorially, the lock and key model of Fischer is usually presented:

$$E + S \underset{k_b}{\overset{k_f}{\Longleftrightarrow}} E\text{-}S^* \xrightarrow{k_2} P + E \qquad (3.55)$$

The rate of the reaction as stated in Eq. 3.45 may be expressed:

$$d[E\text{-}S^*]/dt = v_f = k_f[E][S] \qquad (3.56)$$

$$d[E]/dt = v_f = k_f[E][S] \qquad (3.57)$$

$$d[S]/dt = v_f = k_f[E][S] \qquad (3.58)$$

where E represents the enzyme, S and P are the substrate and the product, respectively. E-S* is a molecular complex (an enzyme-substrate complex), and E-S* is a so-called activated complex, and P denotes a product. As we shall see later (Section 3.2.7), the formation of an E-S* complex is a necessary intermediate in the enzyme catalysis according to the theory of Leonor **Michaelis** and Maud **Menten** (1913).

3.2.5 Effect of temperature on the reaction rate

In the late 19th century, thermodynamic arguments led to a relationship between the equilibrium constant, K, of a reaction and the temperature. The essential equation was

$$d \ln K/dT = E/RT^2 \qquad (3.59)$$

In the integral form, Eq. (3.59) becomes

$$K = A\, e^{-Ea/RT} \qquad (3.60)$$

where A and E are constants. Since $K = k_b/k_f$, where k_f and k_b are the reaction rate constants of the forward and backward reactions, respectively, Svante Arrhenius in 1889 proposed the following empirical relationship between the rate of a chemical reaction and temperature:

$$k = A\, e^{-Ea/RT} \qquad (3.61)$$

where E_a is the so-called energy of activation. Differentiating Eq.(3.61) with respect to temperature one obtains

$$d (\ln k)/dT = E_a/RT^2 \qquad (3.62)$$

or written as

$$d (\ln k)/d(1/T) = -E_a/R \qquad (3.63)$$

and

$$\ln k = \text{const.} - E_a/RT \qquad (3.64)$$

Converting to common logarithms

$$\log k = \text{const} - \frac{Ea}{2.303RT} \qquad (3.65)$$

A plot of log k vs. 1/T should be linear and E_a can be evaluated from the slope (i.e. experimentally, one measures k at several temperatures).

Q_{10}. Values of E_a are used to compare biological rate processes. Another quantity, the temperature coefficient or Q_{10} is also used for this purpose. The Q_{10} is the ratio of the rates of reaction measured at two temperatures 10 °C apart:

$$Q_{10} = k_{(t+10)} / k_t \qquad (3.66)$$

(Note: the temperatures are expressed in degree Celsius, not in the absolute temperature units for T in Kelvin). The Q values for most biological rate processes fall in the range 1.1 to 4. Generally, values of 2 or above indicate chemical reactions; values close to 1 indicate physical processes such as the diffusion. Both Q_{10} and E_a vary depending on the temperature range over which they are measured.

3.2.6 Absolute reaction rate theory

As mentioned (Section 3.2.5), the relationship proposed by Arrhenius, although empirical and exceedingly useful, is not based on thermodynamic or reaction mechanism theory. The concept of E_a is novel but it did not make any statement or assumption about its significance. For example, for a reaction to occur, the two molecules must collide in a right way. In the 1930s, H. Eyring and M. Polanyi introduced a new idea that not only explains how may reactions take place, but correlates observed reaction rates with thermodynamic functions. In other words, in the path of the reaction coordinate from reactants to products, the reactants must overcome energy barriers by forming an activated state (Fig. 3.5). Once this has happened, the resulting transition-state is a point of no return for reactants transforming into products.

In order for a reaction to occur, the molecules must have an effective collision, i.e. form an activated complex, a transition-state without which the reaction is not possible. Referring back to Eq. (3.55)

$$E + S \underset{k_b}{\overset{k_f}{\Longleftrightarrow}} E\text{-}S^* \xrightarrow{k_2} P + E \qquad (3.55)$$

where * indicates the activated complex or the transition-state. In a group of molecules there is a distribution of energies, because individual molecules are subjects to collisions with other molecules, and external energy sources (e.g. light). Most molecules however have energy near the average kinetic energy (kT), not enough to jump over the potential energy barrier. Once a large number of molecules have attained the transition state, the reaction is frequently self-sustaining and proceeds at a characteristic rate, depending solely on the temperature.

From Eq.(3.23), the equilibrium constant, K, for the reaction is given by

$$K = [ES^*]/[E][S] = k_b/k_f \qquad (3.67)$$

and

$$k_2 = \kappa\, kT/hK^* \qquad (3.68)$$

where κ (kappa) is the transmission coefficient which indicates the probability that the formation of the activated complex will lead to reaction, k = the Boltzmann constant (1.38×10^{-16}) = R/N, h = Planck's constant (6.62×10^{-27} erg sec^{-1}). The term kT/h is the frequency of breakdown of the activated complex to products. The beauty of Eq.(3.68) is that it can be applied to chemical, physical and physiological processes. The lifetime of the activated complex is estimated to be on the order of 10^{-13} sec (0.1 picosec or 100 femtosec). From Eq.(3.68), a number of equations can be written in terms of thermodynamic functions:

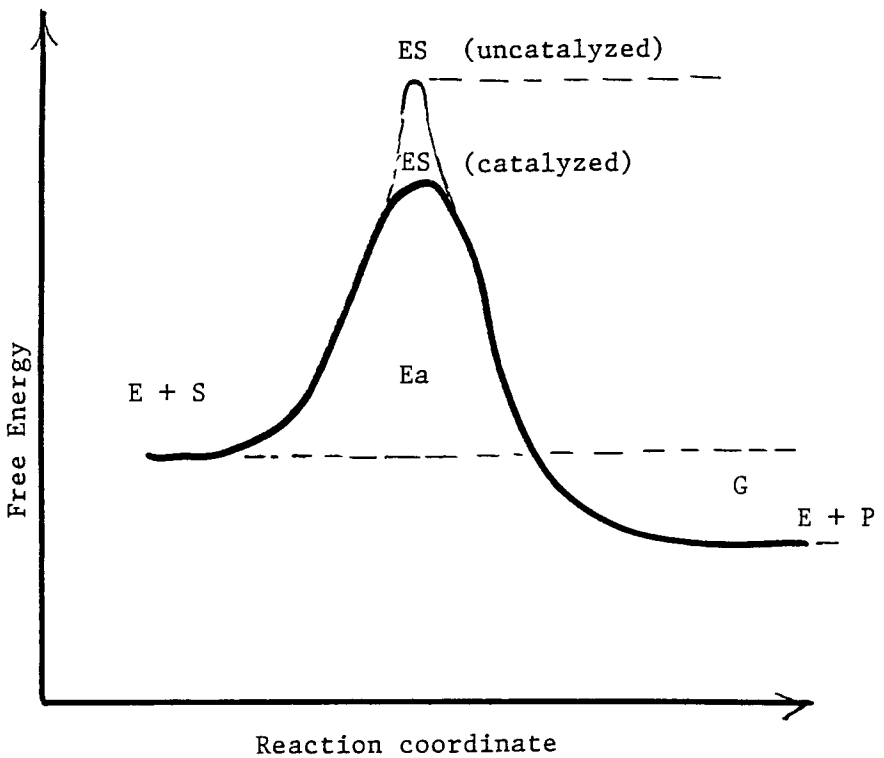

Fig. 3.5 Reaction coordinate. This is an energy diagram for a reversible chemical reaction. All reversible reactions tend to proceed in the direction that decreases the energy of the participants. However, even in this direction the reaction may not proceed very quickly because very few molecules and make the transition toward the lower energy state.

$$\Delta G^* = -RT \ln K^* \tag{3.69}$$

$$\Delta G^* = \Delta H^* - T\,\Delta S^* \tag{3.70}$$

By appropriate substitutions into Eq. (3.68)

$$k_2 = \kappa\,(kT/h)\, e^{-\Delta G^*/RT} \tag{3.71}$$

and

$$k_2 = \kappa\,(kT/h) e^{\Delta S^*/R}\, e^{-\Delta H^*/RT} \tag{3.72}$$

Also, it can be shown that

$$\Delta H^* = E_a - RT \tag{3.73}$$

and at room temperature, RT $\simeq$ 300 cal/mol., which is << ΔH^* , therefore

$$\Delta H^* \simeq E_a \tag{3.74}$$

Finally, we obtain

$$k_2 = \kappa\,(kT/h) e^{\Delta S^*/R}\, e^{-Ea/RT} \tag{3.75}$$

The advantage of Eq.(3.75) is that from a measurement of k_2 and E_a, the entropy of activation, ΔS^*, can be evaluated (Note: the pre-exponential factor in the Arrhenius equation, $A = \kappa\,(kT/h)(e^{\Delta S^*/R})$. This is a very useful number because the entropy changes are related to conformation changes and the sign of ΔS^* indicates whether the transition state is more or less complex than the reactants, and thus enables one to make an intelligent

guess about the structure of the transition state, hence, the mechanism of the reaction.

3.2.7 Michaelis-Menten Kinetics

To account for enzymatic reactions, the model proposed by Michaelis and Menten is the simplest. The central idea is the formation of an enzyme-substrate complex:

$$E + S \underset{k_{-1}}{\overset{k_1}{\Longleftrightarrow}} E\text{-}S^* \xrightarrow{k_2} E + P \qquad (3.76)$$

By this model, saturation means that all of E is converted to E-S*. Since the product P is formed only from E-S*, it is clear when [E-S*] is maximal, the velocity (rate) is also maximal. The rate of P formation is given by

$$d\,[P]/dt = V = k_2\,[E\text{-}S^*] \qquad (3.77)$$

Next, we need to express [E-S*] in terms of known quantities: the rate of formation of E-S* is given by

$$d[E\text{-}S^*]/dt = k_1\,[E][S] \qquad (3.78)$$

and the rate of breakdown of E-S* is given by

$$d[E\text{-}S^*]/dt = k_{-1}\,[E\text{-}S^*] + k_2\,[E\text{-}S^*]$$

$$= (k_{-1} + k_2)\,[E\text{-}S^*] \qquad (3.79)$$

In the steady-state approximation, i.e. the rate of formation is equal to the rate of breakdown of [E-S*], Eq.(3.78) may be equated to Eq.(3.79), hence

$$k_1 [E][S] = (k_{-1} + k_2)[E\text{-}S^*] \qquad (3.80)$$

Solve for [E-S*], which is given by

$$[E\text{-}S^*] = [E][S]/\{(k_{-1} + k_2)/k_1\} = [E][S]/K_m \qquad (3.81)$$

where $(k_{-1} + k_2)/k_1 = K_m$. This K_m is known as the Michaelis constant. Now let us examine [E] and [S] in Eq. (3.81):

$$[E] = [E]_{total} - [E\text{-}S^*] \qquad (3.82)$$

where $[E]_{total} = [E] + [ES^*]$, consisting of free [E] and bound [E-S*]. Substituting Eq.(3.82) into Eq.(3.81)

$$[E\text{-}S^*] = \{[E]_{total} - [E\text{-}S^*]\}[S]/ K_m \qquad (3.83)$$

Now solving Eq.(3.83) for [E-S*]

$$[E\text{-}S^*] = \{[E]_{total} [S]/K_m\}/\{1 + [S]/K_m\}$$

$$= [E]_{total} [S]/\{[S] + K_m\} \qquad (3.84)$$

Combining Eq.(3.84) and Eq.(3.77)

$$V = k_2 [E]_{total} [S]/\{[S] + K_m\} \qquad (3.85)$$

The maximal rate is obtained when all sites are saturated with substrate, that is $[S] >> K_m$ (in the denominator)

$$V_{max} = k_2 [E]_{total} \quad (3.86)$$

By substituting Eq.(3.86) back into Eq.(3.85),

$$V = V_{max} [S]/\{[S] + K_m\} \quad (3.87)$$

One obtains the famous Michaelis-Menten equation. Experimentally, when one plots the velocity as a function of [S], the following is usually obtained: Values of K_m: 10^{-5} to 10^{-2} M. A large value of K_m indicates a high [S], which is required to obtain half-saturation of the enzyme. The Michaelis-Menten equation (Eq. 3.87) describes the reaction rate at all values of [S] as long as $[S] >> [E]_{total}$.

Significance of Km and Vmax. These two parameters define the kinetic behavior of an enzyme as a function of [S]. From Eq. (3.81)

$$K_m = \frac{k_{-1} + k_2}{k_1} \quad (3.88)$$

When k_2 is very small ($k_2 << k_1$), E-S* is less likely to go to P. Eq. (3.76) becomes

$$E + S \underset{k_{-1}}{\overset{k_1}{\Longleftrightarrow}} E\text{-}S^* \quad (3.89)$$

Hence, the equilibrium constant for Eq. (3.79) is a measure of how tightly the enzyme binds to the substrate. In other words, Km is an approximate measure of the affinity of the enzyme for the substrate. In summary, 3 points should be noted:

1. At high [S], i.e. when $[S] >> K_m$, $V = V_{max}$. The rate is independent of [S]. This is because all enzyme molecules are combined with substrates in the E-S complex, whose [S] concentration determines the rate.

2. When [S] << K_m , V = V_{max}[S]/K_m. The rate is proportional to [S]. This is because [E-S*] is proportional to [S], and [E-S*] determines the rate.
3. When V = ½ V_{max}, then [S] = K_m. Thus, K_m is the substrate concentration at which the reaction rate is ½ maximal, V = V_{max}/2.

Procedure for determining K_m and Vmax. These two parameters can be determined, when one has an assay for the enzyme activity. Experimentally, the following steps are involved:

- Carrying out a series of experiments with constant $[E]_t$, varying [S], and measuring V (initial rate of reaction).
- Plot initial velocity V vs. [S].
- Estimate V_{max} from the graph.
- Determine V_{max}/2.
- Read K_m from the plot.

However, V_{max} is difficult to decide if data are plotted this way, since the plot is hyperbolic. It is hard to extrapolate to infinite [S] and estimate V_{max}. For this reason, the Lineweaver-Burke plot is put to use (see below).

The Lineweaver-Burke Plot. When an enzyme is being studied, the first goal is to evaluate K_m and V_m. One approach is to use the method developed by Lineweaver and Burke (1934), since it is usually difficult to assess the saturation level, or V_{max} directly from experiments. This is done as follows: taking the reciprocal of Eq.(3.87) and rearrange algebraically, we have

$$1/V=1/V_{max}+K_m/V_{max}\ 1/[S] \qquad (3.90)$$

which has the form of a straight line, when a plot of 1/V vs. 1/[S] is made from a relatively few experimental points. Fig. 3.6 illustrates such a

Lineweaver-Burke plot, having a y-intercept of $1/V_{max}$, an x-intercept of $-1/K_m$ and a slope K_m/V_{max}.

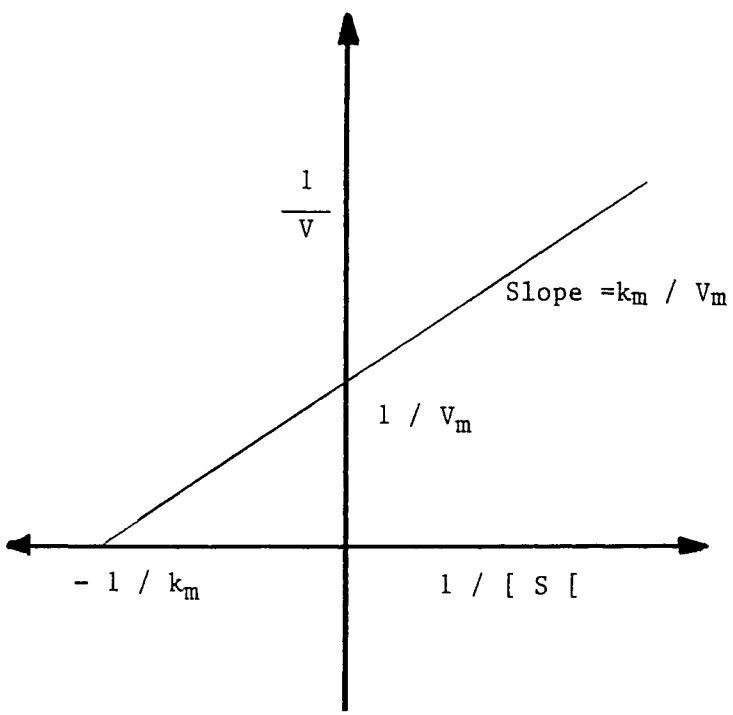

Fig. 3.6 Lineweaver-Burke plot. From this type of graph, it is easy to estimate K_m and V_{max}.

Turnover number. The maximal rate, V_{max} reveals the turnover number (k_2) of an enzyme , if the concentration of active sites $[E]_t$ is known, because

$$V_{max} = k_2[E]_{total} \qquad (3.86)$$

The turnover number of an enzyme (catalyst) is the number of substrate molecules converted into product per unit time when the enzyme is fully saturated with the substrate. Hence, it has the units of a first order reaction. A turnover number is obtained by dividing V_{max} by the enzyme active site concentration and it ranges from 10^2 to 10^7 per second. For example, in the case of a 10^{-6} M solution of carbonic anhydrase, [E], the enzyme catalyzes the formation of 0.6 M H_2CO_3/sec. When it is fully saturated with substrate,

$$k_2 = V_{max}/[E]_{total} = 6 \times 10^5 \text{ /sec} \qquad (3.91)$$

It should be noted that, for enzyme assays, a common unit is μmoles/ min/mg of enzyme, which can be converted to k_2 by multiplying 1.667 x 10^{-5} x (molecular weight/site) x units.

3.2.8 Enzyme inhibition

The mechanism of enzymatic reaction and the chemical nature of the catalytic sites can be studied by various agents that inhibit the enzyme action. The action of a drug can be learned this way. Inhibitors may be classified as reversible or irreversible; the latter, by covalent modification of functional groups on the enzyme. We shall only be concerned with reversible inhibitors within the framework of Michaelis-Menten kinetics. There are 3 types of reversible enzyme inhibition.

competitive (see Fig. 3.7A)
uncompetitive (Fig. 3.7B), and
non-competitive (Fig. 3.7C).

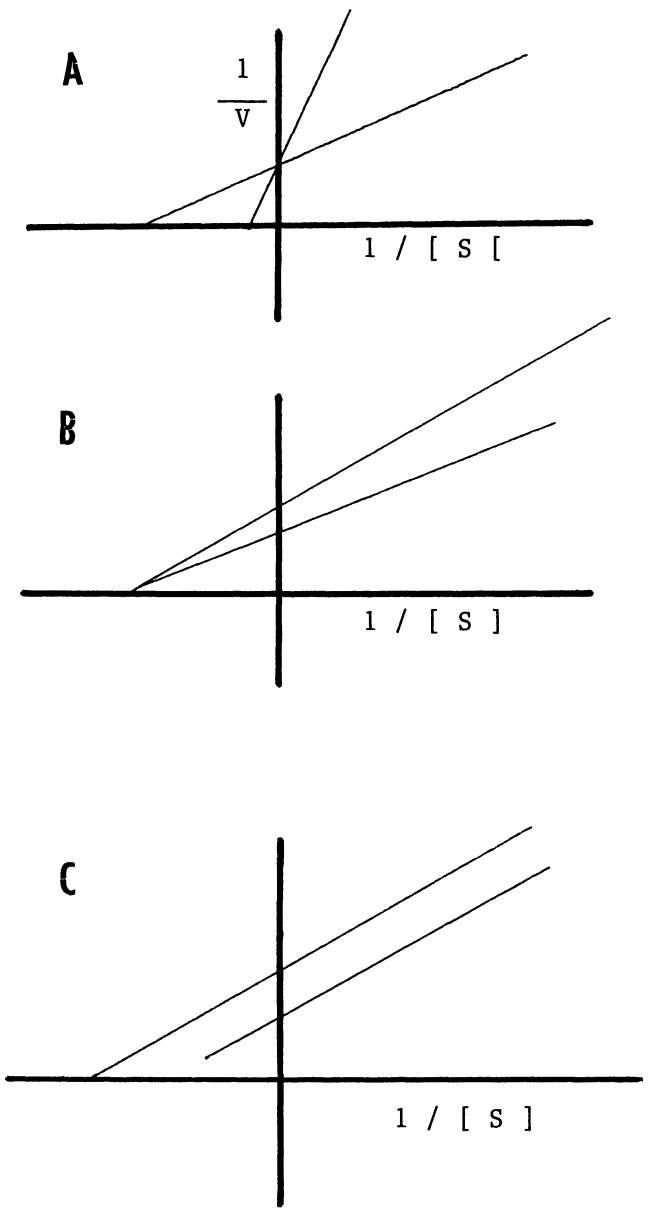

Fig. 3.7. Enzyme inhibition. A. competitive B. uncompetitive C. non-competitive.

Competitive inhibition. The inhibitor competes with the normal substrate for binding site:

$$E + S \equiv\equiv\equiv ES; \quad E + I \equiv\equiv\equiv EI \quad K_I = [E][I]/[EI] \qquad (3.92)$$

It forms an enzyme-inhibitor complex essentialy not different from the formation of [ES]. If [S] is made large enough, the E will be saturated with S only. It can be easily recognized by a set of the Lineweaver-Burke Plots, where slope = $(1 + [I]/K_I)$

Uncompetitive inhibition. The inhibitor combines with ES to form an enzyme-substrate-inhibitor complex, not with free enzyme.

$$E + S \equiv\equiv\equiv ES + I \equiv\equiv\equiv ESI \qquad (3.93)$$

Increasing values of [S] does not restore the reaction to an uninhibited form.

Non-competitive inhibition. Some enzymes contain a second binding site other than that which binds the substrate. Some inhibitors can bind to this site on E and prevent formation of ES and can bind to the same site on ES to form ESI. Thus there are two inactive forms, EI and ESI:

$$E + I \equiv\equiv\equiv E_I \qquad K_{I,EI} = [EI]/[E][I] \qquad (3.94)$$

$$ES + I \equiv\equiv\equiv E_{I,SI} \qquad K_{I,ESI} = [ESI]/[ES][I] \qquad (3.95)$$

where $K_{I,EI}$ and $K_{I,ESI}$ are two inhibition constants which are not necessarily equal. K_m is not affected. In this case, slope = K_m/V^i_{max} and x = $-1/K_m$, the constancy of the x-intercept. This kind of inhibition cannot be overcome by increasing [S]. The details of these reversible inhibitions may be found in the general references listed at the end of this chapter [Metzler, 1977; Gutfreund, 1995]. Here we will illustrate graphically the three types of inhibition (Fig. 3.7).

3.3.1 Interfacial Chemistry

Interface

It is no distortion that modern investigation of interfacial chemistry began in the kitchen sink! In 1891, A. Pockels reported in *Nature* how surface films could be enclosed by means of physical barriers to about 20 A^2/molecule.[1] This was followed by a quantitative investigation of Langmuir in 1917 using a setup now known as Langmuir's film balance, who deduced the dimensions of fatty acid molecules at the air-water interface. As already described in Chapter 2, our current understanding of the structure and function of biomembranes can be traced to the studies of these experimental interfacial systems such as soap films and Langmuir monolayers, which have evolved as a direct consequence of applications of classical principles of colloid and interfacial chemistry.[1] In this connection, surface and colloid scientists have known for decades that amphiphilic compounds such as phospholipids can self-organize or self-assemble themselves into supramolecular structures of emulsions, micelles, and bilayer lipid membranes (planar BLMs and spherical liposomes). Hence, it is worth noting that the process of self-assembly occurs due to the thermodynamics. If the molecules of an amphipathic phospholipid are in water (or other polar solution) the hydrocarbon chains will want to be 'away' from the aqueous solution. They could all go to the top (like oil on water), or they could have the hydrocarbon chains point toward each other. With the hydrocarbon chains pointing toward each other, this could form two different configurations. First would be a micelle that would be like a ball with the phospholipid polar groups on the outside and the hydrocarbon chains pointing together or in the form of a lipid bilayer. Fig. 3.8 depicts schematically some well-established supramolecular structures of colloid and interface chemistry, to which we will devote the entire Chapter 4 (*Planar BLMs and Liposomes*). Here one is reminded that the arrangement of atoms and molecules at the surface or interface of a substance differs from that in the bulk owing to its surroundings. Gibbs and Young formulated the basic principles of the interfacial chemistry. The former set down the thermodynamics of interfaces, whereas the latter introduced the concept of the membrane surface tension. It is thus useful in many fundamental and practical applications such as molecular films, cell

membranes, and lipid-based biosensors to have some knowledge concerning the behavior of substances at the interface. The nature of interfacial phenomena is inherently interdisciplinary involving physics, chemistry, biology, and engineering. Our approach to study the phenomena at interfaces is the membrane biophysics; the main focus of this book. Here we shall be concerned with some of the basic properties of certain interfaces in the following paragraphs.

Oil-water interface. In terms of the three states of matter (solid = *S*, liquid = *L*, gas = *G*) there are 5 distinct interfaces (*G-L; G-S; L-L; L-S; S-S*). An interface, according to Young and Gibbs, is likened to that of a hypothetical stretched membrane having an interfacial tension, and may be described mathematically by a geometrical plane. Properly speaking, when two liquids meet (e.g. olive oil and water) an interphase is formed. Because an interphase has a certain thickness, there is a gradation of property in going from the oil to the water phase, and also a free energy change associated with its formation. The basic principles of interfacial physical chemistry relevant to the topics under discussion can be summarized as follows. At the air-water interface the experimental evidence supports that the water is qualitatively different from the bulk water and an interfacial or surface tension, γ, is associated with it. Since the interfacial layer is a material system with a well defined composition and thickness, thermodynamic treatments can be applied (e.g. $d\gamma/dT = -S$, an entropy term which measures surface orderliness). For interfacial active substances (phospholipids, certain proteins, detergents), the molecules of these compounds adsorbed at the inter-
face generate a pressure which is given by

$$\pi = \Delta\gamma = \gamma - \gamma^{o} \qquad (3.96)$$

where π is the so-called surface pressure, γ and γ^0 are, respectively, the tension of the interface with and without absorbent molecules, and $\Delta\gamma$ is directly related to Gibbs' free energy, ΔG. As an interface is increased, the free energy of the interface increases. It takes, for instance, about 50 dynes or ergs to create 1 cm^2 area of water-hydrocarbon (oil) interface. Of

interest to note here is a simple **wettability** test for the hydrophilicity (or hydrophobicity) of the surface. When drops of water are sprinkled on a hydrophilic surface, they flatten or spread to cover as much area as possible. On the other hand, if the surface is hydrophobic, water droplets form round beads that minimize the area of contact. It is truly astonishing that a single, coherent monolayer made from an amphipathic substance (e.g. phospholipid!) without pinholes can change the nature of the substrate from a hydrophilic type to a hydrophobic type or vice versa, depending which ends of the phospholipid molecules stick on the substrate first. To wit, self-assembled monolayers and supported BLMs are outstanding examples.

Table 3.3 The Science of Dichotomy (or The Science of Yin and Yang or The Tao of Interface Sciences)

Yin	Yang
Earth	Sun
Water	Fire
Female	Male
Negative charge	Positive charge
•	•
•	•
•	•
Oil (ε = 2-5)	water (ε = 80).
(hydrophilic)	(hydrophobic)

Amphihilic (amphipathic) molecules

Interface

Amphiphilic molecules at interfaces. Amphiphilic (amphipathic) substances at interfaces can exhibit unique properties. Understanding and manipulating those properties is difficult because of the minute quantities of material present at the interface. The thickness of an interfacial film may be estimated from optical reflectance measurements. However, when the film is ultrathin (< 10 nm), optical metods will not be very sensitive and precise, since the wavelength of light is much larger than the film. There is another problem associated with the index of refraction; it is a bulk phase property, as it is evidenced with the thickness of the film which varies linearly with the number of monolayers extrapolated to zero layers, it is negative. Additionally, an amphiphilic molecule such as a phospholipid has a hydrophilic and a hydrophobic part in the same molecule; it thus has the unique ability to bridge the two worlds of disparate dielectric constants of water and oil (*see* Table 3.3).

Here, for relaxation, let us digress for a moment. Exobiologically speaking, the ancient view concerning the formation of the universe, from different cultures, has one central theme; it may be stated as '*the view of opposites*'. This point is illustrated in Table 3.3. The most singular property of amphiphilic molecules makes life, as we know it, possible as well as enjoyable! You may ask 'How so?' It would be difficult to imagine that life without soaps, detergents, mayonnaise, sauces, paints, cosmetics, deordorants, etc. When compounds such as a phospholipid or detergent (also known as a surface or interface-active agent or a surfactant) is added to a water-oil interface, molecules of phosphatidylcholine (lecithin), for example, tend to concentrate themselves at the interface and dramatically lower the interfacial free energy.This interface excess concentration, designated by the symbol Γ, is given by the Gibbs adsorption equation:

$$\Gamma_i = \frac{-1}{RT}\frac{d\gamma}{d \ln a_i} \cong \frac{-1}{RT}\frac{d\gamma}{d \ln C_i} \qquad (3.97)$$

where subscript *i* denotes the surface or interface-active species *i*.

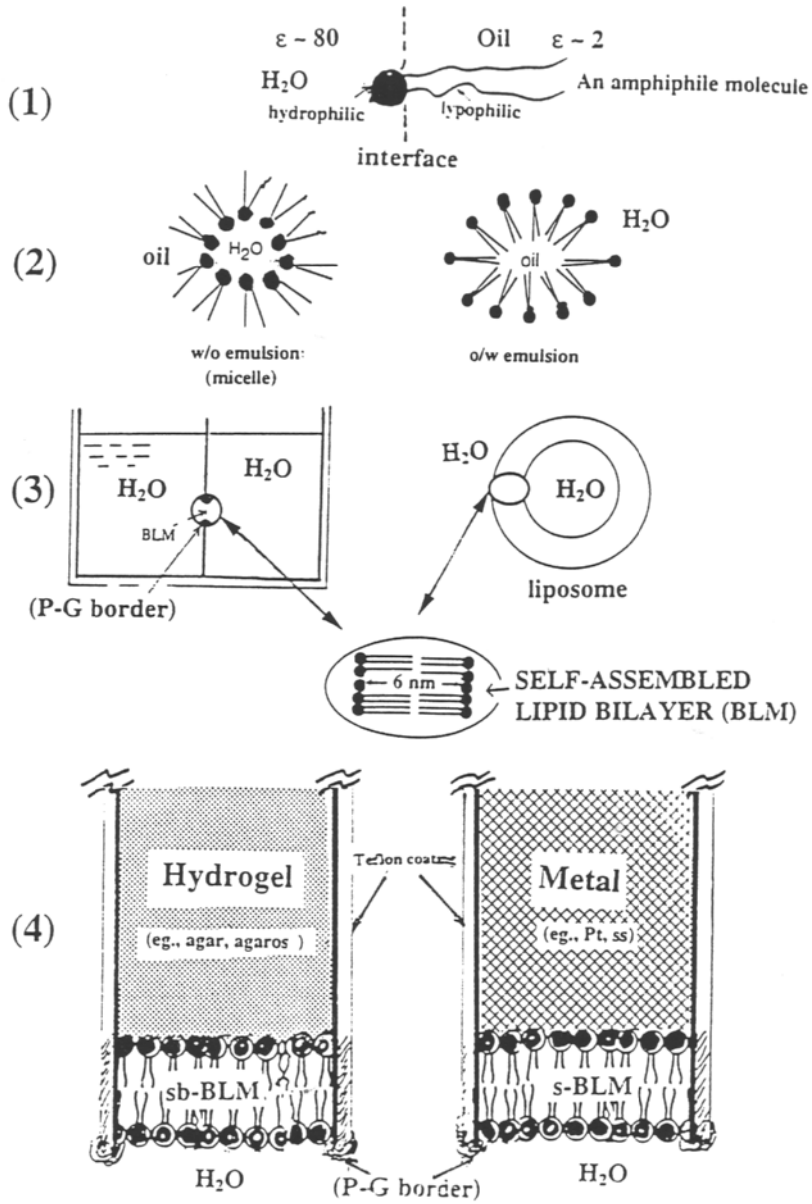

Fig. 3.8 Supra molecular structures at interfaces. (1) Oil-water interface (2) Emulsions (3) Planad lipid bilayer (BLM) and Liposomes (4) Supported BLMs on substrates

The energetics of interfaces. Across any curved interfaces there must be a difference in pressure as a direct consequence of the existence of an interfacial tension. This pressure will be greater on the concave side than on the convex side. When the curved interface is displaced parallel to itself to a new position, its area must change, if the curvature is to remain the same. Consider a cell (or a liposome) with a radius *r*. Its total interfacial free energy, G, is given by

$$G = 2\gamma(4\pi r^2); \quad dG = 16\pi\gamma r\, dr \tag{3.98a}$$

The factor 2 is introduced because a cell, soap bubble or a lipid vesicle (e.g. the liposome) has two interfaces. If the radius of a liposome is to be enlarged by dr (i.e. r + dr), the work W done is

$$W = P\, dV = P\, 4\pi r^2\, dr \tag{3.98b}$$

where V denotes the volume of the liposome. At equilibrium, the interfacial free energy change is $W = dG = 2\gamma\, dA$, which is equal to the PdV work, we have

$$PdV = 2\gamma\, dA$$

or

$$P(4\pi r^2\, dr) = 16\gamma\pi r\, dr \tag{3.98c}$$

Hence

$$P = \frac{4\gamma}{r} \tag{3.98.d}$$

or

$$\gamma = \frac{Pd}{8} \qquad (3.98e)$$

where d (= 2r) is the diameter of the liposome. Eq. (3.84e) is the experimental basis for the so-called maximum bubble pressure method based on the Young-Laplace equation for measuring the bifacial tension of a planar BLM (where *d* is the diameter of the aperture on which a planar BLM is formed).[3]

Electrified interfaces. The very existence of an interface between two immicible phases necessarily implies a basic anisotropy in the forces operating on the species in the interfacial region. Insofar as is known, almost all interfaces are electrified. If so, a potential difference (p.d.) will develop and an electrical double layer will be formed. The origin and characteristics of the potential across the interface have been exhaustingly investigated, and perhaps may be summarized in terms of the electrical double layer theory. There are two aspects of the electrical double layer: (a) the electrical aspect, which is concerned with the magnitude of the excess charge densities across the interfacial region, and (b) the structural aspect, the arrangement of constituents (electrons, ions, dipoles, neutral species). These two aspects are obviously intimately related. We will consider in more detail the theories of electrical double layers in Chapter 6. This section will only consider some potentials at the interfaces, their origins and relationships. First, what are some of the potentials involved at the interface? They are: (1) the surface potential, χ, due to the orientation of dipoles at the interface, (2) the outer potential, ψ, due to the presence of excess free charges separated by the interface, and (3) the inner (Galvani) potential, $\phi = \chi + \psi$. Let us now consider the potential difference between the two phases in contact (examples: oil-water, metal-electrolyte solution, metal-metal, membrane-electrolyte, etc.). The surface potential difference $\Delta\chi$, which is equal to the work of unit charge transfer through the surface layer, cannot be experimentally measured. The absolute potential difference between two phases - the inner potential difference, $\Delta\phi$ or Galvani potential difference is equal to the sum of $\Delta\psi$ and $\Delta\chi$:

$$\Delta\phi = \Delta\psi + \Delta\chi \qquad (3.99)$$

$\Delta\phi$, the Galvani potential difference, may be thought as a measure of chemical affinity of the species under consideration in the two phases (oil and water, O/W). It should be pointed out once more that this so-called Galvani potential which can not be measured experimentally. The difference across the biface, however, is experimentally determinable (see Eq. 3.99). As will be seen later, in studying *W / BLM / W* systems, the polarized biface gives us an external control of the potential drop across the bilayer lipid membrane.

Metal-water interface. Fig. 3.8(4) shows the interface between a metal and planar lipid bilayer. An interesting question is, 'why/how does a BLM self-assemble on a freshly cleaved metallic surface'? An explanation is that a freshly created metallic surface is hydrophilic, which attracts the polar head group of lipid molecules to form a 'condensed' monolayer at its surface. Why a condensed monolayer? This is presumably due to attractive forces among the hydrocarbon (HC) chains of amphiphilic molecules. Upon immersion of a lipid solution-coated metallic surface into an aqueous solution, a second monolayer is attached to the first adsorbed monolayer, leading to a lipid bilayer formation on the metal surface. This second lipid monolayer is also tightly packed so that the contact with water is avoided, since the hydrophobic HC chains of lipid molecules are energetically unfavorable in relation to water.[4]

3.3.2 Electrocapillarity

The connection between the surface tension of an interface and its electrical state may be related by extending the Gibbs adsorption equation by including an electrostatic term. Thus

$$d\gamma = \sum \Gamma_i \; RT \, d \ln a_i + \sigma \, dE \qquad (3.100)$$

where σ is the interfacial charge density, E is the interfacial potential difference, and the other symbols have their usual meanings. If the

composition of a given system is kept constant, i.e. d ln a_i = 0, Eq. (3.100) becomes

$$-\frac{d\gamma}{dE} = \sigma \qquad (3.101)$$

Eq. (3.101) is known as the Lippmann-Helmholtz equation of electro-capillarity, which has been applied to the BLM system.

3.3.3 Membrane Interfaces or Bifaces

***Question*: What is meant by a biface?**

This goes back to the formation of a BLM separating two aqueous solutions in the early 1960s that involved in essence a simultaneous creation of two *co-existing* aqueous solution/BLM interfaces, or a biface.[1] Thermodynamically speaking, a biface is an 'open' system, similar to that of a living cell. In other words, a biface may be represented as follows:

Aqueous solution (*W*) | *BLM* | Aqueous solution (*W*) (3.101)

where | denotes an interface, and BLM is a bilayer lipid membrane (planar lipid bilayer, lipid bilayer membrane or black lipid membrane). On each side of the BLM, there is an interface. The word biface is introduced to emphasize the two coexistent solution/membrane interfaces, through which material, charge, and energy transfer are possible. For that matter the term of biface may be applied to any ultrathin membrane or organic film less than 10 nm thick and liquid-crystalline in nature, separating two co-existing interfaces. Because of its ultrathinness, such an ultrathin film (membrane) structure is capable of supporting an electrical field strength of 250,000 volts/cm or more, and through which electrical (electronic and ionic) transport processes are possible (Chapter 6, *Membrane Electrochemistry*).

Other Definitions

Interface—An interface is the junction of two substances, it is also possible to have an interface of two phases of the same substance.

Thin film and ultrathin film—A thin film is a material of macroscopic thickness (visible to the naked eye); an ultrathin film is about 0.01 thick of the wavelength of the visible light in one dimension, and macroscopic in the two other dimensions.

Thus, a BLM is an example of ultrathin films; it is so thin that it has no homogeneous bulk phase. So when we say a BLM biface it is meant that the properties of the system are influenced by the proximity of its interfaces. In this sense, an interface and an ultrathin film are an associated concept. A BLM biface is unique in that the basic relations between the constituent molecules at, as well as across, the biface and their organizational assembly can be investigated electrically, optically, and by other means (e.g. mechanical). Since a number of interesting phenomena are size-dependent and appear only in tiny systems. Therefore, BLM bifaces, because of their ultrathinness, are good candidates to display these quantum-size phenomena.

Formation and Properties of a Biface: Listed below are a number of outstanding properties which have been investigated over the years [see Davison, 1973-1995].

Techniques

Over the years a number of techniques have been developed for characterizing the liquid/BLM/liquid biface, including the following:

- Optical method for thickness determination
- Maximum bubble method for bifacial tension measurements
- Electrical methods for investigating the biface
- Photoelectrospectrometry for events associated with light and electrical parameters — quantum size effect

With an *'aqueous solution | BLM | aqueous solution'* biface, a number of well-established experimental techniques are applicable. These include optical, mechanical and electrical methods. For example, a BLM is considered as a free standing film, and being as such conventional optical methods have been used to determine its thickness [Mittal, 1986]. Further, a BLM is analogous to that of a soap film, where an *'air | soap film | air'* biface exists. Hence the maximum bubble pressure method can be applied to obtain its bifacial tension. Since, insofar as is known, almost all interfaces are electrified, it is expected that a biface should possess similar characteristics. Indeed, the system of an *aqueous solution | BLM | aqueous solution* biface is set up perfectly for electrical as well as for photoelectric investigations. All one has to do is to place a pair of reference electrodes in the bathing solution across the biface, i.e. *Ref. electrode | **Liquid** | **BLM** | **Liquid** | Ref. electrode*, as will be elaborated later (Section 3.4). The connections between the basic properties of BLM bifaces and biotechnology are particularly close (see Chapter 10. *Applications*). It is now possible to exploit the wealth of information on BLMs that has been accumulated over the past two decades or more.

Phenomena at bifaces

For basic scientific studies, interfaces are of paramount importance. For biosciences in connection with biomembranes, ***Liquid | BLM | Liquid bifaces*** are of pivotal concern. A *liquid | BLM | liquid* biface is a dynamic one. How to control the dynamic character of the *liquid | BLM | liquid* biface, so that desired functions may be achieved? This has been accomplished over the years by embedding a host of compounds into the BLM. For translocating ions and molecules, carriers and channels have been embedded into BLMs (Chapters 5-7). For transferring information or signals, receptors and light absorbers have been incorporated into BLMs (Chapters 7-9). The *liquid | BLM | liquid* biface can also be used as a transducer to actuate a response received from the surrounding. For example, a fullerene C_{60} doped BLM is light sensitive. The light-induced coupled redox reactions will be discussed later (Chapter 10, *Applications*).

Ideally, one would like to develop a liquid/BLM/liquid biface system that function as a transducer-actuator. That is a suitably modified BLM-biface can receive appropriate information, act upon it, and initiate a response. In physiological terms, a ligand interacts with a membrane-bound receptor resulting in a perturbation or a signal. This signal is transduced from the contact interaction into an electrical output, which in turn actuates a chemical or a physical process. A ligand-gated channel is an example, where ligand (i.e. a hormone) binds with a receptor embedded in the lipid bilayer of the membrane. After this contact interaction, the 'gates' of ion-channels are opened to allow ions flowing into or out of the cell. It should be mentioned that the stimulus for interactions might be electrical, mechanical, light, or chemical, with the electrical perturbation most elegant and easy to control and manipulate. Externally applied electric fields across the BLM/biface may induce transient or permanent breakdown of the BLM, depending upon the intensity and duration of the field. The electric field across the BLM/biface is very sensitive to bifacial tension and BLM thickness, which are in turn susceptible to the embedded compounds. Externally applied electric fields act on the BLM/biface by inducing surface charge and by creating pores, although the exact process is still obscure.[6-8] the nature and origin of the signal may be electrical, mechanical, and optical as well as chemical. The challenge task is how to design a liquid/BLM/liquid biface system that will self-assemble to function as a transducer-actuator.

Quantum size effect.[8] According to solid-state physicists, when electrons are confined in a narrow space comparable to an electron wavelength, the electrons are subject to interrelated quantum effects, size quantization and resonance. The former causes the continuum of energy levels that usually exists in the conduction band of a solid to become articulated into discrete energy quanta or states. It has been realized for sometime that a liquid/BLM/liquid biface system is a dynamic one and possesses unexpected properties. By introducing a lipid solution interposed between two aqueous phases, a planar lipid bilayer (BLM) is self-assembled into a supramolecular structure which is microscopic in thickness (~ 5 nm). Such a structure is in a liquid-crystalline state, and inherently dynamic. Upon modification with compounds such as TCNQ, TTF, and fullerene C60,

non-linear electronic behavior and photoelectric phenomena have been observed.[7,9]

It should be noted that photoelectrochemistry of pigmented BLMs, a liquid/BLM/liquid biface system of about 5 nm in thickness, is a research area of many exciting possibilities. In this connection, it is the dynamic lipid bilayer surface that enable our senses to contact with the environment. Examples are seeing (vision), smelling (olfaction), hearing, tasting (gustation), and touching. For all these senses, membrane-bound receptors are involved. These are rod and cone receptors for vision, olfactory bulbs for smelling, tectorial cells for hearing, taste buds for tasting, and nerves for touching. From environment to the brain, signal transduction and information processeing must be transmitted in a language that the brain can understand. Insofar as can be acertained, this language is electrical, for most part based on the translocation of ions and electrons. For ions, ion-channels embedded in the lipid bilayer are the key to our understanding. There are two main classes of ion-channels, voltage-gated and ligand-gated, which by opening and closing regulate the flow of ions. As ions move across the ion-channels embedded in the lipid bilayer, they alter its electrical potential. This transmembrane potential results from a separation of charge across the liquid/BLM/liquid biface. The electric field that give rise to this transmembrane potential is due primarily to the ultrathin hydrophobic portion of the lipid bilayer. The elelctrical capacitance of BLM is easily determined. It has been established that the electrical properties of unmodified BLMs are essentially due to the molecular organizatioin and structure of the lipid bilayer.[7]

In concluding this section, it should be stated that manipulating and controlling conduction processes of the liquid/BLM/liquid biface remains a challenge for both experimentalists and theoreticians.

3.4 Bioelectrochemistry

Question: What is bioelectrochemistry?

First, what can we say about electrochemistry? Electrochemistry is an interface science. Therefore, the structure and composition of the interfacial area are of paramount importance. For example, electrochemistry involves a charge separation and a charge transport or a current (a charge movement as a function of time), which is expressed in ampere per unit area (the current density). In bioelectrochemistry, the unit area in cm^2 will be used for both the area of electrodes and membranes. The aim of bioelectrochemistry is to investigate the electrochemistry of charge separation and the movement in biosystems, in particular in biomembranes and their models at the molecular level. We are interested in the following topics:

- Thermodynamics and kinetics of electron- and proton-transfer processes (photosynthesis and respiration)
- Charge separation and transport
- Electrokinetic phenomena at, as well as cross, interfaces
- Electroanalytical chemistry (biosensors and devices)

The knowledge thus gained through experimental investigations will be used for the development of basic and applied electrochemistry. It is informative here, therefore, to summarize some of the fundamental principles of electrochemistry relevant to biosystems.

3.4.1 Electrochemical cells and membrane potentials

The best starting point of our discussion, perhaps, are electrochemical cells and how do they work. Fig. 3.9 illustrates the so-called Daniell cell that serves as an excellent energy source. By linking a series of electrochemical cells together, you have a battery (e.g. Pb/H_2SO_4 car battery), the importance of which to modern life cannot be overstated. Nowadays batteries of all kinds of design and shape are used in laptop computers, cellular phones, portable medical devices and many others.

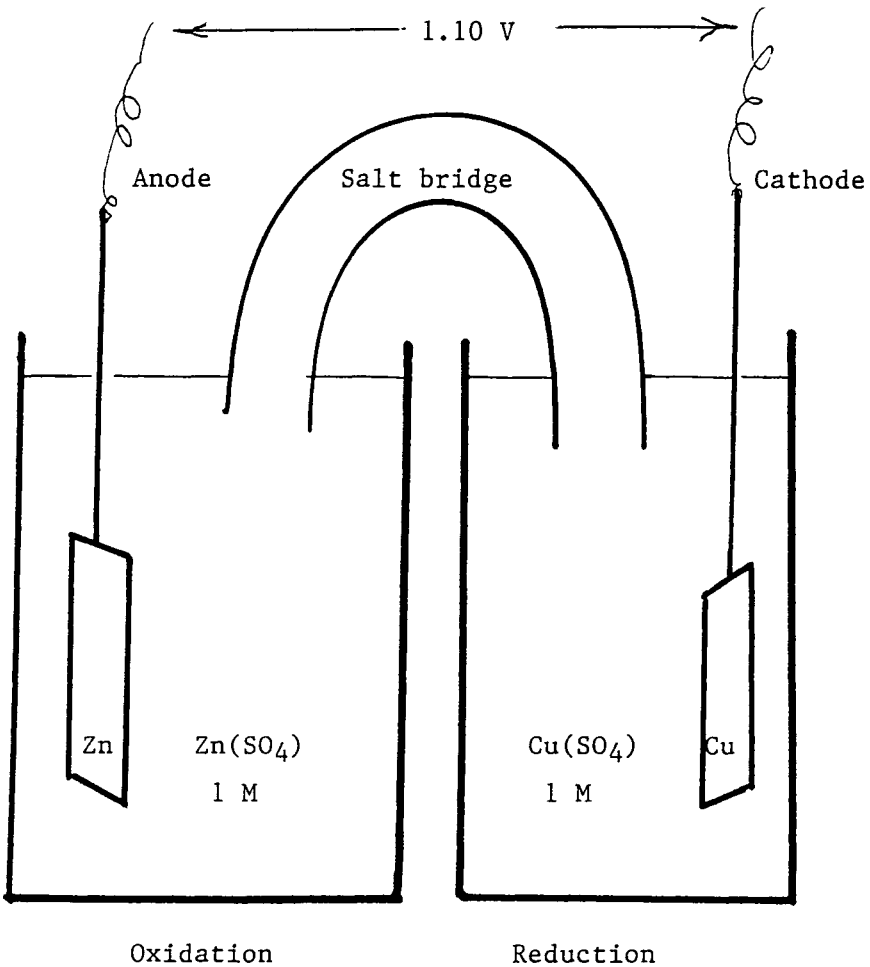

Fig. 3.9 The Daniell cell (1836) illustrating the basic principle of electrochemical cells using copper and zinc. However, instead of Cu/Cu^{2+} and Zn/Zn^{2+}, almost any combination of two different metals connected by a solution of electrolyte, in fact, will produce a voltage and an electric current in an external circuit.

Electrochemical cells, similar to living cells, depend on chemical reactions. With an appropriate arrangement, the chemical energy may be converted into electrical energy or vice versa. Through the application of thermodynamics we know how much energy is absorbed or released during chemical reactions. When electrochemical cells generate a potential difference (PD) or voltage, this is a direct measure of the thermodynamic quantity, and is related to Gibbs' free energy (ΔG, Eq. 3.22 and see below). The Daniell cell shown in Fig. 3.9 may be represented as two half cells connected by a conducting but 'inert' salt solution (bridge) as follows:

(left chamber)		(right chamber)	
outside		inside	
electrode 1	salt bridge	electrode 2	(3.102)
and its solution		and its solution	

Since we can measure only the potential difference (voltage) but not a single potential, we can nonetheless calculate what the single potential should be compared with each other, if we set up some standard state, a reference half cell, and always make measurement against it. Thus, by convention the standard reference half-cell is the hydrogen electrode where $H^+ + e \longrightarrow \frac{1}{2} H_2$, in which activities of all species are equal to unity in contact with a Pt metal. The reference potential of a standard half-cell is constant because the half-cell always has the same reacting species at a stated temperature. The arrangement given in Eq. (3.103) is in fact very useful in evaluating the species in other half-cell reactions and in designing practical biosensors (Chapter 10, *Applications*).

3.4.2 The nature of driving forces

When something moves or a reaction takes place, a driving force is usually implied. The force is related to a gradient of a potential. As with many forces in physics, the gradient of a potential has to be found. For

example, the rate of heat transfer is proportional to the gradient of temperature, and the force on the unit electrical charge is given by the gradient of electrical potential. The appropriate potential for a material species (e.g. for sugar, non-electrolytes, etc.) is the chemical potential, μ, as already described by Eq. (3.22). For ions or charged species, the term electrochemical potential ($\underline{\mu}$) is used. The force is the gradient of electrochemical potential ($d\underline{\mu}/dx$).

The most unique feature about the biomembrane is that it has two solution-membrane interfaces or a biface. Most interfaces are electrified as evidenced by the presence of a potential difference across the membrane. It is worth noting that, like a half-cell potential, the electric potential between the membrane phase and its bathing solution can not be easily measured. However, if we treat each membrane-solution chamber according to Fig. 3.10 as a half-cell, the potential difference between the left chamber and the right chamber can be readily measured with the membrane playing the role of a **bipolar** electrode. That is the membrane is not a passive element but rather each side of the membrane acts as a working or indicating electrode with its own half-cell potential. Hence the word bipolar electrode is introduced [Tien, 1974]. In order to measure the potential difference (voltage) of such a system as depicted in Fig. 3.10, a pair of reference electrodes are placed on opposite sides of the membrane, which may be represented as follows:

reference electrode	outer chamber solution 1	membrane (BLM)	inner chamber solution 2	reference electrode

(3.103)

With the lead wires of the reference electrodes connected to a high impedance voltmeter or an electrometer, the potential difference is then easily measured.[4] The origins of the observed potential difference (voltage) of the system given in Eq. (3.89) depend on the molecular organization of the membrane, which in turn involves its constituents (see Chapter 2, *Biomem branes*). In the following paragraphs we will consider the origins of membrane potentials.

3.4.3 The origins of membrane potentials

By placing a pair of reference electrodes on opposite sides of a biomembrane, a potential difference (voltage, V) on the order of tens of millivolts (mV) is usually detected. This voltage suggests an unequal distribution of charges across the membrane. These charges may be ions or free charges such as electrons and holes, or they may be dipolar molecules. This charge imbalance across the membrane is a result of charge separation, and may be due to one or a combination of several of the following situations:

- Preferential adsorption of ions
- Orientation of dipolar molecules
- Movement of ions from one side to the other
- Deformation of molecules
- Oxidation-reduction (redox) reactions
- Perturbation of the membrane by external sources (light, applied voltage, pressure or temperature difference, and others)

In addition to the membrane voltage (V or E_m) there are other electrical parameters associated with the membrane. Prominently among these are membrane capacitance (C_m), resistance (R_m), current (I_m), and breakdown voltage (V_b). From basic physics, $V \propto q$ (the fundamental charge associated with an electron), one can write

$$q = C\,V \tag{3.104}$$

where C is the proportionality constant, termed capacitance. Thus, we have the familiar formula:

$$C = \frac{q}{V} \tag{3.105}$$

The unit for C in membrane biophysics is defined in microfarad (μF) per unit area in cm^2. Recalling in Chapter 2 , Fricke determined the capacitance (C_m) of the RBC membrane using a parallel plate condenser formula (Eq. 2.2). It should be noted here that a capacitor can be discharged, and therefore there is a capacitive current (i_c) connected with it, which is given by

$$i_C = \frac{dq}{dt} = C\frac{dV}{dt} \tag{3.106}$$

and

$$\int dV = V = 1/C \int i_C\, dt \tag{3.107}$$

This capacitive current, i_c, differs from the current, I, expressed in Ohm's law ($E = IR$). The capacitive current is a displacement of charges on opposite sides of the membrane, therefore, it does not involve a direct translocation of charges (ions) through the membrane. We will mention the capacitive current in Chapter 7 when the action potential of the nerve membrane is discussed. One needs to remember that electrical current is expressed in amperes (coulombs per second). Hence, one can find out the total q by integrating the current from the time t = 0 to $t = t$, which is given by

$$q = \int i_C dt = nFN \tag{3.108}$$

where the various terms have the usual significance.

3.4.4 The electrochemical potential, μ

The Nernst Equation and Electroneutrality Principle

Returning to Eq. (3.103), the solutions in the two chambers, left and right, may be considered, respectively, as an extracellular fluid and intracellular fluid of a cell, and the two sides may be considered being connected by the cell membrane. In order to characterize the non-electrolytes in each chamber, as already mentioned, the chemical potential

is used (Eq. 3.26). For charged species, the driving force is the gradient of electrochemical potential ($d\underline{\mu}/dx$). Thus, from Eq. (3.26) one can add an electrical term associated with the chemical potential to each side of the bathing so lution, that is

$$\underline{\mu} = \mu^o + RT \ln a = \mu^o + 2.303\ RT \log a + zF\psi$$

$$\simeq \mu^o + 2.303\ RT \log \gamma C + zF\psi \qquad (3.109)$$

where z is the valence of the ion, F is the Faraday constant and ψ is the potential. Therefore, at equilibrium $\underline{\mu}_o = \underline{\mu}_i$, that is

$$\mu^o + 2.303\ RT \log \gamma C_o + zF\psi_o = \mu^o + 2.303\ RT \log \gamma C_i + zF\psi_i \qquad (3.110)$$

or

$$\psi_i - \psi_o = E_m = \frac{2.303\ RT}{zF} \log \frac{[C]_o}{[C]_i} \qquad (3.111)$$

where E_m is the membrane potential at equilibrium, and subscripts *o* and *i* refer to, respectively, the outer (left chamber) and inner side (right chamber) of the membrane. According to Eq. (3.111), the **Nernst** equation, there are two points which need to be kept in mind: (i) the amount of

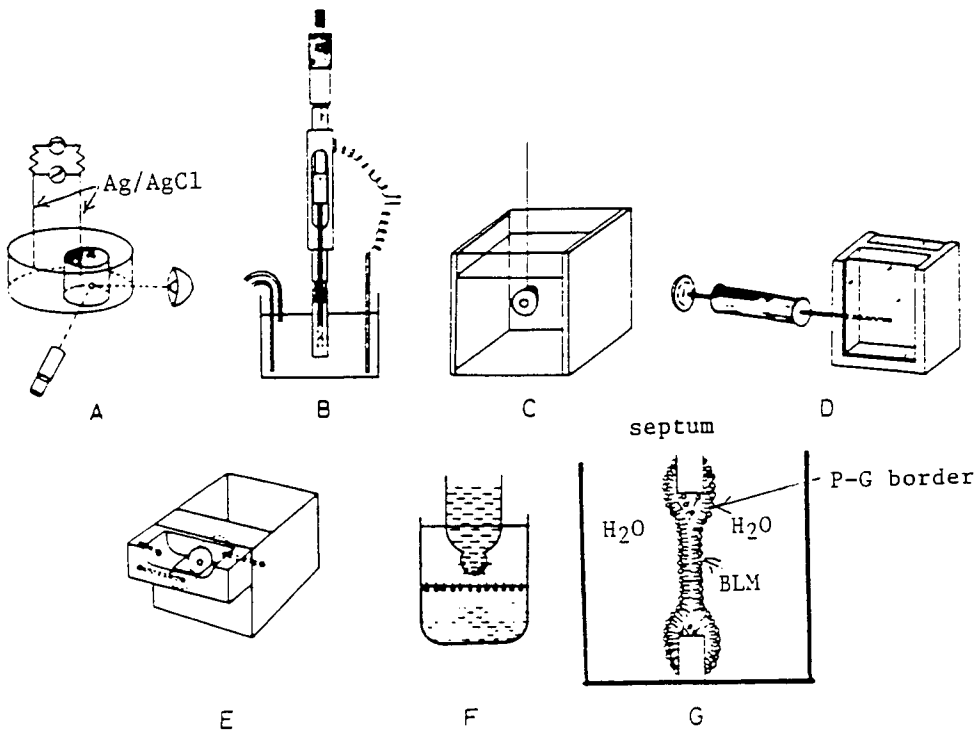

Fig. 3.10 Various cell designs for investigating planar lipid bilayers (BLMs). **A**. Rudin et al (1962) **B**. Hanai & Haydon (1966) **C**. Huang & Thompson (1966) **D**. Vreeman (1966) **E**. Andreoli et al (1967) **F**. Tsofina et al (1966) **G**. Diagram of a free-standing BLM (By courtesy of A. D. Bangham).[1]

charges required to generate tens of mV is exceedingly small, on the order of 10^{-14} M of ions, a quantity that cannot be easily determined by any means except electrically, and (ii) inside of the cell as well as outside, the principle of electroneutrality is, for all practically purposes, maintained. In other words, the amount of charges to be separated at a short distance in order to generate a potential difference, say 70 mV, may be calculated by treating a membrane as a parallel plate condenser of 1μF/cm^2. Accordingly, the amount of monovalent ions *n* is given by

$$n = C_m VA/F \qquad (3.112)$$

where *C* is in farads (1F = 10^6 μF), *A* is Avogadro's number (6.02 x 10^{23} /mole) and *F* is Faraday's constant (96,500 coulombs/mole). Substituting these quantities into Eq. (3.111), the number of ions involved is about 4 x 10^{11}, which is a very miniscule number, when compared with the number of ions that are present in a 100 ml of 0.1 M KCl (it has 10 billion times more than the calculated number!). Therefore, apparently across or at the interface, the condition of electrical neutrality is violated. As illustrated in Fig. 3.10, at or across each of the solution-membrane interfaces, it has practically the same chemical composition but different electrical potentials. As we shall discuss later in Chapter 7 (*Membrane Physiology*), it is this local violation of the electroneutrality principle that makes life, as we understand it, possible!

A living cell is the most unique in that its plasma membrane separates *two* aqueous solutions, which gives rise to a voltage or an electrical potential difference (PD) on the order of tens of millivolts (mV). This small PD is essential for functioning of the cell. This brings immediately to the problem as how to measure it. Fortunately, electrochemists have provided us with a variety of reference electrodes such as Ag/AgCl and Hg/Hg_2Cl_2. The purpose of a reference electrode is to supply a constant potential without changing it with respect to time. A good reference electrode should not be easily polarized during a measurement. Further, to prevent a contamination, a salt bridge made of a piece of tubing filled with agar gel (e.g. 0.3 g of agar/15 ml of 3 M KCl) is

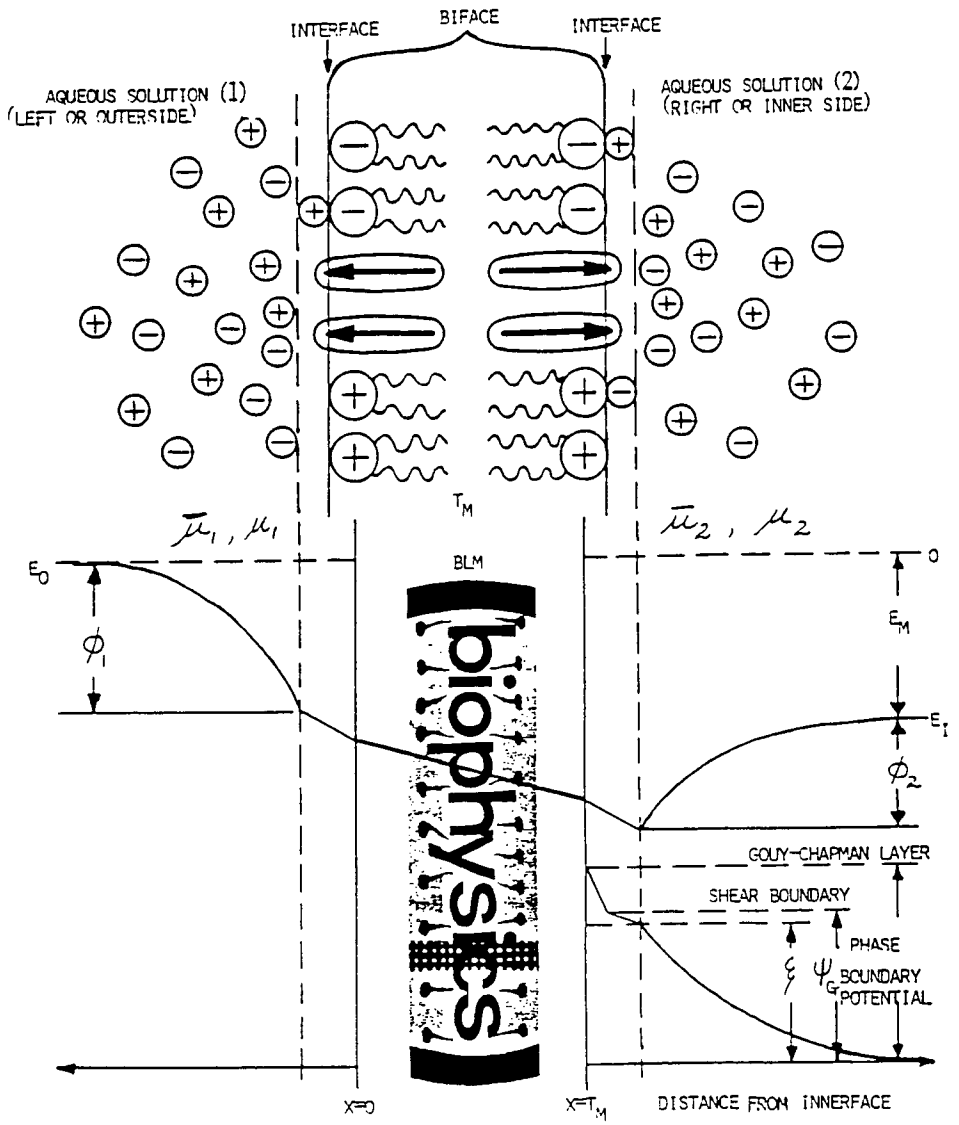

Fig. 3.11 Interfacial potentials of the ***Liquid*** | ***BLM*** | ***Liquid*** biface.

usually attached to the electrode. For example, Hg/calomel Hg_2Cl_2/ saturated KCl/agar gel represents a so-called saturated calomel electrode (SCE). The standard potentials (*vs.* NHE, normal hydrogen electrode) for Ag/AgCl and Ag/Hg_2Cl_2 are 0.222 and 0.268 mV, respectively. Thus, when a pair of these reference electrodes are placed across the cell membrane (for that matter across any physical barriers including a bilayer lipid membrane (BLM) (*see* Eq. 3.103), the resulting potential difference (PD) observed is owing to the contribution of the membrane and its bathing solutions only, since the reference electrodes themselves are invariant. It is worth remembering that we cannot measure a single potential of an electrode but only the PD. The voltage (V) or the PD of a cell is measured when nearly zero current is passing through the contacting reference electrodes. Nowadays, it can be easily accomplished. All one needs is a high impedance voltmeter or an electrometer. Having made these remarks on some practical aspects of electrochemistry, we will then ask the question what is the meaning of this observed PD? Simply answered, it is a manifestation of electrical activities across the barrier membrane, which in turn is a measure of the Gibbs free energy change (ΔG):

$$E_m = -\frac{\Delta G}{nF} \tag{3.113}$$

where E_m is the membrane voltage (PD), n is the number of electrons involved in the reaction, and F is the Faraday constant (96,486 coulombs/ mole). From Eq. (3.23) the following may be obtained:

$$E^0_m = \frac{RT}{nF} \ln K \tag{3.114}$$

where E^0_m is a potential at the standard conditions. It should be pointed out that, when a pair of reference electrodes are placed across the cell membrane, one is actually measuring the sum of two half-cells:

$$E_{cell} = E_m = E_{in} - E_{out} \qquad (3.115)$$

where E_{in} and E_{our} denote the inside and the outside of the cell, respectively. By convention, the inside of the cell is taken as negative. In this connection the two sides of the membrane actually serve as working, redox or indicating electrodes. In general terms, one can express a redox reaction:

$$OX + ne^- \longrightarrow RED \qquad (3.116)$$

where OX and RED represent oxidized and reduced species, respectively. Through the Nernst equation, the values of half-cell potentials can be related to the activities (or concentrations) of the species involved in the solutions bathing the membrane. Then we can obtain

$$E_{cell} = E^0 + \frac{RT}{nF} \ln \frac{[OX]}{[RED]} \qquad (3.117)$$

where [OX] and [RED] are concentrations of active species, not necessarily redox compounds, expressed as moles/liter. All activity coefficients are taken as unity. On the basis of information given in Fig. 3.11, a PD of 58-60 mV would be expected for 10-fold difference in concentrations at room temperature. If the membrane is selective, for example, it prefers cations over anions, then the more concentrated side will be negative.

General References

E. A. Guggenheim, *Thermodynamics*, 2nd ed. Wiley, New York, 1950

A. W. Adamson, *The Physical Chemistry of Surfaces*, 2nd editon, Wiley, NY , 1967

H. T. Tien, *Bilayer Lipid Membranes (BLM): Theory and Practice*, Marcel Dekker, Inc., New York, 1974

D. E. Metzler, *Biochemistry: The Chemical Reactions of Living Cells*, Academic Press, NY, 1977

S. G. Davison (ed.), *Progress in Surface Science*, Vols. **4,8,19(3),23(4), 30(1/2),41(4),47(1/2),49(2),** Pergamon Press, NY, 1973, 1985, 1986, 1989, 1992, 1994, 1995

M. Blank (ed.), *Electrical double Layers in Biology*, Plenum, NY, 1986

I. M. Klotz, *Introduction to Biomolecular Energetics*, Academic Press, New York, 1986

A. A. Marino (ed.), *Modern Bioelectricity*, Marcel Dekker, Inc., New York, 1988

K. L. Mittal and D. O. Shah (eds.), *Surfactants in Solution*, Vols. **8, 11**, Plenum Press, NY, 1986, 1991

H. Gutfreund, *Kinetics for the Life Sciences*, Cambridge University Press, 1995

Specific References

1. M. Kerker (Ed.), Surface Chemistry and Colloids, Vol. 7, MTP International Review of Science (A. D. Buckingham, Consultant Editor), Butterworths, London, 1972, Chapters 1 and 2
2. K. Gawrisch, J. A. Barry, L. L. Holte, T. Sinnwell, L. D. Bergelson and J. A. Ferretti, *Mol. Memb. Biol.*, **12** (1995) 83-88
3. R. P. Rastogi, R. C. Srivastava and S. N. Singh, 'Nonequilibrium thermodynamics of electrokinetic phenomena', Chem. Rev., **93** (1993) 1945-1990
4. B. Pethica and D. Hall, J. Colloid Interf. Sci. 85 (1982) 41
5. S. Ohki, in Comprehensive Treatise of Electrochemistry, Vol. **10**, Bioelectrochemistry, S. Srinivansan, Yu. A. Chizmadzhev, J

O'M. Brockris, B. E. Conway, and E. Yeager (Eds.), Plenum Press, NY, 1985, Chapter 1
6. K. Miyano, 'Interfaces as a field for arranging organic molecules', Japan J. Applied Phys., **24** (1985) 1379-1388
7. I. B. Ivanov (ed.) *Thin Liquid Films: Fundamentals and Applications*, Marcel Dekker, Inc., NY, 1988, pp. 527-1057
8. R. T. Bate, *Scinetific American*, March 1988, pp. 96-123.
9. H. T. Tien and A. l. Ottova, *Colloids and Surfaces A: Physicochemical and Engineering Aspects*, 149, 217-233 (1999).
10. F.Adams and G. Laughlin, *The Five Ages of the Universe*, The Free Press, Simon & Schuster, London and NY, 1999.

Some recent references pertinent to this chapter are cited below.

Kalinowski S, Ibron G, Bryl K, et al. BBA-Biomembranes 1369: (2) 204-212,1998
Evtodienko VY, Antonenko YN, Yaguzhinsky LS FEBS LETT 425: (2) 222-224, 1998
Osman P, Martin S, Milojevic D, et al. LANGMUIR 14: (15) 4238-4242,1998
Sato H, Hakamada H, Yamazaki Y, et al. BIOSENS BIOELECTRON 13: (9) 1035-1046,1998
C. Lemaitre, N. Orange, P. Saglio, N. Saint, J. Gagnon and G. Molle, Euro. J. Biochem., 240 (1996) 143-149
S. Matile, N. Berova and K. Nakanishi, Chem. & Biol., 3 (1995) 379-392
G. Prat, E. J. Holtzman, D. Brown, C. C. Cunningham, I. L. Reisin, T.
A. R. Kleyman, M. McLaughlin, G. R. Jackson, Jr., J. Lydon and H. F. Cantiello, J. Biol. Chem., 271 (1996) 18045-18053
I. Ismailov, B. K. Berdiev, A. I. Braford, M. S. Awayda, C. M. Fullerand and D. J. Benos, J.Memb. Biol., 149 (1996) 123.
Y. Nagaoka, A. Iida, T. Kambara, K. Asami, E. Tachikawa and T. Fujita, Biochim. Biophys.Acta, 1283 (1996) 31-36
Y. A. Ermakov, Makhmudova SS, Averbakh AZ ,COLLOID SURFACE A 140: (1-3) 13-22,1998.

http://www.msu.edu/~ottova/membrane.biophysics.html

Chapter 4

Experimental Models of Biomembranes

"... in a society in which manual labor is demeaned and thought fit only for slaves,...the experimental method does not thrive."
--Carl Sagan in The Demon-Haunted World, p. 312

"...an understanding of biomembranes in physicochemical and physiological terms requires an assessment of the contribution of specific molecules and ...supramolecular structures to various configuration details and functional properties. Such correlation are difficult to accomplish owing to the complexity of the biomembranes."

General References (cited by name in brackets in the text)
Specific References (cited by number in superscript in the text)

Summary. *Knowledge on membrane-bound processes is key to an understanding of living cells. The discovery of how to make experimental bilayer lipid membranes and to impart simple functions such as ion selectivity, ligand-receptor interaction, and light sensitivity to these lipid bilayers was an important step forward. In this chapter we will provide the know-how on forming experimental planar lipid bilayers and liposomes as well as techniques for incorporating a variety of materials such as polypeptides, proteins, ion channels, receptors, light-sensitive compounds, photosynthetic and visual pigments, and others into such lipid bilayers. In addition to conventional BLMs and liposomes, sufficient details will also be given for fabricating supported BLMs of long-term stability on metal and gel substrates for biotechnological applications.*

4.1 Introduction

In the recent past, two principal types of experimental bilayer lipid membrane systems have been developed and extensively employed as models of biomembranes. The first consists of a planar bilayer lipid membrane (BLM) interposed between two aqueous solutions, where a diversity of properties associated with the lipid bilayer can be readily investigated electrically. The second system consists of lipid microvesicles (LMV) popularly known as liposomes, in which a bilayer lipid membrane of spherical configuration encloses a volume of aqueous solution. As we shall discuss shortly, these two experimental bilayer membrane systems are complementary to each other and have contributed enormously to our understanding of the passive properties and dynamic functions of biomembranes. Both types of bilayer lipid membranes will be discussed under separate headings in this chapter. To begin, let us pose and answer a few questions.

***Question*: Why do we study models?**

Apart from a few gifted individuals, most of us need analogies and models to understand the physical world, especially those not readily apparent to the naked eye. Thus, when we do research, in a sense we are making models of the physical world. For example, Niels Bohr used the solar system as a model for understanding the structure of the atom, which

later led to the development of quantum and wave mechanics. There are at least three different classes of models:

- Pictorial or diagrammatic representations, which are mainly descriptive,
- Mathematical models, which attempt to account the properties of real systems, and
- Experimental models; they can be either artificial or natural systems. they are used to test a given hypothesis.

The first two classes of models do not have the same impact as experimental models do, especially if it is a working model. The rationale behind the experimental model membrane research, the main thesis of this book, may be stated as follows: an understanding of biomembranes in physicochemical and physiological terms requires an assessment of the contribution of specific molecules and molecular aggregates (i.e. supramolecular structures) to various configuration details and functional properties. Such correlations are difficult to accomplish owing to the complexity of the biomembranes.

***Question*: What can be learned about biomembranes by studying experimental model systems?**

Some answers are that we can have a better knowledge of:

a) structural-functional relationship of lipids, proteins, carbohydrates, pigments, and their complexes,
b) mechanisms of transport, energy transduction, signal processing, and
c) our common senses such as vision, olfaction, hearing, gustation, and touching sensations.

***Question*: What are some of the criteria of a good experimental biomembrane model?**

a) Chemical composition
b) Dimensional requirements (membrane thickness)

c) Environmental factors (aqueous solution/membrane/aqueous solution)
d) Physical state (fluidity, viscosity)
e) Simplicity of operation (ease of manipulation and modification)

***Question*: What attributes should a good experimental biomembrane possess?**

- The 'railroad' track (trilamina) appearance of biomembranes as seen in electron micrographs.
- The electron density profile across the membrane as determined by x-ray analysis.
- A good model should be able to relate dimensionally, for example, the lipids and proteins invoked in the model to the constituent molecules in the biomembrane.

In brief, the general idea of a model is to provide an appreciation and/or understanding of the subject by stressing unique aspects without unnecessary complexity, which tends to obscure the main feature. Further, a good model must not only explain a large body of known facts (observations and findings) but also must lead to new facts and predictions. As will be shown later in this chapter and the remainder of this book, the experimental lipid bilayers (BLMs and liposomes) have provided us with an excellent tool in the initial testing of working hypotheses which have generated guidelines leading to a better choice of appropriate *in vivo* and reconstituted membrane experiments. However, it should be kept in mind that studies on artificial model membranes should be regarded as complemen-tary to studies on real biological membranes.

4.2 Bilayer Lipid Membranes (BLM)

In Chapter 2, we have seen the overwhelming evidence that the cell membrane of all living systems is a lipid bilayer modified with proteins, carbohydrates, and their lipid complexes as well as other constituents for specific functions. Fig. 1.2 of Chapter 1 illustrates an idealized, grossly simplified, and highly schematic representation of a cell

together with its major structural and functional components. To understand such a variegated conglomerate in physical, chemical, and physiological terms is seemingly beyond any let alone, a single experimental approach. Fortunately, the key to biomembrane understanding is through the lipid bilayer. This key was fortuitously found about four decades ago through playing with child's soap bubbles.[1,2] Experimentally, to make an artificial lipid bilayer in the test tube is exceedingly uncomplicated. Indeed, *'there is not a lot to it!'* as we will see shortly. Nevertheless, such a simple experimental system has made possible, for the first time, the investigations of electrical properties and transport of matter across human-made lipid bilayers separating two aqueous phases.

4.2.1 Historic Perspectives of BLMs

Those whose work has no direct connection with cell membranes, perhaps are not acquainted with the experimental lipid bilayers, commonly referred to as bilayer lipid membranes (planar lipid bilayers or BLMs for short) and spherical liposomes. The seminal work on the self-assembly of planar lipid bilayers or 'black' lipid membranes was carried out by Rudin and his associates in 1959-1963.[2] They first investigated lipid monolayers and multilayers of the Langmuir-Blodgett type. The idea of planar lipid bilayers started while one of the authors was reading a paperback edition of *'Soap Bubbles'* by C. V. Boys.[3] From this source, the early researchers then toyed with soap bubbles and films. These early researchers realized that a soap film in air in its final stage of thinning has a structure, which may be depicted as two monolayers sandwiching an aqueous soap solution. That is a system that may be represented as

$$\textit{air} \mid \textit{black soap film} \mid \textit{air} \qquad (4.1)$$

where the vertical line, | , represents an interface. This picture of the so-called 'black' soap films had been suggested many years ago by Gibbs, Overbeek, Mysels, Corkill, and others [*see* Davison, 1985 and references therein] Once they recognized this arrangement together with its molecular organization, Rudin and colleagues simply proceeded to make an under water 'lipid film' interposed between two aqueous solutions, i.e.,

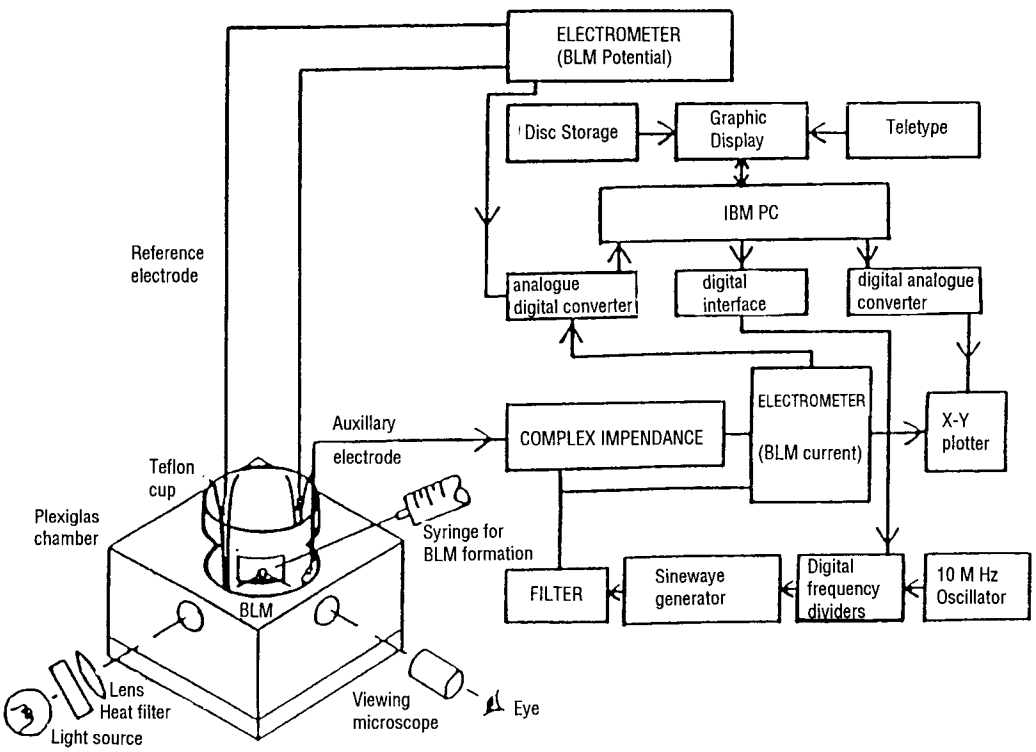

Fig. 4.1 The BLM technique. Shown here is a recent version of the setup for planar lipid bilayer studies.

aqueous solution | BLM | aqueous solution (4.2)

Further, Rudin and collaborators showed that an under water lipid film (i.e., a BLM) formed from brain extracts was self-sealing and resistant to puncture. Upon modification with a certain protein (dubbed as EIM, see Chapter 7), this otherwise electrically 'inert' structure of about 6 nm thick became excitable displaying characteristic features similar to those of action potentials of the nerve membrane.[2] Experimentally, insofar as forming a BLM is concerned, there is not much to it. In fact, as we will see later, it is far easier to form a BLM than spreading a monolayer at an air-water interface.[1]

Rudin and associates,[4] then at Eastern Pennsylvania Psychiatric Institute in Philadelphia, reported an earlier account of planar lipid bilayers (BLMs), dubbed as 'man-made plasma membrane', in 1963. Shortly afterwards, BLMs have found widespread use as model membrane systems, since they have permeability characteristics and other properties similar to those of biomembranes. Planar lipid bilayers have provided the opportunity to study the relation between the structure and function of biomembranes such as transport phenomena via reconstituting membrane proteins into the lipid bilayer. Further, by embedding a variety of compounds into the lipid bilayer domain, modified BLMs can be used as ion and molecular sensors, light converters, and detectors. Thus, in the three plus decades since its inception, the BLM along with the liposome[5] has been extensively used as models of biomembranes. In particular, the BLMs have been adopted to elucidate the molecular mechanisms of biomembrane function such as ion sensing, electron transfer, electric excitability, gated channels, antigen-antibody binding, signal transduction, and energy conversion, to name a few [Tien, 1974; Rosoff, 1996]. It is the aim of this chapter to provide a conceptual as well as practical basis for forming and investigating artificial lipid bilayers (BLMs and liposomes).

4.2.2 Formation and basic characterization of BLMs

Since the pioneering work on BLMs in the early 1960s, several generations of membrane bioscientists including physiologists and biophysicists have exploited the conventional BLM system for biophysical

and reconstitution studies [Antonov et al., 1979; Antolini et al., 1982; Frangopol and Sanduloviciu, 1996]. Experimentally, a BLM is formed by painting a lipid solution onto an aperture separating two aqueous solutions. To date, the original method is still one of the simplest techniques available. Typically either a 1% phosphatidylcholine (lecithin) in n-decane or glycerol dioleate in squalene is used. Oxidized cholesterol in n-octane, which generates stable BLMs, is often used either alone or in combination with a phospholipid. [6-8]

The principle of a BLM experiment is simple. Fig. 4.2 shows such a setup. The BLM may be formed by brushing a solution of phospholipids across a small hole (~ 1-2 mm diameter) in a hydrophobic cup made of either polyethylene or Teflon immersed in an aqueous solution (e.g. 0.1 M NaCl). The Teflon cup is held in a much larger glass dish also filled with an aqueous solution. Because the aperture (hole), where the BLM is being formed, is rather small, a low power microscope is used to observe its formation. Initially, the lipid film interposed between two aqueous solutions is relatively thick, which may show intense rainbow colors as thinning occurs. Depending on the lipid solution used, 'black' spots suddenly appear in the film after a few seconds to several minutes. These low reflecting black spots grow and come together and eventually fill the entire aperture, except at the bright rim, giving an appearance very much like a total solar eclipse. Hence, the BLM is sometimes referred to as the 'black' lipid membrane. Various measurements have shown that the BLM at this stage, corresponds closely to the postulated bilayer leaflet model of the plasma membrane of red blood cells. Detailed procedures as well as instrumentation and apparatus common to many studies with BLMs including formation techniques, BLM-forming solutions, optical thickness determinations, permeability evaluations, electrical measurements including patch-clamp techniques, bifacial tension assessments, spectroscopy, and light-induced characteristics may be found in the monographs on BLMs [Tien, 1974; Hanke and Schlue, 1993]. In the paragraphs below, the essential aspects of relevant methods for forming and studying bilayer lipid membranes of planar configuration are presented. For convenience, hereafter the term planar lipid bilayers or simply BLM(s) will be used interchangeably.

To have a good and workable setup for BLM experiments devoted to straight-forward electrical and photoelectrical measurements, only minimal equipment is necessary. Indeed, a simple BLM setup published in the Journal of Chemical Education is a good starting point (Fig. 4.2).[6,71] Before giving the technical details of BLM experiments, let us have an overview pertaining to the arrangement shown in Fig. 4.2.

Chambers for BLM formation. The materials that are suitable to construction of BLM chambers and supports are limited by the requisites of chemical inertness to both aqueous and organic solvents, electrical insulation and optical transparency. Glass components, because they possess these requisites, are useful when they can be incorporated into the system. Cast Lucite (Plexiglas) is electrically nonconductive, transparent, and resistant to many organic solvents. Because Lucite may be easily machined and cemented it has frequently been used in lieu of glass. However, Lucite should not be used when halogenated solvents such as chloroform and methylene chloride are used as lipid solvents. Teflon, polyethylene, and polycarbonate have the requisite chemical and electrical properties and may be machined or cast, but lack transparency and rigidity. Teflon has proven particularly useful in aperture-containing sheets or cups for the BLM support. As to the size of the aperture for supporting the BLM, diameters ranging from 0.1 to 2 mm and larger have been used. For thin Teflon sheets (~ 10 μm thick) as the partition between the two chambers, diameter of the hole is usually less than 0.3 mm.

Platform for BLM chambers. A planar lipid bilayer separating two aqueous solutions is truly an incredible structure. As such the fragility and short life expectancy of the BLM are to be expected, especially when it is under mechanical or/and electrical stress. In order to avoid premature breakdown of the BLM, the membrane chamber is frequently placed on a vibration isolation platform. One way to construct such a platform economically is by placing a heavy block made of cement, stone or metal on tennis balls or a partially inflated inner tube from a car's tire.

Reference electrodes. To make electrical contacts between the two sides of a BLM and external instrumentation, a pair of reference electrodes must

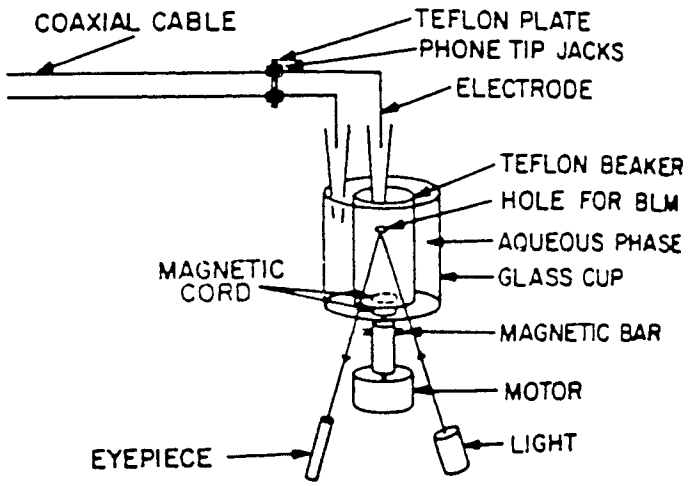

Fig. 4.2 A simple arrangement for investigating the electrical properties of conventional BLMs.[6]

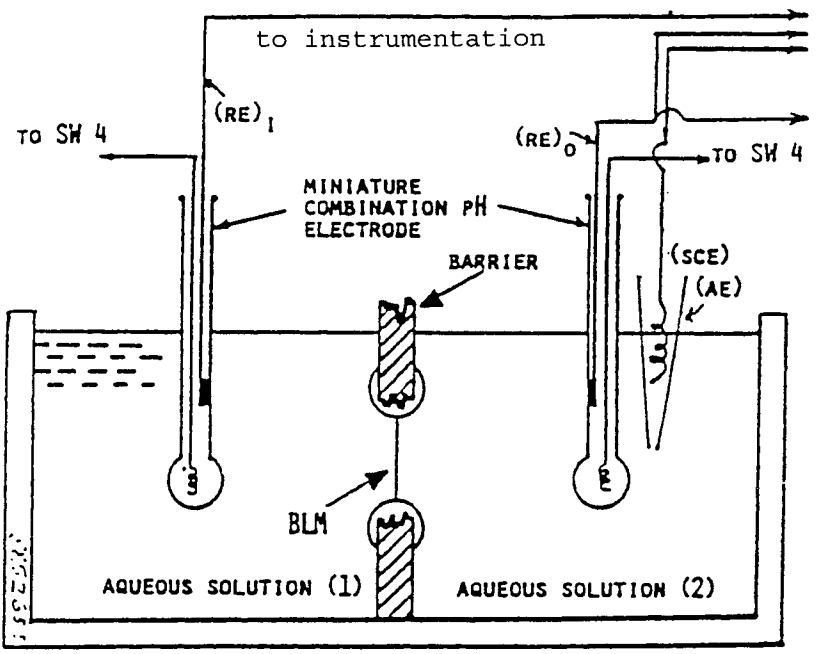

Fig. 4.3 Setup used in BLM electrical and pH measurements.

be used. Simple Ag/AgCl wire electrodes with or without agar salt bridges or saturated calomel electrodes (SCE) are usually used. Agar salt bridges can be easily made from a glass or plastic tubing (~ 2 mm diameter) filled with a hot agar solution. In our laboratory we have found that two miniature combination pH electrodes serve the purpose very well (Fig. 4.3). One advantage of using the reference electrode from a combination pH electrode is that the H^+ ion activity of the solution in each chamber can be monitored in the usual way, if desired, during an experiment.

Stirring devices. It is sometimes necessary to stir the solutions bathing the BLM, especially after an addition of a test compound under study. The stirring can be easily accomplished by polyethylene or Teflon-coated magnetic stirrers placed in each chamber, which are driven by a small DC motor underneath the chambers.

Light source and viewing microscope. For observing a BLM in formation under reflected light, a low power microscope (10-50 x magnification) together with a tungsten lamp is used. For comfort and manipulation, the focal distance of the viewing microscope should be 5-10 cm. For observing light-induced photoelectric effects, a 250-500 watt tungsten light source with simple lens focusing is useful. In photo-transient studies, flash lamps have been used.[10] For labs well endowed with funds, video cameras with TV monitors have been used to display the delightful psychedelic colors leading to 'black holes' formation in BLMs.

Instrumentation. Unmodified BLMs have very high electrical resistance. One critical factor is, therefore, how to measure BLM's exceedingly low current at a given applied voltage. If one is only interested in measuring the potential difference generated by a BLM, any good pH meter with a mV readout will do. For more advanced investigations of BLMs, for examples, such as membrane reconstitution and redox reaction experiments, commercial turnkey workstations are readily available. The levels of BLM currents range from picoamperes (pA) to microampere (μA) or more. To measure current at pA level, it is necessary to use I/V (current/voltage) convert of high sensitivity.

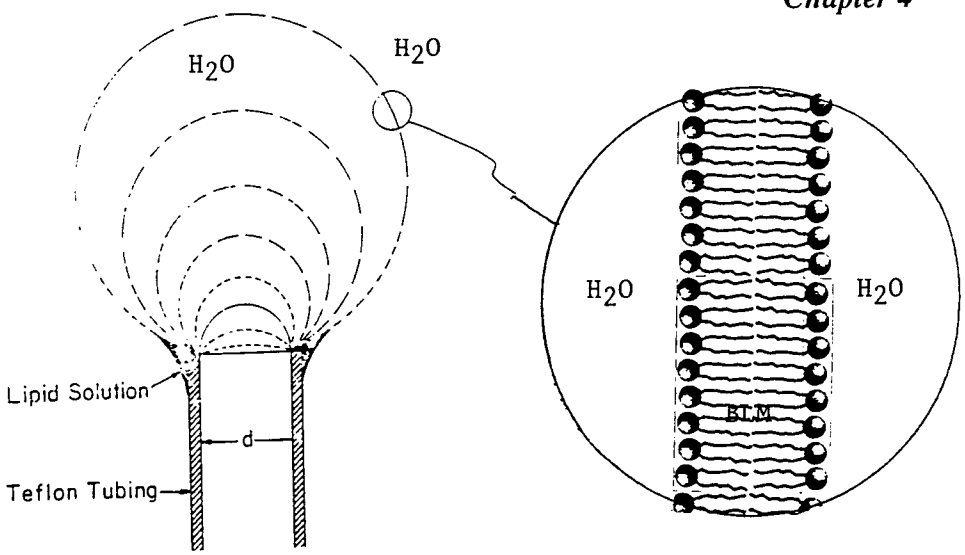

Fig. 4.4 A giant liposome used for studying mechanical and other properties of conventional BLMs.[11,51]

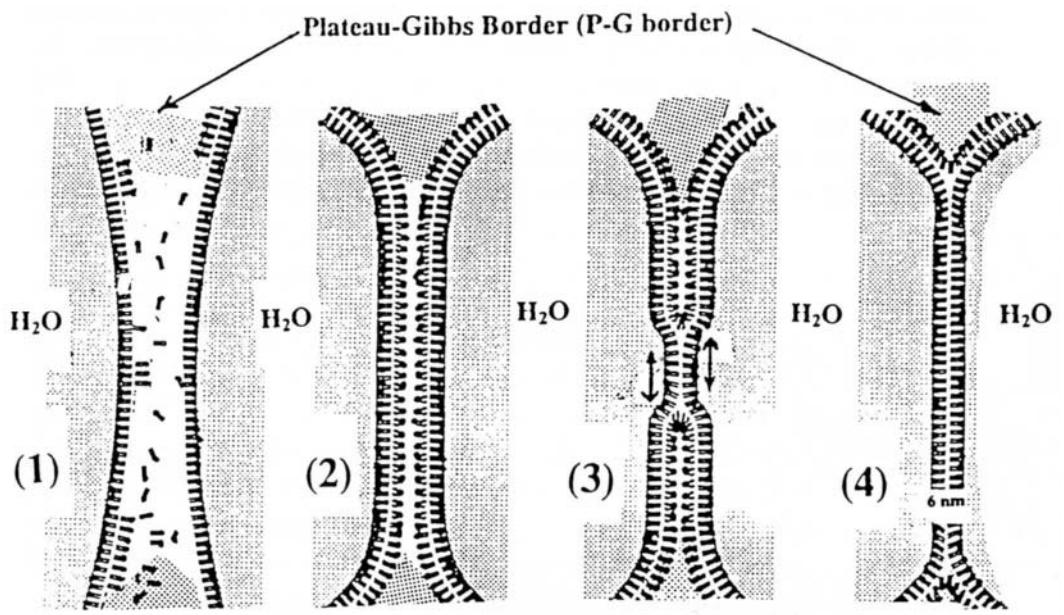

Fig. 4.5 Formation of a conventional BLM. Steps 1 to 4, a 'zipper-like' action is believed to be involved. For such a mechan-ism to work, the presence of a Plateau-Gibbs (P-G) border is essential.[25]

Faraday cage. Electrical stress is more lethal to the well being of a BLM, as compared to the mechanical vibration mentioned above. With the reference electrodes in place, and even with the lead cable well shielded, the BLM acts as a sensitive detector of electrostatics. A simple movement of a hand near the BLM may generate 10s to 100s of mV, which could easily exceed the breakdown voltage of a planar lipid bilayer. The problem can be solved simply by enclosing the BLM chambers and associated components in a Faraday cage made of copper mesh or sheet metal.[6]

In concluding this part, it should be mentioned that, with the advances in electronics, a number of 'turnkey' instruments can be purchased. For example, a commercial instrument designed specifically for the BLM research is available. The setup for measuring the electrical properties of BLMs consisted of an electroanalysis system (Model LB-BLM 1, Jinke Electronics, Ltd.) which include a function generator, a voltammetric analyzer, an electrometer and a picoampermeter. The system is used in conjunction with a printer/recorder and is controlled by a PC. The CV voltammogram may also be generated by means of a BLM simulator, a compact box containing various electrical components so connected for simulating the BLM system.[40,71] Further, this simulator covers various R_m, C_m,and their combinations ranging from 0 to 10^9 ohms and 0 to 30 μF, respectively. This so-called BLM simulator may also be used to test the measuring system as well as to check the reliability of the membrane model suggested in the experiments.

a. Formation techniques

The BLM separating two aqueous solutions may be formed using a number of methods including the brush technique, the dipping technique, the bubble technique, the syringe technique, and the monolayer technique. Conceptually and experimentally, preparation of a BLM is very simple; it involves the creation of two coexisting oil/water interfaces (or a biface) stabilized by appropriate amphipathic compound(s) such as phospholipids. Referring to Fig. 4.1, a 10 ml Teflon cup with a 1 mm hole in the side is held in a Lucite (plexiglass) block, which has two chambers of about the same volume. Both the cup and the chamber are filled with aqueous

solution. Next, a small amount of lipid solution is introduced in the hole with the aid of a small syringe or pipette. Since the area of a lipid membrane is usually small, it is necessary to observe it with a low power (20-60x) microscope in reflected white light.

The BLM of spherical configuration, or giant liposomes up to 1 cm or more in diameter shown in Fig. 4.4, can also be produced, as will be described later (Section 4.4). Contrasting to these giant BLMs, long-lived BLMs of μm diameter have been reported. These micro BLMs are made by filling the smooth circular pores of known diameter and density in a commercially available polycarbonate membrane (Nuclepore filters).[12-14] Under an ideal situation this new BLM system can be visualized as tens of thousands of micro BLMs simultaneously generated in the polycarbonate support. The membranes formed in this manner exhibit far superior stability and manipulability as well as having longer lifetimes and larger areas than can be achieved with a single BLM. The existence of an intact BLM is easily monitored by observing a change in electrical capacitance or resistance on the measuring instrument.

BLMs via Langmuir-Blodgett (L-B) technique. Conventional BLMs can also be formed by the L-B technique, first introduced by Tagaki et al. [see Tien, 1974]. Essentially, it is a combination of the monolayer technique and the dipping method.[18] A partition made from a sheet of Teflon (25-500 μm thick) with a hole (0.25-1 mm) at the center is placed between the two halves of a trough, with the hole above the aqueous phase. The trough is first filled with an aqueous solution. After the surface has been cleared, a monolayer of a suitable lipid solution is spread in the surface in the usual manner. After evaporation of the solvent, the Teflon partition is then lowered slowly into the aqueous solution. A BLM is thus formed over the hole (see Fig.4.5). Conversely, with the Teflon partition bearing a hole in place, the aqueous solution on either side is covered by a monolayer. Then, the levels of aqueous solutions are raised simultaneously above the hole thereby forming a BLM from the aposition of the hydrocarbon chains of the two lipid monolayers. Another variation of the monolayer-dipping technique is by having a closed chamber used in the water permeability studies. The closed chamber with an aperture on its side is held in place. The chamber, while immersed in aqueous solution below its aperture, is

filled completely with aqueous solution. A few drops of BLM-forming solution (n-hexane or n-octane as lipid solvent) is introduced to the surface of the outer aqueous solution. After the solvent has evaporated, the level of outer aqueous solution coated with a lipid monolayer is slowly lowered below the aperture and then raised carefully above it, thereby forming a BLM.

Osborn and Yager[15] reported the formation of planar solvent-free BLMs by the L-B transfer of monolayers to micromachined apertures in silicon. It should be mentioned, however, there is a major difference between the BLM and multilayers formed by the L-B technique. A BLM, formed either by the conventional 'painting' method or self-assembled on a substrate (e.g. a freshly cleaved metallic wire or agar gel, see Section 4.3) is a dynamic liquid-like structure that is capable of accommodating a host of modifiers. In contrast, a Langmuir-Blodgett multilayer of *bimolecular* thickness, albeit much more stable than a BLM, usually contains pinholes and is in a solid state. In this connection, efforts to stabilize BLMs by using polymerizable lipids have been successful. However, the electrochemical properties of these BLMs were greatly compromised. For example, ion channel phenomena could not be observed (*see* Chapter 7, *Membrane Physiology*)[16] Concerning this, Rolandi et al.[17] have reported the electrical properties of polymerized BLMs and found that polymerization in the alkyl chain of the lipid results in a stabilization of the BLM by a factor greater than three, whereas polymerization near the polar head group results in a minor improvement.

It should be mentioned as well that a conventional BLM can also be formed in a horizontal way, which was initially used to 'blow' a single, spherical BLM or a giant liposome.[11,18] The so-called 'solvent-free' BLMs, are a misnomer at best. For example, the L-B technique for planar BLM formation introduced by Tagaki et al. necessitates the pretreatment of the aperture by a lipid solution or petrolatum gel in order to form a stable BLM, which serves the function of a Plateau-Gibbs border.[18]

b. <u>BLM forming solutions</u>

Critical to the success of a stable BLM is the proper formulation of BLM-forming solutions. During the past decades of BLM research,

Table 4.1 Some Typical Lipid Solutions for BLM Formation*

Composition	Aqueous Phase	References
Bovine brain white matter extracts in various mixed solvents (squalene, tetradecane, etc.)	0.1 M KCl	*J. Phys. Chem.* **67** (1963) 534
Phosphatidylcholine (PC) (lecithin 2% in n-decane or squalene)	0.1 M KCl	
Glycerol mono-oleate (GMO) 0.016% + 0.6% cholesterol in n-decane	0.1 M KCl	*J. Coll. Interf.* **22** (1966) 438
Oxidized cholesterol (4%) in n-octane	0.001 to 0.1 M NaCl or KCl	*Nature*, **212** (1966) 718
Cationic, anionic, and non-ionic amphiphilic compounds and cholesterol	0.1 KCl Ringer's solution	*Nature*, **215** (1967) 1199
Chlorophylls, porphyrins visual pigments, etc.	various	*Nature*, **224**, (1969) 1107; **227**(1970)1232
PC + TCNQ or TTF in n-alkanes	various	*J. Phys. Chem.* **88** (1984) 3172
PC + C_{60} in Squalene + toluene		*Electroanalysis* **8** (1996) 1020

*For an extensive list of compounds and procedures, *see* [Davison, 1985; Ivanov, 1988, and references # 25-27]

Ivanov, 1988, and references # 25-27]
the choice depends on the interest and purpose of individual investigators. The widely used materials for BLM formation include synthetic lipids, oxidized cholesterol, interface-active agents, carotenoid pigments, and extracts of brains, eggs, chloroplasts, mitochondria, red blood cells, and of bacteria. In addition to these materials, liquid hydrocarbons (hexane to hexadecane, squalene, etc.) and/or other organic solvents (chloroform, methanol and butanol) are generally required. For new investigators, oxidized cholesterol is highly recommended.[6] This compound, although commercially available (P-L Biochemicals, Inc., Milwaukee, Wis.) is easily prepared by bubbling air or oxygen through a solution of 4% cholesterol in *n*-octane at reflux temperature (~ 125 ^{o}C) for about 4-6 hours, depending on air flow rates. BLMs formed from oxidized cholesterol solutions are known to be stable even after one month's storage.[7] Table 4.1 lists some typical solutions that are known to form fairly stable BLM.

c. Formation characteristics

With an appropriate lipid solution at hand and other apparatus properly arranged, as shown for example in Fig. 4.2, we are ready to observe an under water 'black soap film' or a BLM in formation. As mentioned above, a conventional BLM apparatus consists of two compartments each containing an aqueous bathing solution, usually 0.1 M KCl, separated by a hydrophobic septum. The septum contains a small hole approximately 1 mm or less in which the lipid bilayer will be formed. A lipid solution is applied to this hole using an artist's brush or a syringe with a short length of plastic tubing attached at its end. The process of forming a lipid bilayer in this way first begins with the formation of a thick lipid film. When first formed, the lipid membrane at the biface is usually thick (~ 1 μm), and interference colors may not be visible, as viewed through a 10-60 power microscope in reflected white light. Under suitable conditions, the thick lipid film begins to thin spontaneously. Interference colors soon appear as horizontal bands, at either the top or the bottom of the aperture, depending on the density of the solvent used for the lipid. Initially, only faint pinkish and greenish bands appear. These bands usually increase in breadth and brightness. At other times,

depending on the lipid solution, as the lipid membrane thins, bright swirling patterns of interference colors are displayed. Finally, the 'black holes' (not of the cosmic variety) are seen, either singly or several at once, growing at a fairly rapid rate. The appearance and rate of growth of 'black holes' depend greatly on experimental conditions.

These 'black holes' grow continuously until they cover the entire aperture, resulting in a black, bimolecular, or bilayer lipid membrane (hence the acronym BLM). When viewed by reflected light at a large angle of incidence, the BLM appears as a faint gray sheen. At random intervals colored spots swirl in the black membrane then disappear, demonstrating fluidity of the structure.[2,21] Thus, even to a cursory observer the formation characteristics of the lipid membranes in aqueous solution are strikingly similar to those of soap films in air.[22-24] These phenomena are not entirely unexpected, since, from structural points of view, both soap films and lipid membranes involve two interfaces (*see* Eqs. 4.1 and 4.2).

It should be pointed out once again the significance of the Plateau-Gibbs (P-G) border and the role it plays in BLMs, conventional or supported. The P-G border essentially connects and supports the bilayer membrane to the perimeter of the aperture. As the lipid layer thins, the molecules along with the solvent move from the relatively thick film to the Plateau-Gibbs border. It appears as a torus of lipids surrounding the BLM. Ultrathin lipid films of bimolecular thickness appear 'black' when viewed against a dark background because the light reflected from the front interface undergoes half a wavelength phase shift and interferes destructively with the light reflected from the back interface, which experiences essentially no phase shift. In contrast to L-B monolayers and multilayers, a BLM is a fluid-like, dynamic structure in a metastable state. The process of the BLM formation may be followed visually or by monitoring its electrical properties. During the initial thinning process the membrane exhibits "rainbow" colors that gradually give way to 'black holes'. These 'black holes' eventually coalesce to cover the aperture that separates the two aqueous chambers. This "black hole" formation can be accelerated by applying a voltage (50-100 mV) of short duration (a few msec).[10,20] Of importance to note here is that substances dissolved into the lipid solution (i.e. the P-G border that supports the BLM) will also be

present in the BLM, since the two are in equilibrium with each other. However, due to their differences in quantity, a small concentration changes in the P-G border will lead to a more significant change in the BLM. The most important and hardest variable to control is the actual BLM's composition. Theoretically, the quantity of lipids in the membrane can be estimated by obtaining the product of the membrane thickness and area. The area of the BLM may be estimated by optical and/or electrical methods. The area of the bilayer lipid membrane is very large in comparison to its relative volume and thickness. Therefore, the movement of substances between both aqueous medium and the membrane is very rapid. In fact, gradients of composition may actually exist between the center of the BLM and its P-G border.

As to the mechanism of BLM formation, it has been suggested that, in the final step of spontaneous thinning, a chance contact between the two monolayers situated at opposite sides of the lipid film, may initiate a process analogous to a 'zipper-like' action, leading eventually to the formation of a BLM (see Fig. 4.5). These chance contacts could come about from a number of causes such as thermal motion, mechanical vibration, impurities such as dust particles, and local variation of interfacial tension. The two key components of the thinning process are the actual BLM being formed and the Plateau-Gibbs border. This border serves to support the bilayer and also collects the lipids as they are removed from the lipid film during the thinning process. Stable cupola-shaped BLMs with mobile Plateau-Gibbs border have been reported by Antonov and colleagues.[43] They have found that changes in the lipid bilayer area depend on the temperature at the phase transition of the lipid. Additionally, by applying hydrostatic pressure, giant bilayers were obtained with an area up to two orders larger in magnitude compared with the initial area. Also, they reported a significant shrinkage of the bilayer at temperatures below the main phase transition. Since the BLM is in a dynamic equilibrium with the Plateau-Gibbs border at all times. a large number of molecules, providing various chemical and physical properties, are then incorporated into the lipid bilayer. These molecules are termed *modifiers*. A BLM is altered by adding a modifier to either the bathing solution or the BLM-forming solution. To make a significant change in the membrane composition, only trace amounts need to be added. We will

now in the next section consider the BLM modifiers whose presence in the lipid bilayer domain will transform an otherwise chemically inert structure into a dynamic entity that makes life as we know it more exciting.

4.2.3 Properties of BLMs

BLM Modifiers

A comparison of properties of BLMs, liquid hydrocarbons and biomembranes is presented in Table 4.2. A planar lipid bilayer formed from a typical phospholipid such as lecithin, oxidized cholesterol, or for that matter, formed from brain extracts possesses the following characteristics. Physically, such a BLM is self-sealing to puncture and liquid-crystalline in structure having a thickness about 6 nm. Electrically, an unmodified BLM interposed between two aqueous solutions (e.g. unbuffered 0.1 M NaCl or KCl) has a capacitance (C_m) about 0.5 $\mu F/cm^2$, resistance (R_m) greater than 10^8 ohm cm^2, and a dielectric breakdown strength (V_b) more than 250,000 V/cm. Additionally, a phospholipid BLM has a very low bifacial tension (<1 dyne/cm or interfacial free energy about 0.5 erg/cm^2), whereas it exhibits a relatively high permeability to water (~ 4 x 10^{-3} cm/s). Except the remarkable values for interfacial tension and water permeability, the other properties are to be expected for a liquid hydrocarbon layer of equivalent thickness. As we have discussed in Chapter 2, the lipid bilayer is the principal component of all biomembranes, while their functions come forth from other membrane constituents such as proteins, pigments, carbohydrates, and their lipid complexes. Thus, soon after the seminal work of self-assembling lipid bilayers (under water 'soap bubbles') was accomplished *in vitro*, Rudin and co-workers attempted to modify the basic properties of planar lipid bilayers with a large number of compounds including a proteineous material dubbed as EIM (exciting inducing material). Upon modification with the EIM, an otherwise electrically 'inert' BLM became excitable displaying characteristic features similar to those of the action potential of the nerve membrane.[2]

In the intervening years, a vast number of materials, natural and

synthetic, have been embedded into these so-called unmodified or 'pure' BLMs or planar lipid bilayers.[25-27] Materials include the following:

- polypetides, channel proteins, receptors, and tissue extracts
- pigments, electron acceptors, donors, and mediators, some of these are highly conjugated compounds such as meso-tetraphenylporphyrins (TPP), metallo-phthalocyanines (PLC), TCNQ (tetracyano-p-quinodimethane), TTF (tetrathiafulvalene), and fullerenes (C_{60}, C_{70})
- redox proteins and metalloproteins such as cytochrome c, and iron-sulphur proteins (ferrodoxins and thioredoxins)
- inorganic semiconductors, nanoparticles (Chapters 9 and 10)
- stuff partaking in ligand-receptor contact interactions (Chapters 7-10).

In the last mentioned category, the ligand may be a substrate, an antigen, a hormone, an ion, or electron acceptor or donor, and the corresponding receptor embedded in the BLM may be an enzyme, an antibody, a protein complex, or a carrier.

Methods of Embedding

As summarized in Table 4.3, there are four principal methods for incorporating non-lipid materials into BLM. The ultimate aim of these methods is to reconstitute cell membrane *in vitro* so that the structural-functional aspects of biological membranes may be understood in physico-chemical terms at the molecular level. The absorption method, being the first developed, has been the one more extensively employed than the other three.[2] The monolayer-bilayer interaction method and its variations are based on the formation of a monolayer at the air/water interface. The essential feature consists of the adsorption of non-lipid material on preformed monolayers. This otherwise elegant technique is marred by difficulties in forming planar BLM from monolayers. Hence, only a few studies have been reported. The third method based on lipid-protein complex dispersion is traceable to the procedure due to Folch-Pi, who used a chloroform-methanol mixture to extract brain proteolipids [Tien, 1974]. The addition of surfactant and/or use of sonication greatly enhance

Table 4.2 Comparison of properties of BLMs, liquid hydrocarbons and biomembranes[51]

Property	Unmodified BLMs	Liquid Hydrocarbons	Biomembranes	Modified BLMs
Thickness (nm)	4-10	10	5-7	5-7
Resistance (ohm cm)	$> 10^8$	$> 10^9$	$10^3 - 10^5$	$10^3 - 10^5$
Capacitance(μF cm^{-2})	0.4-1	1	1	0.5-1
Breakdown V (V/cm)	$10^5 - 10^6$	$10^5 - 10^6$	$10^5 - 10^6$	$10^4 - 10^6$
Die-lectric const.	2-5	2-3	2.5-5	2.5-5
Refractive index	1.4-1.6	1.4-1.6	1.6	1.37-1.66
Water Perm. (μM/s)	8-24	35	0.25-400	8-50
Interfacial tension (ergs/cm^2)	0.2-6	50	0.03-3	0.1-6
Membrane Potential (mV)	0	0	0-70	0-100
Electrical Excitability	no	no	yes	yes
Redox reactions	no	no	yes	yes
Photoeffects	no	no	yes	yes
Electronic (non-linear)	no	no	yes	yes

the attractiveness of the method. With a judicious selection of organic solvents (butanol, hexane, ether, etc.) to preserve the biological activity, this method definitely has many advantages over the two just described. The BLM-liposome fusion method is a combination of the adsorption and dispersion methods. Proteins or lipid-protein complexes are first incorporated into liposomes by sonication and subsequently transferred to the BLM by fusion. That is, a fusion of two BLMs is involved. For this fusion process to occur, certain divalent cations such as Ca^{2+} and Mg^{2+} are beneficial. A suggested mechanism is that, as a result of the osmotic swelling of liposomes in contact with a BLM, and subsequent fusion, is responsible. At physiological pH, the surfaces of membranes are negatively charged, hence fusion may also be facilitated through electrostatic interactions (Table 4.3).

The membrane constituent(s) to be incorporated into the lipid bilayer may be added to the lipid solution prior to the assembly of the BLM. If modification is desired after the BLM has formed, then the modifier may be added to the bathing solution. The bilayer membrane can be sufficiently modified by the addition of only trace amounts of the modifier. The reason for this is a result of the large ratio between the surface area and thickness of the BLM. Proteins including ion-channel formers may be reconstituted in the BLM by incorporating the protein first in a liposome then by fusing it with the BLM, which takes place readily. In a sense, the lipid bilayer as existing in BLMs and liposomes may be considered as a solvent for a number of hydrophobic materials including pigments, receptors, channels, carriers, and fullerene C_{60}. In this connection it should be mentioned that unmodified or pure liposomes can also induce channel-like activities in BLMs.[25-27]

Many materials of interest may be incorporated into cells via a phenomenon known as *electroporation* and has been reported by a number of investigators[28-31] and elegantly discussed.[29] This phenomenon usually occurs by applying electric pulses up to 10^6 V/cm with a duration between μsec and msec to membranes including BLMs and liposomes in close contact. One of practical applications is cell transfection for transient gene expression. Other applications include encapsulation of drugs in controlled-release and insertion of proteins in living cells.[80-83] For

example, Genco and colleagues reported electroporation in symmetric and

Table 4.3

Techniques for the incorporation of non-lipid materials into BLMs

Method	Description	Examples	References
Absorption	A BLM is first formed; this is followed by adding non-lipid material to one side of the bathing solution	EIM Surfactants	Mueller et al.,1962; Tien, 1974
Monolayer-bilayer interaction	A BLM is formed by two adjoining monolayers at air/H_2O interface, with the aqueous solution containing non-lipid material	Rhodopsin	Takagi et al., 1965; Tien, 1974
Lipid-protein complex dispersion	Non-lipid material and lipid are co-dispersed in organic solvents by sonication, from which a non-lipid containing BLM is formed		Schein et al., 1976; Stillwell and Tien, 1981; Lopez & Tien, 1980
BLM-liposome fusion	A BLM is first formed; non-lipid material are then added to the solution complexes		Miller & Racker1976
		Bacteriorhodopsin containing liposomes	Rayfield, 1982; Duzgunes and Ohki, 1981 Gyulkhandanyan & Manukian, 1982

asymmetric BLMs.[30] In this connection, mention should be made concerning the work reported by Troiano and associates.[31] They studied the effects of a nonionic surfactant, octaethyleneglycol mono n-dodecyl ether (C12E8), on the electroporation of planar lipid bilayers formed from the synthetic lipid 1-pamitoyl 2-oleoyl phosphatidylcholine (POPC). When high-amplitude rectangular voltage pulses (~ 100-450 mV) were used to electroporate the BLMs, followed by a prolonged, low-amplitude (65 mV) voltage clamp to monitor the ensuing changes in transmembrane conductance, they found that the addition of C12E8 at concentrations of μM to the solution surrounding the membranes decreased the electroporation threshold monotonically. Using a different surfactant (Poloxamer 188), Tung and associates[31] have discussed in an earlier paper the dramatic effects of the compound on the BLM's capacitance, suggesting that surfactants can be used to manipulate the electroporation threshold of lipid bilayers and their usefulness in the *in vivo* chemical treatment of tissues to reduce electrical shock-induced injury.

Measurements with a modified BLM can begin once the electrical parameters such as membrane resistance or capacitance have reached a steady-state value. Changes regarding membrane properties in response to a stimulus from the bathing solution may change the electrical potential across the lipid bilayer that will generate a signal to be sensed by the BLM. In the paragraphs below, a consideration of several BLM parameters are discussed.

a. Optical Properties

There are two optical parameters, which must generally be provided for, in any conventional BLM system: an optical path for visualization of the membrane and provision of shielding to eliminate extraneous light. Visualization of the membrane requires an optical path such that the incident and reflected light ray lie in a plane that is perpendicular to the plane of the BLM. Shielding can be accomplished by painting the apparatus black, or by constructing the apparatus of black Lucite (or black Delrin plastic). Where possible, optical surfaces should be inclined to prevent spurious reflections, and stray or transmitted light from the light source should be trapped. The color and intensity of light

reflected from a BLM depends on its constituent molecules. Techniques have been developed for measuring BLM thickness and refractive index based on reflectance measurements. Optical reflectance when used in conjunction with electrical methods can be used to investigate the structure of BLM. For reflectance measurements, any intense and stable white light source may be used, in combination with an interference filter. With the availability of lasers, the light beam can be focused to a very small spot (0.02 mm). Further, the advantage of high intensity and long-term stability makes laser a superior light source.

The hole (0.1-3 mm diameter) for the BLM is bored in the side of the Teflon beaker (10 ml) below the level to which the aqueous solution is added. The BLM is formed by applying a small amount of the lipid solution across the hole with the aid of a microsyringe with dispenser. To view both the membrane and to measure its reflectance, the microscope-detector is adjusted. The membrane thins spontaneously, first to a thickness about the wavelength of light, then to a thickness less than 100 nm, and finally to an ultrathin film which is about 0.01 of the wavelength of light. When the membrane has reached a thickness of about 200 nm, observation through the microscope at an angle with the normal to the membrane that is equal to the angle of incidence of the illuminating light exhibits interference fringes.

The thickness of a BLM can be measured by three different methods, which give values in fairly good agreement. These methods are (i) the reflectance method, (ii) the electrical method, and (iii) the electron microscopy method. The electron microscopy of BLM is a complicated and involved procedure, and the results obtained are subject to artifacts. The other two methods are generally preferred, but important parameters of dielectric constant and refractive index of the BLM are uncertain. It should also be mentioned that for a membrane about two molecules thick, the meaning of dielectric constant (and refractive index) is ambiguous, since these quantities refer to macroscopic systems.

The BLM thickness is determined from the reflectance measurements, using either a homogenous, single-layer model, or an inhomogeneous, triple-layer model. In the single-layer model, it is

necessary to assume that the membrane is isotropic and transparent, and either to determine the refractive index of the membrane, by measurements of the Brewster angle, or assuming a value for the refractive index (n_b). In the triple-layer model, the polar portions of the lipid molecule situated at the biface are regarded as having a thickness, t_p and a refractive index n_p, and the liquid hydrocarbon core is regarded as having a thickness t_h and a refractive index n_h. The overall BLM thickness, t_m, is thus equal to $(2t_p + t_h)$. According to the definitions used in thin film optics, a thin film is a layer with parallel faces whose thickness is of the order of the wavelength (λ) of light used. An ultrathin film has a thickness less than 0.01λ. By this definition BLMs belong properly to the class of ultrathin films. Hence, the optical properties of lipid membranes in aqueous solution are fundamentally similar to those of ultrathin transparent solid and black soap films. Theoretical considerations developed for the latter are logically extended to the BLM system.[10]

It should be mentioned that for supported BLMs, it has not been possible to observe the formation characteristics visually.

b. Mechanical Properties

In order to appreciate the formation characteristics and stability of BLMs, a basic knowledge of the nature of aqueous solution/BLM bifaces as well as the BLM itself is required. The problem of dynamic changes in the mechanical properties of lipid bilayers have been studied [Hianik and Passechnik, 1995]. At present, the most well-known mechanical property accessible to direct experimental measurement is the bifacial tension of the BLM. Since a BLM possesses a biface (meaning two coexisting *aqueous solution / membrane / aqueous solution* interfaces. *See* Section 3.3.4, Chapter 3), a modified maximum bubble pressure method has been used.[10] A BLM is formed on a 2 mm hole separating two aqueous solutions, each of which is connected to one side of a differential pressure transducer. The hydrostatic pressure on one side is increased until the BLM becomes hemispherical, at which point the bifacial tension can be determined..

In a different approach, the communicative function between two BLMs may be studied by a number of investigators.[32] Melikyan et al.[33]

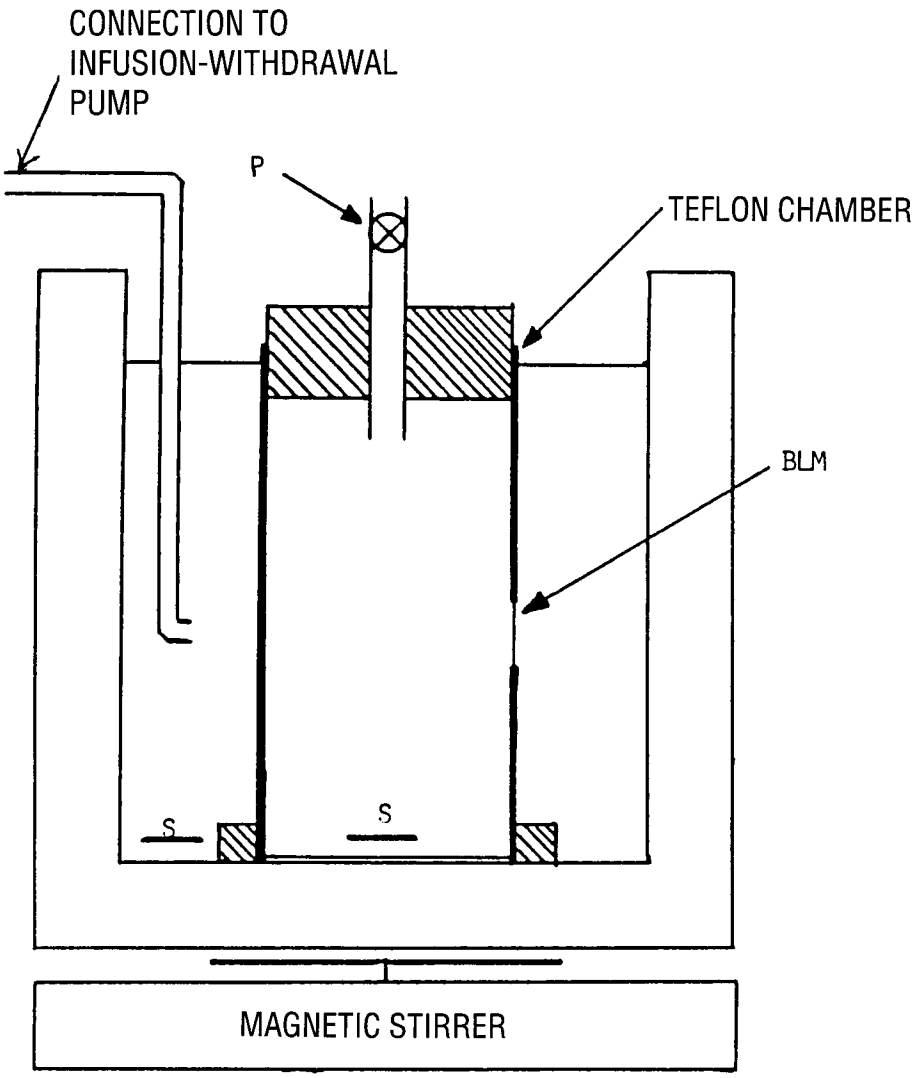

Fig. 4.6 A cell chamber used for permeability measurements. P, to micrometer; S, stairring bar; A connection is made to the outer chamber by an infusion-withdrawal pump, which permits the formation of a BLM from monolayers.[51]

investigated the fusion of two BLMs and proposed a method for measuring the BLM's interfacial tension. Concerning interfacial tension measurements and related properties, Winterhalter and Helfrich[34] and others[35,64] have reported interesting findings. For instance, Feller and Pastor[35] have carried out computer simulations of lipid bilayers with applied surface tensions and contended that the surface tension evaluated from a simulation is expected to be significantly greater than the macroscopic surface tension. They conclude that an applied non-zero surface tension is required when modeling (see Section on Molecular Dynamics Simulations of Planar Lipid Bilayers below). Regarding these highly physical studies, Fang and Yang[36] reported the growth of bilayer defects and the induction of interdigitated domains in the lipid-loss process of supported phospholipid bilayer. The lipid-loss process has been studied with in situ atomic force microscopy (AFM) at six different temperatures for supported dipalmitoylphosphatidylcholine (DPPC) bilayers. A typical structural characteristic is the creation and the growth of bilayer defects as lipid molecules are lost from the bilayer. The rate of the lipid loss has an Arrhenius behavior, with an activation energy of 37 kT, where kT is the thermal energy at room temperature. For the lipid-loss processes at temperatures above 45° C, interdigitated membrane domains are induced and are mostly in contact with some bilayer defects. These domains disappear at the increase of the area of bilayer defects. Possible mechanisms of these phenomena are also discussed.

c. Permeation and Transport Properties

An unmodified BLM is effectively impermeable to solute, but fairly permeable to water.[21] Therefore an osmotic gradient will parallel the existence of any concentration gradient across the membrane. Experimentally, a cell of the type shown in Fig. 4.6 is often used for the osmotic flux measurements. The cell consists of a closed inner chamber, made from a 5-10 ml Teflon beaker. The volume of the inner compartment can be adjusted by manipulation of a precision micrometer syringe. After the membrane has become 'black' (optically non-reflective), a known quantity of a concentrated salt solution is added to the outer compartment. The osmotic pressure gradient will cause the efflux of water, from the inner chamber across the BLM into the outer solution. This efflux is

manifested by the inward bulging of the BLM. The BLM is observed visually, and a planar membrane of constant pattern of reflected light is maintained by manipulating the micrometer syringe. The rate of water flux is determined. From this rate, the permeability coefficient is then calculated. For the details of techniques and apparatus, consult the original references [Davison, 1985;1992].

d. Electrical Properties

An unmodified BLM displays a high D.C. resistance and low permeability for ions. The electrical properties of BLM are usually measured under direct current. A small voltage is impressed across the BLM separating two aqueous solutions via a pair of reversible electrodes. Briefly, a known voltage is applied to the input resistors, the BLM, aqueous solutions, and the electrodes. The portion of this voltage across the BLM is monitored with a high impedance electrometer, and is recorded. A low impedance picoammeter may also be connected in series to the BLM. The general arrangements of the cell, for measurements of electrical properties are shown in Figs. 4.2 and 4.3, may be represented as follows:

(left-side or outer chamber) | | *(right-side or inner chamber)*
ref. electrode | *aq. solution* | ***BLM*** | *aq. solution* | *ref. electrode* (4.3)

The aqueous solutions serve essentially as ohmic contacts to the membrane, and salt bridges are used to avoid possible contamination. In the circuit shown in Fig.4.7, the resistor (R_i) can be selected as 0 or 10^5 - 10^{10} ohms by factors of 10. The applied voltage (E_i) can be variable from ± 1000 mV. The BLM is represented by an equivalent circuit consisting of a capacitor (C_m) in parallel with a resistor (R_m) and the BLM voltage (E_m). Thus, the voltage (E) is related to the other parameters in the circuit by

$$E = \frac{E_m}{R_m/(R_m + R_i)} - \frac{E_i}{1 + R_i/R_m} \qquad (4.4)$$

If R_i is much larger than R_m, which is done in practice by setting it at infinity, one will measure E_m. If R_m is much larger than R_i, one can obtain the applied voltage at intermittent values for R_i and obtain several values for the BLM resistance through the equation

$$R_m = R_i \frac{E_m - E}{E + E_i} \tag{4.5}$$

The capacitance of the BLM can be obtained by measuring the RC decay curve. For a given charging curve, one obtains

$$E(t) = E_{max} [1 - \exp (- \frac{t}{R_p C_m})] \tag{4.6}$$

where E(t) is the charging curve voltage at time t, E_{max} is the final charging curve voltage, and $R_p = (R_i R_m)/(R_i + R_m)$. The voltage change appeared across the BLM and C_m is then calculated by the equation

$$C_m = \frac{t}{\ln [1-E(t)/E_{max}] R_p} \tag{4.7}$$

With a pair of reference electrodes in place as shown in Fig. 4.1, electrical properties of the BLM may be measured with various instrumentation, ranging from a pH meter to a PC-controlled workstation. Often times, home-assembled components have worked very well in many laboratories.[71] For BLM experiments involving cyclic voltammetry (CV), to be considered in the next section (also in Chapter 6, Membrane Electrochemistry), a Lucite block containing two adjacent 2 cm diameter chambers, one of which holds a 10 ml Teflon cup, has been used. The Teflon cup is referred to as the inside, and the other chamber as the

outside. A three-electrode system for obtaining voltammograms has been used in the following configuration: one calomel electrode (SCE) is placed in the Teflon cup and two other calomel electrodes are on the outside. For investigating membrane reconstitution, electrical and other properties of BLMs, both simple and advanced instrumentation have been employed.[6,40]

The voltammograms of the BLM are obtained using an X-Y recorder fed by a picoammeter and the voltage generator (e.g. Princeton Applied Research, Universal Programmer, Model 175). The voltage from the programmer is applied through the potentiometer to the calomel electrode (SCE) immersed in the inside solution. Another SCE immersed in the outside solution is connected to the picoammeter. The important feature of the setup is a very weak dependence of its input voltage on the current being measured. This means that the current is measured under 'voltage clamp' with accuracy $\pm$ 1 mV. A three-electrode system for obtaining voltammograms has the following configuration: one calomel electrode (SCE) is placed in the Teflon cup and two other calomel electrodes are on the outside, one of which may be an Ag/AgCl reference electrode .

Cyclic Voltammetry of Planar Lipid Bilayers (BLMs)

Insulating nature of the lipid bilayer. Before discussing the application of cyclic voltammetry to BLM research, let us consider two factors: the non-conducting nature and intrinsic electrical conductivity of the lipid bilayer. As already mentioned, unmodified BLMs (i.e. formed from either phospholipids or oxidized cholesterol) have exceedingly high electrical resistance ($> 10^8\ \Omega\ cm^2$) and capacitance ($\sim 0.5\ \mu F\ cm^{-2}$). These findings are consistent with the electrical equivalent circuit of a parallel resistor and a capacitor (Chapter 2, Fricke's experiments on erythrocytes). The very high resistance value of unmodified BLMs reflects the insulating nature of the lipid bilayer. Hydrated ions such as Na^+, K^+, and Cl^- are not able to diffuse freely across the lipid bilayer for which presents a gigantic energy barrier. This was first analyzed by Finkelstein and Cass[19] using the Born equation which is given by

$$E_{(r)} = -\frac{q^2}{2r}\left(\frac{1}{\varepsilon^o} - \frac{1}{\varepsilon^w}\right) \qquad (4.8)$$

where $E_{(r)}$ represents the free energy of solvation (ΔG), necessary to transfer a charge, q, associated with an ion with a radius r, from a medium of dielectric constant (ε^w) to one of ε^o. (For those interested in a detailed account of applying the Born equation, see Volkov et al., 1998, cited in Chapter 1). To appreciate Eq. 4.8, we need to substitute known values for ion size r, electrical charge q, dielectric constant for water ($\varepsilon^w = 80$), and for oil or the lipid bilayer ($\varepsilon^o \simeq 2$). As an approximation, $E \simeq 50$ kcal/mol. This high value of Born energy translates to mean a very low probability (as related by the Boltzmann's distribution law) of about 10^{-40} for an ion to be in the lipid bilayer or oil phase. That is why a hydrated ion prefers to be in an aqueous environment. On the other hand, the Boltzmann's law states

$$C^o = C^w e^{-E(r)/kT} \qquad (4.9)$$

where C^o and C^w are, respectively, the concentration of ions in oil and water, k is the Boltzmann constant, and T is the absolute temperature. Hence, if the size of r is changed, say, from 0.2 nm to 0.6 nm, there is a profound effect on E, which in turn alters the probability (or partition coefficient, $P = C^o/C^w$) by a factor of 10^{17}!

The very high electrical capacitance of the BLM is the result of its ultrathin lipid bilayer structure, as can be seen from the parallel plate condenser formula (Eq. 2.2, Chapter 2). Other physical properties, in addition to electrical parameters, of unmodified BLMs are given in Table 4.2. Note the breakdown voltage (V_b) of unmodified BLMs, which is determined by applying a potential difference across the lipid bilayer until the membrane ruptures, is greater than 250,000 volts/cm. This significant fact of V_b has been investigated by several researchers[10] and is useful in the technique of electroporation and transfection studies, as already alluded to above.[28-31] It is worth noting here that under applied voltages greater than 150 mV (field strength $\cong 3 \times 10^5$ V/cm) a significant increase of BLM conductance is often observed. This is explained in terms of 'transient' pores that are being created under high field strength in the

BLM. The simple Ohm's law is no longer obeyed, which often leads to the rupture of the lipid bilayer.

Intrinsic electrical conductivity of the lipid bilayer. Upon inspection of Table 4.2, another anomaly, besides dielectric breakdown strength, is noted. It is the permeability of unmodified BLMs to water, which is comparable to biomembranes. This being so is consistent with the relatively high water solubility in liquid hydrocarbons (*see* Chapter 5, *Membrane Transport*).[21] Assuming water dissociates according to the usual equation:

$$H_2O \longrightarrow H^+ + OH^- \qquad (4.10)$$

where at room temperature $K_{sp} = [H^+]\,[OH^-] = 10^{-14}$. Hence the quantity of ions available for charge transport should be on the order of 10^9 ions. An even greater amount of ions may be present in the BLM under high field strength conditions.[13] Hence, the intrinsic electrical conductance of the BLM may very well be due to dissociated H^+ and OH^- ions in the lipid bilayer.

Cyclic Voltammetry. Having covered the two basic properties of the BLM, we are now ready to continue our consideration on the application of cyclic voltammetry to lipid bilayer research. In voltammetry, the potential of the cell is varied and the corresponding current is monitored. One type of voltammetry is called cyclic voltammetry (CV) and employs a triangular voltage waveform. As a means of investigating redox reactions, CV has been widely used and has been termed the equivalent of spectroscopy.[25] The graph with the current plotted on the vertical axis vs. the potential on the horizontal axis is called the voltammogram, which is characterized by several parameters. The working electrode (WE) may be made of Pt, Au, or carbon paste, glassy carbon, or SnO_2. An Ag/AgCl or a saturated calomel electrode (SCE) is used as the reference electrode (RE). The potential scan or sweep is carried out between two potential values of interest (e.g. from about 1.2 to -0.8 V vs. SCE). The scan rates can be anywhere from 0.1 mV to 100 V or more per second but values between 10 mV to 400 mV s^{-1} are frequently used. The current response of

processes at a metal electrode are indicative of the nature of the redox reaction at the interface. Experimental results derived from measurements of this kind permit the elucidation of mechanism and the thermodynamic parameters of the process (e.g. charge transfer reaction). Frequently a 'duck-shaped' voltammogram is obtained for redox reactions. The underlying physical mechanism responsible for the 'duck-shaped' profile is based on the interplay between the kinetics of the charge transfer process and mass transport of the charge carriers (oxidants and reductants). These basics of CV and its elegance and simplicity are well known to electrochemists.[37,39]

By treating a modified BLM-containing TCNQ (see Table 4.1) as a bipolar redox electrode, the powerful CV technique was applied in 1984 for the first time to lipid bilayer studies with stimulating results. For example, in the presence of ascorbic acid in the outer solution and equal molar ferri/ferro cyanide in the inside (*see* Eq. 4.3), the observed electrical properties are such with R_m decreasing by 2 orders of magnitude, C_m increasing by 25%, E_m developing from zero to about 180 mV, and with the ascorbic acid side positive. The highly asymmetrical current/voltage curves (voltammograms) are reminiscent of those of a *p-n* junction diode that permits an electron current in a forward-bias direction only. The peak current (i) for the transfer of charges from one side of the BLM to the other side is given by

$$i = k\, n^{3/2}\, A\, D^{1/2}\, \upsilon^{1/2}\, C \qquad (4.11)$$

where k is a constant, n is the charge of the species, A is the interfacial area, D is the diffusion coefficient, v is the scan rate (mV/s), and C is the concentration of the redox species in solution.

The CV technique has been used in studying many BLM-based systems,[39-42] the details of which will be taken up in Chapter 6 (Membrane Electrochemistry).

Relaxation studies of ion transport in BLMs. For investigating ion transport processes in BLMs, relaxation techniques have been used in

recent years.[16,44] The essential feature of relaxation techniques is that an external variable such as temperature or voltage is quickly altered and the time course of an internal parameter of the system such as concentration or transmembrane current is measured, while the system relaxes toward a new steady state. For the generation of the voltage jump commercial signal generators are available (< 10 nsec risetimes). The resolution required to record single channel events, requires careful electronic design and extensive shielding, since current pulses of about 10 pA amplitude and msec duration from a source impedance of about 10^6 megaohms. The time resolution of the voltage-jump method is restricted, however, by the R_mC_m of the BLM, which is as usual represented by a simple equivalent circuit of a parallel arrangement of the membrane resistance ($R_m = 10^5 - 10^9$ Ω cm^2) and the membrane capacitance ($C_m = 0.3 - 0.8$ μF cm^{-2}). This gives R_mC_m in the range of 0.8 to 3 sec. The higher value is the actual time-resolution of the voltage-jump current-relaxation technique, since the charging current has to decline to a small fraction of the crucial value before relaxation currents can be measured. A variation of the voltage-jump technique is the so-called voltage-clamp method used extensively in electrophysiology (*see* Chapter 7, Membrane Physiology). In this case the BLM voltage is kept constant, which is most effectively controlled by a negative feedback circuit, while the current time course which reflects the change of BLM resistance is monitored.[16,44] Another technique is the charge-pulse voltage relaxation method in which the BLM capacitance is charged to some initial voltage (10 mV) by a short current pulse of 10-100 nsec duration and then switched to essentially infinite resistance (open-circuit). A commercial pulse generator with a short risetime and a low output impedance may be used. Alternatively, a high input impedance electrometer or a fast FET switch which has an impedance greater than 10^{12} ohms in the open-state and less than 100 ohms in the closed state may be used. The time course of voltage decay, which results from transmembrane charge movement is recorded. The actual time resolution by this technique is limited by the bandwidth of the voltage amplifier and stray capacitance of the circuit. Also the photoeffects in pigmented BLMs which result from light flashes have been investigated by these relaxation techniques (*see* Chapter 9, *Membrane Photobiology*). The light-induced signal may be recorded either in the form of photovoltage under open-

circuit conditions or as a photocurrent with short-circuited external solutions. The kinetics of the pigmented BLM can be investigated by recording either the transient voltage or current signals following the flash. In principle both techniques provide the same information.

AC Impedance Spectroscopy of Lipid Bilayers. It is worth pointing out that, although D.C. measurements have the inherent advantages such as simple instruments and straight forward interpretation, the dynamics of transport processes are not readily accessible. Therefore, AC impedance spectroscopy methods have also been used. For example, a frequency range of 0.2 kHz to 1000kHz, a capacitance bridge is coupled to an external oscillator. Sometimes electrical connection to the aqueous solutions is made via two sheet Pt electrodes (1 cm^2) coated with Pt black, or Ag/AgCl electrodes [Tien, 1974]. Impedance spectroscopy, also referred to as EIS (electrochemical impedance spectroscopy), is a well established technique for investigating the dynamics of membranes including planar lipid bilayers and spherical liposomes.[45-49] The principle of the EIS technique is based on the choice of an appropriate equivalent circuit, which represents the main features of the membrane system. The instrumentation for AC impedance spectroscopy is a gain/phase analyzer (Solartron Instruments, UK) controlled by a personal computer. In recent experiments using the EIS technique, for example, Alonso-Romanowski et al.[45] reported a BLM-containing gramicidin-A that exhibits two time constants, one of which can be assigned to the BLM and the other to the channel-BLM contributions, whereas Vallejo and colleagues[46] investigated the ion transport in the same type of channels in liposomes as a function of temperature. Earlier, Yamada et al.[41] have studied electron transfer with three different redox couples through a BLM-containing TCNQ using AC impedance spectroscopy. It is claimed[46] that the impedance spectroscopy technique can resolve perturbations in the molecular organization of membranes down to 0.1 nm resolution, and may be used to monitor perturbations in the molecular structure due to external influences (e.g. the presence of pharmacologically active molecules in the external environment adjacent to the membrane). This technique is being used to study the dielectric properties of proteins. Also applicable are examinations of the effects of intense electric fields on cells and cell membranes, electro-mechanical properties and stability of biomembranes,

electrical breakdown phenomena and electroporatiion,[28-31] as already mentioned above. We shall see in Chapter 10 (*Applications*) how a combined AC-DC method may be applied to supported BLMs.

Molecular Dynamics Simulations of Lipid Bilayers. The structure of BLMs, which serve as important model biomembranes, is very difficult to determine experimentally because of their fluidity and disorder. As discussed by Feller and colleagues,[35] the techniques mentioned in Chapter 2 (Section 2.4) such as Nuclear Magnetic Resonance (NMR) experiments can probe the average orientation of the CH vectors in the hydrophobic chains of the lipid molecule and X-ray Diffraction experiments can give a profile of the electron density as a function of position in the direction normal to the membrane surface, but neither can probe the absolute value of the lateral separation between lipids, i.e. the surface area per lipid molecule. Estimates, based on models used to interpret the X-ray or NMR data, vary widely even for fully hydrated dipalmitoylphosphatidylcholine (DPPC), the most extensively studied lipid bilayer system. Thus, a more sophisticated technique, known as molecular dynamics (MD) is needed, the results of which will be used in the interpretation of NMR experiments that probe the dynamics of lipid motion.. Feller, Zhang, and Pastor[35] carried out a series of MD simulations of lipid bilayers at areas per molecule of 62.9, 65.5, and 68.1 $Å^2$/molecule and concluded that from their MD data that changes in area of a few square $Å^2$ led to observable differences in the simulation results. Comparison of the simulation results for the three different surface areas showed that the simulation is consistent with the experimentally determined order parameters and diffraction profile at an area of 62.9 $Å^2$/molecule. Interested readers should consult their latest publications. It is worth noting here that a 60 $Å^2$/molecule for the phospholipid is typically assumed for the BLM.[10,51]

e. Light-Induced Effects in Pigmented BLMs

The photoelectric effects in pigmented bilayer lipid membranes (p-BLMs for short) was discovered in 1968 and subsequently used to elucidate the mechanisms of photosynthesis,[18,51-59] in particular the primary quantum conversion step, in which light-induced charge separation into electrons and holes led to redox reactions on the opposite side of the BLM. This is so principally owing to the ultrathin lipid bilayer

(~5 nm) which can withstand an electric field strength of more than 250,000 volts/cm. Further, the insulating nature of the lipid bilayer (an unmodified BLM's typical resistance is greater than 10^9 Ω cm^2) prevents the thermodynamically favored back reaction (i.e. electron and hole recombination), which otherwise would not be possible in the production of oxygen and carbohydrate in the natural photosynthesis. Thus, on the basis of pigmented BLM studies over the past decades, numerous investigators have been attempting some practical applications by mimicking natural visual receptor and photosynthetic membranes for solar energy utilization, as evidenced by many publications.[10] As a recent example, the retina of the eye contains a transparent and weakly reflecting structure known as the retinal nerve fiber layer (RNFL). In order to gain insight into the spectral and directional reflectance of the RNFL, Zhou and Knighton[83] have developed a numerical method to calculate the scattered field from complex cylindrical membranes that are thin relative to wavelength with a reflective index close to that of the medium. It is said that their method is applicable to light scattering by cell membranes in bundles of nerve axons. In this connection artificial retinal membranes using BLMs have been reported by Yamaguchi and Nakanishi,[84] who have paid special attention to the preparation and characterization of a planar BLM for the visual process.

In the mid 1980s, electron transfer in the dark was demonstrated in BLMs doped with either organic 'metals" or semiconducting nanoparticles formed *in situ*. These phenomena were explained in terms of light-induced charge separation, field-driven charge transport and subsequent redox reactions on opposite sides of the BLM. In the absence of light, the theory of electron tunneling was invoked.[10] (see above on the TCNQ-containing BLMs[41,42]). When a s-BLM doped with Zn-phthalocyanine was excited by light, a voltage and a current were recorded, with the action spectra paralleled closely to that of the absorption spectrum of the photoabsorber.[51] In this connection, Bianco and Haladjian[85] have reported the electron transfer reactions between c-types of cytochromes and a lipid-modified electrode. In view of the sensitivity and sophistication of spectroscopy techniques, and their utility in elucidating certain aspects of the structure and dynamics of membranes, attempts have been made to apply absorption, fluorescence, and impedance spectroscopy (see the

paragraphs above) to the BLM system. Additionally, by combining electrical methods with those of spectroscopy, a photoelectric action spectrum of a pigmented BLM may be obtained. This technique of measuring action spectra of pigmented membranes, termed ***photoelectrospectrometry***,[50] is several orders of magnitude more sensitive than conventional absorption spectroscopy. Photoelectric effects from BLM in the presence of pigments and dyes may be investigated by two basic types of setups. One type uses the electrometers to detect the so-called open-circuit voltage, while the other monitors transients in feedback circuit that clamps the membrane voltage. The advantage of the latter is large responses at the monitor for photocurrents of short duration. The 'open-circuit' voltage method offers advantages of measuring smaller photocurrents of long duration.

By combining electrochemical methods with spectroscopy techniques, the so-called 'action' spectrum of a pigmented BLM can be obtained, which may be recorded in either the voltage or the current mode. In the voltage mode, photo-emfs on BLM are measured by two different procedures. The first procedure consists of moving continuously the wavelength cam with a synchronous electric motor whereas the output voltage is recorded. The second, point-by-point procedure, is preferred for more accurate work. In this method, the photovoltage (or photocurrent) is measured at 10 nm intervals, starting from 800 nm. The wavelength setting should be made without disturbing the optical alignment of the monochromator, by the use of the same synchronous motor and switch. This method of obtaining "action" spectra, as already mentioned as photoelectrospectrometry, is useful in elucidating certain aspects of the structure and dynamics of a photoactive BLM.

Rapid electrical transients of a pigment-containing BLM in response to flash excitation can also be obtained. Essentially the same instruments and techniques as those developed for research in photobiology and photochemistry are employed. An apparatus in detail has been described for recording the flash induced voltage transient with 10 ns resolution.[70] The open-circuit method is limited by the resistances of aqueous solution and electrodes used, the electrometer and oscilloscope speed, the flash duration, and the noise superimposed on the open-circuit

voltage. With 10^{-3} M NaCl, for example, as the bathing solution, the electrometer resolution is limited to about 1 sec, whereas with 1 M NaCl, electrometers follow BLM voltage variations with 100 nsec resolution, and BLM current is proportional to the derivative of the electrometer output [Davison,1989].

Some recent reports on light-induced phenomena in BLMs and related systems are available[52-59] and will be taken up, along with the other topics, in Chapter 9 (*Membrane Photobiology*).

4.3 Supported Bilayer Lipid Membranes

Since its inception in 1960, many modifications have been made to the original BLM system, with notable exceptions to be described in this section, but the essential principle has remained the same. A BLM formed in the conventional manner (as described in Section 4.2) is an extremely fragile structure with a limited lifetime. For long-term basic studies as well as for technological applications, the common concern has been the mechanical stability of the BLM. Although a number of improvements have been made to prolong the lifetime of the BLM, they rarely last longer than 8 hours. For protracted basic studies and practical utilization such as in biosensors and molecular electronic device development, a long-lived BLM is a prerequisite. For this reason, it is not only desirable, but also imperative that a method be found so that long-lasting BLMs can be generated. In 1989, a simple and novel method was reported for the formation of self-assembled BLMs on solid substrates, which possessed the desired dynamic properties and the requisite mechanical stability.[25-27] The origin of non-conventional or supported BLMs, however, dates back, many years when a number of researchers were interested in developing a model system for the thylakoid membrane with sufficient strength and size for use as a solar energy conversion system [Davison, 1989] and other purposes (*see* Chapter 9, *Membrane Photobiology*). Later, supported BLMs were formed on metallic wires, conducting SnO_2 glass, gel substrates, and on microchips, as described below under separate headings.[60,61] These self-assembled, supported BLMs, not only have

overcome the long-term stability problem of the conventional planar lipid bilayers, but also have opened a range of possibilities in manipulating interfacial ultrathin films as well as in developing practical biosensors (*see* Chapter 10, Applications).

4.3.1 BLMs on microporous filters and SnO_2 glass

BLMs on polycarbonate and cellulose filters. As mentioned above, a BLM formed in the conventional manner is a very fragile structure and difficult to work with; it is not suitable for practical applications. A novel BLM system with a longer lifetime, a larger surface area and greater stability in the face of chemical and mechanical disturbances was reported in 1978.[12] This new BLM system was achieved by filling the smooth circular pores of a polycarbonate film (known commercially as microporous Nuclepore filters) with a standard BLM-forming solution. The polycarbonate-BLM system was supported in such a manner that an aqueous solution could be easily added to both sides. In an ideal situation this Nuclepore-coated membrane may be visualized as tens of thousands of micro BLMs simultaneously generated *in situ*. For example, pigmented BLMs in these microporous filters could exhibit photoeffects lasting a period of days. It was then concluded that an extension of this type of non-conventional BLMs to other areas of membrane biophysics was anticipated. Indeed, BLMs were formed later in microporous filters made of polycarbonate and cellulose materials for antigen-antibody interaction studies (*see* Chapter 10). Other investigators, notably Thompson et al.[13] and Yoshikawa and colleagues[14] have reported related systems using this type of supported BLMs with interesting results. Kocherginsky, Osak, and their colleagues[62] have also reported lipid-treated filters and concluded that their system may be useful in modeling a variety of water-filled membrane channels.

SnO_2 glass. Electrical conducting SnO_2-coated glass (Nessa glass) has been employed as a substrate for BLM support.[63] As such, a piece of glass coated on both sides with SnO_2 is prepared by covering all but a small area ($\sim 2\ mm^2$) with hot wax on one side. Upon cooling, the barrier created by the wax on the Nessa glass is curved and facilitates the formation of the proper contact angle between the lipid solution and the barrier. A drop of BLM-forming solution is deposited within the barrier, while the other side

is left free as a control, serving the purpose of the reference electrode (see Fig. 4.8).

4.3.2 Metal-supported s-BLMs

Although the conventional BLM proved to be very artistic and useful, for instance, for graduate students in certain fields to obtaining their Ph. D. degrees, it does have one major deficiency, namely, fragility. Due to the nature of the ultrathin membrane, the conventional BLM septum provided an unstable support. The lipid layer could suddenly rupture at any time. This was very frustrating for researchers to deal with. With the advancement of modern electronics came the solid supported BLM (s-BLM). The s-BLM is formed on the tip of a freshly cut metallic wire, and has proven to be much more suitable and longer lasting than the conventional BLM, as detailed below.

Preparing a Solid Supported BLM on Metallic Substrates

The procedure developed in generating a s-BLM is quite different from that used to form the conventional BLM. This new technique provides incomparable support for the stability of the BLM enabling the membrane to last much longer. The formation of a s-BLM is accomplished in two basic steps (Fig. 4.7). In the first step, a metal wire, either platinum or stainless steel, is immersed in a lipid droplet. The wire is usually coated with some type of insulation, generally Teflon. It should be noted that if the wire has had sufficient time to react with the oxygen in air, it is normally covered with an invisible layer of oxide that is hydrophobic. On the other hand, if the metallic wire is submerged in the lipid solution, the tip of which is cut off using a sharp knife or a miniature guillotine,[60] the nascent surface of the freshly cut metal tip is highly hydrophilic and microscopically rough. The rough surface has many pits and crevices in it that makes difficult for the polar heads of the lipid molecules to bind to the support. However, the 'fluid' and dynamic nature of the lipid bilayer obviates this problem. So, a first lipid monolayer with the hydrocarbon chains sticking outward is readily formed on the metallic surface. This modified surface, now hydrophobic, is ready to interact with other lipid molecules in the lipid solution.

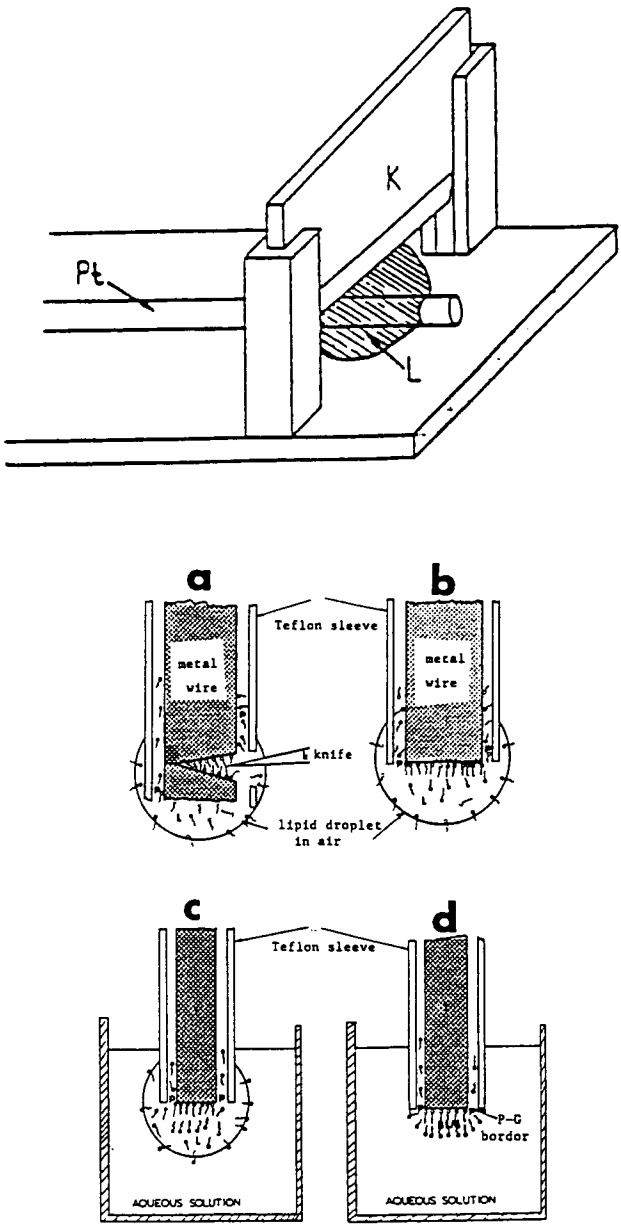

Fig. 4.7 Illustrations of supported planar lipid bilayers (BLMs).

In the second step, the freshly cut metal wire with the lipid droplet is submerged in an aqueous solution (see Fig. 4.7). After a few minutes, a stable lipid bilayer will be formed on the tip of the wire. Electrical properties are utilized to monitor the thinning process of the membrane, as a lipid bilayer is being assembled, the capacitance of the membrane is increasing, whereas the conductance is decreasing towards steady values. The hydrocarbon interior of the bilayer membrane is responsible for these electrical properties. It is important to note that the bilayer formed here is liquid-crystalline in structure, which can be modified to suit the purpose intended by the investigator.

Similar to conventional BLMs, the structural state of s-BLMs and therefore many of the mechanical and electrical parameters can be modified by applying a D.C. voltage. Further, a s-BLM formed in the manner described is remarkably sturdy; it can not be removed by simple washing or mechanical agitation. A s-BLM may be detached from its metallic substrate, however, by strong measures such as sonication, electrolysis or by drastic chemical treatments. Although usually depicted lipid molecules in a planar lipid bilayer are oriented perpendicular to the metal surface, they are most likely tilted in some angle from the normal. To cover entirely of any surface by a layer of lipid molecules at the molecular dimension is an extremely difficult task, since the morphology of the substrate is not likely to be 'smooth', as described above. As an experimental fact, monolayers and multilayers of lipids prepared by the L-B technique are often full of pinholes. These defects are hard to avoid owing to the nature of the substrate at the atomic level. Thus, a freshly cleaved metal surface is not smooth at the atomic level; it is most likely to be very rough with grain and edge boundaries. However, the lipid solution used, being a fluid, is able to interact with the bumpy terrain of the newly cut metal surface and to form an intimate bond within its indentations, pits, and crevices. The lipid monolayer adjacent to the solid metal support is assumed to be stabilized by hydrogen bonds arising between the hydrophilic groups of the monolayer and the electronegative metal surface. The hydrophobic alkyl tails of the amphipathic lipid molecules are arranged in such a way, which allows the polar head groups to pack more closely. The final self-assembled lipid bilayer is stabilized because of intermolecular forces. The breakdown voltage of s-BLMs under these

conditions is several fold higher than those of conventional BLMs (up to 1.5 V or more). The most important factor in the process of the s-BLM preparation seems to be the time the cut end of the wire is allowed to remain in the membrane forming solution (~ 10 min) prior to its transfer into the aqueous solution for a supported BLM to securely self-assemble.[25-27,60]

The most extensively studied system of s-BLMs is made of phospholipid molecules (phosphatidylcholine or PC for example). The molecule has two long hydrocarbon chains with a polar group (esterfied phosphoric acid) at one terminus (see Section 2.3, Chapter 2) . The diameter of the polar group adsorbed on the metal substrate is about the same as the cross-sectional diameter of the rest of the molecule (hence rod shaped), and the PC molecules pack together, generating what is essentially a two-dimensional liquid crystal on a supporting substrate. Like all amphiphilic molecules, one end of which is the polar group that interacts strongly with the hydrophilic surface of a freshly cut metal, whereas at the other end of the phospholipid molecule, hydrocarbon chains stick out, thereby altering the properties of the metal surface formed by the adsorbed monolayer. When planar lipid bilayers formed in this manner, it is envisioned that the first monolayer of the lipid is 'sorbed' onto the substrate thereby forming a *fixed* half-BLM. The second half-BLM is then self-assembled onto the anchored lipid monolayer. As a result of hydrocarbon-chains interactions, and being fluid, the second half-BLM is relatively free to move with respect to the anchored half-BLM; a situation which is not unlikely that of 'oil' used in lubrication. This s-BLM is a simple prototype and practical substructure for a novel type of molecular devices and biosensors, which exemplifies the design principles that materials scientists may find advantageous in their research (*see* Chapter 10, *Applications*).

Supported lipid bilayers or s-BLMs on solid support can also be formed by a number of other methods,[49,60,86-89] besides the two-consecutive step technique described above. A s-BLMs may be formed from a lipid droplet deposited at an air-water interface by the method of Wardak et al.[60] The second method, reported recently by Raguse, Cornell and their colleagues,[49,87] is based on a combination of both monolayer and

bilayer techniques (*see* Table 2.1, Chapter 2). This method, known as the tethered BLM technique (or t-BLM),[87] also consists of two steps: an alkanethiol monolayer is first assembled on gold; which is followed by the formation of the BLM from phospholipid molecules. Apparently, a clean gold surface is modified by gold-sulfur interactions, so that a 'conventional' BLM can self-assemble in the second step. It remains to be seen whether the first step in the t-BLM technique is indispensable, as expounded by its proponents.[49,87] (*see* references therein). Last, but not least, is the method reported by Puu and co-workers;[84] they formed stable lipid bilayers by a combination of L-B and liposome techniques with biological activities. The efficacy of these novel methods[60,86-89] for biosensors and molecular devices development will be further considered in Chapter 10 (*Applications*).

4.3.3 Gel-supported sb-BLMs

Although s-BLMs on metallic substrates are attractive for certain purposes, as briefly described above and in detail later (Chapter 10, *Applications*), the metallic substrate, however, precludes ion translocation across the lipid bilayer. Therefore, the pursuit of a simple method for obtaining long-lived, planar BLMs separating two aqueous media has been elusive until a few years ago.[65-67] A description of forming a planar BLM on hydrogel substrates, which overcomes the deficiency of ion transport encountered in s-BLMs is given below.

The formation procedure practiced in the authors' laboratory consists of three steps. In the first step, a chlorided Ag wire (Ag/AgCl) is inserted into a small diameter (~ 0.5 mm) Teflon tubing which has been previously filled with a hot hydrogel solution (e.g. 0.3 g agar in 15 ml 3 M KCl saturated with AgCl). For electrical connection as well as serving as a reference electrode, an Ag/AgCl wire is inserted at one end. The AgCl electrode and the agar-filled Teflon tubing are glued together with wax at the point of insertion. In this way an Ag/AgCl-Teflon tubing salt bridge (sb) electrode is constructed. In the second step, the tip of the other end of the Teflon salt bridge is cut with a sharp knife, while immersed in a BLM-forming solution as is done with the s-BLM technique.[60] In the third and

Formation of bilayer lipid membrane on rigid supports

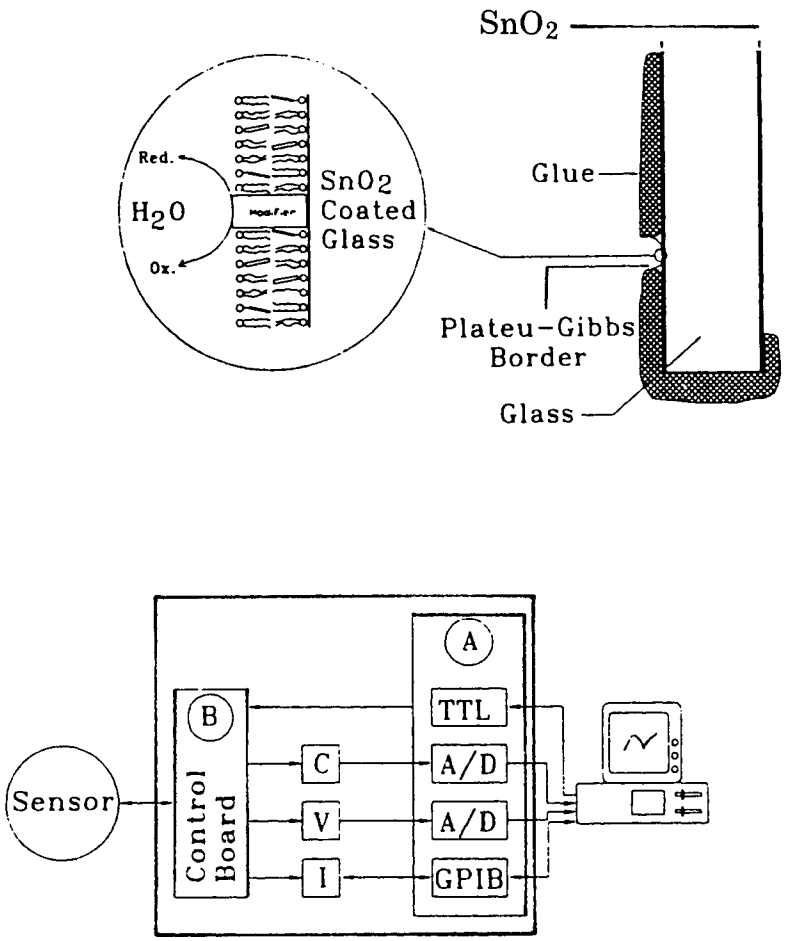

Fig. 4.8 *Upper*: Diagram of the working electrode (SnO_2) with a deposited BLM. *Lower*: The measuring system used for the study.[63]

last step, the Ag/AgCl-Teflon salt bridge with the tip freshly coated with the lipid solution is then immersed in a buffered aqueous solution in the cell chamber, where the experiment is to be conducted. Alternatively, the second step described above may be carried out in air and then the freshly cut end of the salt bridge is immediately immersed in the lipid solution for a few minutes. In either case, the cell chamber filled with an appropriate aqueous solution (e.g. 0.1 M KCl) contains an Ag/AgCl-Teflon salt bridge and an Ag/AgCl-Teflon salt bridge with a self-assembled BLM at its end. The lead wires of the two electrodes are connected to the measuring instrumentation. In this conjunction, it should be noted that the salt bridge electrode without the BLM serves as a reference electrode, as shown in Fig. 4.9, thereby eliminating one of the chambers in a conventional BLM setup.

The sb-BLM system relies on the idea of finding a substance that can act as a support and still possesses properties allowing for the translocation of ions and other compounds across the lipid bilayer. The substances found to be suitable are hydrogels (agar, agarose, etc) commonly used for salt bridge purposes in electrochemistry.[66] These gels not only proved to be viscous enough to provide a stable support for the lipid bilayer, but also watery enough to function as an aqueous substrate. This new planar lipid bilayer system permits for the passage of materials across a stable ultrathin membrane as well as having the electrical properties of its conventional BLM ancestor. Therefore, the sb-BLM system is highly beneficial to researchers interested in practical applications, and in basic studies such as the mechanisms involved in membrane transport, ion selectivity, voltage and ligand gated channels, electron transfer, as well as in signal and light transduction.[25-27]

BLMs on interdigitated electrodes

In recent years, numerous attempts have been made to exploit the BLM system's potential in practical applications in molecular devices and biosensors. Advances in microelectronics and interest in ultrathin organic films, especially the newly developed self-assembled bilayer lipid membrane (s-BLM) on a nascent metallic surface, have resulted in a unique fusion of ideas towards the development of intelligent biosensors and transducers. Furthermore, recent trends in interdisciplinary studies in

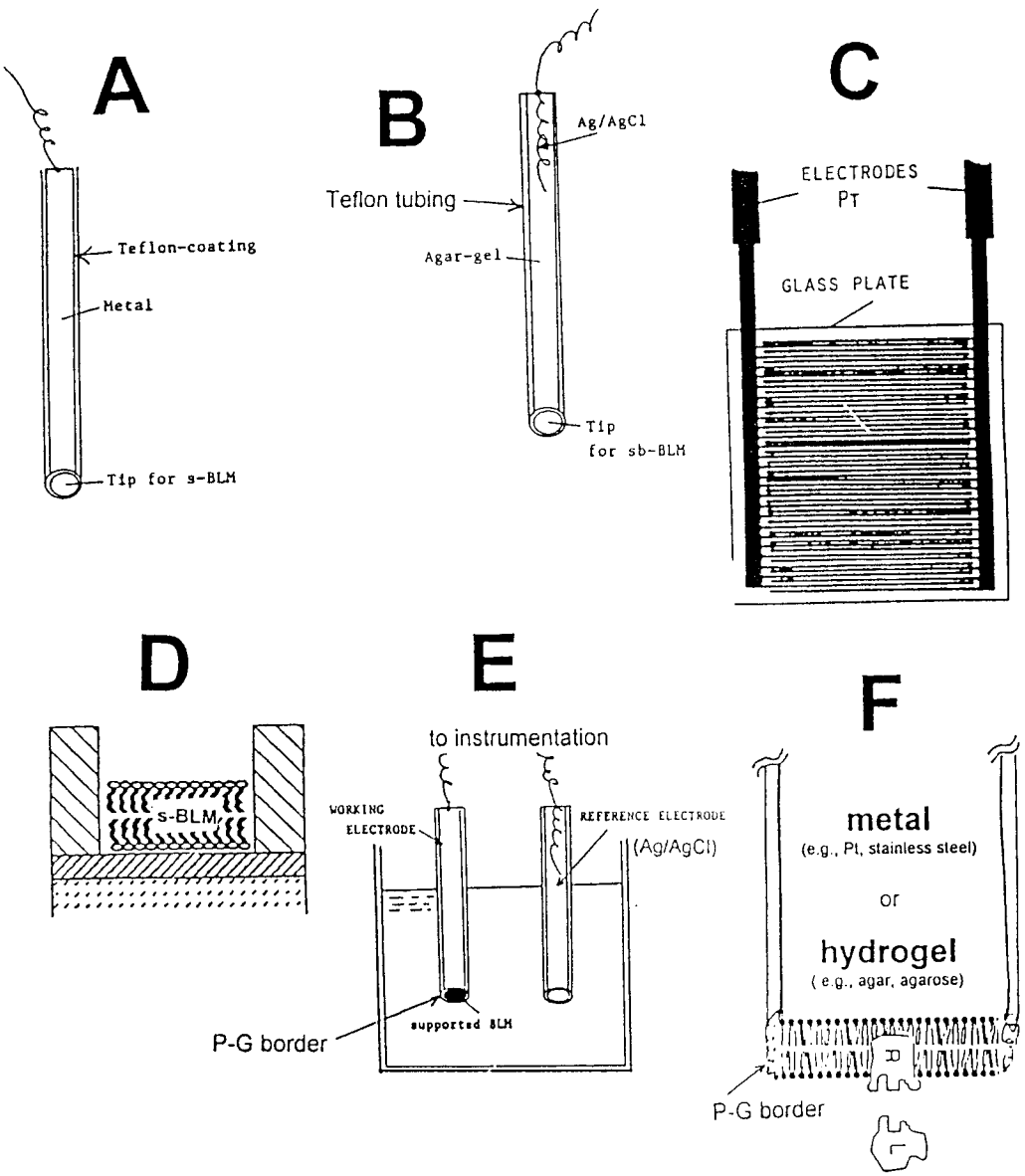

Fig. 4.9 Representations of: **A**. s-BLM probe **B**. sb-BLM probe **C**. interdigitated structure **D**. microsystem for s-BLMs **E**. cell for electrochemical measurements **F**. receptor– ligand interaction.

chemistry, electronics, and molecular biology have led to a new field of scientific/technological endeavor which is a part of a more general approach toward the development of a new, post-semiconductor electronic technology, namely, molecular electronics with a long-term goal of molecular computers [Roberts, 1988; Hong, 1989; Birge, 1994]. In this connection, as already referred to above, BLMs have been deposited on a variety of substrates including SnO_2 (conducting glass), freshly cut metal, and hydrogel. Recently, the technique has been extended to the interdigitated structure (IDS).[61,69] IDS are finger-like electrodes made by microelectronic technologies and used in micro-chip applications.

As demonstrated by a number of investigators,[25-27] the solid supported BLM system (s-BLM) not only possesses the advantages of a conventional planar lipid bilayer structure but additionally gains new important properties such as (a) an anisotropic, highly ordered, yet very dynamic liquid-like structure, (b) two asymmetric interfaces, and (c) this type of probe is directed towards for microelectronics fabrication (*see* Fig. 4.9). Thus, forming of supported BLMs on planar chip with thin-film electrodes have opened broad possibilities for the development of miniaturized biosensors as well as for basic research of electrical and mechanical properties of biomembranes.[61,69]

4.4 Liposomes (Lipid-Micro-Vesicles, LMV)

Presently, the second widely used model system for biomembranes consists of enclosed spherical bilayer lipid membranes or lipid microvesicles formed by mechanically agitating (or sonicating) a suspension of hydrated amphipathic lipids. Since their initial description in 1965, liposomes have been extensively studied[72-73] and comprehensively reviewed [Tien,1974; Ostro, 1983; Rosoff, 1996]. The origin and history of liposomes parallel closely with those of planar bilayer lipid membranes (BLMs), as will be described in the next section. Particular mention should be made that the ability to form self-assembled lipid bilayers (BLMs and liposomes) is not restricted to natural phospholipids. Many synthetic surfactants and amphiphils (amphipathic molecules), some of them with structures not found in biomembranes have been reported.[68] In

this section we will be only concerned with the basic physical, chemical, and biomedical aspects of liposomes including some of their practical applications. Certain other aspects of liposomes, not covered here, will be taken up later in appropriate chapters in the book concerning membrane transport, physiology, bioenergetics, and membrane photobiology.

4.4.1 Background of Liposomes

In Chapter 3 (Section 2.1.3 on Self-assembly) a brief consideration is given on the formation of liposomes when natural lipids with one polar group and two hydrocarbon chains are placed in aqueous solution. Due to the bulkiness of the phospholipid molecule, it becomes difficult to pack this unwieldy molecule into a micelle. Instead, phospholipid molecules form lipid bilayers of spherical configuration called liposomes, which are much larger than micelles. These liposomes (also known as lipid microvesicles, spherules, or smectic mesophase) are of special interest, since their limiting structure is also of bimolecular thickness; they offer a much larger surface area and more stability than a planar BLM, described in the preceding sections. One drawback with liposomes is that highly sensitive electrical methods, with a few exceptions, can not be readily applied to their characterization.

The discovery of liposomes is also a fascinating story, since it is closely tied with the BLM research. For those interested in an *ex cathedra* story, the one written by A. D. Bangham, at Cambridge University, UK, the principal discoverer of the liposome, is highly recommended. In 1995, in an autobiographical account,[5] Bangham writes,

> " (circa 1959)...*the biological community was reacting to the then current claim by Robertson that all plasma and intracellular membranes were accountable in terms of a bimolecular leaflet of phospholipids...*" Bangham continues,
>
> "*... a preprint of a paper was lent to me by Richard Keynes, then Head of the Department of Physiology... They* (Rudin and his collaborators) *described methods for preparing a membrane,... The physiologists went mad over the model, referred to as a 'BLM', an*

acronym for Bilayer or by some for Black Lipid Membrane. They were as irresistible to play with as soap bubbles." Bangham then continues,

"*... I could follow microscopic shape changes, e.g. swelling and shrinking, taking place in my smetic mesophases* (liposomes)...". Finally, in the summary section, Bangham concludes the story of liposomes,

"*... from the perplexity of a blood smear to the growth of a multi-million pound* (dollar) *business.*"

Indeed, in the 1980s, an explosion of research on liposomes began as evidenced by a plethora of conferences and symposia, and publications devoted to the topic (*see* for example [Ostro, 1983]). These activities reflect, to a large extent, prevailing interests in the clinical and commercial applications of the targeting of liposomes as delivery systems in cancer chemotherapy and in pharmacology. Several recent reports,[72-76,79] comprehensive reviews and treatises on liposomes covering current literature have been prepared by many active investigators.[74-76,78,88-90] Further, the use of these liposomes as models for biomembranes, as a tool in molecular biology, in immunology and in therapeutic applications may also be found in a monograph [Rosoff, 1996], the details of which are beyond the scope of this book. Instead, this section will serve as an introduction to the subject matter and highlight some recent developments in this dynamic field.

4.4.2 Types and Preparation of Liposomes

Unlike fatty acid soaps, which undergo phase transitions in water, forming spherical micelles in most cases, phospholipids and the like, form continuous, or 'closed', bilayer structures separating two aqueous solutions. These structures are called liposomes, which are microscopic lipid vesicles. When mixed in water under low shear conditions, the phospholipids arrange themselves in sheets, the molecules aligning side by side in similar orientation, with hydrocarbon chain "tails" up and polar group "heads" down. These sheets then join tails-to-tails to form a lipid

bilayer that encloses some of the water in a phospholipid shell. A liposome may contain one or more lipid bilayer. Typically, several of these vesicles will form one inside the other in diminishing size, creating a multilamellar structure of concentric phospholipid shells separated by layers of water. Similarly to BLMs, liposomes can be prepared from a wide range of natural and synthetic lipids[74] among which phospholipids are most commonly used. These phospholipids can be neutral, or positively charged phospholipids (such as phosphatidylcholine, phosphotidylethanolamine, etc.). Cholesterol is frequently used in liposome formulations to increase the stability by preventing the leakage of contents. Stability is important because when liposomes are employed intravenously they can be disintegrated by the high density lipoproteins (HDL) in the blood stream. In contrast to the BLM, it should be mentioned that alkane, or organic solvents are not required during the final stage of formation of the liposomes. Moreover, liposomes can be prepared in sizes varying from 20 nm to 100 μm or more in diameter, according to the desired purpose.

Procedures and raw materials for formulating liposomes must be considered with care to avoid adverse effects on liposome stability. In general, liposomes should be added to a formulation below 39° C using low shear mixing. The addition of liposomes should also be the last step in the formulation's process. Ethyl alcohol concentration should be kept below 5%, solvents should be kept below 10% and high levels of salts should be avoided. Detergents in general should also be avoided, but low levels (~ 1%) of non-ionic high hydrophilic-lipophilic balance (HLB) surfactants are usually used. Acceptable preservatives for liposome formulations may be added. For most liposome formulations, the storage temperature between 20-25° C is recommended.

Types of liposomes

Multilayer liposomes

They were the first liposomes to be prepared.[5] The method is exceptionally easy requiring only simple equipment. Briefly, the lipids (or a phospholipid preparation) are deposited from an organic solvent (e.g.

chloroform) in a thin film on the wall of a round-bottom flask by rotary evaporation under reduced pressure using a water aspirator. Then, the dried lipids are allowed to swell in a buffered electrolyte solution with gentle agitation above the transition temperature of the lipid (> 30° C). Mechanical agitation facilitates fragmentation of the micelles into microvesicles, producing liposomes of varying sizes, in the range of 5 to 50 μm in diameter. Instead of using mechanical agitation, sonication can be used, which produces microvesicles of a much smaller size (50 nm or less in diameter). The procedure is as follows: lyophilized phospholipids are suspended in a 0.1 M NaCl buffer with tris at pH 8.5. The suspension, at a 3% concentration, of phospholipids is ultrasonicated under nitrogen for 160 minutes at 2° C. The resulting suspension is then isolated by molecular sieve chromatography on large-pore agarose gel or polycarbonate filter. Although multilayer liposomes are easily prepared in large quantity, their main disadvantages are their complicated morphology and inhomogeneity in size, which can be reduced by extrusion at high pressure through a press. However, multilayer liposomes have been used in fusion studies with planar BLMs.

Single-layered liposomes

These bilayer lipid membranes of spherical configuration may be prepared, for example, by evaporating a chloroform solution containing up to 120 moles of phosphatidylcholine (96%) and phosphatidic acid (4%) in a 100 ml round bottom flask. After dryness, 0.6 ml of 0.16 M NaCl or other salt such as ammonium acetate is added to the flask filled with nitrogen. The viscous suspension is then transferred to a 1.3 cm diameter flat bottom tube, and sonicated under an atmosphere of nitrogen for 0.5 to 1.5 hours in a bath-type sonicator at 80 Kc/sec until the suspension becomes clear and bluish. The method is said to yield a homogeneous fraction of lipid microvesicles that are bound by a single lipid bilayer.

To prepare single-bilayer or unilamellar liposomes of large diameter, a so-called reverse-phase evaporation method is available. The lipids are first dissolved in an organic solvent mixture such as diisopropylether/ chloroform (1:1). An aqueous solution is then introduced directly to the organic solution to achieve 1:6 ratio of aqueous phase to

organic phase. A homogeneous emulsion is then obtained by sonication. The organic solvents are then removed under vacuum until the gel state is reached. At this point, a buffered solution is added and the process continued by rotary evaporation under reduced pressure to form a homogeneous suspension of liposomes. This method is particularly useful for encapsulation purposes. A variation of the reverse-phase evaporation is by solvent-injection. Lipids dissolved in ethanol or ether are rapidly injected into a buffer solution where they form unilamellar liposomes of small diameters (20-50 nm). These liposomes are osmotically active and have a high trapping efficiency.

For membrane reconstitution studies, a so-called detergent dialysis (removal) method has been developed for preparing single-bilayered liposomes. The detergent such as sodium cholate is either added to dried lipids before sonication or to preformed single-bilayered liposomes. The mixture is then passed through Sephadex G-25 column to remove the detergent. Alternatively, the mixture is dialyzed against detergent-free buffer, so as the detergent leaves the dialysis bag. Liposomes of fairly uniform size (30-40 nm) form spontaneously and if proteins or other materials are present, they will be incorporated into the liposomal membrane [Ostro, 1983; Rosoff, 1996].

Giant Liposomes

Giant liposomes or vesicles, also known as spherical BLMs, were studied since mid 1960s. The formation of a giant liposome of a diameter of 5 mm or more is as follows. The method consists of attaching a short length of Teflon tubing to a hypodermic needle of a syringe filled with aqueous solution, dipping the needle into a BLM-forming lipid solution, placing the needle in a beaker containing aqueous solution, and 'blowing' a bubble. Thus, within a few minutes either a hanging or free-floating giant liposome is formed [Tien,1974]. Berndl and colleagues[74] have reported shape transformation of liposomes of more than 10 μM and found that a change in temperature can lead to a large change of the volume-to-area ratio. Two different routes are found including (i) symmetric-asymmetric transitions from a dumbbell to a pear-shape state, and (ii) with a wide variety of shape transformations. Using a voltage-sensitive dye (di-

4-ANEPPS) incorporated into liposomes that formed from oxidized cholesterol, Loew and colleagues[11] have reported the effect of medium and membrane conductance on the amplitude and kinetics of membrane potentials induced by externally electric fields. The fluorescence from a potentiometric dye is said to afford a direct measurement of the time course and the amplitude of the induced potential. Both are modulated by changes in membrane or external medium conductance and by the size of the giant liposomes. More recently, stable giant liposomes, formed from a variety of phospholipids, were prepared by Miyata and his associates.[47] They characterized these liposomes under a phase-contrast microscope. Akashi et al[47] suggest that their liposomes are useful in investigating the mechanical properties of the lipid bilayer, as well as in studying mechano-sensitive channel kinetics.

Other types of liposomes

The above two types of multi-layered and single-layered vesicles are known as conventional liposomes; they are the ones that were originally developed.[5] Usually, conventional liposomes are made from: (1) natural lecithin (PC) mixtures, (2) synthetic identical-chain phospholipids, and (3) glycolipid. As such, they are rapidly cleared from the circulation after an systemic administration so they are not much used for clinical purposes. A number of other types are known as specialty liposomes. These include liposomes containing bipolar fatty acids, antibody-directed, methyl/methylene-x-linked, lipoprotein-coated, carbohydrate-coated, multiple-encapsulated, and emulsion-compatible ones. Further, cationic, stealth (sterically stabilized), and targeted liposomes have also been prepared for medical purposes.[78,88-90]

4.4.3 Basic properties of liposomes

The structural characteristics of liposomes generated from various phospholipids have been investigated by optical techniques, electron microscopy, x-ray diffraction, and NMR. The phospholipid liposomes in the light microscope exhibit birefringence. The size of birefringence depends upon the surface charge of microvesicles and the ionic strength of

the aqueous phase. X-ray diffraction of liposomes shows the presence of multilamellar structures, with repeating distances, varying from 5.4 to 7.5 nm, and depending upon the lipid used. The electron micrographs of liposomes, stained negatively with ammonium molybdate, show concentric lammellar layers, each approximately 5 nm thick. In the case of liposomes prepared from bovine brain lipids fixed with OsO_4, electron-micrographs indicate that the boundaries consist of a single, or a few, bilayer leaflets having a peak-to-peak distance of 4.5 ± 0.5 nm per bilayer. The size distribution of the lipid microvesicles in a given preparation has been determined by electron microscopy, and turbidity measurement using light-scattering techniques.

Lipid microvesicles, similar to planar BLMs, are about 100 million times more permeable to water than to electrolyte, and are therefore osmotically active. Liposomes made from charged phospholipids behave as almost perfect osmometers, when alkali metal salts, glucose, or mannitol are used as solutes. The water permeability coefficients for lecithin microvesicles are about 44 μm/sec at 25°C, and 70 μm/sec at 37°C. From these data, the activation energy for water permeation is estimated to be 8.2 kcal/mole, which is interpreted in terms of a solubility mechanism. It is interesting to note that liposomes containing cholesterol show lower water permeability, which has also been observed in the BLM system.[21]

Other solutes, such as erythriotol, malonamide, urea, glycerol, propionamide, ammonium acetate, ethylene glycol, methylurea, ethylurea, etc. are also permeable. The rapid volume changes, combined with the measured total external surface area, are used to calculate solute permeability coefficients. Values in the range of 0.8 to 16 μm/sec have been reported [Rosoff, 1996].

Liposomes or LMV containing positively charged lipids, such as long-chain secondary and quaternary amines, are very impermeable to univalent cations (e.g. Na^+ and K^+), but are permeable to anions. The early workers have found that the diffusion rate for anions follows the sequence $I^- > Cl^- > F^- > NO_3^- > SO_4^{-2} > HPO_4^{-2}$. The diffusion rate for cations is largely controlled by the size and magnitude of the surface

charge. However, in contrast to anions, no significant differences are found for the cation series Li^+, Na^+, Rb^+, and choline.

Owing to the minute size of liposomes, any direct measurements of electrical properties have thus far been precluded, except in the case of single 'giant' liposomes.[11] Nevertheless, a resistance value of 10^7 ohms-cm^2 has been estimated, using the Cl^--flux data. This estimated value, although 1 to 2 orders lower than that of BLM, is consistent with the postulated lipid interior and the osmotic properties of liposomes.

The electrical capacitance of a suspension of liposomes has been measured using a frequency range from 1 kHz to 100 MHz, with the results that (i) at low frequencies the liposomes undergo a counterion-induced relaxation (movements of counterions tangentially to the membrane surface), and (ii) a Maxwell-Wagner dispersion results at high frequencies (above 1 MHz). The dispersion indicates a dielectric constant value of 10 or higher for the liposomal membrane. It is further stated that the water inside of the microvesicles is of the 'free' type, and is entirely comparable to that of the outside. This conclusion is at variance with the electrical properties of the red blood cell, as discussed earlier (*see* Fricke's experiment, Chapter 2]. However, it must be remembered that these LMVs contain no proteins and other RBC constituents inside.

Effects of Modifiers on Liposomes

A variety of modifying agents such as surfactants, steroids, antibiotics, certain proteins, and anesthetics, can significantly increase the permeability of liposomes [Rosoff, 1996]. For instance, the effects of a large number of steroids and other lytic agents can be summarized as being of two kinds: those agents that increase the permeation, and those that retard the permeation. The first group includes diethylstibestrol, deoxycorticosterone, testosterone, progesterone, filipin, nystatin, amphotericin B, and others. Compounds that reduce the permeability or stabilize the lipid microvesicles are cortisone, corisol, chloroqunine, and 17-β-estradiol.[78,88-90]

The effect of a very well known surfactant, triton X-100 (a mixture

of *p*-t-octyl poly[phenoxyethoxy] ethanols) accelerates anion release from liposomes and causes substantial ultrastructural changes. Other modifiers that exhibit pronounced effects are bacterial toxins that rupture both microvesicles and certain natural membranes. Since bacterial toxins possess lipid-like structure (amphipathic), insertion of such molecules into lammellar membranes could produce weak spots and eventually lead to structural failure.

Interactions of liposomes with proteins have been reported. The presence of cytochrome c, and to a lesser extent bovine serum albumin (BSA), tends to produce finer microvesicles (20 to 100 nm). The presence of proteins on the vesicles appears to increase salt capture in the case of phosphatidyl choline. However, salt capture decreases, in the case of acidic phospholipids such as phosphatidylserine, in the presence of cytochrome c. This phenomenon is explained in terms of complex formation thereby diminishing the available ionic groups which presumably are involved in the salt capture process. BSA, when absorbed upon the exterior boundary of these structures, enhances glucose diffusion from the interior, through the bilayer-like walls. A pH-dependent conformational change in the albumin is offered as an explanation.

In the presence of local anesthetics, such as n-butanol, n-octanol, diethyl ether, chloroform, and cocaines, permeability of liposomes is increased. The effect of temperature on the K^+ permeability, with and without the above mentioned compounds has been investigated. The following conclusions have been reached: i) the main barrier to cation permeation is located at the solution membrane interface, (ii) near this interface, the structure of water is highly ordered, and (iii) the effect of local anesthetics increases the disorder at the interfacial region. It is worth noting that very similar suggestions have been made earlier concerning water permeability in the BLM systems [Davison, 1985; Rosoff, 1996]. In this connection, the effects of dibucaine, tetracaine, cocaine, lidocaine, and procaine on the efflux of $^{22}Na^+$ across liposomes formed from a phosphatidylserine-phosphatidic acid mixture have been studied. The most interesting observation is that, in the presence of Ca^{2+}, the calcium-induced Na^+ efflux is completely inhibited by these compounds, which is said to be comparable to the effect observed in nerves. For medical

applications such as drug carriers, the liposomes can be injected intravenously and when they are modified with lipids which render their surface more hydrophilic, their circulation time in the bloodstream can be increased significantly. The above-mentioned so-called "stealth" liposomes are being particularly used as carriers for water-soluble anticancer drugs like doxorubicin, mitoxantrone, and others.[89]

Ultrasonic Spectroscopy of Lipid Bilayers

Biomembranes represent dynamic structures with a large variety of motions of lipids and proteins. The time scale of these motions cover the interval from several hours (flip-flop movement of lipid molecules between monolayers) to less than 10-12 s (vibration movements of certain groups in lipid and protein molecules). The character of these movements depends on structural states of lipid bilayers and can be changed as a result of protein-lipid interactions. A number of experimental methods such as NMR, EPR and fluorescence spectroscopy have been frequently applied to the study of the molecular motions in phospholipid bilayers (see Chapter 2, Section 2.4). However, other macroscopic methods such as ultrasonic spectroscopy and dielectric relaxation have not been so often used [Hianik and Passechnik, 1995; Rosoff, 1996].. One of the most important advantage of the latter methods is that they do not require any probes (e.g. spin or fluorescence marker) to monitor the physical properties of membrane. Thus, they do not perturb the structure of lipid bilayer. The study of mechanical properties of biomembranes requires the measurement of elastic parameters. This is, however, rather difficult owing to the complex nature of membrane structure. In particular, using erythrocytes (RBC) there is difficult to distinguish the contribution to the mechanical properties of biomembranes separately from that of lipid bilayer and the contribution of proteins to membrane rheological parameters. For such purpose the liposome is a suitable system [Hianik and Passechnik, 1995; Rosoff, 1996]. For example, the technique has been successfully used to probe liposome membrane phase equilibria by the measurement of the absorption coefficient over appropriate frequency range. Also, the technique is very effective for studying lipid-cholesterol, lipid-polysaccharide, and protein-lipid interactions, as well as membrane fusion. Thus, the above-mentioned examples present clear evidence about

importance and wide possibilities of molecular acoustics as well as dielectric relaxation spectroscopy to study the physical properties of liposomes.

Before going to the next section on practical applications of liposomes, two remarks must be made. First, in the first 15 years following the introduction of the liposome system by Bangham and his colleagues,[5,] liposomes have been used extensively, along with the BLM system, as models of biomembranes and much fundamental information concerning membrane properties has been obtained. In this connection mention should be made concerning a short communication on a liposome system containing iron oxide particles.[79] These Fe_3O_4–containing liposomes are sensitive to magnetic field. The author suggests that magnet-containing liposomes have certain advantages: (i) a magnetic field can be used for liposome targeting (e.g. in liver) and (ii) microwave radiation can be used for releasing a drug. If so, magnetic liposomes may have great potential as a drug delivery system. Indeed, this brings us to the second remark proffered in the following paragraph.

Although the early promise of liposomes as specific drug carriers remains to be fulfilled, owing to the destruction of liposomes in the circulation along with their predominant uptake in the spleen and liver, the following ingenious experiment was tried in the 1980s on the tails of rats with a biophysics twist. The question asked was '*how to deliver medicine to specific targets where it will do the most good*'? The so-called 'magic bullet' approach was attempted by a group of researchers. They first planted tumors in the tails of rats. They then injected the rodents with liposomes containing an anticancer drug along with particles of iron oxide, a paramagnetic compound. Finally, one group of rats had their tails fixed with tiny magnets so that iron oxide-containing liposomes could be localized. Some very impressive results were obtained: (i) in magnet-equipped rats, tumors either stopped growing or began to shrink in 90% of the rodents, 75% of this group were completely cured. But, all the rats in the group given the same liposomes without placement of magnets died!

4.4.4 Applications of liposomes

Liposomes are the smallest man-made lipid vesicles of spherical

shape that can be produced from natural non-toxic phospholipids and cholesterol. As described below, liposomes can be used, besides models of biomembranes, as drug carriers and be loaded with a great variety of molecules, such as proteins, nucleotides, small drug molecules, and even plasmids. Liposomes are extremely adaptable, and due to the diversity of their composition, they can be utilized for a large number of applications [Rosoff,1996].

Recently, liposomes have been evaluated as delivery systems for drugs, vitamins, and cosmetic materials.[74,78,88-90] They can be custom designed for almost any need by varying the lipid constituents, size, surface charge, and method of preparation (see above). The preparation of liposomes requires careful attention to the formulation, encapsulation efficiency and long-term stability. In biomedical applications, one outstanding advantage of liposomes over systems such as emulsions is that liposomes enable water-soluble and water-insoluble materials to be employed together in a formulation. Water soluble materials are dissolved in the aqueous medium in which the phospholipids are hydrated, and when the liposomes form, hydrophilic molecules can be encapsulated in the internal aqueous volume whereas lipophilic ones can be incorporated in the lipid bilayer phase. Using a high-shear process, stable, unilamellar (single bilayered) liposomes with specifically designed structural characteristics may be produced. These liposomes hold the normally immiscible materials together in a microsphere with controllable release of the encapsulated ingredients. The liposomes, and the otherwise immiscible ingredients they contain, can then be used in formulations without the need for interface-active agents or emulsifiers, eliminating the drawbacks associated with the use of such. Thus, the properties of liposomes yield a variety of additional benefits. To name a few, liposomes can be made into controlled delivery system, carry both water and oil-soluble cargos, and solubilize recalcitrant compounds; they can stabilize proteins and prevent undesired oxidation. Additionally, liposomes are usually non-toxic and biodegradable.[74]

When employed *in vivo*, liposomes have been utilized by intravenous, intramuscular, subcuteneous, intrathecal, intratracheal, oral, and topical routes. For example, in topical applications, liposomes are

used in cosmetics for skin and variety of mucosal tissues since 1986. Other applications of liposomes are as controlled release systems and in transfection experiments. Clinical trials and studies in experimental animals are being conducted for applications in therapeutic and preventive medicine, which include antimicrobial and cancer therapy, metal detoxification, blood transfusion, vaccine, hormone and gene therapy.[81,82] When liposomes are applied by way of intravenous route, they are eventually cleared by phagocytic cells, mostly the fixed macrophages, which result in the localization in spleen and liver. This property can be used by a liposome for passive targeting to deliver the drugs to phagocytic cells and entrapped immuno-modulators, thus activating macrophages and increasing their cytotoxicity to invading cells.

Cosmetics. Liposomes are most useful for being able to transfer and deliver active ingredients to the application site of cosmetics. The lipid bilayer of the liposomes is very similar, physiologically, to the material of cell membranes. For example, when a cosmetic containing liposomes is applied to the skin, the liposomes are placed on the skin and begin to merge with the cellular membranes. In the process, the liposomes release their goods of active materials into the cells. As a consequence, not only is delivery of the compounds very specific, which goes directly into the intended cells, but the delivery takes place over a protracted period of time. Cosmetic ingredients in liposomes display better stability, permeation and efficacy at lower usage levels.

Pore formation in bilayer lipid membranes. A multitude of lipid bilayer-active agents can induce pores (channels) so that vital hydrophilic molecules and ions may be readily transported across the hydrophobic (apolar) core of a lipid bilayer. In this regard, Grigoriev and colleagues reported recently the effect of panosialins on BLMs.[77] They studied the effect of these enzyme inhibitors whose molecular structure is amphipathic (i.e., with a polar and non-polar aliphatic group at each end). Their results suggest that panosialins have two dramatic effects on the planar lipid bilayer: pore formation (as evidenced by the increased BLM conductance) and enhanced action on ion transport by enniatin B (a K^+ carrier). This work of Grigoriev et al is of interest and may shed light on the mode of the action of panosialins on cell membranes. A pertinent

experiment in the case of liposomes and cells utilizes the release of a suitable marker substance. The efflux is measured in the course of time by means of monitoring a characteristic physical signal, preferentially a change of fluorescence. Schwarz and Arbuzova have worked out a theoretical procedure to evaluate the original data so that the effective rate laws of pore formation can be derived.[72] Further, the underlying molecular machinery with emphasis on the relevant reaction kinetics may be investigated. This is expected to provide not only knowledge how pore activation and inactivation (channel gating) could possibly be manipulated but also gives insight into fundamental principles of lipid bilayer-associated penetration and translocation steps. Schwarz and Arbuzova further reported that, using a self-quenching fluorescent dye the average retention factor of a single pore (related to the pore lifetime) for a number of different peptide-lipid vesicle systems (a quantitative measure of 'all-or-none' or graded efflux) was determined.[72] Subsequently, the pore formation rate was evaluated and discussed in the light of the actually lipid associated peptide concentration. Analogous studies with a pore forming protein of influenza virus are in progress.

One final comment on applications. Since it was introduced in the late 1960s, the practical use of liposomes as a drug delivery system has its ups and downs. However, with sustained efforts by many active investigators, the trend is definitely on the upswing.[88-90] Current applications involve in the specific targeting and delivery of informational molecules such as anti-sense oligonucleotides, DNA plasmids (i.e. genes), topical delivery, vaccination, and diagnosis. Other applications include delivering lipid-based carriers or anti-fungal agents by conventional liposomes, and systemic anti-cancer therapy using long-circulating liposomes. Bangham might be right once more;[5] only this time the liposome venture would become *a multi-billion dollar business.*

4.5 Planar BLMs (Lipid Bilayers) *vs.* Spherical Liposomes

Before ending this chapter on experimental lipid bilayers, it may be useful to point out the relative merit of the liposome and BLM systems. *First*, both BLMs and liposomes come about by a process of self-

assembly. But *what is meant by self-assembly*? A simple answer is that an organization, device or a nonliving entity put together with little human intervention. If any human effort is involved, it merely acts as a 'catalyst' to speed up the process. The concept of self-assembly is not new; it is carried out in nature since the time primeval, where entities as simple as a snowflake or as intricate as a living cell arise from thermodynamic principles (*see* the discussion on entropy in Chapter 3, *Basic Principles*), or instructions implicit in their constituents and surroundings. Outstanding examples are BLMs and liposomes, described at length in this chapter and elsewhere in this book, in which amphiphilic molecules arrange themselves into ordered, functioning entities. In other words, we may design the process, and initiate it, but once under way it proceeds according to its own layout, either toward an energetically stable configuration or toward some order whose form and function are inherent in its components (e.g. amphiphilic nature of phospholipid molecules).

Second, in connection with the living cell, its membrane plays a pivotal role, as described in Chapter 2. The principal component of all cell membranes is the lipid bilayer. Thus, the experimental lipid bilayers have played a leading role in the study of biomembranes.[25-27,78,80-82] The liposomes provide large surface areas, and therefore are well suited for the study of transport properties of ultrathin lipid membranes. The uniformity of size of liposomes offers an opportunity to investigate lipid-protein interaction, using the well developed physical chemical methods. Since the liposomes are very stable and can be made easily in quantity, they are ideally suited for studies of permeability, conventional spectroscopy, chemical reactions, and oxygen evolution. Other techniques, such as electron microscopy, x-ray diffraction, NMR, ultrasonic spectroscopy, ESR, using spin labels and more recently MD (Molecular Dynamics), may also be applied. Further, fluxes of many compounds across the liposomal membranes may be monitored by a variety of methods, including tracer influx with the time resolution of seconds and fluorescent-probes for following fluxes down to milliseconds [Antolini, 1982; Rosoff, 1996].

The main drawback of liposomes as an experimental model for the biomembrane is that, owing to their minute size, the powerful electrical methods can not be applied at the present time. In contrast, the ease of

access to both sides of the membrane is a distinct advantage of the planar BLM system for electrical measurements, which have higher sensitivity and time resolution than flux methods. Perhaps one of the best approaches is to carry out the studies concurrently, using both BLM and liposomes. These two model systems are not mutually exclusive; on the contrary, they are complementary to each other, since both types of membranes are derived from a common substance: the amphipathic phospholipid.

General References

S. G. Davison (ed.) *Progress in Surface Science*, Vols. **4** (1973); **19** (1985); **23** (1986); **30** (1989); **41** (1992); **47** (1994); **49** (1995).

H. T. Tien, *Bilayer Lipid Membranes (BLM): Theory and Practice*, Marcel Dekker, Inc. NY. 1974.

V. F. Antonov, Y. G. Rovin, and L. T. Trofimov, *A Bibliography of BLMs*, All Union Institute for Scientific and Technical Information, Moscow, 1979.

R. Antolini, A. Gliozzi and A. Gorio (eds). *Transport in Biomembranes: Model Systems and Reconstitution*, Raven Press, New York, 1982.

J. H. Fendler *Membrane Mimetic Chemistry*.. John Wiley, NY, 1982.

M. J. Ostro, *Liposomes*, Marcel Dekker, Inc., NY. 1983.

G. G. Roberts (ed.) Special issue, *Symposium on Molecular electronics and Biocomputers* (MEBC), 24-27 August, 1987 Supplement to *J. Molecular Electronics* Vol. 4 (1988) s1-s108.

F. T. Hong (ed.) *Molecular Electronics: Biosensors and Biocomputers*, Plenum Press, N. Y. (1989). pp. 259-270.

W. Hanke and W.-R. Schlue, *Planar Lipid Bilayers*, Academic Press, NY. 1993

R. R. Birge (ed.) *Molecular and Biomolecular Electronics,* Advance in Chemistry Series No. 240, American Chemical Society Washington, D.C. 1994

T. Hianik and V. I. Passechnik, *Bilayer Lipid Membranes: Structure and Mechanical Properties*, Kluwer Academic Publishers, Dordrecht,, Boston, London, and Bratislava, 1995

P. T. Frangopol and M. Sanduloviciu (eds.) *Current Topics in Biophysics*, A. I. Cusz University Press, Romania, 1996.

M. Rosoff (ed.), *Vesicles*, Marcel Dekker, Inc., NY, 1996

Specific References

1. R. M.Burton (ed.), *Proc. Am. Oil Chemists' Soc.*, **45** (1968) 201
2. P. Mueller, D. O. Rudin, H. T. Tien, and W. C. Wescott, *Nature*, **194**, (1962) 979; *J. Phys. chem.*, **67** (1963) 534
3. C.V. Boys, *Soap Bubbles: Their Colours and the Forces which Mould Them*, Dover, New York, 1959.
4. *Medical World News* (cover story), February 15,1963. Pp. 64-70.
5. A. D. Bangham, *Surrogate cells or Trojan horses*, BioSystems, **17** (1995) 1081-1088
6. W. A. Huemoeller and H. T. Tien, *J. Chem. Edu.*, **47** (1970) 469-470
7. R. L. Robinson and A. Strickholm, Biochim. Biophys. **509** (1978) 9
8. I. I. Ismailov, B. K. Berdiev, V. G. Shlyonsky and D. J. Benos, *Biohys. J.* **72** (1997) 1182; *J. Gen. Physiol.* **106** (1995) 445
9. H. T. Tien, *Journal of General Physiology*, 52(1,pt.2) (1968). 125-144
10. I. B Ivanov (ed.) *Thin Liquid Films*, Marcel Dekker: New York and Basel, 1988; p. 927.
11. Z. Lojewska, D. L. Farkas, B. Elrenberg, and L. M. Loew, *Biophys. J.*, **56** (1989) 121
12. M. Mountz and H.T. Tien, *Photochem. Photobiol.*, 28 (1978) 395
13. M. Thompson, R.B. Lennox and R.A. McClelland, *Anal. Chem.*, 54 (1982) 76.
14. H. Yoshikawa, Hayashi, T. Shimooka, H. Terada and T. Ishii, *Biochem. Biophys. Res. Commun.*, **145** (1987) 1092
15. T. D. Osborn and P. Yager, *Langmuir*, **11** (1995) 8
16. R. Benz, R. Elbert, W. Prass, H. Ringsdorf, Euro. *Biophys. J.*, 14 (1986) 83
17. R. Rolandi, D. Ricci and O. Brandt, *J. Phys. Chem.*, **96** (1992) 6783-6790; *Prog. Coll. Polym. Sci.* **81** (1990) 222-224

18. H. T. Tien (ed.) *Photochem. Photobiol.*, **24** (1976) 95
19. A. Finkelstein and A. Cass, *J. Gen. Physiol.*, **52(1,pt.2)** (1968) 145
20. L. V. Chernomordik, G. B. Melikyan and Y. A. Chizmadzhev, *Biochim. Biophys. Acta*, **906** (1987) 309-352
21. G. Benga (ed.) *Water Transport in Biological Membranes*, CRC Press, Inc., Boca Raton, FL, 1989. Pp. 41-75
22. D. Exerowa and D. Kashchiev, *Black Films, Contem. Physics*, **27** (1986) 429
23. D. Gallez, N. M. Costa Pinto and P. M. Bisch, *J. Colloid & Interface Science*, **160** (1993)141-148
24. Z. Zhang and Y.-Q. Liang, *J. Coll. Int. Sci.*, **169** (1995) 220-225
25. Y. Umezawa and S. Kihara (eds.), *Molecular Recognition at liquid-liquid Interfaces: Fundamental and Analytical Applications*, Special Issue of *Analytical Science*, Vol. **14**, February, 1998. Pp. 1-248
26. D. P. Nikolelis, U. J. Krull, A. L. Ottova and H. T. Tien, *in Handbook of Chemical and Biological Sensors* (R. F. Taylor and J. S. Schultz, eds.) Institute of Physics Publising, Philadelphia, 1996. Chapter 9.
27. J.-M. Kauffmann (ed.), Special issue on *Electrochemical Biosensors, Bioelectrochem.Bioenerg.* **41** (1997) 1
28. U. Zimmermann, *Biochim. Biophys. Acta*, **694** (1982) 227-277
29. T.Y. Tsong, *Bioelectrochem. Bioenerg.*, **24** (1990) 271; *Biophys. J.*, **60** (1991) 297-306
30. I. Genco, A. Gliozzi, R. M. Robello, E. Scalas, *Biochim. Biophys. Acta.* **1149** (1993) 1024.
31. G. C. Troiano, L. Tung, V. Sharma, and K. J. Stebe, *Biophys. J.*,**75** (1998) 880-888
32. .P. Vassilev, Tien, H. T. In *Artificial and Reconstituted Membrane Systems, Subcellular Biochemistry*; Harris, J. R.; Etemadi, A.-H., Eds.; Plenum Press: New York, 1989; Vol. **4**, pp 97-143.
33. G. B. Melikyan, M. M. Kozlov, L. V. Chernomordik and V. S. Markin, *Biochim Biophys.Acta,* **776** (1984) 169
34. M. Winterhalter and W. Helfrich, *Physical Rev.*, **36** (1987) 5874
35. S. E. Feller and R. W. Pastor, *Biophy. J.* **71** (1996) 1350-1356
36. Y. Fang and J. Yang, *Biochim. Biophys. Acta*, **1324** (1997) 309
37. H. T. Tien, *J. Phys. Chem.*, **88** (1984) 3172; *J. Electroanal. Chem.*, **174** (1984) 299; *J. Electroanal. Chem.*, **211** (1986) 19

38. A. Ring, *Pflugers Arch*, **420** (1992) 264-268.
39. M. Blank (ed) *Biomembrane Electrochemistry*, Adv. Chem. Series, No. **235**, ACS, Washington, DC, 1994.
40. L.-Q. Gu, L.-G. Wang, J. Xun, A. Ottova-Leitmannova, et al. *Bioelec trochem. Bioenerg.*, **39** (1996) 275
41. H. Yamada, H. Shiku, T. Matsue and I. Uchida, *J. Phys. Chem.* **97** (1993) 9547-9549
42. Y. Cheng, V. J. Cunnane, A.-K. Kontturi, K. Kontturi and D. J. Schifrin, *J. Phys, Chem.* **100** (1996)15470; V. J. Cunnane and D. J. Schiffrin, *J. Electroanal.Chem.* **243** (1988) 455
43. V. F. Antonov, E. V. Shevchenko, E. Y. Smirnova, E. V. Yakovenko, A. V. Frolov, *Chem. Phys. Lipids*, **61**(3) (1992) 219-22444.
44. P. Laeuger, *Angew. Chem. Int. Ed. Engl.* **24** (1985) 905
45. S. Alonso-Romanowski.; Gassa, L. M.; Vilche, J. R. *Electrochim. Acta* **40** (1995) 1561-1567. Vallejo and colleagues[46]
46. D. R.Laver, J. R.Smith, H. G. L.Coster, *Biochim. Biophys. Acta*, **772** (1984) 1-9; H.G.L. Coster, T.C. Chilcott & E.P. George, *J. Membrane Sci.*, 100 (1995) 77-86
47. K. Akashi, H. Miyata, H. Itoh, K. Kinosita, Biophys. J. 71 (1996) 3242
48. C. Steinem, A. Janshoff, H.-J. Galla, and M. Sieber, B*oelectrochem. Bioenerg.*, **42**, (1997) 213
49. B. A. Cornell, V.L.B. Brssch-Makavytis, L. G. King, P. D. J. Osman, B. Raguse, L. Wleczorek, and R. J. Pace, *Nature*, **387**, (1997) 580
50. J. R. Lopez and H. T. Tien, *Biochim. Biophys. Acta*, **597** (1980) 433
51. A. Ottova-Leitmannova and H. T. Tien, *Prog. Surface Science*, **41**(4) 337-446 (1992).
52. G. Paillotin, A. Dobek, J. Breton, W. Leibl and H.-W. Trissl, *Biophys. J.* **65** (1993) 379
53. Z.-C. Bi, Y.Y. Qian, J.-P. Huang, Z.-J. Xiao and J.-Y. Yu, *J. Photo chem. Photobiol. A: Chem.* **77** (1994) 37
54. Y. N. Antonenko, T. I. Rokitskaya, E. A. Kotova and A. S. Taisova, *FEBS Lett.* **337** (1994) 77
55. A. Dobek, G. Paillotin, J. Gapinski, , J. Breton, W. Leibl and H.-W. Trissl, *J. Theoret. Biol.* **170** (1994) 129
56. B. Fuks and F. Homble, *Biophys. J.*, **66** (1994) 1404.
57. M. Tanaka, Yonezawa Y., *Mat Sci Eng C-Biomem.*, **4**: (1997) 297
58. J. H. Yang, J. Zhang, D. J. Wang, *J. Photoch Photobio A* **112** (1998)

225-229
59. N. S. Naser, Planner A, Frackowiak D., *J Photoch Photobio A* **113**: (3) 279-282 1998
60. A. Ottova-Leitmannova, T. Martynski, A. Wardak, et al. *In Adv. Chem. Series* No. **240**, ACS, Washington, D. C. (1994) 439-454
61. V. Tvarozek, H. T. Tien, I. Novotny, T. Hianik, J. Dglugopolsky, W. Ziegler, A. L. Ottova, J. Jakabovic, Rehacek and M. Uhlar, *Sensors and Actuators* B, **19** (1994) 597
62. N.M. Kocherginsky, I.S. Osak, L.E. Bromberg, V.A. Karyagin and Yu.Sh. Moshkivsky, *J. Memb. Sci.*, **30** (1987) 39-46.
63. M. Zviman and H. T. Tien, *Biosensors & Bioelectronics*, **6** (1991) 37
64. A. D. Petelska and Z. A. Figaszewski, *Bioelectrochem. Bioenerg.* **46** (1998) 199-204
65. H.-P. Yuan, A. Ottova-Leitmannova and H. T. Tien, *Mat'l Sci. & Eng.* :C 4 (1996) 35
66. X.-D. Lu, A. L. Ottova and H. T. Tien, *Bioelectrochem. Bioenerg.* **39** (1996) 285
67. W. Ziegler, M. Gaburjakova, J. Gaburjakova, V. Tvarozek, and T. Hianik, *Biologia*, **51**, (1996) 683
68. N. Kimizuka, T. Wakiyama, A. Yanagi, S. Shinkai, T. Kunitake, *Bull. Chem. Soc.Jpn.*, **69** (1996) 3681-3684
69. A. Ottova, V. Tvarozek, J. Racek, J. Sabo, W. Ziegler, T. Hianik and H. T. Tien, *Supramolecular Science*, **4** (1997). 110J. S. Huebner, A. E. Popp and K. R. Williams, *J. Chem. Ed.* **65** (1988) 102-108
70. J. Kutnik and H. T. Tien, J Electrophysiol Tech., **14** (1987) 211-221
71. Schwarz and A Arbuzova, *Biochim. Biophys. Acta*, **1239** (1995) 51-57
72. R.A Schwendener, Horber, D.H., Rentsch, K., Hänseler, E., Pestalozzi, B., and C. Sauter, *J. Liposome Res.* **4** (1994) 605-639
73. J. R. Philippot and F. Schuber (Ed). *Liposomes As Tools in Basic Re sarch and Industry*, 1995
74. K. Berndl, J. Kas, R. Lipowsky, E. Sackmann and U. Serfert, *Europhysics Lett.* **13** (1990) 659
75. P.S. Brookes D. F.S, Rolfe,. & Brand, M.D. *J. Memb. Biol.* **155** (1997) 167-174
77. P. A. Grigoriev, R. Schlegel, and U. Graefe, , *Bioeletrochem. Bioenerg.*, **46** (1998)151-154
78. G. Gregoriadis, *Liposomes in drug targetting*, Cell Biology (1994)

79. M. Babincova, *Bioelectrochem. Bioenerg.* **32** (1993) 187
80. Q.-Y. Zhou and R.W. Knighton, *Applied Optics*, **34** (1995) 2354
81. H. Yamaguchi and H. Nakanishi, *Sensors & Actuators, B*, **13/14** (1993) 376
82. P. Bianco and J. Haladjian, *Electrochim. Acta*, **39** (1994) 911
83. P. B. Contino, C. A. Hasselbacher, J. B. A. Ross and Y. Nemerson, *Biophys. J.*, **67** (1994) 1113
84. .P.-A. Ohlsson, T. Tjarnhage, E. Herbai, S. Lofas and G. Puu, *Bioeletrochem. Bioenerg.*, **38** (1995)137
85. L. Dei, E. Ferroni and G. Sarti, *Colloids & Surfaces*, **4** (1995) 433
86. S. H. White, *Science* , **207** (1980) 1075-1077
87. B. Raguse, V. Braach-Maksvytis, et al. *Langmuir*, **14** (1998) 648
88. B. McCormack and G. Gregoriadis (eds.) Strategies for Stealth Therapeutic Systems, Vol. 300, Plenum, NY and London, 1998
89. D. D. Lasic and D. Papahadjopoulos (Eds.) *Medical Applications of Liposomes*, Elsevier Science, Amsterdam, 1998.
90. A. S. Janoff (Ed.) Liposomes: Rational Design, Marcel Dekker, NY, 1999

http://www.msu.edu/~ottova/blm/bilayers_liposomes.html

Chapter 5

Membrane Transport

".... for any open system such as a living cell to be continuously functional; there must be an input (source) and an output (sink). Otherwise, the system would either implode or explode. In either case, the system is not a viable one."

General References (cited by name in brackets in the text)
Specific References (cited by number in superscript in the text)

5.1 Introduction

The historical experiments of Pfeffer and Overton were referred to in Chapter 2 (Section 2.2). The former observed that, when plant cells were placed in concentrated salt solutions, the protoplasm shrank away from the cell wall. Pfeffer concluded that an 'invisible' membrane existed. Further, he proposed that the cell behaved as an osmometer. Overton, some two decades later, confirmed Pfeffer's postulation, and suggested the lipid (olive oil-like) nature of the plasma membrane, based on his permeability studies. As also described in Chapter 2, these and other pioneering investigations led eventually to the lipid bilayer as the central structural component of all biomembranes. This lipid bilayer structure, embellished with functional entities, separating two aqueous solutions, is shown in Fig. 5.1, which will be our main focus in discussing membrane transport. In this chapter a physical and chemical description of transport processes in experimental bilayer lipid membranes (planar BLMs and liposomes) and their natural systems will be given. To establish a correlation between the membrane structure and its thermodynamic properties as related to biochemical and physiological functions, it is essential to compare the behavior of model membranes with their biological counterparts. In this sense, a simple question has to be answered:

Question: ***Can the formalisms deduced for model membranes be applied to biomembranes?***

In an attempt to answer this question, the next two sections of this chapter will be concerning the definition of terms and general principles as applied to membrane transport phenomena, based mostly on the behavior of experimental membranes. Next, the specific features of biomembrane transport will be discussed, with emphasis on the permeation of water and electrolytes. In the last section, the results obtained with experimental bilayer lipid membranes (planar BLMs and spherical liposomes) will be considered. Special attention will be paid to the limitations and the assumptions that apply to the general principles of membrane transport phenomena when they are used to interpret the data from biomembranes

and lipid bilayers and to identify the structural features responsible for permeability properties.

5.2 Osmosis, Water Movement, and Ion Translocation

Diffusion, permeability, transport, and other terms defined

Diffusion. The diffusion of solute in a solvent or, for that matter, a solvent molecule itself, may be thought of as jumping from one quasi-equilibrium site to the next, in terms of molecular scale, perhaps 0.1 nm (10^{-8} cm) away. There will be greater probability of a molecule jumping from a region of higher concentration to a region of lower concentration than the other way around. Thus, the diffusion process, likened to that of random walk, will lead toward an equalizing of concentration. That is, at equilibrium, the chemical potential, μ, is the same throughout the system. Diffusion is a very rapid, 'down hill' process when it occurs within a single living cell. Because of their kinetic energy, solvent and solute molecules are in constant motion. However, on a *macroscopic* scale, the motion may be very slow if stirring and convection are absent. For example, if one puts molecular iodine crystals (I_2) into a beaker of water, the iodine will sink to the bottom. Soon, there will be a thin layer of water saturated with iodine (dark brown color). For the water in the beaker as a whole, it may take days for iodine to distribute itself uniformly throughout the beaker in the absence of stirring. However, on the microscopic scale of living cells, diffusion becomes very rapid. The time required for diffusion throughout a cell is estimated to be about 1×10^{-3} second (1 msec).

Osmosis. If a membrane is permeable to water but only to certain substances, it is called a semipermeable membrane. If the concentrations of a substance to which the membrane is impermeable are different on the two sides of the membrane, water will tend to move toward the higher concentration (osmotic pressure). When a species which cannot pass through the membrane is charged, an electrical potential, ϕ, may be developed across the membrane.

Osmolarity. A one molar or 1 M solution is defined as one mole of dissolved species per one liter of water. The chemical potential of water is higher in more diluted solution. If the solutions across the membrane have the same osmolarity, they are **isotonic**; they have little effect on the cell volume. A solution that causes the cell to swell is called a **hypotonic** solution, whereas a **hypertonic** solution causes the cell to shrink.

Permeability. At the boundaries between two solutions separated by a membrane, natural or artificial, the rate of diffusion may be markedly slow. Here one speaks of 'permeability' in connection with the rate of diffusion through the membrane. In living cells, there is much movement of matter across cell membranes, which is termed collectively as 'transport'.

Passive transport. Movement of species by diffusion down the electrochemical concentration gradient ($\Delta\mu$) across the membrane.

Flux (J). The traffic of molecules across a membrane, in units of amount per unit area per unit time (e.g. $mol/cm^{-2}/sec^{-1}$).

Net flux (ΔJ). The net movement in a given direction (unidirectional flux); at equilibrium $\Delta J = 0$, the free energy of the whole system is at a minimum.

Facilitated Diffusion. Transport process that is helped by a carrier or a channel for a membrane otherwise impermeable to the species (e.g. glucose).

Active Transport. A transport process apparently contrary to the thermodynamic principles. That is the translocation of a species from a lower concentration to a higher one. Active transport is accomplished at the expense of metabolic energy. There is a coupling between a transport system and cell metabolism. Hence, certain compounds (poisons, e.g. 2,4-dinitrophenol) can decouple or inhibit the active transport process.

Purposes of transport processes

The most important purposes of transport are the following:

- Regulate cell volume.

- Maintain the intracellular pH and ionic composition (essential for enzyme activity).
- Concentrate metabolic components.
- Extrude toxic substances.
- Generate electrochemical potential gradients for energy transduction and excitability (nerve and muscle) and ATP synthesis.

To illustrate the system of transport graphically in practical terms, a living being such as an earthworm, at one end are its mouth and the other end anus. The foodstuff the worm ingests, going through its digestive tract, and finally discharges from its body as excrement. During this process, many principles of membrane transport are involved, as will be discussed in this chapter. In brief, the central purpose of transport is, for any open system such as a living cell to be continuously functional; there must be input (source) and an output (sink). Otherwise, the system would either implode or explode. In either case, the system is not a viable one.

Factors governing permeation and transport

Transport through membranes is generally through diffusion, a process of mass transfer that occurs as a result of the movement of individual molecules and ions. This movement may be affected by:

1. A concentration gradient, dc/dx.
2. An electrical field (for charged species), du/dx.
3. A thermal gradient, dT/dx.
4. A pressure gradient, dP/dx.
5. Other means (e.g. gravitation).

A porous medium or barrier that permits *unrestricted* hydrodynamic flow is not a membrane by our definition. All of the membranes which we are going to be concerned with have, in widely varying degrees, the property known as "permeability", which is a numerical measure of the rate at which the transfer of a stated species occurs under specified conditions.

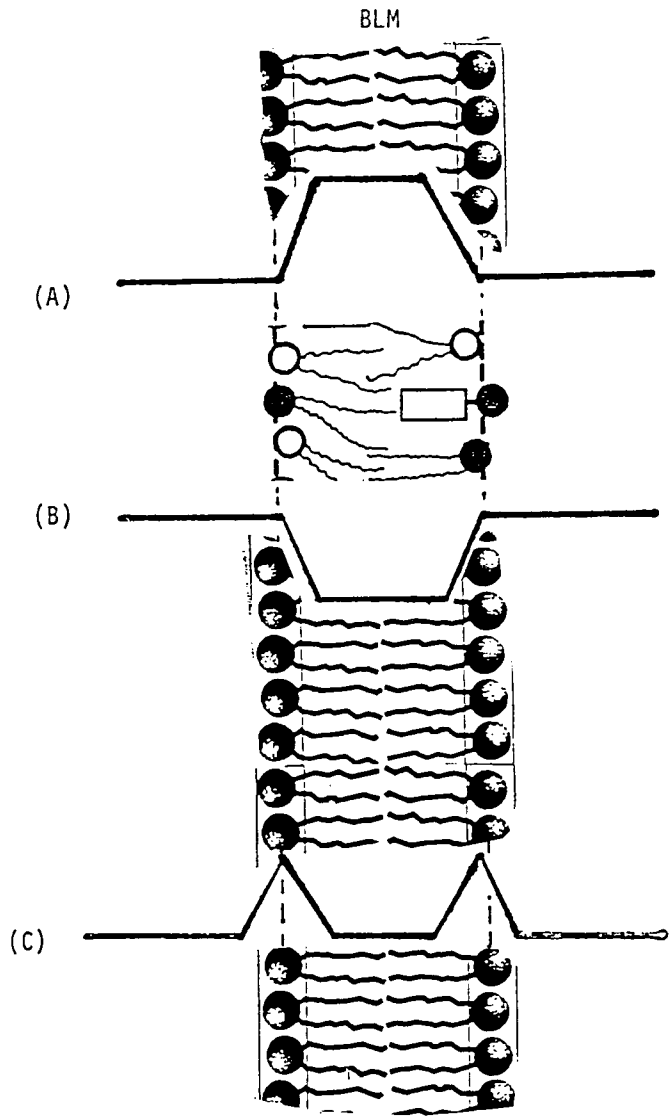

Fig. 5.1 Profiles of membane permeability barriers. Encountered by (A) hydrophilic solutes, (B) hydrophobic solutes.(C) Schematic representation of an interfacial barrier.

With the smorgasbord (or chop-suey) model for the structure of biomembranes in mind (see Fig. 2.7 and Fig. 5.1), there are at least three ways in which a solute can pass through such a membrane: (i) simple diffusion in the lipid bilayer phase, (ii) by way of carriers or channels (facilitated diffusion), and (iii) metabolically-coupled translocation (active transport). The rate-limiting factor in all the above processes is usually the lipid bilayer of the membrane. Properties of the membrane which govern permeation and transport are thickness, solubility, the sign and density of interfacial charges, viscosity, and width and tortuosity of the channels (pores).

5.3 Theories of Membrane Transport

We shall begin with a brief consideration of the fundamental principles of diffusion in liquid, and the nature of driving forces, since these are the basis of membrane permeability and transport [Lakshminarayanaiah, 1969; Davison, 1985; Benga, 1989; Weiss, 1996; Van Winkle, 1999; Deamer, Kleinzeller, and Fambrough, 1999]. Current theories for studying transport processes in membranes will be discussed next. Depending upon the nature of the flux equation used, the theories governing the membrane behavior may be divided roughly into three groups: (1) those based on the Nernst-Planck equation, (2) those based on the concept of the absolute reaction rate processes,[1] and (3) those using the principle of irreversible thermodynamics.[2]

5.3.1 Basic Principles

Permeation processes across biomembranes are discussed here in terms of classical diffusion equations, in which the membrane is assumed to be in a steady state. For the transport of water and nonelectrolytes through membranes, the rate-limiting step is usually within the lipid bilayer, whereas the two interfacial processes are assumed to be rapid. The osmotic water permeability (P_o) is related to membrane porosity. The reflection coefficient, σ, a measure of membrane selectivity between solvent and solute, is used in discussing convective and osmotic water flow. Molecular mechanisms of permeation of both passive diffusion (simple and facilitated) and active transport are considered. Illustrative

examples of both natural and experimental bilayer lipid membranes will be given later in the hope that transport phenomena may be understood in physical and chemical terms.

Many transport experiments have been conducted to measure diffusion rates and permeability. Behind each of these experiments is the mathematical theory of diffusion and permeability. Without it, the experiments would be meaningless. Perhaps the best way to approach this topic is to start with simple idealized situations that can be described exactly by mathematical formulas.

The nature of driving forces

When something is in motion, an active force is usually indicated. The force is related to a gradient of a potential. As with many forces in physics, the gradient of a potential has to be found. For example, the rate of heat transfer is proportional to the gradient of temperature. The appropriate potential in material species translocation for water and non-electrolyte, for example, is the chemical potential, μ, which is given by

$$\mu_i = \mu^0 + RT \ln a_i \simeq \mu^0 + RT \ln C \qquad (5.1)$$

where a is the activity; it is equal to activity coefficient (γ) times concentration (C). Usually the activity is assumed to be equal to the concentration in dilute or ideal solutions ($a \cong C$; $\gamma \rightarrow 1$). For charged species such as Na^+ and K^+ ions, the electrochemical potential, $\underline{\mu}$, is a suitable term as follows:

$$\underline{\mu}_i = \mu_i + z_i F \psi_i \qquad (5.2)$$

where subscript indicates permeant species i, and other terms have the usual significance, as discussed in the following section.

Fick's Laws of Diffusion

Consider a one-dimensional diffusion along the x-axis (horizontal) direction at molecular dimensions shown in Fig. 5.2. Diffusion is a process in which molecules of a liquid or solute disperse or intermingle by virtue of their thermal energy and chemical potential. It is a spontaneous process which leads a system ultimately to thermodynamic equilibrium and is accompanied by an increase in total entropy (or, when it takes place isothermally, by a decrease in total free energy). The gradient (du/dx) of the partial free energy of a diffusing species may be considered to be the equivalent of a driving force upon the molecules that causes them to move against a drag or resistance (identified with the viscosity of the medium).

According to the Nernst-Planck equation, the flux per unit area, J, in words is stated as follows:

$$\text{Flux} = \text{mobility} \times \text{concentration} \times \text{force}$$

and is given by

$$J = U \times C \times \left(-\frac{du}{dx}\right) \qquad (5.3)$$

where the negative sign denotes the direction of decreasing concentration gradient. Upon substitution of Eqs. (5.1 and 5.2) into Eq. (5.3), one obtains:

$$J = -UCRT\left[\frac{dC}{C\,dx} - \frac{zF\,d\psi}{RT\,dx}\right] \qquad (5.4)$$

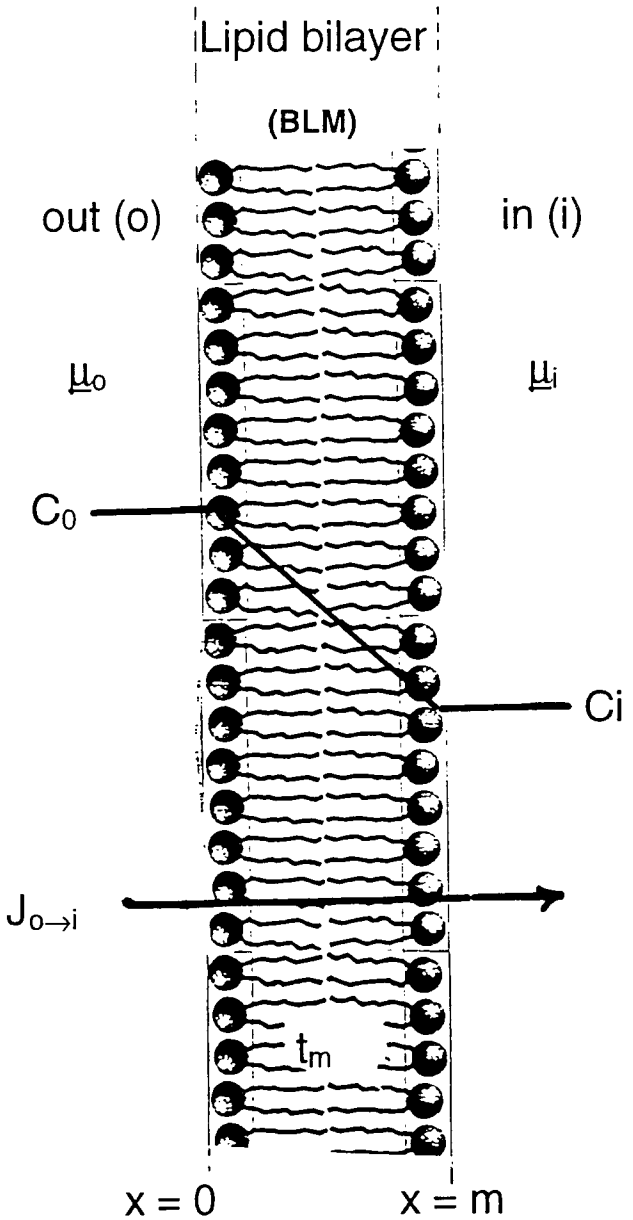

Fig. 5.2. Membrane transport. $\underline{\mu}$, μ, C and J denotes, respectively, electrochemical potential, chemical potential, concentration, and molecular flux. Subscripts: o = outsice, I = inside, I = chemical species i. t_m = membrane thickness (~ 6 nm for lipid bilayer)

The mean velocity (v) of the diffusing species is given by:

$$v = f\ U \quad \left(\text{units: } \frac{g\ cm\ sec}{sec^2\ g}\right) \tag{5.5}$$

where U = the mobility of the ion (proportionality constant). The force, f, is associated with a gradient of chemical potential (i.e. a function which measures the potential energy of a molecule of solute.)

$$f = -\frac{d\mu}{dx} = -\frac{RT\ da}{a\ dx} \cong -\frac{RT\ dC}{C\ dx} \tag{5.6}$$

Upon substitution of Eq. 5.6 into Eq. 5.5, it gives

$$v = -\frac{URT\ dC}{C\ dx} \tag{5.7}$$

or

$$J = vC = -URT\frac{dC}{dx} = -D\frac{dC}{dx} \tag{5.8}$$

where D = URT, as was shown by Einstein. Eq. (5.8) is an expression of Fick's first law of diffusion, where D is a proportionality constant. It can be readily verified that Eq. 5.8 is a special case of the Nernst-Planck equation, since for nonelectrolytes such as water and glucose, $z = 0$, $\psi = 0$. At very low concentrations, D tends to increase slightly. Hence, D is called a diffusion coefficient rather than a constant. The negative sign denotes the direction of decreasing concentration gradient as before.

For diffusion across the membrane as shown in Fig. 5.2, from outside (left) to inside (right), the molecular flux is given by

$$J_{o\rightarrow i} = k_f C N\lambda \tag{5.9}$$

Similarly from right to left

$$J_{i\rightarrow o} = k_b\left(C + \lambda \frac{dC}{dx} \right) N\lambda \tag{5.10}$$

The net flux is given by

$$\Delta J = J_{o\,i} - J_{i\,o} = -k\lambda^2 \frac{dC}{dx} \tag{5.11}$$

where $k = k_f N = k_b N$. The net movement of solute molecules is in the direction of decreasing concentration gradient ($C_i < C_o$), therefore

$$J = k\lambda^2 (C_i - C_o) = k\lambda^2 \frac{\Delta C}{\Delta x} \tag{5.12}$$

where $\Delta C = C_i - C_o$, and $\Delta x = x_i - x_o$.

The molecular flux, J, in Eq. 5.8 is difficult to evaluate experimentally. Instead, one determines the time rate of change of concentration, which is given by:

$$\frac{dC}{dt} = -\frac{dJ}{dx} \tag{5.13}$$

Introducing Eq. 5.8 into Eq. 5.13, one obtains

$$\frac{dC}{dt} = -D\frac{d^2C}{dx^2} \qquad (5.14)$$

Eq.(5.14) is a form of Fick's second law, which represents an expression in terms of concentration, a quantity experimentally measurable, instead of molecular flux, J. Eq.(5.14) is used for solving most diffusion problems encountered in membrane biophysics. It should be noted that for an ultrathin lipid membrane such as a BLM, diffusion is very rapid, so when $dC/dt = 0$, $dJ/dx = 0$, J is a constant.

Since one does not know all the necessary boundary conditions to integrate the flux equation when applied to diffusion through a membrane (*see* Chapter 6, Membrane Electrochemistry), further assumptions have to be made: (i) the concentration gradient across the membrane is homogeneous, (ii) the diffusion path is straight and perpendicular to the plane of the membrane so that its length is equal to the thickness of the membrane, ($t_m = n\lambda$), and (iii) $\Delta C/\Delta x = dC/dx$, since λ has a very small value, Eq.(5.8) may be rewritten as

$$\frac{dC}{dx} = \frac{C_o - C_i}{t_m}$$

or

$$J = -\frac{D}{t_m}\Delta C = -P\Delta C \qquad (5.15)$$

where $P = D/t_m$, the permeability coefficient and $D = k\lambda^2$.

5.3.2 Absolute Reaction Rates[1]

A membrane may be regarded as a series of potential barriers across which the permeant must pass. In order to do so, the permeant must have a minimum amount of energy. Thus, the kinetics of transport can be analyzed in terms of the theory of absolute reaction rates. This simple and elegant theory rests upon two basic assumptions: (i) no reaction can occur until the species involved are transformed into an activated state, and (ii) once transformed, they proceed at a characteristic frequency independent of the reactants and type of reaction. This frequency (f) is given by

$$f = \frac{kT}{h} = \left(\frac{1.38\times10^{-16}\text{erg/deg}}{6.62\times10^{-27}\text{erg/sec}}\right)T = 2.08 \times 10^{10}T \qquad (5.16)$$

According to Erying, Zwolinski and colleagues,[1] the diffusing species passes through the membrane in a series of jumps. As an approximation, the membrane may be considered as a triple-layer system, i.e. a *solution / membrane / solution* sandwich shown in Fig.5.2. Note once more that t_m is the membrane thickness (= $n\lambda$), k is the specific rate constant (the number of times per second a molecule jumps). From the theory of absolute reaction rates, a specific reaction rate constant (k) for any process is given by

$$k = \kappa \frac{kT}{h} \exp\left(-\frac{\Delta G^*}{RT}\right) \qquad (5.17)$$

where kappa, κ, the transmission coefficient, is usually taken as unity, k = the Boltzmann constant, h = Planck's constant and ΔG^* is the free energy change of activation required for the process. In comparison with Eq.(5.15), the permeability P can be expressed in terms of the free energy of activation (ΔG^*), i.e.

$$P = \frac{k\lambda^2 kT}{t_m h} \exp\left(-\frac{\Delta G^*}{RT}\right) \qquad (5.18)$$

This relation has been applied to the transport of solutes through biological membranes and lipid bilayers, specifically water and polar nonelectrolytes, as will be discussed in Section 5.7.

The rate equation can be written in terms of the entropy and enthalpy of activation. In these terms the permeability is given by

$$P = \frac{\lambda^2 kT}{t_m h} \exp\left(\frac{\Delta S^*}{R}\right) \exp\left(-\frac{\Delta H^*}{RT}\right) \qquad (5.19)$$

According to the absolute rate theory,[1] $\Delta H^* = E_a - RT$, where E_a is the empirical activation energy. Equation (5.19) assumes that the permeation process is a point to point jump. These points are separated by a distance λ which is a property of the network of the membrane. Thus, the membrane is assumed to be homogeneous and the kinetic constant in the bulk and in the membrane are equal. In addition, P is independent of concentration and the flux is in the steady-state condition.

In order to explain the transport of molecules from one solution to the other across the lipid bilayer, other kinetic rate constants have to be considered, that is, those corresponding to the jump from the bulk to the membrane phase (k_{sm})and from the membrane to the bulk solution (k_{ms}). As k_{SM} and k_{ms} are not readily measurable, their ratio can be estimated, i.e. $K = k_{sm}/k_{ms}$. The overall permeability coefficient has been shown to be equal to

$$P = \frac{\lambda\, k_{sm} k_m}{2\, k_m + n k_{ms}} \qquad (5.20)$$

An application of Eq.5.20 will be presented in Section 5.7 in conjunction with water permeability in planar BLM. Suffice it to state here three limiting cases can be identified; they are schematically shown in Fig.5.2.

5.3.3 Irreversible Thermodynamics[2]

A lipid bilayer acts as a barrier to the movement of various chemical entities and maintains differences of concentration, pressure, temperature and electric potential across it. If the solutions on both sides of the membrane are well stirred, uniform values of these variables prevail throughout each of the two solutions and the whole gradient acts only across the membrane. The forces denoted by χ (i = 1, 2 ...n) which cause the flows or fluxes J_i (i = 1, 2,...n) are μ, P, T and E. The basic theorem of nonequilibrium thermodynamics is that the forces and the fluxes are so chosen as to satisfy the equation

$$\Phi = T\theta = \Sigma J_i \chi_i \geq 0 \qquad (5.21)$$

and the phenomenological coefficient L_{ik} (i,k = 1, 2,...n) in the equations

$$J_i = \sum_{i}^{n} L_{ik}\chi_k \qquad (5.22)$$

satisfy the Onsager relations

$$L_{ik} = L_{ki} \qquad (5.23)$$

θ in equation (5.21) is the rate of entropy production d_iS/dt due to irreversible processes within the system, and Φ is called the dissipation function. The description of transport processes in a system of n components requires the measurement of only n(n+1)/2 coefficients not all n^2 coefficients. Therefore, it should be mentioned in passing that the two

main purposes of non-equilibrium thermodynamics are: (i) to provide general relations between experimental effects which would be independent of molecular models (the Onsager relation is of paramount importance), and (ii) to establish certain criteria which would remain valid for dissipative systems which are not in equilibrium.

Evaluation of θ allows us to write the appropriate forms of the forces χ_i and requires the use of the laws of conservation of mass and energy, the second law of thermodynamics, and the Gibbs-Duhem equation.[2] For the purposes considered here, we restrict the analysis to membranes whose structures are completely homogeneous in terms of their hydrophilic and hydrophobic character. Hence, the flux of water J_W and solute J_S are described by

$$J_W = P_W \Delta C_W = \frac{D_W K_W \Delta C_W}{t_m} \qquad (5.24)$$

$$Js = P_S \Delta C_S = \frac{D_S K_S \Delta C_S}{t_m} \qquad (5.25)$$

where P_W, D_W, K_W, P_S, D_S, K_S are the permeability, diffusion and partition coefficients of water and solute, respectively. ΔCw and ΔCs are the concentration differences of water and solute between the adjacent compartments of the membrane.

The more realistic situation is found when a membrane admits both water and solute, establishing a ternary system. In consequence, the fluxes J_W and J_S can no longer be considered independent because water-solute interaction as well as the membrane-water and the membrane-solute interactions have to be accounted for. The interference of water and solute

fluxes in the bulk of the membrane is the principal reason to study membrane transport on the scope of the thermodynamics of irreversible processes.[2] This is expressed in Eqs. 5.24 and 5.25. In our case, the J_i will represent the fluxes of water and solutes and χ_i, the forces as the gradients of their chemical potentials.

For the case of water and solute permeation, the dissipation junction can be expressed by

$$\Phi = J_S\chi_S + J_W\chi_W \tag{5.26}$$

The forces can be given in terms of the respective chemical potential gradient as follows:

$$-\frac{\partial u}{\partial x} = -RT\frac{\partial \ln C_W}{\partial x} - V_W\frac{\partial P}{\partial x} \tag{5.27}$$

$$-\frac{\partial u}{\partial x} = -RT\frac{\partial \ln C_S}{\partial x} - V_S\frac{\partial P}{\partial x} \tag{5.28}$$

Then,

$$\Phi = (J_W V_W + J_W V_S)\,P + \left(\frac{J_S}{C_S} - \frac{J_W}{C_W}\right) Dpi \tag{5.29}$$

where $\underline{C}$ and $\underline{V}$ are the mean concentration between the adjacent compartments and V the molar volumes. This treatment allows us to define different types of permeability depending on the experimental

design chosen for its determination, i.e. the election of the force driving the flux.

As will be demonstrated forthwith, Eqs. 5.24 and 5.25 illustrate a particular case of a more general situation. Before entering into details, it must be emphasized that several assumptions are introduced to obtain Eqs. (5.29) and (5.30). These sometimes impose important limitations on the application of this formalism.[2] The most important limitation is that the concentrations (besides the gradients) must be very low in order to assume the Gibbs-Duhem relation ($n_w u_w - n_s u_s = 0$) to be valid with n_i the average moles of water and solute. This facilitates the expression of the concentration of water in terms of concentration of solute, and it changes the logarithm term to a linear one

$$\ln C = C_s/C_s \tag{5.30}$$

and

$$\ln C_w = C_s/C_w \tag{5.31}$$

5.4 Passive Transport

On the basis of experimental findings, various modes or mechanisms of membrane transport have been established [Kotyk and Janacek, 1977; Weiss, 1996]. Generally, two broad categories of biomembrane transport are recognized: passive and active. Since the driving force for membrane transport is the chemical potential gradient for water and nonelectrolytes which is related to the change in free energy (ΔG^0); for passive transport, ΔG^0 is negative, whereas for active transport, ΔG^0 is positive. The former is spontaneous and is discussed in this section, whereas for the latter the process must be coupled to a metabolic energy source, as will be considered in the next section. Before doing so, let us define some of the most frequently used terms in passive membrane transport (*see* Fig.5.3). These are:

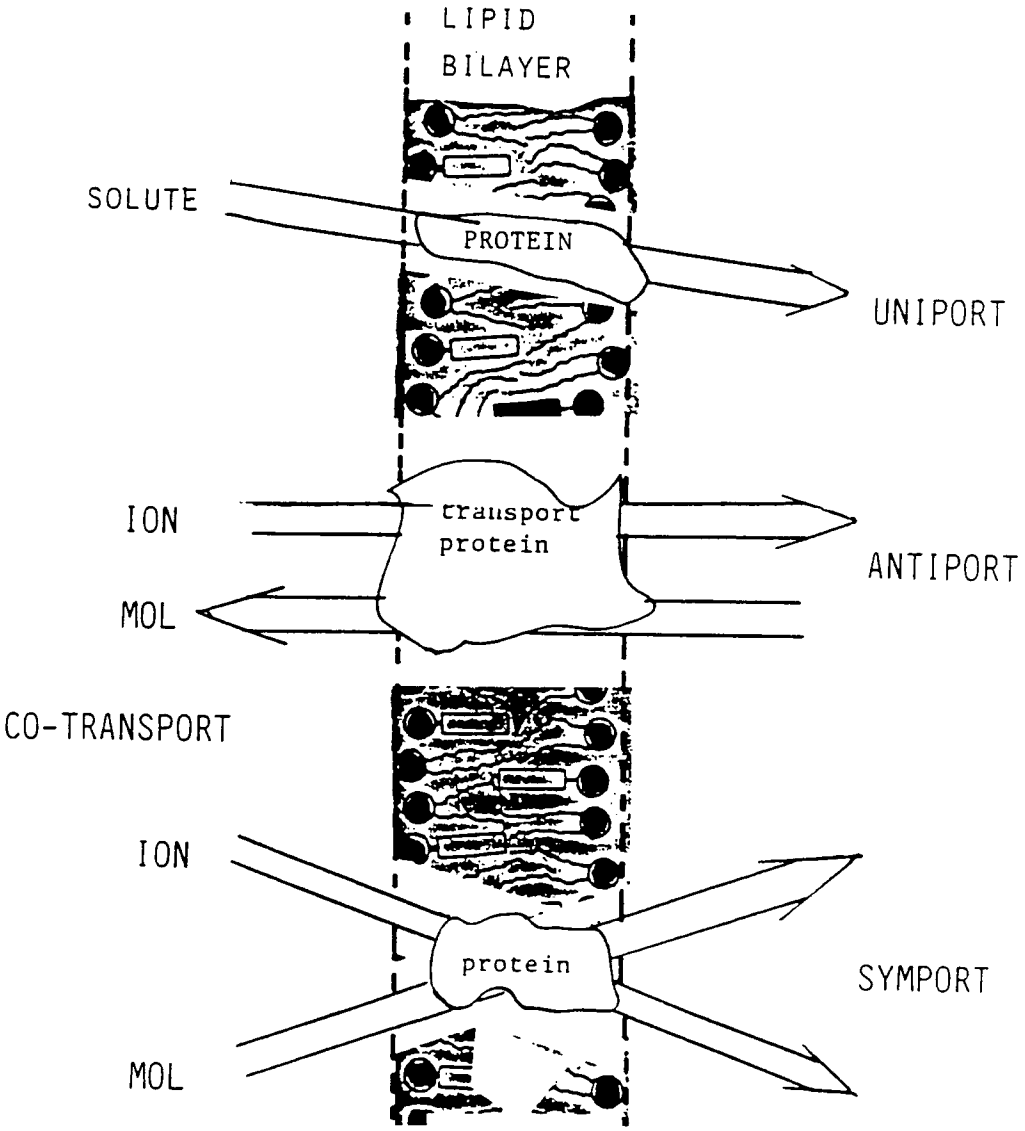

Fig. 5.3. A classification of biomembrane transport systems. A uniport membrane protein moves one solute across the membrane. In cotransport systems there are two types: antiport, in which the movement of one permeant depends on the transfer of another solute in opposite direction (e.g. the Na^+/K^+-ATPase pump) and symport, in which there is a simultaneous transfer of two solutes in the same direction (e.g. H^+ and sugar transport in bacteria).

Exchange Diffusion. The rapid exchange of permeant molecules across a membrane by facilitated diffusion.

Co-transport systems. In which the movement of one substance is dependent on the simultaneous movement of a second substance.

Counter transport. A phenomenon in which the flow of permeant in one direction drives the accumulation of another in the opposite direction.

Symport. In a co-transport system, the movement of one substance involves the movement of a second substance in the same direction.

Antiport. The opposite of symport, as defined above.

Passive Transport of Water

Water Permeability. There are two passive or dissipative transport processes by which water moves through membranes: diffusion and hydrodynamic flow. The Fick's first law, as applied to water transport across the membrane by passive diffusion, is usually written as

$$J_d = -P_d \Delta C_w \qquad (5.32)$$

where $P_d = D/\Delta x$ = the diffusion permeability coefficient. P_d is measured with THO (tritiated H_2O). The rate of passage (v_w) of a water molecule across a membrane is proportional to the force χ_w.(Eq. 5.5)

$$v_w = U_w \chi_w \qquad (5.33)$$

where U_w is the mobility of water in the membrane domain. The thermodynamic force is defined as the gradient of the minus chemical potential, and since the velocity is related to the flux J by the relation:

$$v_w = \frac{J_w}{C_{w(x)}} \qquad (5.34)$$

where $C_{w(x)}$ is the local concentration of water in a region (x) of the membrane. Thus, knowing that the chemical potential μ_w can be expressed in terms of the activity a_w and the pressure P, then

$$\frac{\partial u_W}{\partial x} = - RT \frac{\partial \ln C_W}{\partial x} - V_W \frac{\partial P}{\partial x} \qquad (5.35)$$

assuming concentrations equal to activity. V_w is the molar volume of water. The force driving the water flux has two contributions: the gradient of water concentration and the gradient of pressure. Hence, choosing the appropriate conditions, the flux of water can be determined by means of two different types of experiments. One for which $P/ x = 0$ and the other, $\ln C_W/ x = 0$.

The second type of dissipative transport process is viscous or bulk flow (a quantitative term). $J_v = -L_p A \Delta P$, where J_v = volume flow (ml/s), L_p = filtration coefficient or hydraulic conductivity (cm/s/atm), and ΔP = hydrostatic pressure difference. In order to compare Lp with Pd, Lp is expressed as P_f and is given by

$$P_f = L_p \frac{RT}{V_w} \qquad (5.36)$$

where P_f = cm/s and V = the partial molar volume of H_2O. It can be shown that water transport through membrane-containing pores (channels) is proportional to the square power for the pore radius for diffusion flow and to the fourth power of r for hydrodynamic flow (from Poiseuille's law $Lp = r^4/8\eta Dx$).

The osmotic phenomenon. If the membrane is permeable only to water, not to solute, Van't Hoff's relationship applies (*see* Chapter 2, Sectioin 2.2):

$$\Delta\pi = RT\Delta C_S \qquad (5.37)$$

where π is the osmotic pressure. The van't Hoff equation states a pressure difference must exist at equilibrium across a semipermeable membrane (e.g. the plasma membrane) separating dilute solutions.

Thermodynamically, when a cell is bathed in a dilute saline solution, the chemical potential of water, μ_W, is the same in the outer or extracellular fluid and intracellular fluid: that is μ_W (out) = μ_W (in). For an uncharged species, such as H_2O (or sugar), the chemical potential depends not only on concentration, but also on hydrostatic pressure. Thus, water diffusion may be driven by ΔC as well as ΔP. That is

$$\Delta\mu_W = (\mu_W)_{in}\text{-}(\mu_W)_{out} = V\Delta P + RT(\Delta \ln C_W) \qquad (5.38)$$

The movement of water can be stopped if an opposing hydrostatic pressure is applied; at equilibrium $\Delta\mu_W = 0$, solving Eq. (5.38) for ΔP and rearranging

$$\Delta P = \pi = - \frac{RT}{V_W} \Delta \ln Cw \qquad (5.39)$$

Equation (5.39) can be reduced to van't Hoff's Eq.5.37, since the hydrostatic pressure of the concentrated solution is greter than that of the dilute solution. Also note, this equation is identical in form to the Nernst equation (for ions) in terms of electrical potential and concentration gradients ($\Delta E = RT/F\ \Delta \ln C$).

Isotopic permeability. Another way of determining the permeability of a membrane to water is measuring the rate of diffusion in the absence of a macroscopic gradient. The system consists of the two compartments filled with water. In one of them, traces of tritiated water (THO) are added in a small amount so that no difference of pressure is created. The labeled molecules (THO) diffuse to the opposite compartment and the rate of

appearance of tritiated water is a measure of the diffusion flux. Thus, it is proportional to the difference in the specific activity ΔC^* of water:

$$J_D = L_D \Delta C^* \qquad (5.40)$$

L_D is named isotopic permeability coefficient.

Permeability to Nonelectrolytes

On the basis of classical studies of Overton, mentioned in Chapter 2 (Section 2.2), it was concluded that the rate of permeation of most nonelectrolytes across almost all cell membranes is governed by their lipid solubility relative to their water solubility. This conclusion has been extensively confirmed and modified since.[3] The concept of lipid solubility implies that, if permeability is governed totally by lipid solubility, a regular increase in permeability coefficient and in reflection coefficients must be accompanied by an increase in the lipid water partition coefficient (the equilibrium ratio of the test solute concentration in a lipid solvent to its concentration in water provided the two phases are in contact and mutually immiscible). The concept further implies that the rate-determining step in the permeation of a solute is the diffusion in the membrane phase and the mechanism of nonelectrolyte diffusion is the same through natural membranes as through a bulk lipid phase, and that the following expressions should hold:

$$P = \frac{KD_m}{t_m} \qquad (5.41)$$

and

$$K = \exp\left(-\frac{\Delta G}{RT}\right) \qquad (5.42)$$

where P stands for permeability coefficient, D, the diffusion coefficient for the solute in the membrane interior. K denotes for partition coefficient, t_m,

membrane thickness, and ΔG denotes for the free energy change associated with permeation. A similar type of general mechanism has been proposed by Diamond and co-workers.[3] for the diffusion of nonelectrolytes across membranes, in the form of solubility diffusion model, According to this model, the membrane resistance to permeation of solute (1/P) is the sum of two interfacial resistances (R) and the diffusional resistance of the membrane interior, i.e.

$$\frac{1}{P} = \frac{2\lambda}{D_{sm}} + \frac{t_m}{KD_m} \qquad (5.43)$$

As the mechanism of nonelectrolyte diffusion through membranes is treated the same as through a bulk lipid phase, the following conditions should be fulfilled up to a reasonable approximation. For small molecules

$$DM^{1/2} = \text{constant} \qquad (5.44)$$

and for large molecules

$$DM^{1/3} = \text{constant} \qquad (5.45)$$

where M is the molecular weight of the substance. Thus, the permeability coefficient (P) and the reflection coefficient (σ) should correlate closely with $KM^{-1/2}$ in a homogeneous, bulk lipid membrane. In fact, this relationship has been the guideline for most of the studies on nonelectrolyte permeability and on the basis of observations gathered by numerous ivestigators. The main characteristics of non-electrolyte permeation summarized as follows:

- P increases conspicuously with increasing K, but also increases somewhat with decreasing M at constant K.

- Measured reflection coefficients do not become negative even when the partition coefficient is increased ten times over the values at which σ is already virtually zero. It may be recalled that, under a given set of conditions, σ is 1 for an impermeable solute and 0 for a solute as permeable as the solvent itself. Thus, for solutes with very high lipid

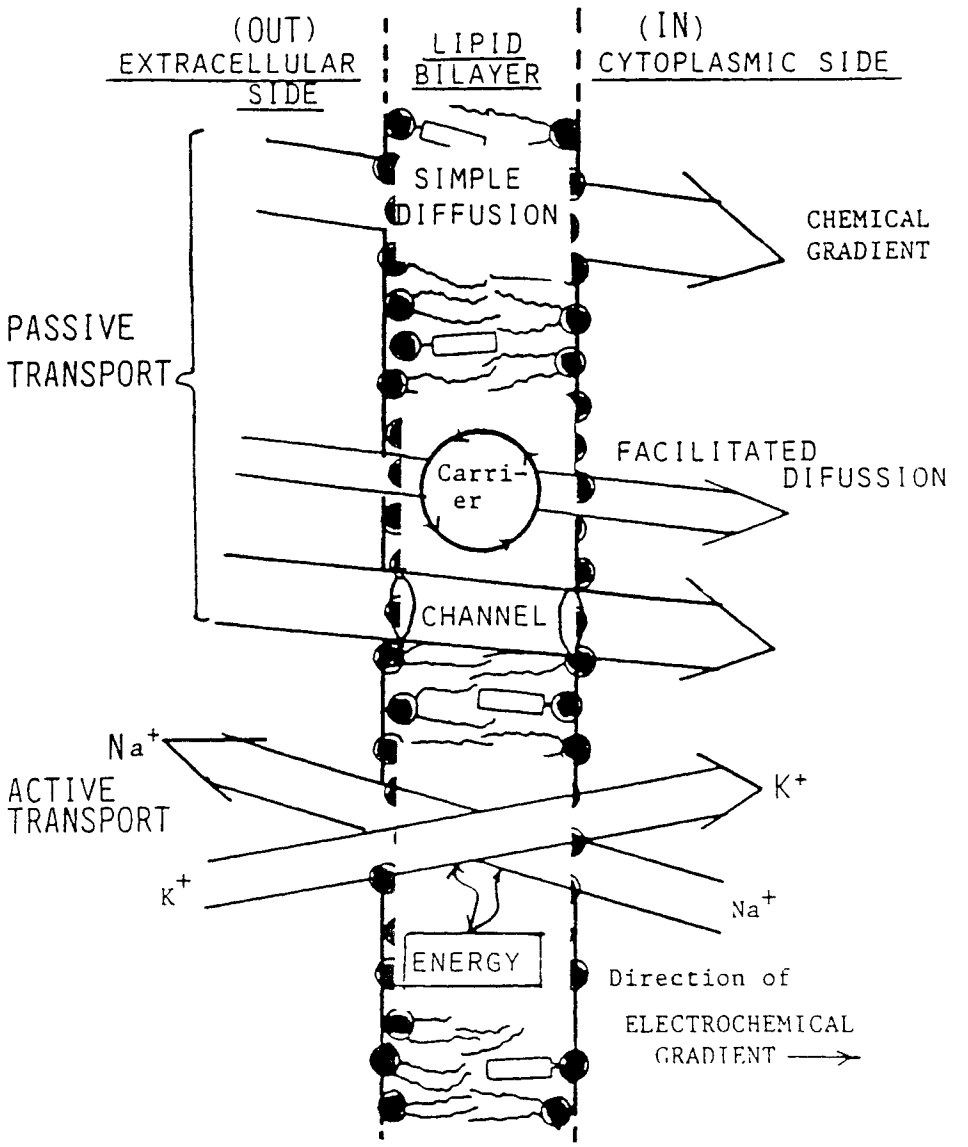

Fig. 5.4 Mechanisms of biomembrane transport.(1) Passive transport in the direction of chemical, u, or electrochemical, u gradient. Two types of (1) are distinguished: simple diffusion and facilitated diffusion. (2) Active transport in the direction opposite to the μ (or $\underline{\mu}$) gradient. A supply of energy is required.

solubilities, diffusion through the unstirred layers probably becomes rate limiting.

- There are significant exceptions to the main pattern of nonelectrolyte permeability: small molecules permeate relatively more rapidly and branched molecules permeate relatively more slowly. It has been found that small polar molecules of low lipid solubility permeate more rapidly than one would expect on the basis of their molecular weights and the inverse relation between σ and temperature is less steep for them than for other solutes and is little affected by a decrease of pH, which increases the value of σ for other solutes

- The transmembrane flux of molecular species which can undergo association-dissociation reactions, such as acids and bases, is generally proportional to the concentration of uncharged species, which may be a function of pH. For molecules having large lipid moieties, such a correlation is not observed. In fact, changing pH has little effect on the permeability of higher fatty acids. At low pH there is significant deviation in the permeability of even neutral molecules, possibly because of altered charge and packing of membrane lipids.[3]

Two possible explanations have been considered for the above-mentioned anomalies: (a) these solutes may follow the same route through membrane lipid bilayers as do other solutes, and their enhanced permeation may be an expression of the sieving properties of oriented membrane lipids or (b) these solutes may follow a separate route through the cell membrane, interacting with polar groups rather than with the hydrophobic chains of the lipid bilayer.

Mechanism of transport of nonelectrolytes

The water permeability of lipid bilyers has been measured using the osmotic properties of the liposomes. In this case, the lipid bilayer behaves as a selective membrane. The permeation of nonelectrolytes such as polyalcohols, urea, and short chain alcohols can also be determined by means of the optical changes. However, the interpretation of the experimental results is not straightforward. They are discussed in the following paragraphs.

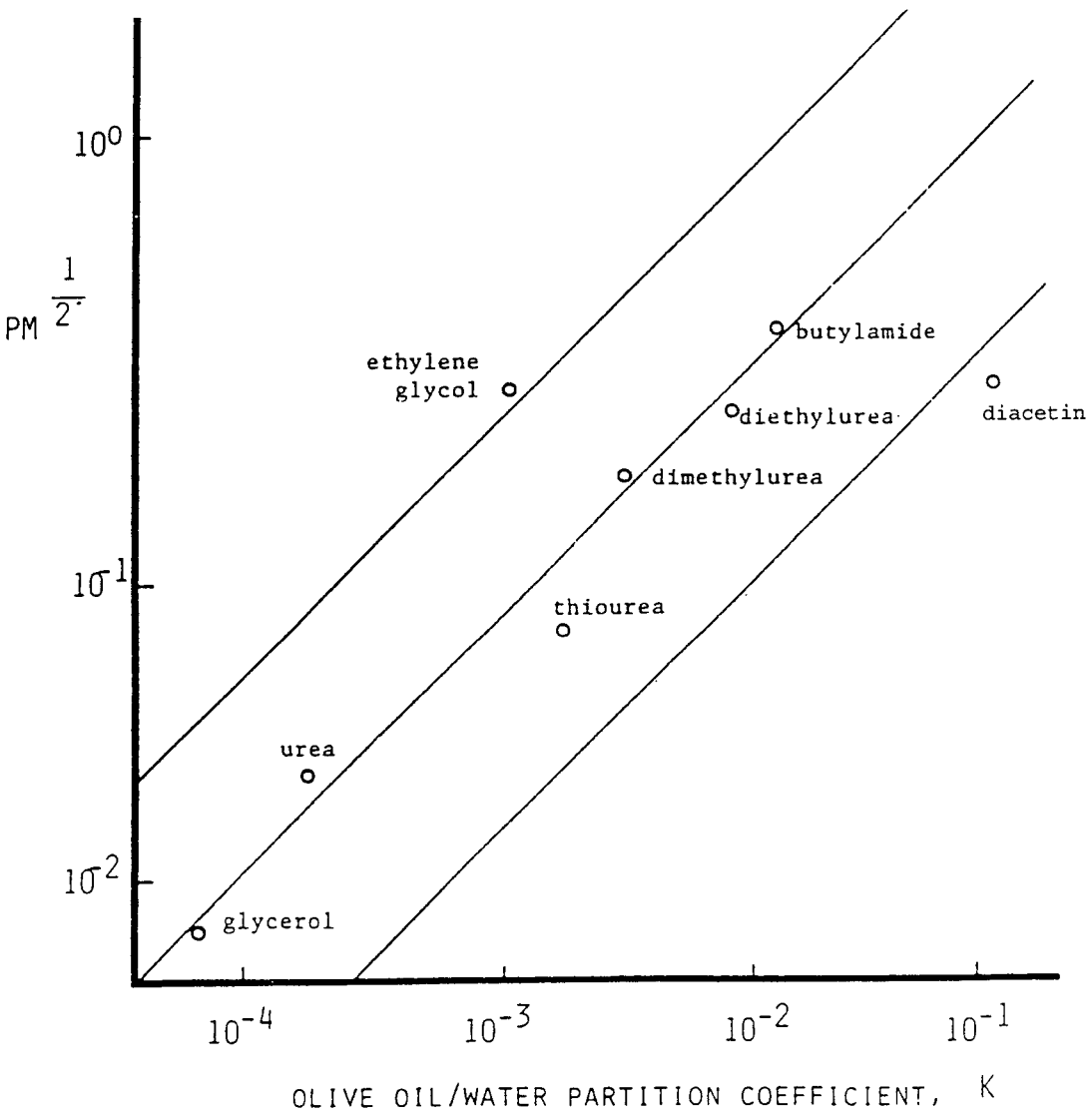

Fig. 5.5 Selected data of permeability of Cell of Chara ceratophylla to nonelectrolytes.[22]

Permeability and partition coefficient. The correlation between the permeability (P) and the partition coefficient (K) of a great number of polar solutes are shown in Fig. 5.5. The permeability of different biomembranes follows this general pattern. For many species, however, the data in Fig.5.5 show a considerable scattering. Therefore, at first glance, natural membranes behave as a solubility membrane in which the nonpolar bulk structure plays a significant role. This suggests that the hydrocarbon-like interior of the membrane is not the main barrier determining the permeability for all solutes. The fluidity of the lipid bilayer interior is much greater than near the glycerol backbone. Thus, this backbone region together with the polar head groups may contribute to the rate-limiting barrier for certain polar solutes. Furthermore, in order to mimic the permeation pattern, octanol seems to be the adequate nonpolar phase in comparison to olive oil and hexadecane. Thus, partition of the polar solutes takes place between water and a partially polar solvent phase.

The discrimination of polar solutes by chemical character of size and shapes is exemplified in Tables 5.1 and 5.2. The permeability coefficient of egg lecithins is directly related to the partition in the hydrocarbon-like phase. Thus, for these compounds the bilayer behaves as a solubility diffusion barrier that is identified as the interior of the hydrocarbon lipid bilayer region. In contrast, compounds listed in Table 5.2 do not correlate with the partition coefficient of octanol/water [Benga, 1989]. It is worth interesting that permeability decreases as a function of the size of the halogenated group linked to the acid molecule. The shape of the molecule as it is the case for the valeric acid (from the straight chain *n*-valeric to the globular *t*-valeric) also decreases the permeability.

Table 5.1 Permeability coefficient (P) of egg lecithins as a function of the partition coefficient (K)

	$\mathbf{P} \times 10^4$ (cm sec^{-1})	$\mathbf{K}_{octanol}$
Formid acid	2.34	0.29
Acetic acid	2.38	0.49
Propionic acid	6.1	1.8
Butyric acid	11.5	6.2

Table 5.2 Permeability coefficient of egg lecithins as a function of the solute shape

	$\mathbf{P} \times 10^4$ (cm sec^{-1})	$\mathbf{K}_{octanol}$
Chloracteic acid	11.6	1.3
Bromoacetic acid	12.3	2.6
Iodoacetic acid	10.9	4.5
Valeric acid	18.0	18.1
Isovaleric acid	13.3	21.2
t-Valeric acid	2.4	29.2

Kinetic-molecular description of solute transport. The movement of molecules across membranes can be described on the basis of the kinetic molecular theory in terms of the thermal fluctuations in the membrane chains of the lipid bilayer [Finkelstein, 1987; Benga, 1989]. The thermal motion of the hydrocarbon chains results in the formation of conformational isomers, so-called kinks. "Kinks" are described as mobile structural defects whose diffusion coefficient is calculated to be 10^{-5} cm^2/sec. Small molecules can enter into the free volume of the kinks and migrate across the membrane together with the kinks. As seen before, this description is suitable for water permeation. An extension to the diffusion of large nonelectrolyte molecules can be done on the basis of the formation of transient pores (channels) inside the lipid bilayer. However, more channels will be available to small molecules than to large molecules.

Another important factor to take into account in the permeation of nonelectrolytes is the presence of water in the lipid bilayer structure. The amount of water in the bilayer varies considerably below and above the phase transition temperature.[4] In parallel, the expected numbers of kinks per fatty acid chain are very small below the trasition point. Thus, the kink diffusion should be hindered by the rigidity of the lipid bilayer matrix. In addition, the fluidity of the hydrocarbon chains in the lipid region increases with the phase hydration. This is consistent with the water permeation data in lipid bilayers in the gel state, which is several times

lower than that in the liquid crystalline state. From a non-equilibrium thermodynamic viewpoint,[2] the water dependence of the diffusion of polar compounds across the polymer-like structure of the bilayer is a strong suggestion to consider the coupling of water and nonelectrolyte fluxes. The mutual influences among lipids, water, and solute make the membrane a ternary system. Hence, the water-solute interaction should be taken into account for an adequate description of transport.

In concluding this section, it should be mentioned that experiments on the permeability of lipid bilayers to small electrolytes have been performed over the years. The results of these experiments, taken together with water permeability measurements, give considerable insight as to the mechanisms by which small molecules pass through the lipid barrier. Many studies over the years have supported "Overton's hypothesis" that the membrane permeability of a molecule correlates well with its oil/water partition coefficient. The bulk oil which seems to give the best correlation is hexadecane [Finkelstein, 1987]. While Overton's hypothesis works remarkably well over a range of 10 in permeabilities and partition coefficients, recent studies on a number of small nonelectrolytes indicate that the membrane interior may be better modeled as a "soft polymer" than as a bulk liquid hydrocarbon.[5] In particular, the permeabilities of very small nonelectrolytes (including water) are 2- to 15-fold higher than would be expected on the basis of the liquid hydrocarbon mode. Moreover, the steep decrease in permeability with increased size for very small molecules does not agree with results in bulk hydrocarbon liquids. Both results do agree, at least qualitatively, with the permeation of small nonelectrolytes in "soft polymers" such as rubber and polyurethane.

The above situation is akin to what has been seen in water permeation. The liquid hydrocarbon model in both cases works very well overall in predicting the permeabilities of the lipid bilayer. When one looks more closely, however, some differences between the bilayer and bulk hydrocarbons appear. While there are several different models of the organization of alkyl chains in liquid hydrocarbons,[5] there are always definite differences in the alkyl chain organization in the bilayer and bulk liquid.[6] The obvious constraint, that one end of the lipid molecule is fixed at the water/membrane interface, results in an overall anisotropy and some

ordering of the alkyl chains in the direction perpendicular to the plane of the membrane. This difference between bilayer and bulk phase organization would be expected to have some effect on solute permeation. Models of solute permeation depend on details of the molecular dynamics and organization of the membrane. It should be possible in principle then, to infer something about the dynamic molecular structure of the lipid bilayer from permeability measurements. Indeed, Trauble proposed an attractive model of water permeation many years ago.[5] In this model, water molecules traverse the membrane by riding along with diffusing free-volume pockets created in the membrane interior by thermally generated gauche-trans-gauch 'kinks' in the alkyl chains. This model predicts an activation energy of about 16 kcal/mol for water permeation in monoolein-hexadecane bilayers vs. the observed value of 15.6 kcal/mol.[6] On the other hand, it predicts the same activation energy for monoolein-triolein whereas the observed value is 9.8 kcal/mol (*see* Tables 5.3 and 5.4). In the 'kink' model, the alkyl chains are quite ordered; subsequent experiments and theoretical models have revealed considerably more disorder in the alkyl chains, especially near the tails of the alkyl chains.[7] As Trauble pointed out in discussing his model,[12] it is no longer valid when the interior of the bilyer "resembles a fluid more than an ordered structure". The fact that the monoolein-hexadecane bilayer is considerably more ordered than the monoolein-triolein bilayer may be relevant here. Trauble also pointed out that the kink model is not relevant when the diffusing solute is considerably larger than the volume of a CH_2(methylene) monomer unit. In this case, one would expect large distortions of the alkyl organization associated with the passage of the solute. This is consistent with the observation that for the premeation of the larger nonelectrolyte molecules, the membrane interior becomes more like a hydrocarbon liquid.[5] Several models exist for the diffusion of solutes through liquids, polymers, and bilayers,[8] as well as several detailed models of the dynamic molecular structure of the lipid bilayer have been developed.[9-13] Combining such theoretical models with experimental studies of the molecular organization of the bilayer and with detailed measurements of the permeation of water and nonelectrolyte molecules should lead to a detailed picture of the molecular mechanisms of water and nonelectrolyte permeation through the lipid bilayer.[14]

5.5 Facilitated diffusion

In contrast to passive water transport by simple diffusion, discussed in the last section, where the pathway is through the lipid bilayer, observed rates of permeability for certain solutes (for example, glucose) across biological membranes are considerably greater than might be predicted from a consideration of their oil/water (o/w) partition coefficients. These findings led to the suggestion of pores and/or carriers in the membrane. Transport processes of this type are referred to as facilitated diffusion (Fig.5.4). For this type of diffusion, a much lower activation energy is indicated (E_a < 16 kJ/mol), the process has been found to be less temperature dependent (Q_{10} = 1.0 to 1.3), not a linear function of substrate concentration and inhibited by reagents capable of attacking proteins.

As facilitated diffusion requires some specific component of the membrane, such as carriers or proteins, the kinetics of such systems have been analyzed in terms of Michaelis-Menten's equation. The permeant (P) is believed to combine with the membrane protein component (M), to form a complex (P-M) as follows:

$$P + M \text{ --- } P\text{-}M \qquad (5.46)$$

If C_1 and C_2 are the concentrations of the permeant in solutions 1 and 2, separated by a membrane, then the fluxes can be given as

$$J_{1\to2} = \frac{J_{max} \cdot C_1}{K_m + C_1} \; ; \; J_{2\to1} = \frac{J_{max} \cdot C_2}{K_m + C_2} \qquad (5.47)$$

where $J_{1\rightarrow2}$ and $J_{2\rightarrow1}$ are the one-directional fluxes of the permeant, J_{max} is the maximum rate at saturation (i.e. when all M's are bound by P), and K_m is Michaelis-Menten constant. The net flux, ΔJ, is given as

$$\Delta J_{net} = \Delta J = J_{max} \left(\frac{C_1}{k_m + C_1} - \frac{C_2}{k_m + C_2} \right) \qquad (5.48)$$

In case the concentration of permeant in solution 2 is very small in comparison to that in solution 1, Eq. 5.48 becomes

$$\Delta J = J_{max} \left(\frac{C_1}{K_m + C_1} \right) \qquad (5.49)$$

On taking the reciprocal of both sides of Eq. 5.44, one obtains

$$\frac{1}{\Delta J} = \frac{K_m + C_1}{J_{max} \cdot C_1} = \frac{K_m}{J_{max}\, C_1 \cdot} + \frac{C_1}{J_{max} \cdot C_1}$$

$$= \frac{K_m}{J_{max}} \cdot \frac{1}{C_1} + \frac{1}{J_{max}} \qquad (5.50)$$

and the values of K_m and J_{max} can be obtained from the slope and intercept, respectively, of the straight line by plotting $1/\Delta J$ against $1/ C_1$ (a Lineweaver-Burke plot, *see* Fig.5.6).

Table 5.3 Experimental activation energies and derived quantities from the absolute reaction rate theory for various systems.[7]

System	E_a (kcal/mol)	ΔS^* (cal/mol/deg.)	ΔH^* (kcal/mol)	ΔG^* (kcal/mol)
Water	4.6	2.5	4.0	3.9
n-Hexadecane	3.4	-0.2	2.8	3.4
Cell membranes	15-22	16-39	14-21	9.7-10.1
BLM[a] (t_m =70A)	6.8	-12.2	6.2	10.1
BLM[b] (= 3A)	6.8	-15.8	6.2	11.4
BLM (= 1A)	6.8	29.1	6.2	-2.4

[a] The derived quantities were calculated according to Eq. 5.19, where l = 5 A. [b] BLM thickness: T = 40 A unless otherwise noted.

Table 5.4 Energies of activation for the permeation of water in different phosphatidylcholine liposomes [Benga, 1989]

System	Energy of activation (kcal/mol)	
	T > Tc	T < Tc
PC/PA(96:4)	9.3 ± 1.3	- -
	12.1 ± 0.9	27.4 ± 3.9
PC/PA(96:4)	11.3 ± 3.4	20.5 ± 1.9
	7.3 ± 1.1	26.6 ± 0.9
PC/PA(92:8)	7.0 ± 1.5	26.0 ± 2.1
PC/PA(96:4)	6.6 ± 0.4	28.5 ± 2.2
	9.5 ± 1.2	26.4 ± 0.9

Note: T_c, phase transition temperature.

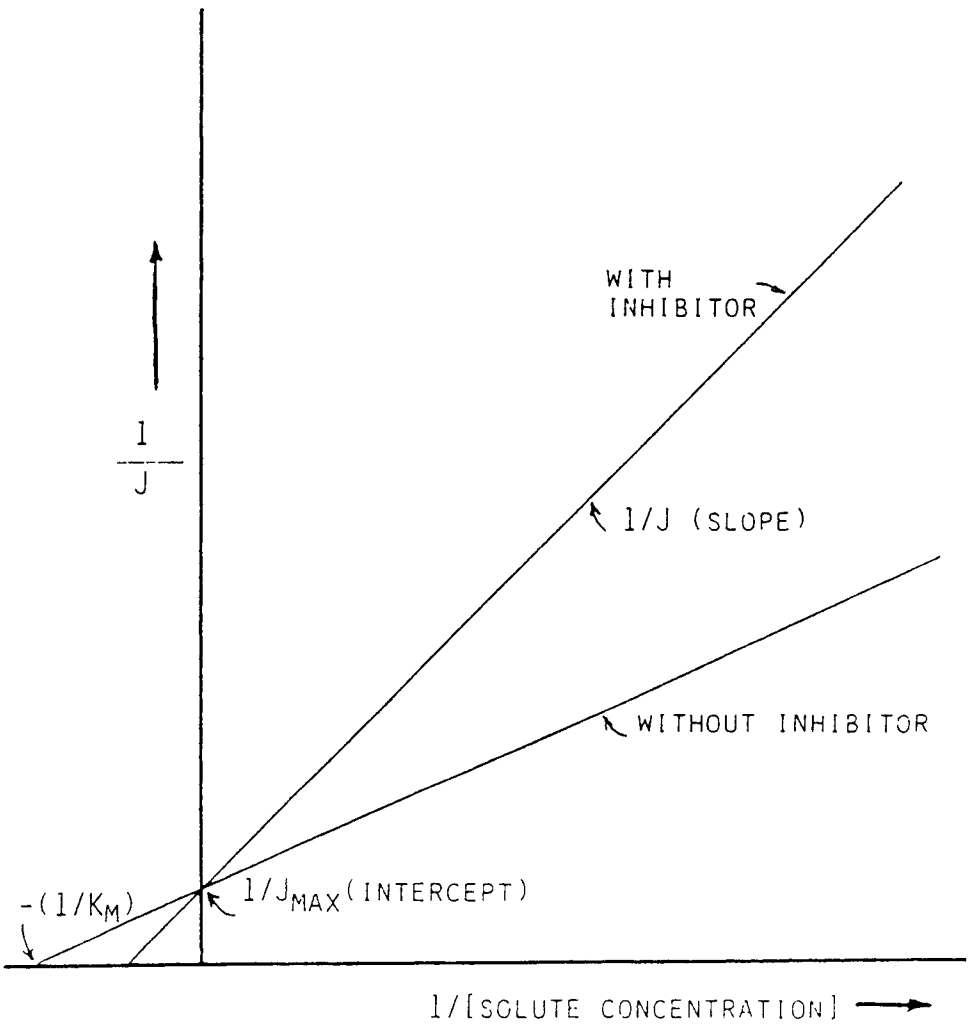

Fig. 5.6 A Lineweaver-Burke plot for the determination of various constants for facilitated transport. From such a plot, the slope yields k_m / J_{max}, whereas from the intercepts at the horizontal and vertical axis, $-1/k_m$ and $1/J_{max}$ are obtained, respectively.

However, polypeptides, the basic units of proteins, can act either as carrier or channels and may be distinguished experimentally by measuring the rate of permeation as a function of temperature (Fig.5.6). We will consider membrane transport by carriers and channels, as well to illustrate the facilitated transport system using experimental lipid bilayers, under separate headings below.

Facilitated diffusion by way of carriers

Selective carriers allow translocation of certain ions and molecules in both directions across the memrbane. Essential characteristics of facilitated diffusion by carrier mechanism are that: (1) with a given carrier it is specific to certain ions or molecules, (2) this passive process is driven by concentration gradients, and (3) the system may become saturated when all carriers are loaded; the rate of movement can become saturated. Transport of bicarboate (HCO_3^-) and Cl^- in red blood cells are two outstanding examples. By this mechanism, the cell can prevents buildup of unwanted materials. Experiments discussed in Sectiion 5.7 with model membranes (BLMs and liposomes) will clearly illustrate facilitated diffusion by carriers.

Channel-mediated diffusion

It is evident that the basic lipid bilayer structure of biomembranes is impermeable to hydrophilic species whereas lipophilic compounds in an aqueous environment must find their way to the membrane in order to be transported into the cell. Nature has solved these paradoxically situations by having carriers and channels in the lipid bilayer of the membrane, which usually exist in a liquid-crystalline, fluid state (see Fig. 5.1). The lipid bilayer of biomemrbanes serves as a very effective barrier to prevent the passage of polar or water-soluble substances from translocating an intact cell membrane. This is consistent with the evolutionary hypothesis that living organisms orginate from an aqueous environment. In order for a cell to be viable, a variety of mechanisms by which water-soluble substances cross the lipid bilayer have evolved. The two most outstanding ones are: the above-mentioned facilitated diffusion via carriers and diffusion through channels, listed here.

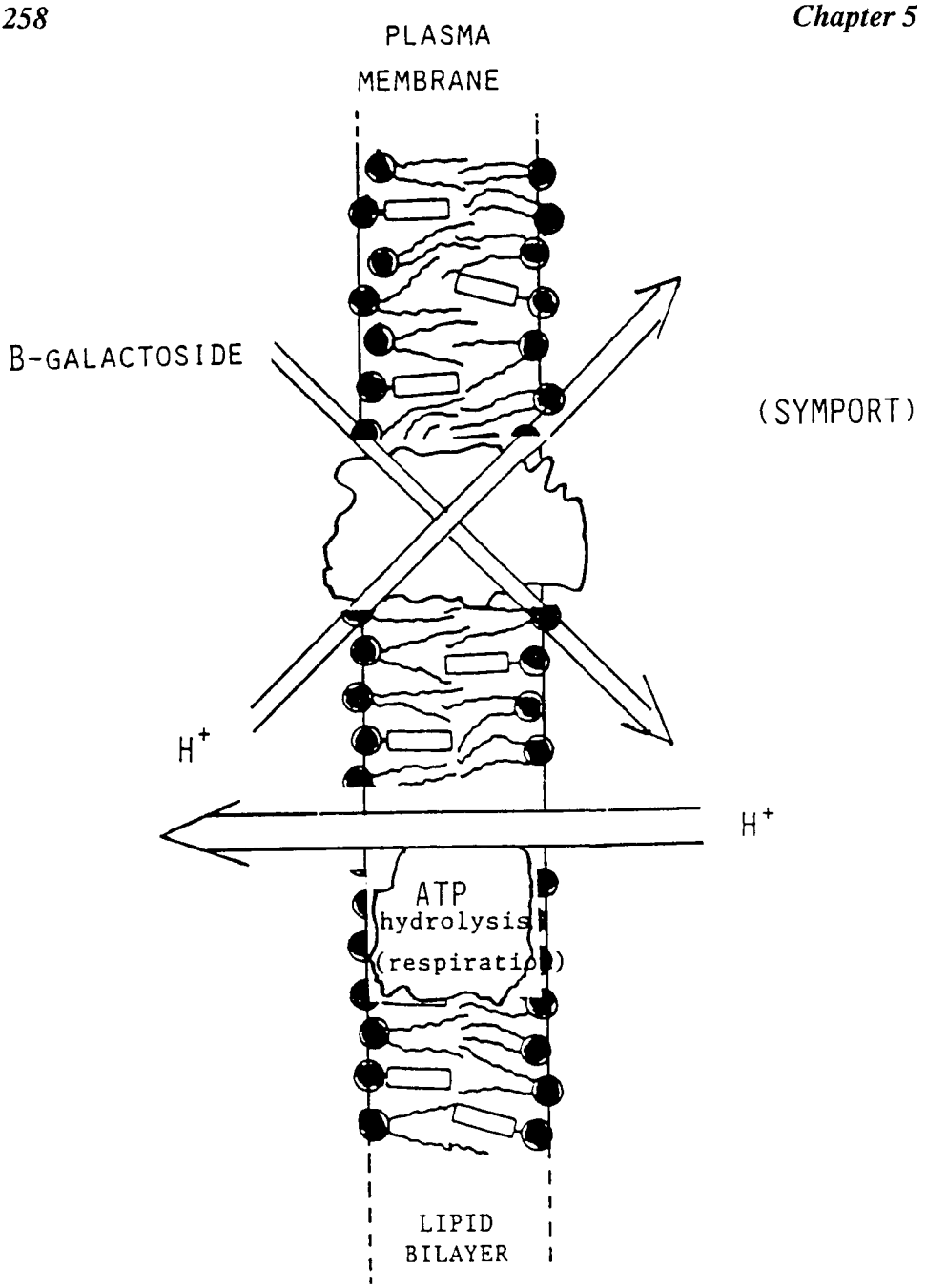

Fig. 5.7 A simplified scheme for the transport of β-galactoside of *Escherichia coli*.[15]

For channels, they are usually proteinous compounds, some of them span the entire lipid bilayer comprising, for example, a water-filled pore for ions. The channels have 'gates'; their openings and closings for ion transport are operated by a number of mechanisms. There are so-called voltage-gated channels, ligand-gated channels and store-operated channels (see Fig. 1.3A, Chapter 1).

The incisive question to raise here is 'how does one go about to investigate the membrane biophysics of carriers and channels in the absence of in vitro lipid bilayer'? A short answer to this question is: "It cannot be done !", for the phenomena under consideration are lipid bilayer-depedent. Insofar as membrane functions are concerned, bilayer lipid membranes (planar BLMs and spherical liposomes) provide a most unique approach and have been so used in studying transport carriers and channels. The two key experiments in bilayer lipid membranes are: (a) ion carriers (*The Valinomycin Experiment*), and (b) ion channels (*The Gramicidin Experiment*). We will deal with the mechanisms of membrane transoprt by means of BLMs and liposomes in Section 5.7.

5.6 Active transport

Facilitated diffusion will continue only for as long as the concentration gradient for the transported material is maintained. However, many substances are transported against a concentration gradient. Therefore, energy must be provided. It should be mentioned that ionic gradients, in terms of H^+ and Na^+ across the membrane, can provide the necessary free energy for the so-called secondary active transport. In terms of irreversible thermodynamics, the flux, J, is 'active' if it is coupled to a chemical reaction; otherwise, it is referred to as passive. In living systems active transport is driven by a chemical reaction (i.e. the hydrolysis of ATP, which is catalyzed by the ATPase). The enzyme, ATPase, is embedded anisotropically in the fluid lipid bilayer, which consumes reactants on one side and discharge products on the other side of the membrane. Active transport systems are best illustrated with examples. We will confine ourselves to three specific cases.

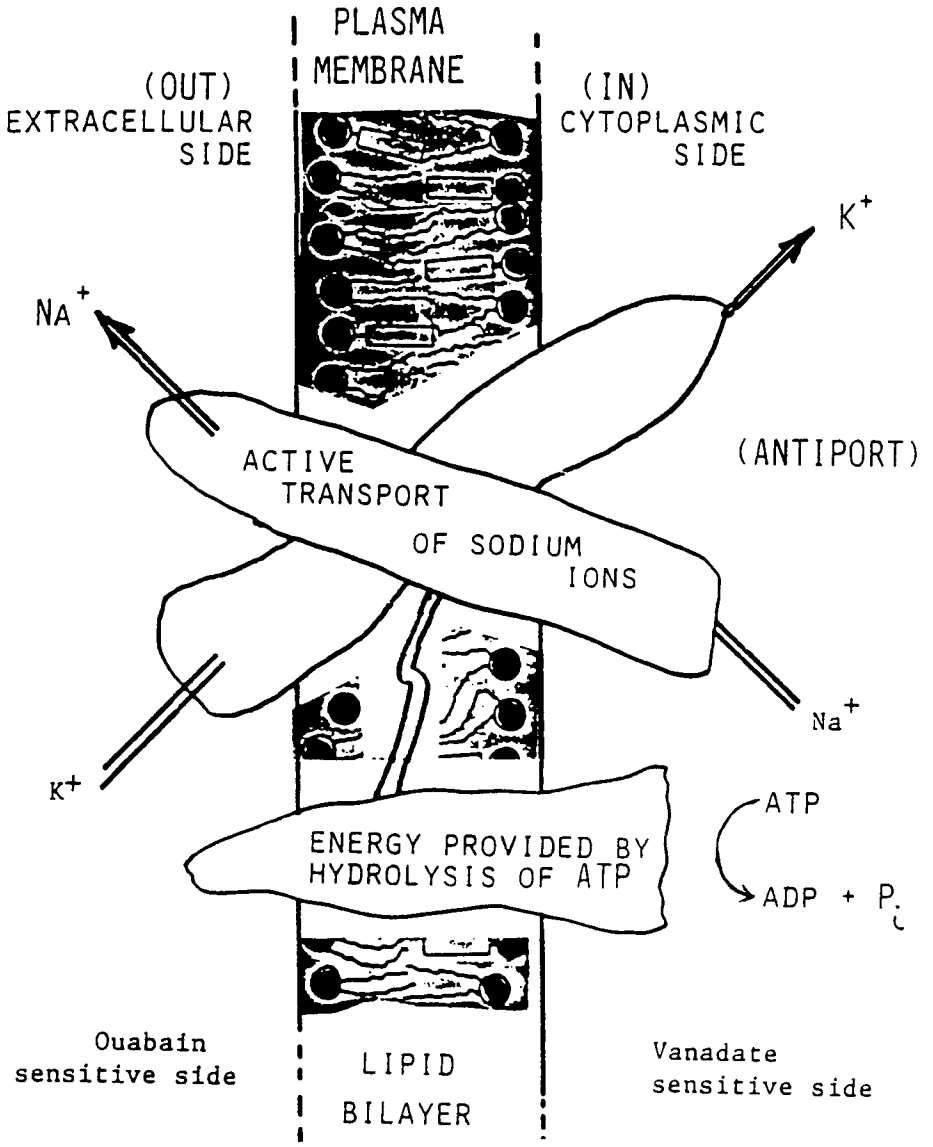

Fig. 5.8. The Na^+/K^+ ATPase pump, one of the most important transporters in biomembranes. The membrane-bound ATPase translocates 3 Na^+ out and 2 K^+ in against their respective electrochemical gradients per molecule of ATP hydrolyzed (*see* ATPase pump reconstitution in BLM.[16,27]).

a. β-galactoside uptake in Escherichia coli

This is a well-characterized active transport system at the molecular level using the proton (H^+) gradient as the driving force. The characteristics of the system, in particular the transport of lactose, were established by Monod, Cohen, Fox, Kennedy, West, and Mitchell. The suggested mechanism is shown in Fig. 5.8..

In terms of the thermodynamic approach, the fluxes of H^+ and lactose are linked. At equilibrium, the differences of electrochemical potential of H^+ and lactose are equal. Although lactose is electrically neutral, the uptake of it would be driven by the membrane potential in the absence of a pH gradient in accordance with the chemiosmotic hypothesis.[15]

b. The Na^+/K^+ ATPase pump

To maintain a high concentration of K^+ and a low concentration of Na^+ inside of the cell relative to the extracellular fluid, the plasma membranes of cells contain a machinery known as the Na^+/K^+ pump which actively transports Na^+ out of the cell and K^+ in, against their electrochemical potential gradients. The Na^+/K^+pump is made of protein, the Na^+/K^+ ATPase, with the energy supplied by the hydrolysis of ATP. To fuel this pump, about one third of a cell's energy is used to translocate K^+ in and Na^+ out of the cell. These ion concentration gradients are essential in maintaining the cell's membrane potential and volume as well as in active transporting in the cell's nutrients (sugars, amino acids, etc.). Clearly, an appreciation of the Na^+/K^+ pump in terms of its structure and mode of operation is in order.

The studies of red blood cells (RBC) and their ghosts have shown that the Na^+/K^+ ATPase is closely associated with the plasma membrane with specific orientation. The translocation of Na^+ and K^+ requires the hydrolysis of ATP and can occur only when Na^+ and ATP are present inside the RBC ghosts and K^+ is on the outside. The pump is specifically inhibited by ouabain (a cardiac glycoside at 10^{-8} M) which also poisons the Na^+/K^+ ATPase. For each ATP hydrolyzed, 3 Na^+ are pumped out and

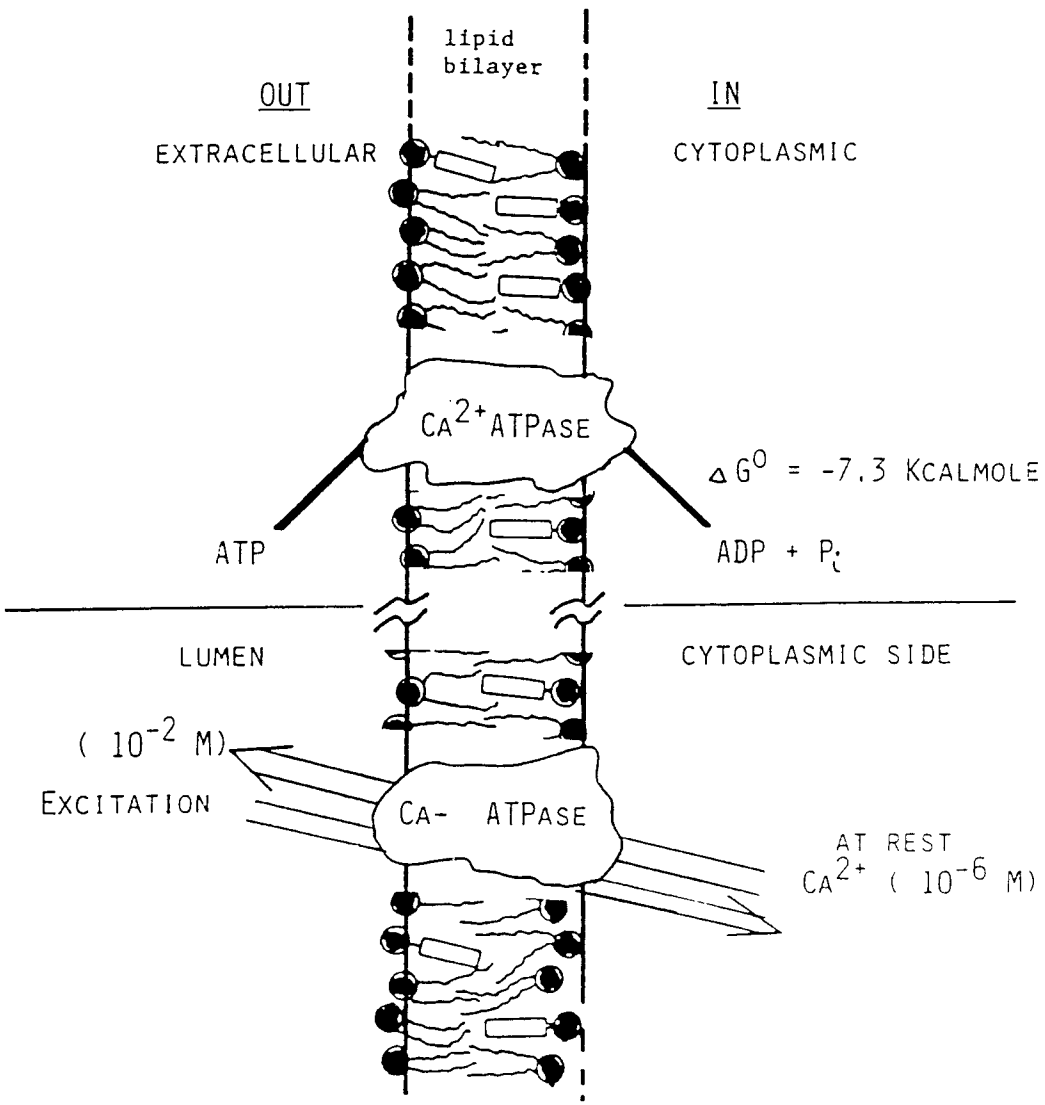

Fig. 5.9 The Ca^{2+}-ATPase pump. *Upper portion*: in the plasma membrane. *Lower portion*: in the sarcoplasmic reticulum The Ca^{2+}-ATPases of SR have been incorporated into BLM and liposomes.[17,18]

2 K^+ pumped in with the turnover rate of 100 ATP per second per ATPase. Finally, the most remarkable feat is that the Na^+/K^+ pump can operate in reverse by synthesizing ATP from ADP and P_i. Figure 5.8 shows the structure and orientation of the Na^+/K^+ pump, where suggested mechanism of operation of the Na^+/K^+ pump is also indicated. An attempt to reconstitute an ATPase pump in BLM has been reported.[16]

c. The Ca^{2+} pump of sarcoplasmic reticulum

The sarcoplasmic reticulum (SR) is associated with skeletal and other muscles. The Ca^{2+}-ATPase of the plasma membrane of erythrocytes (RBC) exhibits a high affinity for Ca^{2+} and calmodulin (a lower molecular weight protein) located on the cytoplasmic side. The Ca^{2+}-ATPase of sarcoplasmic reticulum (SR) is much better characterized, that has a mol. wt. 1.0 to 1.5 x 10^5, constituted about 80% of the structural membrane protein occupying about 30% surface area. Generally, Ca^{2+} is translocated into the SR. During excitation of the SR membrane, Ca^{2+} is relased. Depolarization of the SR membrane leads to translocation of sequestered Ca^{2+} from the SR to the myofibrils providing the connecting link between excitation and contraction of the muscle. The 'heart' of the Ca^{2+} pump is the Ca^{2+} activated ATPase (mol. wt. 100,000) spanning the SR membrane, which constitutes about 60 to 80 percent of its total protein. The Ca^{2+}-ATPase located on the outer surface is capable of binding 40 mol Ca^{2+}/mol of protein. At rest, Ca^{2+} ions are pumped into into SR so that Ca^{2+} concentration around the muscle fiber is very low. A suggested mechanism is depicted in Fig. 5.8.

5.7 BLM and Liposome Experiments

Returning now to the question of 'how does one go about to investigate membrane carriers and channels' using experimental lipid bilayers? Before going into details of the experiments with planar BLM and spherical liposomes, it is worth remembering that biomembranes are composed of lipids in the form of a bilayer, to which protein and nonlipid constituents are embedded (Fig. 5.1). It is evident that these constituents

determine the rates of translocation of matter across biomembranes. Two kinds of permeability properties of biomembranes have been discussed in the preceding sections; those that depend on specific pathways (pores or channels) and those that do not. However, even the relatively simple plasma membrane of RBC ghosts presents an extremely complex lipid-protein composition which makes it very difficult to relate the permeability properties with the structural features. More difficult is to identify the molecular entities playing the key role in the transport of complex solutes. As already considered in Section 5.3, the thermodynamic and kinetic formalisms have been outlined concerning the mechanisms of permeation of water and nonelectrolytes in biomembranes transport. In this section we will be mainly concerned with the nonspecific pathway, that is, the lipid bilayer core, for the movement of water and nonelectrolytes across experimental BLMs and liposomes.

5.7.1 Planar lipid bilayers

Insofar as we know, the functional unit of living systems is the cell whose existence depends on water. Water plays the pivotal role in the self-assembling of lipid bilayer and membrane structures via hydrophilic and hydrophobic interactions. Thus, besides the electrical measurements on BLMs, the process of water transport was among the earlier topics investigated [Benga, 1989].

The virtual impermeability to ions is consistent with the insulating hydrocarbon interior of the BLM. This fact may be illustrated by a simple calculation, which reveals that, for a 1 mm diameter BLM in 0.1 M KCl with a resistance of 10^8 ohm-cm and a potential difference of 50 mV, about 3×10^{10} ions or 5×10^{-14} equivalents of charge move across the lipid bilayer in 1000 sec. On the basis of this analogy, the permeability of unmodified BLM to water and to nonelectrolytes may be predicted from their solubility and diffusion data in liquid hydrocarbons or in olive oil. The latter is of special interest, since Overton and others deducing the lipoid nature of the plasma membrane (Chapter 2, *Biomembranes*) have used the data obtained with olive oil. In the case of water permeability in liquid hydrocarbon, for example, a value of 35 μm/sec is estimated from

the solubility and diffusion data, which we shall see to be in good agreement with measured values.

Permeability to Water

Experimentally, permeability to water in a BLM can be measured by setting up an osmotic gradient and measuring the volume of water flow per unit time or by using a labeled water on one side to find the rate of diffusion. In the latter, the flow of isotopically tagged water through the BLM is determined in the absence of an osmotic gradient. For the osmotic flux method. a cell consists of a closed inner chamber made from a 10 ml Teflon beaker (*see* Chapter 4). The volume of the inner compartment can be adjusted by manipulation of a precision micrometer syringe. After the membrane has become black, a known quantity of a concentrated salt solution is added to the outer compartment. The osmotic pressure gradient will cause the efflux of water, from the inner chamber across the BLM into the outer solution. This efflux is manifested by the inward bulging of the BLM. The BLM is observed visually, and a planar membrane of constant pattern of reflected light is maintained by manipulating the micrometer. The rate of water flux is determined. From this rate, the permeability coefficient is then calculated. For the details of the techniques and apparatus, consult the original references cited.[7,21]

The units of permeability coefficients, P (μm/sec), have the dimensions of velocity. We may, therefore, consider that 1/P is a measure of the resistance, R, offered by the BLM to water permeability. The total resistance, R, encountered by a water molecule, transferring from one side of the lipid bilayer to the other side, may be viewed as consisting of five separate resistances in series. These are two resistances at the membrane/solution interfaces (R_{sm} and R_{ms}), one due to the membrane (R_m), and two bulk-phase resistances. Since the self-diffusion coefficient of water is several orders of magnitude larger than the other coefficients, we need only to consider the resistances due to the membrane and the membrane/solution interfaces. Therefore, this total resistance may be expressed as:

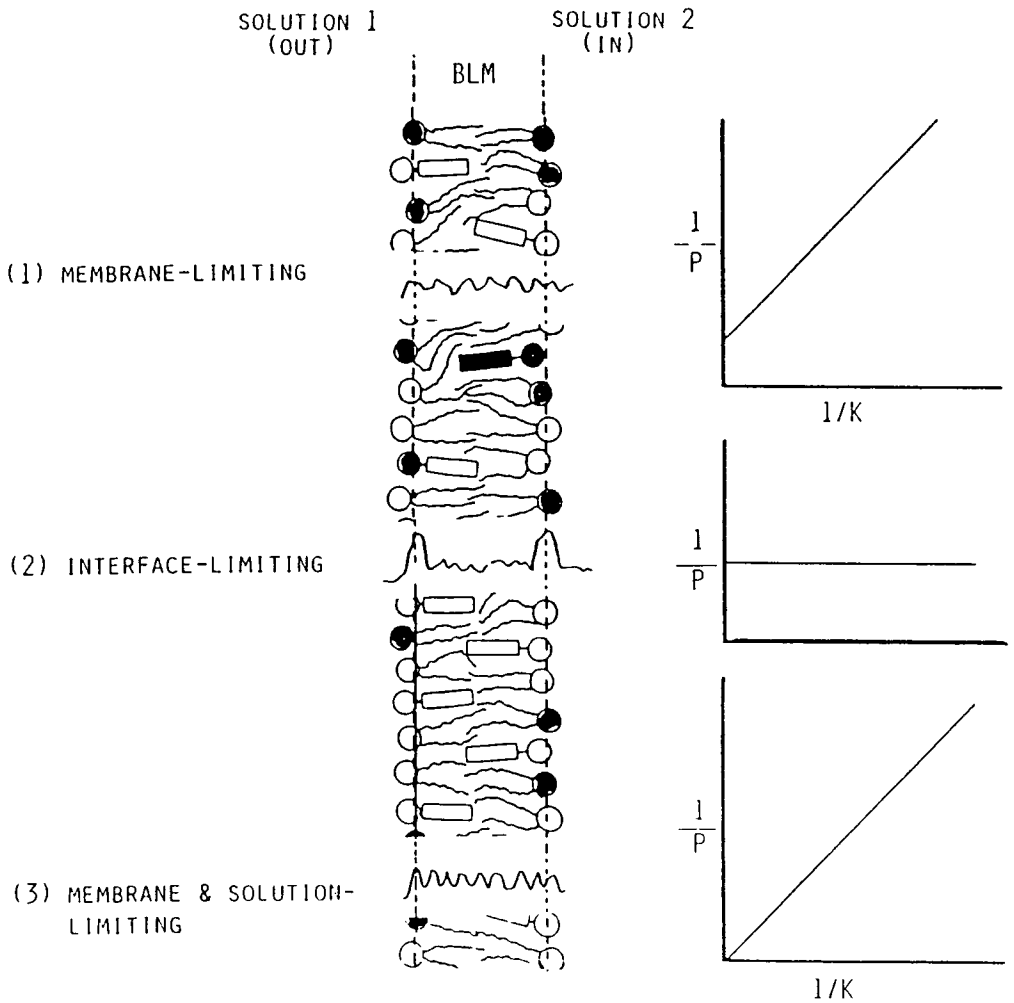

Fig. 5.10. Three limiting cases of permeation of water across biomembranes and experimetnal lipid bilayers according to the theory of absolute reaction rates: (1) $k_{ms} >> k_m$, (2) $k_m >> k_{sm}$, and (3) $k_m \simeq k_{ms}$.

$$\frac{1}{P} = R_{sm} + R_m + R_{ms} \qquad (5.51)$$

where the subscripts s and m refer to the solution and membrane, respectively. According to the Eyring absolute reaction rate theory discussed previously (Section 5.3), there is a specific rate constant k_i associated with each step (Fig. 5.10). Here k_m refers to the rate constantfor the BLM, while k_{sm} and k_{ms} are, respectively, the rate constants for diffusion in the solution/BLM and BLM/solution interfacial region.

Although the magnitude of P provides us with some clues concerning the permeation barrier, it is not possible to assess the relative contribution resulting from each resistance. Hence, it is necessary to measure the permeability coefficients of water through the BLM, as a function of the temperature. If it is assumed that permeation of water through an unmodified BLM takes place by a molecular process, the energy of activation may be evaluated from an Arrhenius equation of the form:

$$\ln P_O = A - (E_a/RT) \qquad (5.52)$$

where A is a constant (frequency factor), E_a is the activation energy involved in the rate-controlling step in the process, and R and T are the gas constant and the absolute temperature, respectively. It is expected that, if the assumption were correct, a standard plot of ln P vs. 1/T should give a straight line. The slope and intercept of the plot yield the activation energy E_a and the constant A. This has been found to be the case for a BLM system studied in the temperature range 22.5 to 44.0 ^{0}C.

In light of the above considerations, the permeability coefficients of water through the BLM as a function of temperature, and the ionic composition of the bathing medium are of interest. These data permit an evaluation of the various derived quantities from the absolute reaction rate theory. Recalling Eq. 5.20 given in Section 5.5.2, the permeability coefficient can be re written as

$$\frac{1}{P} = \frac{2}{k_{sm}\lambda} + \frac{n}{k_m\lambda\,(k_{sm}/k_{ms})} \qquad (5.53)$$

where k_{sm} and k_{ms} are the rate constants for diffusion across the solution/BLM interface, respectively, k_m is the rate constant for diffusion in the BLM, λ is the length of the diffusing jump, and n is the number of jumps across the BLM (note here the thickness of BLM, $t_m = n\lambda$). Since the partition coefficient, K, is defined as the ratio of k_{sm}/k_{ms} and the diffusion coefficient, $D_i = k_i\lambda^2$, where k_i refers to either k_{sm} or k_{im}, Eq. (5.53) becomes

$$\frac{1}{P} = \frac{2\lambda}{D_{sm}} + \frac{t_m}{D_mK} \qquad (5.54)$$

Three special cases may be considered: (1) the membrane limiting, (2) the interface limiting, and (3) both membrane and interface limiting. We shall consider each case separately in the following paragraphs. For all cases considered, $K = k_{sm}/k_{ms} << 1$ will be assumed.

1. *The membrane-limiting case* ($k_{ms} >> k_m$)

The rate-limiting step is diffusion through the BLM, where the first term of Eq. (5.54) is negligible, and we have

$$P = \frac{KD_m}{t_m} \qquad (5.55)$$

Indeed, experimental results indicate that P varies approximately as the reciprocal of the BLM thickness. From Eqs.(5.17) and (5.18), one can interpret ΔG^*, the free energy of activation for permeability, to mean the difference in free energy between the initial position of the permeating

water molecule in the aqueous solution bathing the membrane and the top of the higher energy barrier the water molecule must overcome within the BLM. One can use Eq. (5.18) to obtain entropies of activation (ΔS^*) for the BLM. The larger value of ΔS^* may imply that water permeation through the BLM requires a relatively greater disruption of the alkyl chains than is necessary in the bulk hydrocarbon (*see* Table 5.3).

2. *The interface-limiting case* ($k_m >> k_{sm}$)

Here, the controlling step is diffusion through the solution/BLM interface, Eq. (5.54) becomes

$$P \simeq \frac{\lambda k_{sm}}{2} = \frac{D_{sm}}{2\lambda} \qquad (5.56)$$

The permeability coefficient, in this case, is independent of t_m and K. This is evidently incorrect for bulk liquid hydrocarbon, since $P = D_m K/t_m$ is known to be valid. It is worth remarking that the possibility of the slowest step being diffusion through the solution/BLM interface is not likely. It would be of interest to study the dependence of P as a function of BLM thickness to access the contribution of this limiting case.

3. *The membrane-interface limiting case* ($k_m \simeq k_{ms}$)

The controlling step is also diffusion through the solution/BLM interface modified by diffusion through the BLM. In this case Eq. (5.54) becomes

$$P = \frac{nKD_m}{(2K + n)t_m} \qquad (5.57)$$

In theory, by plotting 1/P *vs.* t_m or 1/K, one might be able to evaluate the two contributions to the overall process. The difficulty in obtaining useful information from Eqs. (5.18) and (5.54) lies in the fact that there are too many unknown parameters in them. K and t_m might be varied. However, one has to assume that all other kinetic parameters (k_m, k_{sm}, k_{ms}) remain unaltered. Much work is still needed in this area.

Finally, one other remark should be made regarding the water transport that is frequently associated with ion translocation through channels embedded in the lipid bilayer. Under such conditions, the transport of water and ions may proceed by a single-file fashion, i.e. water molecules and ions cannot pass each other within the narrow channel. In the absence of a channel, low ion permeation coupled with a high water movement across BLM is also explainable by this single-file proces.[19]

Facilitated Diffusion in Planar Lipid Bilayers

The two key experiments in bilayer lipid membranes are: (a) ion carriers (*The Valinomycin Experiment*), and (b) ion channels (*The Gramicidin Experiment*). They are discussed under separate headings below. Before doing so, let us consider the barrier properties of unmodified BLMs.

The lipid bilayer is a thermodynamically stable structure for several natural phospholipids that constitute biomembranes. When dispersed in an aqueous medium, phospholipid molecules self-assemble into bilayers. The bilayers of biomembranes are mainly composed of phosphatidylcholines (PC), phosphatidylethanolamines (PE), and phosphatidylserines (PS). One of the peculiar properties of lipid bilayers is that they have a transition temperature, which is dependent on the fatty acid composition (Chapter 2, *Biomembranes*). Below the transition temperature the bilayer is in the gel state which resembles a 'solid' structure. Above the transition temperature the hydrocarbon region is similar to a liquid hydrocarbon and is called the liquid-crystalline state.[9] An interpretation of the permeability of water in lipid bilayers focuses on the fact that the permeability values at constant temperature depend on the

fatty acid composition. When a lipid bilayer goes from the gel to the liquid crystalline state through the transition point, the degrees of freedom of the hydrocarbon chains are increased in several orders of magnitude. The different conformational arrangements of the fatty acid residues make possible the formation of free spaces or holes in the bilayer structure. These holes, known as 'kinks', are able to admit a water molecule.[12,21,22] Thus, the permeability of water can be calculated in terms of the diffusion of water molecules from kink to kink.[6,8] The values obtained by the theory are quite acceptable, but it must be emphasized that this may be the case for permeating molecules having a similar size to the kink volume. Bigger solutes would need a concentration of kinks at one point or to enlarge the volume of the kink requiring an additional activation energy. Then, the kinetic-molecular picture for water permeation cannot be extrapolated to permeation processes in which other compounds beside water participate. In connection with the liquid crystalline-gel transition of the lipid bilayer, it has a profound effect on carrier- and channel-mediated diffusion, as will be discused below.

The Valinomycin Experiemnt

A number of polypeptide antibiotics and crown ethers have been well characterized as ion carriers (complexing agents) in experimental BLMs. These include:

- valinomycin -- a macrocyclic compound with alternating α-hydroxy acids and amino acids.
- gramicidin -- as typified by gramicidin A, is a linear pentadecapeptide consisting mainly of hydrophobic amino acids.
- alamethicin -- a linear polypeptide with 20 amino acids, isolated from *Fungus Trichoderma viride*
- crown ethers -- with lipophilic and anion-cap hydrophilic groups

It was discovered in the earlier days of BLM research that certain peptide additives, including alamethicin, can induce activation of ionic movements by a change in membrane potential (gating) in otherwise 'inert' lipid

bilayers. These compounds, capable of gating, are special examples of a larger class of substances, which enhance ion permeability in BLMs. They are known as ionophores, some of which form channels like alamethicin and gramicidin.[22,37] These compounds can span the planar lipid bilayer, while others carry ions across the membrane by forming permeant complexes. Here, only valinomycin- and gramicidin-modifed BLMs and liposomes will be decribed as illustrative examples. Some applications of these compounds in biosensors may be found in Chapter 10 (*Applications*).

The formation of the BLMs is carried out in a hole (~ 1 mm diameter) in the Teflon partition separating two aqueous solutions (e.g. 0.1 M KCl). A 1.5 % phosphatidylcholine (PC or lecithin) in n-decane is a good BLM-forming solution. With two reference electrodes in place, a droplet of the lipid solution is smeared over the hole using either a small paint brush, plastic spatula, or a Hamilton syringe whose needle is covered with a Teflon or polyethylene tubing. Under favorable conditions, rainbow colors will be first seen leading to 'black holes' then to a BLM. The formation of a BLM may be followed optically or electrically by monitoring its resistance (R_m) or capacitance (C_m). BLMs formed from the above PC solution should exhibit R_m and C_m, respectively on the order of 1-10 x 10^8 ohm-cm and 0.5 $\mu F\ cm^2$. To see the effect of valinomycin on the BLM, aliquots of valinomycin are added to the bathing solution at a constant 0.1 M KCl, while resulting resistances are measured (it does not matter whether valinomycin is added to the bathing solution or to the lipid solution, since the lipid phase prefers the carrier about fifty thousand times over the aqueous phase). By plotting R_m *vs.* valinomycin concentraton, a linear relationship with a slope of unity is obtained. Holding the valinomycin constant at 10^{-7} M , while the KCl concentrations are varied. By plotting R_m vs. KCl concentration, again a straight line is obtained having a slope of one. The effect of valinomycin on R_m is most noteworthy; it dropped by six orders of magnitude (~ 10^3 ohm-cm). Further, if there is a concentration gradient of KCl across the BLM, the observed potential difference obeys the Nernst equation. If one side of the bathing solution contains only KCl and the other side NaCl, the valinomycin-doped BLM is about 2000 times more sensitive to K^+ over Na^+, as evidenced by the observed bi-ionic potential measurements. That

is the valinomycin-containing BLM behaves as a K^+-selective electrode. These dramatic results illustrate a carrier (*C*) mechanism with 1:1 *C*-K^+ complex being translocated across the bilayer lipid membrane. The essence of the carrier mechanism is shown in Fig. 5.11. Valinomycin, as an ion carrier in the lipid bilayer phase, binds the K^+ at the left-side of the solution/BLM interface to form a C-K^+ complex which drifts across the BLM to the right-hand side. The complex dissociates itself at the right-hand side of the BLM into K^+ and the empty *C*. The latter moves back to the left side as indicated in Fig. 5.11. A simplified kinetic scheme with four rate constants for the valinomycin experiment have been estimated. These are: (i) formaton of the *C*-K^+ complex, (ii) transport of the complex across the BLM, (iii) dissociation of the complex, and (iv) back-transport of the empty *C*. The values for these rate constants are between 2-5 x 10^5 M/s, with the back-transport being the rate-limiting step. From the kinetic experiment, a unique parameter of the turnover number (f = 1/k's $\simeq$ 2 x 10 10^4 K^+ per sec) has been obtained, which is the maximum rate of transport per carrier, meaning that a single valinomycin molecule is able to transport more than 100,000 K^+ ions per seceond across the BLM!

In conclusion of the valinomycin experiment above, the following are worth noting. To achieve efficient transport by carrier mechanism, it is advantageous to have large rate constants which is limited by the free carrier size, the viscosity of the lipid bilayer, and by the height of the dielectric energy barrier, which in turn are determined by the electrical charges and dipole moments of the constituent lipids. The solution/ membrane interface of most biomembranes are negatively charged (because of the presence of phospholipids PS and PI). Oriented dipoles, on the other hand, inhibits the transport of cations owing to its positive interior potential relative to the aqueous solution and favors anion selectivity. However, the molecular structure of the valinomycin indicates that the polar core of the molecule, resulting from the carbonyl groups, are completely in favor of alkali cation selectivity over inorganic anions. The transmembrane potential measurements yielding a theoretical Nerstian slope, along with other experimental evidence, firmally establish the proposed carrier mechanism of ion transport across the BLM.

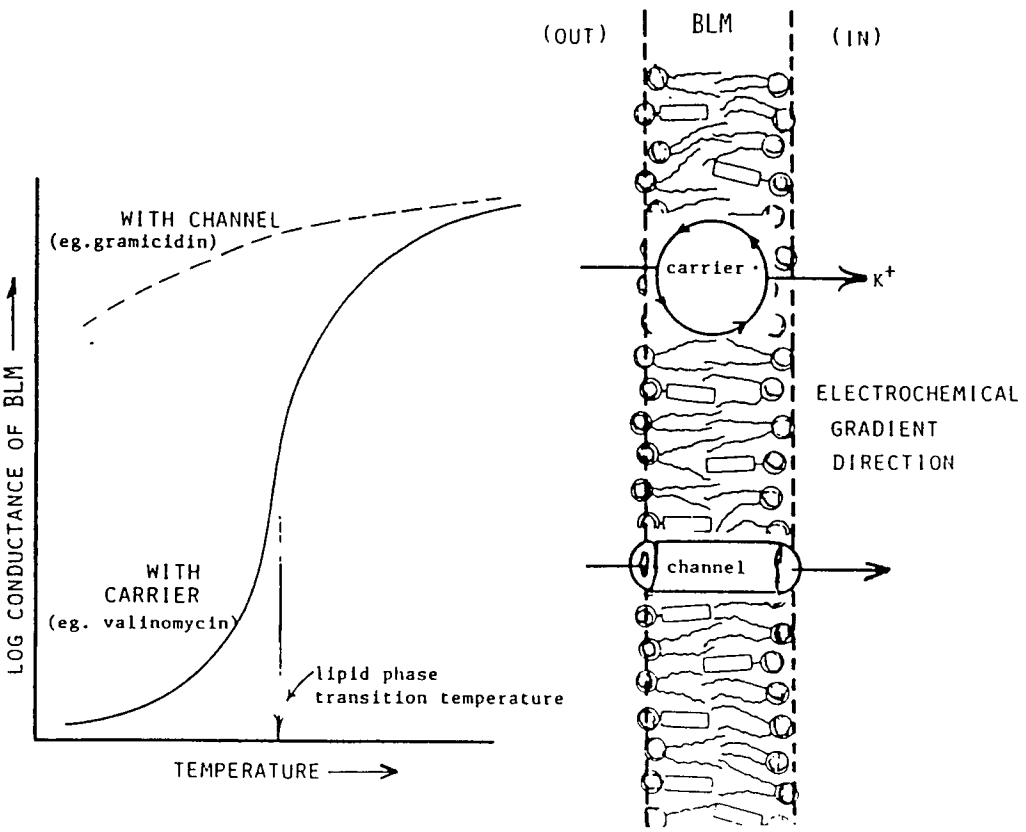

Fig. 5.11 Comparison of facilitated transport by carriers and channels in BLM as a function of temperature in terms of membrane conductance. The liquid hydrocarbon core of the BLM changes from a gel state to a liquid crystalline state at a certain lipid transition temperature. The experimental data are for valinomycin (a carrier) and gramicidin A (a channel former).

The Gramicidin Experiment

Evidence for single ion-channel activities in biomembranes were first suggested in 1969. Bean and colleagues reported that in the BLM containing a bacterial fermentation product, called "EIM" (Excitability Inducing Material) discrete conductance steps were observed. They ranged from 2 to 6 x 10^{-10} Ω^{-1} and suggested the formation of stable transmembane channels (*see* Chapter 7, *Membrane Physiology*). Indeed, later investigations in particular with gramicidin *A*, one of the simplest known linear pentadecapeptide with antibiotic activity from *B. brevis*, forms ion channels in BLMs. A single event brought about by the opening of a channel can be measured. Experimentally, when a BLM containing a very small amount of gramicidin is held under a constant voltage (e.g. 100 mV), stepwise, discrete variations of the membrane current are observed. When increasing amounts of gramicidin are added to the BLM, current fluctuations are superimposed on top of each other. Eventually, with enough gramicidin in the BLM, the membrane conductance reaches a macroscopic conductance value, which is 3 to 4 orders of magnitude higher than the maximum rate based on the carrier mechanism. The simplest explantion of these findings is that:

- gramicidin (not as a carrier) form an ion channel in the lipid bilayer,
- the observed current fluctuations result from the opening and closing of single ion channels, and
- the height of the discrete current step corresponds to a single-channel conductance.

The most significant fact emerged from the gramicidin experiment is that a molecular event of a single ion-channel conductance can be observed in a BLM whose extraordinarily high intrinsic resistance has made this possible. Later, the development of the 'patch clamp' technique to isolate small high impedance patches, has made it practical to study single ion-channels in a variety of biomembranes. This important topic will be discussed in Chapter 7 (*Membrane Physiology*).

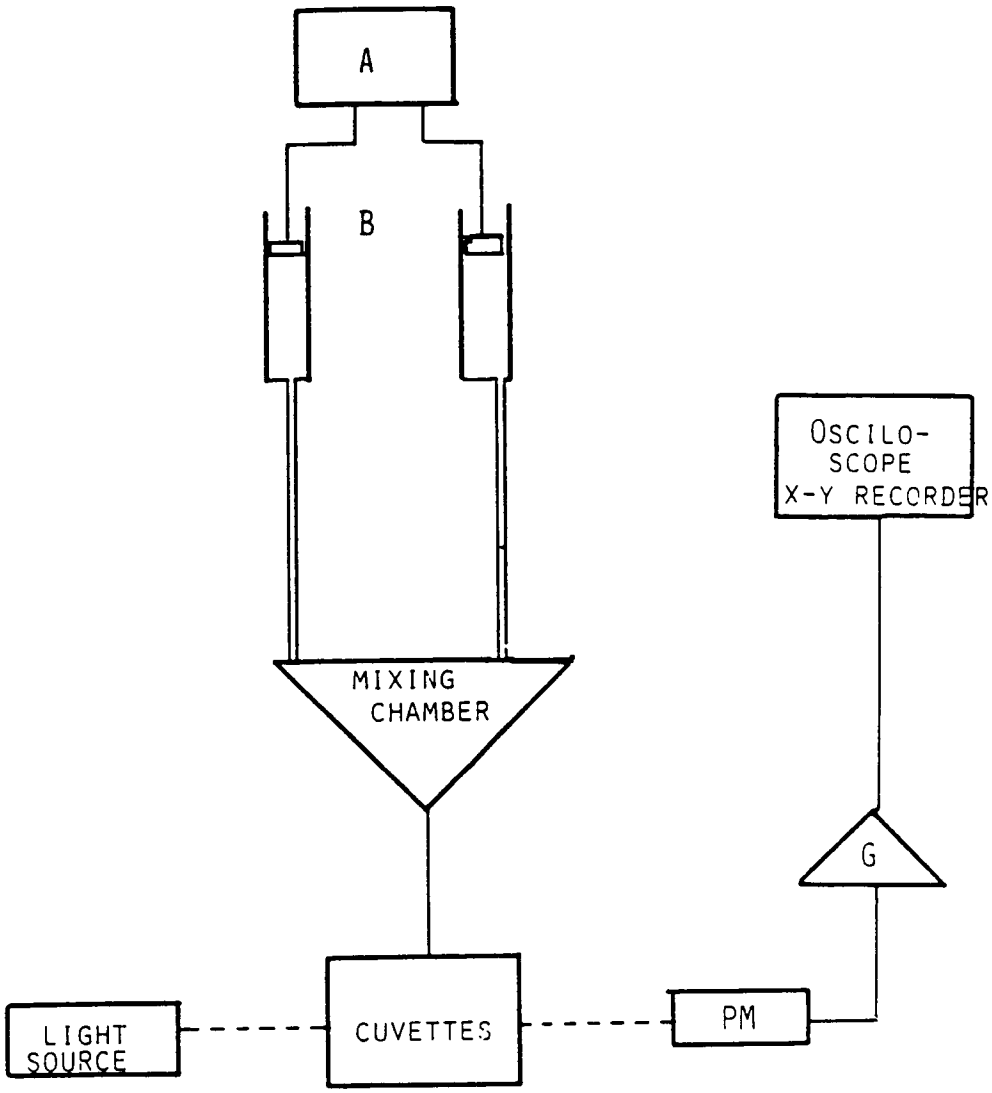

Fig. 5.12 Simplified diagram of a stop-flow spectrophotometer for permeability measuremets in erythrocytes and liposomes. (A) Automatic system of injection.(B) Syringes: one with liposomes and the other with test solutions. PM = photomultiplier, G = amplifier [Benga, 1989, p. 65].

5.7.2 Liposomes (Spherical vesicles)

The determination of the permeability of the lipid bilayer to water and nonelectrolytes requires following changes of volume by means of fast methods [Benga, 1989; Rosoff,1996]. One of the methods frequently employed consists of a stop-flow spectrophotometer for fast reactions (Fig.5.13). Absorbance increases when the liposome (or cell) volume shrinks by the outflow of water. In hypotonic solutions, they swell with a corresponding decrease in the absorbance. The interpretation of the increase (or decrease) of the absorbance with the decrease (increase) of the volume of the vesicles in the dispersion is related to their refractive properties.

The rate of volume change at zero time is related to the concentration diffenence by

$$\frac{dv}{dt} = \frac{d(1/A)}{dt} = Kk_W S(C_i^S - C_0^S) \qquad (5.58)$$

where K is a constant taking into account the optical properties of the dispersion, V is the volume of the liposomes, k_W is the permeability of water, S the area of the membrane (which is proportional to the concentration of liposomes). C_0^S and C_i^S are the outer and the inner concentrations of impermeant, respectively. R and T have the usual meanings. Equation (5.58) can only be used in the case of a selective membrane, i.e. when only water permeates the lipid bilayer. Therefore, it is important to obtain the information from shrinkage or swelling experiments using highly impermeable solutes. In swelling experiments, a leakage of the inner solute solution may appear as a consequence of the changes in area and thickness of the bilayer. Thus, shrinkage experiments are more suitable to avoid that risk. In addition, the changes in the area and thickness of the lipid bilayer in correlation to the permeation process is an important point that has already been alluded to in considering the barrier properties of lipid bilayers above (*see* Facilitated Diffusion in Planar Lipid Bilayers).

Some other relevant experiments related to membrane transport

The permeability of BLM to nonelectrolytes, such as urea, glucose, and sucrose, has also been studied. Generally, the values of permeability coefficients obtained for other compounds are appreciably lower than that of water. However, permeability of BLM to NH_3 and NH_4^+, of vital importance to many living systems and organelle membranes of chloroplasts and mitochondria, has not been extensively investigated.[28] In a series of papers, Gutknecht and Walter[29] reported transport of HSCN, histamine, theophylline, tryptamine, and HCl through phospholipid BLM and effects of cholesterol were noted.[30,31] For example, Gutknecht and Walter reported that addition of cholesterol to phosphatidylcholine (1:1 molar ratio) reduces P_{HA} by a factor of 0.4, but has no effect on P_{A^-}. Their results suggest that SCN^- combines with H^+-forming undissociated HSCN, thereby facilitating its diffusion across the BLM. In this connection, Orbach and Finkelstein [Finkelstein,1988] have found that the permeability of phosphatidylcholine BLM to neutral species obeys Overton's rule. That is, $P = DK_{hc}$, where P is the permeability coefficient of a solute through the bilayer, K_{hc} is its hydrocarbon/water partition coefficient, and D is the diffusion coefficient in bulk hydrocarbon. The partition coefficients are by far the major determinants of the relative magnitudes of the permeability coefficients; the diffusion coefficients make only a minor contribution. They conclude that the recent emphasis on theoretically calculated intramembraneous diffusion coefficients (D_m's) has diverted attention from the experimentally measurable and physiologically relevant permeability coefficients (P's) and has obscured the simplicity and usefulness of Overton's rule. In this connection, mention should be made of the organization of *n*-alkane solvents in BLM and their effects on the water permeability. The partition coefficient between water and the BLM interior, for charged and polar species, depends directly on the energy barrier. The presence of double bonds (unsaturation) may also alter significantly the water solubility in the BLM. The solubility of *n*-alkanes in BLMs has been investigated by Gruen and Haydon.[32] They reported that the *n*-alkanes dissolve primarily into the central core of a BLM and alter significantly the thickness of BLM. *n*-Alkanes with increasing chain length have less solubility, contrary to the expectation. This phenomenon has been also considered at length by

McIntosh et al.[33] based on the results obtained by the combined use of differential scanning calorimetry, X-ray diffraction, and monolayer techniques. Finally, mention should be made about diffusion in the plane of the BLM, i.e. the lateral diffusion. Fahey and colleagues[34] reported the lateral diffusion coefficients (D) of a fluorescent lipid analogue 3,3-dioctake- cylindotri-carbocyanine in BLM. In all BLM, $D \simeq 10^{-7}$ cm^2 sec^{-1} with only weak temperature dependence, even near the phase transition temperatures. Cholesterol in phosphatidylcholine BLM (molar ratio of 1:2) reduces D about twofold, while retained hydrocarbon solvent can increase it two- to threefold. Sopranzi and Calvallott[35] have reported the effect of bombesin (a tetra-decapeptide) on glucose transport in BLM. In this connection, transport by facilitated diffusion is a common feature in the human RBC membrane, of which glucose permeation has been extensively studied.[16] The central idea is that there are membrane-bound proteins with specific binding sites for glucose, which facilitate its transport across the plasma membrane. Attempts to reconstitute a glucose transport system into BLM goes back to 1968. In that year, Jung[36] reported that the BLMs made from crude total lipid extracts of human RBC were about 100 times more permeable to glucose than were the BLMs made from more purified lipids. Recently, several groups[23-26] have reported successful reconstitution experiments with BLM. In a series of papers, Jones and associates[24-26] have aimed for the identification of the monosaccharide transport system of the RBC membrane using both BLMs and liposomes. Their data indicate that the transmembrane polypeptides of band 3 of the electrophoretogram of the erythrocyte membrane proteins are implicated in D-glucose transport, although the possibility that a relatively minor component of the membrane could be responsible for glucose transport cannot be eliminated.

Concluding Remarks

In this chapter, we have focused primarily on the principles of membrane transport, particularly in relation to water and nonelectrolyte permeability. Our treatment on the subject is not exhaustive, but sufficiently detailed. Hopefully, it has been useful to the general reader interested in experimental bilayer lipid membranes as a model for biomembrane transport studies.

General References

N. Lakshminarayanaiah, *Transport Phenomena in Membranes*, Academic Press, New York, 1969.

S. G. Davison (ed.) *Progress in Surface Science*, Vols. **4, 8, 19, 23, 30, 41**, Pergamon Press, NY, 1973, 1985, 1986, 1989, 1992, 1994.

H. T. Tien, *Bilayer Lipid Membranes (BLM): Theory and Practice*, Marcel Dekker, New York, 1974. Chapter 6 (Water and Solute Permeability) and Chapter 7 (Antibiotics and Ion Permeability)

A. Kotyk and K. Janacek, *Membrane Transport, An Interdisciplinary Approach*, Plenum Press, New York, 1977.

R. Antolini, A. Gliozzi and A. Goris (ed.) *Transport in Biomembranes: Model Systems and Reconstitution*, Raven Press, NY. 1982.

A. N. Martonosi (ed.), *Membranes and Transport*, Plenum Press, New York, 1982.

A. Finkelstein, *Water movement through lipid bilayers, pores, and plasma membranes: Theory and Reality*, Wiley-Interscience, NY. 1987.

G. Benga (ed.) *Water Transport in Biological Membranes*, CRC Press, Boca Raton, FL 1989. pp. 41-75.

E. A. Disalvo and S. A. Simon (eds.), *Permeability and Stability of Lipid Bilayers*, CRC Press, Boca Raton, 1995

T. F. Weiss, *Cellular Biophysics*, MIT Press, Cambridge, 1996

M. Rosoff (ed.), *Vesicles*, Marcel Dekker, Inc., NY, 1996

L. J. Van Winkle, *Biomembrane Tranport*, Academic Press, NY, 1999

D. W. Deamer, A. Kleinzeller, and D. M. Fambrough, *Membrane Permeability*, Academic Press, NY. 1999

Specific References

1. B.J. Zwolinski, H.Eyring, and C. E. Reese, Diffusion and membrane permeability, *J. Phys. Colloid Chem.*, **53** (1949) 1426,.
2. R. P. Rastogi, R. C. Srivastava and S. N. Singh, 'Nonequilibrium thermodynamics of electrokinetic phenomena', *Chem. Rev.*, **93** (1993) 1945-1990
3. R. G. Males, P. S. Phillips, and F. G. Herrig, *Biophys. Chem.*, **70** (1998) 65-74
4. J. M. Diamond, G. Szabo, and Y. J. Katz, J. Memb. Biol., 17 (1974) 148
5. D.C. Petersen, Water permeability of the lipid bilayer, in Water and Ions in Biological Systems, Pullman, A., Vasilesce, and Packer, L., (eds.), Plenum Press, New York, 1985, p.409.
6. Seelig, J. and Seelig, A., Q. Rev. Biophys., 13, pp.19, 1980.
7 Tien, H.T. and Ting, H.P., J. Colloid Interface Sci., 27, pp.702, 1968.
8. Pace, R.J. and Chan, S.I., J. Chem. Phys., 76, 4241, 1982.
9. Nagle, J.F. and Scott, H.L., Physics Today, pp.38, 1978.
10. Meraldl, J.-P. and Schlitter, J., Biochim. Biophys. Acta, 645, pp.193, 1981.
11. Gruen, D.W.R., Biophys. J., 33, pp.149, 1981.
12. Day, J. and Willis, C.R., , J. Theor. Biol., 94, pp.367, 1982.
13. Van der Ploeg, P. and Berendsen, H.J.C., J. Chem. Phys., 76, .3271, 1982.
14. Kobayashi K, Mittler-Neher S, Spinke J, et al. BBA-Biomembranes: 35-40 1998
15. I. C. West, The Biochemnistry of Membrane Transport, Chapman and Hall, London, 1983
16. K. Bauer, A. Schmid, W. Boos, R. Benz and J. Tommassen, Eur. J. Biochem., 174 (1988) 199-205.
17. Stewart, P.S., MacLennan, D.H., J. Biol. Chem., 249, p.987, 1974.
18. Shamoo. A.E. and Tivol, W.F., Curr. Top. Membr. Transport, 14, p.57, 1980.
19. Andersen, O.S., in Membrane Transport in Biology, Springer-Verlag, New York, 1978.
20. Fettiplace, R.L. and Haydon, D.A., Physiol. Rev., 60, pp.510, 1980.

21. Storelli, C., Vogeli, H., and Semenza, G., FEBS Lett., 24, p.287, 1972.
22. Collander, R., Physiol. Plant., 2, pp.300, 1949.
23. Nickson, J.K. and Jones, M.N., Biochem. Trans., 5, pp.147, 1977.
24. Jones, M.N., Nickson, J.K., Biochim. Biophys. Acta, 509, p.260, 1978.
25. Phutrakul, S., Jones, M.N., Biochim. Biophys. Acta, 550, p.188, 1979.
26. Jain, M.K., Strickhom, A., and Cordes, E.H, Nature, 222, p.871, 1969.
27. Kovbasnjuk O.N., Antonenko Y.N., Yaguzhinsky L.S,Febs Lett 289: (2) 176-178, 1991
28. Gutknecht, J., Walter, A., Biochim. Biophys. Acta, 685, p.233, 1982.
29. Graziane, Y., and Livne, A., J. Mol. Biol., 7, pp.275, 1972.
30. Lippe, C., J. Mol. Biol., 35, p.635, 1968.
31. Gruen, D.W.R. Haydon, D.A., Pure Appl Chem., 52, p.1229, 1980.
32. McIntosh, T.J., Simon, S.A., and MacDonald, R.G., Biochim. Biophys. Acta, 597, pp.445, 1980; ibid., 645, pp.318, 1980.
33. Tancrede, P., Paquin, P., Houle, A., and LeBlanc, R.M., J. Biochem. Biophys. Meth., 7, pp.299, 1983.
34. Sopranzi, N. and Cavallott, C., Experientia, 36, pp.956, 1980.
35. Pohl P, Saparov SM, Antonenko YN, BIOPHYS J, 75: 1403,1998
36. Jung, C.Y., Fed. Proc., 27, p.286, 1968; J. Membr. Biol., 5, 200, 1971.
37. Janas T, Tien H. T., Biochim Biophys Acta 939: (3) 624-628, 1988
38. Phutrakul, S. and Jones, M.N., Biochim. Biophys. Acta, 550,.188, 1979.
39. G. D. Mironova, T. V. Sirota, L. A. Pronevich, N. V. Trofimenko, G P. Mironov, P. A. Grigorjev and M. N. Kondrashova, J. Bioenerg. Biomemb., 14, (1982) 213-225 ; 25 (1993) 307-312.
40. Trauble, H., J. Membr. Biol., 4, pp.193, 1971.
41. Minami H, Sato N, Sugawara M, et al., , Anal Sci 7: (6) 853-862 Dec 1991
42. Orbach, E., and Finkelstein, A., J. Gen. Physiol., 75, pp.427, 1980.
43. Jones, M.N. and Nickson, J. Biochim. Biophys. Acta, 509, pp.260, 1978.
44. Kobayashi K, Mittler-Neher S, Spinke J, et al. BBA-Biomembranes 1368: (1) 35-40, Jan. 5 1998
45. Antonenko YN, Pohl P, Denisov GA, , Biophys. J. 72: 2187, 1997

Chapter 6

Membrane Electrochemistry

"... Almost all interfaces are electrified. The key concept to describe these electrified interfaces is the electrochemical potential, μ, an extension of which leads to the ***Nernst-Planck equation*** *— the crux of membrane electrochemistry"*

General References (cited by name in brackets in the text)
Specific References (cited by number in superscript in the text)

6.1 Introduction

There is one commonality between electrochemistry and biomembranes; they are both interface science. Electrochemistry is a well-established discipline dealing with electrical phenomena at, as well as across the interfaces. The study of biomembranes, on the other hand, is a relatively new endeavor, whose investigations involve the use of powerful physicochemical techniques based on electrochemistry. Hence, membrane electrochemistry may be defined as the application of electrochemistry to membrane studies, including both artificial and natural systems.

The goal of this chapter is to introduce to the reader the subject of membrane electrochemistry; it addresses, first of all, a few basic principles of electrochemistry. For example, in Section 6.2, we will consider the potential differences between two phases and the electrical double layer on which all electrostatic and electrokinetic phenomena are based. This is important since all living cells and certain subcellular organelles exhibit a potential difference (PD) across their membranes. This PD suggests an unequal distribution of charges across the interfaces (Section 6.2, Electrical Double Layer Theory). How do charged species (e.g. ions) move through a membrane? And how does a membrane discriminate one kind of ion from the others? We will see that the force moving charges and charged species across the membrane is the gradient of electrochemical potential, which is influenced by the properties of the membrane. The traditional view of electrical PD in a membrane system is based upon the *Nernst-Planck* equation which will be considered in Section 6.3. Discussed in Section 6.4 are transmembrane potentials and planar lipid bilayers (BLMs), whereas their experimental aspects are presented in Section 6.5. Electronic processes in membranes in relation to electron transfer and redox reactions are considered next (Section 6.6). In the last section of this chapter there is a synopsis of some recent BLM and liposome experiments.

In perspective, it should be emphasized that biomembranes are about 5-7 nm thick and consist mainly of lipids, proteins, carbohydrates and their complexes. The unique aspect of the biomembrane structure is that the lipids are organized in the form of a bilayer with the hydrophobic portions (hydrocarbon chains) sequestered away from the aqueous

environment and the hydrophilic groups (polar heads) exposed to water. Experimentally, a simple bilayer lipid membrane (BLM) separating two aqueous solutions may be readily formed, which, upon suitable modification, may be used as a model of biomembranes. Indeed, the first direct observations of membrane transport, through either single ion channels or mobile ion carriers, were accomplished through bilayer lipid membrane investigations. These and other topics on BLM electrochemistry may be found elsewhere in this book. For examples, Chapters 7 and 8 deal with, respectively, *Membrane Physiology* and *Membrane Bioenergetics*.

6.2 Interfacial Electrochemistry

In order to describe the most prominent features of biological membranes, e.g. their energy storage and transduction abilities, it is necessary to give a brief insight into interfacial electrochemistry. The importance of such an approach is evident, since we realize that these features are both accomplished by electrical charge separation and transfer occurring at the solution-membrane interface. Since almost all interfaces are electrified, the key concept describing these electrified interfaces is the electrochemical potential, an extension of which leads to the Nernst-Planck equation — the crux of membrane electrochemistry (Section 6.3). Here, let us consider the separation of charges that is usually as a result of:

- preferential adsorption of ions,
- adsorption and orientation of dipolar molecules,
- transfer of charge from one phase to another, and
- deformation of polarizable atoms or molecules (anisotropy).

Hence, these charges may be ions, dipolar molecules such as phospholipids, or they may be free charges such as electrons and 'holes'. Let us consider potentials at interfaces, and their origin and relationship under separate headings below.

Elements of membrane electrochemistry

The principles of membrane electrochemistry may be discussed in terms of two types of measurements. The first is called membrane potentiometry in which the potential is measured under conditions when no current is detected across the membrane. The second is called membrane amperometry in which a current is measured when a potential difference is applied across the membrane. One can also define a third type of measurement, known to electrochemists as voltammetry, in which a scanning voltage is impressed across the membrane and the resulting current is recorded. Of voltammetry, which is a combination of the first two types, the so-called linear sweep voltammetry (LSV) and cyclic voltammetry (CV) are practiced. In the former, a linear voltage scan is used, whereas in the latter the potential is scanned back and forth between two limits. Applications of CV to membrane research, in particular to the BLM systems, will be discussed in Section 6.5

Potentials at the interfaces[2]

We assume that the solid phase in a vacuum possesses an excess of electric charges, generating the electric field around the phase. Let us now transfer slowly a dimensonless test unit charge from infinite distance to this phase. The electrical forces interacting with the unit charge on its way to the phase interior may be divided into two types. One of these is the long range Coulomb forces, which originate from the phase charge. The second type, called the image forces, have their source in the approaching unit charge, which induces, in the solid or liquid phase, its image charge of equal value but of opposite sign. The image forces are acting only on a very short distance from the phase surface (usually less than 100 nm). Accordingly, the external potential ψ of any phase in the vacuum may be defined as equal to the work required for the transfer of a positive test unit charge from infinity to the point nearby the given phase surface, but still beyond the image forces range [Krysinski and Tien, 1986].

The potential defined as equal to this work (the work of overcoming the image forces), is called the surface potential, χ. The sum of

external potential ψ and surface potential χ is the inner potential of a given phase:

$$\phi = \psi + \chi \qquad (6.1)$$

In other words, the inner potential of any phase is equal to the work of bringing a dimensionless test unit charge from infinity to the phase interior. The assumption is made that all points inside the phase have the same potential and all interactions are only electrical.

Let us now consider the potential difference between the two phases in contact (e.g. metal-electrolyte solution, metal-metal, membrane-electrolyte, etc.). The surface potential difference $\Delta\chi$, which is equal to the work of unit charge transfer through the surface layer, cannot be experimentally measured. The absolute potential difference between two phases, the inner potential difference, $\Delta\phi$ or Galvani potential difference is equal to the sum of $\Delta\psi$ and $\Delta\chi$, i.e.

$$\Delta\phi = \Delta\psi + \Delta\chi \qquad (6.2)$$

Let us now consider the work required for bringing the real electric charge, e.g. the positive ion, from infinity to the phase interior. Unless this ion does not interact chemically with the molecules of the phase, the work required for the transfer is only electrical and is equal to the work required for the test charge. For one mole of ions, this work (W_{el}) is equal to

$$W_{el} = z_i.F.\phi \qquad (6.3)$$

where z_i = valency of ion (dimensionless), F = Faraday constant (Coulombs.mol^{-1}), and ϕ = inner potential (volt). When the ion penetrates the phase interior through the interface, it interacts chemically with the phase molecules (e.g. ion-solvent interactions resulting in solvation). This type of interaction is specific and depends on the nature of the penetrating ion or particle and on the nature of the phase (*see* Chapter 3, *Basic Principles*). The specific (chemical) interactions are of short range in contrast to electric (Coulomb) interactions. The work connected with them

is called the chemical potential of species i in the phase and is denoted as μ_i.

$$\mu_i = \mu_i^0 + RT \ln a_i \qquad (6.4)$$

where μ_i^0 = chemical potential of species i in standard conditions (standard chemical potential), R = gas constant, and a_i = chemical activity of species i within the phase. Thus, the total work required for ion transfer is a sum of chemical and electrical work and is called the electrochemical potential $\underline{\mu}_i$

$$\underline{\mu}_i = \mu_i + z_i F\phi \qquad (6.5)$$

Note that the distinction between chemical and electrical work in the formulation of the above equation is purely formal because of uncertainty of ϕ and μ_i, but as we shall see later, the electrochemical potentials are powerful tools for treating the interfacial reactions of charge transfer and separation not only in electrochemistry, but also for biomembrane systems.

Electrical Double Layer Theory

The very existence of an interface between two immicible liquids necessarily implies a basic anisotropy in the forces operating on the species in the interfacial region, a potential difference (PD) will develop and an electrical double layer is formed. There are two aspects of the electrical double layer: (1) the electrical aspect, which is concerned with the magni-tude of the excess charge densities across the interfacial region, and (2) the structural aspect, the arrangement of constituents (ions, electrons, dipoles, neutral molecules). These two are obviously intimately related. This section will consider the following: (A) potentials at the interfaces, their origins and relations, (B) electrical double layer theory, Stern synthesis, boundary conditions and further development, (C) electrokinetic phenomena as a manifestation of the electrical double layer, and (D) non-equilibrium (irreversible) thermodynamics, under separate headings.

Potentials at the interfaces

One of the fundamental factors determining all electrochemical phenomena occurring at the phase boundaries is the electric charge and potential distribution in these regions. The simplest model reflecting the real electrical structure of the phase boundary region is the electrical double layer (EDL) model. The EDL is an interfacial region between two homogeneous phases, in which (a) the charge constituents have been separated so that (b) each side of the interface is electrified, (c) the charges on the two sides are equal in magnitude but opposite in sign, (d) the interfacial region as a whole is electrically neutral, and (e) it is impossible to measure the absolute value of the EDL potential difference (PD) but changes in PD may be determined. The processes occurring at membranes are closely related to the structure of the region of the solution that is nearest to the membrane, which is the electrical double layer. Theories about the electrical double layer have been developed over the past 100 years [Milazzo, 1983; Blank, 1986]. It can be said that an appreciation of the EDL. is a "must" in order to understand the properties of biomembranes both at, as well as across, their solution/membrane interfaces.[1,2,15]

The electrical double layer (EDL) occurs at all interfaces and its structure depends on the properties of the contacting phases. Knowledge of charge and potential distribution in the EDL is very important since it contributes to such membrane phenomena as ion permeability and selectivity, membrane potentials, enzymatic activity and others. In all these phenomena, the EDL is either the primary energy barrier which distinguishes between the various species due to electrostatic interactions, or affects membrane functions by modifying the spatial organization of membrane enzymes and their substrates.

Once the charges are separated, the electrical potential difference is set up across the interface and EDL is formed. The EDL. is defined as an interfacial region between two homogeneous phases, in which the charge constituents have been separated so that each side of the interface

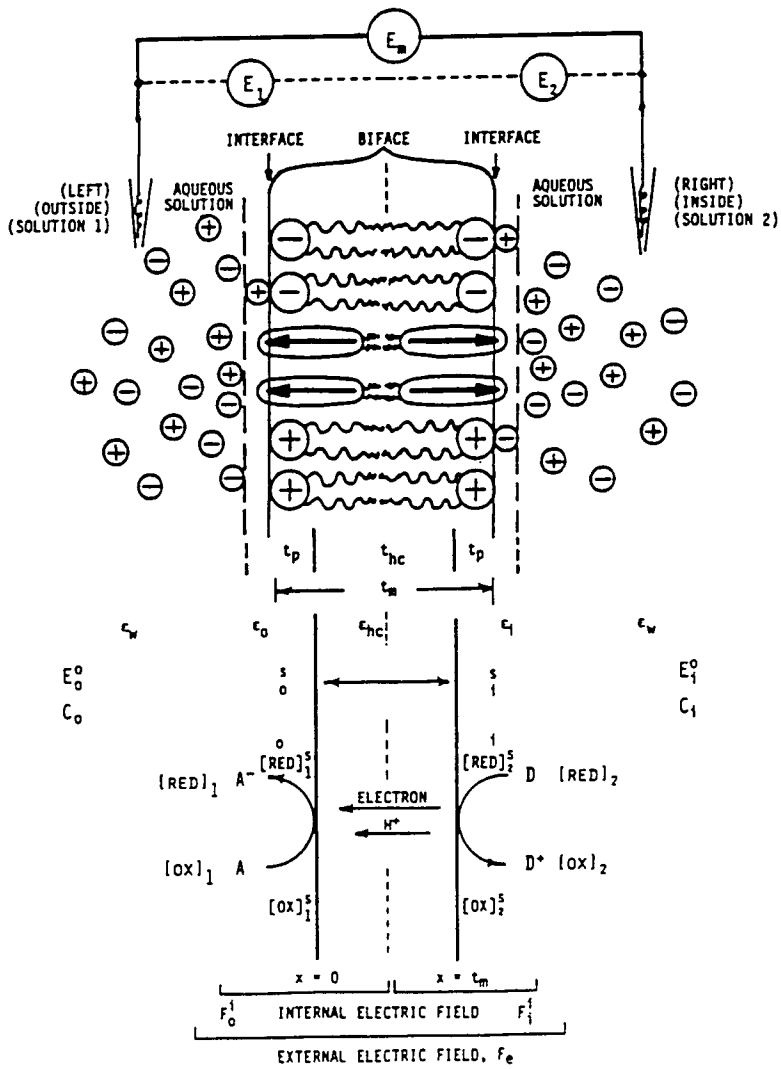

Fig. 6.1 The electrical double layer at the metal/electrolyte interface. IH = Inner Helmholtz Plane, OH = Outer Helmholtz Plane, S = plane of shear, b_M = surface charge density of metal phase, b_H = charge density of Helmholtz layer, b_D = diffuse charge density, ϕ_M, ϕ_D = potentials at the metal surface and Outer Helmholtz Layer (Helmholtz Plane), respectively, ξ = electrokinetic potential [Ivanov, 1988; Osa and Atwood, 1991].

is electrified. The charges on the two sides are equal in magnitude but opposite in sign, thus the interface region as a whole is electrically neutral.

There were several approaches to qualitative and quantitative decription of the EDL structure based on different assumptions. It is beyond the scope here to account the historical development of the EDL Model. Our focus is on Stern's approach that takes ion size into consideration. In 1924, Stern made a synthesis of all previous models and considered two electrified homogeneous phases: metallic electrode in contact with electrolyte solution [*see* Blank, 1986 and references therein]. During the formation of EDL two types of forces affecting the mobile charges or dipoles in the solution should be considered: electrical or ordering forces leading to EDL formation and thermal-disordering forces acting against the electrical forces and 'diffusing' the rigid arrangements of charges in the interfacial region. The rigid arrangement of adsorbed dimensionless charges was the basis of parallel-plate condenser model of Perrin-Helmholtz (1879), which is a good approximation for concentrated electrolyte solutions. The diffuse-charge model was originally developed by Gouy and Chapmann (1910) and is valid for dilute electrolyte solutions. Thus, the Stern synthesis leads to the potential and charge distribution as shown in Fig. 6.1.

Due to electroneutrality of interfacial region as a whole, the charge of the metal surface (or cell membrane surface), for example negative, should be compensated with ions in the electrolyte solution part of the electrical double layer (EDL). It is achieved partially by adsorbed (fixed) solvated ions forming the so called Helmholtz Plane (also called inner or Stern layer) of thickness equal to the radius of the fixed solvated ions, and partially by diffuse charge in the solution. The electrical potential drop between the metal surface and Helmholtz plane is linear, just like in the parallel-plate condenser. To obtain the potential profile in the diffuse layer we have to use the Boltzmann distribution of ions (or any charges) in the region of given electrical potential ϕ

$$n_i = n_i^0 \exp(-z_i e\phi/kT) \qquad (6.6)$$

where n_i = number of ions of type i per unit volume, at a distance x from the surface. At this position the potential has a value φ relative to the

solution at very large x. Note that both n_i and ϕ are functions of coordinate x. n_i^0 is the value of n_i in the bulk of solution, where $\varphi = 0$, e = elementary charge (C), k is Boltzmann constant, T = absolute temperature (K), z_i is the valency of ions, including their sign. The net charge per unit volume of solution at a distance x from the surface, the space charge density ρ amounts to:

$$\rho_i = n_i z_i e \qquad (6.7)$$

In the case of an univalent z_+/z_- (symmetric) electrolyte ($|z_+| = |z_-| = z$, $n_+^0 = n_-^0 = n^0$), Eq.(6.7) may be rewritten

$$\rho = ze(n_+ - n_-) \qquad (6.8)$$

Substitution of (6.8) into (6.6) leads to

$$\rho = -2zen^0 \sinh(ze\phi/kT) \qquad (6.9)$$

An additional relationship between x, ϕ and ρ is given by the Poisson equation:

$$\text{div}(\text{grad}\ \phi) = \nabla^2 \phi = -\rho / \varepsilon \varepsilon_0 \qquad (6.10)$$

where ε = dielectric constant of the medium, assuming its independence of field strength, ε_0 = dielectric constant of free space (F m^{-1}). Combing Eqs.(6.9) and (6.10) gives the Poisson-Boltzmann equation

$$\nabla^2 = (2zen^0/\varepsilon \varepsilon_0)\sinh(ze\phi/kT) \qquad (6.11)$$

This equation forms the basis of Gouy-Chapman theory. The exponential factor $ze\phi/kT$ represents the ratio of electrical and thermal energies of an ion at the given distance from the electrified surface. Taking into consideration that Helmholtz Plane is a flat plate, Eq.(6.11) takes the form

$$\frac{d^2\phi}{dx^2} = (2zen^0/\varepsilon \varepsilon_0)\sinh(ze\phi/kT) \qquad (6.12)$$

where x is the coordinate perpendicular to the plate. In order to express ϕ in terms of x, Eq.(6.12) has to be integrated twice. The first integration upon the boundary condition $\phi = 0$ and $d\phi/dx = 0$ at $x \rightarrow \infty$ gives

$$d\phi/dx = -(8n^{o}kT/\varepsilon\,\varepsilon_{o})^{1/2} \sinh(ze\phi/kT) \qquad (6.13)$$

We can now easily have an expression for the total diffuse charge density σ_D in the electrolyte solution in terms of the potential of the Helmholtz Plane ϕ_D ($x = 0$):

$$\sigma_D = \varepsilon\,\varepsilon_o \left(\frac{d\phi}{dx}\right)_{x=0} = -(8n^{o}kT\varepsilon\,\varepsilon_o) \sinh(ze\phi_D/kT) \qquad (6.14)$$

The diffuse charge density σ_D is of course equal but opposite in sign to the sum of metal surface charge density σ_M and the charge density of Helmholtz layer σ_H :

$$\sigma_D = -(\sigma_M + \sigma_H) \qquad (6.15)$$

In the absence of a Helmholtz layer $\sigma_D = -\sigma_M$, and consequently Eq.(6.14) becomes

$$\sigma_M = (8n^{o}kT\varepsilon\varepsilon_o)^{1/2} \sinh(ze\phi_M/kT \qquad (6.16)$$

where ϕ_M is the potential on metal surface. Eq.(6.16) is the original form of Gouy-Chapman theory relating the surface charge density σ_M and potential ϕ_M. Let us now refer again to Eq.(6.13) to obtain the final form of potential *vs.* distance expression. Integrating this equation using the boundary condition $\phi = \phi_D$ at $x = 0$ gives the following:

$$\tanh(ze\phi/4kT) = \tanh(ze\phi_D/4kT)\exp[-(2n^{o}e^{2}z^{2}/\varepsilon\varepsilon_o\,kT)^{1/2} \qquad (6.17)$$

This equation represents the general solution of the Poisson-Boltzmann equation for flat plates. At this stage, for small potentials, that is in the case $ze\phi_D/4kT \ll 1$ (which is valid for most of biosystems), the

approximation $\tanh(ze\phi/4kT) = ze\phi/4kT$ can be made and Eq.(6.17) reduces to

$$\phi = \phi_D /4kT)\exp[-(2n^0e^2z^2/\varepsilon\varepsilon_0 kT)^{1/2} x] \qquad (6.18)$$

or

$$\phi = \phi_D \exp(-\kappa x) \qquad (6.19)$$

In Eq.(6.19) an abbreviaton $\kappa = (2n^0e^2z^2/\varepsilon\varepsilon_0 kT)$ has been introduced. Here κ has the dimension of a reciprocal length. When $x = 1/\kappa$ then $\phi = \phi_D \exp(-1)$. This dependence shows why $1/\kappa$ is considered to be the effective thickness of the diffuse part of electrical double layer (EDL). An increase of κ (due for instance to the concentration n^0 increase) makes the double layer thinner and causes the potential to change more rapidly with the distance.

From Eqs.(6.18) and (6.19) we see that the potential also decays exponentially within the diffuse part of EDL (see Fig.6.1) until it reaches the value of bulk electrolyte potential (assumed to be zero, at $x \rightarrow \infty$).

A direct consequence of the Stern model is that an interface may be represented by two capacitors in series. According to Stern the total potential drop in the EDL may be expressed in terms of its constituents, i.e. the sum of potential drop within the Helmholtz layer $\sigma_M - \sigma_D$ and diffuse layer $\phi_D - \phi_B$:

$$\phi_M - \phi_B = (\phi_M - \phi_D) + (\phi_D - \phi_B) \qquad (6.20)$$

Differentiating Eq.(6.17) with respect to surface charge density of the metal phase σ_M, one can obtain the general equation for the (differential) capacitance C per unit area of the EDL

$$\frac{d(\phi_M - \phi_B)}{d\,\sigma_M} = \frac{d(\phi_M - \phi_D)}{d\,\sigma_M} + \frac{d(\phi_D - \phi_B)}{d\,\sigma_M} \qquad (6.21)$$

thus

$$\frac{1}{C} = \frac{1}{C_H} + \frac{1}{C_G} \qquad (6.22)$$

where C_H = capacitance of Helmholtz layer, and C_G = capacitance of the diffuse (Gouy) layer. Eqs.(6.21) and (6.22) describing capacitance, or differential capacitance, of double layer are formally identical to a diffuse layer plane condenser with plate distance $1/\kappa$ connected in series with a Helmholtz layer parallel plate capacitor with plate distance equal to the closest approach of hard sphere ions to the metal surface.

Let us now see what happens, when concentration n^0 of bulk electrolyte and/or surface charge of the metal phase varies. At high concentrations. C_D increases. But as C_G becomes greater than C_H, then $1/C_G << 1/C_H$ and total capacitance is then equal to the Helmholtz layer capacitance. This means that at high salt concentrations, the Helmholtz region stores almost all EDL charges. A similar situation occurs at a high surface charge of the metal phase. Conversely, for low concentrations or low surface charge, the diffuse layer capacitor dominates total behavior.

Stern's approach has since been refined, particularly by Grahame [for references, *see* Blank, 1986], who introduced the concepts of inner and outer Helmholtz planes. The specifically adsorbed ions (without their solvation spheres) form the Inner Helmholtz Plane (IH), while the diffuse layer ends at the Outer Helmholtz Plane (OH), and these two planes are in general not identical (Fig. 6.1). For a detailed treatment of these notions, the paper by Sparnaay[1] is recomended. New theories include asymmetry of ions in charge and size, ion-ion hard-core interactions and solvent effects. The latter have their origin in the discrete distribution of solvent molecules. Owing to this, it is better to consider the solvent as a set of hard spheres of a given diameter with embedded point dipoles of a given dipole moment rather than represent the solvent as a dielectric continuum as is done in Stern's model. The charge neutrality condition may also be invalid, particularly if the ions are of different size, since in this case there are regions which are accessible only to some of the ion species. The influence of electrical double layer (EDL) on electrical properties of planar lipid bilayers (BLMs) will be discussed later. Here we will consider another phenomenon directly related to the presence of EDL.

Electrokinetic phenomena as a manifestation of EDL

Electrokinetic phenomena are associated with the tangential movement of the solid phase and surrounding electrolyte with the resultant displacement of diffuse charge of EDL relative to surface charge (including adsorbed ions from inner and outer Helmholtz planes). In discussing these processes it is important to know the exact position of the plane of shear and the value of potential, called ξ-potential, at this plane. Unfortunately, no unambiguous statements can be made as to the position of the slipping plane because a complete theory on the slipping process is not available. However, from the numerous experimental data, it may be concluded that the plane of shear does not coincide with the solid phase surface, but is situated at some distance in the solution. Let us refer once more to Fig. 6.1, showing the schematic diagram of EDL at the solid (metal)/liquid (electrolyte) interface. The ions forming the outer Helmholtz plane possess their solvation spheres. While the outer Helmholtz plane crosses the centers of ions, it is reasonable to expect that plane of shear is shifted at least about a radius of fixed solvated ion toward bulk solution (plane S, Fig. 6.1). The position of the slipping plane, usually within the electrical double layer, strongly depends on electrolyte concentration and the viscosity coefficient of surrounding liquid. In extreme situations (high concentration, high viscosity) the plane of shear may outreach the EDL in liquid phase. But for most common situations it remains a reasonable assumption to set equal to ϕ_D. This implies that it is very sensitive to surface charge and structure changes as well as surface potential as is ϕ_D. Since the measurements are relatively simple, they allow us to gain very important information about structure as well as charge and functional properties related to the charge transfer of many biological systems including cell membranes *in vitro*. This will be briefly discussed at the end of this section.

The electrokinetic phenomena are strictly related to the electrokinetic potential. They manifest themselves only when one phase is in motion relative to the other. This relative movement may be on account of: (1) applying mechanical forces acting on the liquid or solid phase, and (2) applying an electric field tangentially to the electrical double layer.

To the first group belong two electrokinetic phenomena: the Dorn effect and streaming potential. The second group consists of two other phenomena: electrophoresis and electroosmosis. These are summarized in Table 6.1 and briefly discussed thereafter.

Table 6.1 Electrokinetic Phenomena at Interfaces

Phenomena	Stationary phase	Moving phase	Mechanical force	Potential difference
Dorn effect	Electrolyte solution	Suspended particles	Cause	Result
Streaming potential	Walls of capillary	Electrolyte solution	Cause	Result
Electro-phoresis	Electrolyte solution	Suspended particles	Result	Cause
Electro-osmosis	Wall of capillary	Electrolyte solution	Result	Cause

The Dorn effect. It occurs when particles suspended in the electrolyte solution precipitate under the influence of gravity (or centrifugal force), and results in potential difference between the top and bottom of suspension.

Streaming potential. When liquid flows along a narrow tube or capillary, or through a porous plug (a bundle of narrow tubes in parallel or channels in BLMs and biomembranes) under a hydrostatic head, a difference of potential is set up between the ends of the capillary or across the porous plug as the case may be.[32]

Electrophoresis. This is the migration of large molecules (e.g. proteins, polymers), microscopic aggregates of molecules (e.g. colloidal particles)

or cells or liposomes (e.g. erythrocytes) under the influence of an electric field applied to the medium in which the particles are suspended.

Electroosmosis. If a difference of potential is deliberately set up along the axis of narrow tube or across a porous plug, liquid in the tube or plug flows until a hydrostatic head sufficient to prevent continued flow has built-up to the value of the electro-omotic pressure.

In all these phenomena, the EDL and potentials are involved as stated above. By using an appropriate technique it is easy to obtain the value of ξ potential. Since this potential is strictly related to the charge density of the slipping plane of electrical double layer, as follows:

$$\sigma_S = (8n^0 kT\varepsilon\varepsilon_0)^{1/2} \sinh (ze\phi_M /kT) \qquad (6.23)$$

This potential may also be correlated to the immediate surface charge, for instance, of the cell membrane. For a number of cases, this charge is a charge of structural components of biomembranes (e.g. all mammalian cells bear negative charges) like glycolipids, proteins, phospholipids. Therefore, elektrokinetic methods have provided information on membrane surface structure and membrane properties of a diverse range of biological systems. Among electrokinetic phenomena, electrophoresis plays a prominent role. In the form of a special technique, it serves for analytical purposes and as a tool in the investigation of cell diseases and membrane phenomena. For analytical purposes this technique has been used in various forms of paper or gel electrophoresis (two-dimensional electrophoresis, immunoelectrophoresis, isotachoelectrophoresis and others) for preparative separation and identification of fraction components. Besides this, as a microelectrophoresis, the technique may be used to elucidate the nature, number and distribution of charge groups in the peripheral zone of biological cells or to separate subpopulations in a mixture of cells, or vesicles (continuous flow electrophoresis, electrofocusing). Microelectrophoresis has been used for diagnostic tests in medicine as well as for investigations of cell diseases and membrane phenomena. It is also a very important method in the investigation of membrane structure and bioelectrochemical phenomena at the cell membrane/electrolyte solution interface.

One of the efficacy of electrophoresis in all its forms is that the data on the surface of cells or particles may be acquired without measurably altering their surface structure. The surface characteristics of biological membranes or whole cells can be examined without producing significant destruction of structural organization of cell membrane or loss of cell viability. Additionally, the course of any chemical, enzymatic, immunological or viral reaction connected with charge transfer separation which changes the nature or number of surface charge groups may be followed by this technique.

Nonequilibrium (irreversible) thermodynamics[6,31]

In Chapters 3 and 5 we have already touched upon the principles of irreversible thermodynamics. Here an additional reference will be made to the usefulness of the subject for membrane biophysics, e.g. to the electrokinetic phenomena covered in the preceding section, but most importantly to the membrane potentials to be discussed further. The importance of irreversible thermodynamics is due to the fact that metabolic processes of membranes are generally credited with being able to maintain steady nonequilibrium conditions across cell membranes by generating an active transport current of ions or electrons. For instance, in the case of excitable membranes, this active transport of ions across cell membranes generates and maintains nonequilibrium electrolyte concentration gradients, and that electrical excitability is due to transient ion permeabilities, thereby allowing the membrane potential to shift back and forth between the equilibrium potentials of different ionic species. For details, interested readers are urged to consult the cited reference.[31]

The Nernst-Planck Equation[2,5,6]

In a system consisting of an ultrathin membrane (e.g. a planar BLM) separating two aqueous solutions, the law of electroneutrality must be obeyed. That is, the sum of positively charged species is equal to the sum of negatively charged species for the system as a whole. However, as

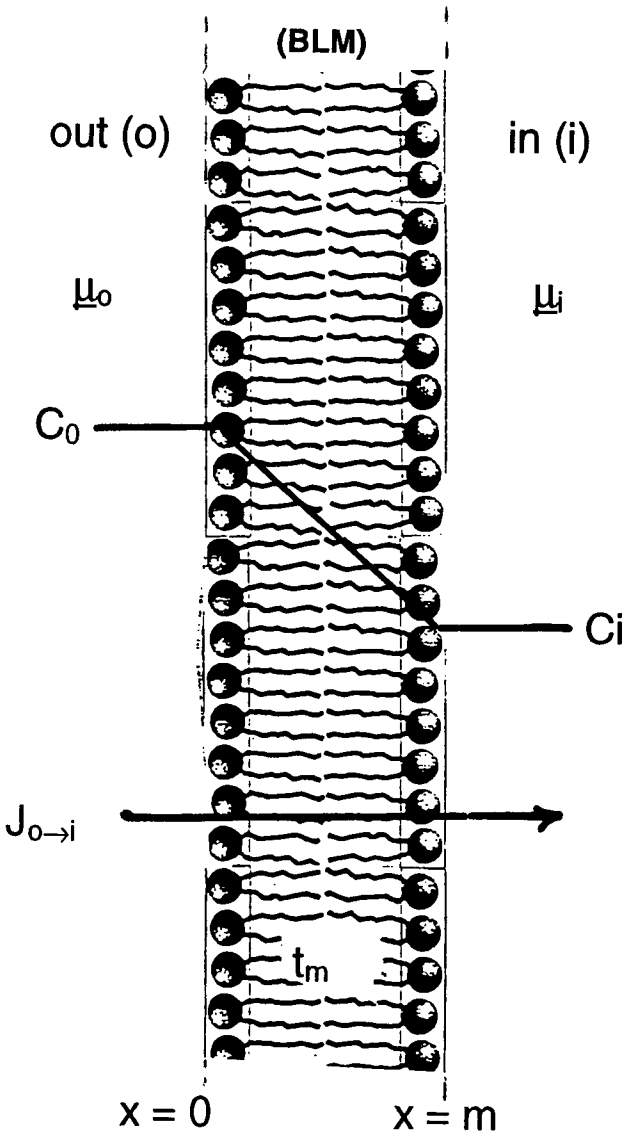

Fig. 6.2 Membrane transport. $\underline{\mu}$, μ, C and J denotes, respectively, electrochemical potential, chemical potential, concentration, and molecular flux. Subscripts: o = outsice, I = inside, I = chemical species i. t_m = membrane thickness (~ 6 nm for lipid bilayer)

pointed out by Guggenheim in 1950 [*see* Atwood, and Osa, 1991; Chapter 3, *Basic Principles*], charge separation on a microscopic scale may occur at membrane/solution interfaces. For example, to develop a potential difference (PD) of 50 mV across a BLM of 5 nm thick, the amount of charged species involved is far too small ($<< 10^{-10}$ M) to be detected chemically, or by any other means, except electrically. Therefore, the PD across the BLM (or a biomembrane, for that matter) cannot be simply related to the composition of bulk solution concentrations.

In order to treat the above-mentioned system thermodynamically, one can use the concept of electrochemical potential defined in the usual manner. Further, it is assumed in our discussion of membranes of molecular thickness and of planar configuration that transport of charged species (flux = J_i) takes place in one dimension (the x direction) perpendicularly to the membrane (Fig. 6.2). As a result of the above considerations, Eq. (6.28) takes the following form:

$$J_i = -kU_i c_i \frac{d\underline{\mu}_i}{dx} \qquad (6.24)$$

Since according to Eqs.(6.4) and (6.5)

$$\underline{\mu}_i = \mu_i + z_i F\phi = \mu_i^{o} + RT \ln a_i + z_i F\phi \qquad (6.25)$$

and $a_i = \gamma_i c_i$, where γ_i is the activity coefficient. Assuming that $a_i \cong c_i$ (i.e. ideal solution) in all further equations of this chapter.

The driving force for moving ionic species across a planar lipid bilayer in the x-direction may be expressed as an electrochemical potential gradient, i.e.

$$\frac{d\underline{\mu}_i}{dx} \cong RT\frac{d\ln [c_i]}{dx} + z_i F\frac{d\phi}{dx} \qquad (6.26)$$

The $\underline{\mu}$ is a fundamental measure of irreversibility as may be deduced from the second law of thermodynamics in the following manner. From the entropy S and $dS \geq 0$, where dS is the change in S for the reversible ($S = 0$) and irreversible processes ($S > 0$), respectively (*see* Chapter 3, *Basic Principles*). With a BLM interposed between two aqueous solutions, it can be shown that, for electrical work (W_{ele}) only,

$$\begin{aligned} TdS &= -\Sigma\, \mu\, dn - d\, W_{ele} \\ &= -(\mu_i - \mu_o)\, dn - \{ zF(\mu_i - \mu_o)\} \qquad (6.27) \\ &= -(\underline{\mu}_i - \underline{\mu}_o) \\ &= -\Delta\, \underline{\mu} \end{aligned}$$

where subscripts i and o denote inside (right = R) and outside (left = L), respectively (Fig. 6.2). From Eq. (6.26), transport of ions and other species is caused by a force equivalent to $-d\underline{\mu}/dx$.

Since the Nernst-Planck equation is central to membrane biophysics (transport, electrochemistry and physiology) phenomena, it is instructive to derive it here. The starting point is to consider the flux (J) across a membrane, which is equal to velocity times concentration (C), i.e. $J = vC$. The flux is also proportional to the mobility (U) and concentration (C) and the driving force of the species involved. One obtains

$$J = kUC\left(-\frac{d\underline{\mu}}{dx}\right) \qquad (6.28)$$

where k is a constant to be evaluated. For simplicity, we have dropped the subscript i. By substituting $\underline{\mu}$ {Eq. (6.5)} into Eq. (6.28), we can write:

$$J = -kUC\left\{RT\frac{d(\ln C)}{dx} + zF\frac{d\phi}{dx}\right\} \qquad (6.29)$$

The value of k is found by rewriting the last term of Eq.(6.35) using for $\mu = v/(-zd\phi/dx)$ because the mobility U of the species is defined as the ratio of the velocity v of the ion and the potential gradient of the field causing the ion's motion. Since vC has the dimension of the flux J, it follows that $k = 1/F$. Eq.(6.29) can then be rewritten in the following way.

$$J = -\frac{UC}{F}\left\{RT\frac{d(\ln C)}{dx} + z_iF\frac{d\phi}{dx}\right\} \qquad (6.30)$$

Eq.(6.30) is the famous ***Nernst-Planck flux equation***, upon which all basic equations relevant to membrane biophysics and electrophysiology depends! Presently we shall discuss the usefulness of the Nernst-Planck equation below. Note here that the first term of the right-hand side of the above equation describes the diffusion force due to concentration gradient, while the second term describes the electrical force due to the electrical gradient developed across the membrane (Fig. 6.2). The Nernst-Planck equation is also fundamental for our next discussion on membrane potentials.

The Nernst Equation

At equilibrium, there is no net transfer of charged species, i.e. $\Delta J = 0$; $d\mu/dx = 0$. therefore, Eq.(6.30) takes the form

$$zF\frac{d\phi}{dx} = -RT\frac{d(\ln C)}{dx} \qquad (6.31)$$

Integration of Eq.(6.31) across the membrane from $x = 0$ to $x = t_m$, gives

$$\phi_i - \phi_o = \Delta\phi\,(PD) = \mathbf{E_m} = \frac{RT}{zF}\ln\frac{[C]^R}{[C]^L} \qquad (6.32)$$

where subscripts o (superscript L) and i (superscript R) refer to the 'outer' and 'inner' (right) side of the membrane, respectively. The potential

difference (PD), or E_m, is called the ***membrane potential***. Eq.(6.32) is the well known ***Nernst equation***.

The Goldman Equation[3]

For biological systems the steady state concentrations of premeant ions are maintained by active 'silent' ion exchange pump (e.g. sodium-potassium). This mechanism is typical for a number of cells. Once the steady-state conditions are fulfilled, we can calculate the difference of the electrical potential between two points inside a continuous layer (membrane) as a function of ion concentrations at these points and ion mobilities inside the membrane, using the Nernst-Planck flux (also known as electrodiffusion) equation, which is cast in the following form:

$$J = -\frac{URT}{F}\frac{dC}{dx} - UC\frac{d\phi}{dx} \qquad (6.33)$$

It turns out that integration of Eq. (6.33) has been difficult owing to uncertainty of events in the membrane phase. Thus, in order to integrate Eq. (6.33) of two variables, many attempts have been made to simplify it. Only two cases will be mentioned here. The first one was by Henderson (1907) who assumed that the concentration gradient is linear within the membrane phase, so that potential gradient is non-linear. This is valid rather for mixed boundaries diffusion potentials (liquid junction potentials). However, for biological membranes and planar BLMs in which the lipid core is a barrier with very high activation energy for ion penetration, the assumption of a constant concentration gradient is unrealistic. The second approach is by Goldman (1944), who assumed the linearity of potential gradient across the membrane phase so that the concentration gradient cannot be linear.[7] For biosystems with various permeant ion species on both sides of the membrane the Goldman approach gives usually better agreement with experiments, so we shall follow this approach in calculations of electrical potential difference across the membrane. However, it is worth noting that the Henderson equation gives the better results for a system with only one simple

electrolyte present in different concentrations on both sides of the membrane. For more complex analysis of all approaches the reader is referred to Goldman,[3] [*see also* Milazzo, 1983 and references therein]. According to Goldman's approximation, Eq.(6.33) after introducing the constant-field condition

$$\frac{d\phi}{dx} = \frac{\phi_i - \phi_o}{t_m} \tag{6.34}$$

will become

$$J = -\frac{RTU\,dC}{dx} - zUFC\frac{\phi_i - \phi_o}{t_m} \tag{6.35}$$

where $\phi_i - \phi_o$ is the electrical potential difference across the continuous membrane phase. ϕ_i describes the potential of the membrane interior close to the interface with solution II, ϕ_o is the same potential nearby the boundary with solution I and t_m is the membrane thickness. After variables separation and integration (from $x = 0$, $C_i = C_{io}$ to $x = t_m$, $C_i = C_{ii}$), we obtain

$$\int dx = -RTU\int \frac{dC}{J + zUF\frac{(\phi_i-\phi_o)}{t_m}C} \tag{6.36}$$

This equation can be solved for J giving the Goldman equation

$$J = -\left\{\frac{URT\,dC}{F\,dx} + \frac{zFC\,(\phi_i-\phi_o)}{RT\quad t_m}\right\} \tag{6.37}$$

This is the expression for a steady-state flux of individual ionic species under the influence of an electric field, as well as concentration gradient inside the continuous layer. Under the constant field treatment,[3] both J and U are effectively constant. The final expression of the Goldman equation is,

$$J = (Py)\left\{\frac{[C_i] - [C_o]^{-y}}{e^{-y} - 1}\right\} \qquad (6.38)$$

where $y = zFE_m/RT$, $E_m = \phi_i - \phi_o$, and $P = D/t_m$, the permeability coefficient. To obtain the value of electrical potential difference in this layer (membrane), which is our aim, we have to take into consideration the electroneutrality condition, which reads

$$\sum_{i=1}^{n} z_i J_i = 0 \qquad (6.39)$$

i.e. the sum of the individual ionic currents across the membrane must be zero. Simple forms of solution may be obtained for ions of the same valency. If, for example, only sodium, potassium and chloride ions are present in our system, the electrical potential difference across the membrane will be

$$\phi_i - \phi_o = \frac{RT}{F} \ln \frac{U_{Na+}[C_{Na+}]_o + U_{K+}[C_{K+}]_o + U_{Cl-}[C_{Cl-}]_i}{U_{Na+}[C_{Na+}]_i + U_{K+}[C_{K+}]_i + U_{Cl-}[C_{Cl-}]_o} \qquad (6.40)$$

Eq.(6.40) relates the concentrations of charged permeant species in the membrane phase close to membrane/solution boundaries with the potential difference developed across the membrane interior.

The Hodgkin-Huxley-Katz equation

It has been shown in Chapter 5 (*Membrane Transport*) that $P = D/t_m$, where P is the permeability coeficient of ionic species (i), Eq. (6.40) now becomes, for a system having Na+, K, and Cl at electrochemical equilibrium, then the so-called Goldman-Hodgkin-Katz equation may be obtained:

$$\phi_i - \phi_o = \frac{RT}{F} \ln \frac{P_{Na+}[C_{Na+}]_o + P_{K+}[C_{K+}]_o + P_{Cl-}[C_{Cl-}]_i}{P_{Na+}[C_{Na+}]_i + P_{K+}[C_{K+}]_i + P_{Cl-}[C_{Cl-}]_o} \qquad (6.41)$$

If the membrane is permeable to only one ionic species, Eq. (6.41) reduces to the Nernst equation of the respective ion (Eq. 6.32). Now we are faced with the problem of relating the ion concentration at the boundaries to those in adjacent electrolyte solutions, as well as including phase boundary potential drop between the membrane and solutions. For this reason, an assumption of equilibrium between the membrane interfacial region and the adjacent electrolyte solution is made to simplify the calculations. The validity of such assumption results from the fact that, usually the diffusion across the lipid bilayer is so slow, that it does not affect significantly the electrical double layer formation.

Assuming that partition coefficients on both sides of a membrane are equal, i.e. $K_i^I = K_i^{II} = K_i$, we may now introduce the so called "modified" permeability coefficients P_i^* for each permeant species

$$P_{Na+}^* = (P_{Na+})^{II} \exp[F(\phi_i - \phi_o)/RT]$$

$$P_{K+}^* = (P_{K+})^{II} \exp[F(\phi_i - \phi_o)/RT] \qquad (6.42)$$

$$P_{Cl-}^* = (P_{Cl^-})^{I} \exp[-F(\phi_i - \phi_o)/RT]$$

where $(P_i)' = RTU_i K_i / F t_m = P_i K_i$ is the permeability coefficient of species i. Finally, equation (64.4) can be written for potential difference across the membrane

$$\phi_i - \phi_o = \frac{RT}{F} \ln \frac{P^*_{Na+}[C_{Na+}]_o + P^*_{K+}[C_{K+}]_o + P^*_{Cl-}[C_{Cl-}]_i}{P^*_{Na+}[C_{Na+}]_i + P^*_{K+}[C_{K+}]_i + P^*_{Cl-}[C_{Cl-}]_o} \qquad (6.42a)$$

Eq.(6.47a) is a modified form of the Goldman-Hodkin-Katz equation. Under special conditions, some terms of this equation may be zero or so small that they can be omitted, which simplifies the equation. Also, ions which have reached complete equilibrium do not contribute to Eq.(42a), since there is no net flux for these ions. Thus, when chloride ions are in an equilibrium or their permeability is negligibly low, Eq.(6.42a) becomes dependent only on the contribution of Na^+ and K^+ ions,

$$\phi_i - \phi_o = \frac{RT}{F} \ln \frac{P^*_{Na+}[C_{Na+}]_o + P^*_{K+}[C_{K+}]_o}{P^*_{Na+}[C_{Na+}]_i + P^*_{K+}[C_{K+}]_i} \qquad (6.42b)$$

Eq.(6.42b) may be easily transformed into

$$\phi_i - \phi_o = \frac{RT}{F} \ln \frac{(P^*_{Na+} / P^*_{K+})_o [C_{Na+}]_o + [C_{K+}]_o}{(P^*_{Na+} / P^*_{K+})_i [C_{Na+}]_i + P^*_{K+}[C_{K+}]_i} \qquad (6.42c)$$

Now, if for some reason $P_{K^+} >> P_{Na^+}$ (e.g. after valinomycin - K^+ ionophore - treatment of human erythrocytes), P_{Na+} / P_{K+} becomes negligibly small, and Eq.(6.41) reduces to the form dependent only on the

potassium concentration ratio on both sides of a membrane. This situation apparently corresponds to resting potentials of nerve and muscle membranes, as will be discussed in the next chapter. Eq. (6.41) was applied by Hodgkin, Huxley, and Katz with great success to the squid axon membrane, as we will take it up again in Chapter 7 (*Membrane Physiology*). Eq. (6.47) has also been applied to the BLM system to estimate the permeability ratio (relative permeabilities) between cations and anions.[8,9]

The Ussing Equation

From the Goldmann equation (Eq. 6.37), we can derive the Ussing equation by separating the right-hand side into two parts as was done by Ussing in his frog skin membrane experiment. Let us write for species i,

$$J_i = (J_i)_{in} - (J_i)_{out} \tag{6.43}$$

where subscript in and out denote inward and outward fluxes, respectively. The ratio $(J_i)_{in}/(J_i)_{out}$ can be expressed as

$$\frac{(J_i)_{in}}{(J_i)_{out}} = \frac{c_{io}\exp[-z_iF(\phi_i - \phi_o)/RT]}{c_{ii}} \tag{6.44}$$

Eq.(6.44) is known as the ***Ussing flux ratio equation*** which can be shown to be equal to $(u_{io} - u_{ii})/RT$ by taking

$$\ln\frac{(J_i)_{in}}{(J_i)_{out}} = \ln c_{io} + z_iF\phi_o/RT - \ln c_{ii} - z_iF\phi_i/RT \tag{6.45}$$

Assuming that standard chemical potentials u_{io}^o and u_{ii}^o are equal, then the final rewriting of the right-hand side of Eq.(6.45) gives

$$\ln\frac{(J_i)_{in}}{(J_i)_{out}} = \frac{\mu_{io} - \mu_{ii}}{RT} \tag{6.46}$$

The Ussing equation (6.44) is often used as an indicator of active transport. When both concentrations c_{io} and c_{ii} for the species i are known, as well as the potential difference (PD) called the membrane diffusion potential (ϕ_i- ϕ_o), we can calculate the ratio of both elementary fluxes. If the result of calculation is in agreement with the results of flux measurements by radioactive isotopes, then the only responsible force is the gradient of electrochemical potential of species i across the membrane. In the opposite case we have to take into consideration the existence of other energetic sources, that may indicate another transport mechanism.

Other Equations related to the Nernst-Planck Equation

As a concluding comment on the Nernst-Planck equation shown below:

$$J = - \frac{UC}{F} \left\{ RT \frac{d(\ln C)}{dx} + zF \frac{d\phi}{dx} \right\} \qquad (6.30)$$

one can also obtain Fick's law of diffusion, $[J = -D(dC_i/dx)]$ by letting z = 0 in Eq.(6.30), and by using the Einstein equation, D = URT/F.

6.4 Transmembrane Potentials and BLMs[2,4,10,15-18,33-34]

Transmembrane potentials

By means of thermodynamics, transmembrane potentials of BLM can be related to the distribution coefficients and electrochemical potentials of species present in aqueous solution and oily membrane phases. Fig.6.3 shows an *aqueous solution/BLM/aqueous solution* system, in which a transmembrane potential E_m is measured. The Galvani potential, ϕ, is plotted on the vertical axis. The BLM thickness is denoted by t_m, starting from x = 0 at the left (outer) or solution(1)/BLM interface to x = t at the right (or inner) BLM/solution(2) interface on the horizontal axis. By convention, the aqueous solution on one side of the BLM is taken to be zero potential.

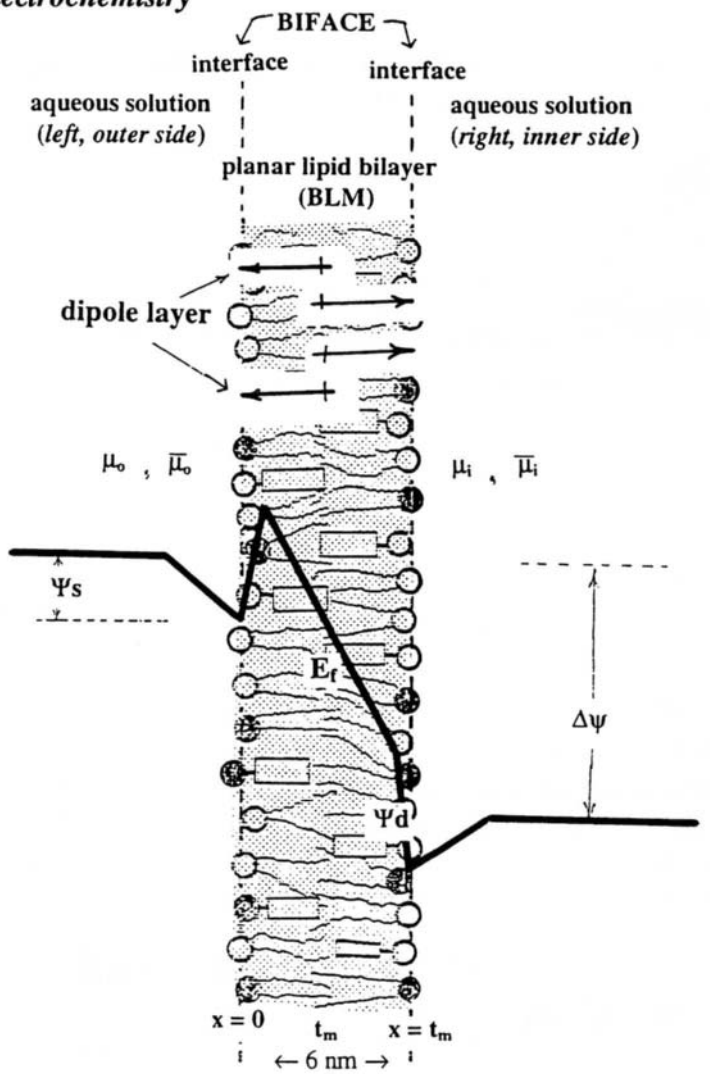

Fig. 6.3 Schematic representation of electric potential profile at the interface and across the BLM of negatively charged lipids, which are also shown as dipoles. t_m = the thickness, less than 100 A. E_o = potential at the outer (left) solution, which is taken to be zero at x = ∞. $E_m = E_i - E_o$, the membrane potential. ϕ_1 and ϕ_2 are the Galvanic potentials at the outer and inner interface, respectively, ϕ_G = Gouy potential, ξ = Zeta potential. Various $\underline{\mu}$'s ans μ's are electrochemical and chemical potentials, respectively as designated by super- or subscripts (see text).

Since single ion distribution coefficients can be related to the classical partition coefficient, K, defined by

$$K = \frac{[Salt]_m}{[Salt]_1} \qquad (6.47)$$

That is, the ratio of salt concentration in the membrane phase $[Salt]_m$ to that in the aqueous solution, $[Salt]_1$, Eq.(6.47) may be rewritten as

$$\phi_1 = \frac{RT}{F} \ln \frac{[K]}{[D_A]_1} \qquad (6.48)$$

since $K = [D_C]_1^{1/2} \times [D_A]_1^{1/2}$.

Referring to Fig.6.3, ϕ_1 and ϕ_2 at each interface, which are not measurable, owing to a lack of suitable contact with the membrane, we nonetheless can measure $\Delta\phi = (\phi_2 - \phi_1)$ by placing a reference electrode (e.g. calomel electrode) in each of the bulk solutions bathing the membrane. For example, NaCl is introduced in the outer aqueous solution (1) and KCl in the inner aqueous solution (2). From Eq.(6.64), we obtain

$$\Delta\phi = \phi_2 - \phi_1 = \frac{RT}{F} \ln \frac{[K_{KCl}]}{[Cl^-]_2} - \frac{RT}{F} \ln \frac{[K_{NaCl}]}{[Cl^-]_1}$$

or

$$\Delta\phi = \frac{RT}{F} \ln \frac{[K_{KCl}]}{[K_{NaCl}]} = \frac{RT}{2F} \ln \frac{D_K}{D_{Na}} \qquad (6.49)$$

where K_{KCl} and K_{NaCl} are distribution coefficients defined by Eq.(6.63). Of interest to note is that, Eq.(6.65), the observed E_m ($\Delta\phi$) is independent of the common anion, Cl^- [see Eq.(6.56) and apply conditions for μ_A^o].

Experimentally, Eq.(6.65) may be readily tested by forming BLM containing valinomycin separating NaCl and KCl solutions.

The Nernst equation [Eq.(6.32)], albeit exceedingly useful in accounting for the transmembrane potential, E_m , does not reveal very much about the underlying mechanism responsible for the observed potential. In the following paragraphs, we will discuss the origin of membrane potentials that have been detected in the BLM systems.

BLM potentials[2,9]

The unique aspect of BLM, similar to biomembranes, is the ultrathin lipid bilayer separating two aqueous solutions (see Fig. 6.3). Membranes of these types have two inter-dependent interfaces (i.e. a *biface*, meaning the two coexistent solution/membrane interfaces, through which material, charge, and energy transfer are possible, Chapter 3, *Basic Principles*). The creation of a biface is the result of two immiscible phases with very different dielectric constants (ε_w = 80; ε_m = 2-5). At each interface, as well as across the ultrathin lipid bilayer (~ 6 nm), powerful electric fields may exist, which facilitate charge separation and transport, as will be discussed later. In this segment, we will consider the origins of BLM potentials.

An observed transmembrane potential in a BLM system may be due to one or a combination of the following potentials:

- Diffusion (concentration) potential, ϕ_d
- Adsorption (surface or interfacial) potential, V
- Distribution (outer) potential, U
- Galvanic (inner) potential, ϕ (= V + U)
- Gouy (Donnan) potential, U_G or ϕ_{Don}
- Electrokinetic potential, U_k
- Thermoelectric potentials, E_t
- Redox (electrostenolytic) potential, E_{RX}
- Photoelectric potential, E_{hv}

In the classification given above, redox potential, thermoelectric, and photoelectric potential in BLM are discussed in Chapter 9 (*Photobiology*), whereas a brief summary has been already given on the electrokinetic potential in this chapter (Section 6.2). Here, we shall describe the first five potentials that are relevant to the BLM systems.

The nature and origin of adsorption, distribution, and Galvani potentials are best described in the language of interfacial chemistry, and have been treated in detail [Ivanov, 1988]. In order to apply these concepts to the BLM system, it is informative, first of all, to define the terms and to summarize some of the general conclusions.

Adsorption potential. Also known as surface or interfacial potential (designated by symbol V), it is opposite to that observed with the diffusion potential. For this interfacial potential to appear, a difference in salt concentrations across the BLM is not required; it depends upon the sorbed species and/or the dipoles. With cationic interface-active compounds, such as hexadecyltrimethylammonium bromide (HDTAB) and phosphatidyl-ethanolamine (PE) at low pH, a negative potential results and vice versa with anionic interface-active compounds, such as dodecyl acid phosphate (DAP) and phosphatidylserine (PS). The magnitude of V decreases with increasing salt concentration. Two other caveats should be noted about this potential: (i) it may have only transient existence, however, the time for its decay can take a long time, and (ii) the law of electroneutrality at the interfaces is not obeyed.

Distribution potential. It is also called outer potential, symbolized by U. The potential arises as a result of a differential distribution of the oppositely charged species across the interface, the magnitude of which is influenced by the diffusion of ions and their concentrations, and increases with increasing salt concentration, but is independent of the nature of the common ion.

The sum of interfacial potential and distribution potential is termed the inner or *Galvani potential*, designated by ϕ. It will be discussed below that the observed transmembrane potential difference, E_m, is due either to ΔV, ΔU, or to ΔV plus ΔU, as defined above. It should be remembered

that there are two components of ϕ (= V + U). Eqs.(6.47-6.49) are concerned with only the distribution potential. If compounds, such as phospholipids and interface-active agents, are preferentially adsorbed at the interface, the so-called adsorption potential (V) may also develop. As shown in Fig.6.3, both adsorbed fixed charge species and dipoles may contribute to the observed potential. The nature and origin of adsorption (or interfacial) potential can be discussed in terms of the classical electric double-layer theory of Gouy-Chapman-Stern-Graham [*see* Osa and Atwood, 1991].

Diffusion potentials. In general, *diffusion potentials* appear always when an electrolyte diffuses down its concentration gradient. However, one prerequisite condition, namely, both cationic and anionic species must have different mobilities. The magnitude and sign of such potential depends on the difference in mobilities between cation and anion (the greater the mobility difference, the greater the potential difference), with the more dilute region having the same sign as the faster ion. In bulk solution these potentials are readily disturbed by convection and may be neglected, but if two electrolyte solutions of different concentrations are in contact in a way that avoids convectional mixing but allows diffusional flow, the diffusion potentials are stable. Such electrolyte contact may be accomplished either in a direct way or by electrolyte separation by semipermeable membrane. The direct contact of two immiscible solutions leads to the so called "liquid junction" potentials which are a possible source of error whenever electrodes with salt bridges are used. The electrolyte separation by a perm-selective membrane is characteristic of biomembrane systems and will be discussed in the present section.

For the sake of simplicity, we will assume that all ion fluxes are constant and independent of time (steady-state conditions). This requires the stable properties of the membrane and constant concentrations at the membrane. The latter may be achieved in several ways. In the case of experiments with bilayer lipid membranes (BLM), the vastness of the two compartments on both sides of the membrane provides practically constant concentrations.

The Gibbs-Donnan potential. The *Gibbs-Donnan potential* occurs when a nonpermeant ion (for biological systems usually a poly-ion such as a

protein) is unequally distributed between the two electrolyte solutions separated by a permselective membrane, which allows certain electrolyte ions to move freely between the two solutions. This movement is restricted by the second law of thermodynamics and the principle of electroneutrality. The first restriction requires that each permeant ion species moves only down its electrochemical potential gradient, the latter requires the sum of all positive charges (cations) to be equal to that of all negative charges (anions) in each solution. When the system reaches its equilibrium, there is no flux of any permeant species i, $J_i = 0$. Eq.(6.30) then takes the form

$$z_i F \frac{d\phi}{dx} = - RT \frac{d(\ln c_i)}{dx} \qquad (6.50)$$

Integration of this equation over the whole membrane thickness at the equilibrium conditions leads to the expression for electrical potential difference developed across the membrane, known as *Donnan potential*,

$$\phi^{II} - \phi^{I} = {}^{II}D^{I}\phi = \frac{RT}{z_i F} \ln \frac{c_i{}^{I}}{c_i{}^{II}} \qquad (6.51)$$

where indices I and II denote the two sides of the membrane. This dependence may be also obtained in another way. The main condition of the equilibrium state is equilibrium of electrochemical potentials of each permeant species on both sides of the membrane

$$\mu_i{}^{I} = \mu_i{}^{II} \qquad (6.52)$$

which leads immediately to the dependence

$$RT \ln c_i{}^{I} + z_i F\phi^{I} = RT \ln c_i{}^{II} + z_i F\phi^{II}$$

or

$$^{II}D^{I}\phi = \frac{RT}{z_iF} \ln \frac{c_i^{I}}{c_i^{II}} \qquad (6.53)$$

being identical with Eq.(6.32). Eq. (6.53) may be useful in the determination of nonpermeant polyion concentration.

Phase boundary potentials. They are also known as ***surface potentials***. Phase boundary potentials, appearing at the interfaces between the membrane and adjacent electrolyte solutions, are attributed mainly to fixed charges within or attached to the membrane phase. These fixed charges which originated from ionic groups are part of the membrane structure and, under special conditions, may change their number through the dissociation of weak acidic groups or conversely through association of ions with binding groups. The electric dipoles (e.g. headgroups of lipid matrix) also contribute to these potentials. The phase boundary potentials do not usually directly add to the transmembrane potential difference, however, they do affect the electrical potential profile within the membrane. Therefore, their presence may alter the permeability properties of membrane (e.g. by affecting organization of integral or peripheral proteins), indirectly affecting in this way, the transmembrane potentials. The relationship between fixed charges and phase boundary potentials can be illustrated by either one of two simplified models: (a) The first model assumes that the fixed charges are adjacent only to both surfaces of a nonpolar membrane interior. This model may represent an artificial bilayer lipid membrane (BLM). It is also close to a biological membrane. In the second model an assumption is made that the fixed charges are homogeneously distributed over the whole membrane. An ion exchange membrane may represent this model.

In the case of ion exchange membrane which is the second model mentioned above, an assumption has been made that its fixed, say negative charges are homogeneously distributed over the membrane phase. In this situation the appearing phase boundary potentials may be treated as two separate Donnan equilibrium potentials at each interface. The role of impermeable polyion from the previous section is now as the fixed charges from the membrane interior. If at the beginning an initial unequal

distribution of permeant ions exists on both sides of such membrane (let us assume that a less concentrated electrolyte solution is on the right side of the membrane), the whole system will proceed toward equilibrium. As a consequence, at equilibrium, the electrochemical potentials must be identical on both sides of each boundary. Since biological membranes do not have a high density of fixed charges in their interior, the effects of Donnan distribution are of smaller magnitude than for ion exchange membrane.

As stated at the beginning of this section, it appears that the permeability and conductance properties of the membrane are strongly influenced by the electrical potential profile. Since the variations of phase boundary potentials may alter the behavior of pores, channels and ion carriers, they may express themselves as alterations of current-voltage relationships, giving indirect information about potential distribution within the membrane and at its interfaces. However, the phase boundary potentials are not usually readily measurable with electrodes due to the thickness of the membrane phase.

Relationship among various potentials[2,15]

Of immediate concern here we have been discussing the observed membrane potential, E_m, which is the sum of all interfacial potentials and diffusion (concentration) potentials at the interfaces and within the membrane. Thus, we have the appropriate name, the so-called ***transmembrane potential***, E_m, which is given by

$$E_m = \Delta\phi + O_d \tag{6.54}$$

or

$$E_m = \Delta V + \Delta U + \phi_d \tag{6.55}$$

or

$$E_m = \Delta U_G + E_p + \Delta U + \phi_d \tag{6.56}$$

For most of these individual potentials, the final expression takes the form of the Nernst equation (Eq. 6.32) Experimental conditions or circumstances can be such, E_m measures one or a combination of these

potentials. Specifically, (i) for a symmetrical BLM, the polarization potential, E_p, is unimportant, (ii) for an unmodified BLM, whose interior is liquid-hydrocarbon like, $\Delta\phi$ is not measured, (iii) for BLM with low interfacial charge density (e.g. $\sigma < 1$, net charge per 100 A^2), $\Delta\phi_G$ contributes very little, (iv) for charged species with substantial solubility in BLM, $\Delta\phi$ may be neglected, and (v) for a BLM with high interfacial charge density (>1e/100A^2), the diffusion potential, ϕ_d, is inconsequential.

It should be emphasized, however, that the above statements are offered as a general guidance only. Even for a relatively simple BLM, the measured transmembrane potential (E_m) could be a result of various potentials. The extent of contributions of these potentials to the overall E_m is dependent upon the nature and properties of BLM-forming constituents, whose charge densities, dipole orientations and relative permeabilities to ions are some of the factors that should be taken into consideration for a careful analysis of the observed membrane potential.

In concluding this section, mention should be made concerning the dipoles of membrane constituents in the BLM. The dipole flip-flop could be important for the voltage-dependent conductance in BLM (e.g. alamethicin-modified BLM). Derzhanski et al[51] have derived an equation for the current as a function of frequencies. Pastushenko and Chizmadzhev[52] have considered the energetic profile of dipole molecules in biomem-branes in general, and in BLM in particular. This topic has been reviewed in detail by Shchipunov and Drachev[29] and by de Levie.[55]

Electrical double layer theory and BLMs

Aspects of the electric double-layer theory discussed above (Section 6.2) have been applied to the BLM system [Milazzo, 1983; Davison, 1992]. The central idea is based on the Boltzmann distribution of the ions in a varying potential field. One important application of the electric double-layer theory is the estimation of ion concentrations, such as

H^+, at the BLM/solution interface. The interfacial $[H^+]_i$ and bulk pH $[H^+]_b$ can be related by the following equation

$$[H^+]_i = [H^+]_b \, e^{-F\phi/RT} \qquad (6.57)$$

By definition, pH = -log $[H^+]$, we have

$$[pH]_i = [pH]_b + \frac{F\phi}{2.3RT} \qquad (6.58)$$

where ϕ is the interfacial potential at x = 0 (or x = t_m, *see* Fig.9.3). For a negatively charged BLM, it can be readily seen that the pH at the interface is lower than the pH in the bulk solution. In general, ϕ may be estimated by measuring the zeta (ξ) potential in the plane of shear. For example, Papahadjopoulos and Watkins[17] have found a reasonable agreement between the values calculated and the electrophoretic measurements on spherical BLMs (liposomes). Vaz et al.[18] using a fluorescent pH indicator (dimyristoyldansylcephalin) estimated the pH adjacent to the BLM interface. They have found that the hydrogen ion concentration is electrostatically enhanced, the enhancement being dependent on the interface charge density and bulk phase salt concentration.

Another approach in estimating ϕ, is by the use of the Gouy equation which may be simplified as follows:

$$\phi_G = 50.4 \sinh^{-1} \frac{134\,\sigma}{\sqrt{C}} \qquad (6.59)$$

C is the univalent ion concentration and σ the interface charge density (charge/A^2). It can be readily shown that, at a fixed salt concentration in the bulk phase for a negatively charged BLM, the interfacial pH should be lower by about 0.6 to 0.7 pH units. By changing the charge density on the BLM and by changing the pH or composition of bathing solutions, it

should be possible to investigate molecular interactions and ion binding in the BLM. In this connection, mention should be made that photochemical reactions[6] may be studied by monitoring a change in ϕ_G ($\Delta\phi = \phi_i - \phi_o$) (*see* Chapter 9, *Membrane Photobiology*).

The Henderson-Hasselbalch Equation

So far we have been concerning hydrogen ions (H^+ or H_3O^+) at interfaces, although pH in the bulk solution is mentoned in passing. It is therefore not out of place here to consider briefly the vital role played by hydrogen ions in the body fluids, both intracellular and extracellular, in cell functions (e.g. enzyme catalysis and periodontal disease). In acid-base physiology, one is concerned with the concentration of hydrogen ions in the bulk phase. The Henderson-Hasselbalch equation of the form given below is of interest:

$$pH = pK + \log \frac{[HCO_3^-]}{[H_2CO_3]} \qquad (6.60)$$

Where pK = 3.6, $CO_2 + H_2O \Leftrightarrow H_2CO_3[0.004] \Leftrightarrow HCO_3^-[24] + H^+[0.00004]$ and with typical concentrations in mM in brackets. For normal healthy people, the pH values of the extracellular and intracellular fluids fall in the range 7.35 to 7.45. When pH values are outside the range between 7.1 and 7.7 for long periods of time, the life as we know it is no longer viable. This narrow 0.6 pH unit appears to be small but actually misleading. From a biophysical viewpoint, the pH values are best expressed in terms of H^+ ion concentration in moles per liter. Thus, a pH of 7.4 represents a 40 nM of H^+ ion concentration. A pH of 7.7 is equal to 80 nM of H^+ ion concentration. Evidently, a change of merely 0.3 pH unit represents a two-fold change in H^+ ion concentration! To better appreciate these numbers, one is reminded of the normal K^+ ion concentration in the extracellular fluid, which is on the order of 5 mM and is of crucial importance in nerve functioning (*see* Chapter 7, *Membrane Physiology*), whereas the H^+ ion concentration is expressed in nM (1 nanomolar = 1 x 10^{-9} moles per liter). Thus, there is a 1,000,000 times difference in magnitude of these two ion concentrations!

Potential difference across BLMs

An unmodified BLM (planar lipid bilayer) made from either oxidized cholesterol or phosphatidylcholine (PC = lecithin), separating two aqueous solutions, presents a very high energy barrier for the transport of common salts, such as NaCl and KCl. This high energy barrier arises mainly from the difference of the electrostatic energies of the ions in the two phases: aqueous solution and oily membrane. Using the Born equation, we have already discussed the insulating nature of the lipid bilayer in Section 4.2.3 of Chapter 4 (*Experimental Models of Biomembranes).* The energy necessary to transport an ion from aqueous solution to the bilayer lipid phase is on the order of 1 - 1.5 eV (about 40 kT), which is much larger compared with kT at room temperatures. Thus, one can conclude, with confidence, as supported by experimental conductivity data, that an unmodified BLM contains few dissolved common ions (e.g. Na^+ or K^+). This being the case, then how does one explain the observed E_m, when such BLM are perturbed by interface-active compounds, such as $HDTA^+$-Br^- and SDS (Na^+DS^-)? Here again, classical interfacial chemistry provides a ready answer.[11]

According to Gibbs' adsorption equation, any substance that has the ability to lower the interfacial free energy tends to be spontaneously adsorbed at the interface. Thus, for example, when $HDTA^+Br^-$ is introduced to one side (say, the outerside) of the BLM, the cation (C) and anion (A) concentrations can be described by the Boltzmann equation

$$[C]_m = [C]_1 \exp\left[-\frac{F(V - \phi)}{RT}\right] \qquad (6.61)$$

$$[A]_m = [A]_1 \exp\left[\frac{F(V - \phi)}{RT}\right] \qquad (6.62)$$

where subscripts m and 1 as before, refer to the membrane and aqueous solution (1), respectively. V is the interfacial potential at the solution/BLM

interface at x = 0 and ϕ is the distribution potential at a distance in the interior of the lipid bilayer, where in principle at least, $[C]_m = [A]_m$. However, at the interface (x = 0 or x = t) the electroneutrality conditions are not observed, Eqs.(6.61 and 6.62) become

$$\phi = RT \ln \frac{D_C}{D_A} = RT \ln \frac{[C]_m}{[A]_m} \qquad (6.63)$$

From the above equations, one obtains, at the condition, where ϕ at x = 0

$$\phi_1 = \phi - (\phi - V) = V \qquad (6.64)$$

Eq.(6.64) shows that at the solution/BLM interface, the inner (or Galvani) potential is determined only by the interfacially adsorbed species and their dipoles.

The dipolar components of interfacial potentials, V, can be analyzed using BLM forming molecules, such as phospholipids (e.g. phosphatidylcholine) and interface-active agents (e.g. HDTABr). These molecules are oriented at the solution/BLM interface. Together with water dipoles (u_w) associated with the fixed charge and polar-head group (u_p), the terminal hydrocarbon chain (u_t) constitutes another dipolar component. The overall contribution to the interfacial potential is given by

$$V = \phi_G + 4 n u_d \qquad (6.65)$$

where ϕ_G is the Gouy double-layer potential due to the fixed charges at the interface, n is the number of dipoles per cm^2, and $u_d = u_w + u_p + u_t$, where u_d is the overall dipole moment of the constituent molecules in the BLM.

6.5 Measurements of Planar Lipid Bilayer Potentials

Up to now, we have used mainly the classical concepts of electrochemistry in describing the various phenomena associated with membranes, involving only hydrated ions and ions surrounded by other ions (ionic cloud). There is no rest for ions in the solution (ceaseless motion or random walk). Ions get nowhere by random walk alone (their time average displacement is zero). A net transport of ions is possible by:

- the presence of an electrical field, and
- a chemical potential gradient.

Thus, a net drift is superimposed on the random walk. When ions reach the interface, properties change abruptly; the anisotropy of the forces compel ions to adopt new configurations unknown in bulk solutions. Here, a variety of phenomena occurs such as charge separation, potential gradient, adsorption, and orientation of H_2O dipole, etc. At present, modern electrochemistry is focused on the transfer of charges across the interface, in particular, the electrified interface. The involvement of the electrical double layer, therefore, is self-evident.

Of special interest to the above topics is the question: 'Experimentally, how does one go about measuring membrane potential such as $\Delta\phi$ (= E_m)?' One may place a pair of identical electrodes, such as (i) Ag/AgCl, (ii) K^+-sensitive glass electrodes, or (iii) saturated calomel electrodes (Hg/Hg_2Cl_2) with salt bridges, across the membrane with fixed negative charges. When the concentration ratio of the solutions bathing opposite sides of the memrbane is 10:1 (say, 0.1 M KCl on the outside and 0.01 M KCl inside), an E_m of about 116 mV would be measured for case (i), about 0 mV for case (ii), and 58 mV for case (iii). Evidently, the choice of the kind of electrodes used to measure E_m is of crucial importance. For BLM and most membrane studies, calomel electrodes with saturated KCl bridges have been extensively employed [Tien, 1974]. A pertinent interpretation to the above data is to liken the membrane as a bipolar electrode rather than merely as a permeating barrier, as will be

considered. First, a summary of the electrical properties of planar lipid bilayers (BLMs) is given as follows.

The usual picture of a BLM interposed between two aqueous solutions consists of a liquid hydrocarbon phase sandwiched between two hydrophilic regions. The electrical properties of BLMs have been extensively investigated, which usually entails measuring membrane resistance (R_m or conductance, $G_m = 1/R_m$), capacitance (C_m), potential (E_m), dielectric breakdown voltage (V_b), and current/voltage (I/V) characteristics. Unmodified BLMs (i.e. BLMs formed from common phospholipids or oxidized cholesterol,[35-39] dissolved in an n-alkane solvent in 0.1.M KCl solution), have typical intrinsic values of R_m greater than 10^8 ohms cm^2, C_m ~ 5000 pF cm^{-2}, E_m ~ 0, V_b < 200 mV, with I/V curves obeying Ohm's Law. With a few exceptions, the results of these measurements have been interpreted by treating the BLM electrically, in a system equivalent to that of a resistor connected in parallel with a capacitor. The structure of the BLM is considered to be a thin slab of liquid crystals in two dimensions, having a fluid hydrocarbon core of about 5 nm thick. This liquid-crystalline structure of BLM is essentially an excellent insulator.[49]

Cyclic Voltammetry[9]

The charges that we are concerned with here are the electronic charges (electrons and holes). For charges of this type to be transported across the interface, electrochemical reactions must take place. In the presence of a membrane that is impermeable to ions, what will happen then? Here, the membrane must serve at least two functions: (1) pathway for electronic charges, and (2) electrode surface for chemical transformation (reduction and oxidation or redox reactions). To probe such a membrane, we will describe a well established cyclic voltammetry method of electrochemists, which was applied to the BLM system in 1984.

Cyclic voltammetry (CV) is an elegant and simple electrochemical technique for studying redox reactions at the metal electrode/solution interfaces and has become increasingly employed in all fields of

chemistry. Until recently, however, the technique has apparently not been applied to any membrane systems including the BLM separating two aqueous solutions. It is instructive, therefore, to give a brief account of the fundamentals of CV and to show how the technique can be applied membrane research.

In conventional CV, one uses immobile working electrode in unstirred solutions and applies a triangular potential waveform between it and a reference or an auxiliary electrode. The working electrode (WE) may be made of Pt, Au, carbon paste, glassy carbon, or semiconductor, SnO_2. A silver/silver chloride or a saturated calomel electrode (SEC) is used as the reference electrode (RE). In the present day practice of CV, a Pt wire or a second reference electrode is employed as auxiliary electrode (AE), the purpose of which is to avoid large currents being passed through the reference electrode during the potential scan, which could change its potential. The potential scan (or sweep) is carried out between two potential values of interest (e.g. from about 1.2 to -0.8 V vs. SCE). The scan rates can be anywhere from 0.1 mV to 100 V or more per second but values between 10 to 400 mV/s are frequently used. During the potential scan, the current is measured at the working electrode. The graph with the current plotted on the vertical axis versus the potential on the horizontal axis is called the ***voltammogram***, which is characterized by several parameters. These are the peak potentials (E_{pc} and E_{pa}, for cathode and anode, respectively), the peak current (I_{pc} and I_{pa}), and the half-peak potential ($E_{p/2}$) and the half-wave potential ($E_{1/2}$). The last parameter is related to the standard redox potential ($E^{o'}$) by the following equation

$$E_{1/2} = E^{o'} + \frac{RT}{nF} \ln \left(\frac{D_{RED}}{D_{OX}}\right)^{1/2} \qquad (6.66)$$

where D_{RED} and D_{OX} are the diffusion coefficients, n is the number of electrons involved and the other terms have the usual significance. Since

$D_{RED} = D_{OX}$, therefore $E \simeq E^{0'}$, which is located exactly halfway between E_{pa} and E_{pc}. Under a given set of conditions, the criteria of reversibility of electron-transfer reactions at the electrode surface is given by

$$E_{pa} - E_{pc} = DE_p = \frac{59\ mV}{n} \qquad (6.67)$$

For a reversible reaction, the ratio of I_{pa}/I_{pc} should be unity and the I_p (peak current in amperes) is expressed as follows

$$I_p = kn^{3/2}AD^{1/2}Cv^{1/2} \qquad (6.68)$$

where A = the electrode area (cm^2), D = the diffusion coefficient ($cm^2\ s^{-1}$), C = the molar concentration, v = the scan rate ($V\ s^{-1}$), and k (= 269) is the so-called Sevick-Randles constant. In Eq.(6.68), it can be seen that I_p increases with C and is directly proportional to the square root of v. For a general redox reaction

$$OX + ne \underset{k_b}{\overset{k_f}{====}} RED \qquad (6.69)$$

where k_f and k_b denote the forward and backward rate constant, respectively, the reaction is said to be reversible if $k_f \sim k_b$. The k's are related to k_S, the standard heterogeneous electron-transfer rate constant, which may be estimated from the value of DE_p [eq.(133.4)] according to the method worked out by Nicholson (see [Osa and Atwood, 1991]). The final results of Nicholson's analysis is that the voltammograms (or current/voltage curves) of CV depend on the three variables, from which a practical relationship between k_S, E_p, and v is obtained, i.e.

$$U \simeq 28.8\ k_S\ v^{1/2} \qquad (6.70)$$

where ψ, as a function of E_p, is available. Thus, known ψ and from experimentally determined DE_p values, k_s can then be estimated.

Cyclic voltammetry and BLM experiments

Before discussing the results obtained on a BLM system using the powerful CV technique, a brief description of the setup used in our work is in order (for more details see Chapter 4). The Teflon cup will be referred to as the inside, and the other chamber will be referred to as the outside. We have used a three-electrode system for obtaining voltammograms in the following configuration: one calomel electrode (SCE) is placed in the Teflon cup and two other calomel electrodes are on the outside. An EC/225 Voltammetric Analyzer (IBM) in the cyclic voltammetry mode in conjunction with an x-y recorder is used throughout in our second setup. The hole of 0.15 cm diameter in the Teflon cup is usually pretreated with the BLM-forming solution to be used later. First of all, in order to demonstrate electronic conduction in BLM in the absence of light, the membrane must be modified to function as a metallic or semiconductor electrode, so that the powerful CV technique can be applied. To impart electronic properties, we have discovered that, by incorporating an organic semiconductor such as TCNQ (7,7,8,8-tetracyanoquinodimethane) or TTF (tetrathiafulvalene) the BLM becomes electron-conducting. (see Table 6.2).

Table 6.2 Analogy between inorganic, organic semiconductors*, and BLM modifiers

	Inorganic Semiconductor	Organic Semiconductor	BLM Modifiers
Base material	Covalent-bonded, crystalline phase (e.g germanium crystal)	Hydrophobic hydrocarbon (e.g. lipid bilayer)	
Electron donor	Group V elements (e.g. As, Sb)	Bioreductant (e.g. cytochromes, ferrous ions, and H_2O)	TTF (tetrathiafulfervalene) C_{60} (fullerenes)
Electron acceptor	Group III elements (e.g. Ga, In)	Biooxidants (e.g. ferredoxins, quinones, and H_2O)	TCNQ (7,7,7,8-tetracyanoquinodimethane); Ferrocene; Iodine (I_2); TPP (meso-tetraphenylporphyrin)
Electron pathway	Crystal proper	Conjugated hydrocarbon chain and ring systems	C_{60} (fullerenes)
Connector	Metallic wire	Electrolyte Solutions	Metal support Electrolytes

*Modified from Table 3, p.988 (Ivanov, 1988)

In order to apply the powerful CV technique to the BLM system, a conceptual effort has to be made, that is to consider one side of the BLM as the working electrode, while the other side is providing the connection to the external circuit. As already mentioned, an unmodified BLM behaves essentially as an excellent insulator (specific resistivity > 10^{14} Ω) and does not function as a working electrode. However, upon incorporation of TCNQ into the BLM and in the presence of ascorbic acid in the outer solution and equal molar (0.001 and 0.01) $K_3Fe(CN)_6/K_4Fe(CN)_6$ in the inside, the observed electrical properties are such (R_m decreasing from 10^8 to 10^6 ohms cm^2, C_m increasing from 0.4 to 0.5 F cm^{-2}, E_m developing to about 180 mV with the ascorbic acid side positive. In the absence of TCNQ in BLM with other experimental conditions the same, the I/V is linear; it practically coincides with the x-axis on the scale used. In the absence of redox couples in the bathing solution, but with TCNQ in the BLM, the I/V curve remains linear. To show more clearly that the redox reactions are occurring across the TCNQ-containing BLM the following experiment was carried out.

To one side of a TCNQ-containing BLM, a high concentration of equal molar ferri-ferro cyanide solution was added, whereas to the other side, aliquots of ascorbic acid of known concentration were introduced. Concurrently, the membrane potentials (E_m) after each addition of ascorbic acid were measured. It is most interesting to note that the extrapolated value of E_m at the equal molar concentrations of the two redox couples agrees very well with the difference of the two standard redox potentials ($E^{O'}$ ~ 300 mV). The highly asymmetrical current/voltage curves are reminiscent of those of a *p-n* junction diode which permits an electron current flow in a forward-bias direction only. In the TCNQ-BLM system, oxidation occurs at the membrane-solution interface contacting the ascorbic acid solution and reduction of ferricyanide to ferrocyanide takes place on the other side of the BLM which has a negative polarity. Implicit in this interpretation is the transmembrane movement of electrons via the TCNQ molecules imbedded in the lipid bilayer; that is, the whole system has the properties of a *p-n* junction with the TCNQ-BLM acting as a rectifier.

To demonstrate that the TCNQ-BLM behaves like a metallic electrode (e.g. Pt which is frequently used in CV), a comparative

experiment was carried out, in that cyclic voltammograms of quinhydrone were obtained using either Pt or TCNQ-containing BLM under very similar conditions. In particular, the cathodic portions of the voltammograms are quite alike, thus substantiating that the TCNQ-BLM functioned as a working electrode. In this connection, a cyclic voltammogram of horse-heart ferricytochrome c was also obtained. Thus, in order to be consistent with the theory of CV, the TCNQ-BLM must function as a redox electrode in the usual practice of electrochemistry.

The significant advantages of the new technique are, besides its simplicity and the good precision of measurement, the involvement of the lipid bilayer and the capability for future development. Since the electron-transfer chain components are known to be closely associated with the lipid bilayer, the values thus determined hitherto by the usual Pt electrode may be quite different from their actual values in the membrane. Conceivably, therefore, the technique described here offers a novel approach to the determination of $E^{o'}$ of membrane-bound biomolecules such as the cytochromes and other redox enzymes, using modified BLM as the working electrode. Further, this new type of electronically conducting BLMs coupled with the CV technique may be useful in the study of membrane bioenergetics (*see* Chapter 8) and in the designing of molecular electronic devices based on ultrathin films.

6.6 Electronic Processes in Membranes

Evidence for electronic processes

More than 40 years ago, Albert Szent-Gyorgyi suggested the idea of the role of solid-state electronic processes in biology. Many attempts have been made during the intervening years to demonstrate that such electronic processes can occur in biomembranes and their constituents such as proteins and lipids (see [Millazo, 1983; Osa and Atwood, 1991]). The origin of the concept of electronic processes in membranes and related systems was first reviewed in 1971, in which the phenomenon known as "electrostenolysis" was stressed. In the language of membrane electrochemistry, electrostenolysis simply means that a reduction reaction

takes place on one side of the membrane (or barrier) where the positive electrode is situated and the oxidation occurs on the other side of the membrane. Although electronic processes in BLM in the dark was mentioned in 1970, no conclusive evidence has been shown. This is because of the fact that an unmodified BLM is an excellent insulator (resistivity $>10^{15}$ ohms) incapable of either ionic or electronic conduction. In order to demonstrate electronic conduction in BLM it seems that the membrane must, first of all, be modified to function as a redox or semiconductor electrode. Secondly, an appropriate method must be found for studies of electronic processes that can be applied to the BLM system. In the following paragraphs evidence of electronic processes in membranes, in particular in BLMs in the dark is described.

Electron-conducting BLMs

Fig.10.4 shows an electron-conducting bilayer lipid membrane (BLM) separating two aqueous solutions containing different redox couples. We will refer to, by subscripts, the left side as the outside "o" (or Aqueous Solution 1) and the right side as the inside "i" (or Aqueous Solution 2). To facilitate the discussion, let's hold the outside constant and consider the interfacial electron transfer reaction on the inside, i.e.

$$D^+ + ne \underset{k_b}{\overset{k_f}{\longleftrightarrow}} D \qquad (6.71)$$

where D and D^+ denote an electron donor in its reduced and oxidized form, respectively, whose concentrations are $[RED]_2$ and $[OX]_2$ in the bulk phase. The corresponding interfacial concentrations are $[RED]_2^S$ and $[OX]_2^S$. The forward and backward heterogeneous rate constants are k_f and k_b, respectively. The observed current is then given by

$$I_{net} = nFA\,(k_f[OX]_2 - k_b[RED]_2) \qquad (6.72)$$

where I_{net} is the net current passing across the interface.

In order for an electron to move from the inside originating from an electron donor (D) to the outside accepted by an electron acceptor (A), it has to transverse at least three energy barriers, two of which are situated at the two membrane/solution interfaces and the third one in the membrane phase, which are labelled E_a^o, E_a^i, and E_a^m, respectively, in Fig.6.6. Clearly, one of the tasks is to evaluate these energies of activation. According to the Arrhenius equation (*see* Chapter 3, *Basic Principles*), one can relate the heterogeneous rate constant, k_s to E_a, which can be related in turn to the free energy of activation (ΔG^*), we have

$$k_s = Ae^{-E_a/RT} \qquad (6.74)$$

and

$$k_s = Ae^{-DG^*/RT} \qquad (6.75)$$

Since the observed current is a measure of the rate of an electrochemical reaction, which may consist of non-faradaic processes (capacitive or charging currents), several equations are available for the evaluation of various parameters including the rate constant. One of the general expressions is the Eyring equation

$$I_{net} = Fk[OX]_2 e^{-F(E-E^o)/RT} - [RED]_2 e^{(1-d)nF(E-E^o)/RT} \qquad (6.75)$$

where d is the so-called transfer coefficient, E^o is the standard redox potential of the couple and E is applied voltage. In this simplified Eq.(6.75), activity coefficients are assumed, n (= 1) and A (= 1 cm^2) to be unity. The Eyring equation (Eq. 6.75) can be expressed in another form known as the ***Butler-Volmer equation***

$$I_{net} = I_0 \{ \exp(-\frac{dFn}{RT}) - \exp[\frac{(1-d)Fn}{RT}] \} \qquad (6.76)$$

where I_0 is the so-called exchange current at n = 0, d is the transfer coefficient as before (under ideal situation d = 0.5), and $n = E - E^0$, the so-called overpotential. Eq.(6.76) has two limiting cases: for small n (< 10 mV)

$$I_{net} = \frac{I_0 F(E-E^0)}{RT} \qquad (6.77)$$

since for small value, exponential terms may be linearized. For large n (> 100 mV), it can be shown that the second exponential term in eq.(6.127) is negligible, thus

$$I_{net} = I_0 \exp[-\frac{dF(E-E^0)}{RT}] \qquad (6.78)$$

Expressing Eq.(6.78) in logarithmic form, we have

$$\ln I_{net} = \ln I_0 - \frac{dF(E-E^0)}{RT} \qquad (6.79)$$

which is known as the ***Tafel equation***. By plotting log I vs. E, various parameters such as I_0 and d may be obtained from the intercept and the slope, respectively. As we will see presently, all afore-given equations, which are well known to physical electrochemists, are highly useful to membrane bioelectrochemistry studies (Blank, 1994; Milazzo, 1983).

To explain the observed membrane potential (E_m), it is best to refer again to Fig.6.6 in which the membrane is assumed to behave like an ideal electron conductor (i.e. Pt). From thermodynamics, the overall free energy change associated with an electrical cell reaction is given by

$$\Delta G = -nFDE \qquad (6.80)$$

where E is the electromotive force (emf) of the cell. Consider the BLM system as an electrical cell shown in Fig.6.6, each solution/membrane interface is assumed to behave as a redox electrode. From Eq.(6.80) the individual free energy terms are denoted by μ. Thus, as indicated on the left side of the BLM $\mu_A + \mu_e = \mu_{A^-}$. Similarly, on the right side

$$D - e \longrightarrow D^+ \qquad (6.81)$$

and

$$\mu_D - \mu_e = \mu_{D^+} \qquad (6.82)$$

In writing these equations the electrons involved are considered as one of the reactants. Since $\mu_i = \mu^0 + RT \ln a_i \simeq \mu^0 + RT \ln [i]$, where μ^0 is a constant, R and T have the usual significance, [i] = the concentration of the redox species when the activity coefficient is taken to the unity. The free energy of the electron u_e, is given by

$$\mu_e = -FE_{out} = \mu_{A^-} - \mu_A = \mu_{A^-}{}^0 - \mu_A{}^0 + RT \ln \frac{[A^-]}{[A]} \qquad (6.83)$$

for the outer (left) solution/membrane interface, where E_{out} = the electrode potential. For the inner (right) solution/membrane interface, we have

$$\mu_e = -FE_{in} = \mu_D - \mu_{D^+} = \mu_D{}^0 - \mu_{D^+}{}^0 + RT \ln \frac{[D]}{[D^+]} \qquad (6.84)$$

At equilibrium, the free energy difference of the electron across the BLM is equal to

$$-\frac{Du_e}{F} = E_m = (E_{A/A^-}{}^0 - E_{D^+/D}{}^0) + \frac{RT}{F} \ln \frac{[A][D]}{[A^-][D^+]} \qquad (6.85)$$

where $[A^-] = [A]$ and $[D^+] = [D]$, we have

$$E_m = E_{A/A^-}{}^0 - E_{D^+/D}{}^0 = E_{redox}{}^0 \qquad (6.86)$$

Eq.(6.86) may be obtained in another way by letting $I_{net} = 0$, therefore Eq.(8.86) is reduced to the Nernst equation

$$E = Eo + \frac{RT}{F} \ln \frac{[OX]}{[RED]} \qquad (6.87)$$

The redox reaction of each compartment may be treated as an electrical cell, thus, one can describe, the electrical potential of each side of the membrane relative to a reference electrode such as to calomel electrode used in our measurement. Therefore

$$E_1 = E_1{}^0 + \frac{RT}{nF} \ln \frac{[OX]_1}{[RED]_1} \qquad (6.88)$$

and

$$E_2 = E_2{}^0 + \frac{RT}{nF} \ln \frac{[OX]_2}{[RED]_2} \qquad (6.89)$$

where E_1 and E_2 are the potentials of Chamber 1 and Chamber 2, while E_1^o and E_2^o are standard redox potentials for the two redox couples. If the membrane is electron-conducting, as in the case depicted in Fig.6.6, we have in essence two electrochemical cells connected in series. The overall potential generated by transfer of electrons from D and A should then be

$$\Delta E = E_2 - E_1 = E_m = E_2^o - E_1^o + \frac{RT}{nF} \ln \frac{[OX]_2[RED]_1}{[RED]_2[OX]_1} \qquad (6.90)$$

In principle, E_2^o and E_1^o, in each chamber should be measurable between the BLM and calomel electrodes, which should be equal to the algebraic sum of E_2 and E_1, if [OX] = [RED] according to Eq.(6.90). Unfortunately, this cannot be done with the BLM separating two aqueous redox solutions. However, the difference can be easily measured. According to Eq.(6.90), we have

$$\Delta E = E_m = E_2^o - E_1^o = E_{op} = E_{ox} \qquad (6.91)$$

where E_m or E_{op} is the membrane potential measured under open-circuit condition (I = 0). This, incidentally, is the proper situation where Eq.(6.91) applies. In carrying out our cyclic voltammetry of BLMs, which involves non-equilibrium conditions, we have to rely on other than the Nernst equation.

In cyclic voltammetry of electron-conducting BLMs, a voltage is applied across the membrane and the resulting current recorded. If redox reactions occur, there are changes of concentration of [OX] and [RED] in the immediate vicinity of the membrane (i.e. $[RED]_2 \neq [RED]_2^S$, etc.). For most experiments described here, we have plotted the logarithm of current as a function of applied voltage, essentially straight lines have been obtained. The results are in accord with Eq.(6.79). Of interest to note is that Eq.(6.79), when written in exponential form, is used in solid-state

physics as the diode equation. In this connection, it should be stressed that as a result of ultrathinness (< 100 A), an electric field gradient of 10^5 V cm^{-5} is easily developed across the BLM (i.e. in the presence of $E_m > 10$ mV). Under high field conditions, two mechanisms may be envisioned for electron translocation across the BLM system; (i) by tunneling, and (ii) by hopping. A straightforward but highly significant experiment would be to measure the electrical conductivity of the doped-BLM system as a function of temperature (also as a function of applied voltage to assess high field effects). With the aid of standard semiconduction equations [e.g. Eqs.(6.88) and (6.89)], the temperature-dependent pre-exponential factor may be determined, from which the nature of electronic processes in the doped-BLM and its related systems may be elucidated.

6.7 Summary of Some Recent BLM Experiments

For the investigation of the properties of BLMs, electrical methods have been applied at the very beginning.[10] In addition to the CV technique, other methods such as electrical impedance spectroscopy (EIS) has been applied. Shortly after the discovery of the BLM system,[19] Hanai and Haydon reported the thickness measurement of a planar lipid bilayer using the impedance technique.[20] Their results are in accord with the value obtained on RBC, estimated by Fricke nearly 4 decades ago (*see* Chapter 2, *Biomembranes*). The impedance technique, nowadays also known as electrical impedance spectroscopy (EIS), has subsequently used by many others.[21-27] The basics of the technique is that a small AC (alternating current) of known frequency and amptitude is applied to the system (e.g. a BLM). The resulting amptitude and phase difference that develop across the BLM are monitored. For a BLM of cross-section area (A), and thickness t_m, the ability of the BLM to conduct and to store electrical charges are decribed by the following:

$$G = \frac{\sigma A}{t_m} \qquad C = \frac{\varepsilon A}{t_m} \tag{6.92}$$

where G and C denote, respectively the conductance and capacitance of the system. σ and ε are constant, representing the electrical conductance and dielectric permittvity, respectively. Note that these two elements, G and C, are connected in parallel. Thus, the impedance (Z) of the system may be expressed as follows:

$$Z(f) = \frac{1}{G + C} \tag{6.93}$$

where f is the frequency. Therefore, a measurement of Z privides estimates of G and C, and is given by

$$G = 1/Z \cos\theta \text{ and } C = -1/fZ \sin\theta \tag{6.94}$$

where θ is the phase angle. It can be shown that Z will disperse as a function of frequency, f. The above equation reveals that the dispersion becomes most conspicuous for f greater than G/C. Typical plots, known as Bode plots (Z *vs.* f; θ *vs.* f) are made, from which the first insights of a BLM separating two aqueous solutioins concerning its thickness and infrastructure are obtained.[20] Additional comments are given below to illustrate the usefulness of EIS (electrical impedance spectroscopy) as applied to the BLM system.

The BLM system, electrically speaking, has two distinct regions, with particular electrical characteristics. These are: (1) the BLM itself which behaves as a resistor (Rm) connected in parallel with a capacitor (Cm), and (2) the two contacting BLM/solution interfaces, which can act as an interfacial capacitor (Ci). When an alternating voltage is applied between the two reference electrodes, immensed in the bathing solutions, and across the BLM, ions flow toward and away from the electrodes, depending on their polarity. At low frequency, the time the ions flow (in one direction, before reversing their flow), is long enough to drive the ions through embedded channels, if present, in the BLM, and into the bathing solutiion on the opposite side.. The interfacial capacitance, Ci, may or may not be of consequence; it depends its size when compared with Cm. Here Rm is the controlling factor. At medium frequency, more ions get a chance to pass through the channels, if present. Once on the other side, the rate of arrival of ions into the BLM/solution interface is slow enough that they can easily disperse away from their entry points at the channel. At medium frequency, the distinguishing characteristic of the BLM circuit is the membrane resistance (Rm). At high frequency, the movement of ions is most affected by the capacitance (Cm) of the BLM. It is informative to mention here the treatment of data as obtaned by EIS, using the Bode plot.

In an idealised impedance spectrum (Admitance or Z *vs.* f) where admitance is defined as the rate at which charges are storred in the capacitor per cycle. The behavior of a pure capacitor, in a Bode plot, forms a line at 45 degrees, whereas a pure resistor forms a horizontal line. The Bode plot is a graph derived from plotting frequency against the admittance of an electrical current. The Bode plot enables us to track the responses of a diverse electrical system by applying and following a range of frequencies. For example, The phase angle between the electrical excitation and the resultant electrical flow is measured at a range of

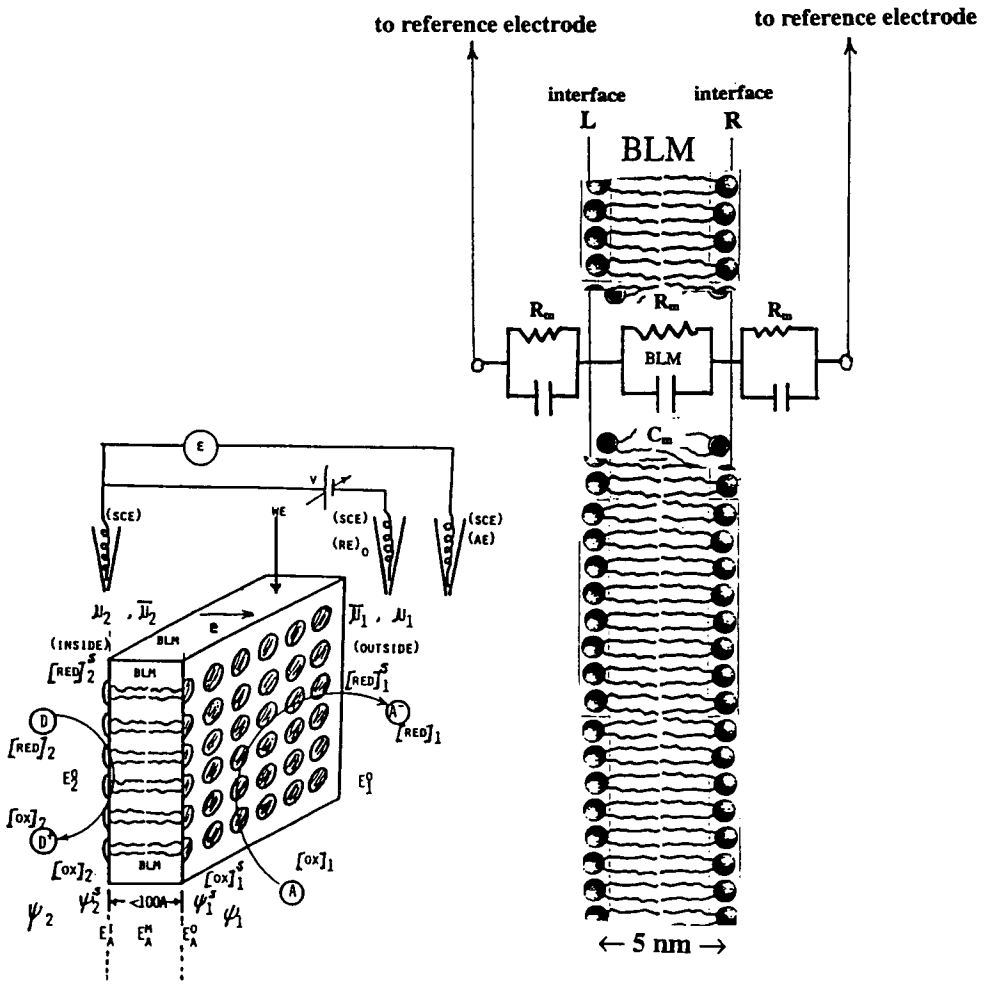

Fig. 6.4 The three domain model of equivalent circuit of a planar lipid bilayer (BLM) system having two interfaces: L = left domain, R = right domain, BLM = membrane domain. R_m = membrane resistance, C_m = membrane capacitance, ϵ = dielectric constant, t_m = membrane thickness. Because of the physical properties of planar lipid bilayer (ultrathinness ~ 5 nm, low dielectric constant ~ 2 to 5), C's >> C_m and R_m >> R's at each interface, the overall DC electrical properties of the system is determined by the BLM domain (*see* text and cited references for further details).

frequencies. The significance of the phase diagram is that if one plots phase shifts over the same range of frequencies that one uses to generate the Bode plot, one can detect when the different electrical characteristics of the circuit are important. On a phase diagram, the behavior of a pure capacitor shows a 90° phase angle, while the more the circuit behaves as a resistor the more it will show up as approaching 0° phase angle.. Thus, if one makes a composite of these graphs, the dip in the phase corresponds to the part of the Bode plot that looks like a resistor trace. From an analysis of impedance data, one may be able to find out specifically the electrical behavior of the BLM, which correlates with the behavior of the modifier (e.g. ion channel) at Rm, and search out specifically changes in the impedance/admittance of the BLM at the point at which the modifier behavior is controlling. In this connection, the results of some recent experiments using EIS are described below.

Alonso-Romanowski, Gassa and Vilche[25] reported the influence of alkali cations on the properties of BLMs doped with gramicidin A, produced by the soil bacteria *B. brevis*. It is well-established that, when two gramicidin molecules align to form a dimer traversing a lipid bilayer, they facilitate the transport of Li+, Na+, K+, and Cs+ across the otherwise ionically impermeable BLM. The impedance spectra of the base system, as typified by the so-called Bode plots (see below), including the BLM and its adjacent aqueous solutions exhibited for all tested cations a single capacitive contribution. The corresponding time constant was discussed in terms of a model which includes a dielectric dispersion in the BLMs. This phenomenon was detected by using either DC or AC voltage perturbations. Data obtained using EIS techniques show two time constants, which can be assigned to the lipid bilayer and to the channel/BLM contributions, respectively. Later, the same group[26,27,56] reported an investigation of the ionic transport phenomena in liposomes made of phosphatidylcholine (PC), with and without the antibiotic Gramicidin A in the presence of Na+, K+ and Cs+ ions. The BLM-Gramicidin A interaction can be characterized by the changes observed in the low frequency range of the impedance spectra. The present EIS data are compared with previous results obtained with BLMs. Their interesting findings are discussed, taking into account the differences and similarities of both model systems, such as time constants and resistance under isotonic, hypertonic and hypotonic conditions, as well as the different

methods of antibiotic incorporation. In connection to the liposome study using EIS, Karolis and colleagues[57] reported low frequency impedance measurements of pure egg lecithin (PC) BLMs have revealed the presence of four layers which can be attributed to the acyl chain, carbonyl, glycerol bridge and phosphatidylcholine regions of the lecithin molecule. Measurements on bilayers formed in the presence of unoxidised-cholesterol revealed that cholesterol molecules were located in the hydrocarbon region of the bilayer with its hydroxyl groups aligned with the carbonyl region of the lecithin molecules. Measurements of oxidised-cholesterol[39,40-42] lecithin BLMs revealed that these molecules protruded less into the hydrocarbon region and their polar hydroxyl group aligned with the glycerol bridge region of the lecithin molecule.

Generally, either alternating current (e.g. EIS) or direct current (DC) is used for investigating BLMs. Recently, a simple setup for measurements of electrical properties of supported planar lipid bilayers (s-BLMs), using a complementary AC and DC method has been reported.[28] The results obtained demonstrated the usefulness of such an approach for studying BLMs. The frequency dependence of resistance and capacitance makes it possible to compare different published data obtained by AC at different frequencies or DC . In some experiments capacitance increases more sharply with the lowering of frequency. As determined, certain s-BLMs modified by AQS or TCNQ[2,48,49] can transfer electrons readily from the bathing solution via the BLM to the supporting Pt surface. Concerning the analysis and interpretation of the experiments, certain assumptions are made about the dielectric constant (ε) and the thickness of the BLM (t_m). For example, a planar lipid bilayer system (aqueous solution | BLM | aqueous solution), is represented by the equivalent circuit shown in Fig. 6.4, where the capacitance (C_m) has been found to be independent of frequency in the range from DC to AC about 10 MHz, directly proportional to the BLM area, and apparently dependent only on the dielectric constant (ε) layer of the hydrophobic interior of the membrane. The C_m of the lipid bilayer, according to the parallel-plate condenser equation is followed. Monitoring the BLM formation, thinning, perturbation, and rupture may be achieved by recording a function of membrane impedance using the equivalent circuit shown in Fig. 6.4. Essentially, a BLM separating two interphases: (*aqueous solution* | *BLM* | *aqueous solution* or *aqueous solution* | *BLM* | *metal support*, or *aqueous*

solution | *BLM* | *hydrogel* substrate, is represented by three R_m-C_m domains connected in series. Each domain has its own impedance due to a difference in constituents and physical attributes.[21] Thus, the BLM domain, owing to its ultrathinness and low dielectric constant, is predominant over the other two adjacent domains. For example, the contribution of the electrical double layer (the so-called Gouy-Chapman layer), which may be two orders of magnitude higher than the lipid bilayer, may be neglected in a serial arrangement. It is worth noting here that, when modifiers are present, they may affect the R_m/C_m signals differently as well as selectively, which may be frequency dependent.

Finally, it should be pointed out that it is simpler, in general, to use the DC method in assessing the planar lipid bilayer (BLM) properties. However, it causes a transient response, owing to the C_m. The advantage of the EIS method is that it permits observation of fast changes when investigating interactions between the BLM and its modifiers. It should be further pointed out that, in using the EIS method, the applied frequency must be carefully chosen so that the effect of capacitative shunting is minimised. Moreover, the selected frequency must not be close to the line frequency (i.e., 50, 60 or 400 Hz). Some preliminary measurements indicate that a frequency around 350 Hz is a suitable one to use. The other advantage with the EIS method is that membrane/electrode polarization is less likely to occur. Perhaps, a complementary AC-DC mode is a method of choice.[28] Insofar as the technique is concerned, it seems evident, on the basis of experimental findings,[20-29,49,56,57] that may open new vista in basic membrane biophysics studies, and offer fresh prospect for biotechnological exploitation (*see* Chapter 10, *Applications*).

General References

Tien, H.T., Bilayer Lipid Membranes (BLM): Theory and Practice, Marcel Dekker, Inc., New York, 1974.

Kotyk, A., Janacek, K., Membrane Transport, An Interdisciplinary Approach, Plenum Press, New York, 1977

Antonov, V.F., Rovin, Y.G., Trifimov, L.T., A Bibliography of Bilayer Lipid Membranes: 1962-1975, All Union Institute for Scientific Information, Moscow, 1979.

Koryta, J., Ions, Electrodes and Membranes, Wiley, New York, 1982

Milazzo, G., (ed.), Topics in Bioelectrochemistry and Bioenergetics, Vol. 5, Wiley, New York, 1983.

S. G. Davison (ed.) Progress in Surface Science, Vols. **19** (1985); **23** (1986); **30**(1989); **41** (1992). Pergamon Press, NY

M. Blank (ed.) *Electrical Double Layers in Biology*, Plenum, NY. 1986.

P. Krysinski and H. T. Tien, *Progress in Surface,* **23**, 317 (1986)

I. B. Ivanov (ed.) *Thin Liquid Films: Fundamentals and Applications*, Marcel Dekker, Inc., NY. 1988. Chapters 14 and 15.

Osa, T., and J. L. Atwood, (eds.), *Inclusion Aspects of Membrane Chemistry*, Reidel Publishing Co., Boston, 1991. pp. 191-274

M. Blank (ed.) *Biomembrane Electrochemistry*, Advances in Chemistry Series, No. 235, American Chemical Society, Washington, DC. 1994. Chapter 24.

Specific References

1. Sparnaay, M.J., Surf. Sci., 13, pp.222, 1969; in Electrical Phenomena at the Mem brane Level, Elsevier, Amsterdam, 1977.
2. Ottova-Leitmannova, A and H. Ti Tien, Progress Surface Science, 41, 1992, 337-446
3. Goldman, D.E., Ber. Bun. Ges. Physik. Chem., 71, pp.799, 1967
4. Amblard, G., Issaurat, B., D'Epenoux, B.,and Gavach, C., J. Electroanal. Chem., 144, pp.373, 1983
5. Scott, A.C.. Neurophysics, Wiley-Interscience, New York, 1977. Chapter 3
6. W. Hughes, Aspects of Biophysics, John Wiley & Sons, NY, 1980
7. Tien, H.T., (ed.), Photoelectric BLMs, Photochem. Photobiol., 24, pp.95-207, 1976.
8. Dely, M., Prager, P., Puppi, A., Studia Biophysica, 85, pp.115, 1981.
9. Tien, H.T., J. Phys. Chem., 88, p.3172, 1984.
10. Bryce, M.R., Murphy, L.C., Nature, 309, pp.119, 1984.
11. R. Pethig and D. B. Kell, Phys. Med. Biol. 32 (1987) 933
12. Bolton, J.R. and Hall, D.O., Ann. Rev. Energy, 4, pp.353, 1979
13. Loew, L.M., Scully, S., Simpson, L., and Waggoner, A.S., Nature, 281, pp.497, 1979.
14. Loew, L.M., J. Biochem. Biophys. Methods, 6, pp.243, 1982
15. Ohki, S., Prog. Surf. Membr. Sci., 10, 117, 1976.
16. Chernomordik, L.V., Melikyan, G.B., Dubrovina, N.I., Abidor, I.G., Chizmadzhev, Yu.A., Bioelectrochem. Bioenergetics, 12, pp.155, 1984
17. Dilger, J.P., Benz, R., J. Membrane Biol., 85, pp.181, 1985.
18. Dilger, J.P., Fischer, L.R., and Haydon, D.A., Chem. Phys. Lipids, 30, pp.159, 1982.
19. Mueller, P., Rudin, D.O., Tien, H.T., and Wescott, W.C., Nature, 194, p.979, 1962.
20. Hanai, T., D. A. Haydon and J. L. Taylor, Proc. Royal Soc., London, Ser. A., 337-391, 1964.
21. Tien, H. T.; Howard, R. E. In *Techniques of Surface and Colloid Chemistry and Physics*; Good, R. J., Stromberg, R. R., Patrick, R. L., Eds.; Dekker, Inc.: New York, 1972; pp 109-211.
22. Ashcroft, R. G.., H. G. L. Coster, D. R. Laver and J. R. Smith, Biochim., Biophys. Acta, 730, 231-238, 1983
23. Laver, D. R.; Smith, J. R.; Coster, H. G. L. *Biochim. Biophys. Acta* **1984**, *772*, 1-9.
24. H. Yamada, H. Shiku, T. Matsue and I. Uchida, J. Phys. Chem. 97 (1993) 9547-9549
25. Alonso-Romanowski S.; Gassa, L. M.; Vilche, J. R. *Electrochim. Acta* **1995**, *40*, 1561-1567
26. Gassa LM, Vallejo AE, Alonso-romanowski, S., Vilche JR, Bioelectrochem. Bioenerg. 42:187-192 1997
27. Vallejo Ae, Gervasi Ca, Gassa LM. Bioelectrochem.Bioenerg. 47: 343-348 1998
28. J. Sabo, A. Ottova, G. Laputkova, M. Legin, L. Vojcikova, and H. T. Tien, Thin Solid Films, 306 (1997) 112-118
29. C. Steinem, A. Janshoff, H. J. Galla and M. Sieber, Bioelectrochem. Bioenerg. 42 (1997) 213-220
30. Tien, H.T. Bioelectrochem. Bioenerg., **5**,.318 (1978); **9**,.559(1982); **13**,.299(1984); **15**, 19 (1986).

31. R. P. Rastogi, R. C. Srivastava and S. N. Singh, 'Nonequilibrium thermodynamics of electrokinetic phenomena', *Chem. Rev.*, **93** (1993) 1945-1990
32. Bockris, J. O'M. and F. B. Diniz, J. Electrochem. Soc., **135**, 1947 (1988)
33. L.-Q. Gu, L.G Wang, J.Xun, A. L. Ottova and H. T. Tien, Bioelectrochem. Bioenerg. 39 (1996) 275-283
34. Bolton, J.R. and Hall, D.O., Ann. Rev. Energy, 4, pp.353, 1979.
35. Davies, J.T. and Rideal, E.K., Interfacial Phenomena, Academic Press, New York, 1961, p. 75
36. V. Aguilella, M. Aguilella-Arzo, P. Ramirez, J. Memb. Sci., 113 (1996) 191-204
37. P. Smejtek, K. Hsu and W. H. Perman, 'Electrical conductivity in BLMs induced by pentrachlorophenol', Biophys. J., **16** (1976) 319-336; P. Smejtek, A. W. Barstad and K. Hsu, Biochim. Biophys. Acta, **902** (1987) 109-127.
38. J. R. MacDonald, Impedance Spectroscopy, Wiley, New York, 1987.
39. H.T. Tien, S. Carbone, and E.A. Dawidowicz, Nature, 212, 718 (1966).
40. R. L. Robinson and A. Strickholm, Biochim. Biophys. **509** (1978) 9
41. E. Gallucci, S. Micelli and G. Monticelli, Biophys. J., 71 (1996) 824-831.
42. I.I. Ismailov, B.K. Berdiev, A.I. Braford, M.S. Awayda, C.M. Fuller and D.J. Be nos, J.Memb. Biol., 149 (1996) 123.
43. Kimizuka, N; Wakiyama, T; Kunitake, T., Chemistry Letters (7). 1996. P.521-522
44. A.W. Dorn And M. Thompson, In *Ion-Transfer Kinetics: Principles And Applications,* By J.R. Sandifer (Ed.) Vch, Ny 1995. Chapter 3.
45. Y.M. Tricot, Z. Porat and J. Manassen, J. Phys. Chem. 95 (1991) 3242
46. R. Rolandi, D. Ricci and O. Brandt, J. Phys. Chem. 96 (1992) 6783
47. P. Bianco and J. Haladjian, Electrochemical Acta, 39 (1994) 911
48. Y.-F. Cheng and D. J. Schiffrin, J. Chem. Soc. Faraday Trans. 90 (1994) 2517
49. T. Miyashita and Y. Ito, Thin Solid Films, 260 (1995) 217
50. X. K. Zhao, S. Basral, R. Rolandi and J. Fendler, J. Am. Chem. Soc. 110 (1988) 1012
51. V. Tvarozek, H. T. Tien, I. Novotny, T. Hianik, J. Dglugopolsky, W. Ziegler, A. L.Ottova, J. Jakabovic, Rehacek and M. Uhlar, Sensors and Actuators B, 19, (1994) 597
52. Derzhanski, A., Petrov, A.G., and Pavloff, Y.V., J.Physique Lettres, 42, 119, 1981.
53. Pastushenko, V.F. and Chizmadzhev, Y.A., Biofizika, 26, pp..458, 1981.
54. Shchipunov, Y.A. and Drachev, G.Y., Biochim. Biophys. Acta, 691, pp.353, 1982.
55. de Levie, R., Adv. Chem. Phys., 39, pp.99-137, 1978.
56. Gassa LM, Mishima HT, Demishima Bal, Vilche JR, Electrochimica Acta 42: (11) 1717-1723 1997
57. Karolis C, Coster HGL, Chilcott Tc, Barrow Kd, Biochimica et Biophysica Acta-Biomembranes 1368: (2) 247-255 Jan 19 1998
58. Y.M. Tricot, Z. Porat and J. Manassen, J. Phys. Chem. 95 (1991) 3242
59. R. Rolandi, D. Ricci and O. Brandt, J. Phys. Chem. 96 (1992) 6783
60. P. Bianco and J. Haladjian, Electrochemical Acta, 39 (1994) 911
61. Y.-F. Cheng and D. J. Schiffrin, J. Chem. Soc. Faraday Trans. 90 (1994) 2517
62. T. Miyashita and Y. Ito, Thin Solid Films, 260 (1995) 217
63. Tien, H.T. and Lojewska, Z.K., Biochim. Biophys. Res. Commun., 119, pp.372-375, 1984

64. Petrov AG, Spassova M, Fendler JH., THIN SOLID FILMS, 285: 845-848, 1996
65. Shirai O, Yoshida Y, Matsui M, Maeda K, Kihara S., Bulletin Of The Chemical Society Japan 69: (11) 3151-3162 Nov 1996
66. Dzekunov SM, Antonenko YN., Bioelectrochem. Bioenergetics 41:187-190 1996
67. Antonenko Yn, Pohl P, Denisov Ga., Biophysical Journal 72: 2187-2195, 1997
68. Sato H, Wakabayashi M, Ito T, Sugawara M, Umezawa Y., Analytical Sciences,13: 437-446, 1997
69. Schwarz, G., and Arbuzova, Biochim. Biophys. Acta 1239, 51-57 (1995).

`http://www.msu.edu/user/ottova/membrane.biophysics.html`

Chapter 7

Membrane Physiology

"...action potential (AP) is a result of the movement of ions...., leading to electrical signaling in a language ...the brain understands. AP is a propagating wave of electrical depolarization... driven by the transmembrane electrochemical potential gradients of Na^+ and K^+. ... maintained by molecular pumps, which derive their energy from the hydrolysis of ATP."

General References (cited by name in brackets in the text)
Specific References (cited by number in superscript in the text)

7.1 Introduction

The molecular organization of biomembranes, as revealed by physical chemical studies, includes an ultrathin lipid bilayer as the pivotal element, associated proteins, glycolipids, and other nonlipid materials as functional entities. This ultrathin plasma membrane, together with cytoskeletal systems, defines and determines the shape of the cell. The lipid bilayer-based membrane similarly surrounds the various organelles and vesicles within the cell that contains chemicals essential for life processes. Of equal importance to life is intercellular communication that takes place across as well as between cell membranes (e.g. through the gap junction). This usually entails the sending, receiving, and decoding of signals. These signals may be chemical and/or electrical in nature predicated upon the presence of an ultrathin lipid bilayer.

A variety of important cellular processes such as excitability, ion transport, and neurohormonal regulation depend on the operation of macromolecular complexes in biomembranes. In view of these diverse and intricate processes, it is not surprising that biomembranes in themselves are very complex functionally. Currently, both the structure of signal transducers and their mechanisms of signal transduction in cells are still obscure. However, a hypothesis of plasma membranes grounded on lipids for the electrical properties of cells and tissues was proposed by Overton and Bernstein at the dawn of 20^{th} century, whose postulates remain essentially correct to this day (see Chapter 2, *Biomembranes*). Instead of stressing on lipids, today we speak of the lipid bilayer as the crucial two-dimensional framework of cell membranes in which carriers, channels and receptors are embedded.

Biomembranes, considered in detail in Chapter 2, are made of, besides the universal lipid bilayer, proteins, carbohydrates, and lipid-protein-carbohydrate complexes. Because of complex structural and environmental factors associated with biomembranes, many investigators recognized in the mid 1950s that approaches using experimental model systems are essential to an understanding of the fundamental membrane processes in physical and chemical terms. Thus resorting to model systems has led to the discovery of a method for forming experimental bilayer lipid

membranes (BLM), whose physical and chemical properties resemble closely to those of biomembranes.[1] The attractiveness of the planar BLM together with its closely related liposome system,[2] unlike any other membrane models thus far devised, lies in the fact that it has made possible, for the first time, the study of electrical events and material transport across an artificially created ultrathin lipid membrane separating two aqueous solutions.

The liquid-crystalline phospholipid bilayer of about 5-6 nm thick, separating two aqueous phases, is central to the understanding of biomembranes. This fluid lipid bilayer plays a vital role in a number of life's processes and serves as the functional environment for other membrane constituents such as proteins that include receptors and ion channels. Concerning the latter, ion channels are crucial in organisms; they are vital for living and defense as well as for attack, and have been investigated for over three decades in reconstituted bilayer lipid membranes (planar BLMs and liposomes). Evidence for single ion-channel activities in biomembranes, for instance, were in fact first demonstrated in BLMs in 1969.[3] Today, ion-channels are found in the plasma membrane of sperm,[4,5] bacteria and higher plants,[6,7] the sarcoplasmic reticulum (SR) of skeletal muscle,[8,9] synaptic vesicle membranes of rat cerebral cortex,[10] and the skin mucus of carps,[11] to name a few. As a weapon of attack, many toxins released by living organisms are polypeptide-based ion-channel formers such as dermonecrotic toxin, hemolysin, brevetoxin, and bee venom.[12-16] With the availability of the patch-clamp technique in the 1980s,[17] the presence of ion-channels have been established in all sorts of biomembranes,[18-25] in addition to those already cited above. It has been assumed from the earlier years of BLM research that membrane-bound channels are polypeptides of proteineous materials.[26] Typically, a simple picture concerning ion-channels in biomembranes is that of an array of cylindrical structures bearing fixed charges and filled with aqueous solution. If so, electrokinetic phenomena based on the electrical double layer theory described in Chapter 6 (*Membrane Electrochemistry*), for instance, should be expected, and have in fact been reported.[27]

The literature on membrane physiology is voluminous and involves several disciplines; it is beyond the scope to cover, let alone to discuss many exciting topics in membrane physiology. In this chapter, for instance, the important quantitative analysis of experimental data on nerve conduction are merely mentioned in passing. Sensory transduction, the well being of living, is barely touched upon. For a detailed treatment on this and other subject matter, the reader is referred to cited papers. Our emphasis here is focused narrowly on ion-channels and their reconstitution in experimental lipid bilayers (planar BLMs and liposomes). Even in this case, our coverage is very sketchy, serving as a guide only. Fortunately, many comprehensive reviews,[26,28-30] current papers[31-49] and monographs are available [*see* General References].

7.2 The Nerve Membrane

In Chapter 6 (*Membrane Electrochemistry*), it is stated that the Nernst-Planck equation is the crux of membrane electrochemistry. If so, it may be said then that the basis of membrane electrophysiology is the nerve membrane of squid axon, upon which Hodgkin, Huxley and Katz (HHK) formulated their keystone theory of the conduction of nervous impulse. Typical concentrations of major ions on the two sides of a cellular membrane are given in Table 7.1.

Table 7.1 Typical intracellular and extracellular ion concentrations

	Extracellular (outside) (mM)	Intracellular (inside) (mM)	Resting potential* (mV)
K^+	4-5	125-140	- 50 to -70
Na^+	120-140	10-12	
Ca^{2+}	2	10^{-4}	
Cl^-	125-140	5-30	
P^-	~ 0	108	

* The potential outside of the cell is taken as zero by convention. 55% of water in the body is inside of the cell.

Membrane properties related to cell physiological functions

One of the main research objectives in membrane physiology is to elucidate the molecular mechanisms of functioning of the ionic channels, using the principles of physical chemistry. The mechanisms of excitability on nerve and muscle membranes are related to the voltage- and time-dependent changes in the electrical properties of the excitable membranes. Here, one is reminded of the Nernst-Planck equation discussed in the previous chapter, i.e. the driving force that determines the movement of charged species across the membrane in the x direction that can be expressed in terms of their electrochemical potential gradients of ions, as we have already in the previous chapter. After integration across the membrane from x = 0 to x = t_m (membrane thickness),[50] an equation for the potential difference (E_m) or PD has been obtained:

$$\phi_i - \phi_o = E_m = \frac{RT}{zF} \ln \frac{C_o}{C_i} \qquad (7.1)$$

where subscripts 'i' and 'o' refer to the "inner" and "outer" side of the membrane and C_o and C_i are the ion concentrations on the "outer" and the "inner" side of the membrane, respectively. After measuring E_m and membrane conductance under different conditions, various membrane characteristics such as transference numbers, ionic mobilities and their related quantities, permeability ratios and ion selectivity may be analyzed. Since the cell membrane under different conditions may be permeable to major ion species present on both membrane sides, it follows that the observed membrane potential must be due to active transport processes, for otherwise, the ion concentration would equalize across the membrane over time on simple thermodynamic grounds. In nerve and muscle membranes, the potential difference is determined mainly by the ratio P_{Na+}/P_{K+} (P denotes permeability), which can be in the range 0.01-1. A simple representation of a squid axon together with its monitoring electrodes is shown in Fig. 7.1.

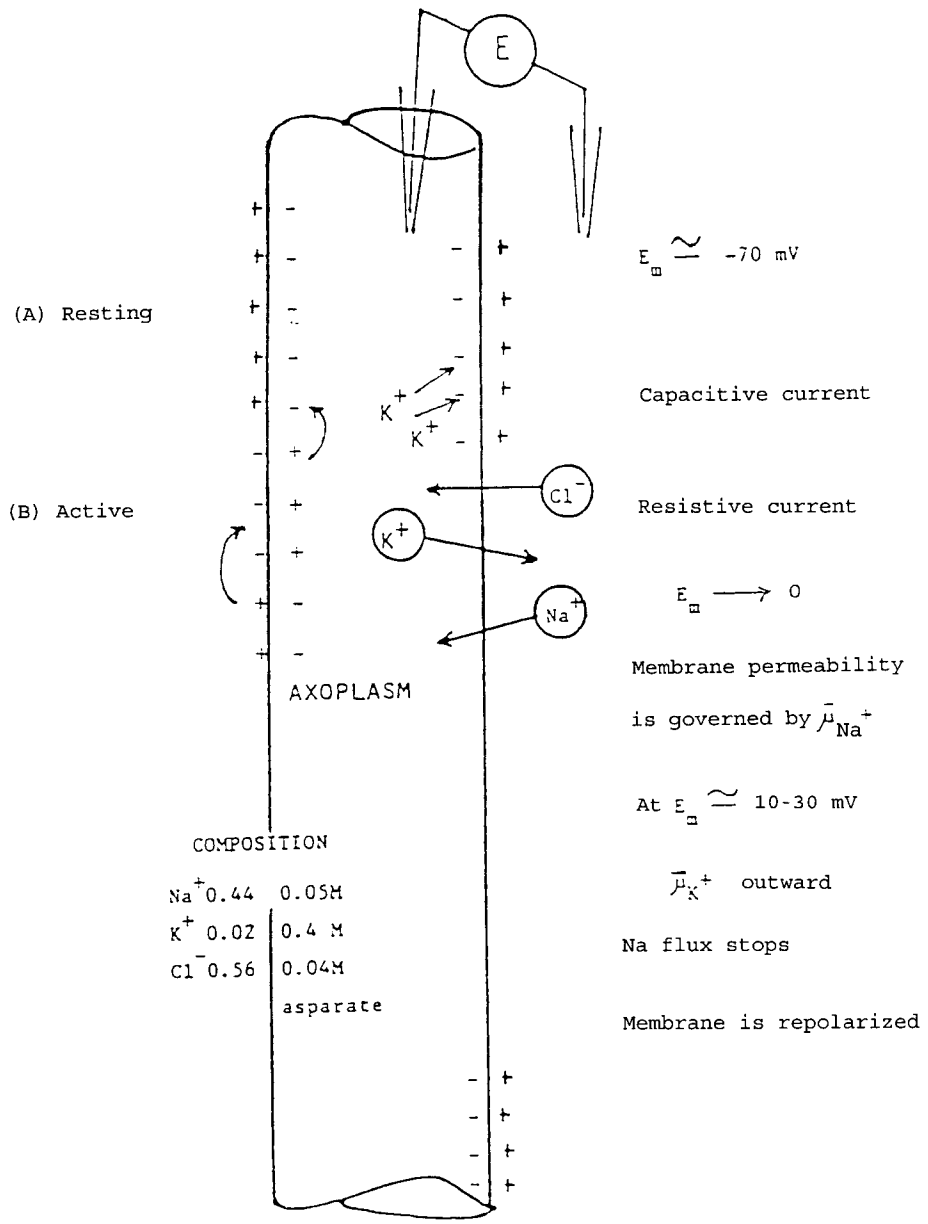

Fig. 7.1 The nerve axon and its associated monitoring electrodes

Resting and Action Potentials

Resting potential. Using the so-called voltage clamp technique (VCT), to be described in more detail in Section 7.4, HHK and others measured the current through the squid axon membrane while holding the voltage at particular levels. The VCT gives us the insight how the action potential is generated. The essence of the technique is that an electronic feedback circuit is used to hold the voltage across a membrane constant, so allowing researchers to measure currents through membrane channels, real or imagined.

The depolarization means a reduction in the membrane potential (E_m) by making the inside less negative, and the hyperpolarization means an increase in membrane potential (E_m) making the inside more negative. HHK postulated that the action potential results from a change in the ratio of Na^+ and K^+ ions in the membrane. Before excitation, a potential difference (voltage) of about –70 mV is observed with the inside of the cell being negative, which is attributed to the equilibrium potential due to K^+. This is the so-called ***resting potential***. Upon excitation, the membrane is depolarized. Na^+ channels then open, allowing Na^+ ions be driven into the cell by their electrochemical potential gradient. The influx of Na^+ further depolarized the inside of the cell allowing even more Na^+ to enter. At some point, however, the feedback mechanism stops Na^+ from entering when the concentration gradient of Na^+ is balanced by the electrical gradient in the opposite direction. The membrane potential is then retired to its resting potential value by an outward movement of K^+, which is driven by its own electrochemical potential gradient. Concerning their elegant work, HHK modestly pointed out that the their description on the action potential is an empirical one and is not based on any particular molecular mechanism. The elucidation of action potential at a molecular level had to wait for almost two decades for membrane biophysics to mature with new and powerful techniques for studying the translocation of ions across reconstituted membrane systems, as will be described later in this chapter.

Action Potential. The action potential is defined as a sequence of potential changes accompanying an impulse in the excitable membrane. Two main

types of potential changes accompany the generation of action potentials in excitable membranes: depolarization and hyperpolarization. The action potential is characterized by:

- An amplitude of more than 100 mV
- A time duration of about 1 msec
- A latent period between the stimulation and the beginning of the action potential is needed.
- A definite threshold stimulating voltage is required. Only suprathreshold stimulus can induce an action potential.

Main events underlying the generation of the action potential according to the work of HHK, and other confirmative findings are as follows:

1) When the nerve membrane potential is reduced suddenly and held at its new value for 10-50 μsec, an initial pulse of current flows through the membrane capacitance.
2) This is followed by large currents, carried mainly by Na^+ and K^+, which traverse the membrane under the influence of their electrochemical gradients.
3) The Na^+-current rises rapidly to a peak followed by a slower decay, and then reaches a plateau value, which is maintained until the membrane potential is restored to its resting level.
4) After initiating the action potential by stimulation (>15mV), the current flowing around the active region depolarizes the adjacent area of the membrane.
5) The membrane potential decrease is accompanied by an inward Na^+-current, which appears because the extracellular $[Na^+]$ is many times higher than the intracellular.
6) The sodium current still further depolarizes the membrane until the membrane potential is reversed in sign and approaches the equilibrium value for Na^+.
7) An outward K^+-current appears as a delayed result of the depolarization. The outward direction is due to the higher intracellular $[K^+]$ concentration in comparison to the extracellular one.
8) Meanwhile, the Na^+ permeability of the membrane decreases after its transient rapid increase.

9) If the K^+-current exceeds the Na^+-current, repolarization of the membrane occurs, and the membrane potential increases back to the resting level that coincides with the potassium equilibrium potential.

The total membrane current, I, consists of two components: a capacitive current C_M (dV/dt), and an ionic (resistive) current I_i. The current is further divided into Na^+ current (I_{Na}^+), K^+ current (I_K^+),and leakage current (I_l). Thus,

$$I = C_m \frac{dV}{dt} + I_i = C_m \frac{dV}{dt} + (I_{Na} + I_K + I_l) \qquad (7.2)$$

where V is the displacement of the membrane potential from its resting value, and C_m is membrane capacity ($\mu F/cm^2$). The ionic permeability is expressed in terms of the ionic conductances (g_{Na}^+, g_K^+, g_l) as follows

$$I_{Na}^+ = g_{Na}^+ (E - E_{Na}^+) \qquad (7.3)$$

$$I_K^+ = g_K^+ (E - E_K^+) \qquad (7.4)$$

$$I_l = g_l (E - E_l) \qquad (7.5)$$

where E is the membrane potential. E_{Na}^+ and E_K^+ are equilibrium potentials for Na^+ and K^+, respectively, E_l is the potential at which the leakage current due to Cl^- and other ions is zero. For practical applications, these equations are rewritten as follows

$$I_{Na}^+ = g_{Na}^+ (V - V_{Na}^+) \qquad (7.6)$$

$$I_K^+ = g_K^+ (V - V_K^+) \qquad (7.7)$$

$$I_l = g_l (V - V_l) \qquad (7.8)$$

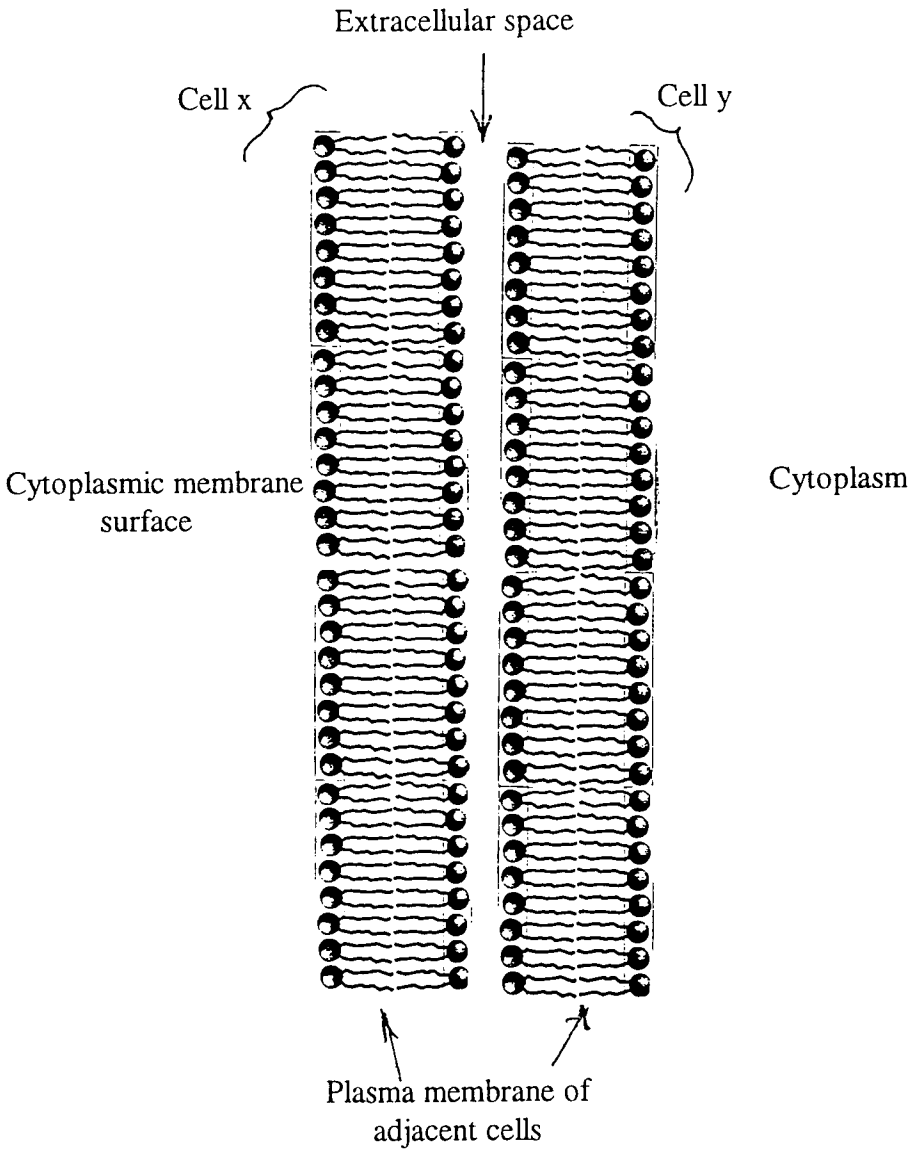

Fig. 7.2 Gap Junction. (for details *see* Beyer, Paul, and Goodenough).[38]

where $V = E - E_r$; $V_{Na^+} = E_{Na^+} - E_r$; $V_{K^+} = E_{K^+} - E_r$; and $V_l = E_l - E_r$. E_r is the value of the resting potential. From experimental evidence, HHK suggested that the conductances g_{Na^+} and g_{K^+} vary with time Further, they have shown, with the aid of all above equations, that they could predict with fair accuracy many of the electrical properties of the squid giant axon:.

- the form, duration and amplitude of the action potential,
- the conduction velocity,
- the impedance change during the spike,
- the refractory period,
- ionic exchanges,
- subthreshold responses, and
- oscillations.

It seems established that the Na^+ and K^+ permeability changes, accompanying the membrane potential displacement, are sufficient to account for most of the electrical phenomena exhibited by the excitable membranes. The conduction velocity is about 20 m/sec. It is instructive to sum up here that the action potential (AP) is a result of the movement of ions across cell membranes, leading to electrical signaling in a language that the brain understands. AP is a propagating wave of electrical depolarization that is driven by the transmembrane electrochemical potential gradients of Na^+ and K^+. These ion concentration differences are maintained by molecular pumps, which derive their energy from the hydrolysis of ATP.

Cyto-organelle Membrane and the Gap Junction

The gap junctioin (GJ) or cell junction is a structure that serves as permeable cell-to-cell ion channels in non-excitable tissues. In excitable cells, the GJ functions as an electrical synapse or coupling between neurons and tissue activities. Dating back to the 1970s, it was supposed that all cells in normal tissues are coupled by permeable cell junctions. Morphologically, the GJ is made of hydrophobic proteins similar to that of the integral type; it is embedded in a lipid bilayer. It has been proposed that each GJ consists of 6 junction proteins termed *connexins* (see Fig. 7.2).[38]

(Electrically, the GJ's properties of gating by ions and charge selectivity are of particular interest; they are eminently suited for planar BLM investigations. For example, connexins vary in their regulatory responses to trans-junctional voltage, enzyme kinases, and intracellular Ca^{2+}. In this connection, mentioned should be made concerning Ca^{2+} ions' involvement in apoptosis (programmed cell death) that is due to a continued Ca^{2+} influx through the plasma membrane (note here that the rupture of the plasma membrane also causes cell death, which is termed necrosis. (*see* Chapter 10, *Applications*, using s-BLMs for studying apoptosis). Here, we shall be mainly concerned with the study of communicative function of cytoskeletal components and the gap junction using two BLMs, and the use of BLMs as models for the plasma membranes, nerve membrane and muscle membranes.

Double-BLM System. Two planar BLMs made from brain lipids were formed in the presence of the brain tubulin; their electrical potentials were simultaneously measured. When electrical pulses were applied across one membrane, displacements in the potential of the other membrane were found, even when the BLMs were not in contact. This effect was observed only in the presence of polymerized tubulin. It was not found in the presence of depolymerized tubulin or in other control experiments. The findings suggest that the microtubule fiber networks may serve as an interconnecting system between membranes.[51]

Microtubule-Dependent Membrane Interactions Studies in Two Types of Double Bilayer Membrane Systems. The microtubules consisting of tubulin subunits are ubiquitous cytoskeletal elements implicated in a variety of cellular functions. It is probable that they play an important role in the integration of the membrane processes and in the structural-functional organization inside the cells by mediating long-range interactions between membranes and by functioning as an intermembrane linking system. This suggestion was tested by using two different techniques for studying the interrelationships between two BLMs. In both systems, evidence for microtubule-assisted interconnections between the membranes was obtained. When electric pulses with amplitude 60-70 mV and duration 30 ms were applied across one of the membranes, a displacement in the potential across the other BLM was observed, even when the membranes

were separated. This effect was found only in the presence of microtubules. It was not observed in the presence of depolymerized microtubule protein, colchicine-treated tubulin, or albumin. On the basis of the data, we suggested that defined configurations of the microtubule fiber networks and bundles may form structural bridges and coupling between membranes and that microtubules may play a similar role in the processes of information transfer in neurons and other cells.[51]

Model for the Plasma Membrane

Different erythrocyte components such as sialoglycoproteins, band 3 protein, were found to induce large changes in the conductance of different types of BLMs. A plant alkaloid, sanguinarine, may inhibit the erythrocyte sodium-potassium pump, but without any influence on the leak for Na^+ and K^+. At the same time, the uncharged form of the compound induces an increased cation permeability in erythrocytes as well as in BLMs made from red cell lipids. The major component of the erythrocyte membrane was defined to be the band 3 protein with a molecular weight of 97,000 daltons. This protein was found to be responsible for one of the main physiological processes in the red cell membrane, the anion exchange mechanism. The latter is related to the transport of nonelectrolytes such as glucose and water. After its reconstitution into BLM, Benz et al[57] found that the band 3 protein provoked an increase in the membrane conductance by several orders of magnitude. This effect was dependent on the fourth power of protein concentration, which was interpreted as an indication that formation of a tetrameric structure is involved in the mechanisms of the ion conduction through the BLM. The voltage did not influence the unit conductance, which was 50 pS. When the protein was pretreated with several different reagents, its action on the membrane conductance was inhibited. The same compounds are known to inhibit water transport through erythrocyte membranes. Other SM reagents that induce such an effect were not able to modify the influence of band 3 protein on BLM conductance. The subunits of this protein may form a tetramer that is involved in water transport across the erythrocyte membrane.

Channel-Closing Activity of Porins from Escherichia Coli BLMs. The opening and closing of the ompF porin from Escherichia coli was investigated by reconstituting the purified protein into planar bilayer membranes. Electrical conductance changes across the membrane at a constant potential were used to analyze the size and aggregate nature of the porin channel complexes and the relative number of opening and closing events. It was found in our laboratory that, when measured at pH 5.5, the channel conductance diminished. The number of closing events increased, when the voltage was greater than 100 mV. The results suggest that the number of smaller sized conductance channels increase, above this potential. There was also an increase in the smaller subunits and in the closing events when the pH was lowered to 3.5, and increasing the voltage further enhanced these changes. It was also proposed in our group that both lowering the pH and elevating the potential across the membrane stabilize the porin in a conformation in which the subunits are less tightly associated and the subunits open in a non-cooperative manner. These same conditions also appear to stabilize the closed state of the pore.[52]

Porins and EIM (excitability-inducing-material).[53-56] The transmembrane diffusion of sugar molecules take place through aqueous pores, since both the specificity and the energy of activation are low. These pores or channels are made of the matrix protein called porin, which has been reconstituted in BLMs. The electron diffraction shows that the reconstituted porins form highly coherent crystalline arrays.[55] Earlier, ion diffusion potentials and electrical rectification across BLMs activated by EIM have been reported. More recently, Ompf porin, a channel-forming protein from E. Coli, has been incorporated into BLMs and extensively investigated. Xu et al[59] found, when measured at pH 5.5, the channel conductance diminished and the number of closing events increased when the voltage was greater than 100 mV.

Kidney plasma membranes

Tosteson and Sapirstein extracted five main proteolipid fractions from the bovine kidney membrane vesicles and inserted them into BLMs

made from diphytanoyl-PC by adding them to the aqueous phase on one side of the BLM. The addition of the proteolipid fractions provoked the appearance of discrete current fluctuations. When using protein concentrations lower than 0.6 ug/ml, the unit channel conductance was about 10 pS in 0.1 M KCl and 3 pS in 0.1 M NaCl. No voltage dependence was observed in this case. At higher protein concentration, 1 μg/ml, a new channel population appeared with about 10 times higher conductance for both types of aqueous solutions, 100 pS and 30 pS, respectively. In the presence of KCl, these channels were voltage dependent. These channels appear owing to the formation of oligomer protein structures in the membrane. The permeability ratio P_{Na+}/P_{K+}, determined from the single-channel experiments, was only 2.5, but the steady-state conductance in the presence of 0.1 M KCl was 100-1000 times higher than that in 0.1 M NaCl. This was explained by assuming that the conformation of apoprotein molecules in KCl is more favorable for incorporation than in NaCl. When protein molecules integrate into the BLM, however, their conformation is changed in a way that always determines a defined permeability ratio. The physiological role of the described channel activities is not clear. Although Na^+-specific channels such as the amiloride-sensitive channels are of particular interest in relation to the functions of the kidney epithelia, other transport mechanisms may also have some physiological implications.

A hormone influencing the transport of sodium and water across the kidney epithelial membranes, vasopressin, was found to induce a decrease in the resistance of BLMs. The effect of this basic polypeptide was more pronounced when it was used at higher doses and at higher salt concentrations in negatively charged PS bilayers. Thus, polypeptide molecules may form channels by the aggregation of four to five polypeptide units.

Model for the Nerve Membrane[72]

Ionic permeability within biomemrbanes are controlled by various ion channels embedded in the lipid bilayer. Each of these channels (examples, Na^+, K^+, Ca^{2+}, and Cl^-) contains charged or dipolar components that sense electrical fields in the membrane and then drive the

conformational change of the channel. These actions result in opening and closing the pore thereby allowing specific ion movement. In voltage-gated ion channels a change in membrane potential difference (PD) causes a change in the conformational state of protein, thereby altering the net charge or location of charge across as well as within the membrane. In doing so, the so-called capacitive current is involved to move an ion from one side of the membrane to the other side, without having physically doing so. It is implicated that different channels play a role in controlling or altering channel proteins as removal of excess ions from cytosols, pH requlation, stabilization of membrane's PD, synaptic transmission, and signal transduction. In certain membrane-related diseases and disorders such as epilepsy, cystic fibrosis, and certain cardiovascular and neuromuscular, ion-channels are also believed to be involved.

Membrane Channels Reconstitution in BLMs. The concept of electrical activity in biomembranes dates back to more than two centuries to the time of Galvani and Volta and their debate on the so-called 'animal electricity'. Today, it is widely accepted by biophysicists and electrophysiologists that ionic channels are the crucial elements in the membranes of nerves and muscles of animals as well as in the other cells such as photoreceptors, plant cells, auditory hair cells, other sensory cells, epithelial cells, and in unicellular organisms. In fact, ionic channels are a unique structure present in all living systems and exhibiting experimentally measured potential difference (PD) across the biomembrane. This experimentally observed PD or transmembrane voltage is best described by the Nernst-Planck equation. Ionic channels are made of macro-molecular proteins embedded in the lipid bilayer of the membrane. Like the phospholipids of the lipid bilayer, these macromolecular proteins are both hydrophilic and hydrophobic in their chemical moiety to allow them to be embedded in the lipid bilayer. The hydrophilic portions of the phopholipid molecules face the aqueous solution (either intra- or extracellular fluid) whereas the hydrophobic portions of the phospholipids interact with each other to form the most unique lipid bilayer structure, whose hydrophobic interior allows the embedding of the hydrophobic portions of channel proteins. The hydrophilic portions of the channel protein is wrapped in such a way which allows forming an aqueous pore or channeling spanning the lipid bilayer of the membrane. Investigations of ionic channels really got underway shortly

after the report of the BLM system.[3] Availability of experimental BLMs allows the membrane channel reconstitution to be carried out under well-defined and controlled conditions. Hence, direct characterization of the properties of single ion channels at a molecular level has become possible. In the following paragraphs a few examples on ion channels are described.

Action of Calcium Channel and beta-Adrenergic Blocking Agents in BLMs.[59-62] The action of beta-adrenergic blockers (propanolol, exprenolol, metoprolol, sotalol, atenolol, timolol) and calcium channel blockers (verapamil, diatiazem) on the electrical properties and fluidity of BLMs and liposomes has been investigated. When antibiotic ionophore substances were used as a probe, electrical measurements showed that many of the drugs inhibited cation transport across the membrane when it was facilitated by the mobile carrier valinomycin, while they had no significant effect on the cation transport through channels formed by gramicidin. The ability of the drugs to decrease carrier-dependent membrane conductance was correlated to their partition into the lipid bilayer and to the magnitude of the transmembrane potential induced by them. In the TEMPO ESR spectral measurements, a number of beta-adrenergic and calcium blockers showed a fluidizing effect on lipsosomes composed of different lipids. The drug concentration required for a detectable change in the TEMPO spectra parameter was rather high (0.01 M verapamil) and the variation of pH from 6.5 to 3.0 did not affect the fluidizing effect of the drugs. In this connection, it should be mentioned that Antonenko and Yaguzhinsky[62] have proposed a mechanism for the generation of the electrical potential on BLMs induced by propranolol and verapamil. In a different kind of investigation, Alekseev and Ziskin[63] reported the effects of microwaves (53-78 GHz) on the capacitance of BLMs modified with gramicidin A, amphotericin B, or tetraphenylboron anions (TPhB), but did not observe any resonance-like effects.

Characteristics of Microsomal Ca Channels.[62,63,72] Single Ca^{2+} channels from brain microsomal membranes were reconstituted in bilayers made at the tips of patch-clamp micropipettes. The single-channel conductance was defined to be 107 pS in 50 mM Ca^{2+}. Channel activity was stimulated by nucleotides and inositol 1,4,5-triphosphate ($InsP_3$); it was inhibited by

ruthenium red. Na^+, added asymmetrically to the membrane bilayer, induced an increase in the Ca^{2+}-channel activity. The described characteristics of these Ca^{2+} channels suggest that they may be responsible for the Ca^{2+} transport across the membrane of the endoplasmic reticulum system, triggering and modulating various neurosecretory and excitatory processes in nerve cells. In this connection, the modulation of ion channels in reconstituted BLMs has been reported by Chung et al and Reinhart.[64] Single channel recordings were made by fusing liposome-containing channel proteins to preformed BLMs. Modulation of the activity of K^+ and other ion channels is an essential functioning feature of the nervous system. The open probability of a Ca^{2+} -activated K^+ channel from rat brain is increased by the addition of adenosine triphos-phate (ATP). These authors conclude that some ion channels may exist in a complex that acontains regulatory protein kinases and phosphatases. It should be mentioned that Tiwari-Woodruff and Cox[5] reported a BLM containing Ca^{2+} channels from a boar sperm plasma membrane and found that these channels share some properties with brain, cardiac and skeletal muscle t-tubule Ca^{2+} channels.

Electrical oscillation in BLMs.[66-68] Of evident interest is the oscillatory phenomena such as frequently observed action potentials of the nerve. Many authors have reported such observations in a variety of systems. In BLMs, the membrane was electrically excitable only when channel-forming materials (excitability-inducing-material – EIM)[3,55] were present. Yoshikawa et al reported electrical potential oscillations using BLMs in a porous filter support and concluded that the periodic change of the ionic current due to the adsorption and desorption at two interfaces results in the oscillation of the transmembrane voltage. Kihara and Maeda[65] have published a comprehensive review on the topic of the ion transport and membrane oscillations. Srivastava, Das and co-workers[65] have reported in a series of papers on oscillatons of electrical potential differences. One of the important points to stress is that the 'fluid' nature of the membrane appears to be crucial. Additionally, the electroosmotic flow needs to be coupled with a pressure-driven back flow across membrane channels. The presence of an electrical double layer within the channels as well as surface potentials may also be necessary for the phenomena of oscillatory transport. Concerning these studies, mention should be made of the work of Antonenko and Pohl[68] and of Chang and Cronan.[54] In transport

processes, unstirred layers near membranes play an important role affecting catalytic reactions. The importance of the unstirred layers of BLMs is stressed. They have proposed an empirical equation for the estimation of the size of the concentration boundary layer, which should be of importance in transport and enzyme kinetics studies.

Muscle membranes[72]

Many similarities exist between the physiological processes in muscle and in nerve membranes. The maintenance of the resting potentials and the ion channel activation and inactivation mechanisms underlying the action potentials share similar characteristics. Substantial differences, however, also exist: for example, much longer action potentials and large Ca^{2+} currents are found in muscle. In most types of muscle cells the membrane processes are particularly complicated in relation to the excitation-contraction coupling process. This key physiological mechanism is dependent upon the coupling between the ionic fluxes across the plasma membrane which has a complex morphology involving the transverse tubular system, and ion transport across the sarcoplasmic reticulum (SR) membrane.[8]

Progress in the field of muscle electrophysiology was previously slow due to the lack of single-cell preparations. Interpretation of the results from experiments on multicellular muscle fiber preparations was more difficult than that of the data on squid giant axon used in neurophysiology. Later single muscle cell preparations were obtained. The patch-clamp method was improved and combined with the whole-cell voltage clamp. The BLM method has also been quite helpful for characterization of the muscle membrane ion channels under well-defined conditions. BLM remains the best technique for characterizing the single-channel activities of intracellular SR membranes and of plasma membrane formations that protrude deeply inside the cell, such as the transverse tubules. The channel mechanisms in these membranes so far cannot be analyzed by direct application of the conventional patch-clamp method.

Sodium channels from skeletal muscle membranes were incorporated into BLM by Moczydlowski et al[73] soon after the experiments on reconstituted nerve membrane sodium channels. The gating, selectivity, neurotoxin modulation, and other properties of the channels were then analyzed and an elaborate model for the voltage-dependent neurotoxin effect was proposed. This model may serve as a clue for understanding the molecular structure of the skeletal muscle sodium channel.

The reconstituted Na^+ channels showed many of the characteristics typical of the batrachotoxin-treated native channels. A steep voltage-dependent activation assessed by measuring the changes in the opening probability as a function of the applied voltage and a negative shift of about 50 mV of the activation curve was observed similar to the batrachotoxin-modified channels in native membranes. It was clearly demonstrated, that at potentials more positive than –60 mV, the channel is almost continuously open, while at –120 mV the openings are very infrequent. The skeletal muscle Na^+ channels showed relatively low unit conductance (20 pS at 0.2 M NaCl), coinciding with that of the Na^+ channels in rat myotubes after taking into account the difference in the temperatures. The sequence of ionic selectivity was as that of the batrachotoxin-treated and of the normal Na^+ channels: $Li^+ \sim Na^+ > K^+ > Rb^+ > Cs^+ >> Cl^-$. The permeability ratio, P_{Na+}/P_{K+}, was close to normal; 14.3 : 1. The channels show specific blocking effects induced by TTX, STX and other neurotoxin analogues. A detailed analysis of the voltage dependence of the block was performed. It was clearly demonstrated that the inhibitory reactions were voltage dependent. The changes of the neurotoxins and their analogues, which varied from 0 to 2, did not influence the block. It seems evident also that the charges of the surrounding lipids do not exert any effect. The applied potential affects both the association and the dissociation rates of TTX. Na^+ competes with TTX, but it competitively inhibits only the association rate. This effect is observed only when Na^+ and TTX are added to the same side of the membrane.[72]

The above-mentioned authors reconsidered the concept of the selectivity filter of the Na^+ channel on the basis of the above data. Krueger and his colleagues[74] suggested that the TTX-receptor site and a Na^+ site are located at the outer mouth of the pore. The Na^+ site operates as a

prefilter, accelerating Na^+ entry into deeper pore regions. The data on the voltage dependence of the toxic effects are better explained by a mechanism in which the neurotoxin molecule does not interact directly with the deeper regions of the selectivity filter; rather, it binds to the receptor site at the outer pore mouth and induces a voltage-dependent conformational change of a polypeptide segment of the protein molecule controlling Na^+ conduction.

Thus, it must be pointed out that most of the data concerning neurotoxin action on Na^+ channels incorporated into BLMs support the supposition that neurotoxin block of Na^+-channel activity is voltage dependent. This property may be characteristic of different kinds of Na^+ channels, because similar results were obtained from experiments on BLMs reconstituted with Na^+ channels isolated from muscles, as well as from nerve membranes. On the other side, the findings in the native membranes are contradictory, especially those in cardiac muscle. Further detailed studies examining, in parallel, native and reconstituted model membranes are needed in order to clarify this question [Harris and Etemadi, 1989].

7.3 Sensory Transduction

Our current understanding in regard to how we see, hear, taste, smell, and touch has been the result by several thousands of researchers, over a period of hundreds of years in numerous laboratories throughout the world. However, during last 20 years progress towards understanding of the above-named five senses at the membrane level has been swift. Indeed, many investigators believe that biomedical science is poised to make important progress toward understanding of the senses (vision, hearing, taste, smell, and touch) at the molecular level. This section summarizes the recent past activities on some of the areas of vision and smell in terms of experimental lipid bilayers in view of anticipated exciting prospect at the next level.

Modified BLMs for the Olfactory System. The average human being is said to be able to recognize some 10,000 different odors. Yet, it is almost imposible to describe how something smells to someone who has not

experienced it. Up to about 1991, little was known about the biochemical process involved in detecting odors [*see* Refs. 75,76 and references therein]. Now it appears that the odorant receptors are quite similar to visual rhodopsin (*see* Chapter 9, *Membrane Photobiology*) consisting of G-proteins criss-cross seven times the lipid bilayer of the plasma membrane. Upon odorant excitation, it seems likely that some sort of conformational changes take place.. This change in the odorant receptor molecule triggers a biochemical cascade, leading most likely to the generation of electrical signals in the brain. To find out how the olfactory system works at the membrane level, researchers have examined the olfactory cells and identified the receptors that actually bind with the odorants. The nature of the molecular structures that encode olfactory information has been a major aim of the study of olfaction. Olfactory receptor cells are bipolar neurons. The extracellular matrix of olfactory neuroepithelium is a highly organized structure in intimate contact with cillia that house the olfactory transducer, certain elements of which have been cloned. The stereochemical conformation of an adsorbed odorant molecule as it binds to a receptor has been proposed to be a critical element for olfactory information. This outstanding past work has further suggested that an odorant molecule can contain more than one of these elements. Thus, an odorant molecule can assume more than one conformation each of that is detected by a different receptor. To investigate this possibility, the response of the bullfrog's olfactory receptors reconstituted into BLMs was studied,[76] using three structurally related odorants: diethylsulfide (DES), thiophene (THP) and diethanolsulfide (thioglycol or DOS). DOS is the dihydroxy derivatives of DES. The two molecules are similar in structure but differ substantially in their odor. THP is a heterocyclic molecule that resembles diethylsulfide in its chemical formula as well as odor. We hypothesized that diethylsulfide may contain a conformation bound by the receptors of diethylsulfide and THP and an additional conformation not shared with these two odorants. To test this hypothesis we presented the odorants sequentially to the reconstituted receptors in BLMs at saturating concentrations. The ordorants were presented in pairs to BLMs containing cilia membrane fragments. DOS induced a response in the presence of either the other two odorants. DES and THP did not induce a response in the presence either of the other two odorants. These observations suggest tha substructures, one common to these odorants and one that is unique to DOS. The results

support the notion that olfactory receptors detect certain molecular segments of odorants. The data also suggest that diethanolsulfide contains a unique binding conformation not shared by the other odorants.[76]

In connection with G-proteins, mention should be made of recent work of Ismailov et al[23,,67] who reported the regulation by Na^+ and Ca^{2+} of renal epithelial Na^+ channels in reconstituted BLMs. They suggest that amiloride-sensitive renal Na^+ channel characteristics are not static, but depend upon the biochemical state of the channel protein and/or its associated G-proteins. The nature of the molecular structures that encode olfactory information has been a major aim of the study of olfaction. Olfactory receptor cells are bipolar neurons. The extracellular matrix of olfactory neuroepithelium is a highly organized structure in intimate contact with cillia that house the olfactory transducers, certain elements of which have been cones. It has been proposed that the stereochemical conformation of an odorant molecule as it binds to a receptor is a critical element for olfactory information. Further it has been suggested that an odorant molecule can contain more than one of these elements. Thus, an ordorant molecule can assume several conformations, each of which is detected by a different receptor.[76] Earlier, the BLM was used for investigating the olfactory receptor function.[78] Homogenates of rat olfactory epithelium were incorporated into BLM made from egg PC by using a new technique based on the Langmuir-Blodgett monolayer method. Single-channel events appeared about 30 sec after the addition of the homogenates. About 20 minutes later, the channel activity decreased and vanished. When adding subsequent nanomolar concentrations of odorous agents, diethylsulfide of carvone, the discrete fluctuations reappeared with changed characteristics. The odorous compounds did not significantly affect the unit channel conductance, which remained in the range of 60-65 pS, but changes in the mean open time and in the probability of opening were observed. Diethylsulfide induced increases in the probability of opening from 0.66 to 0.8 and in the mean open time. The lack of activation in the presence of NaCl and the block of the effect of both odorous compounds by the specific K^+-channel blocker 4-aminopyridine indicate that the channels may be specific for potassium. The authors suggested

correlations with the AchR channels. However, the very long open times and the lack of bursting activity show a quite different behavior.

7.4 Measurement Techniques

Voltage Clamp Technique (VCT)

As its name implies, the voltage is being held constant, while the current is measured. The VCT, developed by Cole and its exploitation later by many investigators including HHK, has had a profound influence on electrophysiology. Fig. 7.3 shows one of the latest arrangement for voltage clamp.[71]

The Patch Clamp Technique (PCT) [17,72]

An ion channel consists of a single protein molecule or a complex of molecules, which forms a mutable, water-filled pore through the lipid bilayer of cell membrane. Some of the ion channels are operated by an electrical signal (voltage-gated), whereas others are activated by chemical signal (ligand-gated). The channel allows specific ion species to flood into or out of the cell. It is believed that opening and closing of the channel is achieved by a minute change in the conformation of the channel protein complex. In the 1970s, shortely after the single-channel activities were demonstrated in BLMs,[3,17,60] a new technique was developed. Briefly, the technique, now known as the patch-clamp (VCT), involves placing a glass micropipette in contact with a patch of cell membrane so as to isolate one or several ion channels of the same type. The membrane-coated pipette is then used as an electrode to record the flow of ions between the inside of fluid-filled pipette and the other side of the membrane fragment. As in planar BLMs, tiny electrical currents at the picoampere (10^{-9} A) level are measured. More specifically, the technique uses a fine glass pipette probe with a tip a few μm in diameter. The pipette is usually filled with a KCl and pressed againt the cell membrane (or BLM or giant liposome). A small suction is then applied so that a tiny patch of the membrane forms a tight

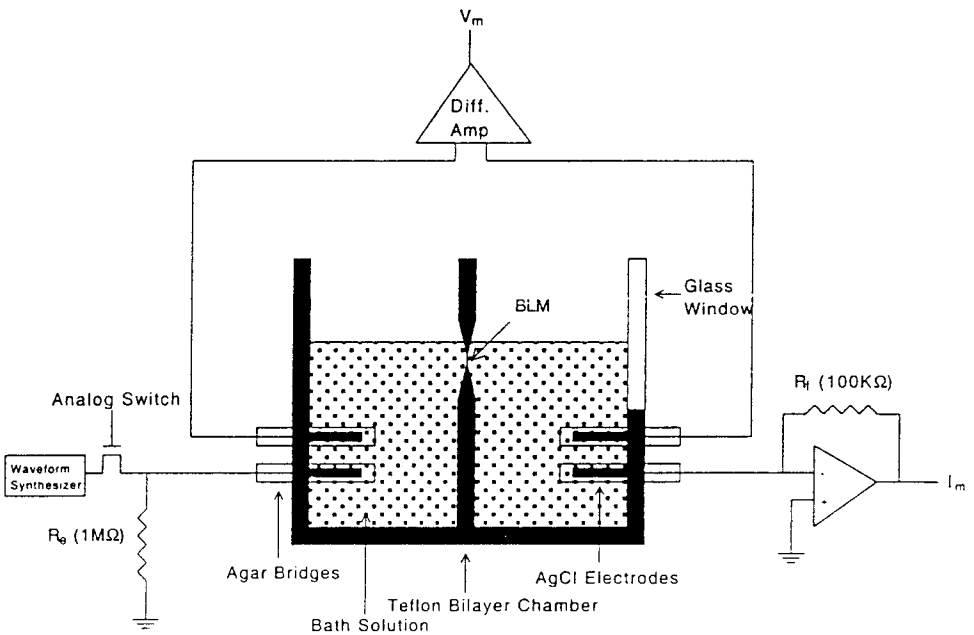

Fig. 7.3 Experiemntal setup for voltage-clamp experiments[71] (Courtesy of Dr. Lesile Tung),

seal around the edge of the pipette tip. Thus, any current through the pippete probe must also flow through the patched membrane. The most crucial aspect of the technique is the formation of a tight seal bwtween the pipette and membrane patch, which is usually on the order of giga ohms ($>10^{10}$ Ω). The technique calls for an electronic feedback circuit, which ensures that the voltage applied across the patched membrane is held at a constant value, so that the monitored currents are proportional to changes in the membrane resistance. If the patched membrane contains an ion channel, a brief pulse of current is observed each time the channel opens. The observed pulses are generally of the same size, monitored as current steps, in a given experiment, suggesting that ion-channels are usually either open or closed, although the time for which the channel is open varies from one opening to the next. From the observed current steps, which are on the order of 10^{-12} A, an opened ion-channel allows a translocation of a few thousand ions across the membrane per msec. It should be pointed out that the openings and closings of channels are random events; they can be predicted only in statistical probabilities. The patch-clamp technique provides experiemnters with a picture at the molecular level how thousands of channels might behave in a given cell membrane. Hence, one of the most exciting development in membrane biophysics and electrophysiology is the availability of the patch-clamp technique (PCT). Prior to the PCT, intracerllulr electrodes used in the voltage-clamp technique (VCT) measure the transmembrane potential across the membrane and through it. The influences of electrical stimuli or of neurotransmitters are described in terms of change in membrane conductance. It has been very successful in accounting and describing the nerve action potential. However, the VCT approach, as practiced earlier, was incapable of giving direct information at a molecular level. In contrast, the PCT brings membrane biophysics to the molecular level, which enables electrophysiological studies to be done on single channels embedded in BLMs, liposomes, or biomembranes. Now, we know that a class of proteins in the cell membrane called pores or ion channels mediates electrical currents in cells, which was first observed in an EIM-modified BLMs.[3,72]

Membrane preparation – the membrane of the cell to be patch-clamped must be clean, free of connective tissue, adherent cells, and basal membranes. The use of a reconstituted BLM, of course, does not have this

problem (see below). A fluid-filled micropipette is lowered onto the surface of a cell so that the contact (or patch) is made with the cell membrane but not to puncture it (area ~ 1 μM^2 or less). If the seal is good between the micropipette and the membrane (~ 10^9 ohms or gigaohms), ions move through the contacted area or patch, which will give rise to an electrical signal, that is transmitted through the reference electrode, bathing solution and to an amplifier. The inside of the pipette electrode is kept at a constant potential with a voltage clamp circuit so that ions flow through the channels in the patch are detected by the circuit as currents. What are actually measured are changes in current caused by abrupt openings of channels in the patch. Instead of measuring the whole cell, a patch of the cell membrane is isolated and studied.

Formation and characterization of planar lipid bilayers (BLMs) – The complex composition and structure of the natural membrane in some cases makes interpretation of the experimental results in this field difficult. Therefore, a quite useful approach is related to the performance of patch-clamp studies on the channel molecular mechanisms by using a model system with well-defined components and characteristics such as BLMs [Harris and Etemadi, 1989]. This approach permits quick progress toward an understanding of the molecular mechanisms of excitability and other membrane phenomena. A BLM with increased mechanical stability may be obtained by using a Langmuir-Blodgett technique for passing a hydrostatically closed Teflon chamber with an aperture of 2 mm through a monolayer. Records with good signal-to-noise ratio are obtained with this method by using a voltage-clamp circuit.[72]

Electrode fabrication – the glass micropipette should be freshly pulled, having a tip diameter of a few μm, which is filled with 1 M KCl solution. An Ag/AgCl wire electrode is place inside the micropipette that connects the excised patch via KCl solution and the instrumention.

Instrument for the patch clamp – The principal part of the instrumentation is the circuits for controlling the membrane potential – a number of such instruments are commercially available (e.g. Axon Instruments, Inc., CA).

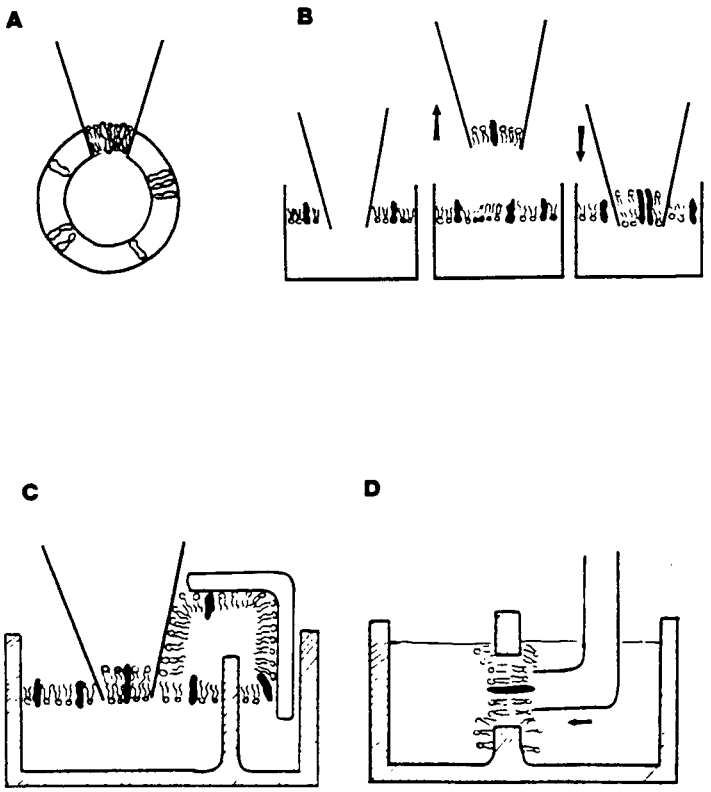

Fig. 7.4 Techniques for formation of bilayers at the tips of patch-clamp pipettes. (A) Formation of bilayers from liposomal membranes. (B) Formation of bilayers from monolayers using the dip-tip technique. (C) Bilayers formed by micropipette guided contact of two monolayers. (D) Formation of bilayers by introducing micropipette tips into preformed planar BLMs.

Software for data analysis - it should be stressed once more here that a tight seal of greater than 10^{10} Ω between the glass pipette and the patch is essential. This is accomplished if a clean glass micropipette surface is available for the attachment of the lipid bilayer of the membrane.

As shown in Fig.7.4(A), macromolecules were inserted in small liposomes, followed by enlargement of the lipid vesicles to about 10 um by using the freeze-thawing method. The tip of a micropipette is brought near one of the blebs formed by the liposomal membrane and, by applying negative pressure, an excised membrane patch is formed on the tip of the pipette. The disadvantages of this method are related to preparation of liposomes with defined size and form as well as the delicate manipulations of the liposomal membranes required by the micropipette. Another method is the so-called dipping technique as demonstrated in Fig. 7.4 B. In this case, a monolayer is formed either by spreading lipid and channel protein molecules dissolved in pentane on the air-water interface, or by absorbing these components on the interface after introducing liposomal suspensions in the aqueous subphase. The tip of a patch-clamp micropipette is immersed in the aqueous solution before forming the monolayer. After formation of the monolayer, the pipette is slowly removed from the aqueous phase to the air and later is cautiously reintroduced into the solution through the monolayer. Depending on different conditions, a BLM is frequently formed on the tip of the pipette by using this simple procedure. A monolayer is formed on the tip when the pipette is lifted to the air after passing it through the interface.

When reimmersing the pipette into the solution, the phospholipid hydrocarbon chains of the monolayers on the tip and on the air-water interface interact when apposed against each other and a BLM is formed on the pipette tip. If the first trial would be unsuccessful, the procedure can be repeated several times. The success rate of BLM formation is usually high, but it depends to a great extent on the lipid composition of the membrane-forming solution, as well as on the ionic composition of the aqueous phases, especially that in the micropipette. BLMs are usually easily formed from different types of phospholipids. The presence of a millimolar

concentration of divalent cations (Ca^{2+}, Mg^{2+}, Ba^{2+}) in the subphase and especially in the pipette increases the chance for high-resistance seals.

To obtain highly reproducible results with a success rate of 80% for BLM formation, the surface pressure of the monolayers must be controlled. The optimal surface pressure during the removal and the reintroduction of the pipette should be about 30 dyn/cm. A special automatic control system is needed in order to maintain the surface pressure at such a constant value. Both fire polished or nonfire polished pipettes can be used. A success rate of 90% for forming gigaseals in the range of 1-10 GΩ can be achieved when controlling the surface pressure of the monomolecular film.[72]

A micropipette guided method which differs from the dipping technique is also available. In this case, the top of the micropipette remains on the interface and the BLM forms by micropipette guided contact of the two monolayers (Fig. 7.4 C). One of the advantages of this method is the facility for investigating channel activities as a function of the surface pressure. The dependence of transport processes on changes in the surface pressure in the range 28-48 mN/m has been studied. This important advantage, however, has not been largely exploited, probably due to the difficult experimental procedure.

A method which differs from the previously described techniques includes the preformation of a standard BLM into which the tip of a patch-clamp micropipette is introduced forming a BLM on the pipette tip (Fig. 7.4 D). In this case, the BLM may contain some solvent, while in the previously described methods the BLMs are 'solvent-free'. Presently, the dipping technique is one of the most convenient and promising methods that have recently been introduced in connection with the modern electrophysiological developments. It is particularly useful when only small amounts of purified proteins and membrane-forming materials are available. All the bilayer techniques are valuable especially for investigating channel activities in reconstituted intracellular membranes, which so far cannot be studied directly in isolated single cells by the standard patch-clamp technique.

Methods for analyzing the properties of reconstituted membranes[72]

The patch-clamp technique may be used for whole-cell current as well as for single-channel current measurements. In the former case, the micropipette interior has free access to the intracellular space, while in the latter case a hemispherically or cylindrically shaped membrane patch with a small diameter is sealed into the micropipette tip by applying negative hydrostatic pressure. Inside-out or outside-out patches can be formed depending on the sealed membrane configuration. One or more channels may be functioning in the patch as a result of varying density of channel molecules in the membranes. The permeation of ions through the open channels can be influenced by electrical potentials applied across the membrane as well as by concentration gradients. The ion transport process can be examined by measuring the single-channel current events, which appear as square-shaped current fluctuations during the transitions of the channels between the different conducting states.

For example, a single-channel current displacement with an amplitude of 1 pA and 1 ms duration may be caused by the flow of 10,000 ions through the open channel across the membrane. So, the single-channel current fluctuation may be characterized by determining its amplitude and its duration. Channels with varying amplitudes and durations may be present in the patch. The amplitude distributions are analyzed by plotting current amplitude histograms, while the open and closed time duration distributions may be estimated after obtaining frequency histograms. The single channel (unit) conductance varies as a function of the concentration of the current carrier. A linear dependence may be observed at a defined ion concentration range, but it usually becomes nonlinear and saturates at high concentrations. For some channels, like the plasma membrane Ca^{2+} channels, the saturating ion concentration can be relatively high (~150 mM), while for other types of channels it is much lower, for example, 18 mM Cs^{+} for the K^{+} channels of the skeletal muscle sarcoplasmic reticulum membranes. The single channel conductance may also vary depending on the charge carrier. For example, the unit conductance of the plasma membrane Ca^{2+} channels is 23 pS in 100 mM Ba^{2+} and 7 pS in 100 mM Ca^{2+}, which means that these channels are significantly more permeable for

Ba^{2+} than for Ca^{2+}. The permeability ratio for any type of channel may be determined after defining the current-voltage relationship and the equilibrium (Nernst) potential under bi-ionic conditions. For example, in the presence of 50 mM Ba^{2+} on one side of the membrane and 80 mM Cs^{+} on the other side, the permeability ratio $P(Ba^{2+})/P(Cs^{+})$ of the muscle sarcoplasmic reticulum Ca^{2+} channels was defined to be 11.4. By determining the reversal potential under bi-ionic conditions in the presence of defined concentrations of monovalent and divalent ions, the ionic selectivity and specificity may be characterized.

The kinetic characteristics of the channels may be analyzed by taking into account the time-dependent transitions of the channels between their closed and open states. The transitions of the channel between only two conductance states, one closed and one open state, can be described by the reaction

$$\text{closed} \underset{k_{-1}}{\overset{k_1}{\longleftrightarrow}} \text{open} \qquad (7.9)$$

where k_1 and k_{-1} are the rate constants for opening and closing of the channel. Some channels, like acetylcholine and other agonist-activated channels, can be opened only after binding of the activating ligands to the receptor region of the channel. In this case, two closed and one open channel states are available and the transitions between them are described as follows

$$\underset{\text{(unbound ligand)}}{\text{closed}} \underset{k_{-1}}{\overset{k_1}{\longleftrightarrow}} \underset{\text{(bound ligand)}}{\text{closed}} \underset{k_{-1}'}{\overset{k_1'}{\longleftrightarrow}} \text{open} \qquad (7.10)$$

The sodium channels are also fluctuating between two closed states and one open state. However, in this case the second closed state is related to the inactivation mechanism of the Na^{+} channels. Transitions may occur between all three different channel states. The characteristics of the simple channel mechanism with transitions between only one closed and one open state will be briefly described. The relation between the rate constants for

channel opening (k_1) and closing (k_{-1})and the difference in energy between the closed and open channel states (ΔE) are given by

$$\frac{k_1}{k_{-1}} = \exp(-\Delta E/RT) \qquad (7.11)$$

where R is the gas constant and T is the absolute temperature. Information about k_1 and k_{-1} can be obtained by taking into consideration the expressions for the distributions of open times, $P_O(t)$, and of closed times, $P_C(t)$, of the channels

$$P_O(t) = k_{-1} \exp(-k_{-1} t) \qquad (7.12)$$

$$P_C(t) = k_1 \exp(k_1 t) \qquad (7.13)$$

For determining the time distributions and k_1 and k_{-1}, the number of opening or closing events as a function of their time duration is estimated. As a result, frequency histograms are plotted. For example, an open state frequency histogram for brain microsomal Ca^{2+} channels is plotted. It is clear that the number of opening events decreases exponentially as a function of the open time duration. In this particular case, the data are fitted by a sum of two exponentials with time constants 1 and 2, which may be due to the presence of channels with two different mean open times. Channels with one or more than two time constants are also described in the literature.[72]

Closed time histograms may be obtained in a similar way by plotting the number of closing events as a function of the closed time durations. The data in this case may be fitted by exponentials, which may differ substantially from those of the open time histograms and may be characteristic of defined types of channels as well as defined blocking effects. When the channel resides in more than one closed state, as shown for some agonist-activated channels, a sum of several exponentials may fit the data from closed time histograms.

In addition to the mean open times that are determined by analyzing the frequency histograms, the channel kinetics are also characterized by their defined open state probabilities. If among a total number of N channels in the membrane patch only n channels are open, then the probability of finding simultaneously open channels $P_{(n)}$ is given by

$$P_{(n)} = \frac{N!}{n!(N-n)!} P_o^n [1-P_o]^{N-n} \qquad (7.14)$$

The probability of the open state (P_o) may be determined by using the equation

$$P = \frac{I}{Ni} \qquad (7.15)$$

where I is the time-averaged current flowing through the open channels for a defined period of time, N is the number of channels functioning independently in the membrane patch and i is the single channel current.

The relation between P_o and the mean open time, t_o, that is, the average time the channel resides in the open state, is given by

$$t_o = \frac{P}{n/T} \qquad (7.16)$$

where n is the number of the channel openings and T is the time period during which the parameters were analyzed. It should be noted that one of the prerequisites of an adequate analysis of the single-channel parameters is to work with patches containing only one functioning channel. This is a considerable limitation. Mention should be pointed out that many of the theoretical considerations of ion selectivity and membrane transport mechanisms are based on BLM experimental background.[79]

7.5 Ion Channels and Their Reconstitution in Planar BLMs and Liposomes[72]

The achievements in the field of electrophysiology were dependent, to a great extent, on the development of modern techniques for measurement of the electrical characteristics of the biomembranes, such as voltage and current-clamp. Although the higher resistance and the size of BLMs imposed some specific requirements concerning the measurement of their electrical parameters, a tendency always existed to apply the most recently developed electrophysiological methods to BLM experiments. On the other side, the achievements in BLM research also influenced, to some extent, electrophysiological developments, so that presently it is possible to state that the electrophysiological and the BLM experimental approaches are complementary [Harris and Etemadi, 1989; Narahashi, 1992]. For instance, the first observation of ionic currents through single ion channels was achieved by using BLM.[3] Discrete conductance fluctuations mediated by polypeptide antibiotics were characterized in other BLM systems. The use of improved voltage-clamp techiques and of folded bilayers, later permitted to obtain single-channel recordings with a better resolution. The small membrane surface area of the BLMs formed from monolayers by the folding method is one of the main prerequisites for improving the signal to noise ratio.

Potassium (K^+) channels

The selectivity of an ion channel depends on a number of factors such as the channel diameter and interacting site linning the channel. For example, the voltage-gated K^+ channel in mammalian cell membranes, about 100 times prefers K^+ over Na^+ owing to the fact that the hydrated Na^+ is larger than that of K^+, which makes it more difficult for larger Na^+ to penetrates the smaller K^+ channel. Further, it seems reasonable that the smaller hydrated K^+ allows a stronger interaction with the sites linning the channel, thereby greater selectivity for K^+ over Na^+.[37]

K^+ channels show considerably more variety than other channels depending on the types of cells, specific regulatory mechanisms, etc. In

addition to several main types, such as inward rectifier, delayed rectifier and Ca^{2+}-dependent K^+ channels, other channels with differing unit conductance in various cells have been described. In this connection, K^+ channels, which are probably responsible for the resting K^+ conductance of brain synaptosomes, were reconstituted in BLMs formed from PE and DPG or PE and PS by Nelson and Reinhardt.[80] A rectification of the current-voltage relationship was observed, which can be described by the Goldman-Hodgkin-Katz equation.[50] A selectivity of K^+ over Cl^- and of K^+ over Na^+ with a permeability ratio, K^+/Na^+, of 3:1 – 5:1 was demonstrated. K^+-channel blockers were tested and it was found that Ba^{2+} (20 mM) provoked a voltage-dependent block, but tetraethylammonium (TEA) did not influence the channel activity. Despite the differences in the actions of inhibitors, the other properties of these reconstituted channels may be interpreted in favor of their specificity for K^+.

An important type of K^+ channel that differs from those involved in resting conductance is *the delayed rectifier channel.* The single-channel analysis of its activity in native membranes using the patch-clamp technique is relatively difficult, but BLM was successfully used for the characterization of this channel. Coronado et al[28] incorporated lobster axon membrane vesicles into BLMs by using an osmotic gradient and observed the appearance of single-K^+-channel events which share some of the characteristics typical for the delayed rectifier channels in a natural environment:

- Bursting behavior with quiescent long duration interbursting intervals.
- Voltage inactivation.
- Lack of Cs^+ permeability and block by Cs^+, TEA, and nonyltrimethylammonium.
- The effects of these blocking agents are exerted only when added to a defined side of the BLM, which is coincidental with their side-dependent inhibitory effects in nerve membranes.

Some differences, however, were also observed. These are:

- The single-channel conductance, 28 pS, was almost three times larger than that of the squid axon membrane K^+ channel. It was suggested that in lobster axon the delayed-rectifier conductance might be lower if a different lipid environment was available. On the basis of data about the dependence of conductance upon the lipid composition of BLMs, it was concluded that decreased amounts of PS or increased amounts of cholesterol in the membranes might cause a lowering of the unit channel conductance.
- There are similarities, but some differences as well, in the bursting kinetics of the reconstituted channels in relation to those of the native channels in squid axons. Temperature was suggested as one of the possible factors influencing the bursting channel lifetimes.
- At high depolarizing voltages a current decrease is observed which remains unexplained.

In addition to the single channels with 6-7 pA current amplitude, which are qualified as delayed rectifiers, another type of a channel with a larger current amplitude, 12 pA, is observed in the recordings, but its behavior is clearly distinguished from that of the delayed rectifier opening events. Data about the ionic selectivity of these channels were obtained on the basis of the reversal potentials and relative permeabilities calculated by using the Goldman-Hodgkin-Katz equation.[50] The permeability ratio P_{Na+}/P_{K+} was defined to be 1:30. Only four ions are highly permeant: $Tl^+ > K^+ > Rb^+ > NH_4^+$. The kinetics of these channels may be described by a scheme which includes one open (O) and two closed states (C_1 and C_2):

$$C_2 \underset{k_{-2}}{\overset{K_2(V)}{=\!=\!=\!=}} C_1 \underset{k_{-1}}{\overset{k_1}{=\!=\!=\!=}} O \qquad (7.17)$$

The voltage-dependent step is supposed to be between the two closed states designated by $k_2(V)$. This scheme may be typical for the channels showing bursting activity. Channels with similar characteristics have also been reconstituted from lobster axonal membranes into BLMs made on the tips of patch-clamp micropipettes.

Using the patch-clamp and the BLM technique, a variety of K^+ channels have been characterized in muscle cells. K^+ channels have been found not only in the muscle plasma membranes but also in the intracellular membranes, such as those of the sarcoplasmic reticulum. Further, K^+ channels from calf cardiac sarcolemma have been incorporated into BLMs from PE/PS and characterized their activity in detail. Three different types of K^+ channels with various unit conductances, 15 pS, 28 pS, and 95 pS were found. The 15 pS channel was shown to be independent of Ca^{2+} concentration. Its selectivity was not very high, the permeability ratio being $P_{K^+}/P_{Na^+} = 3$. The 95 pS channel, on the contrary, was influenced by changes in Ca^{2+} concentration. At Ca^{2+} concentrations lower than 1 mM, the long closing events disappeared. The 28 pS-channel activity was found to be voltage dependent. At –80 mV, the mean open time was 6 msec, but at more depolarizing voltage, -40 mV, it was increased 10 times. The voltage dependence of this channel is quite similar to that of the repolarizing current, i_x, in cardiac muscle. The probability histogram of this channel reveals one open and two closed states. When a fivefold K^+ concentration gradient is created across the BLM, the reversal potential was –34 mV which coincides with the predicted potential for a K^+-selective channel according to the Nernst equation. The permeability ratio, P_{K^+}/P_{Na^+}, of this channel was defined to be relatively low, 5. This low selectivity is also similar to that of the cardiac repolarizing current, i_x.

The Ca^{2+}-activated K^+ channels which were found in a variety of cells, differ substantially from other types of K^+ channels such as the delayed rectifier and the inward rectifier channels. Their opening and closing are regulated mainly by $[Ca^{2+}]$, but the voltage across the membrane also plays a controlling role. Another typical feature of these channels is their very high unit conductance, 200-230 pS, which is substantially higher than that of the other types of channels. The Ca^{2+}-activated K^+ channels incorporated into BLMs shared most of the characteristics of the native channels of this type. A summary of these studies is as follows:[72]

- A high unit conductance.
- Ca^{2+} dependence. Calcium, however, does not influence the conductance, but it does induce substantial changes in the mean open

time. The latter increases as a linear function of $[Ca^{2+}]$, whereas the mean closed time is linearly proportional to the reciprocal $[Ca^{2+}]$. The Ca^{2+} effect depends on the side of addition of the cation.

- Voltage dependence. The voltage also influences the mean open time. It is interesting that in the experiments on the reconstituted transverse tubule membrane channels, where one open and two closed (fast and slow) conductance states were described, the dwelling time of the channel in the slow state increased when applying more positive potentials. An opposite voltage dependence for the fast state was observed.
- Typical ionic selectivity.
- Block by TEA, depending on the side of its addition. This effect is interestingly voltage dependent. The apparent dissociation constant, K_d, decreases as a function of the applied potential.
- Block by Ba^{2+}. The effect of Ba^{2+} shows some similarities, but also some significant differences in relation to that of the inward- and delayed-rectifier K^+ channels. Analysis of the data concerning Ba^{2+} block led to a valuable conclusion about the mechanims of the ion conduction through the different types of K channels.

The results indicate that the Ca^{2+}-activated K^+ channel behaves as a single-ion pore, while the delayed-rectifier channel behaves as a multi-ion pore.

Sodium (Na^+) channels

The investigation of the Na^+-channel activity is one of the most challenging tasks in electrophysiology, owing to the relatively fast kinetics of the activation and inactivation of the Na^+ channels [Harris and Etemadi, 1989; Narahashi, 1992]. They enter an open state during the first several milliseconds after applying depolarizing pulses. Their inactivation also occurs in the range of milliseconds. A special electrical circuit must be used in order to compensate the large capacitance transient appearing in the beginning of the pulse. When using the patch-clamp method, the capacitance transient can also be decreased by coating the glass micropipette with a Sylgard layer about 10-40 um from the tip.

Reconstitution of Na^+-channel activity in a BLM is a difficult task mainly due to the inactivation mechanism. Krueger et al[74] succeeded in incorporating brain membrane components containing Na^+-channel molecules into BLMs and recorded a voltage-dependent Na^+-channel activity by using an inhibitor of the Na^+-channel inactivation. batrachotoxin. The use of batrachotoxin was essential for obtaining Na^+-channel activity. The rat brain membrane vesicles containing the channels were incorporated into the BLM by using the osmotic gradient fusion procedure,[72] which so far has been the most successful method for reconstitution of channel activities in BLM. The authors observed several similarities between the characteristics of the reconstituted and native channel activities. Nanomolar concentrations of saxitoxin (STX) blocked the channels in the presence of 0.5 M NaCl on both sides of the BLM. The same concentrations of STX inhibit the functioning of the Na^+ channels in native membranes. When the concentration of STX was increased, the mean duration of the Na^+-channel openings was shortened. Another interesting observation was the voltage-dependence of the STX-blocking effect, which was more pronounced at hyperpolarizing potentials. The findings concerning the voltage-dependence of the neurotoxin effects in native membranes are rather controversial.[72] A voltage-dependent block of Na^+ channels by TTX was found in the heart which has not been confirmed in later experiments in multicellular preparations. A TTX-induced voltage shift of the inactivation curve of Na^+ channels was obtained by using the patch-clamp single-channel recording technique, indicating that under some conditions the effect of TTX may be voltage-dependent. All these experiments were performed in different types of preparations by using different techniques and therefore it is possible to suppose that the neurotoxins are acting by various mechanisms in defined types of cells. Further experiments in this direction by using other types of reconstituted BLM systems should be particularly helpful in solving this problem, which might facilitate the elucidation of the molecular mechanisms of excitability. The Na^+ channels reconstituted in BLM shared other properties typical of the sodium channels in native membranes such as similar unit conductance and selectivity for sodium over potassium. The unit conductance was 30 pS, which is actually about two times higher than that of the Na^+ channels in native membranes, (15 pS), but in the model system a much higher concentration of NaCl was used (0.5 M) in order to

obtain a good current resolution. The permeability ratio (P_{Na+}/P_{K+}) of 0.06 as well as the lack of Cs^+ permeation are characteristics which also demonstrate the similarities between the properties of the model and native systems.

It should be pointed out, however, that these comparisons are valid for the case when the sodium inactivation is removed by batrachotoxin that modifies the channel kinetics. Further efforts should be made to reconstitute and characterize Na^+-channel activity in BLMs without influencing the inactivation mechanisms. Well-defined purified preparations should be used for the incorporation procedures. Pure synthetic lipids must be employed for preparing the BLM-forming solution. We found channel activities in BLMs prepared from most of the commercially available lipids isolated from brain or other tissues. Although their origin is not known it is possible to suppose that they are due to some proteolipid molecules remaining after the isolation procedures. They may, however, cause misleading interpretations of the results from the reconstitution experiments.[72]

Substantial progress has been achieved toward an understanding of the molecular structure of the sodium channels. Radiolabeled neurotoxins, TTX and especially STX, have been used successfully as molecular probes for purification and reconstitution of brain sodium channel activity in phospholipid vesicles. Homogeneous fractions of sodium channels were purified from rat brains and their molecular composition was defined. Three polypeptide subunits were separated; with a molecular weight of 260,000 daltons; B_1, 39,000; and B_2, 37,000. The B_1 subunit covalently binds scorpion toxin. B_2 and d subunits are covalently linked by disulfide bonds. This trimeric complex has been incorporated into planar BLMs and found that the voltage-dependent Na^+-channel activity was reversibly blocked by tetrodotoxin (K_i = 8.3 nM at –50mV). The unit conductance was 25 pS in 0.5 M NaCl, 3.5 pS in 0.5 M KCl, and 1.5 pS in 0.5 M RbCl. More information about the structure and the properties of the Na^+ channels, and especially about the region of the selectivity filter, was obtained in a study on Na^+ channels incorporated into BLM from rat forebrain membranes. It has been shown that an agent binding to the

selectivity filter, trimethyloxonium (TMO), significantly modified the sensitivity of the channel to the blocking effects of Ca^{2+} and of STX. TMO also reduced the single Na^+-channel conductance from 25 pS to 15.8 pS. Ca^{2+} used at 10 mM 'extracellular' concentration reduced the single-channel current by 60% and induced a decrease in the blocking effect of STX. STX and Ca^{2+} were able to prevent the modification of the Na^+ channels by TMO, which indicates that all of these agents may compete for binding to a common site in the channel molecule. It was suggested that this blocking site may include a specific carboxyl group that is methylated by TMO. The carboxyl group may be important for the toxin binding, but may not substantially affect the access of Na^+ and Ca^{2+} to the pore.

Calcium (Ca^{2+}) channels

Calcium ions entering the cells mainly through voltage-dependent channels and Na^+-Ca^{2+} exchange are involved in the regulation and triggering of many physiological functions. Calcium ions play an important role in nerve cells, triggering the release of neurotransmitters into the synaptic gaps, as well as in the secretion of neurohypophysins, etc. [Harris and Etemadi, 1989; Narahashi, 1992]. Many pharmacological agents were found to exert their effects through modulating the Ca^{2+} currents, which show specific characteristics for different types of cells. Resolution of the single-channel events related to Ca^{2+} transport meets some difficulties owing to the very low unit conductance of the Ca^{2+} channels. By using high calcium or barium concentrations (110 mM or 96 mM in the micropipette solution), however, high-quality single-Ca^{2+}-channel recordings can be obtained in different types of cells. Nelson et al[80] incorporated brain membrane vesicles containing Ca^{2+} channels into BLMs formed from phosphatidylethanolamine (PE) (3.3%) and phosphatidylserine (PS) (2.6%) and studied their characteristics at high concentrations of divalent ions (250mM). The reconstituted channels shared several common properties with Ca^{2+} channels in native membranes:

- The channel activity was voltage dependent. It increased at more positive potentials, but showed saturation at very high voltages.
- A selectivity for divalent over monovalent cations was demonstrated.

- A dose-dependent blocking effect by the following ions was observed: $La^{3+} > Cd^{2+} >> Mn^{2+}$. However, even concentrations higher than 0.5 mM did not completely inhibit the channel activity.
- There was a selectivity among several divalent ions: Ca^{2+}, Ba^{2+}, and Sr^{2+}.
- The unit single-channel conductances were very small, 5-8.5 pS.

Clearly distinguished differences between the unit conductances in the presence of different divalent cations as current carriers were also found. The single-channel conductance carried by Ba^{2+} was much higher, 8.5 pS, than that carried by Ca^{2+} or Sr^{2+}, 5 pS. This means that these two ions are moving through the channel 1.7 times slower than Ba^{2+}. Another peculiar effect induced by Ba^{2+} is the shortening of the mean channel open time, 127 msec, in comparison to those of Ca^{2+} and Sr^{2+}, 454 msec and 385 msec, respectively, at +100 mV. Thus, the order of the mean open times is $Ca^{2+} > Sr^{2+} > Ba^{2+}$. It is noteworthy that it coincides with the order of affinities of the same ions for calcium channels in brain synaptosomes. The data can be interpreted in favor of the supposition that when the cation permeates the channel, it prevents its closure. Some K+ channels in squid axons exhibit a similar behavior. It should be pointed out that the reconstituted Ca^{2+} channels were also functioning in the absence of complete inactivation, similar to the Na^{+} channels reconstituted in the BLM as previously described. The characteristics of Ca^{2+} channels cannot be properly analyzed in excised patches of cellular membranes due to the rapid 'rundown' of the Ca^{2+}-channel activity. The loss of functionally important phospholating enzymes is probably responsible for this phenomenon.

So far the BLM technique has proved adequate for measuring single-channel activity in synaptosomes, which, due to their small size (1 μm in diameter), cannot be studied directly by using the patch-clamp technique. Synaptosomal fractions from rat brain tissue have been used as a source for reconstitution of voltage-dependent Ca^{2+} channels. Several correlations were found between the properties of channels characterized by radioisotopic methods and those of the reconstituted fractions:[72]

- Same order of maximum flux rate of permeating divalents ($Ba^{2+} > Ca^{2+} \simeq Sr^{2+} > Mn^{2+}$).
- Permeation and blocking effect of Mn^{2+}.
- Blockade by organic ions with an order of potency: $La^{3+} > Cd^{2+} >> Mg^{2+} > Na^{+} > K^{+}$.
- The permeant and the blocking ions compete for a single site, the order of their apparent affinities for the site being the same as the orders of maximum flux rate and of blocking potency, respectively.
- Same inhibitory effects by micromolar concentrations of D-600 and verapamil.
- Lack of complete inactivation.

One of the typical features of these channels was the order of the unit conductances for the permeant ions, which was the inverse of the order of their mean open times: $Mn^{2+} > Ca^{2+} = Sr^{2+} > Ba^{2+}$. The blockers reduced the single-channel conductance and affected the mean open times. The blocking effect of Cd^{2+}, which is not a permeable ion, may be explained by its binding to a single site. The mechanism of the Mn^{2+}-induced block, however, is more complicated. In the absence of permeant ions Mn^{2+} can permeate through the channels, the single-channel conductance (4 pS) being lower than that for other divalents (Ba^{2+}, 7.5 pS; Sr^{2+}, 6 pS). When added in the presence of permeant ions, Mn^{2+} can reduce the amplitude of the single-channel fluctuations in a voltage-dependent manner. The existence of more than one binding site is compatible with the data on the Mn^{2+} effect.

The reconstituted Ca^{2+} channels show some deviations from the normal behavior in native membranes. For instance, a shift of their activation curve toward more positive is observed. It has been suggested that this phenomenon is due to the lack of phosphorylating enzymes in the BLM system. These enzymes may be involved in the control of the Ca^{2+}-channel activity *in vivo*. The properties of single Ca^{2+} channels from brain endoplasmic reticulum (ER) membranes reconstituted in BLMs made on the tips of patch-clamp micropipettes have been investigated. They were similar to those of sarcoplasmic reticulum (SR) membranes from skeletal muscle. Large current displacements accompanying the Ca^{2+} channel openings at 50 mM Ca^{2+} (Fig. 7.5 A) were observed and even as low as

$[Ca^{2+}]$ = 3.6 mM. Two exponentials described the open channel kinetics, the first and the second time constants being 14 msec and 39 msec, respectively. The Ca^{2+}-channel activity was inhibited by 1 uM ruthenium red and was stimulated by nucleotides, 1 mM ATP (Fig. 7.5). These Ca^{2+} channels are probably responsible for Ca^{2+} transport across the ER membranes and for the triggering of different processes related to excitability in nerve cells and the release of neuromediators in the synaptic terminals. The similarities between the unit conductances as well as the kinetics of the Ca^{2+} channels in SR and in ER membranes are interpreted in terms of a common Ca^{2+}-channel mechanism controlling the excitation-contraction coupling in muscle cells, as well as the excitation-secretion coupling in nerve and other cells. In a separate series of experiments, it was found that in the presence of brain tubulin (spread on the surface as a component of the monolayer or added to the aqueous subphase underlying the surface film), the brain ER Ca^{2+}-channel activity reconstituted in patch clamped bilayers was substantially increased. The opening probability (P_O) was almost two times higher when tubulin was added. We suggested that tubulin, which is available as peripheral or even as an integral protein in the brain microsomal membranes may be related in some way to the regulation of their Ca^{2+}-channel activity.

In previous studies it was found that microtubules may mediate interactions between two apposed BLMs. Colchicine was shown to inhibit this effect. Dielectric breakdown measurements were carried out which confirmed the evidence that the microtubules can physically interconnect two membranes. Further, brain tubulin may influence the current-voltage relationships, the dielectric breakdown voltage, and other characteristics of brain lipid BLMs. Further experiments were tried to verify that channel activity is available in BLMs containing only microtubule proteins and defined lipid molecules. Some lipid molecular species remain associated to microtubule preparations even after a careful isolation of the proteins. The presence of these lipids may be one of the factors determining the assembly of the microtubule protein fractions into membrane-like sheets and vesicular formations under defined conditions. This finding allowed us to suggest that a hydrophobic fraction containing membrane tubulin and associated lipids may be prepared from isolated microtubule materials.

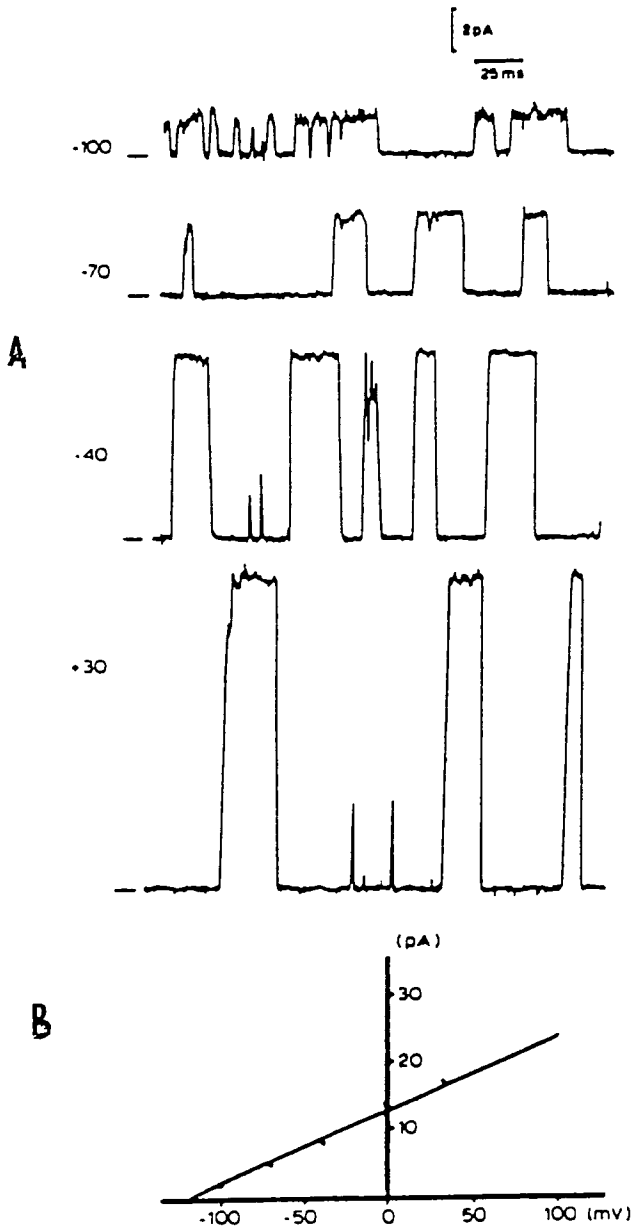

Fig. 7.5 Single Ca^{2+} channels from brain microsomal membrane reconstituted in BLMs. (A) Representative single-channel current traces at four different applied voltage. (B) Single-channel current-voltage relations.[72]

We succeeded in isolating such a hydrophobic fraction from a pellet obtained after two cycles of tubulin polymerization and depolymerization. The BLMs prepared from these materials on the tips of patch-clamp micropipettes were stable and gigaohm seals formed readily. We then studied single-channel activity in these membranes under the same conditions used in previous investigations on reconstituted Ca^{2+} channels from brain microsomal membranes.

Striking similarities were found between the characteristics of the Ca^{2+} channels in BLMs made from materials containing microtubule proteins and those in BLMs from brain microsomal components. The current-voltage relationships, single-channel conductances and the time constants describing the channel kinetics in the two types of membranes were similar. One of the differences was related to the stimulating effects of nucleotides. Guanosine 5'-triphospate (GTP) exerted a more prominent stimulating effect on the Ca^{2+}- channel activity in the BLM containing microtubule components. This may be attributed to the specific role of GTP in tubulin structure and functioning. From these findings we suggest that some microtubule protein fractions may be involved in the regulation of the Ca^{2+}-channel mechanism in intracellular membranes. Further detailed studies shall be needed to define the structural relationships between channel molecules and tubulin subunits as well as those of microtubule-associated proteins (MAPs). It is also noteworthy that low concentrations of Ca^{2+} exert a dramatic influence on microtubule structure.[72] Micromolar [Ca^{2+}] can induce disassembly of the microtubules. Thus, low- as well as high-affinity Ca^{2+}-binding sites are available in the tubulin molecules. The Ca^{2+}-modulated microtubule depolymerization, integration of tubulin molecules into membranes, and defined Ca^{2+}-transport mechanisms may be interrelated events. One of the physiologically important Ca^{2+}-binding proteins, calmodulin, was found tightly associated with microtubule proteins. Calmodulin-dependent protein kinases can interact with the MAPs, and calmodulin antagonists, such as trifluoperazine, were found to influence Ca^{2+}-transport events. A trifluoperazine-induced inhibition of the activity of brain microsomal Ca^{2+} channels which confirms the importance of the cytoskeletal proteins for the Ca^{2+}-channel mechanisms was also observed [Harris and Etemadi, 1989; Narahashi, 1992].

Highly functional Ca^{2+} channels from cardiac sarcolemma were incorporated into BLM in a study by Rosenberg et al. The reconstituted channels shared most of the typical Ca^{2+}-channel properties of the native cardiac cellular membranes:[72]

- Slope conductances of 23 pS in 100 mM Ba^{2+} and 7 pS in 100 mM Ca^{2+} were typical for L-type Ca^{2+} channels in cardiac sarcolemmal membranes.
- Characteristic kinetics of Ca^{2+}-channel gating in the presence of Ba^{2+} and the dihydropyridine Ca^{2+} agonist Bay K8644 were found. The mean open time was 20 msec, with long-lasting opening events being promoted by the agonist.
- A much faster inactivation in the presence of Ca^{2+} was found.
- Steepness and voltage-dependence of activation was typical for the L-type Ca^{2+} channels.
- A full block was produced by 6 μM nimodipine, a dihydropyridine Ca^{2+} antagonist added to both sides of the bilayer in the presence of Bay K8644.
- Block produced by Cd^{2+} induced a noisy open-state current. Cd^{2+} (30 μM) exhibited a 50% inhibition of the single-channel current in the presence of 100 mM Ba^{2+}, which coincides with the findings in cell-attached patches.
- The channels exhibited perfect divalent cation selectivity, the permeability ratio P_{Ba2+}/P_{K+} being 2800:1.

The channel was found to be functionally symmetric under symmetric ionic conditions. Several substantial differences also exist between the characteristics of Ca^{2+} channels derived from cardiac and skeletal muscle sarcolemma:

1. The unit conductance of the skeletal muscle Ca^{2+} channel (10.6 pS) is less than half that of the cardiac membrane channel (22.7 pS).
2. The cardiac and skeletal muscle membrane Ca^{2+} channels display dif ferent gating behavior.
3. The skeletal muscle Ca^{2+} channel shows slower activation and longer mean open times.

On the basis of these findings a structural diversity among Ca^{2+} channels in different membranes may be suggested. Sarcolemmal Ca^{2+} channels from porcine left ventricle were incorporated into patch-clamped bilayers in a study by Ehrlich et al[76] and it was found that, similar to the channels in the native membrane, the reconstituted Ca^{2+} channels are: (1) regulated by voltage, (2) stimulated by Bay K8644, (3) reversibly blocked by nitrendipine (5 μM), (4) selective for divalents with a permeability ratio of $Ba^{2+}Ca^{2+}/Mg^{2+} = 1 : 0.45 : 0.08$, and (5) with a slope conductance of 6 to 9 pS. An interesting effect concerning the blocking action of two stereoisomers of the verapamil analogue, D-600, was also found. One of the stereoisomers, (-) D-600, induced a more prominent block of the Ca^{2+}-channel activity than the other, ($^{+}$) D-600, which correlates with the differences in the binding abilities of the two agents to the channel receptor sites as well as with their physiological actions in heart muscle. Cardiac action potentials are inhibited to a much greater extent by (-) D-600 than by ($^{+}$) D-600. The former agent also induces a 100-fold greater negative inotropic effect in heart muscle. The effect of D-600 on Ca^{2+} channels reconstituted from skeletal muscle transverse tubules was studied by Affolter and Coronado.[28] This agent as well as its charged membrane-impermeable derivative, D-890, substantially reduced the Ca^{2+}-channel activity. Their effects on the reconstituted channels were similar to those found in experiments on cellular preparations:

- D-600 blocked the reconstituted channels with a half maximal blocking dose of 5 μM. In whole skeletal frog muscles this dose was 13.4 μM
- D-600 exerted similar blocking effects when added on either side of the bilayer.
- D-890 effectively blocked the Ca^{2+} current only when added to the "cytoplasmic" side, which correlates with findings in isolated cardiac cells. Its half maximal blocking dose was 3 μM. The mechanism of action of D-890 remains little understood, but obviously the positive charge of its molecule plays some important role.

A different type of Ca^{2+} channel was also shown to be present in skeletal muscle SR membranes by Smith et al [Harris and Etemadi, 1989; Narahashi, 1992]. Similar to their native membrane correlates the SR Ca^{2+}

channels incorporated into BLM were activated by 1 mM ATP and blocked by 1 μM ruthenium red and Mg^{2+}. Their unit conductance, 170 pS in 50 mM Ba^{2+} and 125 pS in 50 mM Ca^{2+}, is much larger than that of the sarcolemmal Ca^{2+} channels. Ca^{2+} channels with similar properties were also characterized in cardiac SR membranes reconstituted in BLM. The channels were activated by micromolar [Ca^{2+}] on the same "cytoplasmic" side of the membrane, and inhibited by ruthenium red and ryanodine.[72]

After analyzing the interrelations between the Ca^{2+} and the voltage dependence of the channels, Vergara and Latorre proposed a model explaining the activation kinetics by two voltage-dependent Ca^{2+}-binding reactions [*see* Harris and Etemadi, 1989; Narahashi, 1992]. The channel transitions between the open and the closed states are due to a conformational change of the channel protein molecule that is not controlled by the voltage.

Anion channels and other channels

Chloride (Cl^-) channels

A Cl^- channel was characterized in BLM reconstituted with calf cardiac sarcolemma [Harris and Etemadi, 1989; Narahashi, 1992]. The analysis of the channel kinetics and of the probability histogram revealed that the channel fluctuates between two closed states and three open states with conductances of 15, 39, and 61 pS. The current-voltage relationship showed that the current saturates at high positive potentials, while at negative potentials it does not saturate, but increases nonlinearly. The reversal potential was almost the same as the expected diffusion potential in the absence of cations. The physiological role of this channel remains unclarified owing to the lack of sufficient information on similar channels in native membranes.

A new method for analyzing channel gating kinetics was proposed by Labarca et al after analyzing the well-defined characteristics of the two-state cholinergic receptor channel and the three-state chloride channel from

Torpedo californica electroplax membrane. Autocorrelation and autocovariance functions were used for obtaining information about the pathways connecting the channel's open and closed states [*see* Harris and Etemadi, 1989; Narahashi, 1992].

A Cl^- channel is available in the cytoplasmic membrane of the electric organ of *Torpedo californica*. It is responsible for the control of the resistance of the electroplax cells serving as a source of the electric current. This Cl^- channel has been reconstituted in BLM and its properties have been profoundly analyzed in several studies [Harris and Etemadi, 1989; Narahashi, 1992]. Several specific features of the channel were demonstrated:

- Bursting activity with four conductance states including two open states, 10 pS, and 20 pS, and two nonconducting states with largely differing lifetimes, 10 and 500 msec.
- Voltage dependence of the gating process.

Specific block by several compounds:

- 4,4'-diisothiocyano-2,2'-stilbenedisulfonate (DIDS),
- 4-acetamino-4'-isothiocyano-2,2'-disulfonic acid (SITS) and SCN.
- Activation by protons.

The effect of low pH is observed only when the pH changes are provoked on the side of the BLM which was exposed to the added electroplax vesicles. DIDS also exhibits inhibitory activity only when added to the same side as the vesicles. About 5 sec after its addition, the higher conductance state disappears and only the 10 pS state resides. The channel activity disappears entirely about 25 sec later. Miller and White interpreted these effects in favor of a model for the Cl^- channel based on a dimeric channel complex spanning the membrane [*see* Harris and Etemadi, 1989; Narahashi, 1992]. They proposed that the Cl^- channel operates as a dimeric complex consisting of two identical subunits, protochannels. Every protochannel opens and closes independently in the range of milliseconds,

but both protochannels may enter and leave an inactivated state on a lower time scale. Further, it has been suggested that another anion-transport complex, the erythrocyte Cl^- exchange system, operates in a similar way as a functional dimer. The oligomeric structures of the transport protein assemblies obviously are quite important for their functional activities.

A Case Study of Anion Channel Reconstitution using the Planar Lipid Bilayer (BLM)[83]

A chloride channel from liver sarcoplasmic reticulum (SR) was embedded into a BLM and its electrical properties determined. Though highly permeable to K^+, the liver ER (endoplasmic reticulum) membrane has been postulated to lack an efficient ion conducting structure for K^+ channel in the SR. The present study was undertaken with the aim to look at the anionic, Ca^{2+} and K^+ permeability pathways present in the ER membrane. The reconstituted system exhibits considerable anionic permeability following the sequence: $SCN^- > I^- > Br^- > Cl^-$ > gluconate. The findings suggest the chloride channels have low field-strength sites. It can be pharmacologically dissected to Zn^{2+}-sensitive and DIDS-sensitive types. The gating of the channel is weakly voltage-dependent and at higher positive or negative voltages the channel prefers the low sub-conductance states. This study is described here in some detail to illustrate how a membrane reconstitution study is carried out using experimental lipid bilayers.

Materials and Methods

Isolation of Rough ER Vesicles from Rat Liver. Adult male PragueDawley rats weighing 200-250 g were used. The animals were fasted for 20 hr before sacrifice. Rough ER vesicles were isolated. Minced livers were homogenized gently in 0.44 M sucrose, 2 g/10 ml, in a Teflon-glass homogenizer (4 x 400 rpm). After the first centrifugation at 10,000 g for 20 minutes, the supernatant was diluted with 0.44 M sucrose to restore the original volume. Of this suspension, 8 ml was layered over 3 ml of 1.31 M sucrose and centrifuged at 105,000 g for 7 hr. 40 min in a Sorvall ultracentrifuge. The upper 0.44 M sucrose phase is removed. The milky layer localized in the upper part of 1.3 M sucrose phase, which is in the

process of sedimenting down, is removed, and recentrifuged at 105,000 g for 90 min after dilution with 0.25 M sucrose containing 0.15 M KCl. It contains the smooth microsomes. The 1.3 M sucrose layer is removed and discarded, but the fluffy layer just above the pellet is left behind and is rehomogenized by hand together with the pellet, after the addition of a few drops of water, and centrifuged at 105,000 g for 90 min. It contains rough microsomes. All the solutions contained the protease inhibitors: 500 μg/ml EDTA, 0.5 μg/ml leupeptin, 0.7 μg/ml pepstatin, 100 μg/ml phenylmethylsulfonyl fluoride. After protein estimation, the smooth and rough microsomes are divided into small aliquots of 100 μl (10 mg/ml), quickly frozen in liquid N_2, and stored at –80 ^{o}C. Protein was estimated using bovine serum albumin as the standard.

Assay for Marker Enzyme. NADPH-dependent cytochrome c reductase (marker enzyme for ER) activity was determined by colorimetric measurement of cytochrome c reduction in the presence of sodium azide and NADPH.

The BLM Setup for Electrophysiological Measurement. Electrical properties of reconstituted BLMs were investigated using a setup shown in Fig. 7.6. Many modifications have been made to the BLM chamber, but the basic idea has remained essentially the same.[2] Ag/AgCl electrodes encased in 0.2 M KCl, 2% agar-filled lengths of polyethylene tubing, are inserted into each chamber for the purpose of applying and recording voltage pulses. Fig.7.6 is a schematic diagram of a data recording, storage, and acquisition system. The command voltage is applied to and current measured across a BLM by a Dagan 8800 total clamp system. The data is monitored on the scope and simultaneously fed to a pulse code modulator (Neurocorder DR 484) and stored on a VCR (Hitachi). The Dagan total clamp system also has a direct current readout monitor. The data from the VCR is acquired off-line using a data acquisition board (Labmaster Scientific Solutions, Inc.), and a data acquisition program (PCLAMP, Axon Instruments). During acquisition, amplified current from the VCR is filtered at 1 kHz through an 8-pole low pass Bessel filter (model 902, Frequency Devices). Output is also acquired in some cases, on a fast strip chart recorder (Gould 2400S).

Cell Chambers for BLM Studies. Two types of BLM cells were used. In the first type, a polytetra-fluoroethylene (PTFE) film of 50 μm thickness, on which a hole (200-300 μm diameter) has been punched by a leveled and electrically sharpened hypodermic needle, is clamped between two communicating Perplex chambers (volume of each is 2 cc). The second type consists of two chambers formed by a polystyrene cup (volume 2 cc) inserted into a doubly cut-away polyvinylchloride (PVC) block. Very clean circular holes can be made on a PTFE film as follows:

(1) A hypodermic needle (27 gauge) is leveled by rubbing on a fine silicon carbide coated paper,
(2) Sharpening is conducted in 5 M HCl solution applying 1.5 V (with the positive pole connected to the needle) and by repeated immersion and removal of the needle tip, and
(3) The PTFE film is supported on a new Plexiglas plate. The needle is mounted on a syringe and is brought down on the PTFE film. The hole is cut by a single turn around the axis. The quality of the hole is checked under a microscope, but the ultimate test is the ease of forming BLMs and their resistance and stability. The films are washed in 5 M KOH; chromic acid; hot water; distilled water; chloroform-methanol, 2:1; and n-hexane and then dried in air before use. Clean circular holes of diameters ranging between 50-250 μm can be made on a polystyrene cup as follows:

a) First make a protrusion on the outside wall of the polystyrene cup (wall thickness ~ 1 mm) by pressing a heated blunt needle (450 ^{o}C) against the inner wall and advancing it forward until a slight protrusion can be felt on the outside wall by touching,

b) Slice off the protrusion with a sharp microtome blade until a circular hole of proper size (100-200 μm) is exposed, and

c) Heat polish the hole to make it smooth. Each cup is inspected under a microscope to ensure that the hole is free from dirt and that cracks have not formed along the edge of the hole. The cup is soaked in 4 percent liquid detergent for 3-4 hrs.; washed under running tap water for ½ hr; soaked in distilled water for ½ hr; given a few more rinses in distilled water and finally dried in air.

A Typical Protocol for a BLM Reconstitution Experiment

BLM Forming Solution. A BLM forming solution is made by pipetting chloroform solutions of lipids into glass vials with a PTFE-lined stopper. The chloroform is evaporated with argon, the vial is evacuated for 20 min., and the lipids are resuspended in n-decane (40 mg/ml). A lipid mixture of PE:PS:PC (5:3:2) was used in all experiments.

Preconditioning the Hole. Before painting a BLM-forming solution across the hole, it is necessary to precondition the hole with a little BLM forming solution to facilitate membrane formation. About 0.5 μl of the BLM-forming solution is squirted into the hole, and a gentle stream of argon is directed toward the hole for 3-4 min.

Bilayer Formation, Fusion and Recording Buffers and Current-Voltage Measurements. The BLM is made in a symmetrical bathing solution of 50 mM choline chloride plus 2 mM calcium chloride that is limited to 2 mM (it is needed to promote the prefusion step), since it is known that ER vesicles aggregate in high concentrations of calcium. ER vesicles that normally need a final centrifugation of about 100,000 g to pellet them, can be pelleted at relatively low speed (27,000 g) by making microsomal aggregates in the presence of 8 mM calcium. To make the BLM, a small amount of BLM forming solution is drawn into a micropipette tip and squirted out. The pipette tip is dipped in one of the aqueous chambers of the BLM setup and pressing the piston of the pippetor blows a bubble. The bubble is then smeared across the hole to make a BLM. The pipette tip is discarded after each use. Initially, a thick layer is formed at the orifice, and in reflected light, interference colors can be seen. At this stage, the capacitance of the lipid film is low. In a few minutes, the lipid film starts thinning to a bilayer state. The BLM looks grayish-dark in reflected light. Sometimes, the multilayer to bilayer transition can be initiated by applying an electrical potential of 100 mV or by poking with one hair of a sable brush. Membrane resistance is measured by applying a potential of $\pm$100 mV and measuring the resulting current. A typical orifice which has a diameter of

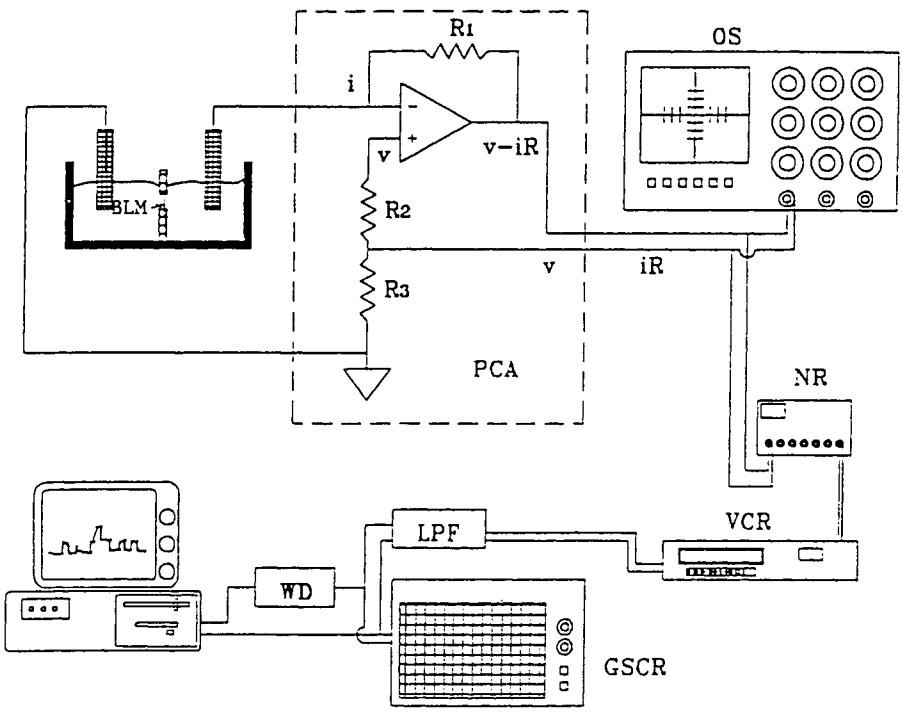

Fig. 7.6 A BLM Setup for Electrophysiological Measurement. R - Feedback resistor; V - Command voltage; i - Measured current; R_2, R_3 - Voltage dividing resistors for command voltage; OS – Oscilloscope; NR - Neurocorder; VCR - Video recorder; WD - Window discriminator; PCA - Patch clamp amplifier; LPF - 8 pole low pass Bessel filter; GSCR - Gould strip chart recorder.

187 μm gives a current of ± 0.4 pA when ± 100 mV is imposed across the membrane. This calculates to a specific resistance of 0.68 x 10^8 Ω.cm which is in good agreement with literature values.[26] The capacitance is measured by applying voltage pulses of 200 μV. An integral of the current divided by the voltage gives the capacitance of the BLM:

$$C = \frac{\Delta Q}{\Delta V} = \frac{\int I\,dt}{\Delta V} \qquad (7.18)$$

The capacitance value is about 0.7 μF/cm^2, again in good agreement with literature values.[26] Before every fusion protocol, the BLM was characterized optically and electrically (measuring capacitance and resistance of the BLM). In some of our initial experiments, to further prove that we had a BLM, we added a small quantity of gramicidin D (the bathing solution was 3 M KCl for gramicidin D experiments) and channel activity was recorded. Gramicidin channels are active only if it is a BLM.The fusion protocol was initiated by raising the *cis* choline chloride concentration to 250 mM, by adding from a stock solution of 2.5 M choline chloride. The stirrer was switched on and after a few minutes, 15-20 μl of rough ER vesicles were introduced into the *cis* chamber. A membrane potential of –40 to –60 mV was applied to the *cis* side to aid fusion. Occurrence of fusion was shown by stepwise abrupt current changes. After fusion had occurred, the stirrer was switched off, and to expose the $InsP_3$-gated and/or ryanodine-gated calcium channels, the *cis* chamber was perfused with a solution of 60 mM pipera-zine-N,N'bis (2-ethanesulfonic acid) (PIPES) + 88 mM bistrispropane (BTP) + 0.1 mM $Ca(OH)_2$ + 0.1 mM EGTA (pH 7.4 and free calcium concentration 2.5 μM). The *trans* side was perfused with a solution having composition: 60 mM PIPES $^+$ 55 mM $Ca(OH)_2$ (pH 7.4). During perfusion, the *cis* side was electrically shorted to the *trans* side. Our success rate of perfusing both chambers and leaving the BLM intact was very low. So, we modified the above procedure and designed a protocol, so that we have to perfuse only the *cis* side of the BLM. In our modified procedure, BLMs were made in a symmetrical solution having the composition: 5 mm N-[2-hydroxyethyl] piperazine N'-[2-ethane sulfonic acid] (HEPES) + 1.3 mM $Ca(OH)_2$ (pH 7.4) or 2.2

mM PIPES + 2 mM $Ca(OH)_2$ (pH 7.4). After resistance and capacitance measurement characterized the BLM, 100-200 µl of 4 M KCl (or K-acetate) was added to the *cis* side making the final *cis* KCl (or K-acetate) concentration 200-400 mM. After fusion, the *cis* solution was perfused with the solution having 2.5 µM free calcium, the *trans* calcium concentration could now be raised to the desired level by adding from a concentrated stock solution of PIPES + $Ca(OH)_2$ or HEPES + $Ca(OH)_2$. The above two-step protocol was necessary to fuse the ER vesicle and look for any calcium channel. For measurement of Cl current, the bathing solution had the composition 5 mM HEPES + 1.3 mM $Ca(OH)_2$ + 2 mM KCl (pH 7.4). After BLM formation and characterization, the *cis* KCl concentration was raised to 200-400 mM by adding 100-200 µl from a stock solution of 4 M KCl. After fusion of one or more vesicles, further fusion is prevented by stopping the stirrer and abolishing the osmotic gradient by adding sucrose solution to the *trans* side. For current measurement under bi-ionic conditions, the other salt solution is added to the *trans* side. In some of our experiments, we have perfused the *cis* side after fusion and have increased the *cis* and *trans* KCl concentration symmetrically by adding from a stock solution of 4 M KCl. In another set of experiments to study the Cl channel, we have used symmetrical 10 mM Tris-HCl as the bathing solution. Fusion of rough ER vesicles with the BLM was achieved by adding 100-200 µl of 4 M KCl solution to the *cis* side (final KCl concentration: 200-400 mM). After one or a few vesicles had fused, the *cis* side was perfused with 10 mM Tris-HCl to stop further fusion. Then, KCl was added from a 4 M stock solution to the *cis* and *trans* side to symmetrically raise KCl concentration from 0 to 500 mM in steps of 50 or 100 mM. The selectivity sequence of the various anions were found by measuring the reversal potential under bi-ionic conditions and applying the Goldman-Hodgkin-Katz (GHK) equation.[50]

Fusion of ER Vesicles with the BLM. The mechanism of fusion is still unknown in detail, but empirical information acquired over the past 15 years has led to a set of conditions under which membrane vesicles or liposomes can be induced to fuse with planar BLMs. In all our experiments, we have designed and followed protocols to directly fuse the liver rough ER vesicles to a preformed planar BLM to delineate the calcium and

chloride ionic pathways of the rough ER membrane.

Fusion of vesicles with a planar BLM has been shown to consist of two experimentally distinguishable steps. In the first, a very tight, close, and irreversible association between the vesicles and the BLM is formed. If the vesicular and/or planar membrane contains negatively charged lipids, the addition of millimolar levels of divalent cations promotes this step. In choosing divalent cation concentration, adsorption of vesicles to the BLM must be weighed against vesicle-vesicle aggregation. Divalent cations induce vesicle aggregation as well as planar membrane adhesion and aggregated vesicles fuse poorly. The association between vesicle and BLM in the "prefusion" step is not a point contact but rather an adhesion of a substantial fraction of the vesicle with the bilayer. Proteins such as fibronectin can also be used to induce adhesion. In the second step, the actual fusion of vesicular and planar membrane takes place. For the second fusion step to occur, in most cases it is necessary that an intravesicular hydrostatic pressure develops within those vesicles that are in the prefusion state. This pressure is routinely induced by osmotically swelling the vesicles and when lysis occurs in the region of contact between the vesicle and BLM, fusion occurs. The osmotic swelling of the vesicle is easily achieved by establishing an osmotic gradient across the planar BLM, *cis* side (the side to which vesicles are added) hyperosmotic with respect to the *trans* side. Water then flows from *trans* to *cis* and a fraction of it enters the vesicles in the prefusion step and causes them to swell. The osmotic gradient can be easily imposed across the BLM by simply adding an osmoticant to which vesicles are added. Since the net role of the osmoticant is to cause swelling of the vesicles, it is necessary that the vesicle membrane be permeable to that osmoticant. Addition of vesicle--impermeant osmoticant will cause net shrinkage of the vesicles and will not promote fusion. The osmoticant also must not be too permeant through the BLM. If the osmoticant is too permeant through the BLM, it will be dissipated across the unstirred layers adjacent to the membrane and there will not be adequate net movement into the vesicle to cause swelling. Urea and glycerol fit into the above criteria and are good osmoticants. If the vesicular membrane has channels that allow salts to enter the vesicles, then permeant salts can be used to osmotically swell the vesicles. A 200-600

μM gradient across the BLM is generally sufficient to induce fusion. Vesicles should be added to the *cis* side with continuous stirring. Stirring promotes adsorption of vesicles to BLMs. Vesicles can also be injected from a micropipette very near to the BLM. The probability of fusion is much higher using this method. When vesicles are added to the bulk aqueous phase, a final concentration of 1-10 μg/ml is generally sufficient.

For fusion to occur, the type of lipid used to make BLM is very important. Phosphatidylethanolamine (PE) is a better phospholipid than phosphatidylcholine (PC) for promoting fusion. On the other hand, PC imparts stability to the BLM. A stable BLM is very desirable so that it can withstand the various manipulations during experimentation. As mentioned earlier, sometimes it is necessary to incorporate a negatively charged lipid like phosphatidylserine (PS) in the BLM-forming solution to promote the prefusion step. BLM-forming solutions are normally made in *n*-decane (or *n*-dodecane) with or without cholesterol. A lipid concentration of 15-50 mg/ml in *n*-decane is normally used as a BLM forming solution. When cholesterol is included in the BLM forming solution, the molar ratio between lipid and cholesterol is kept about 2:1 or 1:1.

An important step in the BLM-vesicle fusion protocol is to stop further fusion after one or more vesicles have fused with the BLM. Fusion is stopped by abolishing the osmotic gradient and by adding the osmoticant to the *trans* compartment. Stopping the stirrer also halts further fusion. After fusion has been stopped, the *cis* solution which contains unfused vesicles can be perfused with fresh solutions.

Results

Assay of Marker Enzyme for ER. NADPH-dependent cytochrome c reductase activity was determined by colorimetric measurement of cytochrome c reduction in the presence of sodium azide and NADPH. The optical density of the incubated mixture at 25 ^{o}C, was routinely measured at 550 nm as a function of time, leveling off after abut 15 min. The mixture contained the smooth ER vesicles. Taking the extinction coefficient for cytochrome c as 18.5 mM^{-1} cm^{-1} and using the initial linear portion of the curve, we can calculate the cytochrome c reductase activity in the smooth

microsomes to be 54 nmoles/min/mg protein. A similar curve was obtained with the cytochrome c reductase activity of the rough ER vesicles at 25 ^{o}C (leveling off after about 70 min) and from the linear portion of the curve, we can calculate a specific activity for cytochrome c reductase in the rough ER membrane as 16.8 nmoles/ min/mg protein. Smooth to rough ratio of NADPH-dependent cytochrome c reductase activity is calculated to be 3.31 and is close to the value 3.5. reported for the above enzyme in the rabbit liver. The specific activity of the enzyme in rat liver microsomes as reported in literature, is 90 nmoles/ min/mg at 30 ^{o}C and assuming a Q_{10} of 2.5 for this enzyme, our values are within reasonable limits.

Characterization of a BLM. A BLM forming solution of PE:PS:PC in the ratio of 5:3:2 in n-decane (40 mg/ml) is used for making the BLM. The BLM is made in symmetrical 50 mM choline chloride solution. It is monitored optically as well as by measurement of electrical parameters like resistance and capacitance. The conductance calculated from the slope of the curve is about 3-5 pS. A typical BLM of 200 μm diameter has a resistance of about 250 GΩ and one can calculate a specific resistance of 2.5×10^7 Ω.cm. The capacitance of the BLM was measured by applying a voltage pulse of 200 μV and measuring the integral of the capacitative current transient. The resultant ΔQ divided by ΔV gives the capacitance of the membrane. Most of our BLMs had a capacitance between 0.55 – 0.7 μF/cm^2. To further prove that we have a BLM, we incorporated gramicidin channels in a BLM. Such current transitions were obtained at 250 mV in 3 M symmetrical potassium chloride solution. From the current amplitudes, one can calculate a conductance of 25 pS which is very close to the value found in literature.

Incorporation of ER Vesicles in a BLM in Asymmetric Choline Chloride Solution. After a BLM formation, the *cis* choline chloride concentration is raised to 250 mM to provide the osmotic gradient. Fusion usually occurs in 1-2 min. Typical fusion events were obtained (not shown), in which the y-axis denotes the current across the BLM and the x-axis the time. The holding voltage is zero mV. At the beginning of the record, the current is almost zero and it changes in stepwise fashion in an outward direction when a vesicle fuses with the BLM. Since there is a choline chloride

gradient from *cis* to *trans* and the current is outward, we can conclude that the majority of the charge carriers are chloride ions. When the choline chloride gradient is abolished by raising the *trans* choline chloride concentration to 250 mM, the current goes back to zero.

A few typical current-voltage curves of BLMs reconstituted with liver ER vesicles in asymmetric choline chloride solution (*cis*-250 mM, *trans* – 50 mM) were obtained. The reversal potential is at 25 mV. If chloride ions are the only charge carriers from Nernst equation, we can calculate a reversal potential of 41 mV. Since the observed potential is 25 mV, it suggests an appreciable choline permeability through the chloride channels. Applying the GHK equation,[50] written for a bi-ionic situation, in which the only species are choline and chloride:

$$V_{rev} = \frac{RT}{F} \ln \frac{P_{choline}\,[choline]_t^{+}\, P_{Cl}\,[Cl]_c}{P_{choline}\,[choline]_c^{+}\, P_{Cl}\,[Cl]_t} \qquad (7.19)$$

where V_{rev} = 25.4 mV at 22 ^{o}C, the subscripts on the concentration terms refer to *cis (c)* and *trans (t)* and P_{Cl} and $P_{choline}$ are the respective permeabilities for chloride and choline ions. A quick calculation shows that $P_{Cl}/P_{choline}$ is about 5. A series of current-voltage curves of a BLM reconstituted with liver ER vesicles in asymmetric choline chloride solution were also obtained (not shown). After reconstitution, when the ionic gradient is abolished by raising *trans* choline chloride concentration to 250 mM, the reversal potential becomes zero.

Perfusion of the cis and trans Chambers with Only Calcium Containing Solutions. The protocol for this is schematically shown in Fig. 7.7. Briefly, after a fusion has occurred, the *trans* side is perfused with a solution containing 60 mM PIPES $^{+}$ 55 mM $Ca(OH)_2$ (pH=7.4) and the *cis* side is perfused with a solution containing 60 mM PIPES + 88 mM BTP + 0.1 mM $Ca(OH)_2$ + 0.1 mM EGTA (pH=7.4). During perfusion, the *cis* and *trans* chambers were shorted. Because of our success rate in obtaining intact BLMs after perfusing both sides, we modified the fusion protocol as

shown in Fig. 7.7. Current-voltage curves were obtained, using choline chloride, potassium acetate, and KCl, respectively as an osmoticant. A general feature of the current-voltage curves is that, there is no true reversal potential. This is expected when choline chloride or potassium acetate or potassium chloride are used as osmoticant, and are not present in the *trans* side. The current-voltage curve approaches voltage axis asymptotically. The apparent reversal potential is between 80-120 mV.

Looking for an $InsP_3$-Gated Calcium Channel in the Liver ER Membrane.

Fig. 7.8 depicts the results of a typical experiment performed to look for $InsP_3$-gated calcium channels in the liver ER membrane. After fusion of a vesicle, the *cis* chamber was perfused with solution having a free calcium of 2.5 μM and a *trans* calcium level which was raised to 23 mM. The conductance of the membrane dropped to about 30 pS. No calcium channels were seen when the membrane was challenged with 10 uM $InsP_3$. But the membrane conductance to acetate remains intact and it comes back to the original level as the potassium acetate concentration is increased in the *cis* side. After repeated attempts (n ~ 100), we failed to detect any $InsP_3$-gated calcium channel in the liver ER membrane. We also failed to notice any rynodine-sensitive Ca^{2+} channels though the appropriate concentrations of Ca^{2+} (2.5 uM) and adaenine nucletides was present (data not shown).

Chloride to Potassium Permeability Ratios of the ER Chloride Channels.

Reversal potential measurements were made in a number of experiments and P_{Cl}/P_K was calculated using the GHK equation in each case. The values (n = 36) are plotted in the form of a histogram in Fig. 7.9. The results indicate that the P_{Cl}/P_K values vary from 4 to 24. If P_{Cl}/P_K is one of the characteristic properties of a channel, our results indicate that we have many different types of chloride channels, or, we have at least two types of channels: one type having a low P_{Cl}/P_K. and the other a high P_{Cl}/P_K. The in-between values are different combinations of these two types of channels.

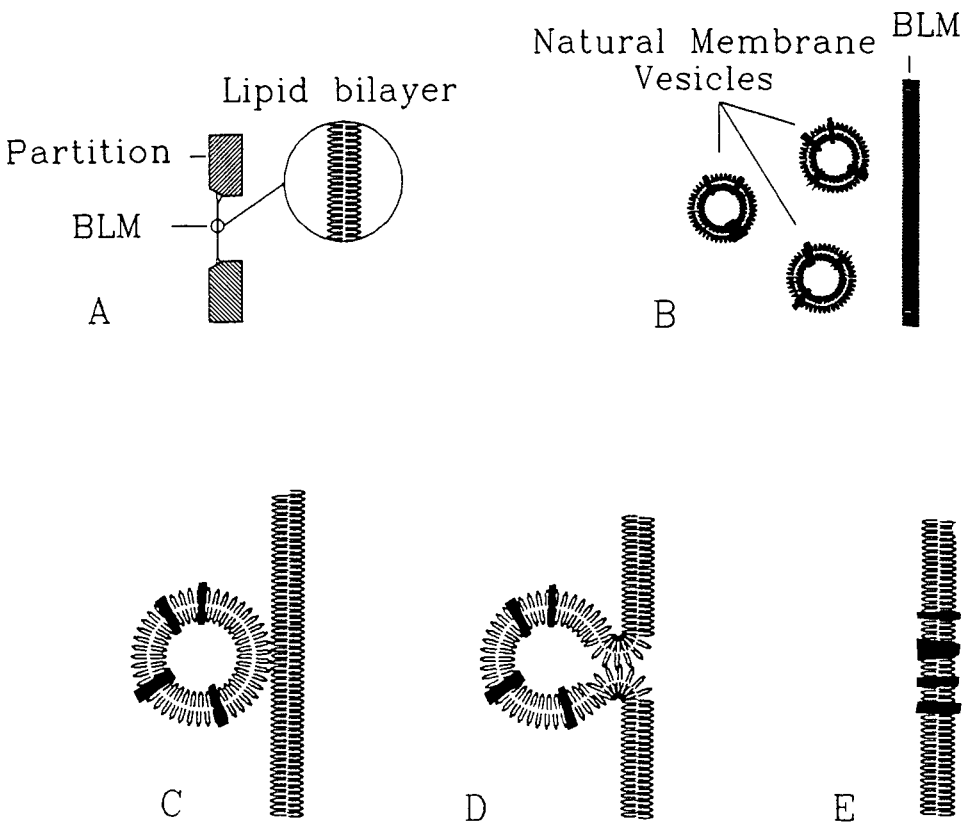

Fig. 7.7 Schematic representation of fusion of vesicles with a planar BLM. A – scheme of a BLM; B – initial stage; C – prefusion state; D – osmotic swelling of the vesicle and fusion; E – final stage: reconstituted BLM.

Permeability Ratios of Halides and Other Anions. A typical current-voltage curve of a reconstituted membrane having initially 402 mM potassium chloride in the *cis* side and 2 mM potassium chloride in the *trans* side is shown in Fig. 7.9. The reversal potential is gradually shifted toward zero mV, when potassium bromide solution is added to the *trans* side in increasing concentration. A (P_{Br}/P_{Cl}) value can be calculated in this case, using the GHK equation and including potassium, chloride and bromide as permeant ions. The results of a series of similar experiments, but having KCl, thiocyanate, and iodide as the permeant ions were obtained. Using the GHK equation, values for (P_{I}/P_{Cl}) and (P_{SCN}/P_{Cl}). can be calculated. Additionally, the results of a control experiment were obtained, in which thiocyanate, chloride and potassium are the ion species present, but the membrane is an unmodified one. In the control experiment the KI solution was one day old and one can see significant current across the BLM. As iodide is permeable through the BLM,[26] it is important that KI solution should be prepared immediately before use.

A compilation of ($P_{test\ anion}/P_{Cl}$) values and the Pauling diameters of the test anions may be found in a paper by Hille.[86] The anionic selectivity sequence follows the sequence SCN^- (2.68) > I^- (1.68) > Br^- (1.32) > Cl^- (1) > gluconate$^-$ (0.11). ($P_{test\ anion}/P_{Cl}$) and is calculated using activities based on available activity coefficients taken from the literature. According to the *Fixed Charge-induction Hypothesis*,[79] the liver ER vesicular chloride channel(s) exhibits a low field-strength permeability sequence for halides in which lower dehydration energy of the larger anions predominates over stronger Coulombic interaction energy of smaller anions in determining selectivity. This selectivity behavior is different from that of the chloride channel from *Torpedo californica* and the cystic fibrosis chloride channel.[83]

Inhibition of Chloride Conductance by Zn^{2+} and DIDS. Since some chloride channels are inhibited by Zn, we have studied the effect of Zn on the macroscopic chloride conductance of a BLM reconstituted with liver ER vesicles. Under our experimental conditions, 3.5 mM $ZnCl_2$ was sufficient to block all Zn-sensitive conductance.

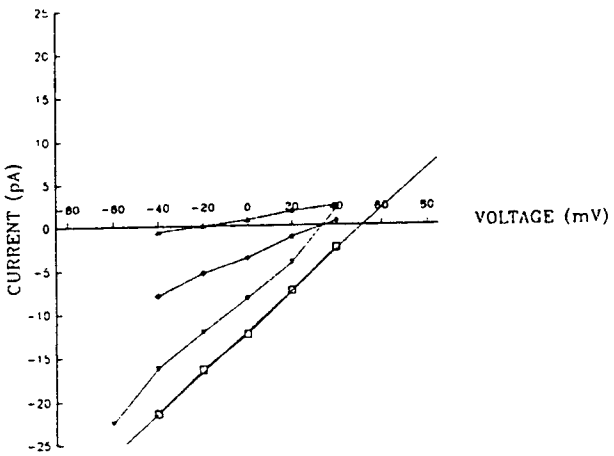

Fig. 7.8 A typical reconstitution experiment to reveal any $InsP_3$-gated Ca^{++} channel present in the liver rough ER membrane. The BLM was made in symmetrical 6.25 mM PIPES $^+$ 5.6 mM $Ca(OH)_2$.

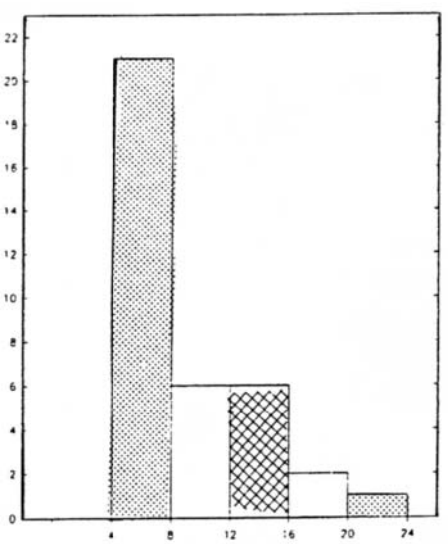

Fig. 7.9 Histogram of P_{Cl}/P_K values. Each value was obtained by reversal potential measurement in bi-ionic condition and calculated using the Goldman-Hodgkin-Katz equation.[50]

Table 7.2 is a As can be seen from the table, saturating concentrations of $ZnCl_2$ can block sometimes totally and sometimes partially, the chloride conductance of the BLM reconstituted with ER vesicles. This suggests that some of the vesicles which fuse with the BLM have only Zn-sensitive chloride conductance and some others have additional Zn-insensitive chloride conductance.

Table 7. 2 Compilation of the chloride conductances blocked by saturating concentrations of $ZnCl_2$. P_{test}/P_{Cl^-}

Test ion	Lobster neuron	Mouse Gly-R	Mouse Gaba-R	CFTR	CFTR (K95D)	SR	This study
SCN^-	n.d	n.d	n.d	n.d	n.d	1.45	2.68
I^-	2.70	1.80	2.80	0.59	1.43	1.39	1.68
Br^-	1.50	1.40	1.50	1.11	1.25	1.00	1.32
Cl^-	1.00	1.00	1.00	1.00	1.00	1.00	1.00
Gluconate$^-$	0.06	n.d	n.d	n.d	n.d	0.04	0.11

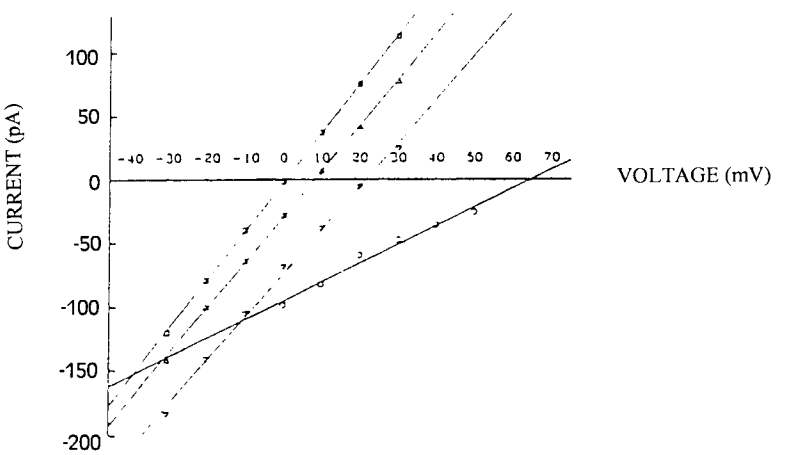

Fig. 7.10 Reversal potential measurement under near bi-ionic conditions (KCl *cis* side and KBr *trans* side) across a BLM reconstituted with liver ER vesicles.

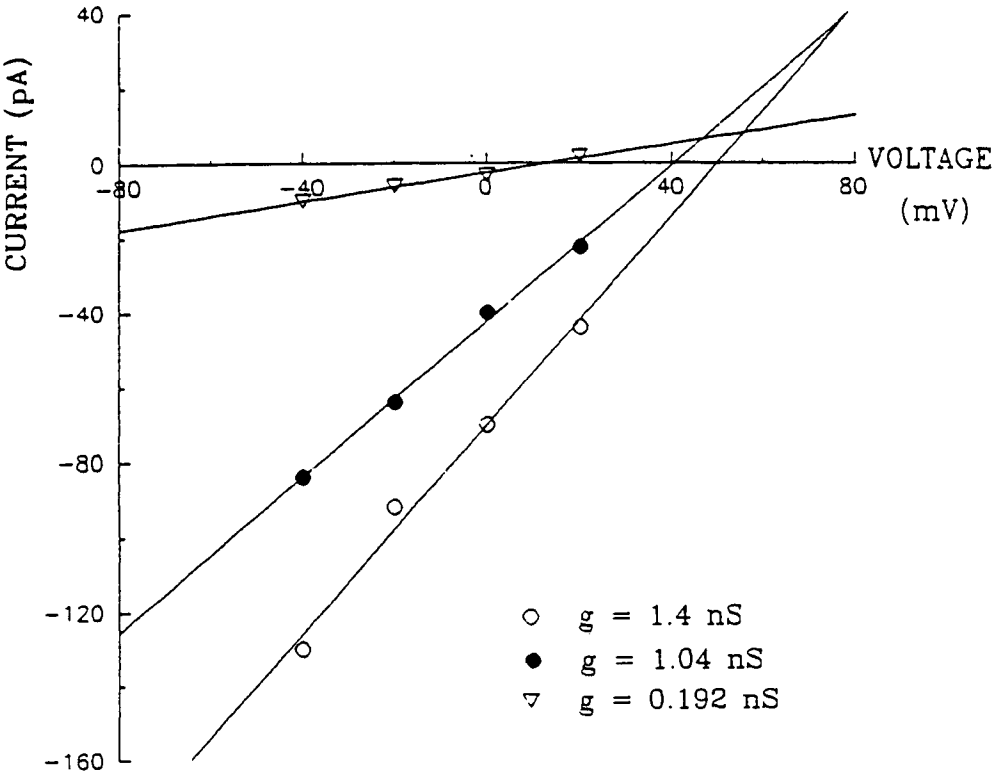

Fig. 7.11. Conductance inhibition by zinc and DIDS: Conductance of a BLM reconstituted with liver ER vesicles (-); Conductance after addition of 2.7 mM $ZnCl_2$ to *cis* and *trans* sides.

Since many anion transport systems and channels are inhibited by disulfonic acid stilbene derivatives, we studied the effect of DIDS 4,4'-diisothiocyanostilbene-2,2'- disulfonic acid) on the macroscopic chloride conductance of the reconstituted BLM. Fig. 7.11 shows a typical finding of the effect of DIDS on the macroscopic chloride conductance. In this particular case, 36 μM of DIDS blocked 75 percent of the chloride conductance and the rest could not be blocked by increasing DIDS concentration even up to 840 μM. This suggests that some of the ER vesicles in addition to having some DIDS- sensitive conductance, have residual DIDS-insensitive conductance.

In about 95% of the cases, we found that DIDS block occurred from the *cis* side. Next, we studied the effect of DIDS and $ZnCl_2$ together on the macroscopic chloride conductance of a BLM reconstituted with liver ER vesicles.

Studies at the Level of a Single Channel. These studies were very difficult to carry out. We followed the usual procedure of dilution and sonication of the ER vesicular sample. Since it is known that the ER vesicles aggregate upon dilution, the diluted and sonicated sample, probably, aggregates again when added to the *cis* chamber. In our fusion experiments, the minimum conductance in 363 mM symmetrical KCl solution which we observed, was between 550 – 600 pS. Some of these conductances could be totally eliminated by DIDS (n=2), and in some cases (n=2), the single channel activity could be totally eliminated by $ZnCl_2$.

Discussion

Typically a cell spends about one-third of its metabolic energy to maintain appropriate ion concentration gradients in ion channel across its membrane that involves ion channels. Ion channels are of paramount physiological importance in information processing and signal transduction such as conduction of nervous impulses, epithelial solute transport and the electrical activity of muscle. However, they are difficult to study *in vivo* owing to a number of factors. For example, the BLM technique has been found very useful in organelle or internal membranes that are not easily

accessible by the patch-clamp electrodes.[72] Earlier, the BLM-liposome fusion technique was used by Miller and Racker who found the so-called b-Cl- (for big chloride) channel* [60] and more recently Kourie, Laver and their colleagues.[9] Discovered the so-called s-Cl (s for small chloride) channel. Therefore, from a biophysical viewpoint, all sorts of ion channels have been embedded and reconstituted in BLMs and liposomes and investigated as such for more than two decades,[26] in particular since the advance of the patch-clamp technique.[72] Reconstitution of ion channels into planar lipid bilayers (BLMs) offers an added advantage in that it provides a practical approach for studying integral membrane proteins in a simple, chemically defined system in which fundamental mechanistic questions may be posed more easily than in the complicated native membrane. Moreover, the intracellular organelle membranes which are inaccessible to direct cellular recording can be studied using electrophysiological techniques after reconstitution in a BLM. In most applications, channels are transferred to the preformed BLM by fusing native membrane vesicles or liposomes containing purified channel proteins. There have also been attempts to make large vesicles from a population of smaller vesicles by repeatedly freezing and thawing the sample and then taking a patch out of the large vesicle. Another approach has been to make monolayers using the proteolipids extracted from native membranes and/or purified phospholipids and then to pick up two monolayers at the tip of a patch clamp micropipette to make a bilayer.[72] The method has been appropriately called "double tip-dip" method. As detailed in this paper, we preferred a combined BLM-liposome fusion method. With the afore-mentioned background and our experimental findings described above, we now discuss the results under separate headings in the following paragraphs.[83]

Fusion of ER Vesicles with a BLM. In asymmetric choline chloride solution, the ER vesicles can be fused with a BLM. Since the reversal potential is 25 mV, when *cis* and *trans* choline chloride concentrations are 250 and 50 mM, respectively, the fusion of ER vesicles impart appreciable chloride conductance to the BLM. The above protocol was used for the fusion of SR vesicles and brain ER vesicles with a BLM. In the above cases, the vesicles fused so that the *cis* side of the BLM is the cytoplasmic side and the *trans* side is the luminal side of the SR or ER. In another study,[83] where cerebellar ER vesicles were fused with a BLM, the *cis* side

was equivalent to the cytoplasmic side and the *trans* side was the luminal side. Consequently, we assumed that the liver ER vesicles will fuse with the same orientation and therefore, accordingly we perfused the *cis* side with a solution having 2.5. uM free calcium and the *trans* side with a solution having 55 or 25 mM Ca^{2+}. The above fusion protocol has one drawback; in order to generate/create/give the calcium gradient across the reconstituted BLM, both the *cis* and *trans* chambers have to be perfused, however the success rate of having an intact BLM is low after perfusing both chambers. Therefore, we have modified the above protocol and have used one in which the perfusion of the *cis* chamber is necessary only to impose a calcium gradient across a reconstituted BLM. Our experimental results demonstrate that it is possible to make BLMs in low ionic strength solution, a choline chloride, potassium acetate and potassium chloride can be used as osmoticants to fuse the liver ER vesicles with a BLM.

In search of $InsP_3$-gated and rynodine-sensitive Ca^{2+} Channels in Liver Rough ER Membrane [83]

Though we made repeated attempts and maintained appropriate conditions (calcium concentration, agonist $InsP_3$ concentration), we were unable to detect any $InsP_3$-gated calcium channel in the liver rough ER membrane. $InsP_3$-gated calcium channels have been observed in the planar BLM after fusion of cerebellar ER vesicles. Our inability to observe $InsP_3$-gated calcium channels in the planar BLM after fusion of liver ER vesicles suggests that the $InsP_3$ receptor/channel is not located in the liver ER. In this regard, the distribution of $InsP_3$ binding sites was investigated in subcellular fractions obtained from rat liver and compared with those of other markers.[83] It was found that the $InsP_3$ binding vesicles were completely distinct from the ER derived vesicles and co-purified with the plasma membrane marker. Though the rynodine-sensitive Ca^{2+} channels have been observed in BLMs after fusion with total brain microsomes and cerebellar microsomes, our inability to observe these channels after fusion of liver rough microsomes suggests that the channel is probably not located in the liver rough ER membrane.

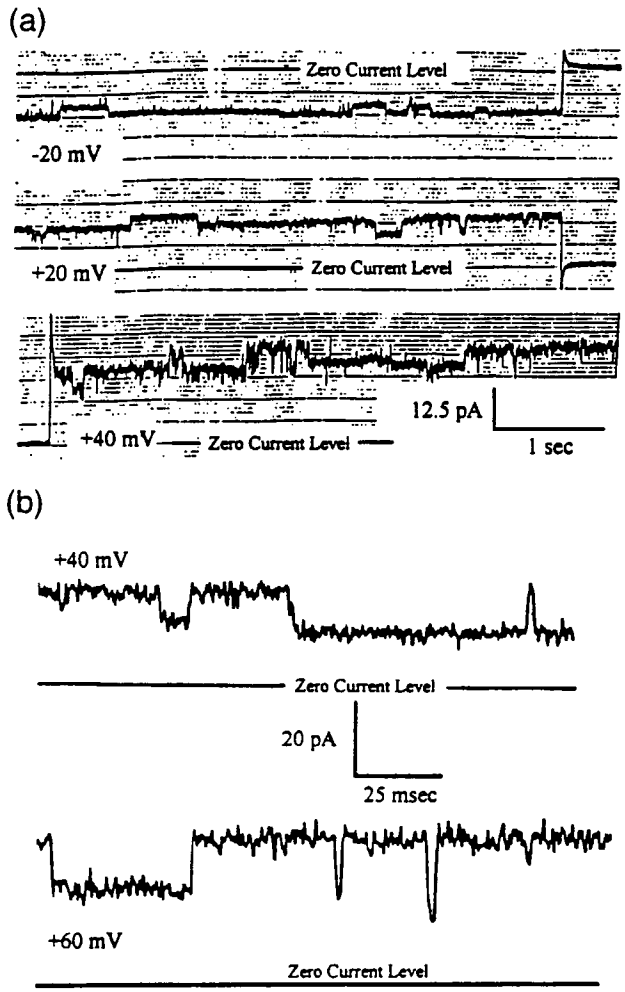

Fig. 7.12 **(a)** shows some of some single channel records in symmetrical 363 mM KCl solution. A maximum conductance transition of 200 pS and many other transitions lower than this value can be seen. Addition of 38 μM DIDS totally eliminated all activity. **(b)** Another set of single channel recordings in which the channel activity could be eliminated by addition of $ZnCl_2$.

Chloride to Potassium Permeability Ratios for Liver Rough ER Chloride Channels. By imposing an asymmetric KCl solution across BLMs reconstituted with the liver ER vesicles, we have measured the reversal potential in each case. By applying a form of GHK equation, we have calculated P_{Cl}/P_K for each case. The calculated values vary from 4 to 24. To explain this variation, we assume that there are existing chloride channels in the ER with different P_{Cl}/P_K values, and that in macroscopic condition, what we are measuring, is a weighted average of the P_{Cl}/P_K values of all the channels that have gotten incorporated in the BLM.

To give a concrete example, if we have at least two types of channels, one type having P_{Cl}/P_K between 4 and 8 and the other type having P_{Cl}/P_K of 20-24. If in a membrane we have only one type, we measure a P_{Cl}/P_K of 4-8 or 20-24. If we have only one channel of one type and one channel of the other type, we would expect a P_{Cl}/P_K of 12-16. We believe the range of P_{Cl}/P_K values that were obtained, can be explained in this way.

Anionic Permeability Ratios. At the outset, we must mention that our anionic permeability ratios are measured under macroscopic conditions. So, if we have different channel types, the selectivity sequence should hold good for all the chloride channel types. The permeability sequence is $SCN^- > I^- > Br^- > Cl^-$ suggesting that the chloride channels present in the liver rough ER membrane have 'low field-strength sites', following the Fixed-Charge Hypothesis.[84] The gluconate permeability of the ER chloride channels seems to be a little bit higher than other chloride channels and is about one-tenth of the chloride permeability. Since the ionic diameter of gluconate is about 0.6 nm, we can assign a similar value as the diameter of the chloride channels. We also studied the permeability of a few other anions and cations. Acetate permeability was almost the same as that of chloride, and fluoride permeability was less than that of chloride. Sulfate seemed impermeable and sodium was about half as permeable as potassium.

No Potassium "Channel" in the ER Membrane. Meissner and coworkers have studied the permeability of various anions and cations using a potentiometric dye.[85] From their studies, they concluded that though the majority of the liver microsomes are more permeable to potassium and

sodium than to magnesium or calcium, they lacked a highly conducting potassium and sodium structure, such as the potassium and sodium channel of sarcoplasmic reticulum. In our studies of direct fusion of the liver ER vesicles with a BLM, we were unable to find any potassium channel.

Pharmacology. We found that the chloride conductance of the rough liver ER membrane can be divided into two components based on their pharmacological sensitivity. One component can be blocked by zinc and the other component by DIDS.

Inhibition by DIDS. The reactive disulfonic acid stilbene (DIDS and 4-acetamide-4'-isothiocyano-tostilbene-2,2'-disulfonic acid) block some chloride channels including a voltage-gated conductance studied macroscopically in squid axon and astrogalia, the low conductance channel of *Torpedo electroplax*, rabbit urinary bladder, lobster neuron and the large conductance channels of A6 epithelial cells, and B lymphocytes.[83] In many of these cases, it was active from the cytoplasmic side. DIDS in 1 μM concentration inhibited irreversibly the macroscopic chloride conductance induced by the *Torpedo* vesicles. Inhibition of lobster neuronal chloride channel by SITS could be fitted to a one-site blocking behavior with a K_I of 53 μM. In our experiments, 36 μM of DIDS can inhibit sometimes totally and sometimes partially the chloride conductance induced by liver rough ER vesicles. We interpret our findings as follows: There are two types of chloride channels in the liver ER membrane. One type can be blocked by DIDS, which we shall call DIDS-sensitive, and the other DIDS-insensitive. During physical disruption of the intact ER (as happens during isolation of ER vesicles), we get a non-homogeneous population of ER vesicles. Some of the vesicles carry the DIDS-sensitive chloride channels, some DIDS-insensitive type and some both types. That is why in our studies involving the inhibition of chloride conductance by DIDS, what we observe amounts to what type of vesicles have fused with the BLM. If a vesicle carrying DIDS-sensitive type channels has only fused with the BLM, we can inhibit the entire conductance by DIDS. If a vesicle carrying DIDS-insensitive type channels has fused with the BLM, we cannot eliminate it by DIDS (we shall show later that the conductance insensitive to DIDS can be blocked by zinc). If both types of vesicles have fused or the third type carrying both DIDS-sensitive and DIDS-insensitive channels

have fused with the BLM, then by application of DIDS, we can inhibit only the DIDS-sensitive portion of the total conductance. In this regard, it is interesting to note that it has been our observation that when the vesicle induced conductance is small (indicating that only one vesicle has fused), the conductance is fully DIDS-sensitive type. When the vesicle induced conductance is large (indicating many fusion events), the conductance can be partially eliminated by DIDS.

Sidedness of DIDS Block. As has been mentioned earlier, in many of the studies involving DIDS inhibition of Cl^- channels, DIDS was active from the cytoplasmic side. In about 95% of our experiments, DIDS blocked the DIDS-sensitive Cl^- conductance from the *cis* side. To induce fusion with the BLM, we add the ER vesicle to the *cis* side. During isolation, if the ER vesicles maintain their normal orientation (we have no reason to believe that it would be otherwise), then, when the vesicle fuses with the BLM, the *trans* side shall be equivalent to the luminal side of the ER and the *cis* side equivalent to the cytoplasmic side. So, we can say that, in our case, DIDS blocks from the cytoplasmic side.

Inhibition by Zinc. In frog skeletal muscle, external zinc decreases Cl^- efflux and reduces Cl^- conductance with a K_1 near 0.1 mM.[83] Thus, there is evidence that 0.1-2 mM zinc in the extracellular solution blocks Cl^- channels of intact muscle. In a recent study of a high-conductance anion channel in adult amphibian skeletal muscle, it was found that 10 mM zinc inhibited the channel activity but DIDS or 9-anthracene-carboxylic acid (another blocker of Cl^- channel) had no effect. In our studies, we found that 2.5 mM zinc can eliminate totally or partially the conductance induced by ER vesicles. In cases where the inhibition was partial, there was no further inhibition by increasing zinc concentration and the residual conductance could be blocked by DIDS. We interpret our data in an analogous way as we have done for the DIDS case. We conclude that the liver ER has two types of Cl^- channels: one type that we shall call DIDS-sensitive and zinc-insensitive, the other type is DIDS-insensitive and zinc-sensitive.

Single Channel Studies. Single channel studies were difficult to perform in our case. In some cases, we have noticed that the single channel activity could be completely eliminated by DIDS (n = 2) and in some other cases, the single channel activity could not be eliminated by DIDS but by zinc. Since "n" is very small, it is not possible for us to draw any definite conclusions about the single channel properties of the DIDS-sensitive and zinc-sensitive channels (Fig. 7.12). We shall limit ourselves to only our observations.[83]

Minimum Conductance Induced by ER Vesicle Fusion with a BLM. The minimum conductance that we observed in 363 mM symmetrical KCl solution was between 550-600 pS. This is most likely due to the fusion of a single vesicle. Sometimes this "minimal" conductance could be eliminated by DIDS and if it could not be eliminated by DIDS, it could be eliminated by the addition of zinc.

Minimal Conductance of a DIDS-Sensitive Channel. Since, in our fusion experiment, the minimum conductance that we observed which could be blocked by DIDS is about 565 pS, and if this is a "minimal" conductance of the DIDS sensitive channel, we wanted to see if at the macroscopic level, the conductance that could be blocked by DIDS is an integer multiple of this "minimal" conductance. In 5 out of 6 of our cases, the conductances were shown to be an integer multiple of a minimal conductance of 0.566 ± 0.021 nS (mean $\pm$ s.d.). The minimal conductance that we observed in our fusion experiments is around this value. As mentioned earlier, this minimal conductance is, most probably, due to the fusion of one vesicle. But is it one channel? It is possible that the vesicle may be carrying more than one channel. If that is the case, the unit conductance of the channel would be lower than 0.566 nS. We then looked at our single channel records in which the minimal conductance of 0.566 nS could be totally inhibited by an application of 38 uM DIDS to the *cis* side. The maximum conductance transition that we observed was about 200 pS and many other transitions occurred which were smaller than this value. We again looked at our macroscopic conductances that could be blocked by DIDS. In all 6 cases, the conductances can be shown to be integer multiples of a "minimal" conductance of 192 pS. Is this the unit conductance of a DIDS-sensitive channel? We do not know. As mentioned earlier our 'n' is too small to

draw any definite conclusions. Further experiments are necessary to clarify this point.

Minimal Conductance of a Zinc-Sensitive Channel. With 'n' also being small (n = 2), we cannot draw any definite conclusions and shall limit ourselves to our observations. The minimal conductance that we observed, which could not be blocked by DIDS, but could be blocked by subsequent addition of zinc, was about 600 pS. We believe that this is probably due to the fusion of a single vesicle. But is it the unit conductance of a single zinc-sensitive channel? It is possible that the single vesicle could be carrying more than one channel. In that case, unit conductance would be lower than 600 pS. We have looked at the macroscopic Cl^- conductance which could be inhibited by zinc. As in the DIDS case, we wanted to see if the macroscopic conductance could be shown to be an integer multiple of a "minimal" conductance of about 600 pS. Since the conductance is a function of the salt concentration, we selected those values in which the *cis* and *trans* KCl concentrations were 363 mM. In all 5 of such cases, the "minimal conductance" comes out to be 0.589 ± 0.0399 nS. We looked at two records in which the single channel activity could be blocked by zinc. There were multiple transitions. There were conductance transitions of magnitude 75 pS, 150 pS, 225 pS, 300 pS and 375 pS. We could not come to any definite conclusion about the unit conductance from our single channel studies. Further experiments are necessary to clarify this point.

Physiological Significance of ER Cl^- Channels. We are unable to state the exact physiological function of these channels. We can only offer speculations. Since the SR is a specialized derivative of ER and a high conductance Cl^- channel has been identified in the SR membrane, we decided to see if the proposed functions for the SR Cl^- channel should offer us any clues. For the SR channel, it has been proposed that a possible function of this anion channel could be to shorten the time course of the Ca^{++} transient and produce a faster twitch. Another physiological function proposed is to provide counter-ion movement during the Ca^{2+} pumping after the SR Ca^{2+} release channels have closed.[83] We know that Ca^{2+} is sequestered in the ER. A Ca^{2+}-ATPase and a Ca^{2+} binding protein

calreticulin have been identified in the liver ER. Since the Ca^{2+} pumping is electrogenic, we believe that the physiological role of the ER anionic channels may be to provide the counter ion movement into the ER, so as to prevent the building up of positive charges inside the ER.

In concluding, the following points can be made concerning this study:

1. The liver rough ER vesicle imparted high chloride conductance to the BLM after fusion, Cl^- to K^+ permeability ratios measured under macroscopic conditions varied from 4 to 24,
2. Anionic permeability follows the sequence $SCN^->I^->Br^->Cl^->>>$ gluconate$^-$, which suggests that the chloride channels have low field-strength sites,
3. The gluconate permeability was observed to be one-tenth of that of Cl permeability. This suggests that the diameter of the rough ER chloide channel(s) is slightly larger than 0.6 nm,
4. The macroscopic Cl—conductance could be pharmacologically dissected to DIDS-sensitive and Zn^{++}-sensitive types,
5. In most cases, DIDS blocked Cl—conductance from the *cis* side (the side to which the ER vesicles are added; equivalent to the cytoplasmic side of the ER).
6. The minimal conductance induced by a vesicle fusion was about 600 pS which could be blocked by DIDS. If not blocked by DIDS, the later addition of the mM concentration of $ZnCl_2$ eliminated the conductance.
7. No conclusions could be drawn about the unit conductance of DIDS-sensitive and Zn^{2+}-sensitive channels from the single channel data,
8. No IP_3-gated Ca^{2+} channel was found, as well as no rynodine-sensitive Ca^{2+} channel was found in the liver rough ER membrane, and
9. No K^+ channel like the one present in SR membrane was found in the rough ER membrane.

7.6 Other BLM and Liposome Experiments[72]

Intracellular Membranes

The reconstitution and characterization of SR membranes in BLM are so far the most adequate approach for obtaining information about their single channel properties. This opportunity was exploited during the first steps of the BLM-reconstitution experiment. The fusion method, which was later used as a reproducible method for reconstitution of various channel activities, has been elaborated to some extent on the basis of studies on sarcoplasmic reticulum components inserted into BLM.[8] Discrete fluctuations of BLM-conductance were observed only when three main conditions for fusion between the sarcoplasmic reticulum vesicles and BLM were available: high [Ca^{2+}], not less than 0.5 mM; osmotic gradient; and the presence of negatively charged phospholipids in the BLM-forming solution. It has been found that the cation channel conductance induced by sarcoplasmic reticulum vesicles in BLM is gated by voltage. This could be related to the physiological mechanism of the excitation-contraction coupling, bearing in mind that the permeability of the sarcoplasmic reticulum membrane is controlled in some way by voltage changes during the coupling of the events occurring in the transverse tubule and the sarcoplasmic reticulum membranes. The voltage-gated K^+ conductance was found to be modulated by some transition metal ions, for example Ag^+, Hg^+, Cu^{2+}, etc. They affect the opening probability rather than the channel conductance. The inhibition effect of one of the agents, mersalyl, is voltage dependent. The results indicated that a sulfhydryl group may be involved in the functioning of the channel. The unit conductance of the channel was 140 pS in 0.1 M K^+.

Later, many other properties of the channel were analyzed in detail It has been found that the channel to be perfectly selective for K^+ over Cl^- and for K^+ over Ca^{2+} -Cs^+ asymmetrically blocked the channel. Increasing [Cs^+] induced several effects, such as reduced channel conductance

increased mean open time and voltage-dependent changes of the open state conductance. Two cholinergic drug agents, decamethonium and hexamethonium, were found to induce blocking effects similar to Cs^+. However, there was some difference between the influences of the two compounds. Decamethonium provoked flickerings from the open state, their rate increasing at higher drug concentrations. The flickering was voltage dependent, which is found only at negative potentials when the drug molecules are driven inside the channels. Hexamethonium, on the contrary, did not induce flickering, but it provoked a decrease in the unitary conductance. The different actions of the two blocking agents may be explained by differences in the lifetime of the open state. These cholinergic blockers were found to induce similar effects on channels isolated from another source, cardiac SR. Some differences, however, were also observed. In the cardiac SR, decamethonium caused flickering from either side of the BLM, while in BLM reconstituted with channels from skeletal muscle sarcoplasmic reticulum, it was effective only when added to the trans side. Nevertheless, in the former type of membrane the voltage dependence of the block was less pronounced when the agent was present on the same side. In both cases, decamethonium probably binds in a bent configuration to a site about 55% of the voltage drop across the channel from the opposite side of the membrane.

In the cardiac membranes there were also channels with differing conductance. Two open states were described, one of them (B) being a fully open state with a unit conductance of 157.2 pS, and the other (d) a substate with a conductance of 100.7 pS. Both states can be blocked by the cholinergic drugs and both of them have the same ionic selectivity sequence which is identical with that of the channels from skeletal muscle sarcoplasmic reticulum. The positive potentials favor the channel opening in both types of membranes. Bell and Miller[72] found the activity of the K^+ channel of sarcoplasmic reticulum to be dependent on the charges of the surrounding membrane phospholipids. The channel conductance is lower in BLMs made from neutral phospholipids than in BLMs from negatively charged phospholipids at a given $[K^+]$, the effect being more pronounced at lower ionic strength. The maximum unit conductance at a saturating K^+ concentration is 220 pS. The charge of the phospholipids does not

influence the ionic selectivity, but it affects the apparent rate constant of the block induced by the divalent channel blocker 'bis Q11'. When a positively charged PC analogue was present in the BLM, the K^+ conductance was lower than that of neutral BLMs. Based on these results, it was suggested that the entry way of the channel is located 1-2 nm from the lipid surface.

The physiological role of the cation channel of the sarcoplasmic reticulum membrane remains unclear. It is probably involved in an antiport system transferring monovalent cations in a direction opposite to that of the electrogenic calcium flux triggered by the action potential. Excitation in the form of an action potential propagates along the transverse tubule cylindric formations (which are part of the muscle plasma membrane) deeply into the myoplasm. In defined regions, the so-called triads, the transverse tubule membrane interacts with the sarcoplasmic reticulum membrane. The excitation of the transverse tubule membrane in these regions in some unknown way is coupled to a very large increase (100- to 1000-fold) in the permeability of the sarcoplasmic reticulum membrane for Ca^{2+}, which is released in the myoplasm and induces contraction of the actomyosin myofibrils. The monovalent cation channel of the sarcoplasmic reticulum may operate as a charge-compensating mechanism in this process of excitation-contraction coupling, countering the charge movements connected with the Ca^{2+} efflux.

Cukierman et al[72] btained valuable information about the structure and properties of the SR K^+ channel in a study on Cs^+ block of the channel incorporated in BLM from rabbit skeletal muscle SR. An early observation about the Cs^+-blocking effect was revised on the basis of these surprising results which showed that the permeability of Cs^+ through the channel is nearly the same as that of K^+ ($P_{Cs^+}/P_{K^+} = 0.7$), but the channel conductance in the presence of Cs^+ is 15-20 times lower than the K^+ conductance. The typical blocker of this channel, decamethonium (150 uM), exhibits inhibition of the Cs^+ current, showing that Cs^+ permeates through the same K^+ channel. A rectification is observed in symmetrical Cs^+

concentrations (18-600 uM), negative Cs^+ current passing more easily than positive, which indicates an asymmetric location of the Cs^+-binding site in the channel molecule. Cs^+ blocks the single-channel K^+ current in a voltage-dependent way. The results are consistent with the view that the Cs^+-binding site is located 40% of the way through the voltage gradient, from one of the membrane surfaces. The diameter of the selectivity filter of the channel is believed to be 0.4 = 0.5 nm, which permits free access of Cs^+ into the pore interior. The low Cs^+ conductance could therefore be explained by tight binding of the ion rather than by a steric hindrance effect. Indeed, the binding of Cs^+ is 20 times stronger than K^+, which may determine the Cs^+-induced block of the single-channel K^+ currents. The structure of the channel can be envisioned as a tunnel, 0.8 nm in diameter, narrowing to 0.4 – 0.5 nm at a point 35-40% of the way down the voltage gradient. A model of the channel with a four barrier energy profile was considered. Bell [72] envisioned the SR K^+-channel mouth to be located 5 to 10 A from the membrane surface in a study of the influence of pH and of surface charge on the functioning of the channel. The protons were found to competitively inhibit the K^+ conductance with an inhibition constant of 0.5 uM. The K^+ conductance is lower in BLMs containing neutral phospholipids than in those composed of charged lipids due to the increased negative surface potential and the higher K^+ concentration near to the membrane surface in the latter type of membrane. The observed effects were attributed to changes in the membrane surface charge, which may influence the permeation of K^+ through the channel. The data are well described by the Gouy-Chapman-Stern theory. Bell [72] suggested that the role of the surface charge should be considered more carefully when interpreting the rectifying behavior and other single-channel characteristics of different types of channels. Gray et al[72] found that the membrane surface charge influenced the blocking effect of a myorelaxant succinyl choline on the cardiac and skeletal muscle SR K^+ channel. Succinyl choline, as well as other positively charged blockers such as the quarternary ammonium compound 'bis Qll', exhibits a more pronounced block of the channel in BLMs containing negatively charged phospholipids. The inhibiting effect of succinyl choline is interestingly larger when added to the cis side of the

membrane, while most of the other blockers (e.g. decamethonium, etc.) are more effective from the trans side. Due to the fact that the succinyl choline molecule is less hydrophobic than that of decamethonium, Gray et al speculated that there are two regions for a blocker to bind on the two sides of the channel molecule and that the region to the cis side is less hydrophobic. The block is voltage dependent and is accompanied by "flickering" events when the channel resides in one of the two open states, d and B. The B state is more susceptible to inhibition by succinyl choline than the d state. They suggested that the single-channel conductance of the d state (100 pS in 75 mM K_2SO_4) is 60 to 70% of that of the B state (184 pS) and may be considered as a substate. One of the typical characteristics of the d state is the noisier open state current. The peculiarity suggests that transient current fluctuations between the open and the closed state underlie the d-state opening events and that 30 to 40% of this time the channel spends in the closed state. Therefore, it may be considered as a gating rather than conducting state, with a characteristic time-averaged conductance. There is evidence that the channel has to be open in order to be blocked. Gray et al observed that the channel resides more frequently in the open state in highly charged bilayers than in neutral bilayers. In neutral bilayers the number of the d-state opening events diminishes when increasing the K^+ activity. A difference between the SR K^+ channels in cardiac and in skeletal muscle was also revealed. The cardiac channel has a higher affinity for K^+ than the skeletal muscle SR channel, although the maximal conductance of the channel is almost the same.

Ligand-gated channels[72]

The hydrophobic core of the membrane lipid bilayer is practically imperable to hydrated ions in aqueous solution. To overcome the high energy barrier of the lipid bilayer, Nature has evolved two stategies: ion carriers and water-filled pores or channels. Membrane pores or channels are made of allosteric proteins. The opening and closing, or gating, of these membrane channels can be divided into two kinds: those controlled by voltages (voltage-gated channels) and those controlled by ligands (ligand-gated

channels). Voltage-gated Channels. They open specifically in response to a change in PD and responsible in propagating electrical trasients (impulses) over long distances in nerve and muscle.

Ligand-gated Channels. They open upon interacting with a ligand such as a hormone or a drug, and are insensitive to voltage change. Ligand-gated chaanels are involved in signal transduction between different neurons and between neurons and muscle across synapses.

Acetylcholine receptor. The acetylcholine receptor (AR) is one of the best-characterized membrane receptor-protein complexes, and experiments on its reconstitution in model membranes progressed relatively rapidly. Using AchR isolated from the electric organ of Torpedo electroplax where this amount is the highest known performed most of these studies. After its isolation and purification from this source, its molecular structure has been well characterized. It was found that the AchR is a pentamer, i.e. it consists of five glycoprotein subunits, d1, d2, B, Y, d. The molecular weight of the entire pentamer is 270,000 daltons. The binding sites for acetylcholine are on the d-subunits, having a molecular weight of 40,000 daltons.

The AchR has been reconstituted in BLM mainly by using the monolayer folding method and the patch-clamp micropipette technique. Several properties which are typical for the AR channels on native membranes have been demonstrated in the BLM experiments. The channels are activated by the cholinergic agonists acetylcholine, carbamoylcholine, and suberyldicholine.The channel stimulating concentrations of these specific cholinergic ligands were similar to those used for activation of the native AchR channels. The channel activity is inhibited by specific inhibitors, d-bungarotoxin, d-tubocurarin, and hexamethonium. Receptors are desensitized under defined conditions.The channels exhibit characteristic unit channel conductance.Concentration and voltage-dependent effect of the local anesthetic derivative of lidocaine, 'QX-222', which is known to block the permeation of ions through the open AR channel on native membranes. It reduces the fast and slow components of the distribution of open times t_{o1} and t_{o2}, respectively.

Voltage-gated channels

In this type of channels, a component of which is sensitive to the sign or magnitude of the PD across the membrane. (Note: a 120 mV PD across a 6 nm thick membrane is equal to a field strength of 200,000 volts/cm.[26,77]

Cytotoxic Agents

Pore-forming bacterial toxins may be broadly divided into two categories: those affecting intracellular metabolisms and those altering the properties of the plasma membrane of susceptible cells. The first category includes cholera, diphtheria, tetanus, and botulinum, whereas S. aureus α-toxin, C. perfringens θ-toxin and E. coli haemolysin belong to the second category. Some differences between the actions of various agonists were found by Suarez-Isla et al[72] For instance, Ach provoked an increase of two lifetimes described by two exponential components characterizing the open-time distribution. At concentrations higher than 10 μM, Ach reduced typical bursting activity. The bursts were interrupted by relatively long quiescent periods. The unit conductance was not changed, 40 pS in 0.5 M NaCl, but the channel open times were longer at higher concentrations of the ligand than at lower concentrations. It is interesting that some agents, such as the disulfide reducing compound dithiothreitol, may alter the ligand affinity of the AR, but at the same time they do not influence the channel activity. Concerning the ion selectivity, Schindler and Quast found that in the presence of CCh the membrane permeability was 7 times higher for K^+ and Na^+ than for Cl^-. Labarca et al determined the conductances for different ions at 0.3 M NaCl: 28 pS for Na^+, 30 pS for Rb^+, 38 pS for Cs^+, and 50 pS for NH_4^+. When the Na^+ concentration is increased, the single channel conductance reaches a maximal value of 95 pS. Two computer simulated models were proposed on the basis of the obtained data.

Acetylcholine receptors from *Torpedo electroplax* membranes were reconstituted in liposomes and their single-channel properties were studied by Tank et al[72] using bilayer patches formed from the liposomal membranes on the tips of patch-clamp pipettes. They observed a main open state level

with a slope conductance of 42 pS in 150 mM NaCl and a subconductance state. A double exponential distribution of the open times with very small time constants (t_{fast} = 0.35 msec and t_{slow} = 2.8 msec) was found. At lower temperatures the amplitude of the single-channel current decreased substantially. Bursting events and desensi-tization effects were observed. The frequency of the opening events decayed with a time constant of 92 sec in the presence of 1 μM acetylcholine. At higher concentrations of the agonist a more rapid inactivation rate was observed. Two inactivation processes were described: a fast (0.1 - 1 sec) and a slow (min) inactivation, which may be influenced in a different way by the agonists. In this connectiion, Murphy and Vodyanoy[72] reconstituted another neurotransmitter-regulated channel, a dopamine-receptor channel, into BLMs and demonstrated the effects of some specific agonists and modifiers of its activities.

Epithelial membranes

One of the most important physiological processes in epithelial cells is the transport of Na^+, which in some cells is stimulated by the hormones aldosterone and vasopressin, and inhibited by such diuretics as amiloride. Sodium-specific channels that could be modulated by amiloride were found in the membranes of such cells. Epithelial membrane vesicles were recently inserted into BLMs from PE/PS (7:3), and the properties of amiloride-sensitive single Na^+ channels were characterized.[72] A broad range of unit conductances were measured, from 4 to 80 pS at 0.2 M NaCl, which was explained by the presence of a variety of stable conductance states similar to the gramicidin A channel. Changes in the applied potential did not influence the channel opening probabilities. There was one long-lived closed state with a mean dwell time of 5 sec and one fast closed state (< 200 msec). Amiloride provoked a dose-dependent decrease in the open state conductance when added to the cis side, and a flickering from the trans side. The influence of Na^+ concentration was studied separately by Olanset al[72] and at high [Na^+] a saturation of the amiloride-sensitive Na^+ channels was observed with Michaelis constants of 17 or 47 mM for maximal conductances, G_{max} of ~ 4 or 44 pS, respectively.

Ciliary membranes

The ciliary formations are responsible for one of the most important physiological functions, the cell movement. The dynamic events accompanying this process depend to a great extent on the transport mechanisms across the ciliary membranes. The ciliary membranes of *Paramecium* are well-characterized biochemically and electrophysiologically. Therefore, they have been used as a source for reconstituting ciliary membrane channel activities in BLMs.[72] Two types of Ca^{2+} channels were identified which were much more permeable to divalent than to monovalent ions: A chel with relatively large unit conductance, 30 pS, was identified, with the following characteristics: (a) Lowic selectivity, the permeability to Mg^{2+} being slightly higher than that to Ba^{2+}.(b) No voltage dependence in the range from –20 to –0 mV. 2. A channel with low unit conductance (1.5 – 2 pS) was found, with properties differing from those of the high conductance channel: Goonic selectivity with Ca^{2+} and Ba^{2+} permeability significantly exceeding that for Mg^{2+} (the permeability coefficient for Ba^{2+} is 10 times higher than that for Mg^{2+}, and (c) Voltage dependence with opening probability increasing steeply with voltage. An *e*-fold increase in opening probability for a potential change of 9 +/- 4 mV was observed, which is similar to that found for native Ca^{2+} currents.

It is worth noting that the applied potential apparently did not influence the mean open time, similar to the intact Ca^{2+} channels. When increasing [Ba^{2+}], a saturating value of the single-channel conductance is reached at concentrations higher than 10 mM. This is another property that the reconstituted Ca^{2+} channels share with the native channels.

Concluding remarks and perspective[72]

Some of the recent studies on BLM were reviewed in an effort to point out the applicability of this model membrane system to the problems related to the structure, properties, and functions of biomembranes. The direct investigation of the cellular membranes meets with considerable difficulties

due to their complex structure. The properties of the experimental bilayer lipid membranes (BLMs and liposomes) and the interactions between their components in relation to defined cellular functions can be studied easier than the more complicated intact biomembranes. For example, investigations of the membrane transport mechanisms in BLM provide a framework of reference to which material transport in the native membranes can be compared. Further developments of BLM research can also facilitate the initial testing of working hypothesis, which may generate guidelines leading to a better choice of appropriate *in vivo* reconstituted membrane investigations.

Looking towards the future of research on BLM systems, it is expected that further achievements are likely in areas connected with cell biology and membrane biophysics such as active transport, oxidative phosphorylation, photosynthesis, vision, immunology, nerve conduction, and energy transduction. The BLM system should also be useful in understanding membrane biogenesis and various membrane-mediated processes.

General References

S. G. Davison (ed.) Progress in Surface Science, Vols. **19, 23, 41**, Per gamon Press, NY, 1985, 1986, 1992

B. Ivanov (ed.) *Thin Liquid Films*; Marcel Dekker, New York, 1988, pp. 927-1057.

J. R. Harris and Etemadi, A.-H. (eds.), Artificial and Reconstituted Membrane Systems, Subcellular Biochemistry, Vol. **14**, eds., Plenum Press, N.Y. 1989. pp.97-143.

T. Narahashi (ed.) Ion Channels, Three Vols. Plenum, NY.. 1988-1992.

B. L. Kagan and Y. Sokolov, *'Use of bilayer lipid memrbanes to detect pore formation by toxins'*, Methods in Enzymology, **235** (1994) 691-705

M. Rosoff (Ed.) *Vesicles*, Marcel Dekker, New York, 1996.

G. G. Matthews, *Cellular Physiology of Nerve and Muscle* (3rd Ed.) Blackwell, 1998.

Specific References

1. P. Mueller, D. O. Rudin, H. T. Tien, W. C. Wescott, Nature, 194, pp.979, 1962; J. Phys. Chem., 67 (1963) 534
2. A. D. Bangham, BioEssays, 17 (1995) 1081.
3. R. C. Bean, W. C. Shepherd, H. Chan and J. Eichner, J. Gen. Physiol., 53 (1969) 741.
4. A. Darszon, P. Labarca, C. Beltran, J. Garcia-Soto and A. Lievano, Methods: A Companion to Methods in Enzymology, 6 (1994) 37
5. S. K. Tiwari-Woodruff and T. C. Cox, Am. J. Physiol., 268 (Cell Physiol., 37) (1995) C1284-C1294
6. L.-G. Li, K.-D. Yin, J.-Q. Yan, Z.-C. Tang, Chinese Science Bulletin, 41 (1996) 1124; Z.-M. Pei, Chinese Sci. Bull., 39(2) (1994) 1923
7. Chernomordik, L. V., G. B. Melikyan and Y. A. Chizmadzhev, Biochim. Biophys. Acta, 906, 309 (1987)
8. A. E. Shamoo and W. F. Tivol, Curr. Top. Membr. Transp., 14 (1980) 57-69
9. J. I. Kourie, D. R. Laver, G. P. Ahern and A. F. Dulhunty, Am. J. Physiol., 270 (Cell Physiol., 39) (1996) C1675-C1686
10. M. Sato, K. Inoue and M. Kasai, Biophys. J., 63 (1992) 1500-1505
11. C. Lemaitre, N. Orange, P. Saglio, N. Saint, J. Gagnon and G. Molle, Euro. J. Biochem., 240 (1996) 143-149
12. O. V. Krasilnikov, V. I. Ternovsky, D. G. Navasardyants and L. I. Kalmykova, Med. Microbiol. Immunol., 183 (1994) 229-237
13. R. Schonherr, M. Broer Hilger, R. Benz and V. Braun, Euro. J. Biochem., 223 (1994) 655-663
14. S. Matile, N. Berova and K. Nakanishi, Chem. & Biol., 3 (1995) 379
15. T. Morita, M. Kasai and K. Mikoshiba, Neurosci. Res., 13 (1992) 207
16. R. L. Baldwin, T. Mirzabekow, B. L. Kagan, B. J. Wisnieski, J. Immun., 154 (1995) 790-798
17. Neher and ; B. Sakmann and E. Neher (eds.), Single-channel Recording, Plenum, New York, 1995.
18. J.-L. Schwartz, L. Garneau, D. Savariat, L. Masson, R. Brousseau and E. Rousseau, J. Memb. Biol., 132 (1993) 53-62
19. L. English, H. L. Robbins, M. A. von Tersch, C. A. Kulesza, D. Ave,D. Coyle, C. S. Jany and S. L. Slatin, Insect. Biochem. Molec. Biol., 24 (1994) 1025-1035

20. A. M. Feigin, E. V. Aronov, B. P. Bryant, J. H. Teeter and J. G. Brand, Neuro. Rept., 6, (1995) 2134-2136
21. A. Gliozzi, M. Robello, L. Fittabile, A. Relini, A. Gambacorta, Biochim. Biophys. Acta, 283 (1996) 1-3
22. A. G. Prat, E. J. Holtzman, D. Brown, C. C. Cunningham, I. L. Reisin, T. R. Kleyman, M. McLaughlin, G. R. Jackson, Jr., J. Lydon and H. F. Cantiello, J. Biol. Chem., 271 (1996) 18045-18053
23. I. Ismailov, B. K. Berdiev, A. I. Braford, M. S. Awayda, C. M. Fuller and and D. J. Benos, J. Memb. Biol., 149 (1996) 123.
24. Y. Nagaoka, A. Iida, T. Kambara, K. Asami, E. Tachikawa and T. Fujita, Biochim. Biophys. Acta, 1283 (1996) 31-36
25. A. Zahradnikova and P. Palade, Biophys. J., 64 (1993) 991-1003
26. Ottova, A. and H. T. Tien, Prog. Surface Science, **41,** 337-445 (1992).
27. V. Aguilella, M. Aguilella-Arzo and P. Ramirez, J. Membr. Sci., 113 (1996) 191-204
28. Coronado, R., Biophys. J., 47, pp.851-857, 1985.
29. P. Smejtek in E. A. Disalvo and S. A. Simon (Eds.), Permeability and stability of lipid bilayers, CRC Press, Boca Raton, 1994, p. 197
30. A. L. Ottova, V. Tvarozek, J. Racek, J. Sabo, W. Ziegler, T. Hianik et al, Supramolecular Science, 4 (1997) 101-112
31. J. Lemmich, K. Mortensen, J. H. Ipsen, T. Honger, R. Bauer and O. G. Mouritsen, Phys. Rev. Lett., 53 (1996) 5169-5180
32. J. Spinke, R. Blankenburg, S. Forster, M. Schmidt, J. Zoller, H. Ringsdorf and W. Knoll, Thin Solid Films, 210/211 (1992) 756
33. R. Sitsapesan, R. A. O. Montgomery and A. J. Williams, Pflugers Arch. Eur. J. Physiol., 430 (1995) 584-589
34. A. Winter, W.-P. Ulrich, F. Wetterich, U. Weller and H.-J. Galla, Bio phys. J, 81 (1996) 21-34
35. L. A. Chung and T. E. Thompson, Biochem., 35 (1996) 11343-11354
37. D. R. Laver and B. A. Curtis, Biophys. J., 71 (1996) 722-731
36. Fujimoto, S. Oiki, T. Kondo, T. Katada, H. Kato, T. Taguchi, M. Ka sai, Y. Okada, K. Mikoshiba and K. Ikenaka, Neurosci. Res., 25 (1996) 229-237
37. L. Y. Jan and Y. N. Jan, Nature, 371 (1994) 119-122.
38. E.C. Beyer , D. L. Paul, and D.L Goodenough, J. Membr. Biol., 116 (1990) 117)

39. Toro, L., L. Vaca and E. Stefani, Am. J. Physiol., **260**, H1779 (1991)
40. Duch, D. S., A. Hernandez, S. R. Levinson and B. W. Urban, J. Gen. Physiol., **100**, 623 (1992).
41. Xiang, T.-X., X. Chen and B. D. Anderson, Biophys. J., 63, 78 (1992).
42. Pohl, P.. T.I. Rokitskaya, E.E. Pohl, S.M. Saparov, Biochimica Biophysica Acta-Biomembranes, 1323 (1997) 163-172.
43. Sassaroli, M., Vauhkonen, M., Perry, D., and Eisinger, J. (1990) Bio phys. J ., 57:281-290.
44. Kunz, H., U. Zeidler, K. Haegele, M. Przbylski and G. Stark, Biochem., 34 (1995) 11895.
45. S.C. Piller, G. D. Ewart, A. Premkumar, G. B. Cox and P. W. Gage, Proc. Natl. Acad. Sci., 93 (1996) 111-115
46. S. Matile, N. Berova and K. Nakanishi, Chemistry & Biology, 3 (1996) 379-392
47. Kobuke, Y., K. Ueda and M. Sokabe, J. Am. Chem. Soc., **114**, 7618 (1992); MEBC, **7**, 33 (1993)
48. Evtodienko, V.Y., O.N. Kovbasnjuk, Y.N. Antonenko, L.S. Yaguzhinsky, Biochimica Biophysica Acta-Biomembranes, 1281 (1996) 245.
49. Gallucci, E. S. Micelli and G. Monticelli, Conf. Biochemistry Cell Membranes (1993) 148
50. Goldman, D.E., Ber. Bun. Ges. Physik. Chem., 71, pp.799, 1967
51. Vassilev,P. Kanazirska, M.; Tien, H. T. *Biochem. Biophys. Res. Commun. 126 (* **1985**) 559; P. M. Vassilev, Kanazirska, M.; Tien, H. T. *Bioelectrochem. Bioenerg.* **1986**, *15*, 395
52. Vassilev, P. Kanazirska, M.; Tien, H. T. *Biochem. Biophys. Res. Commun. 126 (* **1985**) 559; P. M. Vassilev, Kanazirska, M.; Tien, H. T. *Bioelectrochem. Bioenerg.* **1986**, *15*, 395
53. Mauro, A., M. Blake and P. Labarca, Proc. Nat'l. Acad. Sci., 85 (1988) 1071-1075
54. Y.-Y. Chang and J. F. Cronan, Jr., J. Biol. Chem 270 (1995) 7896.
55. B. K. Jap, *J. Mol. Biol.* **1990**, *215*, 429.
56. D. R. Kalkwarf, D. L. Frasco and W. H. Brattain, PNAS, US, 69 (1972) 3765
57. R. Benz, A. Schmid, T. Nakaae, G. H. Vos-scheperkeuter, J. Bacteriology, 165 (1986) 978
58. A. V. Oleskin, Samuilov, V. D. *Biochem. SSR* **1988**, *53*, 1552.

59. Xu, G.; Shi, B.; McGroarty, E. J.; Tien, H. T. *Biochim. Biophys. Acta* **1986**, *862*, 57
60. E. Neher and H. Eibl, Biochim. Biophys. Acta, 464 (1977) 57.
61. Shen, X.-C.; --- *Bioelectrochem. Bioenerg.* **1986**, *16*, 13; B. Shi, and H. T. Tien, *Biochim. Biophys. Acta* **1986**, *859*, 125
62. Y. N. Antnenonko and L. S. Yaguszhinsky, Bioelectrochem. Bio energ. 19 (1988) 499
63. S. I. Alekseev and M. C. Ziskin, Bioelectromagnetics, 16 (1995) 124
64. Chung,S.. P.H. Reinhart, B.L. Martin, D. Brautigan and I.B. Levitan, Neuroprotocols: Methods in Neurosciences, 6 (1995) 72
65. (a) Kihara, S. and K. Maeda, Prog. Surf. Sci., **47**, 1 (1994); O. Shirai, S. Kihara, Y. Yoshida, and M. Matsui, J. Electroanal. Chem. 389 (1995) 61-70
(b) Das, A. K.; Srivastava, R. C. *Langmuir* **1993**, *9*, 3313-3316.
66. Zviman, M. and H. T. Tien, Bioelectrochem. Bioenerg. 36 (1995) 127
67. Ismailov,I. I., B. K. Berdiev and D. J. Benos, J. Gen. Physiol. 106 (1995) 445
68. Antonenko, Y. N. and P. Pohl, Biochim Biophys Acta, 1235 (1995) 57-61
69. Colombini, M. in C. Miller (Ed.), Ion Channel Reconsititution, Plenum Press, New York, 1986, p. 533.
70. (a) Vodyanoy, V. and Murphy, R.B., Science, 220, pp.717, 1983; (b) Vodyanoy, V., Halverson, P., and Murphy, R.B., J. Colloid Interface Sci., 88, pp.227, 1982.
71. Troiano, G. C. L. Tung, V. Sharma, and K. J. Stebe, *Biophys. J.*,**75** (1998) 880-888
72. Vassilev, P. M. Tien., H. T. *In Structure and Properties of Mem branes*; Benga, G., Ed.; CRC Press, Inc.: Boca Raton, FL, 1985; *In Artificial and Reconstituted Membrane Systems, Subcellular Biochemistry*; Harris, J. R.; Etemadi, A.-H., Eds.; Plenum Press: New York, 1989; Vol. 4, pp 97-143.
73. Moczydlowski, E., Hall, S., Garber, S.S., Strichartz, G.S., and Miller, C., J. Gen. Physiol., 84, pp.687-704, 1984

74. Krueger, B.K., Worley, J.F., and French, R.J., Nature (London), 303, 172-175, 1983.
75. Andersen, O.S, in Membrane Transport in Biology, Springer-Verlag, New York, 1978.
76. Ehrlich, B.E., Schen, C.R., Garcia, M.L., and Kaczorowski, G.J., Proc. Natl. Acad. Sci. U.S.A., 83, pp.193-197, 1986.
77. Tsong, T. Y., Bioelectrochem. Bioenerg. 24 (1990) 271; Biophys. J. 60 (1991) 297-306.
78. Edwards, D.A., Schneck, F., Zhang, I., Davis, A.M.J., Chen, H.-M. and Langer, R.: Spontaneous vesicle formation at lipid bilayer membranes. *Biophysical Journal*, **71** (1996) 1208-1214..
79. Eisenman, G. and Horn, R., J. Membr. Biol., 76, pp.197-225, 1983.
80. Nelson, M.T. and Reinhardt, R., Biophys. J., 45, pp.60-62, 1984.
81. Ling, G. N. J. Gen. Physiol., 43(5,pt.2) (1960) 149-174
82. Mountz, J.D. and Tien, H.T., in The Enzymes of Biological Membranes, Martonosi, A., (ed.), Plenum Press, NY. 1976, p.139
83. Tripathy, A., Tien, H.T., Ottová-Leitmannová, A.,44 (1998), pp. 183-199

Complete reference citations of the authors, whose papers referred to in the text, may be found, either in [Harris and Etemadi, 1989; Narahashi, 1992] or on our web page:

http://www.msu.edu/user/ottova/blm/membrane_physiology.html

Chapter 8

Membrane Bioenergetics

"Life is nothing but a movement of electrons!"

A. Szent-Gyorgyi, in *Light and Life*, McElroy and Glass (Eds.) Johns Hopkins, Baltimore, 1961.Page 7

"...two life-endowing enzymes:...the ATP synthase...and the electron/ion translocating Na^+/K^+-ATPase... Both...are constrained to the lipid bilayer of membranes, ... play the pivotal role in bioenergetics."

8.1 Introduction

8.2 Basics of Membrane Bioenergetics

Nature's Energy Transducers

ATP (Adenosine Triphosphate)

8.3 The Cristae Membrane of the Mitochondrion

The Chemiosmotic Hypothesis

ATPase and ATP Synthase

8.4 Relevant BLM and Liposomes Experiments

General References (cited by name in brackets in the text)
Specific References (cited by number in superscript in the text)

8.1 Introduction

Albert Szent-Gyorgyi remarked in 1961 that life, as we know it, is nothing but a movement of electrons. 'Where are these electrons located?' and 'How do they move in the living systems?' Most important of all, 'how is ATP (Adenosine Triphosphate), the universal currency of chemical energy of cells, synthesized?' These are some of the key questions asked by scientists whose domain of research is bioenergetics; it is the branch of biochemistry, that deals with the energy transformation in living organisms. To accomplish the electron movement, Nature has toyed with many possibilities. This has resulted in a variety of energy transducing contraptions (biotransducers) made of lipids, proteins, carbohydrates, pigments, and metallic ions in an aqueous environment. The membranes involved are the cytoplasmic membrane of bacteria, the inner (cristae) mitochondrial membrane, and the thylakoid membrane of chloroplasts (*see* Chapter 9, *Membrane Photobiology*). Reactions take place both in and across membranes, respiratory chain ATP synthesis in cells, photosynthetic ATP synthesis in some bacteria and plants, and also photophosphorylation. Electron transfer chains are involved in the cristae membrane of the mitochondrion, and the thylakoid membrane of the chloroplast for energy transduction and utilization. These electron/ion-transfer enzyme systems or redox chains, made of pigmented protein moieties, are embedded in a matrix of lipids in the form of a bilayer. These biotransducers are the functional entities whose active investigations occupy a central domain in membrane bioenergetics. One approach to the study of these complex enzymes has been resorting to membrane reconstitution using artificial bilayer lipid membranes of both spherical and planar configuration (liposomes and BLMs). For applications of electrochemical and electro-optical methods, the BLM is a system of choice and has been so employed. For example, pigmented BLMs have been studied by photoelectrospectrometry and shown to be capable of light-induced electron transfer and redox reactions (see Chapter 9, *Membrane Photobiology*). In contrast, electronic processes in BLMs in the absence of light have been much more difficult to demonstrate, although they have been repeatedly attempted [Morino, 1988]. In this chapter a brief description of the essential aspects of membrane bioenergetics will be

given. This will be followed by a brief description of the cristae membrane of mitochondrion. Next, a review of the reconstitution experiments using planar lipid bilayers (BLMs) and liposomes. Finally, other lipid bilayer experiments with respect to membrane energetics will be presented.

8.2 Basics of Membrane Bioenergetics

Sources of Bioenergy

The sources of life's energy are limited to:

- The energy of light in the range from 400 to 1000 nm of the spectrum of solar radiation, and

- The chemical energy stored in organic compounds by virtue of their constituent atomic and molecular configuration.

It is worth noting here that the ultimate source of free energy for the living systems on Earth comes from the fusion reaction in the sun that may be epitomized as follows: $4\ H \longrightarrow {}^4He + 2\ e + 2.5 \times 10^7$ eV (1 electron volt = 1.602×10^{-19} joule; 1 calorie = 4.184 J).

However, before the appearance of cells upon which all living organisms are based, energy in the form of lightning, ultraviolet light, and ionizing radiation are necessary to form the molecular building blocks of the cell membrane, from CH_4, NH_3, N_2 and H_2O. For more complex prebiotic compounds, two following examples are relevant: $CO_2 + H_2O + h\nu \rightarrow HCO + HCHO + O_2$, and glutamic acid $\{HOCO(CH_2)_2NH_2CHCOOH\}$ + ATP $\rightarrow$ glutamyl phosphate + ADP + $NH_3 \rightarrow$ glutamine + phosphate. In the second example, the free energy is supplied by the hydrolysis of ATP, the molecular structure of which is shown in Fig. 8.1.

In the above cases, we are referring to electronic energy. In fact, as pointed out by Albert Szent-Gyorgyi, the discoverer of vitamin C, who

said, 'life is nothing but a movement of electrons!', as already qouted under the chapter byline, and

"It is common knowledge that the ultimate source of all our energy and negative entropy is the radiation of the sun. When a photon interacts with a material particle on our globe it lifts one electron from an electron pair to a higher level. This excited state as a rule has but a short lifetime and the electron drops back within 10^{-7} to 10^{-8} sec to the ground state giving off its excess energy in one way or another. Life has learned to catch the electron in the excited state, uncouple it from its partner and let it drop back to the ground state through its biological machinery utilizing its excess energy for life processes."

Cellular energy metabolism

In a cell (or organism), the sum total of all chemical reactions that take place is referred to as metabolism. Through metabolism, cells make use of resources to obtain useful energy and building materials for their continued existence, growth, and replication. In order for these to happen, a large negative free energy change ($\Delta G^0 < 0$) is necessary. For now, a reaction central to cellular metabolism is the oxidation of glucose to the products CO_2 and H_20 (ΔG^0 = - 686 Kcal/mol), whose free energy is conserved in the phosphorylation of ADP to ATP. ATP, also known as the universal currency of cells, is synthesized in mitochondria via a scheme proposed by Mitchell (Chemiosmotic Hypothesis). More specifically, the foodstuff (carbohydrates, fats and proteins) one ingests are broken down enzymatically into simpler molecules in three stages (catabolism) before the cells can make use of them (see Table 8.1). First, carbohydrates, fats, and proteins are broken down, respectively, into sugars, fatty acids and glycerol, and amino acids. Second, sugars and fatty acids upon oxidation are converted into the acetyl groups of acetyl co-enzymes *A* (acetyl Co*A*) in mitochondria. Third, the acetyl Co*A* is degraded to CO_2 and H_2O with the production of ATP. Of interest to note here is that the primary link between carbohydrate and fatty acid metabolism is Acetyl-Co*A*. Carbohydrates can be converted to fatty acids, or vice versa, from which

carbon derived either from fatty acid oxidation or glycolysis can enter the citric acid cycle. [Metzler, 1977; Datta, 1987]. In this chapter, we are mainly concerned with the mechanisms of ATP synthesis and hydrolysis, as discussed from the viewpoint of membrane bioenergetics.

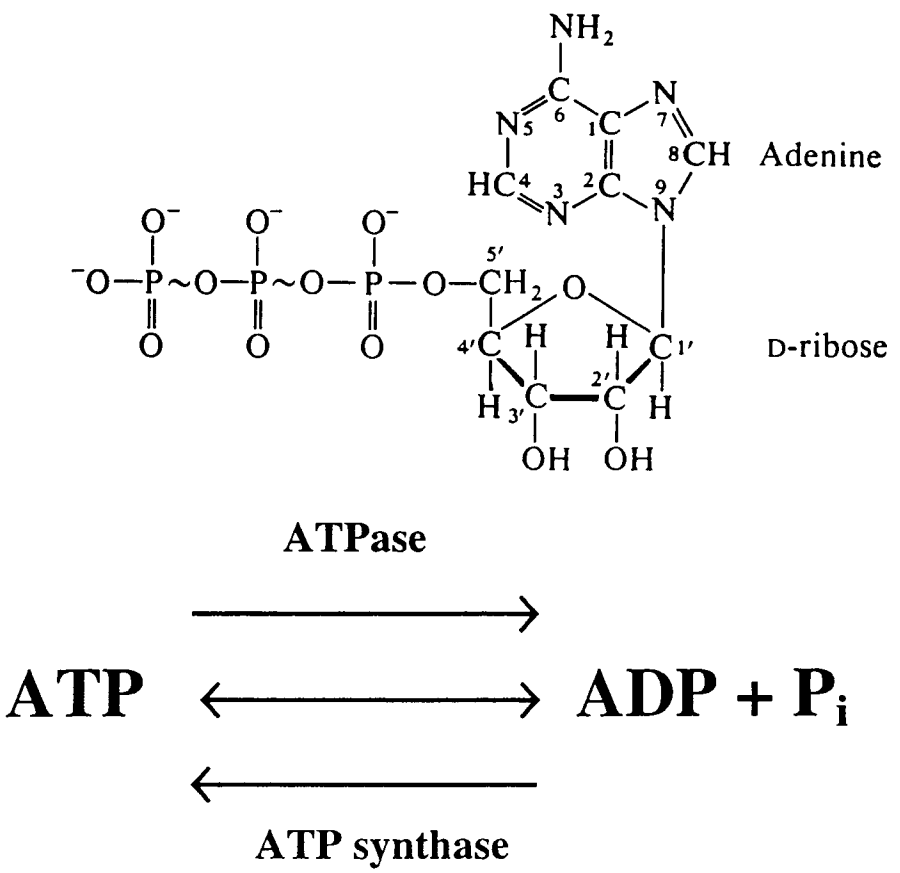

Fig. 8.1 The molecular structure of ATP. Hydrolysis of the outermost phosphate (PO_4) releases 31 KJ (~ 7.4 Kcal) per mol of free energy. As indicated above, the reaction is reversible. This power-rich molecule was discovered in 1929, showed to be the universal energy currency in all living organisms, including humans in 1939, and was synthesized nine years later.

First of all, the flow of matter from organic nutrients to cell constituents (applicable from E. coli to human cells) may be summarized in the following diagram:

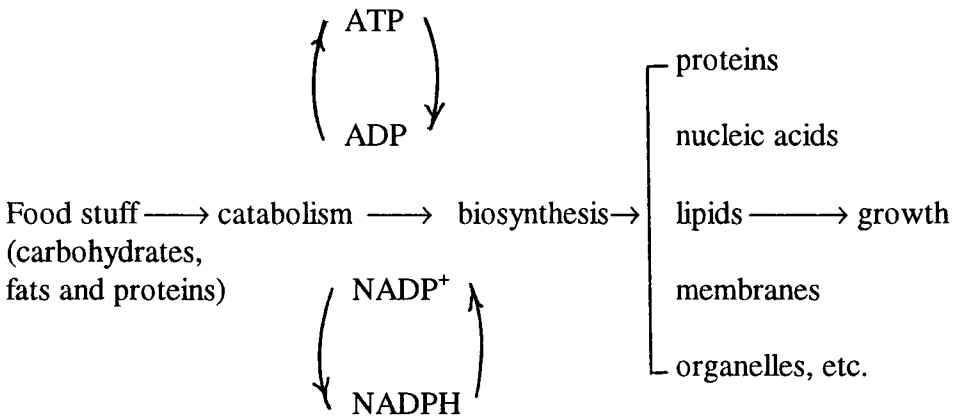

(8.1)

Cellular metabolism may be divided into three domains (or stages), as presented in Table 8.1: (A) Citric Acid or Krebs Cycle (also known as TCA = tri-carboxylic acid cycle), (B) Glycolysis, and (C) Fatty Acid Biosynthesis and Oxidation. In domain (A), some ATP and NADH are produced. But most of ATP is generated via electron flow coupled to the chemiosmotic mechanisms. The ATP thus formed is consumed, on the order of 50%, to transport solutes (e.g. Na^+ and K^+) across membranes.

For controlled energy transduction and material transformation in the absence of oxygen, cells use anabolic metabolism for biosynthetic activities, the pathways of which generate the simple molecules that are the precursors of biomacromolecules such as amino acids for proteins, sugars for polysaccharides, fatty acids and glycerol for lipids, and nucleotides for nucleic acid polymers. Much of biochemical energy for living organisms comes in the form of organic molecules in the environment (proteins, lipids, polysaccharides, and sugars). For the present, consider reduced carbon in the form of D-glucose. A process called glycolysis converts glucose to pyruvate. Pyruvate is then oxidized to CO_2 and most of the electrons are removed as hydride ions (H^-) and stored as molecules of $NADH^+$. This latter process involves the Citric Acid Cycle and one of its intermediate

metabolites is succinate, which is oxidized by the enzyme succinate dehydrogenase. Oxidative phosphorylation is the process cells use to extract the stored free energy in $NADH^+$ and succinate. Before describing the three domains of cellular metabolism, let us ask 'how did living organisms manage to do without oxygen at the beginning? And 'where did oxygen come from?'.

Prior to the evolution of oxidative phosphorylaltion, life was based on anaerobic mechanisms. As such, life proceeded at a much slower pace for millions of years. Then some organisms developed photosynthesis using the energy of the Sun. Once the revolution had started they evolved a mechanism to reduce CO_2 and make use of water as the electron donor. A byproduct of this vital process was oxygen. As O_2 concentrations increased in the atmosphere, it created an opportunity for non-photosynthetic organisms. The standard redox potential for O_2 is about 800 mV. If O_2 could be used as an electron acceptor for partially oxidized organic molecules, they could be completely oxidized and a large amount of free energy would be available to cells. However, there is one problem with using O_2 to oxidize organic molecules, since the amount of free energy released is huge. For example, oxidation of glucose by oxygen to the products of CO_2 and H_20, releases 686 Kcal/mol of energy (ΔG^o is negative). If living cells including humans operate like an internal combustion engine, it would be fine to deal with this quantity of free energy. Since we are not, so cells decided from way back to organize the production of free energy from oxidation and distribute it via transduction to ATP (the so-called universal currency of life). The actual transduction machinery is made of lipid bilayer-based membranes (*see* Item 8 of Fig. 1.2, Chapter 1). The process is called oxidative phosphorylation.

Now back to our discussion on cellular metabolism: In domain (A), a more efficient pathway is catabolic metabolism, as most ATP is generated through electron transport, usually supported by the electrons donated from NADH (a strong electron donor with a negative redox potential) and is used to drive many biosynthetic reduction reactions. The NADH is in turn generated through metabolic oxidation of organic monomers such as carbohydrates and lipids. NADH serves as a common carrier, allowing one membrane-bound electron transport system to accept electrons from a abundance of original sources. NADH is shuttled to the respiratory

Table 8.1 Catabolism of Injested Food Stuff.

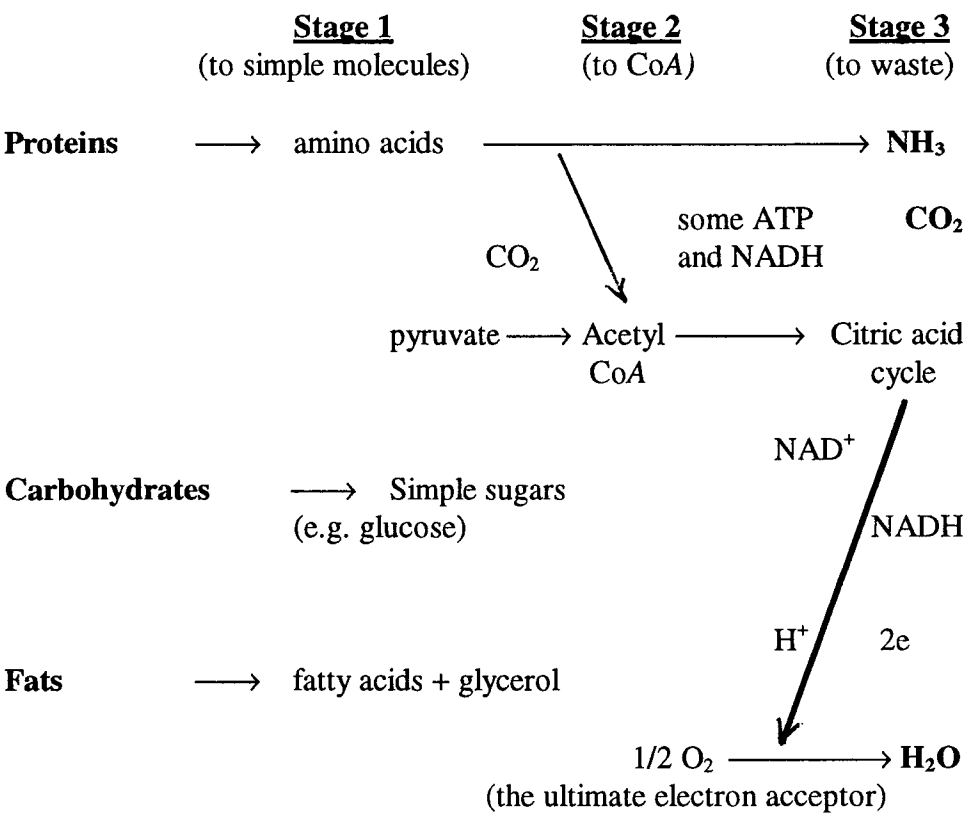

Note: for a 150 lbs (~ 69 Kg) human being, energy expenditure for the following activities (10 minutes): sitting ~ 18 Kcal, walking ~ 30 Kcal, walking upstairs ~ 180 Kcal, and thinking ~ 180 Kcal. In this connection, a recent finding on obesity control is of interest. A gene for a protein, termed UCP (uncoupling protein) has apparently been identified that seems to control the efficiency with which human beings make use of the energy in their food. This newly identified gene is an protein that is capable of 'uncouples' electron transport processes that store and convert energy captured from metabolizing food from the production of ATP, the ultimate energy source for most of the work cells do. A number of UCPs have been known, one of which, for example, is found in the fat of brown adipose tissue. Humans (also small rodents) have a lot of this tissue when they are born but lose most of it before reaching the age of two.

electron transport chain, where its oxidation supports large ATP generation. In aerobic organisms the TCA cycle is used to further oxidize the pyruvate from glycolysis. Pyruvate is first oxidized, releasing CO_2 and a 2-carbon acetate unit covalently linked to an activating carrier molecule, in a complex termed Acetyl-CoA. Acetyl-CoA reacts with a 4-carbon organic acid (oxaloacetate), to form a 6-carbon organic acid (citrate). A sequence of reactions follow, in which electrons are removed from the organic acids and transferred to NADH or $FADH_2$, common electron carriers for many catabolic reactions. At two more points during the cycle CO_2 is released, with the net result that the 4-carbon oxaloacetate acceptor molecule is regenerated, but the 2-carbon acetate is released as 2 molecules of CO_2. In heterotrophic or catabolic systems, the ammonium is released from the amino acid and excreted in urine, while the carbon skeleton is then free to re-enter glycolysis or the TCA cycle.

In domain (B), in aerobic organisms the NADH from glycolysis is available for oxidation by respiration, and pyruvate from glycolysis is further oxidized, releasing much more energy. It should be mentioned that glycolysis is a very ancient cytosolic path and is carried in the absence of oxygen (anobolisim), in which 6-carbon glucose is broken down to two 3-carbon pyruvate molecules, thereby generating two molecules each of ATP and NADH through substrate-level phosphorylations. Organisms derive most of their energy requirements from glycolysis and derivatives by this pathway, the process of which is known as fermentation.

In domain (C), fatty acids are the precursors for lipid biosynthesis, which are of course essential structural molecules for biomembranes. When oxidized, lipids are also a rich source of NADH and $FADH_2$ to support electron transport and ATP generation. In primeval times when food was limited, our progenitors worked hard under difficult conditions and evolved genetically a strong appetite for fats and sweet stuff as valuable energy sources. Today, cravings for such food raise problems for certain people in different areas of the world.

Although not directly related to human cellular metabolism, one other pathway of nitrogen metabolism should be mentioned for

completeness. Some prokaryotes contain an enzyme system that catalyzes nitrogen fixation; the conversion of N_2 to NH_3. This path is very old and widespread among prokaryotes, but requires a very large energy and reductant contribution. Thus, it is activated only when alternate nitrogen sources are not available. No eukaryotes have this capacity, but some plants maintain symbiotic nitrogen-fixing bacteria; the plant provides carbohydrate sustenance and the bacteria fix nitrogen for their own and the plants requirements. Some cyanobacteria contain this full metabolic complement, and rely on products from other organisms to sustain their existence.

The free energy concept

Life, as far as we know in our universe, depends upon spontaneous processes such as flowing of heat from a warmer body to a cooler one, water at the mountain top to its valley below and excited electrons at a higher energy level to the ground state in accordance with the second law of thermodynamics, which is expressed in the entropy function, $S = Q/T > 0$. To assess entropy change (ΔS), which is the sum of $(Q/T)_{system}$ and $(Q'/T)_{surroundings}$, is a difficult task. Experimentally, the free energy function (G) introduced by Gibbs is used, which is obtained by combining the first and second laws of thermodynamics (*see* Chapter 3). The Gibbs free energy change ($\Delta G = \Delta H - T\Delta S$) is by far most useful in bioenergetics, for it can be related to the equilibrium constant (K) of a reaction ($\Delta G^o = -RT \ln K$) and to the standard reduction-oxidation (redox) potential (E^o) of an electrochemical cell ($\Delta G^o = -nFE^o$).

As will be described presently, energy transductions in living cells are membrane-based redox reactions. It should be stated here that ΔG^o and E^o as expressed are in their standard states, usually at one atmosphere of pressure and 25°C, with reactants and products at unit activity. ΔG and E expressed without the superscript 'o' are for reactions other than the standard state conditions. In bioenergetics, $\Delta G^{o'}$ and $E^{o'}$ are used, with all

components present at 1 M, except $[H^+]$ which is at pH = 7. For all spontaneous processes at constant temperature (T) and pressure (P), $\Delta G < 0$, which is the maximum work possible except PV work. For a given process involving one or more reactions, these are called *coupled reactions*, which are crucial in explaining cellular energy transduction. Thus, in bioenergetics the free energy concept is important for it indicates the capacity of doing useful work for which ΔG is negative. This concept applies to a single reaction as well as to a group of reactions so long as the overall ΔG is less than zero. Finally, a remark should be made about useful work which is a product of two terms, intensity times capacity; examples are electrical work (electric potential times charge) and transport work (chemical potential times mass), as already discussed in Chapter 3 (*Basic Principles*).

The electrochemical potential

In bioenergetics the basic unit of action is the cell and its organelles (e.g., chloroplasts and mitochondria) of which the cell's plasma membrane along with its organelle membranes play the central role. For a cell to be viable, nutrients and toxic waste products must be transported across the membrane, for which ΔG must be negative, otherwise metabolic energy must be supplied. Since a compound is a chemical species, an intensive factor called the chemical potential (μ) can be assigned to it. If the chemical species also carries electrical charges, then the term assigned to it is called the electrochemical potential ($\underline{\mu}$). By definition, $\underline{\mu} = \mu + zF\phi = \mu^o + RT \ln a + zF\phi$, where μ^o is a constant, R is a gas constant, T is absolute temperature, a = activity coefficient (γ) multiplied by concentration C, z is the valence, F is the Faraday constant, and ϕ is the electrical potential. It can be shown that $\mu = (dG/dn)_{P,T}$, at constant pressure and temperature. For transmembrane processes of interest, the driving force is the electrochemical potential gradient in the direction (x) perpendicular to the

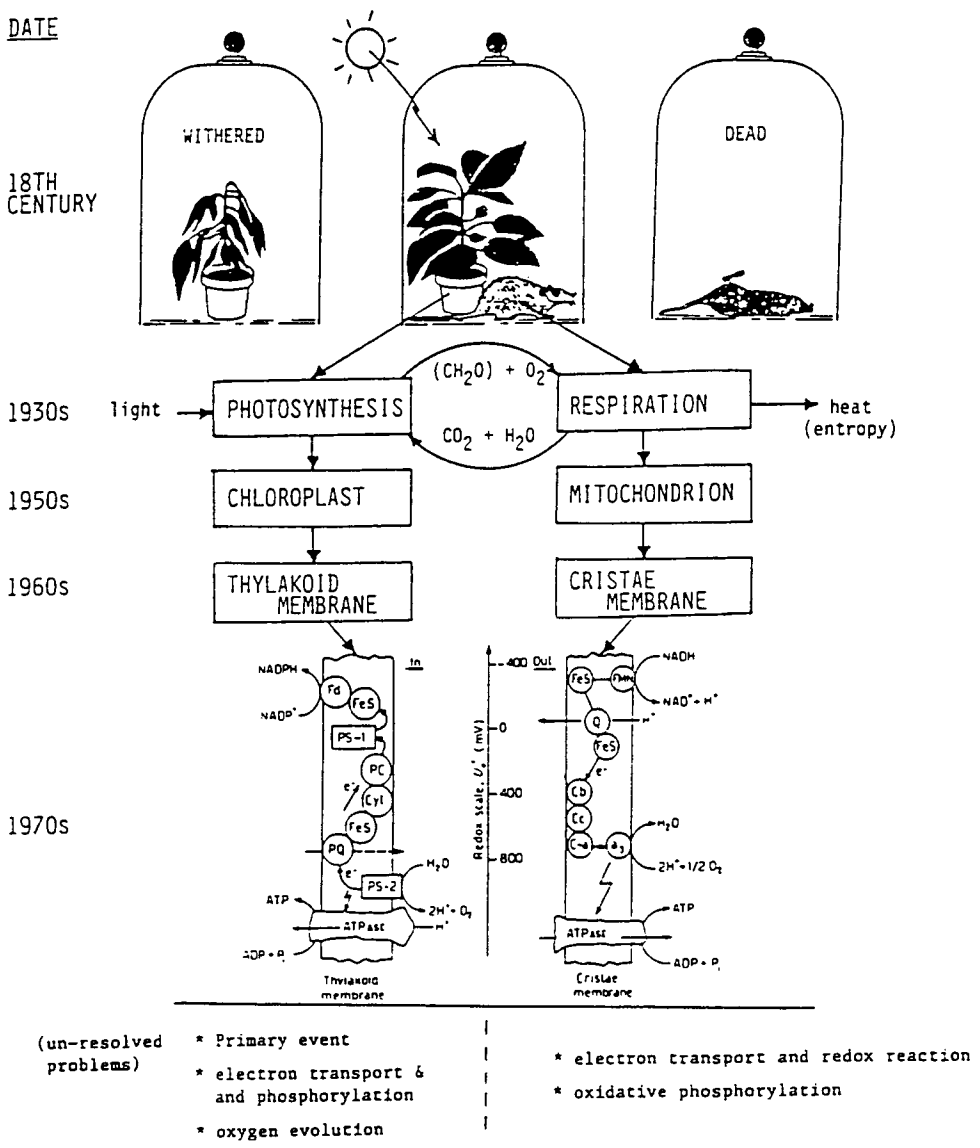

Fig. 8.2 Interdependence of photosynthesis and respiration. Also shown are the major events in membrane bioenergetics research. In the 1930's, new insights were gained by comparative studies. [Dryhurst and Niki, 1988, p.533].

membrane and is given by the well known Nernst-Plank equation, as previously discussed (*see* Chapter 6, *Membrane Electrochemistry*), which is also of central importance in membrane bioenergetics.

Energy flow and coupled processes in bioenergetics

In thermodynamics, one deals with closed and open systems, the difference between the two being that the latter involves the exchange of matter in addition to energy (heat and work). Clearly, a cell is an open system. Similarly, organelles such as chloroplasts and mitochondria are also open systems. Other energy transducing systems of interests are found in bacteria and in visual receptors. We shall mainly focus our attention on the cristae membrane of mitochondria and the thylakoid membrane of chloroplasts. It is particularly noteworthy that energy transduction and material transport in these two systems are coupled; the products of photosynthesis are utilized as the reactants in respiration, and vice versa. Priestley dramatically demonstrated the interdependence of photosynthesis and respiration in 1771. He observed that a green plant in a closed bell jar withered after some time, in spite of sunlight and a mouse in another closed bell jar died. However, when both the plant and mouse were placed in the same closed bell jar in the presence of sunlight, both thrived.

The essential feature of Priestley's experiment is the coupled processes of photosynthesis and respiration in that they represent on a global basis, a steady-state operation brought about by the flow of energy from the ultimate high energy source of the sun to the low potential sink of the earth (Fig. 8.2). It is not the energy itself that makes life possible, but the flow of energy.[1,2] Thus, from the observations of Priestley, a clear picture has emerged after two centuries of research that energy flow and coupling are what bioenergetics is all about; they are accomplished through the energy transducing membranes of chloroplast thylakoids and mitochondrial cristaes [Dryhurst and Niki, 1988].

Nature's Energy Transducers

The fundamental unit of vital cellular functions is the lipid bilayer that provides the structural framework for embedding and intercalating of other membrane constituents. For functions, the most important of which is energy transduction. Thus, a variety of energy transducing apparatus made of lipids, proteins, pigments, and their complexes must reside in the membrane. Some of these energy transducing machineries may be termed as biotransducers listed in Table 8.2.

Experimental problems in membrane bioenergetics

In the 1950s, the ultrastructures of chloroplast and mitochondrion were revealed by electron microscopy. In the 1960s, advances in membrane biophysics and biochemistry together with the chemiosmotic hypothesis of Mitchell, and model bilayer lipid membranes resulted in evermore detailed pictures of the thylakoid membrane of chloroplasts and the cristae membrane of mitochondria in the 1970-1980s. In the 1990s and beyond, what are some of the unfinished problems of membrane bioenergetics? In photosynthesis, there are three, namely (i) the primary steps of photon conversion, (ii) electron transport and oxygen evolution, and (iii) ATP synthesis. In respiration, the main problems appear to be quite similar; they are electron and proton transport, energy coupling, and ATP synthesis. All of these are membrane-bound problems. To date, in view of what is known about the thylakoid membrane, the cristae membrane and other energy-transducing membranes, they are far too complicated for direct experimentation when the structural-functional relationships are considered at the molecular level (see Fig. 8.2). For example, a number of hypotheses have been proposed for photon conversion in green plant photosynthesis, one of which is the mechanism analogous to that taking place in semiconductor silicon solar cells [Barber, 1979]. If so, the most direct kind of experiment would be to place electrodes across the membrane and measure its voltage under illumination. Unfortunately, such an approach is still very difficult owing to the microscopic size of the thylakoid. Similar experimental difficulties are encountered for mitochondria, when one wishes to probe them electrically. Therefore, an alternative approach is

resorting to membrane reconstitution experiments using bilayer lipid membranes (planar BLMs and spherical liposomes). As will be described in Section 8.4, these reconstituted membrane systems are very useful for investigating energy transduction, electron transfer, and other energetics problems.

Mechanisms of membrane transport

Of central importance in membrane bioenergetics are primary particles such as electrons, holes (vacant sites left by electrons) and protons, and a vast variety of chemical compounds. All of these must be transported within as well as across the membrane. The driving force is due to the electrochemical gradient for passive and facilitated transport. Ion 'pumps' driven by metabolic energy from ATP-hydrolysis for active transport are known, an outstanding example of which is the Na^+/K^+ ATPase pump. Four basic mechanisms have been proposed: carrier, channel, hopping, and tunneling. For ions such as Na^+ and K^+, water-filled channels seem to be the most efficient pathways for transport. For electrons and holes a tunneling mechanism is a plausible one. Protons may be transported by a hopping mechanism. It is beyond the scope of this chapter to discuss any of these mechanisms here. The fact is that electron/ion carriers, pigments, and protein 'channels' can be reconstituted into experimental bilayer lipid membranes displaying unique transport characteristics (*see* Chapter 5, *Membrane Transport* and Chapter 7, *Memrbane Physiology*).

8.3 The Cristae Membrane of the Mitochondrion

From an evolutionary viewpoint, mitochondria in mammalian cells are descended from bacteria, and thus mitochondrial respiration is similar to bacterial respiration, except that the autonomous bacteria are more metabolically flexible. In most cases carbohydrates or lipids are the electron donors in both bacterial and mitochondrial aerobic respiration. The process is catalyzed by electron flow from carbohydrates or lipids to

Table 8.2 A classification of biotransducers*

Basic Unit	Membrane Involved	Energy Transduction
Chloroplast	Thylakoid Membrane	Light to Chemical
Mitochondrion	Cristae Membrane	Food to Chemical
Individual Cell	Plasma Membrane	Chemical to Mechanical
Nervous System	Nerve Membrane	Chemical to Electrical
Retina	Rod and Cone Segment Membranes	Light to Electrical
Inner Ear	Tectorial Membrane	Sound to Electrical
Muscle	Plasma membrane (Actomyosin)	Chemical to Mechanical
Fire Fly	Plasma membrane	Chemical to light

*Adapted from [Ref. 3 and Dryhurst and Niki, 1988, p.532]

oxygen (the ultimate electron acceptor) as outlined in Eq. 8.1. It is worth noting here that there are bacterial anaerobic respiration and chemotrophic respiration. In the absence of oxygen some bacteria can use alternate electron acceptors and some others can also extract electrons from alternate inorganic donors such as hydrogen sulfide (H_2S). If inorganic electron donors are used, the system is termed chemotrophy (chemical-eating or lithotrophy, rock-eating), since the respiration does not need organic substrates.

Mitochondria are cellular organelles responsible for the synthesis of ATP; they are commonly accepted as the 'power plants' of aerobic cells, the primary function of which is fatty acid oxidation to the products CO_2 and H_2O, and ATP synthesis. As listed below, there are four types of ATP synthesis system centered on mitochondria. It is, therefore, instructive to describe the essential steps involved in isolating mitochondria. Here we cite the procedure in isolating mitochondria,. for example, from liver. Step (i),

liver is homogenized in isotonic serine (0.25M), Step (ii), the homogenate is centrifuged at 800g for 10 minutes, the supernatant is collected (the pellet contains unbroken cells and nuclei), Step (iii), the supernatant from Step (ii) is then centrifuged at 10,000g for 10 minutes leaving microsomes and cytosol in the supernatant and mitochondria, lysosomes etc. in the pellet, Step (iv) the mitochondria can be separated from other organelles by density gradient centrifugation, and (v) the mitochondria are washed and re-suspended in fresh medium. Now, let us list the major studies of four types of ATP synthesis system:

(1) Mitochondria -- they can transport both external ADP and ATP, but exchange of external ADP for Internal ATP is favored under energized or phosphorylating conditions.
(2) Mitoplasts -- (mitochondria without the outer membrane which has been removed by treatment with digitonin, similar to (1).
(3) Submitochondrial particles (SMPs) that are made by sonication of mitochondria. SMPs carry out efficient phosphorylation but show no respiratory control and high ATPase activity. They are deficient in transport functions. They have a major advantage in that the ATP synthtase and the ATPase are on the outside of the membrane, there is therefore no barrier to substrate or other interacting molecules, and
(4) Vesicles reconstructed from respiring and ATP synthase complexes.

Morphologically, the structure of ATP synthase/ATPase appears as knobs on one side of the membrane, in mitochondria and bacteria they project into the matrix (in SMP's and in isolated thylakoid membranes they project outwards). The synthesis (hydrolysis) of ATP occurs on the side of the membrane with knobs. The ATP synthase complex that performs this task consists of at least 9 different polypeptides. This complex is considered as two parts; a protruding knob like structure which is the catalytic site of ATP synthesis (known as F_1 in mitochondria), and the remainder of the complex, known as F_0, which are highly hydrophobic and conduct H^+ through the membrane. F_1 can be removed from the membrane by several methods (e.g. mechanical disruption, sonication, and chemical agents such as urea, EDTA).

The coupling mechanism of oxidative phosphorylation involves the generation of an electrochemical potential gradient of protons (PMF = protonmotive force) across the inner membrane by the H^+ pumps of the respiratory chain. The PMF, also known as the Central Energetic Intermediate, is the energy currency, and is also involved in the movement of substances across membranes. This PMF, in addition to being the immediate source of energy for ATP synthesis, has a great influence on the transport of cations and anions across the inner cristae membrane, and in a number of cases the membrane potential itself is used to drive transport. There are at least two transport pathways, a cation uniporter, which transport K^+ and other cations, and an anion uniporter that is also called the inner membrane anion channel. The latter uniporter enables mitochondria to pump out salts and the K^+ uniporter allows salts to be pumped in. The balance between these processes is the essence of mitochondrial volume homeostasis. In this regard, electrophysiological methods are eminently suitable to examine the properties of channels extracted from mitochondria and reconstituted into planar BLMs and spherical liposomes in order to identify and purify these membrane-bound channels. In respiratory schemes electrons flow from an electron donor with a relatively low redox potential (low affinity for electrons) to an electron acceptor with a relatively high redox potential (high affinity for electrons), as indicated in Fig. 8.2. The electron flow is not direct; rather the electrons are passed along a series of membrane-bound carriers linking the acceptor to the donor. During the transfer the path of the electrons crosses the membrane several times, and H^+ are carried across during the process. The proton transport across the membrane is driven by localized redox reactions. In one popular mechanism, for instance, a membrane-embedded quinone molecule is reduced on one side of the membrane, accepting electrons and protons. The quinone then diffuses to a site on the opposite side of the membrane, where it is oxidized. The electrons are then passed to another carrier and the protons are discharged from the membrane. Thus, experiments of embedding a quinone in an electron-conducting planar lipid bilayer and measuring its electrical properties are of great interest (see Section 8.4).[26,39]

As mentioned in the Introduction, the chemiosmotic hypothesis of Mitchell suggests that coupled electron and ion movements are crucial to

redox protein-chain energy transduction into ATP formation.[4] The key questions to be answered are: (i) how are electrochemical potential gradients ($\Delta\underline{\mu}/\Delta x$) of protons across the biomembranes generated, (ii) how are electrons, ions, and chemical species transported across the membrane, and (iii) how are such potential gradients used to drive the synthesis of ATP?

The Chemiosmotic Hypothesis

There is a plethora of literature on mitochondria and chloroplasts whose main task is energy transduction. That is, the organelle membranes of mitochondria and chloroplasts produce most of the energy for cellular processes in the form of ATP (adenosine triphosphate). The mechanism of energy transduction has been elegantly explained by Mitchell's chemiosmotic hypothesis.[4] Briefly, mitochondria contain the enzymes and coenzymes that mediate the electron transport from NADH (a reduced nucleotide) down the chain of redox proteins to the ultimate electron acceptor, oxygen. As electrons move down the redox protein chain, an electrochemical gradient of protons is generated. Free energy is conserved in the synthesis of ATP as a result of the discharge of the proton gradient across the cristae membrane of mitochondria. The essential feature of the Mitchell theory is 'energy-coupling' among the various membrane-bound processes: electron transfer, redox reaction, ion and proton gradient, membrane potential and ATP synthesis. Obviously, these membrane-based activities, many of which are electrical in nature, should be probed and investigated by electrochemical methods, as have been carried out on whole cells and nerve axons by electrophysiologists. Unfortunately, mitochondria, along with other organelles such as chloroplasts, are too tiny to stick microelectrodes into them for reliable experiments, although there have been several isolated reports.[5,6] In order to test the chemiosmotic hypothesis, many researchers have in the past resorted to reconstituted membrane studies using artificial bilayer lipid membranes (planar BLMs and liposomes).[8,9]

The Adenosine Triphosphate (ATP) Generating Enzyme

The bulk of ATP in cells is generated through a process of oxidative phosphorylation, which takes place in intracellular organelles, namely, mitochondria and chloroplasts. Briefly, there are two life-endowing enzymes: the adenosine triphosphate synthase that catalyzes the formation of ATP and the electron/ion translocating Na^+/K^+-ATPase that maintains the critical balance of Na^+ and K^+ ions in the living cell. Both ATP synthase and Na^+/K^+-ATPase are constrained to the lipid bilayer of membranes, which play the pivotal role in bioenergetics.

The components of oxidative phosphorylation must be viewed in three separate ways: (a) as a linear assembly of electron transfer components; (b) as a series of components ordered according to their standard reduction potentials; and (c) in terms of their location in the membrane. The linear assembly in terms of standard redox potential (Fig 8.1): NADH $\rightarrow$ FMN $\rightarrow$ FeS $\rightarrow$ Q $\rightarrow$ [FeS·Cyt b] $\rightarrow$ Cyt c_1 $\rightarrow$ Cyt c $\rightarrow$ Cyt a $\rightarrow$ Cyt a_3 $\rightarrow$ O_2.

The transfer of electrons from NADH and succinate to oxygen releases enormous amounts of free energy. Because of the supramolecular arrangement of the machinery in the lipid bilayer-based membrane, the free energy is transduced to an electrochemical potential gradient of protons ($\Delta\mu_{H+}$). The proton gradient thus generated across the membrane is released and the free energy produced is used to reverse an ATPase activity ($ATP + H_2O \rightarrow ADP + Pi$).

The supramolecular architecture of oxidative phosphorylation is ATP synthase that is composed of two parts, the F_0, which is an integral membrane complex which functions as a proton pore, and F_1 which can hydrolyze the catalysis of ATP hydrolysis. When the relative proton concentration on the outside of the membrane in increased by electron transfer reactions (e.g. proton pumping by Q), the F_0 complex can let the protons run down the concentration gradient, releasing free energy. The close association of F_1 with F_0 causes the released free energy to be used to

reverse the hydrolysis of ATP, with the net synthesis of ATP from ADP and Pi.

The ATP synthase or F_1F_0 ATPase is the central energy-generating enzyme in biology, which catalyzes the synthesis of ATP from ADP (adenosine diphosphate) and Pi (inorganic phosphate); it works inside cell mitochondria and chloroplasts as well as in bacterial cell membranes. This process of ATP formation requires 30 to 60 KJ/mole of energy, depending on the experimental conditions. ATP synthesis by electron transport chain, a series of proteins embedded in the membrane lipid bilayer, is coupled to the oxidation of nutrients in eukaryotic cells, that undergo a series of redox reactions. Portion of the free energy released in this process is used to generate an electrochemical potential gradient of protons across the membrane. Energy from the resulting proton gradient is then released back through the membrane (a channel in F_0, a domain of the ATPase), where it is connected to the active sites of the lipid bilayer-bound ATPase (a spherical F_1 domain) to drive ATP synthesis. It should be noted that when an ATPase is coupled to its energy source, it is called an ATP synthase. A question of long-standing is 'how the energy of the proton gradient is coupled to the catalytic sites' ? This question appears to be answered recently through the x-ray crystal structure determination of the ATPase.[9] The hypothesis proposes that the enzyme's three catalytic sites are involved in the following steps: (i) the binding of ADP and Pi to an active site in the '*loose*' state, (ii) the conformational conversion of the site to the '*tight*' state, and (iii) the ATP synthesis with the site converting from a tight to an '*open*' state to a loose state, making it once again capable of binding substrate. To see how these steps work, the structure of ATP synthase (F_1F_0-ATPase) must be mentioned. In the domain of F_1-ATPase, it consists of nine subunits of α (3), β (3) and γ, δ, and ε (one of each) with active sites for ATP synthesis, whereas in the domain of F_0-ATPase, it contains a minimum of three subunits (a, b, and c) and functions as a proton channel. The F_0/F_1 ATP synthase coupling factor is a proton channel that joins the movement of protons across the membrane to drive ATP formation, which exists in all known organisms. This coupling factor is a multi-polypeptide complex, with a similar structure and function. In other words, a rotary mechanism of ATP synthase coupling factor has been suggested. It

involves a transmembrane H^+ flow through the F_0 membrane channel drives rotation of a subunit of the F_1 complex. This rotation forces a sequence of conformational changes in the F_1 catalytic unit. The changes in protein conformation create a tiny cavity where phosphorylation of bound ADP is energetically favored. Further rotation and conformational changes then expel the newly formed ATP from the cavity. Fig. 8.3 depicts a model for the structure of E. coli F_1F_0-ATP synthase. The binding-change mechanism for ATP synthesis is illustrated. The main points of the hypothesis are: (1) the energy stored in the electrochemical potential gradient of protons is used to discharge formed ATP from its catalytic sites, (2) energy-linked substrate binding, formation of tightly bound ATP and product discharge take place simultaneously at three separate but interacting sites that remain 120° out of phase in the catalytic cycle, and (3) the binding changes required for catalysis are driven by the rotation of an asymmetric aggregate of subunits as shown in Fig. 8.3. This last process is likened to that of a truncated bacterial flagellar motor whose rotation is energized by the dissipation of the proton gradient through the F_0-ATPase proton channel. In this connection, Miedema and associates[37] reconstituted a hydrophobic Fo of ATP synthase, purified from bovine heart mitochondria in BLMs, which resulted in a voltage-selective K^+ channel of 18 pS. Venturicidin drastically decreased the channel opening. The Fo preparation is claimed to be very pure and will be used in crystallography studies. Regarding this, functional nonpeptide rigid rod-shaped polyols for transmembrane proton channels have been reported by Weiss and co-workers.[10] Proton flux mediated by polyols are shown to be strongly favored over metal cations and anions. The modest selectivity for monovalent cations ($Rb^+ > Cs^+ > K^+ > Na^+ \simeq Li^+$). Their results suggest that a rigid rod-shaped polyol acts as a functional unimolecular proton wire which mimics the hydrogen-bonded chain mechanism found in bioenergetic systems.

It is worth mentioning here that the work described above provides solid ground for interpreting many experiments done over the past two decades, since previously not much was known about the ATP synthase's atomic structure and the findings have been ususally explained in speculative ways. The structural determination, as pointed out by the authors, will be used in chemical modification and genetic studies; 'detailed

structures of F_1-ATPase and other enzyme complexes involved in energy conversion in mitochondria are likely to be key elements in understanding aging and neurodegenerative and neuromuscular diseases (e.g. Alzheimer's and Parkinson's disease).[38]

8.4 Relevant BLM and Liposomes Experiments

In bioenergetics, electron-transfer and redox reactions play the central role. For example, the conversion of solar energy into chemical free energy in green plant photosynthesis is conducted in special membrane-bound subcellular organelles called chloroplasts, the operational apparatus of which is the thylakoid membrane (*see* Chapter 9, *Membrane Photobiology*). Another outstanding example of energy transduction is the oxidative phosphorylation in the cell respiration, which takes place in the cristae membrane of mitochondria, as described above. Cell respiration involves the overall oxidation by oxygen of the reducing equivalents (e.g., NADH) that have resulted from the metabolic process of ingested foodstuff. As in the thylakoid membrane, the redox proteins embedded in the lipid bilayer of the cristae membrane are poised to perform electron-transfer and redox reactions. In both green plant photosynthesis and cell respiration, the energy-transducing membranes are composed of redox protein components intercalated among lipid molecules that are organized in the form of a lipid bilayer.

To account for the above-mentioned membrane-bound electron-transfer and redox reactions more quantitatively, the components of electron-transfer chains have been placed on a redox potential scale ($E^{o'}$) as in ordinary electrochemical reactions. That is, the redox potential of the components involved in photosynthesis and respiration are expressed in terms of $E^{o'}$ (in volts or mV vs. normal hydrogen electrode at pH 7). Invariably, these redox potentials have been determined by measuring the electromotive force (EMF) in a simple electrochemical cell using platinum electrodes. This lack of membrane participation in these determinations of the membrane-bound bioredox reactions in the past was to be expected since until the early 1960s experimental bilayer lipid membranes (planar

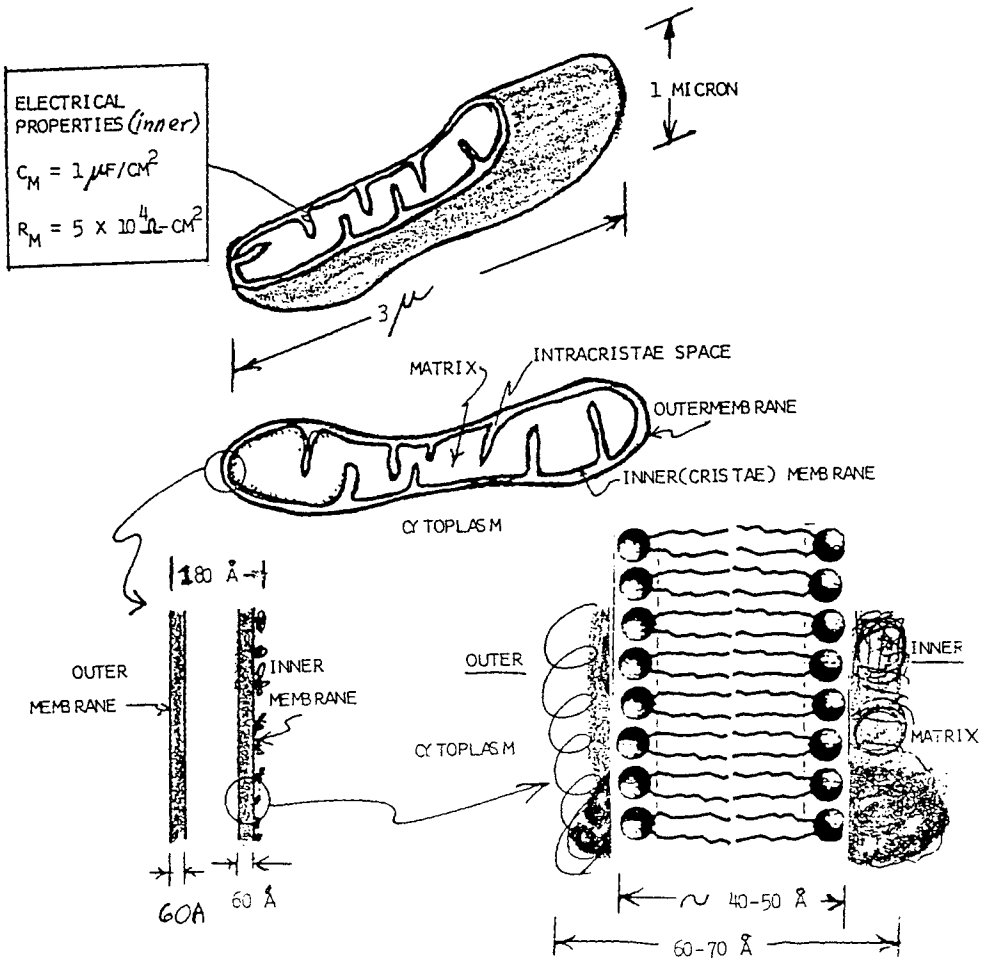

Fig. 8.3 (see N. Rasmussen, Trends Biochem. Sci., 21 (1996) 319-321 cite this with picutre of mitochondrion Fig. 8.3 depicts a model for the structure of E. coli F_1F_0-ATP synthase The binding-change mechanism for ATP systhesis is illustrated in Fig. 8.3.

BLM and spherical liposomes) were not available, and the electrochemical techniques developed by electrochemists were the only ones adopted by life scientists who have since compiled extensive tables of redox potentials of biological compounds using platinum electrodes [Blank, 1994]. Thus, until early 1980s, two factors had been mainly responsible for the lack of success: (a) a modified BLM capable of electronic processes was not available, and (b) a suitable experimental technique with an established theoretical basis was not tried. In a later section, an approach using modified planar lipid bilayers containing organic semiconductors (e.g. TCNQ = 7,7,8,8-tetracyanoquinodimethane, and TTF = tetrathiafulvalene) as a model for the cristae membrane and investigated by cyclic voltammetry will be described. We will first of all describe some prior work on the use of planar lipid bilayers as a model for understanding the cristae membrane of mitochondria.

Bilayer lipid membranes as a model for the cristae membrane

From a biophysical point of view, the use of whole mitochondrion (or chloroplast) to test the 'molecular' theory of Mitchell does not seem satisfying. The translocation of ions, such as protons, across a complex system, such as cristae, is in itself ill defined. The interactions between various fluxes (ion and water movements, electron and hole transport, etc.) are far too complex to be amenable to a simple analysis. At the present time, direct tests with the mitochondrial membranes are difficult. Experimental testing of the chemiosmotic hypothesis, using simpler model systems such as planar BLM and spherical liposomes are, therefore, in order.

Among the first to employ a BLM system to test one aspect of Mitchell's hypothesis were Bielawski, Thompson and Lehninger[11] who studied the effect of 2,4-dinitrophenol (DNP) on the BLM conductivity. The BLMs were formed from a solution of purified lecithin, cholesterol, and n-decane. They found that the uncoupling agent (DNP), at a concentration of 10^{-3} M, decreases electrical resistance of BLM to less than 0.4% of the original values (i.e., from 1.5×10^7 to 6.1×10^4 Ω cm^2). The effects of uncoupling agents of oxidative phosphorylation on BLM were

examined systematically by Liberman et al.[12] The major findings of their work are as follows:

- In general, the uncoupling agents (uncouplers) raise the conductivity of BLM by several orders of magnitude, and the effect depends strongly on the pH of the bathing solution, being most effective at the pK value of the uncoupler.
- The effectiveness of the uncouplers studied follows a series: tetrachlorotrifluoromethylbenzimidazole (TFB) > *p*-trifluoromethyloxy-carbonylcyanide phenylhydrazone (FCCP) > DNP > salicylic acid > acetoacetic ester. The order of effectiveness is similar to that found in the mitochondria.
- The current/voltage curves of the BLM in the solution containing the uncoupler are nonlinear, and depend on pH and the buffer capacity of the solution.
- In the presence of TFB, the BLM behaves as a hydrogen electrode. The modified BLM is said to be more permeable to H^+.
- The uncoupler is considered a carrier of H^+. The operation is described as follows: on one side of the membrane, a proton reacts with the uncoupler in the BLM; this uncoupler-H^+ complex diffuses across the membrane, and to the other side of the membrane discharging the H^+; the uncoupler then returns to the other side.

Liberman, Topaly, et al.[12] suggested that their findings agree with the scheme of oxidative phosphorylation as envisioned by Mitchell, and concluded that BLMs are good models for the mitochondrial membrane.

The pH-dependence of the effect of TFB and other uncouplers on the electrical conductivity of the BLM described above has been studied in detail.[13] The earlier investigators were interested in establishing the relationship between the pK value of the modifier (e.g., DNP) and the conductivity of the BLM and found that the effectiveness of these compounds in lowering the conductivity follows their pK values. The conductivity for picric acid-modified BLM was about 10^{-4} ohm^{-1} cm^{-2}. In this connection, Wardak[14] has investigated the effect of picric acid on the

transport of H^+ and K^+ and found that the salt of picric acid is highly permeable in the BLM.

Other uncouplers such as carbonylcyanide phenylhydrazone (CCP) derivatives have also been reported by Ting, Wilson, and Chance.[15,34] Although they also observed a resistance decrease by a number of compounds, the conclusion they reached is that no simple correlation exists between the relative effectiveness of the uncouplers on the conductance of BLM. Since literally several hundreds of agents are known at the present time, a theory is needed to explain the observed phenomena. Bruner[16] has, in fact, attempted to establish a correlation between the pK value and the membrane potential arising from ion concentration gradients. It has been found that substances, which uncouple oxidative phosphorylation in mitochondrial membranes, usually increase the electrical conductance of phospholipid BLM. Among these uncouplers is a group chemically known as weak acids. For this group, the conductance of the BLM, when measured as a function of pH at fixed uncoupler concentration, shows a maximum at a pH approximately equal to the pK value of the uncoupler used. Corresponding maxima in electrical potential arising from ion concentration gradients are also observed. Bruner then suggested that charge transport is by direct transfer of either protons or anions of the uncoupler. A fixed charge density at the membrane surface is required in Bruner's theory.

As pointed out by Mitchell, all uncouplers are weak acids (HW) with relatively high solubility in the lipid phase of the membrane. In BLMs, weak acids act as carriers for H^+ and the charged translocating species is either the anionic form of the weak acid, W^-, or the complex of the anion, HW_2^- and the undissociated acid, HW. Thus, the concentration of the undissociated HW and W^- should be governed by the pH of the outer and inner bathing solutions.[17] At a steady state in the lipid bilayer phase

$$J_{HW} - J_{W^-} = 0 \qquad (8.2)$$

where the J's denote molecular fluxes. If the two solutions of different pH are separated by a BLM formed from a neutral or zwitterionic lipid, a membrane potential (E_m) should be observed according to the Nernst equation

$$E_m = \frac{RT}{F} \ln \frac{[W^-]_i}{[W^-]_O} = \frac{[H^+]_O}{[H^+]_i} \qquad (8.3)$$

since the anion and its complex (HW_2-) are the only charge translocating species. The behavior of uncouplers is readily understood by considering the following reactions as shown by Finkelstein:[17]

$$HW \longleftrightarrow H^+ + W^- \qquad (8.4)$$

$$K_1 = \frac{[H+][W-]}{[HW]} \qquad (8.5)$$

$$HW_2- \longleftrightarrow HW + W^- \qquad (8.6)$$

$$K_2 = \frac{[HW][W^-]}{[HW_2^-]} \qquad (8.7)$$

Note that $[HW_2-] << [HW] + [W^-]$. Therefore, $[W^-]_{total} = [HW] + [W^-]$. It is further assumed that the concentration $[HW_2^-]$ is directly proportional to [HW] at the interfaces. Experimentally, it has been found that DNP and other uncouplers exhibit a quadratic dependence of conductance on concentration and pH with a sharp maximum conductance at $pK_1 = pH$. Accordingly, it can be readily shown that

$$[HW_2-] = \frac{K_1}{K_2} [W^-]_{total}^2 \frac{[H^+]}{(K_1 + [H^+])^2} \qquad (8.8)$$

Defining the BLM conductance (G) as

$$G = k[HW_2^-] \tag{8.9}$$

we then have, from Eq.(8.8)

$$G = k \frac{K_1}{K_2} [W^-]_{total}^2 \frac{[H^+]}{(K_1 + [H^+])^2} \tag{8.10}$$

Eq.(8.10) indeed predicts that the membrane conductance goes through a maximum at $pK_1 = pH$ and is proportional to the square of the total anion concentration, $[W^-]_{total}$. The results of Wardak[14] are consistent with the analysis of Finkelstein.[17] In this connection, Dilger, Fischer and Haydon[18] suggested that because of the ability of weak acids to transport protons across BLM and to uncouple oxidative phosphorylation in mitochondria, some fraction of the lipid bilayer component of the cristae membrane must have a dielectric constant (ε) greater than 2.2. This conclusion is based on the experiments of Dilger et al., who used chlorodecane as the BLM solvent (ε = 4.5) instead of *n*-decane (ε = 2). In the presence of thiocyanate, the conductance of chlorodecane-BLM is one thousand times larger than *n*-decane-BLM. The specific capacitances, which are proportional to ε/t_m, are 0.73 and 0.39 $\mu F\ cm^{-2}$ for chlorodecane BLM and *n*-decane-BLM, respectively. Thus, the observed increase could be due to either an increase or a decrease in t_m (membrane thickness). Since Dilger et al. have observed, by X-ray diffraction experiments, that there is little difference in thickness, the effect must be due to the increase in BLM dielectric constant.

Electronic Processes in Planar Lipid Bilayers (BLMs)

In the introductory remarks of this section, organic semiconductors such as TCNQ and TTF are mentioned. The selection of TCNQ and TTF for incorporation into the BLM is motivated by the fact that TCNQ

belongs to a class of 'organic metals' whose most unusual properties have great technological potential in the construction of molecular electronic devices, and as components of solar cells.[19] For TCNQ-doped BLMs as a model of the cristae membrane, a brief description of the BLM system along with an experimental setup is given below.

Planar lipid bilayers (BLMs). To facilitate handling, a simple cell assembly is used. This consists of a 10 ml Teflon cup (commercially available), which is held in a Lucite holder, such as shown in Fig. 8.4, having a second chamber of equal volume. A small aperture of about 0.5 - 2 mm in diameter is punched in the side of the Teflon cup. Since electrical measurements can provide the simple means of monitoring the behavior of BLM and its interactions with different modifiers and agents, they are in common use in BLM investigations. Because of the very high resistance of the unmodified BLM ($>10^8$ ohm cm^2) care is needed in the insulation and shielding of the membrane chamber, electrodes, cables, switches, and any connections in order to avoid current leakage and antenna-like action of the setup. Therefore, it is generally advisable to enclose the whole membrane chamber in a Faraday cage. For d.c. measurements, different types of so-called non-polarizable electrodes may be used, including saturated calomel and silver/silver chloride (Ag/AgCl) electrodes. However, for several kinds of experiments using pulse or a.c. techniques, bright platinum or platinum coated with platinum black electrodes, though polarizable, are preferable. The temperature of the cell assembly (Teflon cup and Lucite holder) may be maintained either by placing the whole assembly in a thermostatic chamber or by circulating water from a thermostat through a glass coil placed around the Teflon cup. For effective stirring, a magnetic stirrer with very small stirring bars may be used, if required, but should be switched off during measurements, particularly for cyclic voltammetry (CV) studies. During the experiments, if required, the solution in one or both chambers may be changed with the BLM in place, by using infusion-withdrawal pumps in which closely matched syringes should be used in order to prevent the membrane from bulging and breaking.

BLM formation. The seminal method introduced in the early 1960's is still being practiced with some minor modifications. With the cell chambers

filled with an appropriate bathing solution (usually 0.1 M KCl), a drop of lipid solution is introduced to the aperture in the side of the Teflon cup using a Hamilton syringe with a dispenser attachment (PB-600-1). Owing to the small diameter of the aperture, a low power (20-60x) microscope is used to observe the membrane. After formation of the BLM, the electrical properties can be investigated with the instruments described above. To exchange or add small amounts of solutions on either side of the BLM, a disposable or an adjustable micropipette may be used. If a given amount of a new solution is added to one side, the same amount of bathing solution should be added to the other side of the BLM to maintain equal solution volumes on both sides.

Methods of study. If the BLM system to be investigated is symmetrical, i.e., a symmetrical BLM separates two identical electrolyte solutions of equal ionic strength, then in the absence of external voltage there is no residual transmembrane potential. A transmembrane potential may be generated, however, whenever there is a difference in ionic strength, ionic species or redox compounds across the planar lipid bilayer.[8]

Experimental Findings

Porin Channels. A voltage-dependent anion channel material from Paramecium mitochondria has been incorporated into BLM. The transmembrane voltage is in the vicinity of zero and decreases sharply with both positive and negative voltage. These mitochondrial outer membrane porin channels appear to be anion selective, in contrast to bacterial porin channels.[20-22] Mention should also be made about the incorporation of an invertebrate respiratory protein into BLM. Menestrina et al.[23] reported that keyhole limpet hemocyanin interacts with BLMs increasing their conductance by the formation of cation-selective hydrated channels through the membrane. When the interaction occurs only on one side of the BLM, the membrane conductance is voltage dependent. This showing is a characteristic sigmoid shape similar to those obtained from the mollusk, *Paludina vivipaa*, that has the property of open channels in the BLM. In oxidized cholesterol BLM, channel conductance depends on the type of

electrolyte present (e.g., 0.2 M NaCl, 0.4 M $BaCl_2$, and 0.6 M $CaCl_2$), ranging from about 20 to 500 pS (picosiemens). Menestrina et al. also discussed their interesting results in terms of the Gouy-Chapman electrical double-layer theory (*see* Chapter 6, *Membrane Electrochemistry*) and suggested that molluscan hemocyanins are a class of channel-forming proteins.

Cytochrome c oxidase. One of the important and well-studied cristae membrane enzymes is cytochrome c oxidase,[24] which catalyzes the final reaction of respiration by reducing molecular oxygen to water with the electrons from its substrate. Several investigators have incorporated cytochrome c oxidase into BLM (*see* review by Shamoo and Tivol[25]), and found that, in the presence of oxidized cytochrome c on one side, a potential difference is generated upon reduction of the substrate. This transmembrane potential could be reversed or prevented by cyanide. However, the BLM conductance was little affected by cyanide or ascorbate.

Electron Transfer from Cytochrome c to Cytochrome c Peroxidase across the BLM . Cytochrome c (Cc) is a small, peripheral membrane heme-protein that transfers electrons between the cytochrome b-c_1 complex and the cytochrome oxidase complex in the mitochondrial respiratory chain. As a model for the investigation of the mechanism of electron transfer reactions, the interaction of Cc with cytochrome c peroxidase (Cc P) has been widely studied. There have been two types of experimental approaches: (i) electron transfer within a Cc-CcP complex in solution (the crystal structure of the proteins and a computer model of the complex are known) and (ii) the reduction and oxidation of both Cc and CcP, measured separately at an electrode, in simple electrochemical systems. The first direct demonstration of an electron transfer between Cc and CcP across a modifier BLM has been reported.[55] The calculated rate constant is five to six orders of magnitude lower than that reported for the complex. Further, it has been demonstrated that the formation of the complex is not the necessary condition for the electron transfer and that electron transfer between the two proteins can be mediated by a modified BLM.[55]

Electrical work and membrane capacitance. Let us turning now briefly to the electrical properties of BLMs. Typically a BLM (or biomembrane) has been represented by an equivalent circuit consisting of a combination of resistor (R_m) and capacitor (C_m) in parallel.[8] Thus, it is worth remembering that energy may be stored in the membrane capacitor, as given by

$$dW_{el} = C_m \int E_m \, dE_m \qquad (8.11)$$

or

$$W_{el} = 1/2 \, C_m E_m^2 \qquad (8.12)$$

where W_{el} is the electrical work, C_m and E_m are, respectively, membrane capacitance and potential. In this connection two aspects of cristae membrane from an experimental point of view will be described: electron transport and ATP synthesis. As already mentioned, central to membrane bioenergetics are the transmembrane redox reactions. The process entails the generation, separation, and transport of charges (electrons, holes and protons), leading eventually to redox reactions on opposite sides of the membrane. The energy stored in separated charges and redox compounds may be used to drive vital processes such as oxidative phosphorylation. In the cristae membrane of mitochondria, the redox protein components embedded in the lipid bilayer are poised to perform electron-transfer and redox reactions. The exact location and orientation of these membrane proteins and other components are not known (Fig. 8.5). The generally accepted arrangement, however, is that membrane proteins and other components are closely intercalated among lipid molecules which are organized in the form of a lipid bilayer. It should be of interest to incorporate electron-transfer proteins and co-enzymes into BLMs and to investigate their redox properties (e.g., measurements of $E^{O'}$ values by cyclic voltammetry and/or by photoelectrospectrometry). $E^{O'}$ values in the past have been obtained by the classical potentiometric technique without 'membrane' participation. The potentiometric technique is frequently complicated by the low electron exchange currents at Pt electrodes. Since accurate $E^{O'}$ values are important in determining the sequence of electron

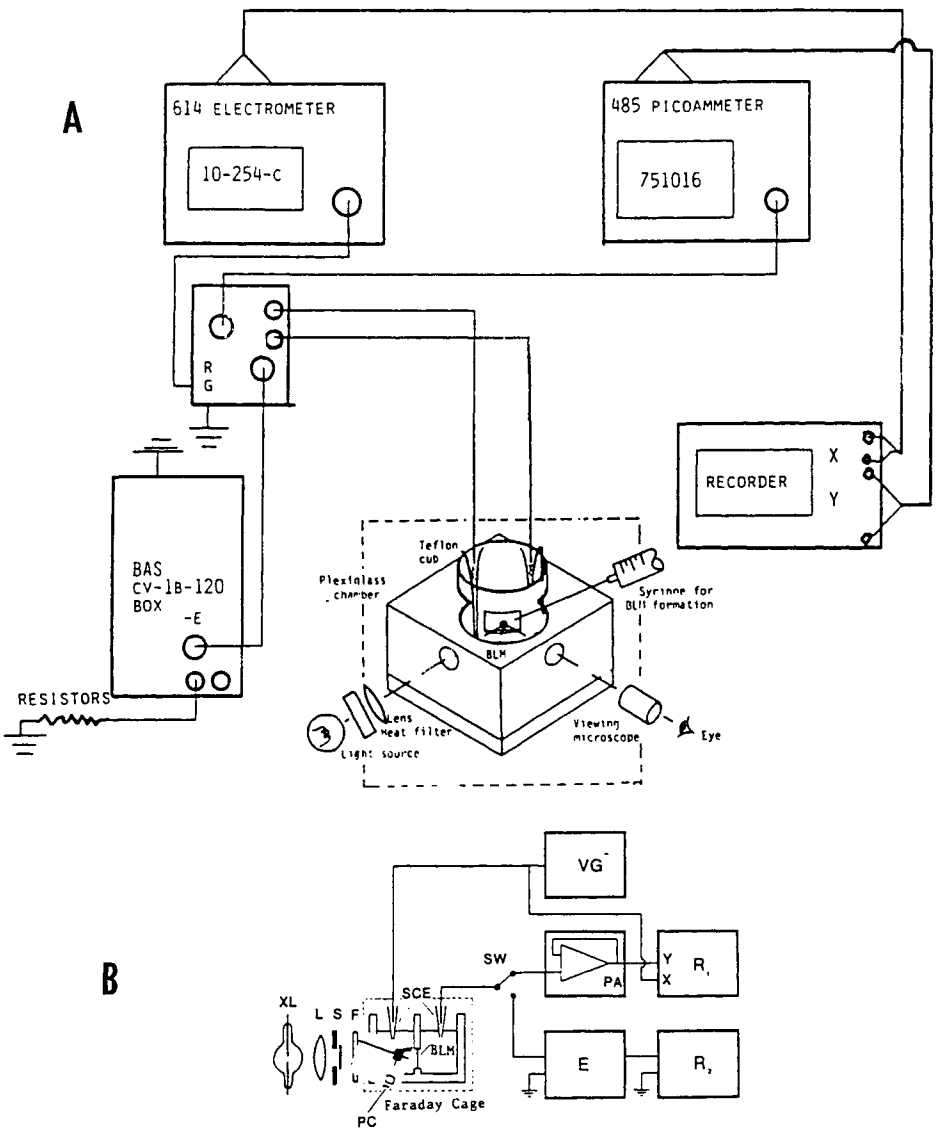

Fig. 8.4 Experimental setup for investigating transport and energy transduction in reconstituted bilayer lipid membranes (planar BLMs). (A) Schematic representation of the setup for electrical measurements. (see [34]). (B) Block diagram for investigating photoelectric effects in pigmented BLM.

transfers among redox enzymes in electron transport chains, their measurements in 'membrane-bound' states are self-evident. Up to now the measurement of $E^{O'}$ values of electron transport chain components in association with lipid bilayers has not been possible, owing simply to the fact that no suitable technique existed. With the availability of electron-conducting BLMs (e.g. doped with either TCNQ or C_{60}) coupled with the cyclic voltammetry technique (CV),[26,59] an entirely new approach is open for unraveling the complicated electron-transfer and redox reactions in the process of oxidative phosphorylation.

It is significant that a suitably modified BLM can function as a redox electrode in relation to the standard redox potentials ($E^{O'}$) of electron-transfer chain components, which, if known have usually been determined by the use of the Pt electrode. Since the electron-transfer chain components are known to be closely associated with the lipid bilayer, the values thus determined by the usual Pt electrode may be quite different from their actual values in the membrane. Conceivably, therefore, the technique described may offer a new approach to the determination of the $E^{O'}$ values of membrane-bound molecules such as the cytochromes using modified BLM as the working electrode. Further, this new type of electronically conducting BLMs coupled with the cyclic voltammetry technique may provide a unique opportunity to probe the mechanisms of biological redox reactions [Blank, 1994].

It is worth noting here that the most unique aspect of the mitochondrial process is ATP synthesis. As proposed by Mitchell, it establishes a proton and/or potential gradient (i.e., $\Delta\mu_{H^+}$) which is used to drive ATP synthesis from ADP and phosphate ions. Racker and Stoeckenius reported photophosphorylation in reconstituted proteo-liposomes from a mixture of bacteriorhodopsin, beef-heart ATPase, and soybean phospholipids (see Oosawa and Imai[27]). This outstanding, often cited experiment does not appear to have been repeated by others. It would be, therefore, of interest to test the chemiosmotic hypothesis using planar BLM. In the BLM system, both pH and applied potential gradients can be easily created.

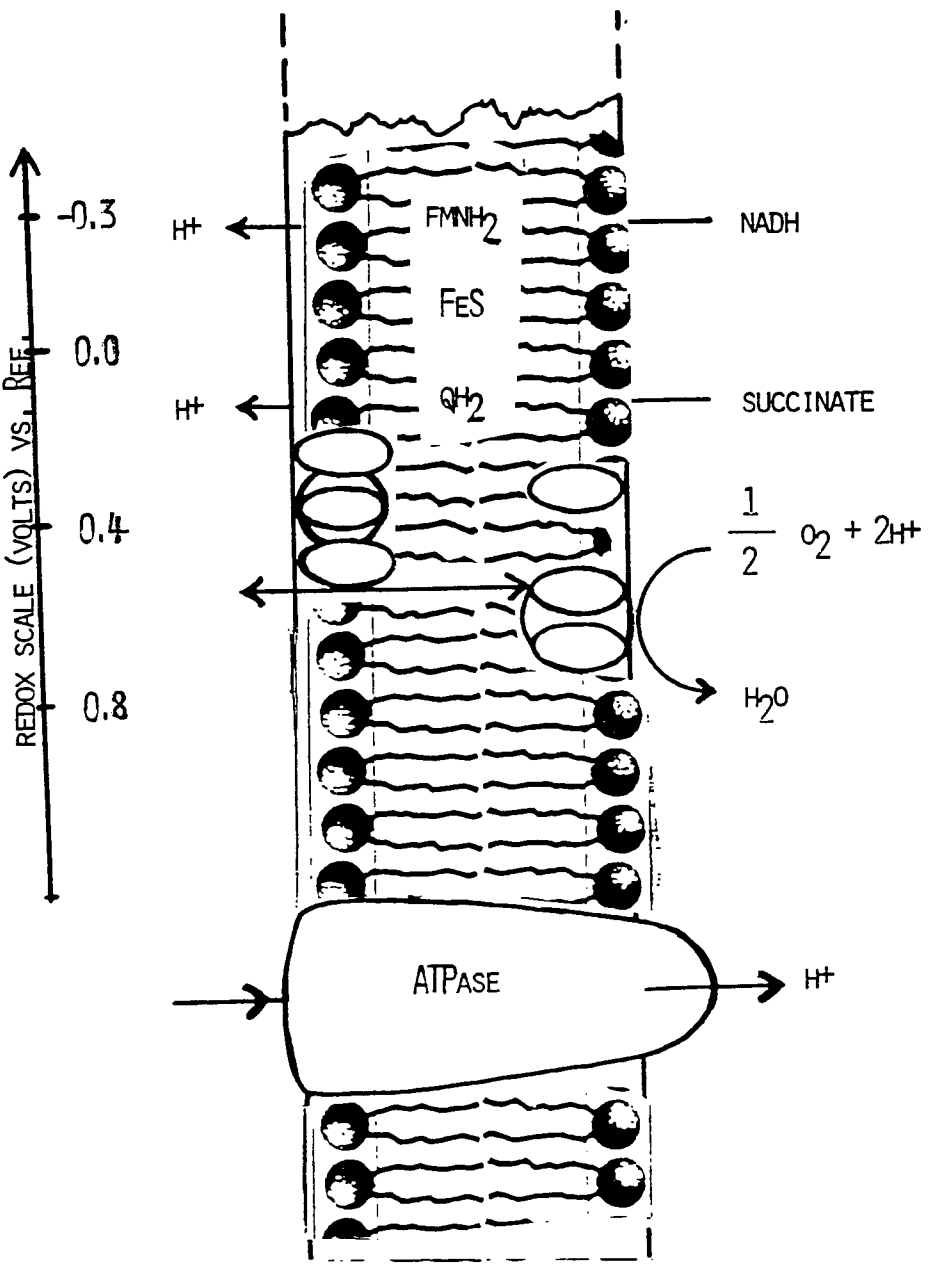

Fig. 8.5 *The Na^+/K^+ ATPase.*

The Na^+/K^+ ATPase

The reverse process of ATP synthesis is hydrolysis, which is used to provide energy for a host of cellular activities such as muscle contraction, nerve impulse transmission, compound synthesis and active transport. The last mentioned process is of special significance, since differential ion concentration gradients are crucial to the living state. For example, almost all cells maintain a high concentration of K^+ and a low concentration of Na^+ inside. The so-called Na^+/K^+ pump has been demonstrated to exist in the membrane, which actively transports 3 Na^+ out and 2 K^+ into the cell against their respective electrochemical potential gradients. The Na^+/K^+ pump, made of protein (the Na^+/K^+ ATPase) is powered by the energy resulting from the hydrolysis of ATP. To test this hypothesis, Jain and associates[40] carried out the first attempts to study the functions of the Na^+ / K^+ ATPase in a BLM formed from oxidized cholesterol,[28] after addition of a membrane-bound form of the enzyme from rat brain synaptic vesicles to one side of the membrane.[29,32] The addition of ATP to the same compartment in which the enzyme was added results in a 1 to 3 orders of magnitude decrease in the electrical resistance (R_m) of the membrane, to a level of 10^6 ohm-cm^2, and the generation of an electrical current across the reconstituted system.[25,41-46] The dependency of this phenomenon on the presence of ATP and Na^+, and its inhibition of ouabain, suggested that it was directly mediated by the enzyme, or more specifically by its α-subunit.[29] In this connection, in order to attain inhibition by ouabain, the inhibitor has to be added to the opposite side of the BLM from that on which the enzyme and the ATP were added.[44] However, it became clear that the site of inhibition by ouabain was located on the opposite side from which the ATP binding site(s) are located, and the same side on which the K^+ binding sites are found.[29,45,56] In agreement with this proposal, the presence of potassium ion in the system appears to antagonize the inhibitory effect of ouabain.[48,49] In contrast, vanadate appears to inhibit from the same side as that on which the ATP binding site(s) are located. However, treatment of the Na^+/K^+ ATPase with trypsin from both sides of the membrane abolished the electrical phenomenon.[51-54] In the experiment of Jain, Strickholm, and Cordes.[28], the BLM was formed in the usual manner. ATP was added to one side of the BLM, and this was followed by

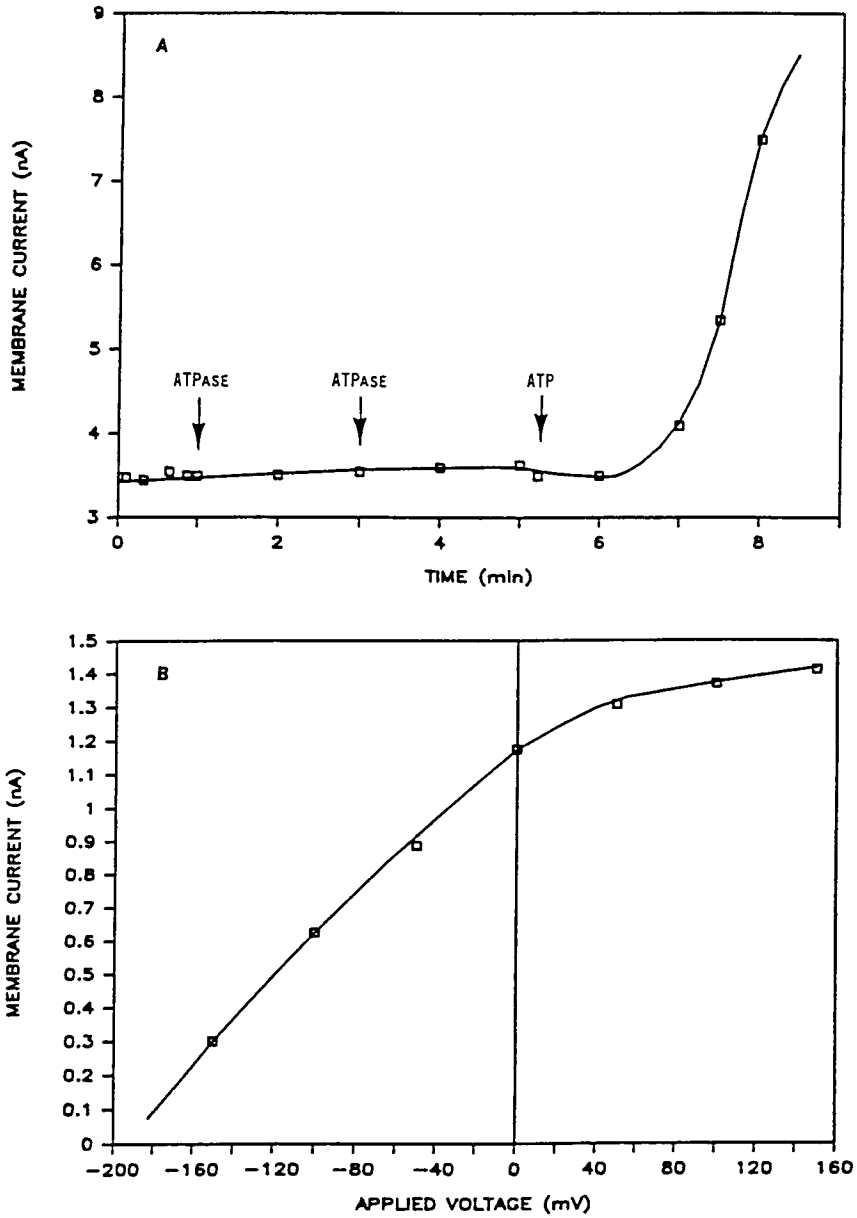

Fig. 8.6 The effect of ATP and ATPase on the electrical properties of reconstituted BLM. (A) Generation of membrane current upon additions of ATPase followed by ATP as a function of time. (B) Current/voltage curve of a reconstituted ATPase-BLM.[8]

the addition of a preparation of membrane-bound ATPase. After these additions, a decrease in the membrane resistance was observed. The current across the BLM and open-circuit membrane potential were monitored. Jain et al. observed a positive current across the BLM. This was interpreted as being due to the transport of Na^+, which was analogous to that found in the natural membrane. The current in their reconstituted system was said to be dependent on the presence of Na^+ in the bathing solution, the magnitude of which depends on ionic strength. Further, the presence of ouabain (a cardiac glucoside), a compound known to block Na^+ transport in red cells, inhibited the current flow across the ATPase-modified BLM. It seems probable that, by introducing ATPase into the bathing solution, 'molecular sodium pumps' might have been inserted into the BLM, which could account for the observed phenomena.

In a different experiment, it was suggested that observed electrical events were due to a particular alignment of ATP molecules on the phospholipied membrane by ions associated at its interphase with the water phase. However, further accumulation of experimental evidence suggested that Na^+/K^+-ATPase isolated from different sources were indeed directly responsible for establishing the ionic currents across the BLM[44,50] The original observations of the electrical events induced by the enzyme on planar lipid bilayers were interpreted as the existence of an electrogenic Na^+/K^+ exchange (not a 1:1 exchange) catalyzed by the Na^+/K^+-ATPase However, the failure of Na^+/K^+-ATPase preparations from different origins in reproducing the results obtained with the rat cortical brain tissue preparations, cast some doubts on the nature of the observed phenomena. Indeed, some reports indicated that the short-circuit current and the open circuit voltage was observed in response to the simple addition of ATP in the presence as well as in the absence of the reconstituted Na^+/K^+-ATPase.

The incorporation of the Na^+/K^+-ATPase into the BLM conferred ion-gated channel properties to the plasma membrane.[41,42] The nature of this gating was described as non-electrical. However, incorporation of the α-subunit of the Na^+/K^+-ATPase demonstrates that the presence of an electrical potential was necessary for sustaining high ATP hydrolytic activity, and the presence of a mebrane potential of 100 mV results in the

closing of the ouabain-sensitive, univalent cation-selective channel. The system appears to operate in two states, one of high conductance, sensitive oubain and vanadate, and the other of low conductance, and insensitive to the inhibitors. The addition of ATP, or the pretreaetment of the enzyme with trypsin prior to its reconstitution into the liposomes did not affect the electrical conductance.[44-46] In this connection, when a small amount of preotein was added to the BLM, it was possible to measure single channel conducatnce of 270 pS. In another approach, the enzyme was first reconstituted into liposomes containing only a mean of one pump per vesicle, and later the proteoiposome was fused with a planar BLM.[42] With this system, the measured sinlge-channel conductance was from 40 to 50 pS; however, it was concluded that such conductance was due to disabled pump molecules. The addition of ATP to a BLM made from a mixture of different phospholipds plus cholesterol to which the Na^+/K^+-ATPase had previously been added resulted in a lag before the short-circuit current was initiated.[44] This electrical current increased over several hours, reflecting a progressive incorporation of individual pump molecules into the planar lipid bilayer. Flat membrane sheets of 0.2 to 1 μm in diameter containing high density Na^+/K^+-ATPase were bound to a planar lipid bilayer.[34] This system produces most probably a fusion of both membranes and could be used to study transmembrane voltage generation using the photolabile derivative, (a caged-ATP) as a substrate, measuring short time-resolution events of approximate 1 ms, upon irradiation with ultraviolet light.[34, 45,46,58]

The operation of the Na^+/K^+-ATPase depends strongly on the presence of Mg^{2+} as seen in the following experiment. A stationary pump current was obtained after addition of the Na^+/K^+ exchanger, monensin, plus the K^+ carrier valinomycin.[29] The pump current was obtained in the presence of Na^+ or Na^+ and K^+ in the presence of magnesium, but not with K^+ alone in the presence of magnesium. When the ATP-binding site(s) of the enzyme were labeled with florescein isothiocyanate no electrical current was observed. Analysis of the transient ionic current presents a biphasic behavior, and shows that a slow non-electrogenic step was followed by an electrogenic transient with a rate constant of 100/s. The intrinsic pump current can be evaluated from the voltage signal, and the dependence of the intrinsic pump current on the concentration of Na^+ permits a kinetic

analysis supporting the assumption that two sodium binding sites have a high affinity and that a third site of lower affinity is rate limiting. Charge-translocation is associated with early events in the normal transport cycle of the enzyme, and it was concluded that Na^+ translocation precedes translocation of K^+. Channel conductance in BLM also has been induced upon addition of the isolated subunits of the enzyme, and with polypeptide fragments obtained after its bromocyanate treatment. In the latter case, two fractions, one with cationic conductance and the other with cationic-anionic conductance without selectivity for Na^+ or K^+ was observed.[25] However, a passive conductance pathway in the Na^+/K^+-ATPase molecule highly selective for Na^+ was first observed in pronase-sensitive, acid-soluble fractions of tryptic-digested membrane fraction from the electrical organ of *Electrophorus*, and from bovine kidney membranes after its reconstitution into a BLM of oxidized cholesterol.[25, 28] It was also suggested that the conductive unit may have an oligomeric nature. The ionophoretic activity was induced by the association of 1 α + 2 β-subunits, since the alpha or the β-sunbunits individually lack ionophoretic activities. Moreover, it was suggested that the Na^+ dependent ionophore was present in the small β-subunit, and the role of the large α-subunit was to induce the opening of Na^+ sites for its ionophoretic properties.[25] This Na^+-ionophoretic activity was subsequently demonstrated in a mixture of intact α+β-subunits of the enzyme at a weight-to-weight ratio of approximately unity. In this connection, mention must be made of the paper by Fendler et al.,[29,57] who investigated the transport activity of purified Na^+/K^+ ATPase incorporated into a BLM [Laeuger, 1991]. Stationary pump currents were obtained after the addition of monensin and valinomycin (ionophores). In the absence of ADP and inorganic phosphate (P_i) the half saturation for the maximal effect was obtained at 6.5 μM released ATP. Further, pump activity was obtained only in the presence of Na^+, K^+ and Mg^{2+}. The electrical response was blocked completely by ouabain and vanadate (ATPase inhibitors). Fendler et al. suggest that their method offers the possibility of studying by direct electrical measurements of Na^+/K^+-ATPase in transport. In this connection the effect of ATPase, followed by the addition of ATP, on the BLM current was observed.[8] In these experiments, open-circuit membrane potentials as large as 130 mV were observed. Development of the membrane potential and short-circuit current is

dependent upon the presence of all the substrates of Na^+/K^+-ATPase as well as the enzyme itself. Further, the short-circuit membrane current thus generated could be diminished by applying voltages of opposite polarity. At about 175 mV positive with respect to the ATPase-free side, the current, presumably due to the Na^+ flux, was essentially zero.

A number of other techniques for embedding the purified Na^+/K^+-ATPase into liposomes have been reported.[41,43,48,50-52] The stated aim is to study further the properties and mechanism of the purified Na^+/K^+-ATPase in proteolipososmes. These experimental techniques were said to be necessary for the study of the functions and physicochemical properties of the resulting liposomes. A first step in this approach has been the understanding of the role of the lipid constituents of the membrane on the Na^+/K^+-ATPase. The activating effect of phospholipids on the ATP hyrolytic activity of the Na^+/K^+-ATPase has been known for some time. Using 90% delipidated and highly inactivated enzyme preparations from rabbit kidney and bovine brain, it was established that addition of sonicated vesicles of phosphatidylserine or phosphatidylglycerol produced its reactiviation, and confers substantial discrimination of K^+ over Na^+ in terms of the permeability of the reconstituted vesicles. Although removal of the native lipids from the enzyme, and its substitution for phosphatidylserine vesicles result in one of the best reactivation of the enzyme, using an enzyme from rabbit kidney it was demonstrated that phosphatidylserine is not an absolute requirement for its activity. When the enzyme was brought in contact with performed liposomes, it was found that it binds to positively electrical charged liposomes made of a mixture of phosphatidylcholine, cholesterol and stearylamine, but not to negativley charged liposomes. However, later experiments demonstrated that full recovery of the ATPase activity was obtained when negative charged phosphatidylinositol plus cholesterol was employed in the reconstitution procedure. Also, it was established that the Na^+/K^+-ATPase also binds to formally neutral sphiongomyelin liposomes, but not to pure phosphatidylcholine liposomes. However, the interaction of the enzyme with preformed liposomes appears to be very weak, since it was easily extracted from the liposomes with high ionic strength solutions, demonstrating that the nature of this protein-lipid interaction does not represent the insertion of the enzyme across the membrane bilayer.[41,43,48,50,51]

To obtain reactivation of the ATP hydrolytic activity of the enzyme, it was also established that no more than six lipid-binding sites of the 30 known to possess the enzyme could be unoccupied. Moreover, the dissociation equilibrium constant for the lipids was determinate to be in the range from .3 to 5 μM, and maximum reactivation was obtained with phospholipids containing unsaturated fatty acyl chains conferring high fluidity to the membrane. Other authors also concluded that to attain good reassembly of the Na^+/K^+-ATPase with the membrane lipid required the addition of diacylphospholipids with fluid acyl-chains and negatively charged polar heads. Furthermore, by modifying the thickness of the membrane bilayer by using phospholipids of different acylchain length, or by the addition of a discrete amount of n-decane, an inverse relationship was demonstrated between enzyme activity and chain length of the saturated fatty acid of different phosphatidylcholine vesicles and maximum activity was obtained with membrane of intermediate thickness.[41,43]

Hybrid reconstitution of the delipidated Na^+/K^+-ATPase from crab nerve into vesicles made of lipids isolated from the brain enzyme increased the sensitivity of the crab enzyme to ouabain inhibition. In contrast, hybrid reconstitution of delipidated enzyme from bovine brain into liposomes formed from the lipids extracted from preparations of the crab nerve enzyme reduced the sensitivity of the brain enzyme to inhibition by ouabain. The variation of the pumping activity with the composition of the lipid membrane results from the different amounts of enzyme incorporated with the correct orientation into the lipid bilayer and to a lesser extent from lipid-dependent variation of the intrinsic turnover rate of the Na^+/K^+-ATPase

The first embedding of an active Na^+/K^+-ATPase into a bilayer liposomal membrane was obtained with the enzyme from bovine brain microsomes solublized by deoxycholate using a mixture of 96% phosphatidylcholine plus 4% phosphatidylserine. Incorporation of the ATPase into the liposome was shown by co-migration of the lipids and the enzyme activity by sucrose density gradient centrifugation. However, no measurement of transport activities was conducted in this earlier work followed by dialysis of the detergent.[41,53,54]

Using proteoliposomes prepared by the cholate-dialysis method, the Na^+ transport function by a purified and reconstituted enzyme isolated from canine renal medulla, and the rectal salt gland of the spiny dogfish shark *Squalus Acanthias* was carried out. The ATP-dependent uptake of $^{22}Na+$ by those vesicles was demonstrated to be against a concentration gradient, increasing the intraliposomal Na+ concentration from 20 mM to 38.4 mM. However, the low efficiency of the transport function was reflected by the low Na^+/ATP ratio, in the order of 0.3 to 0.4. Moreover, the ATP-dependent $^{42}K^+$ efflux by the reconstituted enzyme was negilible.[51, 52]

The low Na+/ATP ratio was attributed to the presence of non-incorporated Na^+/K^+-ATPase molecules. Accordingly, addition of strophantine to the outside medium increased the Na^+/ATP ratio somewhat. Later, ouabain was used to inhibit the non-reconstituted enzyme. The enzyme participating in transport function has been estimated to be on occasion as low as 20% of the total enzyme in the system. However, these data contrast with another report in which it was estimated that only 5% of the enzyme remain non-reconstituted.[51.52]

In those earlier experiments it was also established that ouabain or strophantine inhibits Na^+ transport from the inside of the vesicles, but not from the outside. The inhibition for the transport function of the enzyme by ouabain from the inside of the vesicles is due to the interaction of the inhibitor with ATPase molecules presenting the ATP binding site(s) to the outside of the vesicles, and therefore exposing the K+ binding sites to the vesicular lumen. However, vanadate inhibits the enzyme form the outside of the vesicles, where the ATP-binding site(s) are located int eh enzymes responsible for tranpssort functions since ATP is added to the external media.[53,54]

On the methodological front, a microprocedure for reconstitution of about 200 micrograms of purifired enzyme by the cholate-dialysis method and capable of Na^+ and Rb^+ tranpsort has been developed.[53] Also, an ingenious method to continuously monitor ATP-driven K^+ transport is the use of the sensitive fluorescent probe indocyanine dye in the presence

of valinomycin . Under those conditions the generated K^+ Nernst potential responds to the concentration of potassium ion.[41,52-54]

Analysis of data obtained

Using the relationships $\Delta G^{O'} = -RTlnK$, where $K = [ADP][Pi]/[ATP] = 10^{-4}$, and $\Delta G^{O'} = -nFE_m$, where E_m is the membrane potential at $I_m = 0$, one can calculate the quantity, 'n', the number of protons translocated across the membrane per mol of ATP hydrolyzed. This turns out to be about 3. For ATP synthesis, Lane et al.[30] have reported that the entire mitochondrial electron transport chain (from NADH dehydrogenase to cytochrome oxidase) requires the translocation of at least 12 protons per oxygen atom. How are these results to be correlated remains to be seen.[31]

Channel and ATPase Reconstitutions

Mironova and colleagues[32] have reported BLMs with hydrophobic components extracted from mitochondria and observed Ca^{2+}-induced oscillations in channel activity. The conductance with 10 mM Ca^{2+} was 100 pS or its multiples. Ca^{2+} gradients of 4:1 induced. Oscillating channel activity for several hours, with initial open states of 40 s and closed states of 56 s; the open times gradually decreasing to 8.6 s. No channel activity was seen without added fractions. Nuclear magnetic resonance spectra of the fractions showed the presence of aliphatic chains and carbonyls, but the detailed structure remains to be elucidated. Regarding to Ca^{2+}, Eisenrauch et al.[33] have reported electrical currents generated by a partially purified Na^+/Ca^{2+} exchanger from lobster muscle reconstituted into liposomes and adsorbed on BLMs. One notable aspect of this work is that the caged Ca^{2+} can be activated by photolysis.[33]

General References

H. D. Brown (ed.) Chemistry of the Cell Interface, Academic Press, NY and London, 1971. Pp. 205-254

M. L. Hair (ed.) The Chemistry of Biosurfaces, Marcel Dekker, Inc., New York, pp. 233-348

Metzler, D.E., *Biochemistry: The Chemical Reactions of Living Cells*, Academic Press, Inc., New York, 1977

J. Barber (ed.) Photosynthesis in Relation to Model Systems, Topics in Photosynthesis, 3, Elsevier/North-Holland, NY, 1979, pp.115-173.

Davison, S.G., (ed.), Progress in Surface Science, Vol. 19 (No.3), Pergamon Press, New York, 1985, pp.169-274.

D. B. Datta, *Membrane Biochemistry*, Floral Publishing, Madison, 1987

A. A. Morino, Modern Bioelectricity, Marcel Dekker, Inc. NY.1988

G. Dryhurst and K. Niki (eds.) *Redox Chemistry and Interfacial Behavior of Biologiacal Molecuales*, Plenum Press, NY, 1988. pp. 529-556.

P. Laeuger, *Electrogenic Ion Pumps*, Sinauer Associates, Sunderland, 1991.

M. Blank (ed.) 'Electronic Processes and Redox Reactions in BLMs', in Adv. Chem. Series, No. 235 -- *Biomembrane Electrochemistry*, ACS, Washington, DC, 1994. Chapter 24.

Specific References

1. Morowitz, H.J., Biosystems, 14, pp.14, 1981; Am. J. Physiol., 235, p.R99, 1978.
2. Tien, H.T., Separation Science and Technology, 15, pp.1035, 1980.
3. Weller, P.F., (ed.), Solid State Chemistry and Physics, Vol. 2., Marcel Dekker, Inc., New York, 1973, pp. 847-903.
4. Mitchell, P., FEBS Sym., 28, pp.353, 1972; Palmer, J.M. and Hall, D.O., Prog. Biophys. Mol. Biol., 24, pp.125, 1972.
5. Bulychev, A.A., Andrianov, Kurella, G.A., and Litvin, F.F., Biochim. Biophys. Acta, 420, pp.336, 1976.
6. Kinnally, K.W. and Tedeschi, H., FEBS Lett., 62, pp.41, 1976; Bowman, C. and Tedeschi, Nature, 280, pp.597, 1979.
7. Abrahams,J. P. A. G. W. Leslie, R. Lutter and J.E. Walker, Nature, 370 (1994) 621-628
8. Tien, H.T., Bilayer Lipid Membranes (BLM): Theory and Practice, Mar-cel Dekker, Inc., New York, 1974.
8. Antolini, R., Gliozzi, A., and Gorio, A., (eds.), Transport in Mem Branes Model Systems and Reconstitution, Raven Press, NY, 1982, pp. 57-75.
10. Weiss, LA; Sakai, N; Ghebremariam, B; Ni, CY; Matile, S., J. Am. Chem. Soc., 119 (1997) 12142-12149
11. Bielawski, J., Thompson, T.E., and Lehninger, A.L., Biochem. Biophys. Res. Commun., 24, pp.948, 1966.
12. Liberman, E.A., Topaly, V.P., Tsofina, L.M., Jasaites, A.A., and Skulachev, V.P., Nature, 222, pp.1076, 1969.
13. Takeguchi, N., Saitoh, T., Morii, M., Yoshikawa, K., and Terad, H., J. Biol. Chem., 260, pp.9158, 1985;Sotnikov, P.S. and Melnik, E.I., Biofizika, 13, pp.185, 1968
14. Wardak, A., Stud. Biophys., 102, pp.155, 1984.
15. Ting, H.P., Wilson, D.F., and Chance, B., Arch. Biochem. Biophys., 141, (1970) 141; Wilson, D.F., Ting, H.P., and Koppelman, M.S., Biochemistry, 10 (1971). 2897
16. Bruner, L.J., Biophysik, 6, pp.241, 1970.
17. Finkelstein, A., Biochim. Biophys. Acta, 205, 1, 1970.
18. Dilger, J.P., Fischer, L.R., and Haydon, D.A., Chem. Phys. Lipids, 30,

p.159, 1979.
19. Carter, F.L. and Wohltjen, H., (eds.), Proc. 3rd International Symposium on Molecular Electronic Devices, Arlington, VA, USA, 6-8 October 1986, North- Holland, Amsterdam.
20. Schein, S.J., Colombini, M., and Finkelstein, A., J. Membrane Biol., 30, pp.99, 1976.
21. Benz, R., Janko, K., Boos, W., and Laeuger, P., Biochim. Biophys. A. 511,305, 1978.
22. Xu, G., Shi, B., McGroarty, E.J., and Tien, H.T., Biochim. Biophys. A, 862, 57, 1986.
23. Menestrina, G., Maniacco, D., and Antolini, R., J. Membrane Biol., 71, pp.173, 1983.
24. Wikstrom, M., Nature, 308, pp.558, 1984.
25. Shamoo, A.E. and Tivol, W.F., Curr. T. Mem., 14, pp.57, 1980.
26. Tien, H.T., J. Phys. Chem., 88 (1984) 3172; Bioelectrochem. Bioenerg., **9** (1982) 559-570; **13** (1984) 299-316; **15** (1986) 19-38.
27. Oosawa, F. and Imai, N., (eds.), Dynamic Aspects of Biopolyelectro lytes and Biomembranes, Kodansha-Elsevier, Tokyo and Amsterdam, 1982, pp.445-456.
28. Jain, M.K., Strickholm, A., and Cordes, E.H., Nature, 222 (1969) 871
29. Fendler, K., Grell, E., Haubs, M., and Bamberg, E., EMO J., 4(1985) 3079
30. Lane, M.D., Pedersen, P.L., and Mildvan, A.S., Sci., 234, 1986.
31. Wikstrom, M., Nature, 308, pp.558, 1984.
32. Mironova, G. D. T. V. Sirota, L. A. Pronevich, N. V. Trofimenko, G. P. Mironov, P. A. Grigorjev and M. N. Kondrashova, J. Bioenerg. Biomemb., 14, (1982) 213-225 ; 25 (1993) 307-312.; Mironova, GD; Lazareva, A; GateauRoesch, O; Tyynela, J; Pavlov, Y; Vanier, M; Saris, NEL. Journal Bioenergetics Biomemb. 29 (1997) 561
33. Eisenrauch, A; Juhaszova, M; EllisDavies, GCR; Kaplan, JH; Bam berg, E; Blaustein, MP., J Memb. Biol., 145 (1995) 151-164
34. Reinhardt, R., Lindermann, B. and Anner, B.M. (1984) Biochim. Bio phys. Acta 774,147-150.
35. Martonosi, A.N., (ed.), Membranes and Transport, Plenum Press, New York, 1982, pp.165-171.
36. Tien, H.T., Nature, 219 (1968) 272.

37. Miedema, H. H. S. van Walraven and A. H. de Boer, Biochem. Bio phys. Res. Commun. 203 (1994) 1005-1012
38. Pollard, HB; Arispe, N; Rojas, E. Cellular And Molecular Neurobiology, 15 (1995) 513-526
39. Cheng, Y., Cunnane, V.J., Kontturi, A.-K., Konturri, K., Schiffrin, D.J., , *J. Phys. Chem.*, **1996**, 100, 15470-15477
40. Jain, M.J.M. White, F.P., Strickhom, A., Williams, E. and Cordes, E.H. (1972) J. Membr. Biol. 8, 363-388
41. Vilalobo, A., Biochim. Biophys. Acta, 1017 (1990) 1-48
42. Last, T.A., Gantzer, M.L. and Tyler, C.D. (1983) J. Biol Chem. 258, 2399-2404
43. Abeywardena, M.Y., Allen, T.M. and Charnock, J.S. (1983) Biochim. Biophys. Acta 729, 62-74.
44. Issaurat, B., Amblard G. and Gavach, C. (1980) Bioelectrochem. Bio energ. 7, 353-362 (J. Electroanal. Chem. 116, 353-362).
45. Fendler, K., Grell, E. and Bamberg, E. (1987) FEBS Lett. 224, 83-88.
46. Borlinghaus, R. and Apell, H.-J (1988) Biochim. Biophys. Acta 939, 197-206
47. Shamoo, A.E. and Albers, R.W. (1973) Proc. Natl. Acad. Sci. USA 70, 1191-1194.
48. Skou, J.C. (1988) Methods Enzymol. 156, 1-28.
49. Albers, R.W., Koval, G.J. and Siegel, G.J. (1968) Mol. Pharamacol. 4, 324-336.
50. Kimelberg, H.K. and Papahadjoupoulos, D. (1972) Biochim. Biophys. Acta 282, 277-292.
51. Cornelius, F. and Skou, J.C. (1984) Biochim. Biophys. Acta 772, 357
52. Hokin, L.E. (1982) in Membranes and Tranpsort, Vol. 1 (Martonosi, A.N., ed.) pp. 547-551, Plenum, New York.
53. Racker, E. and Fisher, L.W. (1975) Biochem. Biophys. Res. Commun. 67, 1144-1150.
54. Appel. H.-J, Nelson, M.T., Marcus, M.M. and Lauger, P. (1986) Bio chim. Biophys. Acta 857, 105-115.
55. (a) Z. Salamon, Vitello, L. B.; Erman, J. E.; Butko, P.; Tien, H. T. *Bioelectrochem. Bioenerg. 21 (1989)* 213; (b) P. Butko, Salamon, Z.; Tien, H. T. *Bioelectrochem. Bioenerg. 23 (1990)* 153.
56. Broustovetsky, N; Bamberg, E; Gropp, T; Klingenberg, M., Biochem

istry. 36 (1997) 13865-13872
57. Hartung, K; Froehlich, JP; Fendler, K. Biophysical Journal. 72 (1997) 2503-2514
58. Sokolov, VS; Apell, HJ; Corrie, JET; Trentham, DR. Biophysical Journal. 74 (1998) 2285-2298
59. Kauffmann, J.-M. (ed.) Special issue devoted to electrochemical bio sensors, Bioelectrochem. Bioenerg. 42 (1997). pp. 1-104
Mannela, C. A., M. Marko and K. Buttle, TIBS 22 (1997) 37 ;Shao L., Kinnally, KW, Mannella, Biophys. J., 71, (1996) 778.

{Visit the web page at <http://www.msu.edu/user/ottova/chap8.html> where latest references pertaining to this chapter may be found}

Chapter 9

Membrane Photobiophysics and Photobiology

"Without light there can be no life, so let there be hv!"

9.1 Background and Perspective

Solar energy in the form of visible light is what makes life possible on Earth. Light is used by living systems for two main purposes: (i) as a source of free energy, and (ii) as a source of information. To achieve either purpose, light must first be converted into an appropriate form of energy that can be utilized by the organism. To effect light transduction, certain 'machineries' have been evolved in Nature; they are the lipid bilayer-based organelles. The details of these organelles (machineries, devices or transducers) in biological membranes for light transduction are largely uncertain but they are definitely made of lipids, proteins, and pigments including metallic ions. These constituents are believed to be organized in special arrays with lipids in the form of a bilayer, with proteins 'floating' about or spanning across the bilayer, and with the pigments in some ordered lattices. Clearly, until our knowledge of biomembrane transducers (biotransducers) is vastly improved, alternative and conflicting explanations will be offered for almost any experimental findings in work with intact biomembranes. If, on the other hand, one can obtain similar observations in a sufficiently well defined artificial membrane system, the interpretation of experimental results would be much less ambiguous. It is along this line of reasoning that membrane photobiophysics and photobiology with emphasis on pigmented bilayer lipid membranes (p-BLMs and liposomes) are discussed. One way to begin this exciting story of light and life in terms of membranes, perhaps an overview is in order. This is presented in Table 9.1 in which the major events are listed in chronological sequence.

The aim of this chapter is to introduce to the reader the experimental aspects of lipid bilayers in the study of photoactive natural membranes. The principal areas covered include a brief consideration of the law of photophysics and photochemistry (Section 9.2). The essential physical aspects of green plant photosynthesis in terms of the thylakoid membrane of the chloroplast are considered in Section 9.3. The visual receptor membrane of the eye will be described next (Section 9.4). This will be followed by a discussion of the purple membrane of H. halobium (Section 9.5). The applications of artificial lipid bilayers to the investigations of thylakoid extracts, visual rhodoposins, and bacteriorhodopsins embedded in experimental bilayer lipid membranes

(BLMs and liposomes) will be presented at the end of each of the above sections. Section 9.6 reviews miscellaneous studies of photoeffects involving pigmented BLMs, liposomes, and related systems. A common aspect in all the above descriptions is the desire to stimulate studies with a view to improve the understanding of photoactive biomembranes at a molecular level, and to apply the insight thus gained in practical applications such as in artificial photosynthesis for solar energy utilization (see Chapter 10, *Applications*).

The remarkable structures of pigmented organelle membranes enable light transduction by photoreceptors. The two most outstanding examples are the thylakoid membrane of chloroplasts in green plants and the outer segment sac membrane of retinal rods in vertebrate eyes. In the first example of photosynthetic thylakoid membrane, one speaks of photoconversion where the energy of light is transduced and stored as chemical free energy. In the example of visual retinal sac membrane, one speaks of photodetection where light is transduced and utilized as a signal to trigger a sensory response. Consideration will also be given to another example of pigmented membranes, the so-called purple membrane found in *Halobacterium halobium.* This membrane, extensively investigated in the 1970s-1980s, appears capable of both photoconversion and photodetection. Structurally, all these light-transducing membranes, as revealed by electron microscopy, are surprisingly similar in construct in that the principal element is interpreted to be a lipid bilayer in which photoactive pigments are embedded. To quantitate the light transducing process of these systems, one of the ideal approaches would be to measure the electrical properties by placing electrodes across the pigmented membrane, much as has been done for the nerve membrane of squid axon (Chapter 7, *Membrane Physiology*). Unfortunately, due to technical difficulties such an elegant approach is not yet easible. As a result, two types of artificial bilayer lipid membranes have been employed as reconstituted systems for the study of light-induced reactions of natural membranes (Chapter 4). The first consists of a planar bilayer lipid membrane (BLM) separating two aqueous solutions, where photo-effects can be readily measured electrically. The second system utilizes lipid microvesicles, LMV (or liposomes), which are spherical bilayer lipid membranes enclosing a small volume of aqueous solution. Since liposomes are stable and can readily be made in quantity, they are ideally

Table 9.1

Major events in membrane photoscience research

(visible light range 390-760 nm)

Date	Event
1660s:	Robert Boyle: phosphorescence, chemiluminescence, bioluminescence (needs O_2)
19th century:	Photography
20th century:	Organic photochemistry (many interesting photochemical reactions were discovered by Ciamician)
1900:	The quantum theory (Planck); Grothus-Draper's Law – only light absorbed causes chemical reactions
1908:	Einstein - Law of Photochemical Equivalence
1920:	Warburg - quantum yield concept
1920-1940:	Photosynthesis - Molecular spectroscopy; fluorescence lifetime measurement; flash photolysis; visual processes
1950-1960:	Photosynthesis: primary events, photophosphorylation and oxygen evolution; structure of photoactive membranes
1968:	Photoelectric effects in pigmented bilayer lipid membranes
1970s:	The purple membrane of *Halobacterium halobium*
1980s-1990s:	Molecular details of light transduction in photoactive membranes, BLMs and liposomes
21st century:	Lipid bilayer-based electronic sensors and devices activated by light; water photolysis via semiconductor septum photovoltaic cells for solar energy utilization.

suited for studies of permeability, conventional spectroscopy, chemical reaction, and gas evolution experiments. In the following sections, a brief description of experimental aspects of each bilayer system as covered in this chapter will be presented, more detailed discussions may be found in Chapter 4 (*Experimental Models*).

A planar BLM separating two aqueous solutions may be made quite easily in the following manner. A droplet of lipid solution is applied to an aperture in a hydrophobic support (e.g. Teflon). There follows drainage of excess lipid solution towards the perimeter of the aperture, the so-called Plateau-Gibbs (P-G) border. The drainage leads to a thinning of the thick lipid film until there exists a membrane consisting a double layer of opposing lipid molecules, a bilayer. The formation of the bilayer membrane is accompanied by the gradual disappearance of brilliant interference colors leaving an optically 'black' region. Liposomes, BLMs of spherical configuration, are simply obtained when amphipathic lipids such as phospholipids are dispersed in excess water (Chapter 4, *Experimental Models*). By mechanical agitation, the multilamellar vesicles of various sizes and shapes are formed which, upon sonication, break up into a fairly homogeneous population of single layer vesicles. Figure 9.1 illustrates the formation of the lipid bilayer in a schematic way and the bilayer's proposed structure. A variety of lipid membrane forming solutions have been formulated from highly purified phospholipids, surface-active agents, to tissue extracts, etc. Either negative or positive surface charge can be conferred to the BLM by incorporating an anionic or cationic compound, respectively, into the lipid bilayer forming solution.

In photochemical studies, pigments and dyes can be incorporated directly into the bilayer forming solution, or can be solubilized in the aqueous bathing media and permitted to adsorb onto the lipid membrane after formation.[1] Spectroscopic methods, which are useful to photochemical studies, are available.[2] For electrical methods of detection, a heat filter be placed between the light source and the membrane chamber is recommended. Electrical measurements can be readily made using a high impedance electrometer and ordinary calomel electrodes or Ag/AgCl electrodes. If the measurement of transient responses is desired, one can use a fast recording device to record the parameters of interest.[2] Other closely related work pertinent to membrane photochemistry and

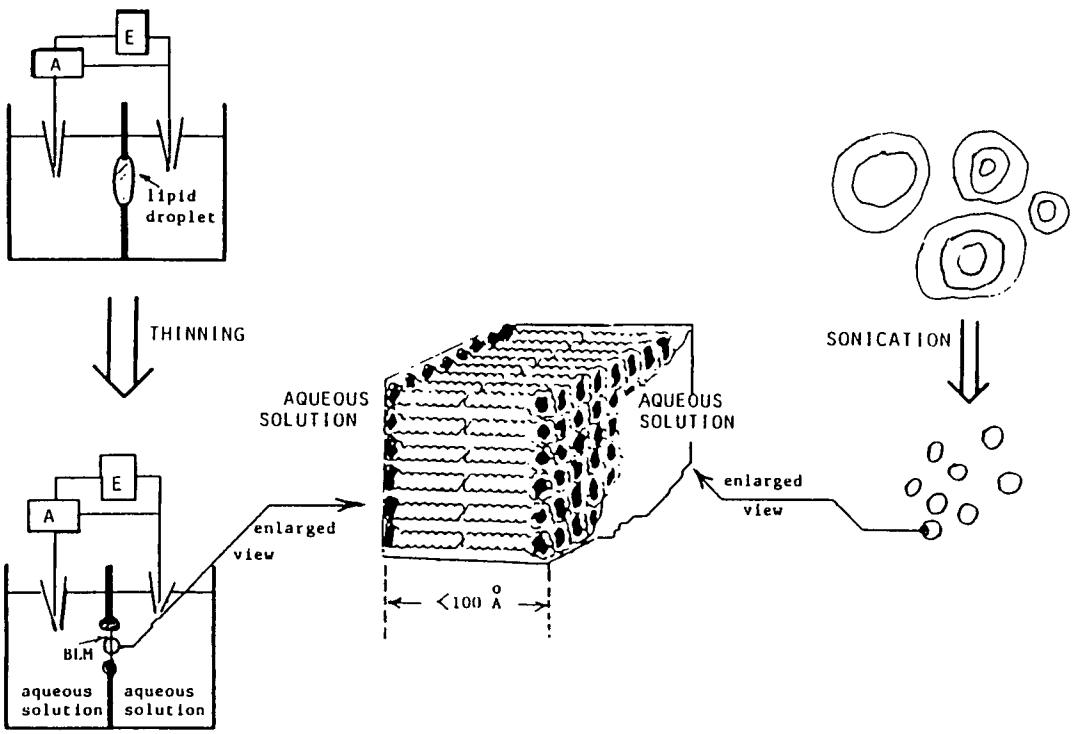

Fig. 9.1.Experimental bilayer lipid membranes: Left, bilayer lipid membrane of planar configuration (BLM). Right, bilayer lipid membrane of spherical configuration (liposomes). A 3-dimensional structure is shown in the middle. An exciting light source is needed for inducing photoeffects in pigmented lipid bilayers. These reconstituted lipid bilayers provided convincing evidence for a lipid bilayer in biomembrane (For an historical perspective, see Chapter 2, *Biomembranes*).

photobiology to be reviewed here are organized multilayers, [3-6] immiscible or semiconductor/electrolyte interfaces,[7-10] micelles,[11] and filters.[12,-17] In searching for a method to transduce light into electrical/chemical energy, many new ideas and novel ways have emerged in the past decades. One approach is to mimic nature's photosynthesis of which several so-called biomimetic systems for solar energy conversion have been investigated. As examples, Miyasaka et al.[6] reported that, by using a Chl-a monolayer-coated SnO_2 transparent electrode as a photoanode, photoelectrolysis with a maximum photocurrent quantum efficiency of 12-16% has been obtained. The physical stability and photochemical activity of Chl-a/synthetic lipid mixed monolayers they reported were described in the BLM study. In this connection, Janzen et al.[18] carried out photochemical electron transfer in monolayer assemblies. Chlorophyll monolayer, together with an acceptor species, such as sublimed chloranil, cause a light-induced electron paramagnetic resonance (EPR) signal. Under steady-state illumination, the rise and decay of this signal was of the order of minutes. Under flash illumination, the decay time of this signal was 0.6 msec and was temperature independent. Schreiber and Dupeyrat.[14] described a different system, using a dye. A lipid membrane, made of oleic acid trapped in a collodion matrix, becomes photoactive when sensitized with methylene blue; its photoresponse in 0.1 M KCl saturated with air, as compared with that given by sensitized collodion membranes without oleic acid, was studied by measuring the photoelectric effect produced by a platinum electrode coated with the membrane. For both kinds of membranes, the greatest photoresponse occurs near their spectral absorption maximum, at about 660 nm. The photoresponse is not instantaneous, a delay of about 10 sec, attributable to the diffusion time of the photochemically generated species being observed. Somewhat similar studies have been reported by Sugimoto et al.[16]

The interpretation of light induced phenomena is based on the theory of photochemical reactions and the quantum theory of radiation and matter. In the next section we will give a short discussion on the general principles of photophysics and photochemistry, and their relationship to reactions at membrane/solution interfaces and in the membrane lipid bilayer. These interesting findings are important in that they provide insights on the subject of photoelectric effects and solar energy utilization

[Tien, 1976; Metzner, 1978; Barber, 1979; Oosawa and Imai, 1982; Mittal and Fendler,1982; Davison, 1989; Ginley, 1996].

9.1 Basic Laws of photophysics and photochemistry

The nature of light and matter as particle waves

The electromagnetic radiation spectrum of which ultraviolet (uv) rays, visible light, infrared (IR) radiation, and microwaves are examples, extends through 10^{16} different wavelengths. Visible light from about 390 nm to about 760 nm, constitutes a tiny segment, on which life as we know it depends. The basic equation of electromagnetic radiation due to Planck (1900) is given by

$$E = h\nu \qquad (9.1)$$

where E = energy (Kcal/mol or eV; where 23.1 Kcal = 1 eV), h = Plank's constant (6.6 x 10^{27} erg sec), ν = the frequency (cycles per sec). Eq.(9.1) expresses the quantitization of energy, i.e. any atom or molecule has available to it only a discrete set of energy levels. The particle-like nature of radiation is the basis of the photoelectric effect, in which shining light on a metal under suitable conditions causes electrons to be ejected from it. The kinetic energy of the emitted electrons depends linearly on the frequency of light, but not on the light intensity, and is given by

$$\tfrac{1}{2}\, m\nu^2 = h\nu - W \qquad (9.2)$$

where the left side of Eq.(9.2) represents the kinetic energy of the electron of mass, m; W is the work function, the minimum energy necessary to remove an electron from the metal. Since $\nu = c/\lambda$ where c is the speed of light (3 x 10^{10} cm sec^{-1}) and λ is the wavelength of light (nanometer, nm; 1 nm = 10 A), by substituting v into Eq.(9.1), we have

$$E = h\, c/\lambda \qquad (9.3)$$

The duality of particle-wave nature of light was dramatically demonstrated by de Broglie in 1924, who combined the Einstein equation ($E = mc^2$) with the Planck equation [Eq.(9.1)] resulting in

$$\lambda = h / p \qquad (9.4)$$

in which the momentum, p, of the particle (m) and velocity (v) is $p = mv$ (note: for photons $v = c$). Thus, there is a characteristic wavelength associated with each particle (for a ping pong ball traveling at 45 miles/hr, the de Broglie wavelength is about 1.6×10^{-26} nm which is exceedingly small, exhibiting essentially no wave character. As we will discuss later, the wave nature of particles is essential in the understanding of electron transfer via tunneling in certain biomembranes. The particles of light are called photons (or quanta). From Eqs.(9.1) and (9.2) we can see that the frequency of radiation is inversely proportional to wavelength; the shorter the wavelength, the greater the energy. To bring about a photochemical change, Einstein postulated that all the energy of a single photon is transferred to a single electron of matter. This is known as Einstein's law of photochemistry, which is applicable to dissociation, isomerization, fluorescence, phosphorescence, radiationless transitions, and other reactions involving excited species.

Transitions

The common transitions encountered in biomolecules are n—s*, n—n*, T—T* and charge-transfer (CT), where n, s, and T denote, respectively, nonbonding, sigma, and (pi) orbitals. Their respective antibonding orbitals are indicated by *. The charge-transfer or CT transition is due to the presence of an acceptor-donor complex whose absorption band is generally broad and structureless. The absorption spectrum (optical density vs. wavelength or frequency) of most biomolecules show two or more bands, exhibiting that there are two or more distinct electronic excited states. Instead of displaying sharp and well-defined lines as in the case of an atom, the lines of biocompounds tend to fuse and form a broad band because of interactions between the compound and its surroundings. This is shown in Fig.9.2 for chlorophyll. At room temperature in thermal equilibrium, most electrons are in the

lowest or "ground states" of these respective orbitals. Upon absorption of light, they may be excited or in a higher energy state.

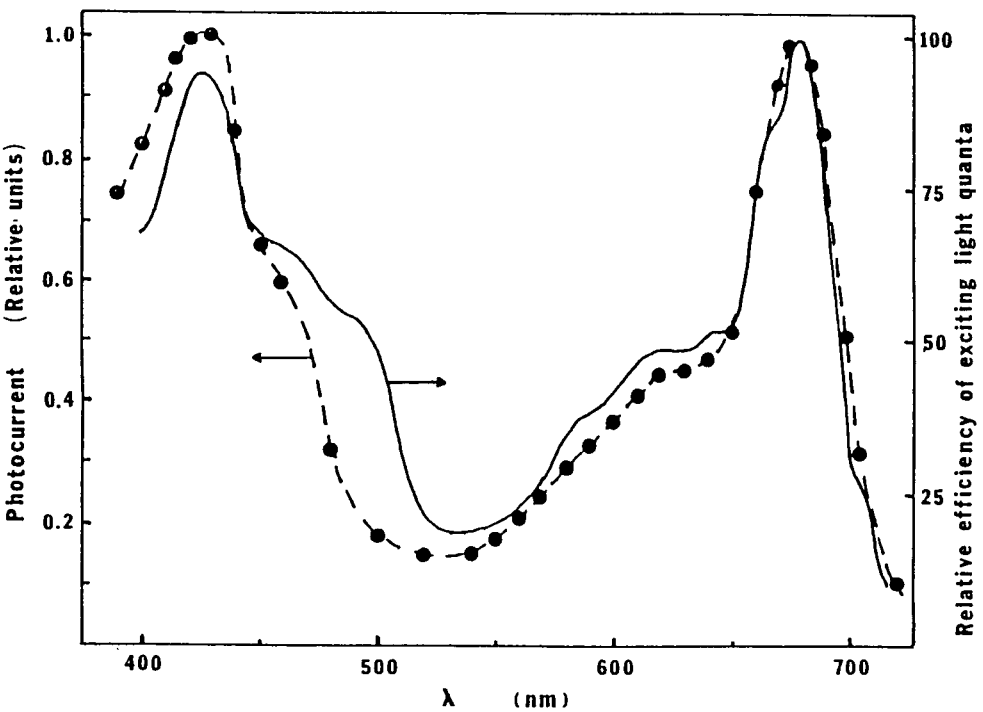

Fig.9.2 The absorption spectrum (right ordinate) is from the Photosystem I (PS-I) reaction center shown in a solid line. Also shown is the photoelectric action spectrum of a BLM containing a PS-I reaction center.

The fate of the excited state

Light consists of photons, which are absorbed by electrons of pigment molecules, which in turn become excited. Various deexcitation processes are possible for excited molecules. These are: radiationless decay (generates heat), fluorescence (releases a new photon), conversion from singlet to triplet (electrons develop same spin), and phosphorescence (see text for details). Energy and electron transfer (e.g. redox reaction in photosynthesis) is also possible. In general, the overwhelming majority of atoms or molecules are in the lowest energy or ground state. If a molecule is induced to undergo a transition to an excited state, it will eventually return to its ground state via some energy deactivation mechanism. Photochemical reactions, which proceed from these energetically more favorable excited states, must compete with these de-excitation processes. The various photophysical chemical processes of energy deactivation are described in terms of a transition (state) energy diagram due to Jablonski (see Fig.9.3) and extended by others [*see* Barltrop and Coyle, 1978]. The singlet states are arranged in order of increasing energy. All the physical processes involved in the interconversion of the states can be represented on such a diagram. The overall efficiency of any particular process is determined by the relative magnitude of a number of individual rate constants and can be expressed in terms of the quantum yield (Φ) in Eq. (9.5)

$$\Phi = \frac{\text{rate of conversion}}{\text{rate of absorption}} = \frac{c/dt}{I_0 A \Delta e} \qquad (9.5)$$

where c = the pigment concentration, I_o = the incident light intensity, A = the fraction of light absorbed, and Δe = a difference in extinction coefficient (units: moles $cm^{-3}sec^{-1}$/einstein cm^{-3} sec^{-1}). The emission and nonradiative decay from a triplet to a singlet state is forbidden on the basis of multiplicity and therefore occurs with low probability. This means that if the molecule can be induced into a triplet state, it will remain there for a relatively long period of time. This is desirable from the standpoint of photochemistry since it allows the excited state molecule more time to react chemically. This is understandable, since an excited state of a molecule (or species) can be expected to exhibit quite different properties from the ground state, owing to a shift in electron-density distribution.

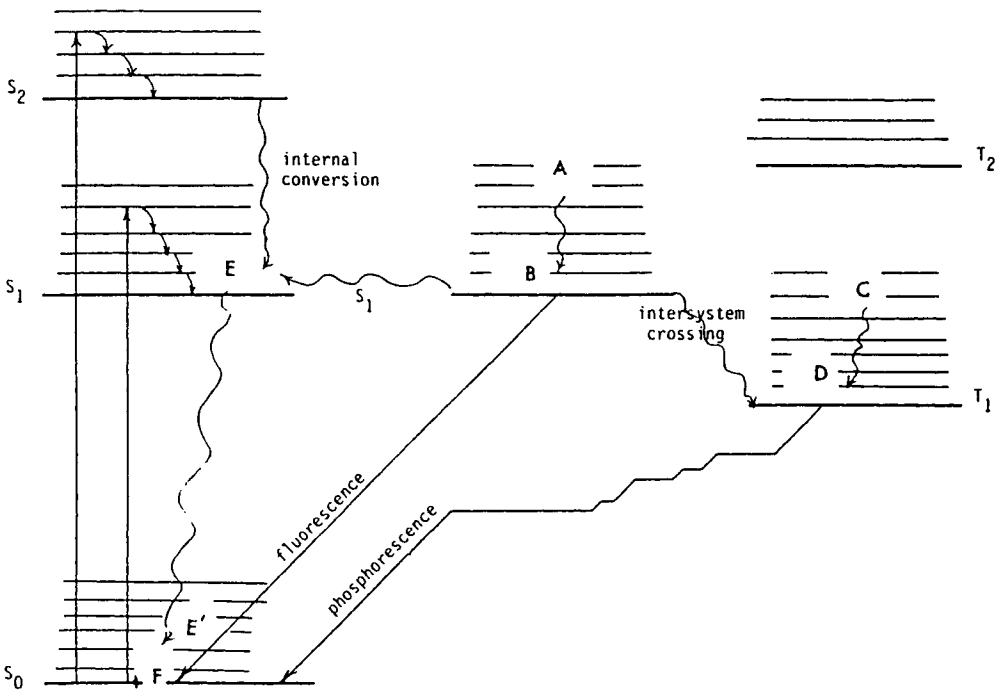

Fig.9.3 A Jablonski energy level diagram. S_0 = the ground singlet electronic state. S_1 and S_2 are the first and second excited state. T_1 = the first triplet state (see text for details).

Energy transfer processes

When a molecule is excited, another molecular species reacts photochemically. Such a process is said to be sensitized and is indicated by the reaction, D* + A → D + A*, and A* is an excited species. The mechanism of such type of reactions varies and proceeds via radiative and non-radiative (analogous to the intramolecular de-excitation described above) processes. The radiative mechanism is quite simply the fluorescence de-excitation of the donor D*, followed by the immediate absorption of the emitted photon by the acceptor, A, as follows: D* → D + hv, and A + hv → A*. Since a photon is exchanged between the donor and acceptor, no fluorescence is observed from D*. Another consequence of the involvement of a photon is the relatively long range of separation between D* and A over which the energy may be transferred.

The basis of non-radiative energy transfer is the perturbation theory of intermolecular forces. When two different molecules interact, the energy of the system can be expressed as a sum of the energies of the individual molecules plus an interaction term. Intermolecular forces are distinguished on the basis of the range of their influence, namely, long range vs. short-range forces. Each of these categories is mathematically derived by a different theoretical formalism. Without delving into the details of the theory, energy transfer occurs because a finite probability exists of a state D-A* in the presence of a state D*-A. In quantum mechanics, one often describes a system as a sum of all the possible states of its components and then computes the relative contribution of each component to the total. At the risk of oversimplification, one can draw an analogy to the problem of energy transfer. The D and A are in some way associated due to intermolecular forces and can be written as resonance structures as D*-A ↔ D-A*. Because of this analogy, one often refers to the process as resonance energy transfer, a special case of which is known as Forster energy transfer. The process requires overlap of the spectra of donor and acceptor species. The resulting coulombic interaction is expressed as multipole-multipole expansion, the leading term of which is the dipole-dipole interaction. According to Forster, the dipole-dipole energy transfer takes place over 2-6 nm distances as compared with the much shorter distance of 0.6-1.5 nm for electron exchange processes. For dipole interactions, the energy involved is proportional to $1/r^2$ and the rate

of energy transfer is $1/r^6$ whereas in exciton transfer the rate of energy transfer is proportional to $1/r^3$. The exciton mentioned here refers to the so-called Frenkel exciton in which a bound electron-hole pair is involved. Frenkel excitons can "hop" from one species to another. The forces of interaction are van der Waals type and relatively small, and may dissociate into a free electron and a positive "hole".

Time scales for photophysical and photochemical processes

From the absorption of light by a pigment molecule in the membrane to the formation of a stable product in bulk solution, there are at least four distinct processes occurring with vastly different time scales. Fig.9.4 shows the time scales in membrane photobiophysical chemistry, beginning with the primary event, preceding to charge separation and dissociation, and ending with the final products, A^- and D^+.

Photochemical reactions

There appears to be a great number of very rapid processes initiating from the excited state of a given molecule. The only way for a reaction to occur from an excited state is for it to take place on a time scale very nearly the same as the processes with which it must compete. The overriding factor of quantum mechanics and its influence on macroscopic behavior is the law of probabilities. It is not enough for a process to yield stable products; it must also be very fast to happen photochemically. Electron transfer is one of the fastest types of chemical processes, therefore, photochemistry consists almost exclusively of charge or electron transfer reactions. Examples include:

<u>*Dissociation*</u>

$$A - B \xrightarrow{h\nu} A + B \qquad (9.6)$$

The energy of visible light is in the range 40-80 Kcal/einstein (1 einstein = 6×10^{23} photons or quantum moles).

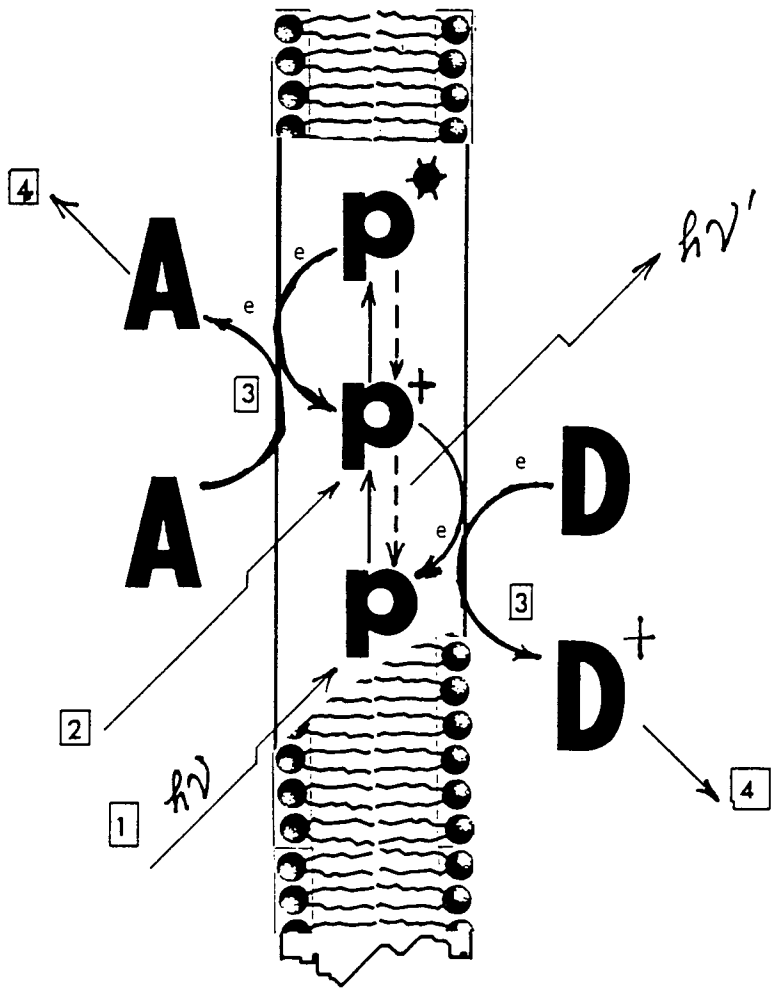

Fig. 9.4 The time scale of membrane photophysico-chemical processes. (1) Photoabsorption. The pigment absorbs a photon. This takes place within 10^{-15} to 10^{-9} sec. (2) Charge separation and dissociation. This happens in about 10^{-10} sec. The presence of an electric field plays a crucial role. (3) Electron transfer and ejection. Interfacial electron transfer and ejection is a relatively slow process and may take 0.1 μsec to 1 msec. (4) Diffusion of products. The time necessary for the products of the primary photophysico-chemical process to diffuse away from the membrane/solution interface is about 1 msec.

Ionization

$$AB \xrightarrow{h\nu} AB^+ + e \qquad (9.7)$$

or

$$AB \xrightarrow{h\nu} A^+ + B^- \quad \text{(radical ions)} \qquad (9.8)$$

Association

$$A \xrightarrow{h\nu} A^* + A \longrightarrow A_2 \qquad (9.9)$$

Photosensitization

$$A \xrightarrow{h\nu} A^* + B \longrightarrow A + B^* \qquad (9.10)$$

Photoisomerization (as in vision)

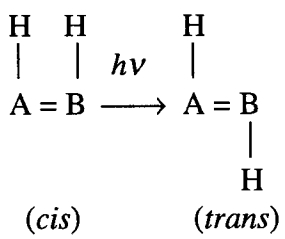

(9.11)

Photoredox Reactions (electron transfer as in photosynthesis)

$$A + D \xrightarrow{h\nu} A^- + D^+ \qquad (9.12)$$

For the purposes of energy conversion, we shall confine our discussion to photoredox reactions, as indicated in Eq.(9.12), although the topics of photosensitization and photoisomerization will be briefly mentioned at appropriate places.

Upon absorption of light by a pigmented molecule in the membrane, it is postulated that an electron-hole pair or a Frenkel exciton is formed, as mentioned earlier. To effect redox reactions, an exciton must dissociate into its components, namely, an electron and a positive hole. There are two types of processes to accomplish this: one-quantum and two-quantum process. In the former, an exciton may be dissociated by thermal energy, field ionization, collision with a dissociation center, or liberation of a trapped carrier. In the two-quantum process, charge carriers may be generated as a result of photon-exciton interaction or collision of two excitons or fusion of two excitons leading to more energetic species for redox reactions.

In a photoredox process, an electron is excited to a higher energy level, altering both the electron donor and electron acceptor properties of the photoactive pigment (P). An excited electron is a stronger reducing agent than an "usual" (ground state) electron. The excitation of the electron leaves a positive "hole" in its previous location in the orbital and may permit the excited molecule (P*) to accept an electron (reduction); a photogenerated hole has a greater oxidizing power. Alternatively, the excited molecule may now have an electron energetically favorable for transfer to another molecule (oxidation). Reverse reactions, which would result in charge recombination and subsequent de-excitation, must be prevented for a photochemical charge transfer reaction to proceed with any efficiency. One means of accomplishing this is by separating the products in some way. A simple example of product separation would be the charge separation process that occurs at semiconductor junctions. If one joins a p- and a n-type semiconductor together, one forms an interface between the two, called a junction. When light falls on the interface, an electron-hole pair is formed across the junction resulting in charge separation and a voltage difference. Charge separation is maintained by migration of the electron and hole away from each other, on opposite sides of the junction.[19] The semiconductor model is analogous to processes of allowing redox reactants and products to separate as quickly as possible.

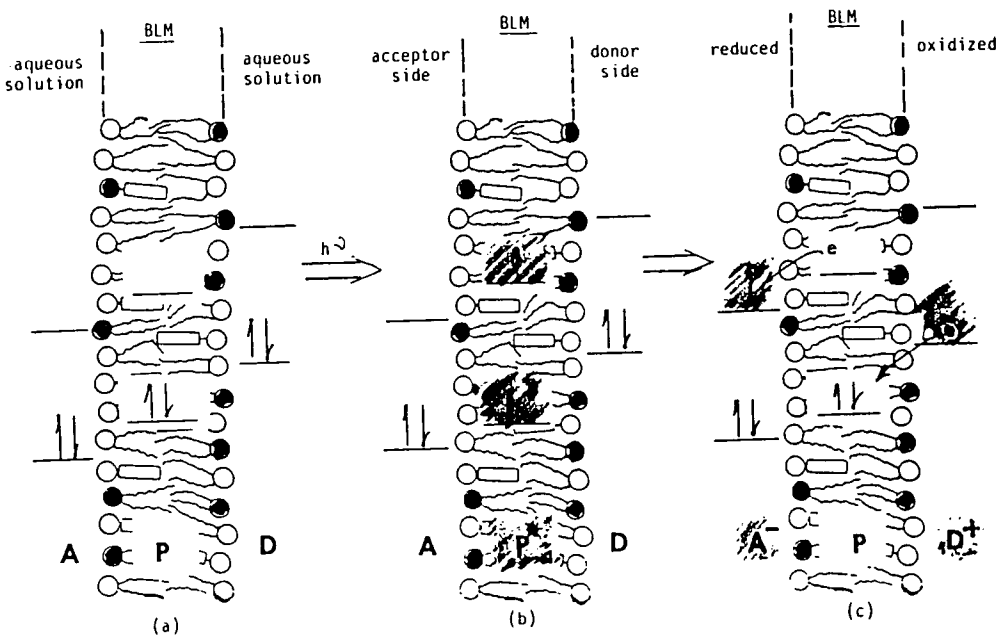

Fig. 9.5. The membrane redox electrode model of electromagnetic energy transduction in a pigmented BLM separating two aqueous solutions. P and P* denote the pigment in the ground and excited state, respectively. A = electron acceptor, D = electron donor, A^- and D^+ are reduced and oxidized forms, (a) the system at the ground state, (b) after absorption of photons by the pigment resulting in charge separation, (c) electron transfer processes (*see* [Bolton, 1977; Metzner, 1978]).

However, the processes of diffusional mass transport or convection are the only means of separating the products in solution, and these are slow compared to the mechanism involved in semiconductors. To enhance mass transport, it is possible to introduce intermediates so that oxidant and reductant are separated by fast electron transfer reactions. Thus, the recombination is prevented by the physical separation of oxidant and reductant using intermediary donors (D) and acceptors (A).

More germane to our discussion is the light-driven photoredox process illustrated in Fig.9.5, in which a membrane provides a barrier to the oxidant (A) and reductant (D), preventing their recombination. Photochemical redox reactions are light-driven in that photoactive pigments are involved in electron transfer from donor molecules (D) to acceptor molecules (A). The net result is that D becomes oxidized (D^+) and A becomes reduced (A^-). The membrane consists of an ultrathin lipid bilayer containing pigments (P). On one side of the membrane are electron acceptor molecules, and on the other side are electron donor molecules. Owing to the presence of the lipid bilayer, there is no overlap on the orbitals of the acceptor and the donor molecules, whereas some overlap of the orbitals between the pigment and acceptor (or donor) are assumed. Upon absorption of a photon ($E_{hv} > E_g$) by the pigment (P), an electron in the highest filled orbital (ground state) is promoted to the lowest empty orbital. The excited electron may return to the ground state or move to the lowest orbital of an acceptor. Concurrently, an electron can be transferred from a donor to the empty orbital left in the pigment. Thus, a portion of the free energy of the photon has been conserved in the form of an oxidized donor (D^+) and a reduced acceptor (A^-) on opposite sides of the membrane (Fig.9.5).

9.3 The thylakoid membrane of photosynthesis

Overview

Most photosynthetic pigments (chlorophylls, carotenoids) act as antenna to capture light energy. All of these pigments are in some fashion in complexes with proteins. Light absorption occurs in 10^{-15} sec, and energy is transferred in about 10^{-11} sec (transferred to Chl a) to photochemical reaction centers where a charge separation takes place in about 1 psec across the membrane, and charge stabilization occurs in about 1 microsec. The electron- carriers are connected to two light systems: Photosystem I (PS-I = P_{700} plus its antenna) and Photosystem II (PS-II = P_{680} plus its antenna). Thus, the so-called photosynthetic apparatus (Z-scheme) consists of PS-I and PS-II together with their electron-carriers. Electrons are driven by absorbed photons across thylakoid membrane by PQ (plastoquinone). An electrochemical gradient of H^+ is converted to ATP by CF_1CF_0 complex. ATP is produced after about 1 msec. Meanwhile, H_2O is oxidized to O_2 and $NADP^+$ to NADPH. In the biochemical domain (in the dark), CO_2 is fixed into organic matter in reactions using ATP and high energy electrons. Fixed CO_2 can be stored in the chloroplast until needed as starch and is transported to the rest of the plant as sucrose.

All photosynthetic organisms, whether they are higher plants, algae or lower bacteria, contain the so-called reaction centers. Higher plants have two kinds of reaction centers, whereas bacteria possess only one. These reaction centers, insofar as we can visualize, are globules of chlorophyll-protein complexes embedded in a phospholipid bilayer that is the site for solar energy-driven photosynthetic processes. In green plants the photosynthetic membrane is a highly convoluted membrane system forming sacs, called thylakoids. Hence the term thylakoid membrane is usually used. Thylakoids, located in a specialized organelle known as the chloroplast, are piled on top of one another in stacks termed grana immersed in a fluid medium called stroma. As will be described presently, photosynthesis consists of two separate but coupled reactions. Thylakoid membranes carry out the light reaction where the photons of sunlight are converted into electrical/chemical energy. The dark reaction takes place in the stroma. Photosynthesis in simplest terms can be, therefore, described

as a process by which *water is oxidized to oxygen and carbon dioxide is reduced to carbohydrates*. This thermodynamic uphill process (Gibbs free energy change, $\Delta G > 0$) is driven by the radiation of the sun and is mediated through the pigmented thylakoid membrane.

Composition

The gross chemical composition of thylakoid membranes consists of 60% proteins, 20% lipid and pigments, 4% nucleic acids and others. The types of lipids present are glycolipids, phospholipids, sulpholipids, and plastoquinones. The two sides of the thylakoid membrane are termed as stroma and lumen. The stroma is analogous to the cytoplasm of the photosynthetic bacteria. The lumen is the region enveloped by the thylakoid membrane. The application of methods designed to interact specifically with a given lipid type has indicated an asymmetrical arrangement of the lipids in the bilayer membrane. On the outer layer, there exist monogalactolipids, sulfolipids, phosphatidylglycerol, lutein, plastoquinone, and some pigments. The inner layer, on the other hand, consists of digalactolipids and pigments. Of particular interest to note is that the acyl chains of the lipids are highly unsaturated (fluid) which allows diffusional processes to occur. At physiological pH (~ 7.6), phospholipids together with sulpholipids are negatively charged.

What we know about the membrane proteins of thylakoids are as follows. On the stroma side, extrinsic proteins such as a water-soluble ferredoxin, ferredoxin-NADP oxido-reductase (a flavoprotein), and ATP synthetase (CF_1) complex are located. On the inner thylakoid surface the water splitting proteins of Photosystem II (PS-II) have been identified. One other extrinsic protein, plastocyanin (copper-containing) is also believed to be loosely bound to the inner thylakoid surface. Numerous intrinsic pigment protein complexes involved in light absorption and subsequent electron transport and phosphorylation are known including Photosystem I (PS-I) complex cytochromes and a complex of ATP synthetase. It should be stated that the precise details of these thylakoid membrane proteins are not known in their native state.

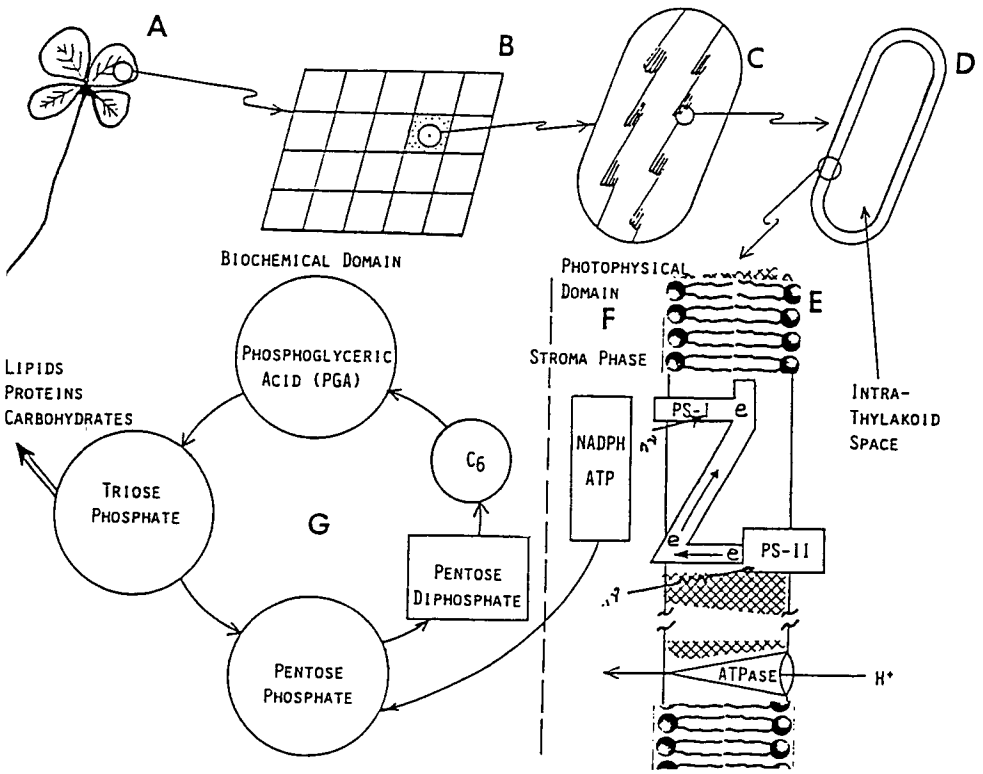

Fig.9.6. Green plant photosynthesis: An overview.[7]
A: a four-leaf clover, B: an enlarged view of mesophyll showing chloroplasts (in dots), C: a chloroplast, D: a thylakoid, E: an enlarged view of thylakoid membrane containing a "Z" scheme of PS-I and PS-II, F: photophysical domain, G: biochemical domain, CO_2 fixation cycle.

Molecular organization

Electron microscopy and freeze-fracture studies have provided information on the structure of the thylakoid membrane. The interpretation of the electronmicrographs has been the subject of some dispute since the methods of fixation and staining often provide conflicting results. Freeze fracture/etch methods have shown that there exist differences in the number and types of particles on different fracture faces. The outer membrane surface on the stromal side is shown to have two populations of particles of about 10 nm and 14 nm, respectively. The larger particles are missing on the fused outer surfaces, which constitute the contact zones of the granal stack and have been shown to be the coupling factor particles. The inner or lumen surface is also populated by particles consisting of subunits. The inner hydrophobic region can also be studied by the freeze fracture method. These fracture faces show a very densely populated collection of particles and the nature of this fracturing lends some support to the suggestion that the particle consists of clusters and aggregates representing multi-enzyme complexes.

The important aspect of these microscopic data and models derived thereof is that there is an organizational aspect of the membrane. An asymmetry of particles has led to a suggestion that the proteins of the photosynthetic membrane are specifically oriented within the membrane and this has further led to the concept of vectorial electron flow as a mechanism of energy transduction. At the molecular level, much of the information known about the primary photochemistry has been derived from bacterial systems because of their relative simplicity.[8] Isolated reaction centers can be induced to undergo charge separation reactions and studied by flash kinetic methods. The reaction center protein may be solubilized in detergent micelles. It will bind quinones, and it can be shown that flash excitation will initiate charge transfer to the quinone acceptors in a reaction similar to that described for photoredox reactions at an interface in general. The quinone may diffuse in and out of the binding site and interchange with a quinone pool. *In vivo*, however, the reaction center is within a membrane in the presence of other electron transfer components such as cytochromes and other metallo-proteins. In a similar vein, the reaction centers of thylakoids are also arranged in a highly organized array of redox active components. As a result, what is known

Table 9.2. Major landmarks in photosynthesis research

Year	Investigator(s)	Insight or Findings
1776	Joseph Priestley	Oxygen evolution
1782	Jean Senebier	Carbon dioxide reduction
1796	Jan Ingenhousz	Carbon dioxide reduction
1845	Julius R. Mayer	Energy 'transduction'
1931	C.B. van Niel	Generalized equation for photosynthesis
1943	S.C.J. Ruben	ATP and NADPH for CO_2 reduction
1949	E. Katz	Semiconduction theory
1951	M. Calvin, A.A. Benson and J.A. Bassham	Dark reactions
1960	R. Hill and F. Bendall	Two light reactions
1961	W. Menke	Thylakoid membrane
1961	P. Mitchell	Chemiosmotic hypothesis
1965	K.Muehlethaler, H. Moor and Szarkowskin	Bilayer leaflet model
1966	A.T. Jagendorf and E. Uribe	ATP synthesis and ΔpH
1968	(*sundry*)	*Photoelectric effects in pigmented BLMs,*[6] *transmembrane electric field in thylakoids,*[9] *and oxygen evolution in liposomes.*[10-12] *(for references prior to 1968, see [Olson and Hind, 1976; Barber, 1979; Metzner, 1978; Bolton and Hall, 1979; Biggins, 1987]*

about individual reaction center reactions only forms a small but crucial aspect of the overall membrane-dependent process. Besides the primary charge separation, the vectorial electron flow taking place among redox components of the energy transducing membrane, is also depicted.[7] Fig. 9.6 shows one of the proposed organizations of the thylakoid membrane depicting the relative spatial relationships of PS-I, PS-II, and other intrinsic and extrinsic membrane proteins. This representation serves as a basis for understanding the various factors governing the light-induced reactions, electron transport, and water splitting of photosynthesis, and may furnish a 'blueprint' for membrane reconstitution experiments and model membrane studies.

Photosynthesis in green plants is by far the most crucial redox reaction on Earth, for life depends upon the transduction of solar energy into biochemical energy. In simplest terms, the overall process of photosynthesis may be considered as light-driven, coupled CO_2 reduction and H_2O oxidation. The important landmarks of modern photosynthesis research are summarized in Table 9.3. It is worth noting that, beginning with Priestley's oxygen evolution experiments in the last quarter of 18^{th} century, to van Niel's generalized equation for photosynthesis in the 1930s, Mitchell's chemiosmotic hypothesis, to Muehlethaler, Moor, and Szarkowskin's bilayer leaflet model of mid 1960s, leading to the discovery of photoelectric effects in pigmented BLMs,[6] transmembrane electric field in thylakoids,[9] and finally to oxygen evolution experiments in liposomes[10-12] in the late 1960s, tremendous cerebral efforts were spent. Yet, in spite of nearly two centuries of labor, we are still far from solving all the major problems of photosynthesis. Among the outstanding problems that remain to be solved at the molecular level are: (i) the primary events of quantum conversion, (ii) electron transport and photophosphorylation, and (iii) oxygen evolution. It appears that all major unsolved problems are intimately connected with the lipid bilayer structure of the thylakoid membrane. To facilitate an understanding and to maximize the effort, photosynthesis research has been operationally divided into two areas: the light physicochemical domain and the dark biochemical domain. An overall view of photosynthesis by green plants may be seen in the flow diagram shown on the next page.

Photosynthesis
(chloroplast)

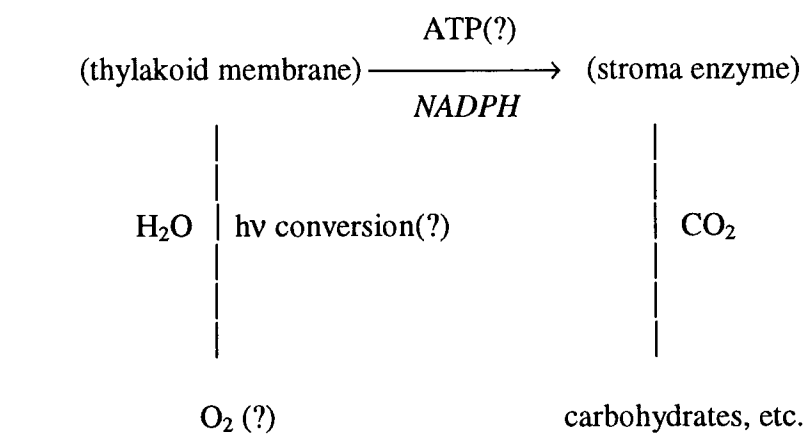

where (?) indicates the details have not been completely established. In the biochemical domain in the absence of light, carbohydrates are formed from CO_2 by a series of enzymatic reactions driven by ATP and NADPH. The process is well understood. In the photophysicochemical domain, the lipid bilayer structure or the thylakoid membrane is strongly implicated in the two different photoreactions. Therefore, the resolution of the three major problems (identified by the question marks in the flow diagram) cannot be achieved without, first of all, having some appreciation of the role of the thylakoid membrane in terms of chemical composition and molecular organization.

Under a light microscope, a green leaf shows numerous cells containing disc-shaped bodies (about 7 μm in diameter, 1 μm in width and about 20 or so per cell). These bodies are called chloroplasts, where chlorophylls (Chl) and other pigments are concentrated. The chloroplast is the site of photosynthetic activity. Under an electron microscope, each chloroplast can be seen to be bound by a plasma membrane envelope in which thylakoids are located. Thylakoids are seen to be highly organized lamellar structures called grana. The thickness of these structures is on the

order of 4-12 nm. Here we come to the limit of resolving power of the electon microscope. So, from here on, it is the end of the "facts" and the beginning of imagination or speculation. To Menke these grana looked like a stack of disc-shaped vesicles, named thylakoids by him. Thylakoids are double membranes closed in themselves, which are embedded either singly or in stacks (grana) in the stroma. The thylakoids are the structural units of the photosynthetic lamellar systems. From the images of electron micrographs, the structure of the thylakoid membrane has been variously interpreted. The membrane consists of an ultrathin lamella with attached globular units, termed quantasomes, which is considered as the morphological expression of the photosynthetic unit. A different interpretation has been given by Howell and Moudrianakis who suggest that the entire membrane is involved in photoreactions. Weier and Benson have interpreted their images in a somewhat unique fashion, and conjured up a highly intricate picture. On the basis of X-ray diffraction studies, the ultrastructure of chloroplast membrane has been analyzed by Kreutz, and the subject reviewed by him. Using the freeze-etching technique, Muehlethaler has suggested a picture for the thylakoid membrane based upon the bimolecular leaflet model [*see* Olson and Hind, 1976; Gregory, 1978; Barber, 1979; Biggins, 1987]. The salient feature in all these proposed models lies in their oriented bilayer lipid core, onto which other important cellular constituents, such as proteins and pigments, may interact through either ionic or van der Waals attraction, or both. Muehlethaler's interpretation is of special interest, in view of the experiments using the pigmented bilayer lipid membrane (p-BLMs) as a model for the thylakoid membrane that will be discussed in a later section.

The equations of photosynthesis

Photosynthesis research may be roughly divided into three periods:

Period I: Major advances were made in the 1930's after R. Hill showed that isolated chloroplasts can evolve O_2 (when a suitable electron acceptor A, or oxidant, was provided).

$$CO_2 + H_2O \xrightarrow{h\nu} (CH_2O) + O_2 \qquad (9.13)$$

Period II: In the 1950's, Arnon and his colleagues demonstrated that isolated chloroplasts can carry out not only photophosphorylation but also CO_2 reduction. Two types of phosphoryla-tion are known: Cyclic - which involves no net electron transport from a donor to an acceptor, and (2) Non-cyclic where:

$$ADP + P_i + NADP + 2H_2O \longrightarrow ATP + NADPH_2 + H_2O + 1/2O_2 \quad (9.14)$$

In this process, ATP formation is associated with NADP reduction (in contrast to NAD oxidation in mitochondria) and O_2 evolution.

Period III: In the early 1960s in order to explain these two types of photophosphorylation and the enhancement effect observed by Emerson in the 1940s--1950's, the so-called "Z" scheme, or two photosystems, was proposed. It is generally accepted that Photosystem I (PS-I) and Photosystem II (PS-II) together provide reduced nicotinamide adenine dinucleotide phosphate (NADPH) and adenosine triphosphate (ATP) for the CO_2 reduction. However, the details of these systems remained obscure and they were the focal point of much research activity. Concurrently, with this development was the proposal of Peter Mitchell [*see* Barber, 1979], which has come to be known as the chemiosmotic hypothesis, to explain energy transduction. In Mitchell's formulation the membranes must be relatively impermeable to ions. The driving force for phosphorylation is due to the electrochemical gradient of protons ($\Delta\mu_{H+}$), which could come about as a result of electron transport. The results obtained by Jagendorf, Neumann, and Hind, with chloroplast suspensions subjected to pH "shock", are generally cited as evidence in support of the chemiosmotic hypothesis [see Olson and Hind, 1976; Akoyunglou, 1981].

In the first period, Eq.(9.13) has been known for over a century; it tells us about the stoichiometry, but nothing about the mechanism of photosynthesis. In articles and books dealing with photosynthesis published in the 1960s, Eq. (9.13) was frequently presented, which we now know to be not valid or at best misleading in at least two respects, from the well-known facts. First, to transform 1 mole of CO_2 into 1 g-atom of carbon in the carbohydrate requires about 112 kcal (~ 5.2 eV). Since this quantity of free energy must come from sunlight, the question one usually asks is: 'Does the sunlight reaching the earth contain energetic

photons of this magnitude?' The answer is 'Negative', since we know that the sunlight which reaches green plants consists of light predominantly in the range of 400-1300 nm (88%) which in terms of energy is between 1-3 eV (~ 20-70 Kcal/quantum). Thus, it is impossible to expect the reaction, as indicated in Eq. (9.13), to be achieved in a single step on the basis of elementary energetic considerations, and second, the work of van Niel and others has conclusively demonstrated that CO_2 does not take part at all in any photochemical reactions. Carbon dioxide reduction involves a series of enzymatic reactions that can and do take place in the dark. Thus, van Niel, using a comparative approach, suggested a generalized equation:

$$CO_2 + 2H_2A \longrightarrow (CH_2O) + H_2O + 2A + \Delta G^0 \qquad (9.15)$$

where H_2A = H_2O, H_2S, isopropranol, etc. (all of these are hydrogen donors). Implicit in Eq. (9.15) is that O_2 comes from H_2O. Further, van Niel proposed that the essence of green plant photosynthesis is water splitting, i.e.

$$H_2O \xrightarrow{h\nu} [H] + [OH] \qquad (9.16)$$

where [H] and [OH] are unspecified reducing and oxidizing entities, respectively. Translating van Niel's Eq. (9.16) into modern terminology, the scheme may be depicted in Fig. 9.7 below.

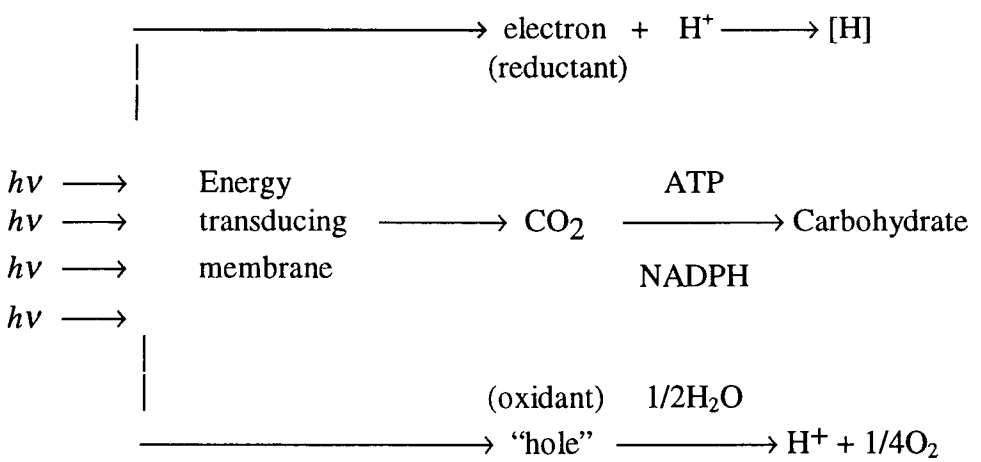

Fig. 9.7 A highly simplified overview of green plant photosynthesis.

Redox reactions

Photosynthesis may also be considered as a coupled redox reaction, in which it is involved in the gain or loss of electrons as follow:

$$A + D \Longleftrightarrow A^- + D^+ \qquad (9.17)$$

where A and D denote an electron receptor and donor, respectively, and A^- and D^+ are the species in their respective reduced and oxidized states. In terms of membrane dynamics, the light-induced redox reactions can be simplified as already shown in Fig.9.5. This membrane system consists of two interfaces with donor molecules on one side and acceptor molecules on the other. The pigment molecules, denoted by P_0 and P_i, at each membrane/solution interface are assumed to be capable of light excitation, charge separation and electron transfer, thereby leading eventually to stabilized products (A^- and D^+). This simplified energy transducing scheme will be considered further in the section on pigmented bilayer lipid membranes.

Visible light is energy in packets called quanta or photons. The energy per quantum is related to λ (wavelength, *see* Eq. 9.3). Photosynthesis uses visible light in the range from blue (~ 400 nm) to red (~700 nm). A photon is absorbed only if its energy exactly matches quantum jump of electron associated with conjugated double bonds (-C=C-C=C-), as in chlorophyll, for example, which is a tetrapyrrole-like heme, but with Mg^{2+} in its center. Once absorbed, the photon is transduced into chemical energy.

For photosynthesis, light-induced electron transfer across membranes is an important subject to investigate. Experimental bilayer lipid membranes (planar BLM, and spherical liposomes) are ideal systems for such investigations. Indeed, photovoltaic effects were observed in pigmented BLMs, using both chloroplast extracts and synthetic porphyrins as early as 1968.[1] The addition of electron acceptors and/or donors to opposite sides of the solution in contact with the BLM greatly enhanced the observed photoelectric effects. In Section 9.3.1, we will be concerned with the mechanisms of light-induced electron transfer across planar

BLMs, since the BLM system is most easily investigated by electrical methods. Other model membrane systems including pigmented liposomes will also be covered in thae next section.

BLM and Liposome Experiments Involving Photosynthesis

One would like to raise the question of why light-induced electron transfer across an ultrathin membrane is of paramount importance in phototransduction? This question can not be satisfactorily answered without referring to natural photosynthesis. It is currently accepted that the primary event in green plant photosynthesis is light-driven charge generation and separation across the thylakoid membrane. The initial step is the absorption of photons, by arrays of chlorophyll molecules arranged like molecular antennae, in the membrane. This results eventually as energetic electrons associated with molecules other than chlorophylls. The positive charge or 'hole' left on the initially excited chlorophyll must be replenished with electrons from other donors, most preferably water molecules. If chlorophylls are merely dissolved in a solution and 'free' to move about, the energy of photons contained in such chlorophylls is not likely to lead to charge separation and electron transfer. This is due to excessive vibration and collision of molecules, which leads to the giving off heat, or at best fluorescence. By forming a lipid bilayer, nature has solved two crucial problems insofar as initial phototransduction is concerned. First, when chlorophylls (together with proteins) are embedded in a lipid bilayer environment; this makes efficient energy or electron transfer possible with minimal loss. Second, by introducing a vectorial property to the molecule such as by association or in contact with other compounds, charge or electron and hole recombination (back reaction) can be hindered or completely prevented. For electron transfer between molecules by a tunneling mechanism, there must be an electron wave function overlap and energy conservation. This may be achieved in membrane-bound molecules in which an electron is transferred from a bound state on one donor molecule (D) to a bound state on an acceptor molecule (A) that has a lower redox potential. Of importance is the distance between D and A. Further, energy must be conserved in order for electron tunneling to take place. For an electron to tunnel to a state of lower redox potential, some energy must be lost. Apparently, nature has

solved this problem by vibronic coupling between the involved molecules [Kavarnos, 1993].

Electron transport

The efficiency of electron transport has a major impact in the achievement of artificial photosynthesis (Secton 9.6). Photoinduced electron transfer in liposomes is a topic of much research following the experiments of pigmented BLMs. For example, Ford et al.[30] demonstrated light-induced electron transfer across a liposomal membrane doped with tris-(2,2'-bipyridine)ruthenium^{2+} separating EDTA (ethylenediamine tetraacetic acid) and MV^{2+} (1,1'-dimethyl-4,4'-bipyriduim salts) on opposite sides of the membrane. Consistent with the findings of pigmented BLMs, they too found evidence to support the theory that pigmented vesicles can transfer electrons. They also concluded that the quantum yield was completely dependent on the Ru^{2+} concentration in the membrane. In this connection Sugimoto et al.[16] have studied electron transfer from EDTA to $Fe(CN)_6^{3-}$, also using Ru^{2+} as a mediator. They reported the complete schematic of the reduction to oxidation reaction. They also reported that EDTA is irreversibly oxidized, leading to efficient transport. When using $FeCl_2$ reverse electron transfer is possible. The use of either probe still provides for the storage of energy. Nagamura et al.[15] have studied the Ru^{2+} complex incorporated into synthetic bilayers and liposomes. Additional development in manufacturing synthetic membranes capable of photosynthetic reactions has been conducted by Nagamura et al.[40] Sudo and Toda[41] studied electron transfer in liposomes incorporating methylene blue as both a pigment and an electron carrier using $K_3Fe(CN)_6$ as an acceptor and ascorbic acid or iron chloride as the donor. They concluded that transfer efficiency is controlled by the E_m of the dye. The higher the dye, the greater the electron transfer. Usui and Gotuo[42] also studied energy transfer in micelles from acridine orange-10-dodecyl bromide to methylene blue. Laane et al.[169] have found the quantum yield can be enhanced by creating potential within the cell. This was done by loading the vesicles with K^+ ions. When the ratio of K_{in} to K_{out} was greater than one the electron transfer was enhanced. Likewise, the converse was true.

Takayanagi[43] et al. have studied the effectiveness of different mediators. They compare Ru^{2+} and N-butylibhenothiazine when placed in various environments. They concluded that the N-butylibhenothiazine is an excellent mediator. This is attributed to its hydrophobicity. They also found that in the synthetic environment of dihexadecyldimethyl-ammonium bromide a high achievement of charge separation was attained. This is an important discovery since charge separation is vital to photosynthesis. Other experiments dealing with photoinduced charge separation include Neumann[44] et al. and Tomkiewicz and Corker.[32] Hurley et al.[45] studied chlorophyll in condensed media. Results of the study concluded that placing chlorophyll-*a* in a rigid environment in contact with an acceptor produced a viable method for energy storage. This work was followed up by Hurley et al. in their study of electron transfer to quinone in liposomes.[45] A two step method of activation has been reported by Matsuo and associates.[40,43,46] Photoinduced electron transfer has been observed at extremely fast rates with the proper choice of mediator. Aso, Kano and Matsuo[47] also studied the reduction of 9,10-anthraquinone-disulfonate by zinc porphinate complex in the presence of various electron mediators.

Energy transfer in membranes

Nomura et al.[48] studied energy transfer in dioctadecyldimethyl-ammonium chloride (DODAC) liposomes. They have shown that efficient energy transfer exists in these vesicles. The donors and acceptors used were pyrene, located in the hydrophobic region, and pyranine, located on the charged outer surface. If the donor and acceptor were placed in alcohol no energy transfer occurred. Schnecke et al.[49] used pyrene to study energy transfer in membranes. His studies are primarily the reaction of hydrated electrons with pyrene. Nomura et al concluded that the DODAC membrane has a remarkable organizational ability.[48] This will strengthen efforts towards development of artificial photosynthesis.

Luisetti, Galla and Mohwald[50] studied energy transfer in chloro-phyll containing liposomes. They related thermal phase change in the vesicle to energy transfer efficiency. They observed a decrease in energy transfer when a vesicle is in the liquid crystalline state. This is an expected result since there is formation of chlorophyll aggregates below the

transition temperature. As mentioned above, Aso, Kano and Matsuo[47] studied the singlet-singlet energy transfer of all oxazines to isoalloxazines in DPPC liposomes. They observed that, in single walled vesicles, the energy transfer is accomplished by efficient Forster resonance energy transfer. Since the mean transfer distance is much smaller in multicompartment vesicles, their energy transfer is much more efficient. Their findings may be summarized as follows: (i) energy transfer efficiency increases with increasing length of the acceptors alkyl chain length, (ii) the most efficient donors are of the intermediate alkyl chain length, and (iii) the energy transfer efficiency increases above the thermal transition temperature.

It should be brought up that the electrical properties of phosphatidylcholine liposomes were measured by Kadoshnikov and Stolovitsky.[31] The membrane's average resistance was found to be 1-3 x 10^6 Ω cm^2. The photoconductivity was found to be 0.9-2.75 x $10^{-7}\Omega^{-1}$ cm^{-2}. The presence of an electric field, pH gradient or an acceptor greatly increased the photoeffects. Dodelet, LeBrech and Leblanc[51] reported the efficiencies of crystalline chlorophyll **a**. The action spectra of chlorophyll **a** absorbing at 700 nm were also determined. Harbich and Helfrich[53] demonstrated the ability to align and open giant egg lecithin vesicles with low power electrical currents.

Membrane spectroscopy

In the preceding paragraphs, we have considered the photoeffect in pigmented BLMs and liposomes (for more details *see* [Davison, 1989]). From the results obtained, it is evident that the presence of photoactive species, either embedded in the lipid bilayer or at the solution-BLM interface, is a prerequisite. To demonstrate conclusively the presence of the photoactive species involved, measurements of the spectra of BLM constitute, in principle, the simplest approach. Experimentally, a number of spectroscopic methods have been applied to membrane studies including optical spectroscopy (UV, visible, IR), polarization spectroscopy, fluorescence spectroscopy, and photoelectrospectrometry.

Additional Experiments involving chlorophylls and related compounds

Planar BLMs and spherical liposomes containing chlorophylls and related compounds have been reported by several groups of investigators.[31, 32-34] Elegant techniques and setups have been described.[1,35] To elicit appreciable photoelectric effects, asymmetrical conditions across the pigmented BLM are necessary. These conditions can manifest themselves in terms of pH difference, electrical potential difference, different composition or concentration of electron acceptors and/or donors present in the bathing solutions. For electron transfer and charge separation studies, Joshi et al.[22] and Seta and others [119] have formed BLM from lipid solutions containing chl or porphyrins with and without added modifiers, such as quinones and carotenes. The additions of quinones and/or carotenes is due to the well-documented evidence that quinones serve as the primary electron acceptor and carotenes as effective light-gathering accessory pigments. In this connection, the experiment reported recently by Rich and Brody is of interest.[143] They found that chl-BLM in the presence of dihydroxy-carotenoids give rise to much greater photocurrents than either the simple carotenes or the diketocarotenoids. BLM formed using pheophytin (a Mg-free chlorophyll) generates very small photocurrent regardless of the carotenoids used. This is explained in terms of lack of interaction between pheophytin and carotenoids. The negligible photocurrent in pheophytin and ferricyanide, thus prevents the latter from being reduced by the former. The interaction between chlorophyll and β-carotene in BLM has also been studied by Vacek et al.[144] They observed a decrease of photopotential upon repeated flash excitation, which might be owing to lipid oxidation. The kinetics of photopotential were studied in more detail by Liu and Mauzerall,[37] who explained the decay by a rate constant that exponentially decreases with distance between pigment cation and reduced acceptor (e.g. ferricyanide). The other conclusion from their study is that the pigment cation does not transverse the BLM in less than 10 msec. Further, Mauzerall and colleagues[145,147] have published several papers stressing the aspects of the aqueous-solution/BLM interface, whose properties may be crucial to many biomembrane processes. Woodle and Mauzerall[145] have found that photoexcitation of Mg-octa-ethylporphyrin-containing BLMs produces ion-radicals in the presence of electron acceptors such as ferricyanide (FeCN) and methyl viologen (MV^{2+}). The photocurrent is decreased by

FeCN, whereas MV^{2+} has the opposite effect when oxygen is present. The kinetics of charge transfer at the solution/BLM interface have been discussed in some details. According to Mauzerall and co-workers,. the observed photocurrent is due to the movement of superoxide anion. In this connection Hofmanova et al[146] reported the involvement of superoxide ions in their Zn-porphyrin-containing BLMs. They found that a strong enhancement of photocurrent is observed when the oxidizing solution is made more acidic, and proposed two mechanisms to account for their finding that: (i) the dual role of the porphyrin acts as an electron as well as proton carrier, and (ii) the excited Zn-porphyrin reduces oxygen which moves across the BLM. Both of these mechanisms are pH dependent.

Instead of using ferricyanide as an electron acceptor in the usual chl-containing BLM experiment, Kutnik and Lojewska measured the photoconductivity of chl-BLM in the presence of $FeCl_3$ with added β-carotene as a function of wavelengths. They obtained the highest efficiency at 541 nm, in good agreement with a value reported using photoelectrospectrometry.[7,109] Photoelectrospectrometry is a technique which combines the classic photoelectric effect with optical spectroscopy. Thus far, only the range of UV and visible wavelengths has been reported using this method. Putvinskii,[149] for example, has reported the influence of UV light on the stability of BLM formed from mitochondrial lipids and explained his results in terms of photoperoxidation of unsaturated fatty acid chains of phospholipids. Sielewiesiuk[150] reported the photooxidation of chl in BLM on the basis of a decrease in photocurrent.

In a novel experiment, Koyama, Komori, and Shiomi[151] obtained a spectrum of carotenoid-BLM by resonance Raman spectroscopy, which should be considered as a major advance in BLM spectroscopy. For efficient charge transfer, the orientation of chlorophyll molecules at the membrane/solution interface is important. Brasseur, Meutter and Ruysschaert[152] have developed a new procedure for conformation analysis to define the position of chlorophyll in BLM. They found that the porphyrin ring is orientated at an angle of 45 $\pm$5 degrees to the plane of the BLM, in excellent agreement with the value reported previously.[7]

In an interesting study, Hattenback et al.[153] raised the question, 'Does phytochrome interact with lipid bilayers'? Phytochrome, a plant

chromoprotein, claimed to respond reversibly to red light of different wavelengths (667 and 725 nm), has been incorporated into a BLM. E. Muller and colleagues have found no detectable change in membrane conductance during illumination with red light (660 nm). Their finding in BLM, however, does not rule out the regulatory role of phytochrome in plant membranes.

A unique feature of the BLM system is that a coupled photosensitized redox reaction may be independently activated at the two interfaces of the BLM, mimicking the 'Z' scheme of photosynthesis. [Bolton and Hall, 1979]. One way to accomplish this is to use ZnTPP (or MgTPP), as the photoabsorber in the BLM, in conjunction with tris-(2,2'-bipyridine) ruthenium ion, $Ru(bpy)_3^{2+}$, methyl-viologen (MV^{2+}, 1,1'-dihexadecyl-4,4'-bipyridium) as electron acceptor, EDTA (ethylene-diamine-N,N,N',N'-tetraactate) as electron donor, and vitamin K (VK_1) as a hydrogen carrier.[7] In one system, the BLM phase contained VK and MV^{2+} with $Ru(bpy)_3^{2+}$ added to one side of the bathing solution and EDTA to the other side. The second system differed from the above by having only ZnTPP added to the BLM-forming solution. All experiments were performed in the absence of O_2 by bubbling Ar (or N_2) through the bathing solution for at least 30 minutes before forming BLM. Photovoltages of the viologen-free side were positive 50 mV and 90 mV, respectively, for the first and second systems. The time course for the photocurrent is as follows: photocurrent rises rapidly, which is followed by a slow increase, then it decays to a steady value. When the light is switched off, the current goes back to the dark value. Since in both systems the photoresponses were observed, $Ru(bpy)_3^{2+}$ must be bound to the BLM. The presence of ZnTPP in the BLM greatly enhanced the response, which implies facilitated electron transport. Photoexcitation of $Ru(bpy)_3^{2+}$ and/or ZnTPP leads to viologen reduction, as evidenced by the polarity of photopotentials. Since acceptor (MV^{2+} or Fe^{3+}) and donor (EDTA) are physically immobilized, some transmembrane redox reactions must take place. The most direct interpretation of the data is that reduction of $Ru(bpy)_3^{2+}$ occurs on the side containing EDTA with transmembrane electron tunneling facilitated by ZnTTP and VK_1. The drop in photocurrent may be caused by the diffusion of reduced MV^+, which could become more soluble in the membrane phase. In analogy to the 'Z'

scheme of photosynthesis, this two-step electron-transfer system should be further studied.

Reconstitution of PS-I into BLM. Toward a more complicated experiment, reconstitution with an entire reaction center (i.e. Photosystem I of green plants) has also yielded a photoelectric effect.[110] Upon illumination, the PS-I reaction center (RC) containing BLM generated transient and steady-state light-induced voltages and currents. The wavelength dependence of the photoresponse matched the absorption spectrum of RC. Before describing this work in more details, it should be mentioned that Barsky et al[155] reported that thin lipid membranes containing RC isolated from pea chloroplasts did not exhibit any light-induced electric effects. In their experiments, the generation of photoelectric effects was observed, however, in the presence of the anion probe PCB^-. This was attributed to either a lack of association between the BLM and the thick (colored) planar membrane or to inactivation of the RCs by the solvent present in the membrane. It may be explained that a thin lipid membrane is simply not a good system for RC reconstitution experiments, since thylakoid membrane fragments isolated from RCs, when incorporated into BLM, generated dramatic photoelectric effects as described in the following paragraphs.

Thylakoid membrane fragments (TMF) were obtained from spinach chloroplasts by gentle osmotic shock.[110] TMF, thus obtained, were incorporated into lipid microvesicles (LMV) called liposomes. Electron microscopy of the LMV revealed that they consisted of closed structures. Two different LMV preparations were used for fusion studies: RC-LMV and TMF-LMV. In both cases the same method was used to achieve fusion. The BLM was formed with a solution that contained a negatively charged phospholipid, phosphatidylethanolamine. A divalent cation, usually Ca^{2+} was present in the bathing solution. With both of these conditions met, addition of either LMV preparation resulted in fusion of the LMV with the BLM. Addition of vesicles containing thylakoid membrane fragment (TMF) to one side of a planar BLM resulted in the generation of light-induced membrane potentials. The generation of the photovoltage required the addition of artificial carriers of reducing equivalents (e.g. PMS = phenaminemethosulfate) to the same side as the vesicles or the presence of vitamin K_3 (V-K_3), a quinone, in the vesicular

membrane. The polarity of the photovoltage indicated that the side containing the liposomes (LMV) becomes negatively charged. This may be due to the reduction of PMS by ascorbate as evidenced by a change in the color of the suspension from light yellow to green. Addition of such chemical agents to the other side had no effect on the system, suggesting that the photoactive species had no access to the other side of the planar membrane.[110]

The photovoltage increased when coenzyme Q_6 (CoQ_6 or ubiquinone-30) or V-K_3 were present in the vesicular membrane, and decreased sharply when *o*-phenanthroline was added to the side containing the LMV. Addition of small amounts of the proteonophorons uncoupler carbonyl cyanide *m*-chlorophenyl hydrazone (CCCP), which is known to increase the permeability of membrane to protons, caused a small decrease in the BLM resistance and a decrease in the photovoltage. However, no significant change in the shape of the photovoltage time course was observed, with the exception that if a quinone was also present the rise and decay time of the slower component decreased. This observation suggests that the slower component may be associated with ion (probably H^+) diffusion across the membrane. The time constant of the slow component was calculated from the time course of the photovoltage and found to be equal to 6 sec. This value is in agreement with the value of 5 sec calculated from the values of BLM resistance (R_m = 1.2 x 10^9) and capacitance (C_m = 4.1 nF) for that membrane. It was also found that the open-circuit photovoltage obtained in the presence of PMS and in the absence of any other exogeneous substance, developed after some time, a slow component. The slow component, as in the experiments with quinones, had the same polarity as the fast component and was superimposed on it. The time course of the short-circuit for a typical membrane consists of a large initial overshoot when the light is turned on, followed by decay to a smaller steady-state current and an undershoot when the light is turned off, followed by a return to the base line. When the conductance of the bilayer to protons was increased with CCCP, the steady-state current also increased. These results, taken together with the fact that no change in conductance was found for the BLM in the presence of the vesicles, indicate that the vesicles remained intact after fusion. The same model has been previously proposed for studies involving the fusion

of planar membranes with LMV containing purple membrane from *H. halobium* (*see* Section 9.5).

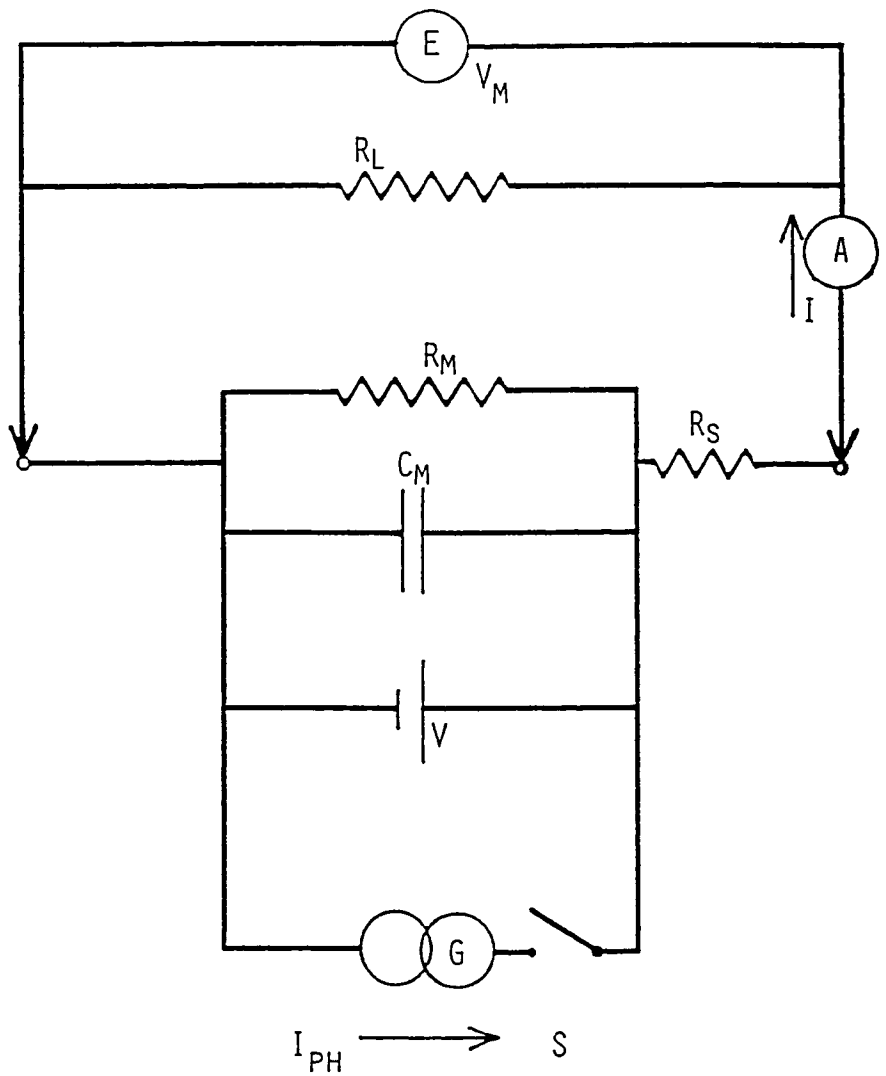

Fig. 9.8 Equivalent circuit representing the liposome-BLM associated system. Under short-circuit conditions, the potential difference is zero (E_m = 0), I_f would represent the short-circuit current induced by light.

In order to test the validity of the proposed model, the system was analyzed on the basis of an equivalent circuit similar to the one used by Rayfield.[49] The equivalent electrical circuit for a single fused vesicle is shown in Fig.9.8. In the diagram R_v and C_v are the resistance and capacitance between the right chamber and the interior of the vesicle. R_f and C_f are the resistance and capacitance between the left chamber and the interior of the vesicle (fused portion). R_m and C_m are the resistance and capacitance of the planar BLM. All the equivalent current generators in one vesicle are designated by I, and V_b represents the potential difference between the interior of the vesicle and either chamber.

The photocurrent is made up of two components, a displacement or capacitive current through C_f and a leakage current through R_f which starts to appear as the light is turned on. As the potential reaches its steady-state value, the displacement current gradually decreases until only the steady-state current is left. When the light is turned off, the membrane begins to discharge (V_b decreases) and this generates a displacement current of opposite sign. However, if the displacement current is larger than the leakage current, the short-circuit current reverses sign and gradually decays to zero. The results discussed here support the idea that under the conditions in which the above studies were done, the closed structure of the vesicles is maintained after fusion of the two membranes takes place. They also show by direct electrical measurements, that TMF reconstituted in such a way are capable of generating photovoltage and photocurrents which are directly related to the absorption of light by the PS_1 reaction center present in the TMF.

In concluding this section, the partial reconstitution of the PS-I reaction center from chloroplasts in BLM was accomplished by two different methods. Reconstitution of reaction centers (i.e. Photosystem I of green plants) in a BLM has also yielded a photoelectric effect. Upon illumination, the PS-I reaction center (RC) containing BLM generated transient and steady-state light-induced voltages and currents. The wavelength dependence of the photoresponse matched the absorption spectrum of reaction centers (RC). The main features of the photoresponse are explained by the redox membrane electrode model. The observed photosignals are due to the transfer of electrons from a donor to an acceptor located on opposite sides of the BLM. This RC-containing BLM

provides direct evidence that the RC is an intrinsic membrane protein that spans the lipid bilayer. In this connection the experiments reported by Seibert et al.[8] on an RC-doped semiconductor electrode and by Chen and Li[131] on chloroplast in liposomes are of interest.

Semiconductor model of green plant photosynthesis

Chronologically, the use of the concepts of semiconductor physics to biosystems was introduced by Szent-Gyorgyi, later with specific application to natural photosynthesis by E. Katz [*see* Barber, 1979 for a review]. Since the photoelectric effects were observed in chlorophyll-containing bilayer lipid membranes (p-BLMs), specific models based on solid-state physics have been suggested.[6,50] Several reviews are available [Bolton, 1977; Metzner, 1978; Marino[161]]. A useful model for the thylakoid membrane of green plant photosynthesis can best be discussed in terms of the theories of *p-n* junctions and Schottky barriers. Fig. 9.9 shows the thylakoid membrane as a *p-n* junction (or two Schottky barriers) interposed between two aqueous solutions. The energy levels in the aqueous solution containing redox couples are governed by their standard redox potentials. The Fermi level in the membrane is determined by the so-called flat-band potential (E_{fb}) which is the potential at which the band-bending is zero. Absorption of photons by the pigments embedded in the lipid bilayer at the two interfaces results in the generation of electron-hole pairs (excitons) which separate at the respective interfaces. Referring to Fig.9.9, for the reduction to occur on the left membrane/solution interface and the oxidation on the right, the redox couples in the bathing solution must possess certain redox potential values such that for the *p*-type membrane interface, the acceptor must be equal to or below the conduction band of the membrane photocathode, whereas for the *n*-type membrane interface, the redox potential of the donor must be equal to or above the valence band of the membrane photoanode. For the photoelectrolysis of water, the interfacial electron transfer (redox) reactions may be written as

$$A + e \xrightarrow{h\nu} A^- \qquad (9.18)$$

or

$$H_2O + e \xrightarrow{h\nu} \tfrac{1}{2} H_2 + OH^- \qquad (9.19)$$

$$(E^{0\prime} = -0.41\ V)$$

and

$$D + h^+ \xrightarrow{h\nu} D^+ \qquad (9.20)$$

or

$$H_2O + 2h^+ \xrightarrow{h\nu} 2H^+ + \tfrac{1}{2} O_2 \qquad (9.21)$$

$$(E^{0\prime} = 0.82\ V)$$

The sums of Eqs.(9.18) and (9.20) and of Eqs.(9.19) and (9.21) are, respectively,

$$A + D \xrightarrow{h\nu} A^- + D^+ \qquad (9.22)$$

and

$$H_2O \xrightarrow{h\nu} H_2 + \tfrac{1}{2} O_2 \qquad (9.23)$$

$$(E^{0\prime} = 1.23\ V)$$

Thermodynamically, the overall reaction for water decomposition as summarized in Eq.(9.23) requires a minimum of 1.23 eV (~ 284 Kcal) for the overall dissociation energy per mole. Natural photosynthesis accomplished this feat by having two photosystems located at the opposite sides of the membrane. Thus, for each electron transferred, the absorption of at least two photons are necessary. This elemental insight derived from study of green plant photosynthesis is of crucial importance in devising a means for water-splitting by artificial photosynthesis (Chapter 10, *Applications*).

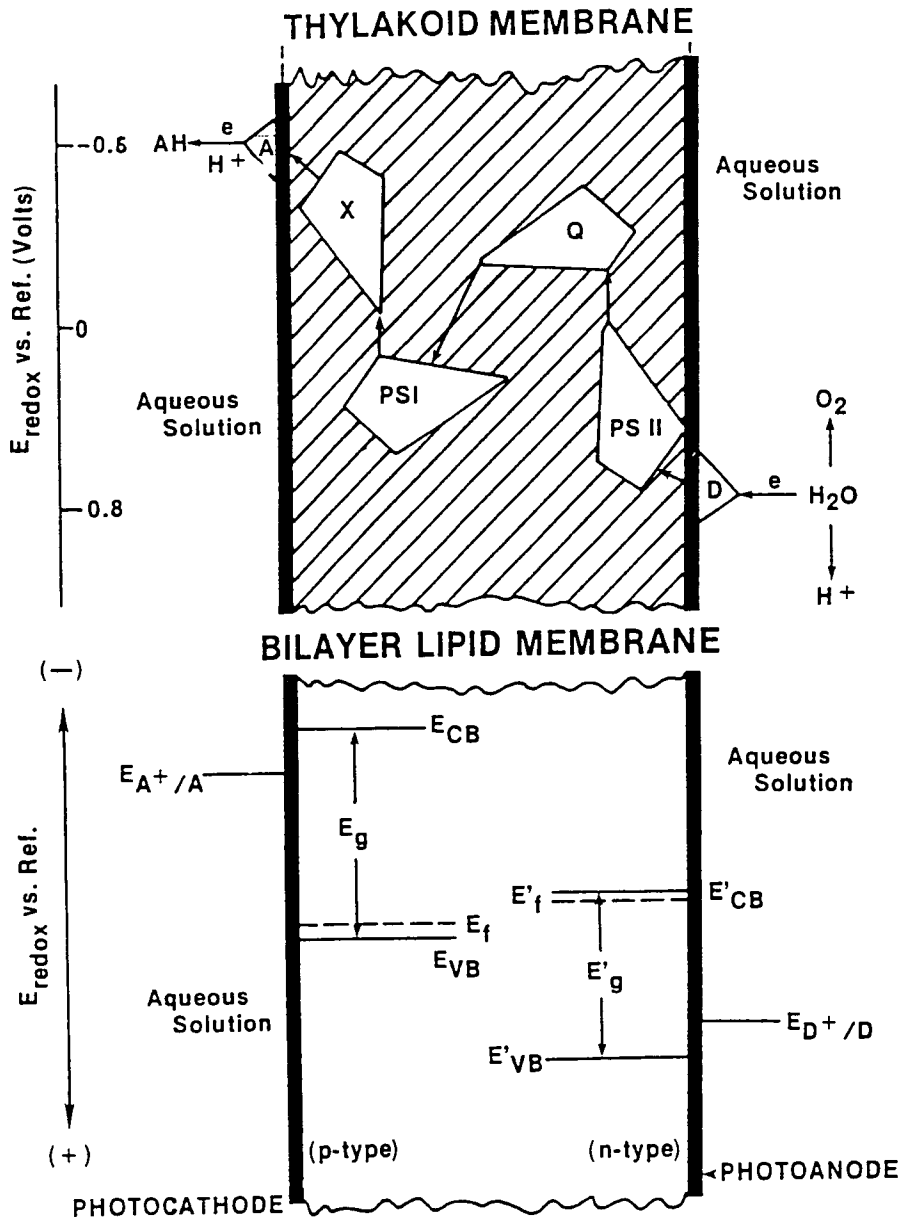

Fig. 9.9 Solid-state model of photosynthesis. *Upper*: scheme depicting a mode of operation of the thylakoid membrane. A = electron acceptor, D = electron donor, X and Q are the intermediate electron acceptors for PS-I and PS-II. respectively. *Lower*: scheme depicting a pigmented BLM.

Pigmented liposomes

The lipid microvesicles or liposomes are much more stable as compared with planar BLMs; they can be made in large quantity and hence are amenable to study by electrochemical techniques. For example, attempts to detect light-induced pH changes and oxygen evolution have been carried out with these pigmented liposomes [Metzner, 1978]. In this section a short summary of relevant papers on pigmented liposomes will be presented. References to earlier work may be found in reviews.[70,160]

Chlorophyll and its derivatives in liposomes

Initially, researchers were interested in finding out the reason(s) for the differences in chlorophyll absorption spectra and photochemical activities *in vivo* and in organic solvents. The rationale was that the liposomes made from plant lipids and chlorophyll could be used in an absorption study to give an absorption spectrum closely similar to that *in vivo*, if the postulated structure of the thylakoid membrane were correct. The reasoning was that the lipid bilayer of the liposomes would provide a favorable site so that the phytol chain of the chlorophyll (chl) would anchor there while the hydrophilic porphyrin ring would orient at the membrane/solution interface.[39] With these thoughts in mind, the following experiments were performed. The chl-containing liposomes were prepared by sonication of a lipid-chlorophyll mixture 0.1 M phosphate buffer at pH 7.5. The sonicated mixture was passed through a Sephadix G-50 column previously in equilibrium with the same buffer. The liposomes collected were those contained in the first 2 ml of the fastest green band to pass down the column. The absorption spectrum (of the chl-liposomes) was taken and the peak was at 673 nm. The results strongly suggested that the chl in liposomes was in an environment more similar to that *in vivo* than when it was simply dissolved in organic solvents. In an elegant study, Oettmeier et al.[34] reported that light induced formation of chlorophyll *a* radicals. In their work they used both quinoids and nonquinoid acceptors. The most satisfactory acceptor was Fe^{3+}. Another important factor in these types of experiments was the exclusion of oxygen from the sample. Exposure times as little as one minute caused the formation of chlorophyll radicals when exposed to light. Electron transfer was studied by Sugimoto et al.[40] and found the effects of asymmetrically located mediators.

Krasnovsky et al.[36] also studied chlorophyll *a* as a sensitizer, however, they used methyl viologen as the acceptor and studied the photoproduction of hydrogen. Tomkiewicz and Corker[32] demonstrated earlier that the photochemistry of chl in liposomes is different from the photochemistry in homogeneous solution and reported a G-value of 2.0026 ±0003 with a line width of 9.0 ± 0.5 G. On the basis of their results Tomkiewicz and Corker concluded that the lipid/water interface is unique in that it imparts some stability to the photochemical charge separation. Besides confirming a 10 nm red shift of the Soret band with respect to organic solvents in chl-liposomes, Mangel[37] reported the appearance of absorbance peaks beyond 700 nm, implying the presence of chl aggregates. Moreover, Mangel also showed that liposomes containing chl and β-carotene are capable of photoinduced electron transfer in the presence of a redox gradient, consistent with the photoelectric effects in chl-BLMs as already discussed above.

Liposomes fused with oxygen evolving complexes

Earlier, some researchers attempted to test the idea of water splitting by light by incorporating photosynthetic pigments into liposomes, very much as was done for the planar BLM. Preliminary experiments showed some O_2 evolution from chl-containing liposomes, as detected by a Clark-type electrode. However, later experiments with better temperature control indicated otherwise. The apparent oxygen evolution as sensed by the electrode was due to heating effects on the electrode itself. This failure notwithstanding, Toyoshima et al.[59] using a similar system, reported light-assisted oxidation of water in chlorophyll-containing liposomes. The rate of oxygen production, as calculated from the initial slope, was 4.2×10^{-4} per mole at 10^5 lux under similar conditions, but employing rigid temperature controls (within ± 0.2^{o} C). However, other investigators observed oxygen consumption instead, as the pigments in the liposomes became irreversibly photooxidized. Much of the work on oxygen deals with studies of the kinetics of oxygen evolution. These studies have led to the formal kinetic model of Joliot and Kok [*see* Metzner, 1978] From this model many general speculations on the mechanism of oxygen evolution have appeared. However, the oxygen evolving complexes have not been isolated or purified and the mechanism of action remains obscure.

Nevertheless, oxygen evolution is definitely a membrane-associated function. The oxygen evolving apparatus of green plants is believed to be associated with the inner thylakoid membrane [Olson and Hind, 1976]. At this site, light is used to split water molecules while generating protons and oxygen with the electrons being driven through Photosystem II. The actual "oxygen evolving enzyme" (or complexes = OEC) is one of the most unstable and elusive entities in all of biology, which is deactivated by mild biochemical treatments. Little is known about this supposed enzyme on a molecular level. Among its properties, it is very sensitive to aging, heat, ultraviolet light, organic solvents and high concentrations of tris buffer. It is stimulated by chloride, bicarbonate and manganese. In fact, manganese is believed to be at the active site of the enzyme. Additionally, the following questions have been posed: (i) Is a sealed membrane, topologically separating two aqueous solutions, a requirement for O_2 evolution? and, (ii) Does the reconstituted system of OEC-containing liposomes respond to compounds known to alter O_2 production *in vivo*?

Experiments have been designed to answer these two questions. For example, chlorophyll-containing liposomes have been shown to undergo photoelectron transfer, including the so-called "Krasnovsky reactions". As already mentioned above, Toyoshima et al.[59] have reported the generation of a small amount of oxygen upon white light irradiation of chlorophyll-containing liposomes in the presence of the Hill acceptor ferricyanide. Since there was some question concerning temperature controls, it seems possible that the observed oxygen was in reality a heating effect on the oxygen electrode. Following the negative results, a different series of experiments were undertaken in which broken thylakoids incapable of oxygen generation, were incorporated into various kinds of liposomes.[70] Evidence indicates that thylakoid membrane, in the form of a sealed vesicle, is an indispensable structure for O_2 evolution and photophosphorylation. Indeed, it has been found that osmotically shocked or broken thylakoids did not readily generate O_2. If, however, these broken thylakoids were sonicated, some of the O_2 evolving ability was revived. Further, it was demonstrated that broken thylakoids fused with liposomes greatly increased the stability of the oxygen evolving complexes to aging. However, it was not clear if the two membranes adhered or actually fused. To differentiate between these two possibilities, liposomes composed of lysophosphatidyl choline and phosphatidyl serine

as well as the normal egg lecithin were made with the Hill acceptor (ferricyanide) internally sequestered. If the membranes did not fuse but only adhered, no oxygen should have been detected since the Hill acceptor was only inside the liposomes. Only upon fusion of the membranes could ferricyanide have been exposed to the oxygen evolving complexes of the thylakoids. When the experiments were conducted oxygen could be detected, indicating at least some membrane fusion. As expected, Ca^{2+} greatly enhanced the rate of fusion. From the experimental results it was concluded that an intact sealed membrane is likely required for the process of oxygen evolution. Oxygen evolution was shown to closely follow the breakage and resealing of the thylakoid membrane. Also, oxygen evolution was demonstrated for broken thylakoids fused with liposomes containing ferricyanide. The requirement for a sealed membrane is consistent with compartmentalization of protons produced from water oxidation (thought to drive ATP synthesis via a chemiosmotic mechanism) and the initial light-driven charge separation known to exist across chl-BLMs.

Fragata et al.[52] performed studies to determine the location of chlorophyll a in phospholipid vesicles and hydrocarbon solutions. They concluded from his studies that the porphyrin ring is exposed to water at the inner and outer surface. Extent of immersion is unknown. In this connection, Leblanc and colleagues[51] have conducted research in the photosensitization of methyl red-ascorbate reaction in vesicles. They concluded that the reaction can occur more easily when the reactants are in the same compartment. Proton diffusion can also be measured using dyes. The Stillwell and Doran[53] method involved the incorporation of sequential pH dyes in the membrane of liposomes. This method yields a simple process to measure perturbations and diffusion in the membrane. Schmidt[55] used flavins to determine rotational motion of flavins in the membrane. Zero field optical detection was performed by Hotchandani et al.[56] They concluded that monoligated and biligated chlorophylls are present in the monolayer. Regen et al.[87] have demonstrated the ability to produce polymerized vesicles. These vesicles are much more stable than phospholipid vesicles, thus they have important biomedical applications. Sudholter et al[88] demonstrated the ability to form closed vesicles from synthetic amphiphiles. Witt and DiFiore[39] developed a method for creating planar BLMs from vesicles in suspension, which may be useful in photosynthesis research. In connection with thylakoid lipids, Fuks and

Homble[89] reported that the addition of thylakoid lipids to glycolipid monogalacatosyldiacylglycerol is sufficient to promote a planar BLM without using n-decane solvent. Further, they found that the BLMs formed from thylakoid lipids are about as permeable as pure phospholipids to H^+, but five orders of magnitude higher than alkali or halide ion permeability. Additionally, the authors suggest that HCl was not trasported as neutral species through the galactolipid-containing BLM.[89]

9.4 The Photoreceptor Membranes of Vision

Overview of the visual process

It seems appropriate to begin the discussion of the membrane biophysics of vision with a rough sketch of the gross anatomy of the eye. From front to back, the eye consists of the cornea, anterior chamber, iris, lens, vitreous humor, retina, and optic nerve. Photons of light enter the eye at the cornea, pass through the pupil like a camera aperture, are focused by the lens and finally reach the retina. The cornea and the lens of the eye form an image of the external world on the layer of photoreceptor cells. It is at the retina where the energy of photons are transduced into other forms of energy, which in turn result in electrical messages eventually decoded by the brain. The task of understanding how the eye transduces electromagnetic radiation into a signal that is ultimately perceived by the brain, requires an integrated knowledge of physics, biochemistry, photobiology, and neuroscience. As yet, the task of understanding vision at the molecular level is far from complete. We will describe what is known, concentrating on those aspects that are amenable to an experimental approach with techniques and instruments now available.

In vertebrates, vision begins when the photons of visible light hit the retina, where photoreceptors are located (see Fig. 9.10). There are rods and cones, so called after their typical shape. Cones function in bright light for color vision, detail and lines and for rapid movement, whereas rods operate in dim light, capable of detecting a single photon as well as shapes, shades and tones. That is, cones are better for temporal resolution and rods for sensitivity. Because of ease of isolation, rods have been extensively studied. A rod consists of two segments, the outer and the

inner. The inner segment is concerned with cellular metabolism, which houses mitochondria, nucleus, etc. The outer segment, the light absorbing body of the photoreceptor, is composed of 1000-2000 or so disc-shaped sacs, neatly packed like a stack of coins (30 nm apart) which are enclosed by the plasma membrane [Knowles and Dartnall, 1977]. Although the term disc has been generally used, the term sac is more descriptive and appropriate because of the presence of intradiscal space. Henceforth, the terms disc and sac will be used interchangeably. The sacs in a rod cell are specialized bilayer lipid membranes that contain the crucial light-sensitive molecule, rhodopsin. As for cones, the visual pigment appears to be located in the infoldings of the plasma membrane.[61,62] There are channels for ion transport located in the plasma membrane as well as ATP-driven pumps for maintaining the ionic balance of Na^+, K^{2+}, and Ca^{2+} across the membrane. The sac membranes where visual pigment rhodopsin is located are physically distinct from the plasma membrane (Fig.9.17). In the dark the chromophore retinal portion of rhodopsin is in *11-cis* form and the plasma membrane is hyperpolarized at about 40 mV with the cytoplasmic side negative. This is due to a net higher outward flux of K^+ and lower inward flux of Na^+ across the plasma membrane. Upon absorption of light, an increase of hyperpolarization of the plasma membrane of the photoreceptor is observed. It is generally assumed that an intracellular chemical transmitter exists that serves as a mediator between photoexcitation of rhodopsin in the sac membrane and gating of Na^+ channels in the plasma membrane. Substances such as Ca^{2+} and cyclic guanosine-3'5'-mono-phosphate (cGMP) have been proposed as mediators.[63,64] Studies in different laboratories have suggested that Ca^{2+} does not mediate visual excitation as evidenced by a decrease rather than increase of the free Ca^{2+} concentration after injecting calcium buffers or cGMP into ROS cells.[65,66] However, certain experiments indicate the key role played by Ca^{2+} in the steps of recovery and adaptation in the overall visual process.[67]

The Ca^{2+} hypothesis of Hagins and Yoshikami predicts a sudden permeability change of sac membrane after light absorption by rhodopsin, whereas the cGMP hypothesis suggests that light leads to hydrolysis of cGMP which in turn triggers the receptor potential. Recent advances definitely favor the crucial role played by cGMP.[70] The earlier suggestion that Ca^{2+} is sequestered within the interior of the sacs remains unclear.

Further, it is fair to state that, at present, little is known about the permeability to ions of the sac membrane. Thus, questions like, "How does excited rhodopsin alter the biophysics and biochemistry of its surroundings to generate an electrical signal eventually perceived by the brain? By what mechanism is the energy of photons transduced?" Rods are not only sensitive to a single photon, but are also able to adjust their sensitivity by light adaptation over five orders of magnitude of light level.

Facts like these are known. However, the details of amplification of the light effect by the photoreceptor and its subsequent recovery as well as the questions posed above have not been completely answered. Since rhodopsin and lipid bilayer are intimately involved, many investigators have resorted to experimental bilayer lipid membranes (BLMs and liposomes) to examine the rhodopsin (and its precursor, retinal) interactions with other components of the visual system.[69,70] What follows first of all is some background information concerning the visual receptor. Experiments using experimental bilayer lipid membranes as a model of the sac membrane of the visual receptor will then be presented.

Biochemical and molecular aspects of visual photoreceptors

The visual receptor membrane of the retina is believed to have evolved from, or have a common origin with, photosynthesis. Much of the evolutionary evidence is based on the similarities between the two systems. For example, the visual receptor cell consists of a stack of membranous discs (sacs) very much like the granal stacks of thylakoids. Both photosynthetic and photoreceptor systems make use of carotenoid pigments which are highly conjugated. Another evolutionary consideration is the association of cilia or microvilli with the photoreceptor cell. All photoreceptor cells are equipped with cilia or a flagellum. It is believed that the photoreceptor membrane develops at the expense of modified cilia, flagella, or microvilli. What is particularly interesting about the evolutionary origin is that animals are unable to synthesize carotenoids, however they may absorb them from foods and that carotenoids, in particular, vitamin A (the deficiency of which causes night blindness) is essential for the structure and maintenance of a ciliated cell.

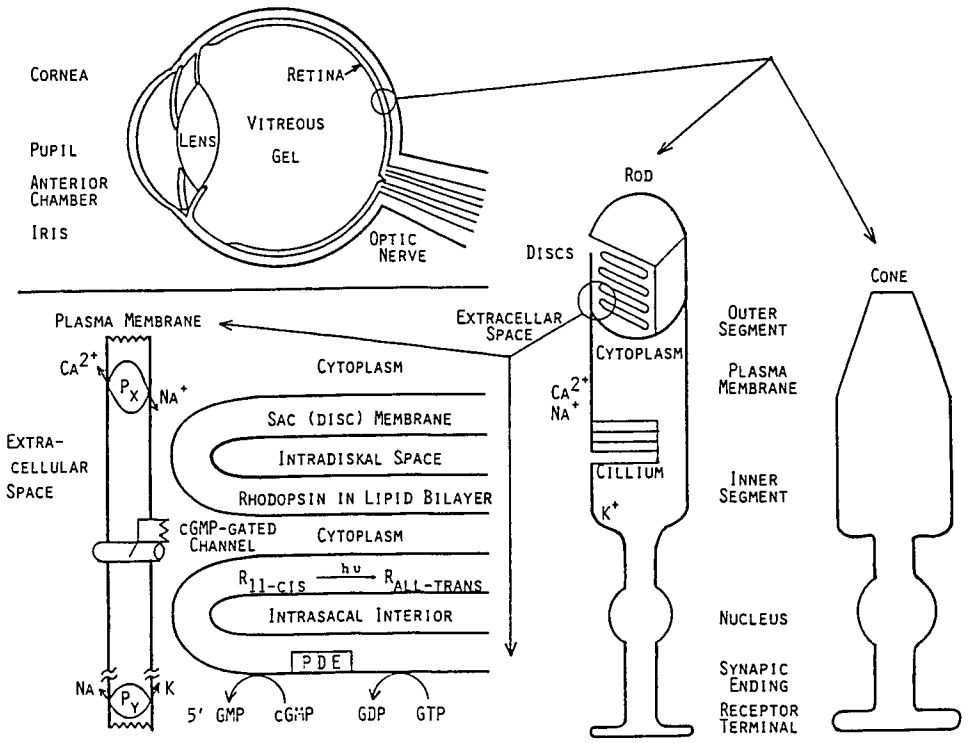

Fig. 9.10. Schematic drawings of the eye and its photoreceptor membranes. (1) Vertebrate eye. (2) The retina, a sheet of light sensitive tissue, consists of two kinds of photoreceptors, rods and cones. (3,4) The structural details of a rod and its photobiophysics and photobiochemistry in terms of the plasma and sac membranes are shown in the lower left. (5) In the dark, Na^+/Ca^{2+} pumps in the outer segment and Na^+/K^+ pumps in the inner segment maintain a high K^+ and low Ca^{2+} concentration inside of the plasma membrane which has a high permeability to Na^+. (6,7) Under illumination, a single photon absorbed by a rhodopsin ® isomerizes it to R*, which initiates the cGMP cascade that blocks the inward flow of Na^+ and Ca^{2+} in the outer segment.[70]

The photobiochemical aspects of visual excitation were first worked out in some details by G. Wald (for reviews, see[69]). So far,all the visual pigments in vertebrates consist of a complex of retinal and opsin termed rhodopsin. The light-mediated biochemistry of rhodopsin and its regeneration is called the visual cycle. The retinals and retinols are highly conjugated systems with a functional group of aldehyde or alcohol, respectively, at one end of the molecule. Both retinals and retinols possess four double bonds in the side chain, each of which might adopt either **cis** or **trans** configuration, producing thereby a number of geometrical isomers. The most stable and prevalent isomer is the **all-trans**, whereas the 11-**cis** isomers are found to be involved in the initial step of light absorption. In organic solvent, retinal absorbs intensely at 380 nm. However, when present in rhodopsin (or rather surrounded by opsin) the absorption peak appears at 500 nm. The initial step in bleaching after absorption of a photon is to isomerize retinal (the chromophore of rhodopsin) from the 11-**cis** to the **all-trans** configuration (prelumirhodopsin). Then the structure of opsin opens progressively, ending in the splitting of retinal from opsin. To regenerate 11-**cis** retinal, NADPH is required. How retinal recombines with opsin forming rhodopsin is not entirely clear at present. Very recently, the conversion of the polyene **all-trans** retinol into 11-**cis** retinol has been investigated by Law et al,[174] and they found that an intact polyene system must be present for appreciable isomerization to take place.

The rhodopsins in vertebrates are located in the highly organized lamellar membranes of the outer segments of rods and cones. From a structural point of view, the photoreceptor consists of three segments: (i) the outer segment membrane where photopigment molecules are located, (ii) the inner segment, which provides the metabolic energy, and (iii) a conducting fiber that takes part in transmitting the excitation to other cells in the retina (Fig.9.10). Under the electron microscope, the outer segment membranes appear to be a stack of double membrane disks. Each disk or sac membrane consists of two triple-layered structures, which could form a closed sac not unlike those found in the chloroplast. The interpretation of electron micrographs in physical and chemical terms is difficult owing to our lack of knowledge about the reactions that take place during fixing and the precise chemical composition of lipids, proteins, and chromophores present in the outer segments. However, using the findings of electron

microscopy, X-ray diffraction, and other experiments, Fig. 9.11 shows a schematic model for a rod.

Although detailed information is still lacking, the structure of the outer segment of rods appears to be a highly ordered array of repeating units, about 55 A thick. Similar to the four types of biological membranes already described, the lamellar membrane of retinal rods is also interpreted in terms of a Gorter-Grendel bilayer model. For instance, Gras and Worthington (for references, see [Stieve, 1986]) have proposed a model to account for their data, derived from X-ray diffraction studies. They suggest that the membrane surface facing the intrasac space is 40 A thick, the lipid region 16 A thick, and the surface facing the cytoplasm 18.5 A thick. Thus, the rod is a highly membranous structure made of lipids, proteins, and pigments. The evidence for a bimolecular leaflet now known as lipid bilayer in these structures was indicated in the studies of Schmidt, as early as 1936, who used polarization microscopy. The gross composition of the rod outer segment is about 40-50% protein, 40-50% lipid, and 4% carbohydrate on a dry weight basis. The visual pigment, rhodopsin, accounts for about 35-50% of the dry weight, the rest being mainly lipids.These lipids, mostly phosphatidylcholine (PC), phosphatidylserine (PS), phosphatidylethanolamine (PE), and phosphatidylinositol (PI), are believed to be of special importance. The protein moiety of the visual pigment opsin composed of 348 linked amino acids, is less stable when isolated from rhodopsin, which has a molecular weight of 41,000 daltons and appears to be composed of seven d-helices linked together by loops.[64] It is believed that 11-**cis** retinal, the principal chromophore, is linked directly to opsin, lying near the center of the sac membrane. The evidence that the rhodopsin molecule is surrounded by polypeptides buried deep in the lipid bilayer is intriguing, and needs to be tested experimentally. Perhaps the use of pigmented BLM and liposomes, described in the section on reconstitution, may prove helpful in such studies.

Biochemical aspects of the visual process have been investigated by many workers. For example, complexes between phospholipids and retinals have been reported. The phospholipid composition and extra stability of bovine rod outer segments and rhodopsin micelles have been studied. In particular, they point out that lipids play a significant role in the visual process, not only through binding pigments, but presumably in

modulation of the membrane potential and permeability properties. In this connection, the earlier paper of McConnell, Rafferty, and Dilley is of interest. These workers have observed that fragments of bovine retinal outer segments, containing intact photoreceptor sacs accumulate hydrogen ions upon illumination. Most significantly, the bleached samples were not able to do so. This finding is seen to be in accord with the results reported by Falk and Fatt[71] who, after investigating suspensions of retinal outer segments with light flashes, suggested that the uptake of protons by rhodopsin was responsible for the observed potential changes in their system. Earlier, Brown and Murakami[72], also using light flashes, had observed a new photoresponse in the monkey eye, which had a latency of about 1 usec and a duration in the msec range. This fast photoeffect is known as the early receptor potential (ERP) The early receptor potential has the following characteristics: (i) it is unaffected by anoxia, (ii) it is less sensitive to the ionic environment, and (iii) it is found in the degenerating rodent eye, from which no electroretinogram can be recorded. At room temperature, the early receptor potential had two components in the frog eye, as was reported by Cone.[73] The first corneo-positive phase was observed to reach a peak value in about 100 μsec, and was followed by the second, corneo-negative phase, with a peak time about 900 sec. Since the sign of two components depends on the position of the recording electrodes, Cone proposed the use of R_1 and R_2 for the first and second components of the early receptor potential, respectively. Pak[74] used R_1 and R_2 for the two components of "rhodopsin response." It is due to this discovery of the biphasic nature of the early receptor potential that the understanding of the mode of its generation has been strengthened, since various experimental conditions are now known to influence R_1 and R_2 independently. For instance, temperature is the most effective and first discovered parameter in controlling the mode of generation of the early receptor potential. A number of investigators have demonstrated the different temperature dependencies of R_1 and R_2 in the albino rat eye, and have discovered that lowering the temperature sufficiently abolished R_2 and isolated R_1, which could be detected even at a subzero temperature of -35 ^{o}C.

At the present time, the early receptor potential has not been obtained with an aqueous suspension of rhodopsin or any other pigments, or even with the aqueous suspension of rods and cones.[70] Instead, the

optimum early receptor potential can only be observed in membraneous structures with high electric resistance and proper orientation of the pigment molecules. Hagins and Ruppel[75] and Govindjee et al.[76] have suggested that early receptor potential is related to displacement currents across the plasma membrane of the rod. Recent studies have shown that the ERP tells us little about the molecular mechanism of visual excitation, since the initial step of rhodopsin excitation takes place in the inner sac membrane. In rods the presence of outer plasma membrane separated from the inner pigmented sacs (discs) is rather inefficient for generation of the early receptor potential.

As has been realized by many investigators, the mechanism for visual excitation cannot be understood without a fuller understanding of the structure and function of the membranes. Recently, several papers have appeared addressing certain aspects of the problem, as will be discussed shortly. In this connection, let us go back to electrical transient phenomena induced by light. It is necessary to examine changes in the membrane properties upon illumination. At present even with the sophisticated intracellular recording techniques advanced by Toyoda, Nosak, and Tomita,[77] it has not been possible to place recording electrodes on either side of the visual receptor sac (disc) membrane, and to explore the basic nature of the early event of phototransduction. It seems that resorting to model systems such as BLMs and liposomes, discussed in the next section, may be a viable approach.

Phototransduction mechanisms

As already alluded to in the introduction, the eye is an outpost of the central nervous system. At the back of the eye is the retina, where the photoreceptor membrane is situated. This is where signal transduction occurs, but we do not know how light signals are actually transduced into nerve impulses, nor is it known that how that activity is transformed into chains of nerve impulses conducted along the optical nerve to the brain. How does the brain decode the received signals to generate visual perception in terms of shapes, colors and movements? These questions have also been raised. In going from the retina to the brain, five types of membraneous structures are involved. These are the rods and cones, the bipolar and the ganglion cells, the horizontal and the amacrine cells and all

of these are connected to one another by synapses. How these structures function electrically and chemically remains obscure. However, important progress has been made in last two decades. We shall now summarize our current understanding of the mechanism of photoreception in its earliest stages in terms of critical membrane processes.[70]

The essential aspects of phototransduction in the vertebrate rod cells of the photoreceptor were generally understood in the 1970s. A rough outline is as follows: rhodopsins embedded in the disc or sac membranes of the outer segment absorb light, change from 11-**cis** to **all-trans** retinal, which sets off a series of biochemical reactions that in turn affect ion channel properties in the plasma membrane leading to altered electrical activities of the photoreceptor. Since the sac membrane where rhodopsin molecules are located and the plasma membrane where the ion-channels are situated are not directly connected, there must be an intermediary or messenger to carry the photoexcitation signal between the two physically distinct membranes. Hagins and Yoshikami, as already mentioned, proposed Ca ions for the role of internal messenger. Before describing the Ca hypothesis, let us consider the electrical properties of the plasma membrane in the dark. If a pair of microelectrodes are placed across the plasma membrane as shown in Fig. 9.11, a resting potential of about -40 mV is measured with the cytosolic side being negative. This observed dark potential can be explained in terms of K^+ and Na^+ ion concentrations according to the Nernst equation. The respective potentials are about 60 ± 5 mV for K^+ and 10 ± 5 mV for Na^+. If one measures the current across the plasma membrane, a value of 50 to 80 pA is detected as a result of greater flow of K^+ ions from the cytoplasmic side to the extracellular space than the flow of Na^+ ions in the reverse direction. This current of ions originates in the inner segment flowing along the rod and reenters the outer segment of the plasma membrane, which is maintained by the ATP-driven Na^+/K^+ "pumps".

According to the Ca^{2+} hypothesis, Ca^{2+} ions are sequestered in the sacs in the outer segment; the free Ca^{2+} is very low in the cytoplasm. Upon illumination, excited rhodopsins cause permeability changes in the sac membrane, thus releasing Ca^{2+} ions into the cytosolic space, which in turn affect the permeability of ion-channels in the plasma membrane. Namely,

the flow of Na^+ ions is greatly diminished due to the presence of Ca^{2+} ions which compete for the same Na^+ sites on the channels. Indeed, recent results indicate that there is a flux of Ca^{2+} out of the plasma membrane under illumination. The critical task, however, necessary to prove the Ca^{2+} hypothesis is to demonstrate that the disk (sac) membranes release the ions under illumination and take up Ca^{2+} in darkness. This has led to a number of light-induced experiments on rod photoreceptor cells in the intervening years since the Ca^{2+} hypothesis was first proposed in the early 1970s, the results of which are described in the following paragraphs.

In darkness, the chromophore embedded in the lipid bilayer is in 11-cis configuration and hyperpolarized (cytoplasmic negative side -40 mV). Absorption of a photon by 11-cis retinal changes it to the all-trans configuration which causes the plasma membrane to be further hyperpolarized (-75 mV). There are cGMP-gated channels as well as Na^+/Ca^{2+} and Na^+/K^+ pumps in the plasma membrane. The hyperpolarization is due to the inward flow of Na^+ and Ca^{2+} ions and the outward flow of K^+ through appropriate channels, some of which are controlled by the presence of cGMP. The ionic balance across the plasma membrane is maintained by the ATP-driven pumps.[70]

From the preceding description of the photoreceptor cell membranes, it can be appreciated that the pre-eminent role is played by the protein rhodopsin embedded in the sac (disc) membrane located in the outer segment. As techniques for manipulating membrane proteins developed in the 1970s, investigators began to study other proteins of sac membranes, especially those activated by light in conjunction with rhodopsin excitation. These light-activated proteins (enzymes) include 3',5' cyclic guanosine monophosphate (cGMP), GTP-binding protein (G-protein or transducin), guanylate cyclase, phosphodiesterase (PDE) and others. These proteins, like rhodopsin R, are also embedded in the sac membrane which has been deduced to be highly fluid with a viscosity of olive oil. This means that these membrane-bound proteins are very mobile within the plane of the sac membrane and able to interact with each other strongly. One of the most exciting findings in vision research in the 1980s was that, when the rod cells of photoreceptors were exposed to light, the current of the Na^+ ions was dramatically increased in the presence of

added cGMP. Further, light excitation of rhodopsin was found to decrease rather than increase the free Ca^{2+} concentration in the rod's outer segment. Additionally, Ca^{2+} ion concentrations in the cytoplasm enclosed by the plasma membrane could be substantially reduced by Ca^{2+}-chelating agent without abolishing the photoreceptor's ability to respond to light. Prior to these recent experiments, it was known that cGMP played an important role in regulating Na^+ channels in the plasma membrane. For instance, light excitation of one rhodopsin molecule is known to result in the hydrolysis of about 10^5 molecules of cGMP. Accordingly, one photo-activated rhodopsin changes more than 100 molecules of G-protein from an inactive form to active form, the latter of which turns on the enzyme PDE that hydrolyzes cGMP to 5'GMP at a rate of 200 per second. Other experiments by Nicol and Miller[79] showed that cGMP injected into rods caused a delayed change in the dark current after illumination as if the system has to wait for the photoactivated enzymes to destroy the added cGMP before responding to light in the usual manner. Thus, cGMP has been shown to be the most likely phototransduction messenger instead of the Ca^{2+} ion. In summary, a description of the current status of phototransduction in the retina's rods of vertebrates is given in Table 9.2.

Light-initiated excitation of rhodopsin molecules in the inner sac (disc) membrane sets off a cascade of enzymatic reactions that lead to the hydrolysis of cGMP, of which the departure from ligand-gated Na^+ channels in the plasma membrane alters the electrical properties of the photoreceptor. cGMP plays the role as the internal messenger between the sac membrane and the plasma membrane. For recovery and adaptation, Ca^{2+} serves the function of a feedback messenger.

Model systems and membrane reconstitution

The photoisomerization of retinaldehyde, the chromophore of the visual pigment rhodopsin, is believed to be the primary event in the visual process. The photoisomerization initiates a sequence of conformational changes in rhodopsin embedded in the sac membrane of the rod outer segment (ROS) leading to cellular excitation mediated by the ionic conductance. The currently accepted hypothesis is that cGMP serves as an internal transmitter between light-sensitive rhodopsin molecules in the sac membranes of ROS and Na^+ channels in the plasma membrane. Owing to

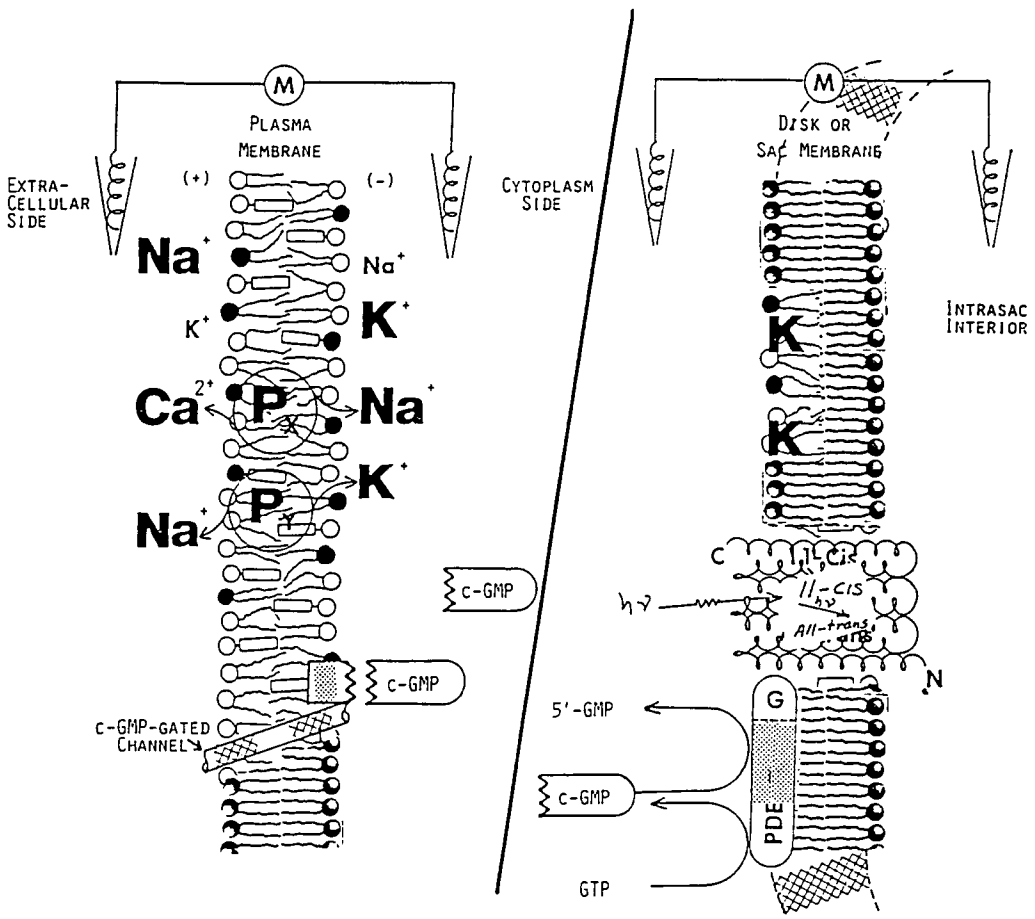

Fig. 9.11. Diagram showing electrical events of a sac (or disc) membrane (right) together with its external plasma membrane (left) of retinal, the rod outer segment (ROS).

Table 9.2 A summary of current status of phototransduction

In Darkness	Under Illumination
Rhodopsin's chromophore, retinal, is in 11-**cis** conformation in the sac (disc) membrane.	Retinal of rhodopsin in **all-trans** conformation.
Na^+, K^+, and Ca^{2+} ions move down their respective electrochemical gradient: K^+ ions move out of the cell in the inner segment whereas Na^+ and Ca^{2+} ions move into the cell.	Excited rhodopsin (R*) interacts with GTP-binding proteins (G-protein), which in turn activate PDE that hydrolyzes cGMP to 5" GMP. The lower concentration of cGMP causes the Na^+ channel to close, blocking the entry of Na^+ ions into the cell in the outer segment. As a result, the plasma membrane is further hyperpolarized to -70 mV.
The ionic balance across the plasma membrane of the cell is maintained by ATP-driven continues, pumps of Na^+/K^+ and Na^+/Ca^{2+}, located in the plasma membrane of the inner and outer segments, respectively, of the rod.	Na^+/Ca^{2+} pumping thereby causing a decrease of Ca^{2+} concentration in the cytoplasm, which may act as a signal for adaptation; Ca^{2+} plays as a feedback messenger for restoration and adaptation.
As a result of ion fluxes across the plasma membrane, the plasma membrane is hyperpolarized at about 40 mV cytosolic side negative; a dark current of 50-80 pA is detected.	cGMP synthesis is catalyzed by guanylate cyclase.
Channels in the plasma membrane are held open by cGMP.	

the greater size and ready availability of rods compared to cones, ROS has been used in many biophysical and biochemical studies.[69] Purified ROS sac membranes are composed mainly of phospholipids and rhodopsin, the lipids of which are known for their high degree of unsaturation. Physical studies (X-ray diffraction, neutron diffraction, NMR, and electron microscopy) have indicated that rhodopsin penetrates into and probably spans the sac membrane. This transmembrane protein rhodopsin can be solubilized and purified. The mechanisms of light-induced changes in rhodopsin embedded in the sac membrane and the resulting membrane electrical activity are obscure, however. This is owing to the fact that, experimentally, it is not yet possible to monitor directly the electrical events across the sac membrane by placing microelectrodes across it, as has been done with the plasma membrane of the ROS. Hence, the reconstitution of an artificial photoreceptor by incorporating rhodopsin into BLM was attempted as far back as 1963. The early investigators of the BLM system extracted rhodopsins from the retinal tissues of the eyes of bees, frogs, and cows. These extracts were added to one side of the BLM but no photosensitivity was observed.[81] One of the difficulties in the earlier studies was membrane instability because of the presence of rhodopsin along with the detergent used in rhodopsin preparation. In contrast, it was discovered later that retinals and β-carotene, being oil soluble, could readily be incorporated into oxidized cholesterol and/or lecithin BLM. Further, these carotenoid BLMs generated appreciable photoelectric effects. A brief summay of these experiments are given under separate headings below.

BLM and Liposome Experiments Related to Vision

Observations with carotenoid BLM. As in the case of photosynthesis, the primary steps of light conversion in the visual process are still obscure at the present time. With the background information described in the preceding sections, the use of BLM containing carotenoid pigments as an experimental model for the visual receptor membrane, appears to be a useful approach and has been, in fact, attempted by a number of investigators.[69] The initial workers observed that the BLM formed from brain lipids or proteolipids became electrically excitable after the adsorption of water-soluble extracts from bacterially fermented retina. Takagi et al.[82] formed BLM by apposition of the hydrocarbon chains of

two lipid monolayers at an air-water interface using the digitonin-free rhodopsin extracted from cattle retina, and observed that the resistance of the membrane was lowered to 10^3 to 10^5 ohm cm^2 in 1.0 M KCl solution, and increased to 10^6 ohm cm^2 when one side of the bathing solution was replaced with isotonic $CaCl_2$. Excitability, however, was not observed with this preparation.

The observation of light-induced effects in carotenoid BLM was reported in 1969. For BLM formation, the early workers[83,84] used various carotenoids (e.g. **all-trans**-retinal, 90-**cis**-retinal, **all-trans**-retinol, and β-carotene), phospholipids, and oxidized cholesterol dissolved in liquid alkanes. The dark dc resistance of the membrane was ohmic, ranging from 10^6 to 10^7 ohm cm^2, which is about 2 to 3 orders of magnitude lower than that of carotenoid-free BLMs. Upon illumination with white light, a maximum photoemf of about 6 mV was observed in a BLM containing a mixture of **all-trans**-retinal and β-carotene. All carotenoid BLM were found to be photoactive. In addition, the photoresponses of these carotenoid BLM have been found to be complex, as the experimental conditions have been altered. Depending upon the carotenoid pigments used, and external factors (e.g. the presence of modifiers and applied voltage), the voltage/time curves can vary from a simple monophasic response to a typical biphasic waveform, not unlike those found in vertebrate retina[84] It was emphasized that not only the presence of photosensitive molecules in the lipid phase, but also the interaction of the molecules with the aqueous phases, seemed to play an important role in the generation of the photoresponses. Subsequently, an intensive investigation was carried out on the mode of biphasic photopotentials of **all-trans**-retinal BLM. The obtained results are described in details elsewhere.[70,85]

Hanke and Kaupp[154] incorporated two types of channels from bovine rod outer segments into planar bilayers and patch-clamped bilayers. Neither of them was sensitive to light, but they did show several specific characteristics. One of the channels had relatively low unit conductance (20 pS in 150 mM NaCl), but was considerably more selective for Na^+ (P_{Na+}/P_{K+} = 6 : 1), and was considered a Na^+ channel. The other channel had a larger conductance (120 pS in 150 mM NaCl), but

had low Na^+ selectivity (P_{Na+}/P_{K+} =1.6 : 1). It was referred to as a cationic channel. One of its specific characteristics was its ability to activate in less than 10 msec and inactivate after applying a negative voltage step. The Na^+ channel was not influenced by Ca concentrations in the range from 1 uM to 1 mM. Tetrodotoxin at concentrations up to 1 uM could not induce any block of the two channels. The channels may originate from disc or plasma membranes, but their physiological significance remains unclear.

Finally, the exciting work of Tanaka, Yonezawa, and Sato should be mentioned.[129] They reported photochemical control of DC current across planar bilayer lipid membranes doped with an amphiphilic azobenzene derivative, 4-octyl-4'-(5-carboxypentamethyleneoxy) azobenzene (8A5). The photoelectric properties of planar BLMs made from soybean lecithin were examined. When a DC voltage is applied across the BLM, the trans-membrane current changes under alternate irradiation with ultraviolet and visible light. A comparative study on the photoresponse of soybean lecithin liposomes doped with 8A5 revealed that the photoelectric properties of the BLM result from the change in the membrane conductivity due to photoisomerization of 8A5.

9.5 The Purple Membrane of *Halobacterium Halobium*

Background

Halophilic microorganisms of halobacteria, salt-loving cells that thrive in the Dead Sea and salt flats all over the world, were first noted on dried salted fish in about 1900 in Scandinavia. The biochemical aspects of extreme halophilism displayed by these organisms have been reviewed by Larsen.[91] These bacteria are the only known organisms that use light to make energy without using chlorophyll. They do this using their own version of the energy-trapping pigment, a purple-colored protein embedded in the plasma membrane. One of the best studied halobacteria is *H. halobium* by Stoeckenius, Oesterhelt, and Blaurock in 1971 [*see* Oosawa and Imai, 1982], who discovered the protein pigment of the purple membrane of the microorganism, called bacteriorhodopsin

(BR).[70,92] The name is derived from the chemical similarity with the visual pigment rhodopsin, discussed in the last section (9.4).

H. halobium is a flagellated, prokaryote with a length of 5-10 um and a diameter of 0.5 μm. Its natural habitat is the salt flats and stagnant puddles at the edge of tropical seas. These salt-saturated puddles and flats are rich in organic material but have a low oxygen content. Moreover, the bacteria are exposed to high temperatures as well as a large solar insolation. In the laboratory *H. halobium* cells require at least twelve percent NaCl; they also need low concentrations of KCl and $MgCl_2$. The discovery of BR by Oesterhelt and Stoeckenius had a strong impact in the research area of bioenergetics and in the study of visual photobiophysical chemistry. Indeed, *H. halobium* is an extraordinary and unusual photosynthetic bacterium. Extraordinary in that *H. halobium* requires an almost saturated NaCl solution for growth. What is unusual about *H. halobium* is that it can photosynthesize ATP when grown under anaerobic conditions. When it is grown in the presence of oxygen and nutrients without light, *H. halobium* thrives by oxidative phosphorylation. Therefore, *H. halobium* is an excellent experimental organism that is being extensively used for studying the structure and function of membranes, the bioenergetics of the cell, and the possible utilization of solar energy [Bolton and Hall, 1979]. For a collection of papers on the application of physical chemical methods as well as model systems of *H. halobium*, the reader is referred to the cited references.[91,92]

Membrane composition and supramolecular organization

The purple color of *H. halobium* is due to a rhodopsin-like complex termed bacteriorhodopsin (BR) in the plasma membrane which occurs when the cells are grown in the absence of a suitable source of nutrients or at low oxygen tension. Unlike its counterpart visual rhodopsin, BR is extremely stable up to 45^{o} C and pH from 0-11. The purple membrane, of which BR is the main constituent, is made of patches covering as much as 50% of the surface of *H. halobium* cells. On the basis of electron microscopy and X-ray diffraction studies, the purple membrane of about 5 nm thick may be considered to be two-dimentional crystals comprising an array of BR which is arranged in a lipid bilayer in a highly ordered hexagonal lattice in patches with vectorial properties. Chemically,

the purple membrane consists of 25% lipids (mostly phospho-, glyco- and sulfolipids) and 75% protein which has a MW of 26,000. This protein contains two chromophores, 13-**cis** and **all-trans** retinals (vitamin A aldehyde), linked as a Schiff base to a lysine residue of the opsin. This pigmented protein of 248 amino acid residues, spanning the lipid bilayer of the plasma membrane, is arranged in an d-helical configuration. This view is supported by circular dichroism studies. The amino acid sequence of various regions of BR has been determined, suggesting the retinal lysine is situated towards the inside surface of the purple membrane. The structure of BR consists of seven rods, each about 3.5 nm in length organized in parallel arrays. The native functioning unit is a trimer. The polypeptide chains of 4.5 nm in thickness span the lipid bilayer. Resultsfrom Ovchinnikov's laboratory suggest a highly hydrophobic nature for the peptide chain. Its amino acid sequence and structure to 0.7 nm aree known.[93]

Mechanism of light transduction and the photocycle

Observations made of whole cell cultures of *H. halobium* have suggested some of the properties of the purple membrane. The halophiles are bacteria which can proliferate in the presence of a high concentration of NaCl which ordinarily is a microbial inhibitor. In the dark, the cells at pH 6.5 display a pH gradient of about 0.5 units with the inside of the cell alkaline, and in the light about 0.65 units. The pH gradient appears to be dependent on the external pH. Also of interest is the finding of transmembrane Na^+ and K^+ concentrations. The interior concentration of K^+ was found to be 3 to 5 M and that for Na^+, 0.5 to 1.2 M. Further, K^+ can be retained for days, even if the cells have been starved or poisoned. This observation strongly suggests the intracellular binding of K^+. Another observation of whole cells of *H. halobium* is that exposure to light diminishes O_2 consumption of starved cells. Starved cells ordinarily require less O_2 to begin with, but light further reduces this need. Cells which are not starved and are at the late-log phase of culture are found to consume less O_2 when illuminated. The oxygen tension has a negative effect on the biosynthesis of purple membrane. Cells grown while being vigorously aerated form fewer purple membranes and it can be shown that as the O_2 tension is reduced, an increase in purple membrane production

is seen. It has been found that dark-adapted respiring cells and illuminated anaerobic cells will acidify the media. One can abolish acidification by illuminated anaerobic cells by the addition of "uncouplers" (compounds which interfere with oxidative phosphorylation by disengaging the coupled reaction of electron transport and ATP synthesis). In the case of respiring cells, both uncouplers and electron transfer inhibitors are effective in halting acidification. It appears that light enables the purple membrane to generate and maintain a pH gradient across itself and thereby acidify the medium.

On the basis of the results described above, the chemiosmotic hypothesis of Mitchell has been invoked to account for all the observations. It is generally accepted that bacteriorhodopsin in the membrane acts as a light driven proton pump which generates a proton gradient and potential gradient across the membrane. This electrochemical gradient is used to synthesize ATP in accordance with the Mitchell's hypothesis. This light driven pump translocates the protons from the cytoplasmic side of the cell to the external medium. This suggestion is based on the light induced pH changes resulting in a net acidification of the medium, oxygen consumption measurements, and light drive ATP synthesis. The photophysicochemical reactions (or the photocycle) of BR accompanying proton translocation were first proposed by Oesterhelt and Stoeckenius; they and others have reported an absorbance change from 560 nm to 416 nm upon light absorption. The absorbance is cyclic and coincides with the release of a proton into the medium and the uptake of a proton from the cytoplasm. BR undergoes a cyclic light-induced reaction with a half-time of a few msec, generating an electrochemical potential gradient of about 200 mV. Under illumination at physiological conditions, the cycle repeats 200 times per second. The cycle can be observed over a broad pH range from 3 to 12. Recent data for the photocycle of purple membrane fragments indicate that there are five intermediates - K, L, M, N, and O. These are shown in Fig.9.12. The connection between the intermediates is probably more complex than indicated in Fig. 9.12. It is interpreted that during the reaction cycle protons are released on the outer surface of the purple membrane and taken up on the inner surface. This release and uptake of protons which accompany the photocycle of BR results in a net acidification of the medium as found experimentally.

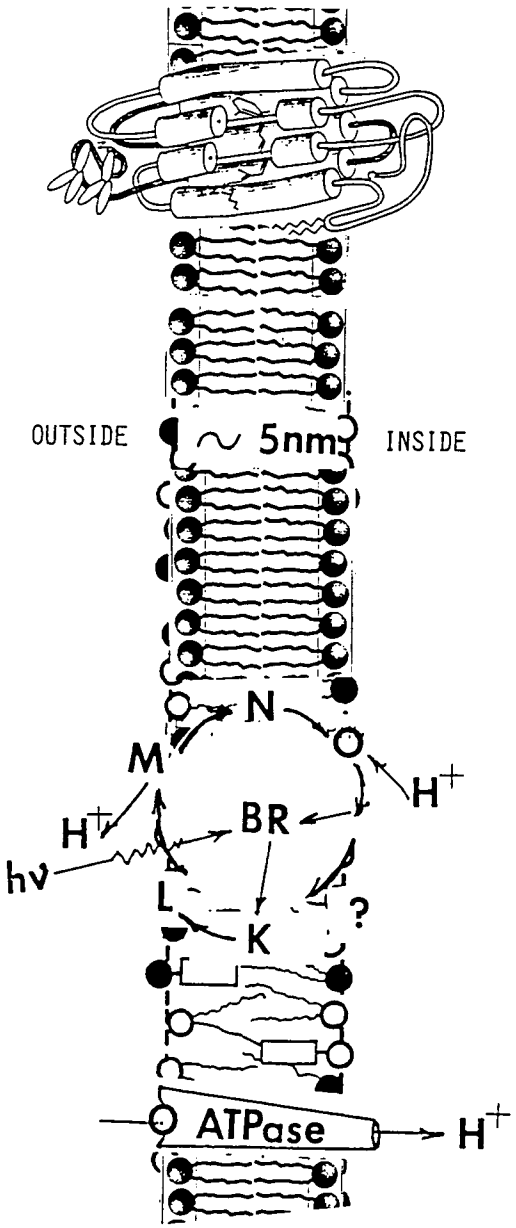

Fig. 9.12. A highly schematic diagram of BR-proton pump in terms of the photocycle. Light reactions start by absorption of photons by BR. Protons are translocated from one side of the membrane to the other side. A membrane potential of about 200 mV is developed.[92]

During the photocycle, it is assumed that the observed 13-**trans** to 13-**cis** photoinitiated isomerization of the retinyl protonated Schiff base in BR is the essential first step in the molecular mechanism of proton translocation.[93] It should be pointed out that the diagram shown in Fig. 9.15 depicts a "helix-bundle" of bacteriorhodopsin, a light-driven proton-pump from the purple membrane of *H. halobium.* The 7 helices are simply drawn to distinguish them in a two-dimensional view. The region of a protein which traverses the lipid bilayer usually consists of an alpha-helix or several alpha-helices each of about 20 residues. In the present case, the helices are connected by loops which are exposed to the aqueous environment on either side of the membrane and which therefore consist of residues with polar side chains. These connecting loops are generally quite short and may consist of hairpins When several helices are bundled, then only the side chains on the outside of the bundle need be hydrophobic. If the central channel between the helices is lined with polar residues, the resulting structure might act as a pore in the membrane through which ions may pass. Thus, one would expect a relatively long, uninterrupted sequence of hydrophobic residues to represent a membrane-spanning channel. There is a large super-family of receptors that adopt the same tertiary structure; as illustrated in Fig. 9.12. It should be noted here that membrane proteins are difficult to crystallize. Because they have significant hydrophilic and hydrophobic surfaces, they are not soluble in aqueous buffer solutions yet they denature in organic solvents. Methods such as Infra-red Spectroscopy, Raman Spectroscopy and Circular Dichroism are used to deduce secondary structure.

In connection with fast photoevents across the purple membrane of *H. halobium*, Mathies et al.[98] reported recently the use of femto second (10^{-15} sec) optical measurement techniques to observe the excited-state **trans** $\Leftrightarrow$ **cis** photoisomerization in BR. Their data reveal the details of the time course of the double-bond isomerization in BR. Further, it is claimed that, as the chromophore distorts on the photoactive surface, excited-state absorption to torsionally flatter surfaces will shift to the blue. The work of Mathies et al. supports the idea that the optical excitation is largely complete by the 28 femtosecond spectrum.[132]

BLM and Liposome Experiments with *H. Halobium*

Several groups have attempted to examine phenomena of the BR photocycle and proton translocation as well as other ion transport experimentally and theoretically using model systems.[92-97] The objective of these approaches is to understand the light transduction and bioenergetics in *H. halobium* at the membrane/cellular level. In this connection, two types of experimental bilayer lipid membranes have been employed. As already discussed, the first consists of lipid microvesicles (liposomes). In this system, a bilayer lipid membrane of sperical configuration encloses a volume of aqueous solution. Since the liposomes are very stable and can be easily made in quantity, they are ideally suited for studies of permeability, ATP synthesis, chemical reactions, and oxygen evolution. The second system is comprised of a planar BLM separating two aqueous solutions where photoeffects can be readily measured electrically, whereas it is not possible to do so in either intact cells or BR-containing liposomes.[93]

Reconstitution experiments started almost immediately after the discovery of BR since it is the widely accepted approach if one wishes to understand any complicated biomembrane system in physicochemical terms. The details of this research up to 1988 have been reviewed.[70]

The story of *H. halobium* is not yet complete. Perhaps the BLM technique and its modification along with other methodologies developed recently[93] may provide further details on the molecular mechanism of light transduction by the purple membrane and the steps involved in translocating protons in BR. Hopefully, the whole puzzle of the energy transduction process of *H. halobium* may be put together in the not too distant future.

9.6 Miscellaneous Studies of Photoeffects Involving BLMs, Liposomes, and Related Systems

Dye-sensitized BLMs

Photoelectric effects from dye-modified bilayer lipid membranes (BLMs) have been widely studied for many years for the purpose of elucidating details of light-induced processes in photosynthesis and vision (*see* Sections 9.3 and 9.4). Charge separation, electron transfer across the membrane and subsequent redox reactions at the membrane/aqueous solution interfaces, induced by light, play a key role in these processes as already discussed. Dyes have often been added as sensitizers to both inorganic and organic semiconductors, for the purpose of understanding the mechanism of photoeffects, and also for the practical application of photosensitive materials as in, for example, photodynamic therapy. Two types of sensitization are known: **intrinsic** and **spectral**. In intrinsic sensitization, the added sensitizer does not alter the basic spectral response of the system, but merely enhances it. In contrast, in spectral sensitization, the spectrum of the system is modified by the sensitizer in the region of the spectrum corresponding to the optical absorption of the added sensitizer.[70] These phenomena, and other aspects of photosensitization as observed in organic solids, are also possible in the BLM systems. Experimentally, photoconductance and photovoltage resulting from the above mentioned phenomena can be easily studied in the BLM system using electrical methods such as cyclic voltammetry and flash excitation. For recording photopotential transients resulting from pulsed light with 10 nsec resolution, Huebner and associates have described such an apparatus in detail and used it to examine a large number of cyanine dyes.[104] The use of dyes, particularly those potential-sensitive ones such as cyanine and merocyanine as optical probes, are important to the understanding of molecular mechanisms at the membrane level. Dragsten and Webb[102] reported that BLM-containing Merocyanine 540 responds to a potential step in two distinct time constants; one is less than 6 usec and the other is 0.1 sec. Both response amplitudes are proportional to applied voltages. The relationship between optical properties and the applied field, known as electrochromism, has been observed by Loew et al.[103] This effect will be reviewed shortly.

A number of reasons can be given as to why one should be interested in studying the dyes and membrane interactions. It is well known that organic dyes are used as biological stains and are often used in biology, physiology, pharmacology and medicine, as well as in industry (their use in the food industry is of special interest). In general, it is known that coloring and staining processes involve adsorption, solubility, penetration, and chemical reaction, but how dyes affect lipid membranes still seems to be a problem. However, as a result of many diverse kinds of experiments, valuable structural information concerning biomembrane surfaces is beginning to emerge. In experiments with BLMs and liposomes, photobleaching and NMR techniques have yielded diffusion coefficients for membrane constituents (lipid, peptides and proteins). Another important application of dyes has been their use as probes of membrane potential.[104] Loew[105] has written an excellent review on the design and characterization of such dyes and their interaction with bilayer lipid membranes. Earlier, Loew et al. [103] have provided evidence for a direct response of an electronic probe (*p*-aminostyrylpyridium-ASP) to the electric field across BLMs. Experiments carried out with liposomes and with the optical BLM apparatus described are consistent with the notion that this dye (ASP) indeed functions electrochromically. These experiments indicate that the transition moment direction is parallel to the BLM fatty acid chains. More recently, the properties of a series of new potentiometric membrane-active dyes (all related to ASP) have been explored.[106] In hemispherical BLMs, the spectral responses to a membrane potential are quite similar for all probes tested. The authors of this publiction conclude that, in additional to potential sensitivity, many of these dyes have properties that make them useful as reporters of other membrane properties.[105,107]

Huebner and co-workers have reported in a series of papers photoeffects in dye and aromatic amino acid sensitized BLMs.[101,104] They reported that voltage transients are generated across BLMs by light flashes, as a result of photophysical processes in sorbed dyes, which displace electrical charges. Experimental results are presented for an azo dye, three carbocyanine dyes, an amino-pyridinium dye, and a zanthene dye (erthrosin, Red Dye No. 3 used in food coloring). Photoeffect quantum efficiency values, obtained by calculating optical absorption cross sections from the dyes' molar extinction coefficients in aqueous

solutions are given. Huebner and co-workers[104] present a hypothesis which suggests that: (i) the fraction of sorbed dye, which displaces charge from one flash can be determined, providing the second flash occurs before dye excited by the first flash returns to its equilibrium condition, and (ii) the photoeffect quantum efficiency can be determined from the fraction of dye displacing charge, the light intensity and the dye's optical absorption cross section. However, the dye's optical absorption cross section values are uncertain, due to solvent and orientational effects in BLMs.

Owing to the importance of dyes, researchers have investigated systematically dye-sensitized BLMs, using the cyclic voltammetry technique. Redox reactions at the BLM-solution interfaces are most conveniently scrutinized by this technique. Fifty-seven dyes of different chemical groups have thus been studied. From the obtained voltammograms, 5 types of characteristic curves have been established.[107,109,111] Electronic processes in, as well as across, the BLM are considered. In the presence of light of known wavelengths, a number of dye-sensitized BLM have also been investigated by photoelectrospectrometry.[110] Ultraviolet light flashes can also induce voltage transients across BLMs, when aromatic amino acids are absorbed to one side of the membrane. These photoeffects varied with the chromophore structure, the aqueous solution salt concentration, pH, and oxygen partial pressure. These photoeffects are attributed to the migration of electrically charged photochemical intermediates in the BLM, and provide a new method for studying the effect of UV light on membranes.

When a pigmented BLM and dye interacted,[109] a photovoltage was observed only when an electrochemical potential difference across the membrane existed and a photosensitizing agent(dye) was present in the system. The combination of Mg-TPP in the membrane phase, dyes such as malachite green and crystal violet). and redox agents (EDTA and MV^{2+}) in the aqueous phase yielded the largest photovoltage but no one of these substances, when present alone in the system, caused the photovoltage to develop. It may be inferred from the results that certain dyes can act either as photosensitizers or as redox agents or both. Interestingly, it was found that only Mg-TPP in the BLM, interposed between properly chosen solutions, generates the largest photoeffect under illumination.

Table 9.3 A classification of dyes in terms of their electron donating and accepting affinity[70,109]

p-type	*n*-type
Merocyanine	Crystal Violet
Phthalocyanine	Victoria Blue B (VBB)
Methyl Orange	Malachite Green
Methylene Blue (MB)	Coumarin
Thionine	Methyl Red
Anthraquinone Sulfonate (AQS)	Pinacyanol
Naphthraquinone Sulfonate (NQS)	Methyl Violet
Aromatic Amines	N,N,N'N' tetramethyl-*p*-phenylene diamine
Eosin	Rhodamine B

Conclusions

It should be stated once more that the essential process of green plant photosynthesis are the coupled redox reactions of carbon dioxide reduction and water oxidation; the end products of which are carbohydrates (reduced CO_2) and oxygen (oxidized H_2O). An overall view in terms of the life cycle is depicted in Fig. 9.13. The photons of solar energy absorbed by pigments embedded in the lipid bilayer of the thylakoid membrane cause the water molecule to decompose into its constituents, namely, electrons, protons and oxygen. Photoinduced electron transfer processes are a crucial aspect of Nature's photosynthesis, which are achieved in an ultrathin pigmented bilayer lipid membrane separating two aqueous solutions. Most of our understanding of the above-mentioned processes has resulted from interdisciplinary endeavors. One such endeavor is the use of a bilayer lipid membrane (BLM) less than 7 nm thick as a model for the thylakoid membrane of the chloroplast. Several publications indicate that the pigmented BLM system is also of interest in the field of solar energy conversion.[70] Further, in recent years there has been a great deal of concerted effort towards mimicking the natural process, which has come to be known as ***artificial photosynthesis*** with the chief aim of generating electricity and/or hydrogen via water

photolysis.The basic arrangement consists of a photoactive membrane separating two aqueous solutions containing redox compounds. Light-induced charge separation in the form of electrons and holes causes a reduction on one side of the membrane and an oxidation on the other side. In this scheme a transmembrane movement of electronic charges is accepted. Pertinent and closely related to the membrane based systems are interfaces, organized multilayers, micelles, and lipid vesicles.[7] Thus, the subject of artificial photosynthesis will be discussed in terms of the photoelectrochemistry of pigmented bilayer lipid membranes and their derived practical systems such as the semiconductor septum-based electrochemical photocell. We will take up the subject matter again on 'Towards Practical Applications' in Chapter 10.

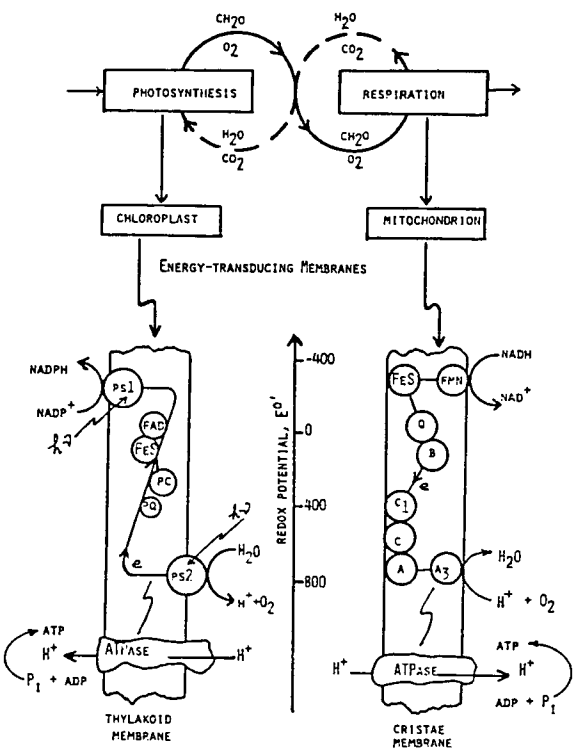

Fig. 9.13 The life cycle in terms of energy-transducing membranes the chloroplast and mitochondrion.

General References

Tien, H.T., (ed.), Photoelectric BLMs, Photochem. Photobiol., 24, p. 95-207, 1976.

Olson, J.M. and Hind, G., (eds.), Chlorophyll-proteins, reaction centers and photosynthetic membranes, Brookhaven Symposia Biology, 28, p.103, 1976.

Oosawa, F. and Imai, N., (eds.), Dynamic Aspects of Biopolyelectrolytes and Biomembranes, Kodansha-Elsevier, Tokyo and Amsterdam, 1982, p.445.

Knowles, A. and Dartnall, H.J.A., in The Eye, Darson, H., (ed.), 2nd ed., Academic Press, New York, 1977, p.425-497.

Bolton, J.R., (ed.), Solar Energy and Fuels, Academic Press, New York, 1977, p.167-225.

Metzner, H., (ed.), Photosynthetic Oxygen Evolution, Academic Press, New York, 1978, p. 411.

Gregory, R.P.F., Biochemistry of Photosynthesis, Wiley, New York, 1978.

Barltrop, J.A. and Coyle, J.D., (eds.), Principles of Photochemistry, Wiley, New York, 1978.

Barber, J., (ed.), Photosynthesis in Relation to Model Systems, Topics in Photosynthesis, 3 Vols.,Elsevier, Amsterdam and New York, 1979.

Bolton, J.R. and Hall, D.O., Ann. Rev. Energy, 4, p.353, 1979.

Akoyunoglou, G., (ed.), Fifth International Congress on Photosynthesis, Balaban Int'l Science Services, Rehovot, Israel, 1981, p.254..

Stieve, H., (ed.), Proc. of the Molecular Mechanism of Photoreception: Dahlem Konferenzen, Springer-Verlag, Berlin, 1986.

Ebrey, T. G., Frauenfelder, H., Honig, B., and Nakanishi, K., Biophysical Studies of Retinal Proteins, U. of Illinois Press, Urbana, 1987.

Dryhurst, G. and Niki, K., (eds.), Redox Chemistry and Interfacial Behavior of Biological Molecules, Plenum, New York, 1988.

Davison, S.G. (ed.), Progress in Surface Science, **30,** Pergamon Press, NY, 1989. P.1-200

Kavarnos, George J., Fundamentals of Photoinduced Electron Transfer, VCH Publishers, NY 1993

Ginley, D., T. Catalano, H. W. Schock, C. Eberspacher, T. M. Peterson, and T. Wada (eds.) Thin Films for Photovoltaic and Related Device Applications, Materials Research Society, Vol. 426, Warrendale, PA. 1996

Specific References

1. Tien, H.T., Nature, 219, p.272, 1968; J. Phys. Chem., 72, p.4512, 1968; and Verma, S.P., Nature, 227, p.1232, 1970.
2. Huebner, J.S., Photochem. Photobiol., 30, 233, 1979; 39, 191, 1984; J. Chem. Ed., 65, 102, 1988.
3. Bhardwaj, R., Pan, R.L., and Gross, E.L., Photochem. Photobiol., 34, p.215, 1981.
4. Dam, R.J., Kongslie, K.F., and Griffith, O.H., Photochem. Photobiol., 22, p.265, 975.
5. Villar, J.-G., J. Bioenerg. Biomemb., 8, p.199, 1976.;Vaillier, J. and Vaillier, D., Clin. Exp. Immunol., 30, p.283, 1977.
6. Miyasaka, T., Watanabe, T., Fujishima, A., and Honda, K., Nature, 277, 638, 1979; Surf. Sci., 101, 541, 1980; J. Am. Chem. Soc., 100, 6657, 1978.
7. Boguslavsky, L.I., Volkov, A.G., and Kandelaki, M.D., Bioelectrochem. Bioenerg., 4, 68, 1977Schreiber, B., Bioelectrochem. Bioenerg., 9, p.265, 1982.
8. Seibert, M., Janzen, A.F., and Kendall-Tobias, M., Photochem. Photobiol., 35, p.193, 1982.
9. Trissl, H.-W. and Graber, P., Biochim. Biophys. Acta, 595, p.82, p.96, 1980.
10. Frackowiak, D., Erokhina, L.G., Jadzyn, Cz., Shubin, L.M., and Shkuropatov, A.Y., Photosyn., 15, p.36, 1981.
11. Szabad, J., Lehoczki, E., Szalay, L., and Csatorday, K., Biochim. Biophys. Acta, 376, p.268, 1975.
12. Pileni, M.P., Lerebours, B., and Brochette, P., J. Photochem., 28, p.273, 1985.
13. Sasaki, H., Anzai, J.-I., and Ueno, A., J. Jpn. Chem. Soc., 6, 1199, 1985.
14. Schreiber, B. and Dupeyrat, M., Bioelectroch. Bioenerg., 6, 427, 1979.
15. Srivastava, R.C., Tandon, A., Kurup, S., Bhise, S.B., and Sharma, R.K., J. Electroanal. Chem., 187, p.325, 1985.
16. Sugimoto, T., Miyazaki, J., Kokubo, T., Tanimoto, S., Okano, M., and Matsumoto, M., J. Chem.Soc. Chem. Commun., p.186, 1982.
17. Yamauchi, A., Itoh, M., Kaibara, K., and Kimizuka, H., J. Chem. Soc. Jpn., Chem. Ind. Chem., 7, p.887, 1983.

18. Janzen, A.F., Bolton, J.R., and Stillman, M.J., J. Amer. Chem. Soc., 101, p.6337, 1979.
19. Govindjee and Govindjee, R., J. Sci. Indust. Res, India), 36, 662, 1977.
20. Fleming, G.R., Martin, J.L., and Breton, J., Nature, 333, p.190, 1988
21. Porter, G. and Archer, M.D., Interdisc. Sci. Rev., 1, p.119, 1976.
22. Joshi, N.B., Lopez, J.R., Tien, H.T., Wang, C.B., and Liu, Q.Y., J. Photochem., 20, p.139, 1982; Photobiophys. Photobioch. 4, 177, 1982.
23. Connolly, J.S. and Bolton, J.R., in Photoinduced Electron Transfer, Fox, M.A. and Chanon, M., (eds.), Elsevier, Amsterdam, 1988.
24. Acuna, A.U. and Gonzalez-Rodriques, J., Ann. Quim., 75, 630, 1979.
25. Ho, T.-F., McIntosh, A.R., and Bolton, J.R., Nature, 286, p.254, 1980.
26. Dalton, J. and Milgrom, L.R., JCS Chem. Commun., p.609, 1984.
27. Nishitani, S., Jurata, N., Misumi, Y., Migita, S., Okada, N., Nataga, T., Tetrahedron Lett., 22, 2099, 1981; JACS, 105, 7771, 1983.
28. Moore, A.L., Dirks, G., Gust, D., and Moore, T.A., Photochem. Photobiol., 32, 691, 1980.
29. Oettmeier, W., Norris, J., and Katz, J., Z. Naturforsch., 31, 163, 1976.
30. Ford, W.E., Otvos, J.W., and Calvin, M., Nature, 274, p.507, 1978; Proc. Natl. Acad. Sci. US, 76, p.3590, 1979.
31. Kadoshnikov, S.I. and Stolovitsky, Yu.M., Bioelectrochem. Bioenerg., 9, 79, 1982.
32. Tomkiewicz, M. and Corker, G.A., Photoch. Photobiol., 22, 249, 1975.
33. Antolini, R., Gliozzi, A., and Gorio, A., (eds.), Transport in Membranes: Model Systems and Reconstitution, Raven Press, New York, 1982, p.57.
34. Stillwell, W. and Tien, H.T., Photobiophys. Photobioch., 2, 159, 1981.
35. Sugimato, T., Miyazaki, J., Kokubo, T., Tanimoto, S., Okano, M., and Matsumoto, M., Tetrahedron Letters, 22, p.1119, 1981.
36. Krasnovsky Jr., A.A. and Semenova, A.N., Photobiochem. and Photobiophys., 3, 11, 1981; and Nikandrov, V.V., Photobiochem. and Photobiophys., 4, 227, 1982.
37. Mangel, M., Biochim. Biophys. Acta, 419, 404, 1976; 430, 459, 1976.
38. Csorba, I., Szabad, J., Erdei, L., Fajszi, Cs., Photochem. Photobiol., 21, 377, 1975.
39. Witt, H.T. and DiFiore, D., FEBS Letters, 128, p.149, 1981.
40. Nagamura, T., Takuma, K., Tsutsui, Y., and Matsuo, T., Chemistry Letters, 503, 1980; ____., Takayanagi, T., and Matsuo, T., Int. J. Quant. Chem., 18, 509, 1980.

41. Sudo, Y. and Toda, F., J. Chem. Soc. Chem. Commun., p.1044, 1979; Sudo, Y., Kawashima, T., and Toda, F., Chem. Lett., p.355, 1980.
42. Usui, Y. and Gotou, Photochem. Photobiol., 29, p.165, 1970.
43. Takayanagi, T., Nagamura, T., and Matsuo, T., Ber. Bunsenges. Physik. Chem., 84, p.1125, 1980.
44. Neumann, S., Korenstein, R., Barenholz, Y., and Ottolenghi, M., Israel J. Chem., 22, p.125, 1982
45. Hurley, J.K., Castelli, F., and Tollin, G., Photochem. Photobiol., 32, p.79, 1980.
46. Matsuo, T., J. Photochem., 29, p.41, 1985;
47. Aso, Y., Kano, K.& Matsuo, T., Biochim.Biophys.A, 599, 403, 1980.
48. Nomura, T., Escabi-Perez, J., Sunamoto, J., and Fendler, J., J. Am. Chem. Soc., 102, p.1484, 1980.
49. Schnecke, W., Gratzel, M., and Henglein, A., Ber. Bunsenges. Physik. Chem., 81, p.821, 1979.
50. Luisetti, J., Mohwald, J., and Galla, H.J., Z. Naturforsch., 34, p.406, 1979; Biochim. Biophys. Acta, 552, p.519, 1979.
51. Dodelet, J.P., Le Brech, J., and Leblanc, R.M., Photochem. Photobiol., p.1135, 1979; ___, J.P., Le Brech, J., and ___, R.M., Photochem. Photobiol., 31, p.145, 1980; ___, R.M., DuPre Werson, B., and Dijkmans, H., Photosynthetica, 15, 109, 1981.
52. Fragata, M., J. of Coll. Int. Sci., 66, p.470, 1978.
53. Harbich, W. and Helfrisch, W., Z. Naturforsch., 34, p.1063, 1979.
54. Stillwell, W. and Doram, K., Biochem. Biophys. Res. Commun., 93, p.326, 1980
55. Schmidt, W., J. Memb. Biol., 47, p.1, 1979.
56. Hotchandani, S., Leblanc, R.M., Clarke, R.M., and Fragata, M., Photochem. Photobiol.,36, 235, 1982.
57. Dratz, E.A. & Hargrave, P.A., Trends Biochem. Sci., 8, 128, 1983.
58. Huebner, J.S. and Tien, H.T., Biochim. Biophys. Acta, 256, p.300, 1972; J. Memb.Biol., 11, p.57, 1973.
59. Toyoshima, Y., Morina, M., Motoki, H., and Sudigara, M., Nature, 265, 187, 1977.
60. Stillwell, W. and Tien, H.T., Biochem. Biophys. Res. Commun., 81, p.212, 1978.
61. Ford, W.E. and Tollin, G., Photochem. Photobiol., 38, 441, 1983; 35, 809, 1982
62. Brann, M.R., Sci., 241, p.845, 1988.

63. Yoshikami, S. and Hagins, W.A., Biophys. J., 10a, 1970; Hagins, W.A., Penn, R.D., and Yoshikami, S., Biophys. J., 10, p.380, 1970.
64. Pugh Jr., E.N. and Cross, W.H., Vision Res., 26, p.1613, 1986.
65. Koch, K.-W. and Kaupp, V.B., J. Biol. Chem., 260, p.6788, 1986; Koch, K.-W. and Stryer, L., Nature, 334, p.64, 1988.
66. Nakatani, K. and Yau, K.-W., Nature, 334, p.69, 1988.
67. Mathews, H.R., Murphy, R.L., Fain, G.L., and Lamb, T.D., Nature, 334,67, 1988.
68. Fesenko, E.E., Kolesnikov, S.S., and Lynbarsky, A.L., Nature, 313, p.310, 1985.
69. Korenbrot, J.I., Ann. Rev. Physiol., 39, p.19, 1977.
70. Tien, H.T., Progress in Surface Science, 30(1/2), p.1-217, 1989.
71. Falk, G. and Fatt, P., J. Physiol., 183, p.211, 1966.
72. Brown, K.T. and Murakami, M., Nature, 201, p.626, 1964.
73. Cone, R.A., Nature (London), 204, p.726, 1964.
74. Pak, W.L., Cold Spring Harbor Sym. Quant. Biol., 30, p.493, 1965.
75. Ruppel, H. and Hagins, W.A., in Retinal Rods Biochem. and Phys. Visual Pigments, Langer, H., (ed.), Springer, Berlin, 1973, 257-261.
76. Govindjee, R., Dancshazy, Z., Ebrey, T.G., Longstaff, C., and Rando, R.R., Photochem. Photobiol., 48, p.493, 1988.
77. Toyoda, J., Nosaki, H., and Tomita, T., Vision Res., 9, p.453, 1969; Quart. Rev. Biophys. Bioeng., 3, p.197, 1970.
78. Liebman, P.A. & Pugh, E.N., Curr. Top. Memb. Transp.15, 157, 1981.
79. Nicol, G.D. and Miller, W.H., Nature, 280, p.64, 1979.
80. Stern, J.H., Knutsson, H., & MacLeish, P.R., Science, 236,1674, 1987.
81. Burton, R.M., (ed.), J. Am. Oil Chemists' Soc., 45, p.201, p.246, 1968.
82. Takagi, M., Azuma, K., and Kishimoto, U., Ann. Rpt. Biol. Works Fac. Sci., Osaka Univ., 13, p.107, 1965; see also Ref. 9, p. 477.
83. Tien, H.T. and Kobamoto, N., Nature, 224, p.690, 1969; *see* also Nature, 223,.885, 1969.
84. Kobamoto, N. and Tien, H.T., Biochim. Biophys. Acta, 241, p.129, 1971; 266, p.56, 1972.
85. Schadt, M., Biochim. Biophys. Acta, 323, p.351, 1973.
86. Tien, H.T., Separation Sci. Tech., 15, p.1035, 1980.
87. Regen, S.L., Czech, B., and Singh, A., JACS., 102, p.6638, 1980.
88. Sudholter, E.J.R., Engberts, Jan B.F.N., and Hoekstra, D., J. Am. Chem. Soc., 102, 2467, 1980.
89. B. Fuks and F. Homble, Biophys. J., 66 (1994) 1404

90. Karvaly, B. and Dancshazy, Z., FEBS Lett., 76, p.36, 1977
91. Larsen, H., Adv. Microb. Physiol., 1, p.67, 1967.
92. Schreckenbach, T., in Photosynthesis in Relation to Model Systems, Barber, J., (ed.), Elsevier/North-Holland, Biomedical Press, New York, 1979, Ch. 6.
93. Hong, F. T., Prog. Surf. Sci., 62, 1-237, 1999.
94. Blok, M.C., Hellingwerf, K.J., and Van Dam, K., FEBS Letters, 76, p.45, 1977.
95. Keszthelyi, L. and Ormos, P., FEBS Lett., 109, p.189, 1980.
96. El-Sayed, M.A., Karvaly, B., and Fukumoto, J.M., Proc. Natl. Acad. Sci., US, 78, p.7512, 1981.
97. Bienvenue, E., Seta, P., and Gavach, C., J. Electroanal. Chem., 140, p.217, 1982; 162, 275, 1985.
98. Mathies, R.A., Cruz, C.H.B., Pollard, W.T., Shank, C.V., Science, 240, 777, 1988.
99. Severina, I.I., Biochem. Biophys. Acta, 681, p.311, 1982.
100. Kouyama, T., Nasuda-Kouyama, A., Ikegami, A., Mathew, M.K., and Stoeckenius, W., Biochem., 27, p.5855, 1988.
101. Arrieta, R.T., Arrieta, I.C., Pachori, P.M., Popp, A.E., and Huebner, J.S., Photochem. Photobio., 42, p.1, 1985.
102. Dragsten, P.R. and Webb, W.W., Biochem., 17, p.5228, 1978.
103. Loew, M., Scully, S., Simpson, L., and Waggoner, A.S., Nature, 281, p.497, 1979.
104. Huebner, J.S., Arrieta, R.T., Arrieta, I.C., and Pachori, P.M., Photochem. Photobiol., 39, 191, 1984.
105. Loew, L.M., J. Biochem. Biophys. Meth., 6, p.243, 1982.
106. Fluhler, E., Burnham, V.G., and Loew, L.M., Biochem., 24, 5749, 1985.
107. Allen, M.J. and Underwood, P.N.R., (eds.), Charge and Field Effects in Biosystems, Abacus Press, UK, 1984, p.123-138;
108. Tien, H.T. and Kutnik, J., Photobioch.Photobiophys., 7, 319, 1984.
109. Kutnik, J. and Tien, H.T., Photochem. Photobiol., 46, 1009, 1987.
110. Lopez, J.R. and Tien, H.T., Biochim. Biophys. Acta, 597, p.433, 1980; . Joshi, N.B., Lopez, J.R., Tien, H.T., Wang, C.B., and Liu, Q.Y., J. Photochem., 20, 139, 1982; Photobiophys. Photobiochm., 4, 177, 1982. Higgins, J., Lopez, J.R., and Tien, H.T., J. Electroanal. Chem., 104, p.509, 1979; Lopez, J.R. and Tien, H.T., Photobiochem. Photobiophys., 7, 25, 1984; .

111. Kutnik, J. and Tien, H.T., Photochem. Photobiol., 46, p.413, 1987.
112. Zhao, X.K., Baral, S., Rolandi, R., and Fendler, J.H., J. Am. Chem. Soc., 110, 1012, 1988.
113. Salamon, Z. and Tien, H.T., Liquid Cryst., 3, p.169, 1988; Mol. Cryst. Liq. Cryst., 154, p.195, 1988; Photochem. Photobiol., 58, p.281, 1988.
114. Chapoy, L.L., Munck, D.K., and Biddle, D., Mol. Cryst. Liq. Cryst., 105, p.353, 1985.
115. Huang, C.C. and Lien, S.C., Phys. Rev., A31, p.2621, 1985.
116. Hautala, R.R., King, R.B., and Kutal, C., (eds.), Solar Energy: Chemical Conversion and Storage, Humana Press, Clifton, New Jersey, 1979, p.419.
117. Meier, H., Organic Semiconductors, Verlag Chemie, GmbH., Weimheim, 1974, p.440.
118. Murthy, A.S.N. and Reddy, K.S., Proc. Ind. Acad. Sci., (Chem. Ser.), 93, p.433, 1984.
119. Seta, P. and Bienvenue, E., Images Chimie, Suppl. CNRS, 65, 1985.
120. Hall, D.O., Biologist, 26, p.67, 1979.
121. Calvin, M., Photochem. Photobiol., 23, p.425, 1976.
122. Harima, Y. and Yamshita, K., J. Electrochem. Soc., 186, 313, 1985
123. Bockris, J.O'M. and Diniz, F.B., J. Electrochem. Soc., 135, p.1947, 1988.
124. Tripathy, A.K. & Tien, H.T., J. Appl. Electrochem., 17, 1098, 1987.
125. Jackowska, K. and Tien, H.T., Solar Cells, 23, p.233, 1988.
126. Bhardwaj, R. and Tien, H.T., Bull. Electrochem., 4, p.667, 1988; Bhardwaj, C. and Tien, H.T., Int. J. Energy Res., 1989.
127. Nosaka, Y., Photochem. Photobiol., 47, p.897, 1988.
128. Worthy, W., Chem. Eng. News, 66(40), p.32, 1988.
129. Tanaka M, Yonezawa Y, Sato T., Thin Solid Films, 285: 833, 1996
130. Semenova, A.N., Wikandrov, V.V., and Krasnovsky, A.A., J. Photochem. B., 1, 1987 p.85,
131. Chen, Q.-S. and Li, S.-J., Acta Physiol. Sinica, 12, p.9, 1986.
132. R.A. Mathies and T. Kakitani (eds.) Biophysical Chemistry of Retinal Proteins, Photochem.Photobiol., 56 (1992) 857-1187
133. Bialek-Bylka, G.E. and Wrobel, D., Acta. Biochim. Biophys. Hung., 21, 369, 1986.

134. Gruszecki, W.I., Studia Biophys., 116, p.11, 1986.
135. Fujishima, A. and Honda, K., Nature, 238, p.37, 1972.
136. Lee, Y.-I., Kwon, H.W., Shin, D.H., Yoon, M., Bull. Korean Chem. Soc., 7, 120, 1986
137. Tabushi, I. and Kugimiya, S.-I., Tetrahedron Lett., 25, p.3723, 1984.
140. Mettee, H.D., Ford, W.E., Sakai, T., and Calvin, M., Photochem. Photobiol., 39, p.679, 1984
141. Tancrede, P., Paquin, P., Houle, A., and LeBlanc, R.M., J. Biochem. Biophys. Meth., 7,299, 1983.
142. Robert, S., Tancrede, P., Houle, A., and Leblanc, R.M., Photochem. Photobiol., 41, p.101, 1985.
143. Rich, M. and Brody, S.S., FEBS Lett., 143, p.45, 1982.
144. Vacek, K., Valent, O., and Skuta, A., Gen. Physiol. Biophys., 2, p.135, 1982.
145. Liu, T.M. and Mauzerall, D., Biophys. J., 48, p.1, 1985
145. Woodle, M.C. and Mauzerall, D., Biophys. J., 50, p.431, 1986.
146. Hofmanova, A., Bienvenue, E., Seta, P., and Momenteau, M., Photochem. Photobiol., 44, 87, 1986
147. Dancshazy, Z., Ormos, P., Drachev, L.A., and Skulachev, V.P., Biophys. J., 24, p.423, 1978.
148. Losev, A. & Mauzerall, D., Photochem. Photobiol., 38, 355, 1983.
149. Putninskii, A.V., Biofizika, 22, p.725, 1977.
150. Sielewiesiuk, J., Stud. Biophys., 96, p.117, 1983.
151. Koyama, Y., Komori, M., and Shiomi, K., J. Coll. Int. Sci., 90, p.293, 1982.
152. Brasseur, R., Meutter, J.D., and Ruysschaert, J.-M., Biochim. Biophys. Acta, 764, p.295, 1984
153. Hattenbach, A., Gundel, J., Hermann, G., Haroske, D., and Muller, E., Biochem. Physiol. Pflanzen., , p.611, 1982.
154. Hanke, W. and Kaupp, U.B., Biophys. J., 46, p.587-595, 1984.
155. Barsky, E.L., Dancshazy, Z., Dracher, L.A., Ilina, M.D., Jasaitis, A.A., Konrashin, A.A., Samuilov, V.D., and Skulachev, V.P., Biol. Chem., 215, p.7066, 1976.
156. Rayfield, G.W., Biophys. J., 38, p.79, 1982
157. .Drachev, A.L., Evstigneeva, R.P., Kaulen, A.D., Lazarova, C.R., Laikhter, A.L., Mitsner, B.I., Skulachev, V.P., Khitrina, L.V., and Chekulayeva, L.N., Biofisica, 50, p.1142, 1984.

158. Fendler, K., Gartner, W., Oesterhelt, D., and Bamberg, E., Biochim. Biophys. Acta, 893, 60, 1987.
159. Mirsky, V.M., Sokolov, V.S., Dyukova, T.V., and Melnik, E.I., Bioelectrochem. Bioenerg., 12, 327, 1984.
160. Tien, H.T., Photochem. Photobiol., 16, p.271, 1972.
161. Marino, A.A., (ed.), Modern Bioelectricity, Marcel Dekker, Inc., NY, 1988, 181-242.
162. Gerischer, H., Topics Appl. Phys., 31, p.115, 1979.
163. Sherratt, A.F.C., (ed.), International Journal of Ambient Energy, Vol. 7, Ambient Press Ltd., Lancaster, UK, 1986, p.3-30.
164. Kalyanasundaram, K., Photochemistry in Microheterogeneous Systems, Academic Press, New York and Tokyo, 1987.
165. Strauss, G., Photochem. Photobiol., 24, 141, 1976; 17, 425, 1973.
166. Weller, H.G. & Tien, H.T., Biochim. Biophys. A., 325, 433, 1973.
167. Mauzerall, D., in Light-induced Charge Separation in Biology and Chemistry, Gerischer, H. and Katz, J.J., (eds.), Dahlem-Konferenzen, Verlag Chemie, Veinheim, 1979, p.241.
168 Trissl, H.-W. & Laueger, P., Biochim. Biophys. A. 282, 40, 1972.
169. Laane, C., Ford, W.E., Otvos, J.W., and Calvin, M., Proc. Nat. Acad. Sci., US, 78, p.2017, 1981.
170. Knoll, W., Bauman, J., Korpiun, P., and Theilen, U., Biochem. Biophys. Res. Commun., 96, p.968, 1980.
171. Dijkmans, H., Leblanc, R.M., Cogniaux, R., and Aghion, J., Photochem. Photobiol., 29, 367, 1979.
172. Walz, D., J. Memb. Biol., 31, p.31, 1977.
173. Lojewska, Z. and Loew, L.M., Biochim. Biophys. Acta, 899, p.104, 1987; Ehrenberg, B., Farkas, D.L., Fluhler, E.M., Lojewska, Z., and Loew, L.M., Biophys. J., 51, p.833, 1987.
174. Law, W.C., Rando, R.R., and Nakanishi, K., J. Am. Chem. Soc., 110, 5915, 1988.
177. Liu, Q.-Y. and Tien, H.T., Photobiochem. Photobiophys., 4, p.73, 1982; 10, p.1, 1985.
178. Bauer, P.J., Bamberg, E., and Fahr, A., Biophys. J., 46,111, 1984.
179. Tomioka, H., Kamo, N., Takahashi, T., and Kobatake, Y., Biochem. Biophys. Res. Commun., 123, p.989, 1984.
180. Srivastava, R.C. and Tandon, A., Biotech. Biol., 31, p.511, 1988.

Chapter 10

Applications

"Life is molecular electronics!"

First International Conference on MEBC, Budapest, 1987

"Which way did the prey go and what are its characteristics? You need a precise answer..." ...the !Kung tracking protocols of magic methods... the general principles (of which are) passed down from generatiion to generation. ---Carl Sagan on hunters-gatherers *in* The Demon-haunted World (1995) p. 313-315

"Of all endeavors in life, the noblest one is practical applications serving humankind". --- Peking University (Beida Summer School) Beijing, July 1998

General References (cited by name in brackets in the text)
Specific References (cited by number in superscript in the text)

10.1 Introduction

For more than three decades surface and colloid scientists have known that amphiphilic molecules such as stearic acid and phospholipids can self-assemble or self-organize into supramolecular structures of micelles, monolayers, or bilayer lipid membranes (lipid bilayers for short or planar BLMs and liposomes). It is therefore informative to mention in this introduction the crucial role played by the science of interfaces. In living cells, the tremendous interfacial areas that exist between the membrane and its surroundings not only provide ample loci for carrying out activities vital to the living system, but afford a clue for our understanding. Planar BLMs, along with spherical vesicles (liposomes), have been used for decades as models of biomembranes. They provide a natural environment for embedding a host of compounds such as ion carriers, peptides, proteins, pigments, receptors, membrane/tissue fragments, and even whole cells for studying membrane functions, and for elucidating the mechanisms of ligand-receptor interactions. One of the main tasks of biomembrane functions is molecular recognition that entails selectivity and specificity. Thus, understanding the principles that lie behind the structural-functional relationship of biomembranes should therefore help to provide the insights of much of the cell's biochemistry.

Physically, an interface is characterized most uniquely by its interfacial free energy which is a result of the orientation of the constituent molecules.[1] Those whose work has no direct connection with biomembanes, perhaps are not acquainted with experimental lipid bilayers, commonly referred to as planar bilayer lipid membranes (BLMs)[2] and spherical liposomes.[3,4] The work began with D. O Rudin and his associates in 1959-61. They first investigated lipid monolayers and multilayers of the Langmuir-Blodgett type, and then they toyed with soap bubbles and films. It was then evident that the structure of a soap film in air, in its final stage of thinning, has a structure which may be depicted as two lipid monolayers sandwiching an aqueous solution. That is a system which may be represented as *'air | soap film | air'*. Once they recognized this structure together with its molecular organization, Rudin and associates simply proceeded to make an under water 'lipid film', i.e. *aqueous solution | BLM*

| *aqueous solution*. Experimentally, it is far easier to form a BLM interposed between two aqueous solutions than spreading a Langmuir monolayer at the air-water interface. Further, the pioneering workers showed that a BLM formed from brain extracts was self-sealing to puncture with the following electrical characteristics: capacitance (C_m) $\simeq$ 1 $\mu F/cm^2$, resistance (R_m) greater than 10^8 ohm cm^2 and dielectric breakdown (V_b) about 300,000 V/cm, as well as very low interfacial free energy (~ 0.5 erg/cm^2).[5]

The background of the membrane biophysics work described has been focusing in understanding of the living organisms in physical and chemical terms. The discovery of planar BLMs and later developed supported BLMs of long-term stability have made it possible for the first time to study, directly, the electrical properties and transport phenomena across a lipid bilayer separating two interfaces. A BLM is viewed as a dynamic system that changes as a function of time in response to environmental stimuli. A functional biomembrane system, based on a self-assembled lipid bilayer and its associated proteins, carbohydrates and their complexes, is also in a liquid-crystalline and dynamic state. In molecular and electronic terms; a functional membrane system can facilitate both ion and electron transport, and is the site of cellular activities in that it functions as a 'device' for either energy conversion or signal transduction. Such a system, as we know intuitively, must act as some sort of a transducer capable of gathering information, processing it, and then delivering a response based on this received information. With the availability of supported BLMs, a host of compounds can now be embedded in the ultrathin lipid bilayer for detecting their counterparts present in the environment. Owing to its long-term stability, ease of formation, and low cost in its construction, a supported BLM offers an approach especially advantageous in the research and development of lipid bilayer-based sensors and devices.

Concerning the interfaces, '*aqueous solution* | *BLM* | *aqueous solution*' and '*aqueous solution* | *BLM* | *metal*' systems are of particular interest from the viewpoint of applications. The reasons being as follows. First, an interface can be thought of as a structure so thin that it has no

homogeneous interior. However, the kind of ultrathin films under discussion here are heterogeneous from their contacting phases. Second, an ultrathin film such as a planar lipid bilayer is a system whose interior is influenced by the proximity of its interfaces. In a sense we speak of two interconnecting membrane-solution interfaces or a *biface*[1] which is defined as any two coexisting membrane-liquid interfaces, through which material, charge, and/or energy transfer are possible. Thermodynamically speaking, it is an 'open' system, similar to that of a living cell. These and other interfacial properties of membranes of a bilayer thickness can be understood to a large extent in terms of the laws of interface chemistry and physics that govern them, in particular electrochemistry. A planar BLM is a 5 nm thick lipid bilayer structure separating two aqueous solutions, which along with the spherical liposomes has been extensively used as an experimental model of biomembranes. In fact, the current understanding of the structure and function of biological membranes can be traced to the investigations of experimental model membranes which have been developed as a direct consequence of the applications of classical principles of interfaces advanced by Langmuir, Adam, Harkins, McBain, Hartley, and others (*see* Chapters 2-4).

In the last decade, there have been a number of reports on self-assemblies of molecules as 'advanced materials' or 'smart sensors'.[6-8] Without question, the inspiration for this exciting development comes from the biological world, where, for example, the lipid bilayer of cell membranes is among the foremost self-assembling systems (Table 10.1). The cogent reason that self-assembled BLMs are of sustained scientific and practical interest is owing to the fact that most physiological activities involve some kind of lipid bilayer-based ligand-receptor contact interactions. For instance, by embedding a receptor or a host of specific entities in a supported BLM, it is possible to create a sensor that will interact with its selected environmental counterpart. Some of recent experiments of planar BLMs together with their closely related systems are delineated in this chapter.

It should be mentioned at the outset that self-assembled and supported BLMs, the main topic under discussion, differ from the much-

studied Langmuir-Blodgett (L-B) films and other thin film systems[6-8] in several major respects. First, a BLM is fluid and self-sealing to puncture. Second, the formation of a self-assembled BLM, either on metal or hydrogel, is exceedingly simple. Unlike L-B films for which elaborate setup such as film balance, clean room, etc, is usually required, whereas supported BLMs may be formed without any special tool (see the experimental section). Third, self-assembled BLMs are reconstituted lipid bilayers as existed in nature; thus they possess all the desired properties and are ideal for ligand-receptor interaction experiments. Supported planar BLMs, therefore, are one of the ideal systems for biosensor technology.

Table 10.1 Self-Assembling Amphiphlic Interface-active Systems[8]

Type	Interface
1. Soap Films	air | soap film | air
2. Monolayers (Langmuir type)	air | monolayer | water[1]
3. Multilayers (Langmuir-Blodgett type)	air | multilayer | solid substrate[2]
4. Planar Lipid Bilayers (BLMs)	water | BLM | water
5. Nucleopore Supported BLMs	water | BLMs[3] | water
6. Gold Supported Monolayers	air | thio monolayer[4] | Au
7. Metal Supported BLMs (s-BLMs)	water | BLM | metal[5]
8. Salt-bridge Supported BLMs (sb-BLMs)	water | BLM | hydrogel[6]

Notes: [1]aqueous solution [2]such as glass [3]tens of thousands of BLMs in a polycarbonate filter [4]such as Au [5]such as Pt, stainless steel [6]such as agar in 3M KCl.

10.2 BLMs in medicine[2,27]

a. Immunology

First of all, a brief synopsis of the topic under consideration is in order. The immune system is found in all higher organisms that possess the capability of self- and non-self recognition and respond to antigens (such as foreign proteins, bacteria, parasites, fungi, or viruses). Lymphocytes, the main constituent of the immune system, of which there are about 2000 x 10^9 of them in humans; they are dispersed throughout the body. There are two types of lymphocyte: B cells and T cells. T Cells are so called because they pass through the thymus before release, whereas B cells do not. B Cells are from stem cells (in the bone marrow) and give rise to what is termed the *humoral immune response*. Produced by B-Lymphocytes they are excreted into the serum. Unlike B Cells, T cells interact directly with the antigens. Of T Cells, there are three kinds that give rise to the *cell mediated response*. The three classes of T cells are: T Helper Cell (TH), T Killer (Cytotoxic) Cell (TC) and the T Suppressor/Self Recognition Cells (TS). The functions of each class of T cells are as follows: TH cells perform antigen recognition, causing the release of interlukins, which aid the B cells and cause them to release antibodies. T Killer cells contact the antigenic cells, and eliminate them - they are macrophages. TC cells recognize antigens on the cell's surface. Normally both B and T Cells are required to destroy antigens. TS Cells suppress production of anti-self antigens by the B Cells.

Further, there is a series of proteolytic enzymes, known as complement, in the serum. Antibodies are 'Y' shaped molecules (IgM, IgE, IgA, IgG, IgD) that recruit complement to help fight bacterial infection; this is called complement mediated cell killing. Complement binds to IgG and IgM, similar behavior is seen in both neutrophils and macrophages. Different antibodies have different effects, for examples, IgE binds to mast cells releasing histamine (causes inflammation) and IgE is involved in hayfever.

One lymphocyte makes one antibody. Before meeting an antigen the antibody is found on the cell membrane of the lymphocyte. Lymphocytes in this state are called virgin lymphocytes. The body contains many virgin lymphocytes, when an antigen binds to a particular cell, the bound cell divides. If there is no antibody in the blood, lymphocytes must be reproduced before the antigen reaction can occur.

A particular antibody responds only to one particular antigen, although an antigen usually has many epitopes. The antibody has (in most cases) two contacts with the antigen. Mixing blood and antigen causes a precipitate to form, this immunoprecipitate is normally most effective when there is a 2:1 ratio of antibody to antigen (as most antigens are bivalent). When the body first reacts to a new infection it must start from no stored antibody and combat the infection. The amount of antigen/antibody present can be tested with immunoprecipitation, using an agar plate. Below, an experimental method based on the BLM is described.

If a foreign substance (antigen) is injected into an experimental animal, such as a rat, the animal's immune system soon generates antibodies that combine to that antigen and eliminate it. Presently, this is the molecular basis of immunity: the recognition of what is "self" from "non-self". The destruction of foreign invading cells (non-self) depends upon recognition sites on their membranes. Indeed, one of the principal defenses of our immune system is to make holes (lysis) in membranes of "non-self" cells, thereby causing their demise. It is not completely understood how the immune system achieves molecular recognition that a particular membrane should be attacked, nor do we know the detailed mechanism of lysis. One thing is clear however, that target cells and their membranes should be closely scrutinized for possible clues. Therefore, several investigators, for their simplicity, have used experimental lipid bilayers (BLMs and liposomes), as target membranes modified with recognition sites for other components of the immune system. Before describing the application of experimental lipid bilayers (BLM and liposomes) for such purposes, a summary of membrane damage by channel-forming proteins as related to immunology is in order.

Membrane damage by complement[13]

Damage to the target bilayer membrane can be effected through two basic mechanisms: direct attack on membrane lipids (e.g. snake-venom phospholipases) and non-enzymatic physical perturbation of the lipid bilayer (e.g. insertion of channel-forming proteins). Concerning this type of membrane damage, the so-called "hydrophobic doughnut" hypothesis proposed by Mayer is of interest. The hydrophobic doughnut hypothesis or the mechanism of immune cytolysis by complement is based on the fluid lipid bilayer model of biomembranes and envisages an annular assembly made up of complement proteins C5b-9, which perturbs the lipid bilayer forming a stable transmembrane channel. It is assumed in this hypothesis that the terminal complement proteins undergo conformational changes when they react with one another and that these changes lead to exposure of hydrophobic peptides from their interior. The complement system comprises at least 12 proteins in blood serum not counting inhibitors and regulatory enzymes which, when activated, can result in cytolytic activity as well as a variety of other biological activities, including opsonization (enhancement of phagocytosis), chemotaxis, leukocyte mobilization, virus neutralization, involvement in blood clotting and fibrinolysis, generation of kinins (small polypeptides which increase vascular permeability), activation of B lymphocytes and macrophages, and the killing of target cells through membrane damage. Eleven of these complement proteins belong to the 'classical' complement system, and the letter C and a number designate these: C1, C2, C3, and so on up to C9. The other three proteins belong to the "alternative" pathway of the complement system. The letters B, D, and P designates these. In the classical pathway, Ag-Ab complexes activate C1q to C1q', which in turn activates C1r to C1r and C1s to C1s (activated enzymes are denoted by underline). C4 and C2 are cleaved by C1s and the C3-cleaving enzyme is converted to the C5-cleaving C4b, 2a, 3b enzyme by uptake of C3b. C3a and C5a are polypeptide fragments (called anaphylatoxins) that mediate release of histamine from mast cells and produce smooth muscle contraction. C5a is also responsible for the oriented migration of leukocytes toward a site of injury (chemotaxis). Cell-bound C3b conveys the property of immune adherence and renders cells more susceptible to phagocytosis (opsonization). Also, C3b activates B-

lymphocytes and macrophages. The formation of C5b-9, which is the cytolytic attack complex of complement is formed by a series of complexing steps not involving enzymatic cleavage. That is, the eventual formation of a transmembrane channel (or doughnut) by C5b-9 in the lipid bilayer. The evidence that supports the hydrophobic doughnut hypothesis includes the following:

The cytolysis by complement is a two-stage event. When complement it swells until the membrane is explosively ruptured and the cell attacks a cell contents spill out. The simplest explanation for this is that complement makes holes in the membrane that are large enough to permit salt and water and other small molecules to pass, but are too small to allow macromolecules to leave the cell.

The one-hit theory of complement lysis. This theory, developed from kinetic statistical and statistical studies, states that the production of a single lesion in the cell membrane is sufficient for complement lysis of a cell.

Electron microscopy. Using the negative staining technique electronmicro*graphs* show lesions in cell membranes as a light ring with a dark central portion. Those produced in red blood cells by guinea pig complement range between 8.5 and 9.5 nm internal diameter; those produced by human complement range between 10 and 11 nm.

The demonstration that complement releases phospholipid from membranes lends support to the transmembrane channel hypothesis because it indicates those hydrophobic peptides are exposed on the interaction of the terminal complement proteins. Further support for Mayer's "doughnut" hypothesis comes from the finding that the C5b-9 complex is an amphipathic molecule that possesses apolar, detergent-binding-surfaces. This evidence was obtained from charge-shift crossed-immunoelectrophoresis. "Neoantigenic" determinants were also found on the C5b-9 complex, which are absent on native C5-C9 molecules. This indicates that the assembly of C5-C9 into the terminal membrane C5b-9 complex is accompanied by conformational changes in the individual

components that lead to the exposure of apolar molecular regions in the complex.

Finally, mention should be made about an interesting study in which a glass microelectrode is pushed up against the cell membrane of a living cell to record individual complement channels. The current recorded by the pipette underwent discrete jumps indicating the opening and closing of channels. The channel currents were uniform in amplitude and suggested a C channel of approximately 0.8 nm in diameter. Control experiments with heat-inactivated C or cells which were not prior Ab-coated had no effect.

Antigen-antibody Complement Reactions on BLM.

The first study of immunologic reactions on an artificial membrane system was that of del Castello and associates.[2] They found that marked transient impedance changes could be observed when a soluble antigen was added to a BLM already sensitized with the appropriate antiserum. No impedance changes were observed if the antigen (Ag) and antibody (Ab) were mixed before they were added separately. Enzymes and their substates gave similar transient effects. This technique was even used in clinical trials to detect antibodies to insulin in patients having diabetes. The ability of BLM to substitute for natural membranes in immune cytolytic phenomena was soon demonstrated by a number of other workers and some information was derived from these studies regarding lytic mechanisms. Wobschall and McKeon reported transient step-wise and permanent changes in membrane resistance and membrane rupture when bovine whole serum and rabbit antiserum against bovine serum were added to opposite sides of the BLM. No conductance changes were observed if the antiserum and complement were heat-inactivated at 56 °C for 30 minutes, or if the complement was added to the side opposite the antibody. Also, no significant reaction occurred if proteins or sera other than bovine were added to either the side containing the antibody and complement or the opposite side of the membrane. However, the membrane stability was less if both the Ag and Ab were present on the same side of the BLM.

By far the most experiments of complement on BLMs were carried out by Mayer and his associates (D.W. Michaels, A.S. Abramowitz, and C.H. Hammer).[13] They report that activated C5b,6 combined with C7 and C8 complement components causes a oderate increase in the ion permeability of BLMs. The resistance was also found to be voltage ependent. The subsequent addition of the complement component C9, however, greatly implified this resistance change. Also, the more C9 added the greater the permeability change, until eventually membrane rupture occured. In addition, the channels formed by the addition of C9 to membranes treated with C5b,6,7, and 8, were found to be voltage-independent. No permeability changes occurred when the complement components were added individually or in mixed pairs to the membrane. This data supports the hypothesis that complement attacks membranes by forming a stable protein channel across the lipid matrix of the membrane. These investigators also report that oxidized cholesterol and monoolein BLMs increase the sensitivity of the complement attack. They suggest that this is due to the decreased thickness of these membranes. In another series of experiments, Michaels and Mayer have found that the permeability of BLMs increases in discrete steps following the addition of C components, suggestive of membrane channel formation, and that the size and stability of the channels increased with sequential addition of C components. Also, prior to the addition of C9, the C5b-8 channel opens and closes continuously. They estimated the size of this complement channel to be greater than 30 A. In this connection, heat-inactivated Ag-Ab complexes and fresh complement individually have no effect on the resistance of BLMs formed from oxidized cholesterol and phosphatidylcholine. When combined, however, the resistance was found to decrease within five minutes. It was also discovered that Ab could be titrated against Ag to restabilize BLMs. One conclusion is that the Ab might be restabilizing the membranes by deabsorbing the Ag from the BLM.[13]

Activation and Attack of Complement on Liposomes:

Haxby and Kinsky reported the activation of complement on liposomes by means of a lipid Ag present in the membrane. They prepared liposomes from a total lipid extract of sheep erythrocyte membranes and

observed 65% release of trapped glucose marker in the presence of rabbit antisheep erythrocyte antiserum (RAS) and guinea pig serum (GPS). Much of the early immunology work done with liposomes has been reviewed. For example, sheep erythrocyte membrane lipids have been employed because the extract contains Forssman Ag and RAS possesses Abs directed against this glycolipid. Liposomes containing purified Forssman Ag were also successful in releasing glucose. In addition, purified complement components and specific anticomponent Abs as inhibitors have been used to demonstrate that immune damage of liposomes involves the same classical sequence responsible for the Ab-induced cytolysis of cells. In this connection, sheep lipid liposomes have also been found to release a variety of other markers upon incubation with RAS and either whole guinea pig, human, or rabbit serum as a source of complement. Other naturally occurring lipid Ag's have been found capable of sensitizing liposomes to Ab and C. Cardiolipin is one such antigen that is of special interest because of the role it plays in the C-fixation test for syphilis.

The phenomenon of "reactive lysis" initiated without Ag-Ab complexes, as in the alternative pathway, has also been studied on liposomes. Weissman and associates found that C5b,6 + C7 + C8 +C9 gave maximal release of trapped markers (glucose or chromate) for liposomes that were either positively or negatively charged showing that the complement molecules probably attack the hydrophobic layer of the membrane directly without regard for the polar groups of the lipids.

Liposomes composed of dimyristoyl phosphatidyl choline (DMPC), cholesterol, stearylamine (SA), and galactosyl ceramide were found by Mold and Gewurz,[4] capable of activating C directly, i.e. these lipids themselves were able to activate C via the alternative pathway. All four types of lipids were required for this unique activation. Another very useful and interesting application of liposomes has been described by Lewis and McConnell. By incorporating spin-labeled lipid haptens into liposomes they were able to study the early recognition and triggering events of C activation as opposed to the terminal lytic destruction. They found that the more fluid the membrane, the better is the complement fixation (binding).

Presumably, in order to activate C, the Ab molecules must be able to diffuse laterally on the membrane surface.

Hsia and Tan used electron spin resonance as a membrane immunoassay. Liposomes with lipid-linked antigens have spin markers trapped in their internal aqueous compartments. In the presence of Ab and C the spin markers leak out so that a sharp, intense signal is detected. The magnitude of this peak intensity in the ESR spectrum is directly proportional to the number of spin-label molecules released from the liposomes. Thus the degree of lysis can be determined accurately by measuring the change in this signal intensity. Richards, Alving and Scher reported that the complement lesion in liposomes may be transient. They have found that the percent of trapped glucose released from multilamellar liposomes was inversely related to the aqueous volume of the liposomes. Also, large unilamellar liposomes released only 35% of their marker. These data suggest that the complement lesion is open only for a transient period since 100% release would be expected from unilamellar liposomes if the complement induced membrane lesion remained open permanently, and a transient complement lesion would result in a greater percentage of release from small liposomes than large ones.

Other Immunologic Events Observed on Planar BLMs

Henkart and Blumenthal used the BLM technique to study Ab-dependent lymphocyte-mediated cytotoxicity. They found that in the presence of Ab against DNP and human lymphocytes, dinitrophenylated lipid bilayers showed rapidly induced increases in membrane conductance of several orders of magnitude without membrane breakage. Such ionic permeability changes were only observed when the membranes' voltage was positive on the lymphocyte side, as would be the case with a target cell membrane. This system is thought to mimic lymphocyte killing of the Ab-coated target cells and the primary event in lymphocyte killing of Ab-coated target cells is the creation of ion-conducting channels in the target membrane. This cell-mediated cytotoxicity is thought to be similar to cytolysis by complement. Both processes exhibit one-hit and colloid-osmotic characteristics, and in both cases the lipid bilayer is implicated as

the target of attack. Mayer and associates propose that by analogy with the cytolytic mechanism of complement, the interaction between a lymphocyte and a target cell may activate membrane-associated proteins of the lymphocyte, leading to exposure of hydrophobic proteins, which then become inserted into the lipid bilayer of the target cell and form transmembrane channels. In order to test this working hypothesis, Mayer et. al. developed a model system in which multilamellar liposomes containing dimyristoylphosphatidyl choline, cholesterol, dicetylphosphate and Forssman hapten in the lipid phase, and $^{86}Rb^{+}$ and ^{51}Cr (Na Chromate) in the aqueous phase, are treated with anti-Forssman IgG and nonadherent cells from mouse spleen. It was found that lymphotoxin, a 45,000 dalton protein, released from activated lymphocytes and responsible for killing target cells nonspecifically, when neutralized with anti-lymphotoxin, is not responsible for the specific killing of target cells which requires intimate contact between the plasma membranes of the target and killer cells. This "membrane contact" is thought to involve the formation of channels in the target cell membranes, and the evidence that anti-Forssman Ab and lymphocytes cause direct synergistic marker release from liposomes containing Forssman Ag supports this hypothesis.

Wolf et al observed that Ab and Ag cause "patching" on BLMs, and that Ab reduces the diffusion coefficient of antigens in the membrane. Similar phenomena were observed using the lectin concanavalin A as the cross-linking probe. The diffusion and distribution of the amphipathic Ags was measured by flourescence photobleaching recovery. Rosenstreich and Blumenthal looked at the ionophorous activity of a number of B cell mitogens (proteins which cause B lymphocytes to divide), and found that with the exceptions of Keyhole Limpet Hemocyanin (KLH) and EIM, none of the B cell mitogens were ionophorous (i.e. able to increase the permeability of membranes) when tested on BLMs. It may be that EIM and KLH act on lipid receptors and the other mitogens require protein receptors in the membrane to function as mitogens.

Deleers, Poss and Ruyssachaert[6] reported that specific glycolipids incorporated into the BLM can be detected by conductance increases caused by the lectin, concanavalin A. The addition of a glycoprotein from

blood group O of human red cell membranes to the solution bathing the outside of the lipid bilayer membrane led to a steady increase of membrane conductance up to 25-fold above that of the control membrane, and when Con A (concanavalin A) was added in the presence of 1 mM Ca^{2+}, a further 7-8 fold increment in conductance was observed. The BLM has, therefore, been used to study several types of immunological reactions in conjunction with the liposome system.

Voltammetric Immunoassay

From the description of antigen-antibody-complement actions on BLM and liposomes presented in the preceding sections, it is evident that a potential sensitive technique may be developed based on a combination of electrochemical measurements and, through use of artificial BLM, immunoassay methodology. This technique may be properly termed voltammetric immunoassay. The basic principle is that any immunological reactions taking place at the BLM will alter the electrical properties which in turn will be converted into an electrical signal useful for assay purposes. Clearly, the successful development of voltammetric immunoassay requires, first of all, a BLM-based sensor, which should be specific, sensitive, and stable. In the following paragraphs the use of Nucleopore and Millipore-supported BLMs in the study of Ag-Ab-complement will be described. Such a study may be considered as the first step towards voltammetric immunoassay.[18,56] Owing to the extreme fragility of the BLM formed in the conventional manner, it precludes any practical application. Therefore, it was decided to form BLMs in commercially available filters (Nucleopore and Millipore membranes) of small diameter pores, since it is known that the stability of a BLM is inversely proportional to its diameter. Indeed, long-lasting micro BLMs of long duration (several days) could be formed in Nuclepore and Millipore filters. With these micro BLMs, it has been found that the conductance of membranes treated with C5b, C7 and C8 was affected markedly by the polarity of an applied field. Further, phospholipid is not required for the action of C5b-9; instead the only requirement is for a hydrophobic lipid bilayer for complement channel formation. From electrical measurements of complement-BLM, the diameter (or the effective size of the channel) has been estimated to be

about 100 A. Additionally, we have also found that these micro BLMs, to exhibit stepwise reductions in electrical resistance in the presence of Forssman antigen, appropriate antiserum and complement. The results appear to support the "hydrophobic doughnut" or transmembrane channel hypothesis. Channel formation in these artificial membranes is believed to be due to the insertion of complement proteins.

Experimentally, the membrane system is constructed by filling the smooth circular pores of polycarbonate membrane commercially known as Nuclepore filter (or Millipore filters) with a standard BLM forming solution.[2,27] This nuclepore filter is first glued with CH_2Cl_2 onto the end of a tapered polycarbonate centrifuge tube of 0.7 cm diameter. After the solvent has evaporated, the nuclepore filter is coated with membrane forming solution containing. Forssman antigen obtained from sheep RBC lipids. The tube is then snugly fitted into a cylinderical hole drilled into a block of plexiglass. The chambers on either side of the membrane are immediately filled with the aqueous bathing solution. This bathing solution is Varonal saline which consists of 145 mM NaCl, 4.9 mM sodium barbitol, 0.5 mM MgCl2 and 0.15 mM CaCl2 buffered a pH 7.4. The temperature of the bath is kept at 37~C. The assembly for the electrical resistance measurements has been described earlier. The results obtained during the course of Antigen-Antibody-Complement reactions on micro BLMs can be summarized as follows. In all the experiments it is found that between 0 and 10 minutes the drop in resistance of the micro BLM is small (3.8×10^7 to 1.2×10^7 ohm cm^2) while between 10-20 minutes the drop in resistance is marked and is of one order of magnitude ($1\ 0^7$ to 10^6). The drop in resistance or conductance is always in discrete steps or stepwise fashion. After 30 minutes the resistance values become constant and it may be assumed that a maximum number of channels have been formed in the membrane. The result obtained may be discussed along the lines proposed by Mayer's group; i.e. the sequential interaction of nine complement proteins. In the presence of antigen and antibody the complement is activated (enzymatic cascade). The C4b,2a,3b enzyme initiates the membrane attack sequence (C5-9) by cleaving C5. The resulting activated C5b fragment is stabilized by combination with C6. Subsequent reaction with C7 generates the complex C5b,6,7 which then becomes embedded in

the phospholipid moiety of the membrane at another site. At the C8 stage, cells begin to lyse, slowly (partial hole). C9 greatly accelerate hemolysis as indicated by "Complete hole".

The results obtained by us using Forssman antigen (sheep RBC lipid) antisheep hemolysin and Guinea pig serum complement show that the electrical resistance Rm of the micro BLM decreases in a characteristic step-wise fashion. This decrease in resistance of the membrane and attainment of a particular value takes different time intervals. This time ranges from a lowest value of 30-35 minutes to the highest value of 170-180 minutes. The values of micro BLM resistance Rm in saline solution on both sides without any antibody and complement varied between 3.2 x 108 ohms-cm^2 to 2.7 x 10^7 ohms-cm^2. In the case of antigen-antibody-complement complex, which forms channels throughout the bilayer, similarities are also found with hemocyanin channels; the results of our studies can be viewed in the light of well-established systems. The formation of additional channels due to electrophoresis of proteins toward the BLM followed by insertion, when the membrane potential is positive on the complement side, and Mayer's group questions ejection of proteins when the side is made negative. This ejection of C5b,6,7 or C5b-8 complex from the membrane seems unlikely. The data confirm the view held by Mayer that electric field can cause conformational changes in the proteins associated with the membrane. Electrically mediated changes may be reversible. Our results with change of polarity show that there is not much change in the resistance in either direction.

Bearing in mind that all above-mentioned immunological studies using conventional BLMs are highly significant. The major drawback for practical applications is their long-term stability. With the availability of stable, supported planar lipid bilayers (s-BLMs), the problem appears to have been overcome, as may be seen later in a feasibility study[56] of an antigen (Hepatitis B) and antibody (HBs-Ab) reaction using s-BLMs.

b. Cancer[2,27]

Since no part of the human body is immune to cancer, it is thus the most dreaded disease. In some forms of cancer, however, effective drug therapies have been found. Whether complete "cure" for all kinds of cancer can ever be discovered is highly uncertain. This is perhaps not surprising, since cells, both normal and cancerous, proliferate in the course of life. To answer several questions about cancer, we need therefore an understanding of how the process of proliferation is regulated in normal cells, which is determined partly by the structure and function of the plasma membrane. Other crucial functions served by the plasma membrane are the site of immunological reactions, phagocytosis, and pinocytosis. Recently, the involvement of the plasma membranes in tumor cells has also been recognized, in view of the crucial role played by the plasma in the processes of cell growth, differentiation and motility. The direction of cancer research, parallel with the development of cell biology, is increasingly molecular and membrane-bound. Thus, to some extent, the problem of cancer is similar to immunity: how does the body deal with the invading (cancer) cells? Before suggesting what role the BLM system can play in the war on cancer, a brief account of the progression of events on cancerous growth (i.e. metastasis, the spread of tumors throughout the body) is in order. A number of hypotheses have been advanced to account for the metastatic process, one of which is that metastatic cells from a primary tumor somehow enter the blood or lymph. Although the overwhelming majority of metastatic cells that enter the bloodstream are destroyed by natural killer cells, a few surviving ones travel in the circulation as single cells or in clumps. After finding a suitable site for attachment, the metastatic cells invade the region between the endothelium and the membrane. Once getting through the membrane, metastatic cells must establish a tumor colony for growth, if it is connected to a blood line for cellular nutrient delivery and waste product removal. For a tumor to become 0.5 cm in diameter in size and a few grams in weight, about 109 cells are needed, a lot of which are potentially metastatic. By then, it may be too late to effect a cure. Thus, one of the problems in treating cancer is early detection so that effective drugs and other therapies can be applied.

From the above description, cancer may be thought of as a membrane-based disease. The BLM system may be used, therefore, as a tool for detecting the presence of metastatic cells in the blood (or lymph), for example. Also, it may be developed into a method for testing the influence of agents (known collectively as biological response modifiers or BRMs) capable of stimulating the body's defense systems. This is due to the fact that the electrical properties of BLM are highly suseptible to alteration as has been shown by many investigators. Before summarizing the studies using the BLM system in cancer research, the following remarks are appropriate.

During the last decade or so, evidence has accumulated showing that natural resistance to tumors involves the activity of natural killer (NK) cells. These cells morphologically identified as large granular lymphocytes, play an important role in anti-tumor defense mechanisms. The cytotoxic effect of the NK cells can be modulated by different factors and agents (biological response modifiers - BRMs), one of the most efficient BRMs being interferon. Other BRMs used in cancer chemoprevention such as selenium compounds may also be involved in modulation of this cytotoxicity. The precise mechanism of the cell-mediated tumor-killing effect is not fully understood. Changes at the level of the membranes of the interacting NK cells and target tumor cells may be involved in this phenomenon. One of the primary events may be a structural modification: changes in the permeability and related electrical parameters of the target cell membranes induced by the activity of the NK cells. In order to provide experimental support for the above hypothesis, the BLM system has been used in the following manner (Fig. 10.1). The BLMs were formed from lipids and proteolipids isolated from K562 cells or phosphatidyl choline (PC) and oxidized cholesterol. After forming the BLM, NK cells pretreated with interferon or selenium were added to one side of the BLM and the changes in membrane conductance were monitored. Fig. 10.1 shows the changes in the specific conductance of BLMs made from lipids and proteolipids isolated from K562 cells. The untreated NK cells were added to the positive side of the BLM at 30 mV applied potential. Several minutes after the addition of the NK cells, the conductance starts to increase gradually reaching a relatively constant value in about 20-30

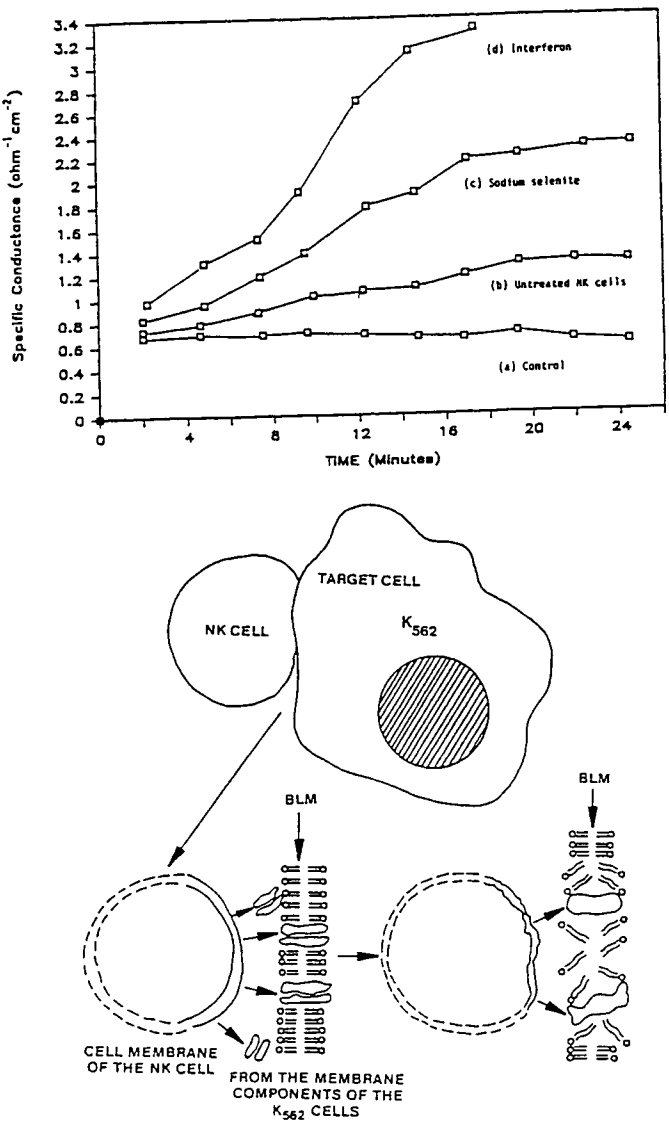

Fig. 10.1 *U*pper: Scheme representing the interaction between the NK cells and the BLM containing target cell components. *Lower:* Changes in specific R_m with added NK cells.

minutes (curve c). A breakdown of the membrane is observed 45-50 minutes after addition of the NK cells in about 50% of the experiments. Under the same experimental conditions, NK cells pretreated with interferon exert a more pronounced effect on the BLM conductance (curve a). A drastic increase of the membrane conductance is observed between 2-10 minutes after the addition of the interferon-treated NK cells. The dielectric breakdown of the membrane occurs within 20 minutes after the beginning of the conductance change. The NK cells pretreated with sodium selenite also induce an increase of the membrane conductance (curve b) which is higher than that in the control, but was less pronounced than that mediated by the interferon-treated cells. A dielectric breakdown of the membranes in these experiments was observed less frequently, although the conductance changes were substantial. The conductance increased at a higher rate in comparison to the untreated NK cells. Stepwise changes in the membrane conductance were characteristic for the selenium effect but similar changes, although less frequent, were also observed when untreated and interferon-treated NK cells were added. The conductance remains unchanged when no NK cells were added (curve d). Furthermore, the effect of the latter type of cells is more significant than that of the untreated cells. In addition to this voltage-dependence, a polarity-dependence of the effects was also observed. When added to the negative side of the BLMs, the cells exert less significant effect than when added to the positive side. The conductance changes were accompanied by alterations in BLM stability. Interferon-treated, selenium-treated NK cells, and the untreated NK cells, provoked a decreased membrane lifetime, which is indicated by an earlier occurrence of dielectric breakdown of the BLMs. The decreased membrane stability in the presence of added NK cells may be due to perturbation of the bilayer structure, an effect which could be involved in the mechanism of tumor-killing. The specificity of the observed cell-ediated effects was tested by performing parallel experiments on BLMs made from PC and oxidized cholesterol (2:1). The treated and untreated NK cells did not induce substantial changes in the electrical parameters in these BLMs. This finding indicates that the observed cell-mediated effects on the BLMs containing components of target tumor cells are specific. The dependence of the observed effects on the concentration of the added cells were added to the positive side of BLM. A larger

number of interferon-treated cells induced a more pronounced effect in comparison to selenium-treated or untreated cells. The described NK cell-mediated changes in the conductance of the BLMs made from components of the target cells can be explained by specific interactions between the membranes of the two types of cells. The added cells may also induce an effect without directly interacting with the model membranes. They may release some substances such as cytolysins, which gradually may integrate into the BLMs and provoke perturbation of the lipid bilayer structure or pore formation as suggested by Henkart. It is difficult at present to differentiate between these possible mechanisms, but the decreased membrane stability as well as the polarity- and the voltage-dependence of the effects may be interpreted in favor of the existence of more than one mechanism. A tentative scheme of the interaction between the cells and BLM is shown in Fig. 10.1. Related to the above is the BLM experiment reported by Henkart and Blumenthal in 1975 on antibody-mediated cellular cytotoxicity, which is dependent upon recognition by the killer lymphocytes of an antibody directed to the antigen of the target cell. This situation has been mimicked in the BLM with the correct specificity. Thus, the usefulness of the BLM system for investigating the cell-mediated tumor-killing effect and its modulation has been demonstrated. The findings support the concept that the NK cells increase the conductance and permeability of the target cell membranes and may be one of the primary mechanisms of the tumor-killing effect. Ion-channel activity modulation as well as local perturbations of the bilayer structure may be involved in this phenomenon. Speaking of ion channels in membranes, especially calcium channels, they are important in cellular functions. For example, the opening of calcium channels during excitation is a crucial step in the initiation of contraction in smooth and cardiac muscles. Since the plasma membrane of most cells are negatively charged, the immediate effect of these charges at the surface is to modulate the activity of ion channels. Recently it has been found that verapamil and other calcium channel blockers can substantially increase the cytotoxicity of different anti-tumor agents such as adriamycin, vinblastine and Cisplatin (cis-diammine dichloroplatium-II) for some kinds of resistant cells. Presently, Cisplatin is one of the most powerful antitumor agents, therefore it should be quite important to analyze the mechanism of resistance of some cell lines to the drug in order to obtain improved

therapies. Of interest to note here is that Cisplatin, the inorganic coordination compound cis-$[PtCl_2(NH_3)_2]$, has revolutionised the treatment of certain forms of cancer. The discovery as an anticancer agent.compound was 'by chance' by B. Rosenberg.[24] In the early 1960s, he decided to investigate the effects of electric fields on cell growth. The bacteria, which he used in the experiments, turned from short rods into long filaments. However, it was not the electric field that caused this dramatic effect but electrolysis products from the platinum electrodes. Further, it was discovered that only *cis* isomers but not the *trans* isomers, possessed the wide range of anticancer activity. In this connection, calcium channels from proteolipid fractions of Cisplatin-sensitive and cisplatin-resistant cells have been reconstituted and characterized in BLMs formed at the tips of patch-clamp micropipettes. The characteristics of the Ca channels are typical for the endoplasmic reticulum (ER) membrane channel activity.[2] They have a relatively large unit conductance and are modified by typical activators (nucleotides) and inhibitors (ruthenium red, verapamil). The mean open time and open state probability of channels reconstituted in BLMs from the membrane components of cisplatin-resistant cells are larger than those in BLMs made from components of cisplatin-sensitive cells. Ruthenium red (2 x 10-7 M) has been found to inhibit the channel activity in both types of membranes to the same level. The observed effects may be explained by an increased Ca release from the intracellular Ca stores (ER system) accompanied by an enhanced intracytoplasmic [Ca] in cisplatin-resistant cells. These changes in the [Ca] level may be responsible for the higher antitumor drug efflux rate and the development of the drug resistance. The information obtained by using the BLM system may help toward understanding the origins of drug resistance of cancer cells, thereby further improvement in the treatment of cancer may be facilitated.

c. Drug testing

Since the basis of life in terms of cells is the membrane, it is logical that an experimental compound to be potent must be compatible with this membrane in order to be readily avaliable to the cell. For testing and quantitating results, electrical measurements, due to their sensitivity and

elegance, is the technique of choice as has been used extensively in studying supported, planar lipid bilayers (or s-BLMs for short). As discussed in Chapter 4 (*BLMs and Liposomes*) and Chapter 5 (*Membrane Electrochemistry*), there are two unique aspects of planar BLMs: (a) preparation of BLM is simple; the membrane composition can be reasonably controlled, which overcomes the uncertainty of natural membranes; and (b) membrane electrical properties may be easily measured, providing a sensitive and rapid source of information. Electrical properties are important characteristics of the biomembranes. Both transport of charged species through membrane and the interaction of electroactive species with membrane cause changes of electric parameters. Some of these changes influence many important physiological functions. Specifically, crucial membrane properties such as E_m (membrane potential), R_m (resistance), I_m (current), C_m (capacitance), I/V (voltammograms), and V_b (dielectric breakdown voltage) can be easily measured. These measurements allow the investigator to determine accurately and correlate even the slightest changes in the s-BLM's electrical properties. Keeping this simple idea in mind, it has been suggested[59] that the use of BLMs in the initial study and screening of prospective compounds such as herbal anti-cancer drugs. It is well known that for years the Chinese have used herbal compounds to treat various diseases. Upon assay of these Chinese elixirs there is usually the recurrence of several compounds. These recurring compounds are usually mixed with sometimes more than 100 other ingredients. Research assays have shown that some herbal remedies contain, among others, vasodilators used for the treatment of coronary disease. It is therefore reasonable to speculate that many of the untested Chinese herbs may contain compounds that produce treatments such as anti-cancer activity. The problem that exists is the ability to find and isolate the few compounds that should be selected for further study in anti-cancer effects. In order for a cancer drug to be effective *in vivo* it has to interact with a cellular membrane. This is the reasoning behind using s-BLMs for the testing of prospective drugs. If a drug is shown to have no membrane activity, in the testing s-BLM, then it may be concluded that the drug in question would have little anti-cancer activity. The use of electrical parameters and the s-BLM, in conjunction with initial tests of natural compounds for anti-cancer activity, is an

extremely effective, and accurate method for screening the many untested Chinese natural compounds. This method can offer quick preliminary tests that separate the membrane active drugs from the inactive ones, which will facilitate further research in the hope of a breakthrough. In this conncetion, a project of screening Chinese herbal compounds for anti-cancer activity using supported lipid bilayers has been in progress.

Previous work done with NK cells and BLMs composed of K562 proteolipids shows that a relationship exists between membrane activity and tumor cell death. A relationship was determined between an increase in BLM conductance and the administration of NK cells. This increase in conductance resulted in a breakdown of the membrane, which could explain the NK cell's anti-cancer activity in vivo. This work is analogous to the above suggestion, for the basis on predicting the activity of Chinese herbal compounds that exhibit changes in BLM electrical parameters. This would allow us to determine which compounds react with the BLM and therefore would react similarly *in vivo*. This evidence will allow the selecting of compounds based on their membrane activity and excluding compounds without membrane activity. The end result is a precise method for screening the vast number of Chinese herbal compounds to facilitate further study, and quantitate the claims of Chinese herbal medicine.

In another approach, the BLM system could be developed into a significant part of a new method for screening chiral drugs.[59] The rationale is as follows: the composition of the human erythrocyte (RBC) membrane is complex, containing many different proteins, cholesterol, phospholipids, and glycolipids, but the experimental BLMs contain only phosphatidylcholine *(*PC*)* and cholesterol, and only phosphatidylcholine has the *chirality* (compounds whose mirror images cannot be superimposed). The chirality of drugs is very important in their function. Many drugs possess chiral selectivity, which is very significant to their bioactivities. For example, fre-quently, only one of the antimers is efficient, whereas the others may be defective. The difference in the transmembrane rates of these optical antimers should be one of the important reasons for their different bioactivities. These two kinds of membranes have the same chiral selectivity and permeability ratio, which demonstrates that the chiral

selectivity of the cell uptake is mainly due to the chirality of membrane lipids, i.e. due to the selective recognition of natural phospholipid's chiral carbon in the chiral molecule. The selectivity can only come from a direct interaction between the chiral carbon of lipid and its antimers. That is the observed selectivity of cell uptake was mainly caused by the chirality of the membrane phospholipid itself. The permeability ratio calculated from E_m was in good agreement with the results from human erythrocyte experiments. But the BLM electrical measurement is more simple, rapid and sensitive than the latter one. The composition of BLMs can be controlled accurately, which eliminates the disturbance of other components, leading to reliable results. Altogether, these above-mentioned advantages make the BLM system a useful tool for studying membrane transport, and drug–membrane interaction, as well as their mechanisms. By studying the permeating behavior of other chiral complexes and the electrical properties of BLMs with different compositions, details of this selective interaction could be further revealed. Thus, the BLM system may be developed into a useful tool for drug screening.[59]

d. Apoptosis

The last phase of a cell's destmy is so-called programmed cell death or commonly refered to as *apoptosis*. A failure of cells to fulfill their destiny has grave consequences on an organism, for a healthy being is an on-going concern; it maintains a balance of life and death of diffentiated cells. There are at least 3 ways to detect apoptosis; one of which is DNA laddering, the others being Annexin binding and the so-called Tunel-based assays. Of course, the most appropriate method will ultimately depend on the tissue type or cell being analyzed.[45] In this connection, a new method based on photoelectrochemistry for analyzing apoptosis of s-BLMs containing MCF-7 nuclei is described. The s-BLM cell responded to white light (200-800 nm). During the apoptosis induced by Taxol (paclitaxel, an anticancer drug), the photoelectric current of the cell decreased, suggesting the degradation of nucleus DNA. Electron transfer along the DNA double helix and along nuclear skeleton is assumed in the interpretation. This novel photoelectric analytical method may provide a rapid and sensitive technique

to evaluate apoptosis.[45] Specifically, a photoelectric method used for analyzing the cell-free apoptosis of human breast cancer cells (MCF-7 line) induced by Taxol. The cell-free MCF-7 nuclei are deposited on self-assembled bilayer lipid membranes (BLMs) on ITO conducting glass.[12] The dark current (light off) was first measured, then the light current was measured with the light on. The light-induced current was determined as the difference between the two measured values. A s-BLM can serve as a physical barrier separating two compartments, as well as acting as a bipolar electrode. That is, there is an anodic oxidation on one side of membrane and a cathodic reduction on the other side, with the lipid bilayer itself providing pathways for electrons and protons. The findings suggest an electron transfer process occurring across the bilayer lipid membrane, and the photoelectric current is intimately involved with the states of nuclei. Fig. 10.2 shows the typical photoelectric current of the assemblage. The photoelectric current of the cell is mainly dictated by the response of MCF-7 nuclei, which have been also confirmed by the apoptosis experiment. Because apoptosis experiment can cause the degradation of the nuclear DNA into oligonueosome chains, so, it is important in apoptosis experiments to observe the influence of the state of nuclei on the photoelectric response. The possibility has been considered that the DNA double helix, which contains a stacked array of heterocyclic base pairs, could be a suitable medium for electron transfer over long distance.. So the nuclear DNA can serve as an "electric wire" for photo-induced electron transfer by "hopping" from base to base.[18] The cleavage of nuclear DNA resulted in the damage of DNA structure as photo-induced electron transfer bridge. So the photoelectric current decreased with the cleavage of nuclear DNA. Moreover, the DNA ladder requires a large amount of DNA to be cleaved by nuclease; the cleavage of a small amount of DNA can not be revealed by agarose gel electrophoresis. However the variance of photoelectric current can reflect any small change about the structure of nuclear DNA. The nuclear skeleton plays an important role not only in the maintaining of nuclear structure, but also in the energy transfer. So, the photoelectric current decreasing was in accordance with the nucleus morphological change. Compared with the traditional techniques used to estimate apoptosis, such as the morphological observation and the agarose

gel electrophoresis, the photoelectric analytical method of apoptotic system may provide a rapid and sensitive way to evaluate the nucleus apoptosis.

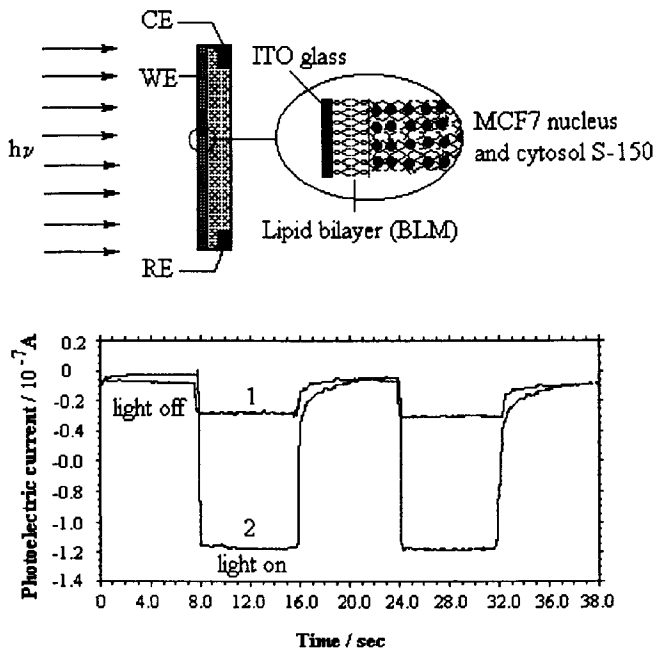

Fig. 10. 2 *Upper*: Experimental arrangment *Lower*: Typical photoelectric current responses.

10.3 Supported Bilayer Lipid Membranes as Biosensors

It is generally accepted that a biosensor consists of two principal parts: a recognition element and a transducer. These two parts must be in intimate contact with each other. As discussed by many investigators [Taylor and Schultz, 1996] and reviewed elsewhere,[6-8,11] we define biosensors as a new class of sensors that incorporate biomolecules as their principal sensing components. The word 'biomolecule' is meant to include

those compounds that exist in nature (chlorophylls, receptor proteins, antibodies, hormones, DNA, etc.) as well as man-made compounds such as TCNQ, *meso*-tetraphenylporphyrins (TPP), phthalocyanines, and fullerenes (C60). A more up-to-date definition of biosensors may be found on the inside cover of the international journal '*Biosensors & Bioelectronics*'; it states that "Biosensors are defined as analytical devices incorporating a biological material (e.g. tissue, microorganisms, organelles, cell receptors, enzymes, antibodies, nucleic acids, etc), a biologically derived material or biomimic intimately associated with or integrated within a physicochemical transducer or transducing microsystem, which may be optical, electrochemical, thermometric, piezoelectric or magnetic. Biosensors usually yield a digital electronic signal that is proportional to the concentration of a specific analyte or group of analytes. While the signal may in principle be continuous, devices can be configured to yield single measurements to meet specific market requirements. Under separate headings below, three main groups of electrochemical biosensors are described.

1. ***Potentiometric Biosenosrs***. They operate on the principle of a potential difference (PD) between a sensing (indicating or working) electrode and a reference electrode. This PD is proportional to the logarithm of the species concentration present in the sample solution. In the early 1970s ion-sensitive field effect transitors (IS-FET) were made, which were sensitive to H+, Na+, and K+. In essence, a sensitive membrane (e.g. a BLM) has modified the gate of the FET. In the usual operating mode, a voltage is applied between the silicon substrate and the gate electrode creating a conducting path between the source and the sink (drain) for the drain current. Thus, the gate potential through capacitive coupling controls the current. It should be pointed out that the essential requirement for a good FET-based biosensor is the solution-membrane interface at the gate terminal, which should be imperable to charge transfer. A s-BLM, with its inherent resistance of more than 10^7 Ω-cm^2, is ideally suited for such a purpose. Fig. 10.3 shows schematically a typical FET sensor. It should be pointed out that the essential requirement for a good FET-based biosensor is the solution-membrane interface at the gate terminal, which should be imperable to charge transfer. A s-BLM, with its inherent resistance of more than 107 Ω-cm2, is ideally suited for such a purpose.

2. ***Amperometic Biosensors***. These are based on the application of a constant voltage (PD) between the sensing electrode and a counter electrode and measuring the current which is a result of an electrochemical

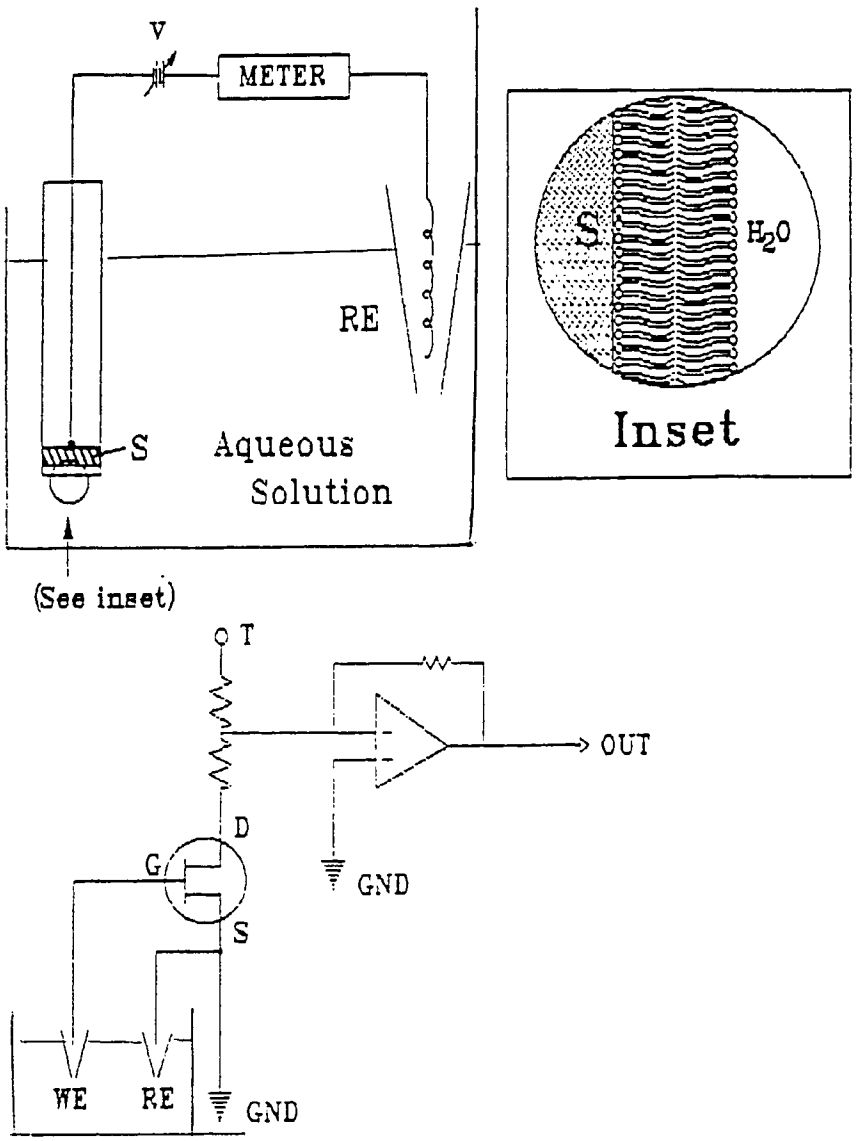

Fig. 10.3 A suggested FET sensor based on s-BLMs..

reaction at the working (sensing) electrode. The resultant current is proportional to the concentration of the species in the sample solution. As in cyclic voltammetry, an amperometric biosensor consists of three electrodes: a working electrode, a counter (auxiliary) electrode, and a reference electrode. Thus, in a typical amperometric chip it consists of three micropatterns: a sensing electrode, a counter electrode and a reference electrode. These micropatterns are produced as operations normally required for making transistors. The additional steps required are the attachment of a biomaterial to the sensing electrode, the conversion of Ag to AgCl for the reference electrode, and the encapsulation step so that only the desired areas of the micropatterns are exposed to the sample solution for redox reactions.

3. ***Conductimetric Biosensors.*** Compared with the two other types discussed above, conductimetric biosensors are by far the simplest. The principle of conductimetric biosensors is based on the measurement of conductivity changes of the test solution as a result of chemical reactions altering ionic species concentration. Hence, the conductance measurement of a testing solution is rather non-specific. However, by modifying the surface of the conductance electrode with compounds capable of undergoing receptor-ligand contact interactions, it may be possible to overcome this lack of specificity inherent in the conductivity measurement. For example, by coating the surface of an interdigitated microarray electrode, commercially available, with an enzyme (e.g. glucose oxidase), this modified conductance electrode should be able to detect the changes in conductivity as a result of the specific catalytic action with its substrate (in this case, glucose). This presupposes that, of course, the resulting 'enzyme-substrate' contact interaction generates ionic species in the test solution.

Biosensors have been applied to a wide variety of analytical problems including in medicine, the environment, food, process industries, security and defence. Thus, supported planar BLMs fit the above remarks quite well, as will be discussed below. Before doing so, a brief history of supported BLMs (planar lipid bilayers) is given here.

The origin of supported BLMs dates back to 1976 when a group of investigators were interested in developing a model system for the thylakoid membrane with suitable strength and size for use as a solar energy conversion device (see Section 10.5). Later, supported BLMs were formed on metallic wires, conducting SnO_2 glasses, gel substrates, and on microchips.[6-8] These self-assembled, supported BLMs, besides overcoming the stability problem of the conventional BLMs, have opened a range of possibilities in manipulating interfacial properties.

The theory behind the development of BLM-based biosensors is remarkably simple: to function in a biological environment the sensing element should be biocompatible. The bilayer lipid membrane (BLM) meets this criterion and is an ideal choice upon which to develop a new class of electrochemical biosensors. These sensors may be developed on the basis of either potentiometric or amperometric measurements. In the former, the potential (V_m) across the BLM is measured under conditions when no charges are flowing. In the latter, a current (I_m) is measured when a voltage is impressed across the BLM. Since the capacitance of a BLM is also readily monitored, the third type is a capacitative BLM-based device. A variation of the above are conductometric BLM-based devices in which the conductivity (G_m or resistance R_m) of the BLM is determined. In addition, simultaneous measurements of the current and voltage of a BLM resulting in a voltammogram may contain data useful for practical applications.

a. BLMs on microporous filters and SnO_2 glass

A BLM formed in the conventional manner, although miraculous, is nontheless a very fragile structure and difficult to work with. The conventional BLM system has one major drawback in that it is notoriously unstable, rarely lasting more than a few hours. As a result, many attempts have been made to stabilize this extremely delicate lipid bilayer structure for fundamental studies and practical applications. In this connection, the first report published in 1978 described the formation of supported BLMs in polycarbonate filters with much improved stability to both chemical and

mechanical disturbance.[26] This effort resulted in creating a membrane system by filling the smooth circular pores of a polycarbonate film (known commercially as Nuclepore filters) with a standard BLM-forming solution. The wet membrane was supported in such a manner that an aqueous solution could be easily added to both sides. In an ideal situation this Nuclepore-coated membrane may be visualized as tens of thousands of micro BLMs simultaneously generated *in situ*.[51] The most suitable pore size was found to be 3 μm. The Nuclepore filter supported BLMs exhibit far greater stability and manipulability than conventional BLMs.

b. Metal-supported s-BLMs[10]

The extreme fragility of the conventional BLM seriously limits its utility as a practical tool since it cannot be easily fabricated and will not endure rugged laboratory handling. This problem of fragility was finally overcome by forming BLMs on either smooth substrates (e.g. hydrogels, *see below*) or freshly created metallic surfaces. The freshly cut metallic surface has a great affinity for lipid molecules, which adhere to the nascent metal surface. After immersing the lipid-coated tip into the bathing solution, it gradually thins to a bilayer structure that is in equilibrium with a thick surrounding annulus referred to as a Plateau-Gibbs (P-G) border. Alternatively, a freshly cut end of the Teflon-coated metallic wire is dipped into the bilayer-forming solution for about 10 min; it is then taken out and immersed into an aqueous solution. The bilayer is considered as completely formed when its electrical conductance or potential have reached a steady-state value. A detailed procedure for s-BLM formation is given below. Unlike conventional BLMs, the structural state of s-BLMs and therefore many of the mechanical and electrical parameters can be modified by applying a d.c. voltage. Further, a s-BLM formed in the manner described is remarkably stable; it can not be removed by simple washing or mechanical agitation. A s-BLM may be detached from its metallic substrate, however, by sonication, electro-chemically or by drastic chemical treatments. Although usually depicted the lipids are oriented perpendicular to the metal surface, they are most likely tilted in some angle from the normal. To cover any surface by a layer of lipid molecules at the molecular

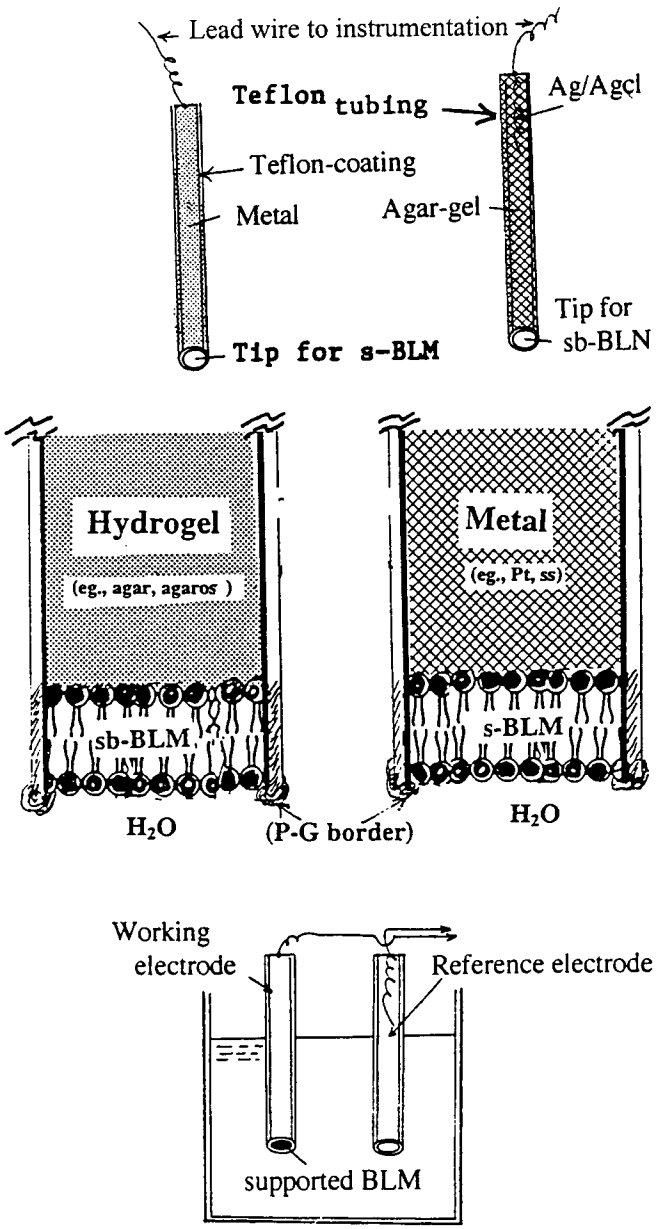

Fig. 10.4 lillustration of planar BLMs on various substrates.

dimension is an extremely difficult task, since the morphology of the substrate is unlikely to be 'smooth'. As an experimental fact, monolayers and multilayers of lipids prepared by the L-B technique are often full of pinholes. These defects are hard to avoid owing to the nature of the substrate at the atomic level. Thus, a freshly cleaved metal surface is not smooth at the atomic level; it is most likely to be very rough with grain and edge boundaries. However, the lipid solution used, being a fluid, is able to interact with the bumpy terrain of the newly cut metal surface and to form an intimate bond within its indentations, pits, and crevices. The lipid monolayer, adjacent to the solid metal support, is presumed to be stabilized by hydrogen bonds, arising between the hydrophilic groups of the monolayer and the electronegative metal surface. The hydrophobic alkyl tails of the amphipathic lipid molecules are so arranged allowing the polar head groups to pack more closely. The final self-assembling lipid bilayer is stabilized because of intermolecular forces. The breakdown voltage of s-BLMs under these conditions is several folds higher than conventional BLMs (up to 1.5 V). The most important factor in the process of the s-BLM preparation seems to be the time the cut end of the wire is allowed to remain in the membrane forming solution (~ 10 min) prior to its transfer into the aqueous solution for a supported BLM to self-assemble. Fig. 10.4 illustrates a planar BLM on the metallic substrate, a sb-BLM , together with other self-assembled systems.

BLMs on Metallic Substrates (s-BLMs)

Modified s-BLMs as pH sensors. Of all the ions crucial to the functioning of cellular processes there is the hydrogen ion (H^+) which plays the leading role in enzyme catalysis and membrane transport. Thus, it is not surprising that, the measurement of pH is of the utmost importance. Currently, the pH glass electrode is routinely used in chemical and clinical laboratories, as well as in a number of situations such as food processing, fish farming, pollution control, etc However, the large size and fragility of pH glass electrodes preclude their use in many situations such as *in vivo* cell studies and in monitoring membrane boundary potentials.It has been known for many years that BLMs formed from chloroplast extracts exhibited Nernstian behavior as a function of pH [Tien, 1974]. These observations

suggest that s-BLMs may be used as a pH probe in biophysical research and in biomedical fields where the conventional glass electrode presents many difficulties. For example, the hydrolysis of membrane lipids by phospholipid enzymes (lipases A and C) changes the boundary potential of BLM (or cell membrane) as a result of the local pH change. To test some of these ideas, a number of quinonoid compounds (e.g. chloranils) have been incorporated into s-BLMs.[9] Indeed, s-BLMs containing either TC*o*BQ (tetrachloro-o-benzoquinone) or TC*p*BQ (tetrachloro-p-benzoquinone) responded to pH changes with a nearly theoretical slope. This new pH-sensitive s-BLM offers prospects for ligand-selective probe development using microelectronics technologies.[10]

Embedding of ferrocene on s-BLMs. An amperometric sensor of ferri-/ferro- cyanide ions. The redox reactions for a solid supported BLM containing vinyl-ferrocene as an electron mediator have been investigated using cyclic voltammetry. The results have shown that (i) ferrocene can be very easily embedded in the lipid bilayer on the surface of a metallic wire (s-BLM) system. This demonstrates that the s-BLM system offers a novel approach to the electrode modification by simple way of immobilization of compounds within BLM, and (ii) ferrocene in a bilayer lipid membrane increases about two orders of magnitude of the potassium ferri-/ferrocyanide ion sensitivity more than that of the platinum electrode. Recently, substituted ferrocenes were incorporated into s-BLMs on Pt and stainless steel support and investigated using cyclic voltammetry.[30]

Hydrogen peroxide-sensitive s-BLMs. The embedding of appropriate active molecules (modifiers) into the matrix of the lipid bilayer should be able to impart the functional characteristics of s-BLMs. We chose TCNQ (tetracyanoquinodimethane) and DP-TFF (dipyridyl-tetra- thiafulvalene) as modifiers because of their properties as typical electron acceptor and donor molecules, respectively. It was found that DP-TTF could improve not only the stability but also increased the range of s-BLM's sensitivity to hydrogen peroxide. In contrast, TCNQ-containing s-BLMs did not show much responses to H_2O_2. This was not entirely unexpected since TCNQ should behave as an electron acceptor.

Modified s-BLMs as ion sensors. S-BLMs containing six different kinds of crown ethers were synthesized and investigated using the cyclic voltammetry.[20,21] In particular, s-BLMs formed from a liquid crystalline *aza*-18-crown-6 ether and cholesterol-saturated n-heptane solution was found to be sensitive to K^+ in the concentration range of 10^{-4} to 10^{-1} M with theoretical Nernstian slope. The specificity for three alkali metal cations and NH_4+ of five different kinds of bis-crown ethers in BLMs were investigated. The order of specificity for most of these bis-crown ethers was found to follow hydrated radii of cations, i.e. $NH_4^+ > K^+ > Na^+ > Li^+$. The results obtained with these s-BLMs compare favorably with conventional BLMs containing similar compounds such as valinomycin.[2]

Modified s-BLMs as Molecular Sensors. Many authors have reported sensors for the detection of the glucose using the glucose oxidase.[48,49] Earlier, we have reported embedding glucose oxidase on a polypyrrole-lecithin BLM with good results.[53] Interestingly, using s-BLMs containing redox compounds and electron mediators but without the enzyme, glucose was detected in a buffered solution. The results are very preliminary and further experiments are in progress. If highly conjugated compounds such as TCNQ is incorporated in the s-BLM forming solution, the resulting s-BLM was able to detect the presence of the ascorbic acid, which is consistent with the findings obtained with conventional BLMs.

Electrochemical Transduction of an Immunological Reaction via s-BLMs. S-BLMs can be employed to embed a host of compounds such as enzymes, antibodies, protein complexes (receptors, membrane fragments or whole cells), ionophores and redox species for the detection of their counterparts, respectively, such as substrates, antigens, hormones (or other ligands), ions, and electron donors or acceptors. In this connection, the first publication on direct electrical detection of Immunological reactions based on transient changes of electrical conductance in conventional BLMs was reported by del Castillo et al. Further studies of antigen-antibody reactions via BLMs have been carried out by others.[13] Using s-BLMs as biosensors with electrical detection, a feasibility study of an antigen-antibody reaction has been reported.[56] The antigen (HBs-Ag -- Hepatitis B surface antigen) was incorporated into a s-BLM, which then interacted with its

corresponding antibody (HBs-Ab -- Monoclonal antibody) in the bathing solution. This Ag-Ab interaction resulted in some remarkable changes in the electrical parameters (conductance, potential and capacitance) of s-BLMs. The magnitude of these changes were directly related to the concentrations of the antibody in the bath-ing solution. The linear response was very good ranging from 1 to 50 ng/ml of antibody, demonstrating the potential use of such an Ag-Ab interaction via s-BLM as a transducing device.[56] Fig. 10.5 illustrates the basic mechanism of ligand-receptor interactions in s-BLMs. Also shown is the constructiion detail of a simple s-BLM probe.

S-BLM-based sensor for iodide. The outstanding properties of geodesic fullerenes C_{60}, C_{70}, etc. appear to be excellent modifiers for investigating electronic processes in BLMs. Thus, to test fullerenes' efficacy as an electron mediator in a lipid bilayer environment, we have chosen an iodine-modified BLM system, since it has been previously shown that such a system was sensitive to iodide.[2,27,58] The results of our new findings are presented as follows. First, the presence of C_{60} greatly strengthened the stability of the s-BLM and dramatically alters its electrical properties. The cyclic voltammograms contain distinct redox peaks, which are not symmetrical. We have found that C_{60} in the lipid bilayer had the opposite effects on membrane resistance (R_m) and capacitance (C_m), respectively; it caused the R_m to decrease and C_m to increase. The presence of iodine in conjunction with C_{60} in the s-BLMs further accentuated the effects. It is apparent that both C_{60} and iodine, when embedded in BLMs, facilitate electrical conduction, thereby lowering the R_m. Since the dielectric constant (ε) of a typical, unmodified BLM is about 2, the presence of C_{60} and iodine should exert a great influence on ε. Since C_m depends on a number of factors such as the surface charge of the BLM, the nature of hydrocarbon chains, and embedded modifiers, an increase in ε, and consequently in C_m , is therefore expected. By incorporating C60 into our s-BLMs, we have found that the presence of C_{60} in the lipid bilayer increased the detection limit for I^- by 100 times (to 10^{-8} M). Thus, C_{60} greatly facilitates the discharge of I_3^- at the metal surface, which demonstrates clearly that the embedded C_{60} is indeed an excellent electron mediator.[18]

c. Gel-supported sb-BLMs[15,16]

Salt-bridge supported lipid bilayers (sb-BLMs) on gel substrates

Although lipid bilayers on metallic substrates are attractive for certain purposes, the metallic substrate however precludes ion translocation across the lipid bilayer. Therefore, the pursuit of a simple method for obtaining long-lived, planar BLMs separating two aqueous media has been elusive until very recently. A brief description of forming a planar lipid bilayer on the agar or agarose gel is given below.

Techniques for hydrogel supported lipid bilayers.

Although s-BLMs on metallic substrates are attractive for certain purposes (e.g. certain biosensors), the metallic substrate however precludes ion translocation across the lipid bilayer. Therefore, until a few years ago the pursuit of a simple method for obtaining long-lived, planar BLMs separating *two* aqueous media has been an elusive one. The procedure for forming a planar BLM on agar or agarose gel has been published. Briefly, a small diameter (~ 0.5 mM) Teflon tubing is filled with a hot hydrogel solution (e.g. 0.3 g agar in 15 ml 3 M KCl). For electrical connection as well as serving as a reference electrode, an Ag/AgCl wire is inserted at the one end. The other end of the agar-filled Teflon tubing is cut in air and then immediately immersed the cut end in the lipid solution for about 10 minutes. The next step is to put the lipid-coated tip into an aqueous solution for a sb-BLM to self-assemble. Fig. 10.4 illustrates a planar BLM on a hydrogel substrate.

Syringotoxin-induced channels in a sb-BLM. Of special interest is that cation channels in BLMs can be induced by a number of toxins such as δ-endotoxins. With the availability of highly stable sb-BLMs, certain phytotoxic substances (e.g. syringotoxin, S-toxin) has been embedded into the lipid bilayer, since the dimensions of this S-toxin are almost in the same range as the lipid bilayer thickness. Indeed, the single ion channel activities of this S-toxin-containing sb-BLM were observed, which appear as a square-shaped current fluctuation during the transitions of the channels between different conducting states. From plots of frequency vs. single-channel conductance histogram, and the current-voltage curve, a linear

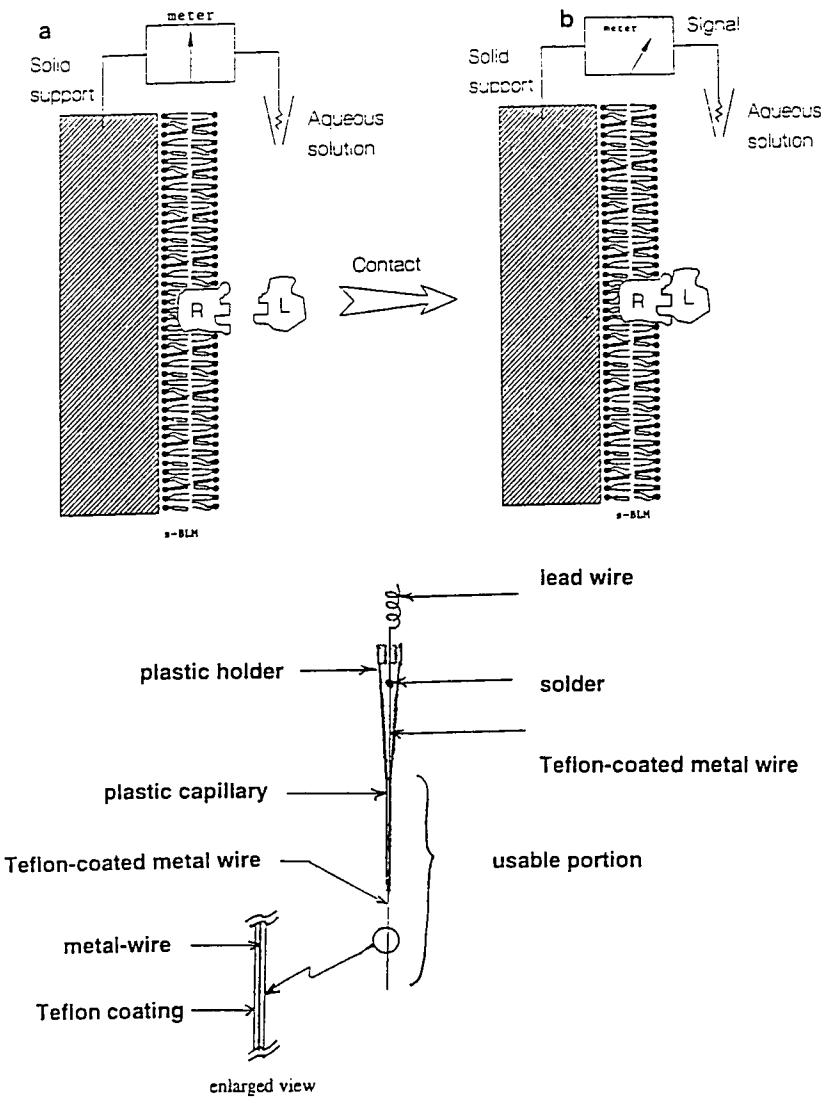

Fig. 10.5 *Upper.* Basic mechanism of ligand-receptor interactions in a s-BLM (L = ligand, R = receptor). As a result of L-R contact interac-tion, an event is produced, which is then transduced into an electrical signal, amplified, detected, and displayed by appropriate state-of-the-art technology *Lower.* the constructiion detail of a simple s-BLM probe.

relationship was obtained. In the latter case, the slope conductance was found to be 125 pS for the S-toxin-modified sb-BLM, which is in accord with known values.[6-8]

Photoelectric responses of supported BLMs modified with fullerenes

Electron transfer across biomembranes is central to vital processes such as photosynthesis and mitochondrial respiration, and has been the focal point of numerous BLM studies. This is owing to the fact that BLMs and s-BLMs represent the simplest self-assembled structure that separate two phases (liquid/liquid or liquid/solid). Indeed, certain electron mediators can modify the electrical parameters of supported BLMs.[6,18] Thus, the insights gained in these findings may facilitate the future perspective in the use of s-BLMs for practical applications. For instance, fullerence (C_{60})-containing sb-BLMs have been found that C_{60} can function both as a mediator and a photosensitizer. A comparison of properties between planar lipid bilayers (BLMs) and biomembranes is given in Table 10.1.

Table 10.1 Properties of Planar Lipid Bilayers and Biomembranes*

Property	BLMs	Biomembranes
Thickness (nm)	4-7	5-7
Resistance (Ω cm2)	> 10^8 (unmodified)	10^3- 10^5
Capacitance (μF cm^{-2})	0.3-1.3	~ 1
Breakdown voltage (V/cm)	2-10 x 10^5	10^5 to 10^6
Dielectric constant	2.1 to 5	2-3
Water permeability (μM/sec)	8-24	35
Interfacial tension (dynes/cm)	0.2-6	< 1
Potential difference per 10-fold concentration (e.g. KCl) (mV)	> 50 (modified BLM)	> 50
Electrical excitability	observed (modified BLM)	observed
Photoelectric effects	observed (modified BLM)	observed
Electronic (non-linear)	observed (modified BLM)	observed

*For more details see Refs. 1,6-8,10.

d. BLMs on complex substrates

S-BLMs on interdigitated electrodes by microelectronics techniques.[17] The results of recent research have confirmed a broad spectrum of possible areas of BLM applications.[6-8,40] All of these possibilities are based upon the fact that a lipid bilayer structure can be deposited on a solid substrate. This novel manner of lipid bilayer formation overcomes two basic obstacles in the way of the practical utilization of the BLM structure, namely: (i) its stability and (ii) its compatibility with a standard microelectronics technology. The solid supported BLM system (s-BLM) not only possesses the advantages of a conventional BLM structure but additionally gain the new important properties such as (a) long-term stability, (b) an anisotropic, highly ordered, yet very dynamic liquid-like structure, (c) two asymmetric interfaces, and (d) this type of probe is predestined for microelectronics fabrication. On this last mentioned property, we extended the experiment described above to the interdigi-tated structures (IDS). IDS are finger-like electrodes made by microelectronics technologies and used in micro-chip applications. By forming s-BLMs on IDS made of platinum with a window of 0.5 mm x 0.5 mm, we obtained the following interesting results. First, when an IDS coated with a BLM is formed from asolectin, it responded to pH changes with a 15 $\pm$ 2 mV/decade slope. The conductance of s-BLMs on IDS was about 50 times higher than the usual s-BLMs. Second, when an IDS coated BLM formed from asolectin plus TC*O*BQ (or TC*P*BQ), the pH response was linear with a 50 $\pm$ 1 mV slope. This very interesting finding suggests that (i) the lipid bilayer, the fundamental structure of all biomembranes, can be attached to an IDS with responses not unlike those found in the s-BLM, (ii) this type of structure (i.e. s-BLM on interdigitated electrodes) can be used to investigate ligand-receptor contact interactions, and (iii) s-BLMs on an IDS can be manufactured using microelectronics technologies which already exist without the explicit need of special modification. We consider this finding as a major 'breakthrough' in biosensor development. In this connection it should be mentioned that the experiment on the IDS-chip modified with a BLM is based on a common basic aspiration. That is to self-assemble a lipid bilayer containing membrane receptors so that a host of physiological activities, such as ion/molecular recognition can be investigated. At the molecular level, most

of these activities may be termed collectively as receptor-ligand contact interactions. The structures we have been reconstituting are inherently dynamic. Receptors and ligands in such close contact normally will vary as a function of time, frequently resulting in non-linear behavior. With the IDS-chip modified with BLMs, we now have at last a most unique system for an extensive experimentation that will be only limited by our imagination. Thus, insight gained from these studies will guide the preparation of functional BLMs on the IDS support.

Cyclic voltammetry of s-BLMs modified with redox species.[30,53] In one application of the self-assembled BLM on a solid support, the redox reactions of embedded pigment-protein complexes are of interest, where the transfer of electrons is assumed from a pigment to a substrate. To model these processes we have studied the electron transfer from cytochrome c to a Pt electrode covered with a modified s-BLM. The water soluble cytochrome c is often denatured on the clean metallic surfaces. In the case of s-BLMs modified with AQS, the cytochrome c in the solution gives no observable current responses. When 1 mM was added to the cytochrome c solution, the cyclic voltammogram with corresponding oxidation and reduction peaks was recorded. The redox potentials did not change with the different scan rates. In another experiment, the heights of the cyclic voltammogram peaks increased, when only diaminodurene has been present in the solution. The current was changed independently from the concentration of the cytochrome c, when the s-BLM has been modified by AQS and with diaminodurene (DAD) present in the solution. It is reasonable to assume that cytochrome c is physically adsorbed onto the BLM and thereby effectively excludes the DAD molecule from the s-BLM surface. The analogous experiments were also carried out with s-BLMs modified by 4,4'-bipyridyl and with ferricyanide present in the solution.[53]

S-BLMs stabilized by trehalose.[19] From an experimental viewpoint, the stability of BLMs has been a common concern. Recently, we have investigated the effect of trehalose and glucose on the elasticity modulus perpendicular to the membrane plane (E_l) and the electrical capacitance (C_m) of s-BLMs on Teflon-coated Ag wire. Addition of the saccharide (trehalose) into the electrolyte resulted in decrease of elasticity modulus of

the s-BLM formed from soybean phosphatidylcholine in n-hexadecane, while C_m did not change. Further, trehalose had considerable stabilizing effect on the other parameters of the s-BLM, consistent with earlier findings. Treatment of the s-BLM in electrolyte containing 300 mM trehalose allowed s-BLMs to be kept in dry conditions and stored for several days in a refrigerator with subsequent recovery of membrane parameters after dipping the wire into the electrolyte. After initial sharp changes of C_m and E_l, these parameters were stabilized after about 25-30 min. The 'step-like changes' of C_m and E_l probably reflect the dynamic nature of lipid structure as well as certain cooperativities in forming the bilayer during the hydration process. Removing the trehalose is accompanied not only by creation of hydrogen bonds between water molecules and phospholipid head groups, but also by changes in ordering of the hydrophobic part of the lipid bilayer. These results, especially the stabilization of the s-BLM parameters open additional possibility for practical application of s-BLMs.

Owing to its long-term stability, ease of formation, and low cost in its construction, a supported BLM offers an approach especially advantageous in the research and development of lipid bilayer-based sensors and devices. Some of the advantages of supported BLMs are listed in Table 10.2.

10.4 Liposomes, Liquid Crystals, and Nanoparticles

Applications of liposomes[3,4]

Liposomes, along with planar lipid bilayers (BLMs) have been extensively used as an experimental model of biomembranes. Some aspects

of practical applications of liposomes have been covered in Chapter 4. More details and references may be found in a review by Bangham.[4]

Table 10.2 Advantages of the supported (s-BLM) system*

Attribute	Remarks
1. Formation -- a self-assembled lipid bilayer	very easy to prepare
2. Thickness -- a nanostructure	~ 5 nm
3. Junction -- 2 interfaces	aq. solution |BLM| aq. solution agar gel |BLM| aq. solution metal |BLM| aqueous solution
4. Stability	long-term, very durable
5. Manipulation -- very simple	a host of compounds has been embedded in BLMs
6. Properties -- electrical	easily measured
7. Dielectric strength	> 250,000 volts/cm
8. Cost -- very low	disposable

* For more details see Refs. 6-8,26.

BLMs formed from liquid crystals[76-80]

Liquid crystals are compounds that have more molecular organization than liquids and less than solids. In a classical melting of a solid to a liquid, the molecules undergo dramatic changes, usually very sharp, in positional, rotational and orientational order at the melting point. Compounds that exhibit liquid-crystalline behavior, however, "melt" in a stepwise manner with increasing temperature. There are a number of

intermediate, thermodynamically stable phases comprising the so-called thermotropic liquid-crystalline, mesomorphic state. The three main phases are: smectic, nematic, and cholesteric. The last type are compounds derived from cholesterol which by itself is not mesomorphic, however. Liquid-crystalline mesophases can be formed in a mixture of surface-active compounds and solvents (e.g., a common soap in water). Thus, in the first papers published in the early 1960s on BLMs, the term "smectic (neat) mesomorphic phase" was used to describe the structure of this new type of artificial membrane.[2] In the intervening years, liquid crystals have found many important applications in technology. In view of their molecular orientation and other intriguing aspects, liquid crystals should be investigated in the form of BLMs. The following paragraphs summarize some of findings in this facinating area.

In this research, a simple approach was adopted to form BLM using thermotropic liquid crystals such as nematic (4'-hexyl-4-cyanobiphenyl-6CB), and smectic (4'-octyl-4-cyanobiphenyl-8CB) compounds. Cholesteryl palmitate (ChP) was also used as a cholesteric liquid crystal. All of the liquid crystals were dissolved in decane with butanol (1:1 v/v) before the BLM formation. Electrical properties of liquid crystal (LC) BLM were examined by the usual methods and are given in Table 10.3.

Table 10.3 Electrical properties of liquid crystal BLMs[80]

No Sample	R_m [ohm cm^2]	C_m [$\mu F\ cm^{-2}$]	Breakdown Voltage [mV]	Lifetime [min]
6CB	10^4	0.80	80 - 120	30 - 60
8CB	10^4	1.00	90 - 120	40 - 80
ChP	10^8 - 10^9	0.70	150	
BLM (lecithin)	10^7 - 10^9	0.35	200	

As may be seen in Table 10.3, the capacitance of liquid-crystal BLMs is much higher than unmodified lecithin BLM. Likewise, the resistance of cyanobiphenyl BLM is several orders of magnitude smaller than that of lecithin BLM. Such large differences between those two types of membranes, in both parameters (C_m and R_m), were expected on the basis of known properties of pure hydrocarbons (dielectric constant $\varepsilon \sim 2.1$ and specific resistivity $\Omega = 10^{15} - 10^{19}$ ohm-cm) in comparison to pure cyanobiphenyls (dielectric constant depends strongly on macroscopic orientation of molecules and in most common cases. The data shown in Table 10.3 are within experimental error independent of the amount of liquid crystal material ejected into the hole for membrane formation. This observation indicates that the final stage of LC-BLM formation is independent of the amount of material used, suggesting that this stage always has the same structure. Taking into consideration the overall picture of liquid crystal BLM, one can view the data as follows: (i) either from the standpoint of ε, being the same in both macroscopically ordered liquid crystal films, so that a LC-BLM permits one to estimate the thickness of a 'black' liquid-crystal membrane, or (ii) from the assumed value of BLM thickness which allows us to estimate the average value of ε. Under the given experimental conditions it seems probable that ε is decreased (in comparison to liquid crystal films) by some amount of solvent molecules which might be present in the BLM.

The effects of light on LC-BLMs were also investigated with a view to the understanding of the relationship between the capacitance and its surface charge density. There are two ways of treating pigmented BLM (p-BLM): (i) as an organic semiconductor, and (ii) as two double layers connected by an ionic pathway. If the first case is granted, the observed photoelectric effects of p-BLM are easily explained in terms of the band theory of semiconductors, with the particular reference to the charge functions between metals and semiconductors (p-BLM). The second scheme is based on a macroscopic molecular model and the Gouy-Chapman double layer theory (Chapter 6, *Membrane Electrochemistry*). In such a model the p-BLM system involves two interfacial photoreactions coupled by transmembrane diffusion of pigment molecules (ionic current).

Using cyanobiphenyl liquid crystalline materials together with a 7,7,8,8-tetracyanoquino-dimethane (TCNQ) as photosensitizer, the BLM capacitance could be enhanced as much as five times in comparison with the usual BLM just described. Interestingly, the BLM capacitance increase under light is drastically altered by the presence of redox compounds in the bathing solution. The photocapacitance changes under conditions with redox agents usually occur in one direction, namely, the dark capacitance drops under light exposure. Additionally, with redox compounds such as methylene blue (MB), generation of a photovoltage under light exposure can be observed. With the high affinity of TCNQ molecules for electrons, one can suggest that the electron exchange between the charge transfer complex and methylene blue (MB) as the acceptor might be the limiting step. The excitation of MB molecules increases their electron accepting ability, thereby facilitating the electron flow through the membrane. As a result one can see an increase of negative potential within the MB compartment. At the same time the membrane capacitance decreases because of the increase of the CT complex dissociation probability. On the basis of this explanation of photoprocesses of the p-BLM membrane, one can also understand that, under the appropriate experimental conditions a biphasic signal of photocapacitance changes might be observed. Results obtained with LC-BLMs show that, under appropriate conditions, it is possible to design a unique photoactive BLM system in which one is able to produce the photochanges of all main electrical parameters (conductivity, capacity and voltage across the membrane) in a controlled way. Therefore, we believe that the photoactive LC-BLM system is a promising one and might be especially useful for the future experimental study of photoelectronic process and factors that control the overall quantum yield of all kinds of photoinduced changes.

Nanoparticles

BLMs containing inorganic semiconductors. In order to demonstrate electronic processes in BLMs in the absence of illumination, at least three fundamental questions have to be answered: (i) is there any experimental evidence to support the idea of electron conduction; if so, (ii) what is the source of electrons, and (iii) what is the pathway for electrons in the

membrane? Answers to these questions have been provided by a number of experiments such as electrostenolysis in BLMs.[2,27] Even more direct experimental evidence can be seen in BLMs containing semiconductor polycrystallites (semiconductor nanoparticles). For example, CdS crystallites were formed *in situ* in the pores of a polycarbonate (Nuclepore) membrane separating two aqueous solutions.[80] When the CdS-membrane was irradiated, open-circuit photopotentials up to 500 mV were obtained.

To take a closer look at the membrane coating phenomenon, the cyclic voltammetry technique was used for the investigation of photoelectrical and electrochemical properties of BLMs. A number of substances, such as Cu, CuS, CdS, FeS, and AgBr having typical metallic or semiconducting features were selected. Suspensions of AgBr and CdSe particles in BLM in the absence and presence of pigments were also examined.[77,80] Although inorganic substance deposition onto the BLM has been reported earlier, the results obtained in later work shed more light on this interesting phenomenon. The experiments showed that mechanical, electrical and optical properties of the BLM can be drastically altered by deposition of a metallic or semiconducting layer (or both) onto its surface. Extremely low membrane resistance ($< 10^5$ ohm cm^2) observed in the case of FeS- and Cu-coated BLMs has not been previously reported. Voltammograms recorded for metallic Cu-coated BLM and combined Cu/CdS-coated BLMs displayed rectifying diode characteristics. It can be explained by considering that in the case of Cu deposition, the CuS/Cu_2S layer is produced first and further reduction to the metallic Cu follows. In such a way, a *p*-type semiconductor/metal junction is generated. Similarly, in the case of combined Cu/CdS (or CdS/Cu), depositing *n*-type semiconductor/metal junctions are formed thereby endowing the membrane rectifying properties. It should be emphasized that coated BLMs show very good stability in comparison with unmodified BLMs, which usually lacked satisfactory durability. Metallic or semiconducting layers deposited onto the BLM surface can serve as electrodes directly contacting the membrane, which eliminates electrolytic contact with the lipid bilayer and may be useful in biomolecular electronic devices development.[77,80]

Similar studies in semiconductor-containing BLMs have been carried reported. Zhao et al.[81] have described preparation and characteriza-

tion of stable BLMs and their potential utilization in membrane mimetic chemistry. Zhao and associates formed BLMs from bovine brain phosphatidylserine, glyceryl monooleate, and a polymerizable surfactant, [n-$C_{15}H_{31}CO_2(CH_2)]_2\ N^+(CH_3)CH_2C_6H_4CH{=}CH_2]Cl^-$. These BLMs were then used to provide matrices for the *in situ* generation of microcrystalline CdS, CuS, Cu_2S, PbS, ZnS, HgS, and In_2S_3. Semiconductors were formed by injecting appropriate metal ion precursors and H_2S into the bathing solutions on opposite sides of the BLM. Their presence was established by voltage-dependent capacitance measurements, absorption spectroscopy, and optical microscopy. Subsequent to the injection of H_2S, the first observable change was the appearance of fairly uniform white dots on the black film. These dots rapidly moved around and grew in size, forming islands that then merged with each other and with a second generation of dots, which ultimately led to a continuous film that continued to grow in thickness. These data were interpreted in terms of an equivalent RC circuit that made possible an assessment of the semiconductor penetration depth into the BLM.

10.5 Solar Energy Transduction via SC-SEP cells

Artificial photosynthesis

The essential process of green plant photosynthesis is the redox reaction of carbon dioxide and water, the end products of which are carbohydrates (reduced CO_2) and oxygen (oxidized H_2O), as described in Chapter 9 (*Photobiology*). The photons of solar energy absorbed by photoactive pigments embedded in the thylakoid membrane cause the water molecule to decompose into its constituents, namely, electrons, protons and oxygen. Photoinduced electron transfer processes are a crucial aspect of Nature's photosynthesis, which are achieved in an ultrathin pigmented bilayer membrane separating two aqueous solutions. Most of our understanding of the aforementioned processes have resulted from interdisciplinary endeavors. One such endeavor is the use of a bilayer lipid

membrane (BLM) less than 10 nm thick as a model for the thylakoid membrane of the chloroplast. Recent publications indicate that the BLM system is also of interest in the field of solar energy conversion.[28,29,61,62,65] Further, in recent years there has been a great deal of concerted effort towards mimicking the natural process, which has come to be known as ***artificial photosynthesis*** with the chief aim of generating electricity and/or hydrogen via water photolysis. For instance, the use of membrane-based photoelectrochemical systems for solar energy conversion was attempted by several groups of investigators (for reviews of early work, *see* Bolton, 1977; Davision, 1989). The basic arrangement consists of a photoactive membrane separating two aqueous solutions containing redox compounds. Light-induced charge separation in the form of electrons and holes causes a reduction on one side of the membrane and an oxidation on the other side. In this scheme a transmembrane movement of electronic charges is assumed. Experimental support for these photoinitiated transmembrane redox reactions has been provided by a number of laboratories. Pertinent and closely related to the membrane-based systems are interfaces, organized multilayers, micelles, and lipid vesicles. Therefore, the subject of artificial photosynthesis will be discussed in terms of the photoelectrochemistry of pigmented bilayer lipid membranes and their derived practical systems such as the semiconductor septum-based electrochemical photocell.

Semiconductor septum electrochemical photovoltaic (SC-SEP) cells

With the essential principles of the primary steps in green plant photosynthesis and the photoelectronic processes occurring in pigmented bilayer lipid membranes established, these insights thus gained have been applied in constructing practical "membrane-based" photoelectrochemical cells (PECs) for artificial photosynthesis. A conventional PEC consists of a photoactive semiconductor electrode, a counter electrode, and an electrolyte, all of which are contained in one compartment. The single-compartment construction of a conventional PEC limits the maximum photoelectrical response to the degree of band bending and is controlled, therefore, by the Fermi level for a given semiconductor and redox couple. This major drawback has been overcome in a novel semiconductor-liquid junction PEC, called semiconductor septum electrochemical photovoltaic

(SC-SEP) cell. The basic idea of a SC-SEP cell is that the photoactive compounds (e.g. pigments, semiconductors) in the form of a 'membrane' or pellet can act as a bipolar septum electrode between two redox solutions (Fig. 10.6)..

Description of the SC-SEP cell

The principal components of a semiconductor septum electrochemical photovoltaic (SC-SEP) cell consists of a semiconductor 'membrane' in place of the pigmented BLM, two contacting electrodes, and two aqueous solutions containing the same or different redox couples. Fig.10.3 shows a diagrammatic representation of a semiconductor septum electrochemical photovoltaic cell. The semiconductor septum serves as the photoactive bipolar electrode through which light-generated electrons and holes are translocated under the influence of an electric field. The semiconductor (SC) septum bipolar electrode used in our cells has been either a *n*-type SC or *p*-type SC or a SC on a metallic substrate (Pt, Ti, Ni). A *n*-type and *p*-type SC jointed back to back has also been tried. In this last case, the SC septum bipolar electrode mimics precisely a pigmented BLM separating two aqueous solutions. As a specific example, a typical SC-SEP cell may be represented as follows:

Contacting Electrode	Redox Solution	Semiconductor bipolar electrode	Redox Solution	Contacting Electrode

Illumination of the CdSe septum bipolar electrode with light from a halogen-tungsten lamp at 80 mW cm^{-2}, open-circuit photovoltage ($V_{oc}^* = V_{light} - V_{dark}$) and short-circuit photocurrent ($I_{sc}^* = I_{light} - I_{dark}$) of 1.8 V and 40 μA cm^{-2}, respectively, have been obtained in preliminary experiments. As shown in Fig.10.6, exposure of CdSe to light induces electron/hole separation within the SC depletion layer. The holes thus created are driven and used for polysulfide oxidation at the left electrolyte/ CdSe interface, whereas electrons move through the bulk of SC to the other side of the CdSe septum to effect a reduction.

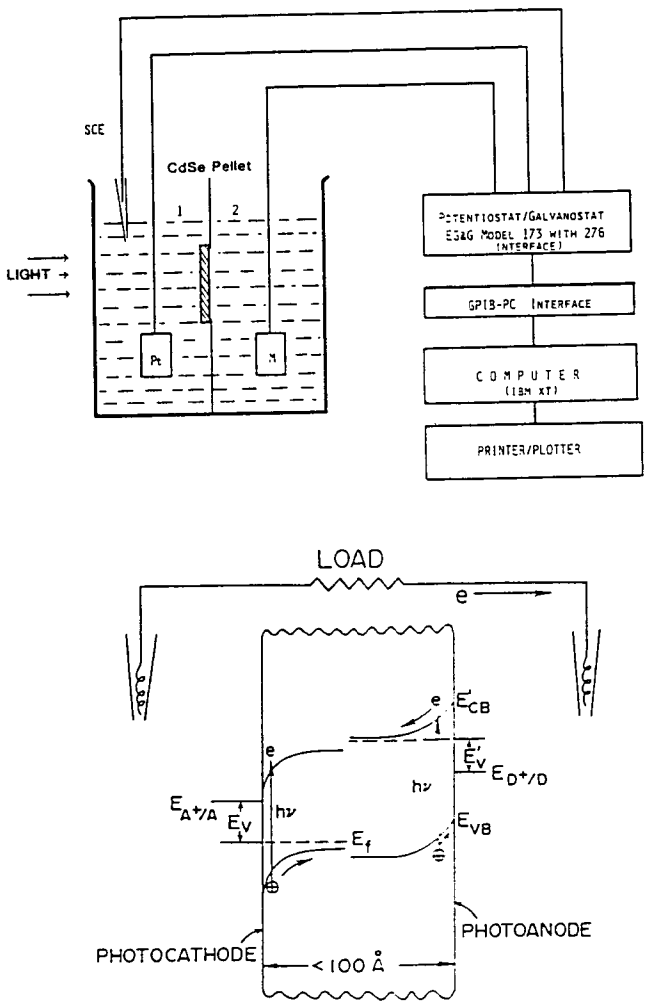

Fig. 10.6 *Upper.* Diagrammatic representation of a semiconductor septum electrochemical photovoltaic (SC-SEP) cell. *Lower.* Mechanism of operation.

Reactions complementary to the ones just described take place at the respective contacting electrodes. Additionally, the SC-SEP cell possesses its own redox potential and can, therefore, operate as a battery in the dark with storage capability. These initial findings offer a novel approach to photovoltaic cell design and, in addition, display a photo-to-electrical energy conversion efficiency of about 10 percent. Instead of using a CdSe pellet as the septum electrode, polycrystalline CdSe powders deposited on various metals (Ti, Ni, graphite, etc.) have also been tried obtaining essentially similar results.

Water photolysis via SC-SEP cells

The ultimate goal of experiments for the photochemical conversion and storage of solar energy in the 1980s and beyond is the photolysis of water modeled after green plant photosynthesis.. The overall reaction for water splitting requires a minimum redox potential of 1.23 V. However, various energy losses such as electrode overpotentials and back reactions have to be considered, which are inherent in the process of quantum conversion. Therefore, the minimal energy is estimated to be around 2.0 eV. The aforementioned backward reactions (i.e. charge recombination) can be prevented by creating an electrical field to facilitate charge separation and collection. The latter can be further enhanced by the presence of suitable redox couples. Moreover, in order to put the reaction indicated in Eq.(9.23) to work, the hydrogen and oxygen produced should be separated from each other as a first step by, for example, a membrane (*see* Chapter 9 *Membrane Photobiology*). Since a minimum of two photons are required for each molecule of H_2 generated and four photons for O_2, the scheme of two coupled photosystems, as employed in natural photosynthesis, is a logical choice. With the development of SC-SEP cells in the 1988s, we are now in a position to explore the feasibility of water photoelectrolysis via a variety of semiconductor septum electrodes covered with suitable catalysts. Thus, by using SC-SEP cells and their modifications, the dream of generations of energy-conscious scientists and engineers may perhaps at last be realized (Fig. 10.7). This would be accomplished by not merely mimicking but actively improving on Nature's photosynthesis process, namely, the photolysis of water into hydrogen and

oxygen (or their equivalents) at opposite sides of the semiconductor septum electrode via solar energy.

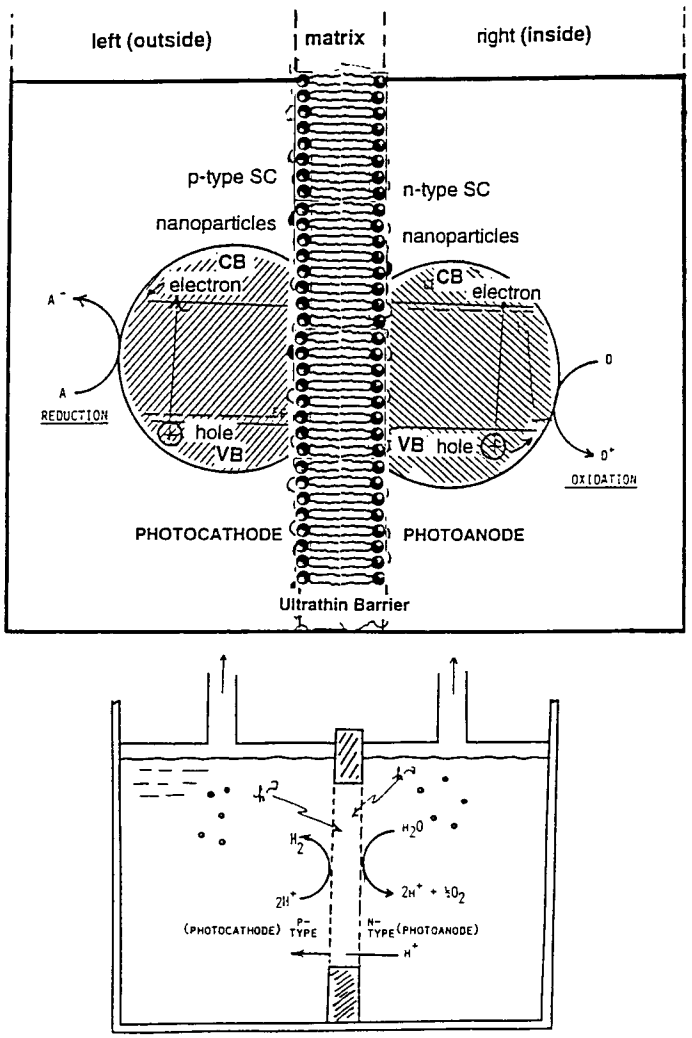

Fig. 10.7 A proposed SC-SEP cell for water photolysis using semiconductor nanoparticles. The concept of the SC-SEP cell is derived from natural photosynthesis. The overall thickness of the septum bipolar electrode (*p*-SC / metal substrate / *n*-SC) should be less than 10 nm [Ginley et al, 1996, p. 547].

CONCLUDING REMARKS

The development of BLMs, and later s-BLMs and sb-BLMs have made it possible for the first time to study, directly, electrical properties and transport phenomena across a 5 nm ultrathin cell membrane element separating two aqueous solutions. As a result of extensive studies over past decades, biomembranes have now been recognized as the basic structure of Nature's sensors and molecular devices. For example, the plasma membrane of cells provides sites for a host of ligand-receptor contact interactions such as the antigen-antibody formation. To impart relevant biofunctions in BLMs, a variety of compounds such as ionophores, enzymes, receptors, etc. have been incorporated. Some of these incorporated compounds cause the BLMs to exhibit non-linear phenomena. A modified BLM (or s-BLM, sb-BLM) is viewed as a dynamic system that changes both in response to environmental stimuli and as a function of time. This is best described by the *dynamic membrane hypothesis* as a basis of the biomembrane function. The self-assembled lipid bilayer, the crucial component of biomembranes, is in a liquid-crystalline and in a dynamic state. A functional cell membrane system based on self-assembled lipid bilayers, proteins, carbohydrates and their complexes should be considered in molecular and electronic terms; it is capable of supporting ion or/and electron transport and is the site of cellular activities in that it functions as a 'device' for either energy conversion or signal transduction. Such a system, as we know it intuitively, must act as some sort of a transducer capable of gathering information, then processing it, and delivering a response based on this information. In the past, we were limited by our lack of sophistication in manipulating and monitoring such a system. Today, cell membranology is a matured field of research as a result of applications of many elegant techniques including membrane electrochemistry, patch-clamp techniques, spectroscopy, and membrane reconstitution. We now know a great deal about the structure of cell membranes, 'ion pumps', electroporation, and membrane channels. In membrane reconstitution experiments, the evidence is that intracellular signal transduction begins at membrane receptors. The work summarized here offers new and exciting opportunities for the preparation of a variety of supported lipid bilayer (BLM) probes with potential applications in membrane biophysics, biochemistry, physiology and biotechnology. For example, the membranes

can function in such important processes as electron-transfer, signal transduction and cellular environmental sensing. Without doubt, these ideas will be pursued by researchers in the coming years.

In conclusion, the research area covered in this chapter is highly interdisciplinary. Emphasis has been placed on fundamental research. Past work and new ideas described in these pages have been benefited by cross-fertilization of ideas among various branches of sciences. It seems likely that the devices based on 'smart materials' may be constructed in the form of a hybrid structure, for example, utilizing both inorganic semiconducting nanoparticles and synthetic lipid bilayers. The biomimetic approach to ***materials science*** is unique and full of exciting possibilities. In this connection, the rationale of membrane biophysics, as viewed from planar lipid bilayers and liposomes, has been to understand the living organisms in physical and chemical terms. Hence, in a sense, we have been mimicking Nature's approach to 'smart' materials science or life, as we understand it, which may be summarized by one word *'trial and error'*. This approach was fine for Nature but not a viable one for us now, since we do not have unlimited time and resources at our disposal. Nevertheless, we can glean the design principles from Nature's successful products and apply to our search for better materials from which advanced devices and biotechnology ultimately depends.

General References

S. G. Davison (ed.) Progress in Surface Science, Pergamon Press, NY. 19 (1985) 169; 23 (1986) 317; 30 (1989) 1; 41(1992) 337

Bolton, J.R., (ed.), Solar Energy and Fuels, Academic Press, New York, 1977, p.167-225.

Metzner, H., (ed.), Photosynthetic Oxygen Evolution, Academic Press, New York, 1978,

Kalyanasundaram, K., Photochemistry in Microheterogeneous Systems,

Academic Press, New York and Tokyo, 1987.

Marino, A.A., (ed.), Modern Bioelectricity, Marcel Dekker, NY. 1988,

K. L. Mittal and D. O. Shah (eds.), Surfactants in Solution, Plenum, NY, 8 (1989) 133 ; 11 (1991) 61

F. T. Hong (Ed), Molecular Electronics: Biosensors and Biocomputers, Plenum Press, NY, 1989.

Blank, M. and Findl, E., (eds.), Mechanistic Approaches to Interactions of Electric and Electromagnetic Fields with Living Systems, Plenum Press, New York and London, 1987, p.301-324.

R. Birge (Ed.) *MolecularElectronics and Bioelectronics*;.; Adv. Chem. Series No. 240, ACS, Washington, D.C., 1994.

R. F. Taylor and J. S. Schultz (eds.) Handbook of Chemical and Biological Sensors Institute of Physics, Publising, Philadelphia, 1996.

Ginley, D., T. Catalano, H. W. Schock, C. Eberspacher, T. M. Peterson, and T. Wada (eds.) Thin Films for Photovoltaic and Related Device Applications, Materials Research Society, Vol. 426, Warrendale, PA. 1996.

Specific References

1. H. T. Tien and A. l. Ottova, *Colloids and Surfaces A: Physicochemical and Engineering Aspects*, 149, 217-233 (1999)
2. A. Ottova-Leitmannova and H. T. Tien, "Bilayer lipid membranes: An experimental system for biomolecular electronic devices development", Prog. Surface Science, 41(4), 337-446, 1992.
3. A. D. Bangham, "Surrogate cells or Trojan horses: the discovery of liposomes", BioEssays, 17(12), 1081, 1995
4. M.Rosoff (ed.) Vesicles,Marcel Dekker,Inc. New York 1996
5. P. Mueller, D. O. Rudin, H. T. Tien and W. C. Wescott, Nature, 194, 979 (1962).
6. Kauffmann J.-M.(ed.) Special issue devoted to electrochemical biosensors, Bioelectrochem. Bioenerg. 42 (1997). p. 1-104
7. Umezawa , Y. S. kIHARA, K. Suzuki, N. Teramae and H. Watarai (Eds.) Molecular recognition at liquid-liquid iterfaces: fundamentals and analytical applications , Analytiacal Sicences, 14 (1998) p. 1-245
8. Brett, C. M. A. and A. M. Oliverira-Brett (eds.) Electroanalytical Chemistry, A Special Issue, Electrochimica Acta, 43(23) (1998) 3587
9. W. Ziegler, et al, and W. Ziegler, D. Remis, A. Brunovska, J. Jakabovic and H. T. Tien, in Proc. 7th C-S Conference on Thin Films (V. Tvarozek and S. Nemeth, Eds.), L. Mikulas, Slovakia, June 1993. p. 304-311
10. A. Ottova-Leitmannova, T. Martynski, A. Wardak, H.T. Tien, in: R. Birge (Ed.), Molecular Electronics and Bioelectronics, Advanced Chemistry Series, vol. 240, American Chemical Society, Washington, DC, 1994.
11. R. S. Sethi, Biosensors Bioelectronics., 9 (1994) 243
12. M. Zviman and H. T. Tien, Bioelectrochem. Bioenerg., 36 (1995) 127
13. K. O'Boyle, F. A. Siddiqi, and H. T. Tien, "Antigen-antibody-complement reaction studies on micro BLMs," *Immunol. Commun*, **13**, 85 (1984).
14. Tien, H. T. *J. Clinical Lab. Analysis* 1988, *2*, 256; Mat'l Sci. & Eng. C:, 1995, 3,7
15. Yuan, H.-P. A. Ottova-Leitmannova, H. T. Tien Mat'l Sci. & Eng. :C 4 (1996) 35
16. Lu, X.-D. A. L. Ottova and H. T. Tien, Bioelectrochem. Bioenerg. 39 (1996) 275
17. Tvarozek, V.; Tien, H. T.; Novotny, I.; Hianik, T.; Dlugopolsky, J.; Ziegler, W.; Ottova, A.; Jakabovic, J.; Rehacek, V.; Uhlar, M. *Sensors and Actuators B.Chemical* **1994**, *19*, 597.
18. L.-G. Wang, X. Wang, A. L. Ottova, H. T. Tien, *Electroanalysis*, 8, 1996, 1020
19. Hianik, T., J. Dlugopolsky, M. Gyeppessova, B. Sivak, H. T. Tien, and A. Ottova-Leitmannova, Bioelectrochem. Bioenerg.. 39 (1996) 299
20. Z.H. Tai, L. Cun, and C.-Z. Yang, 'Pt supported BLMs modified by ferrocene", Mol. Eng., 2 (1994) 215-220
21. He, Y., E. M.,G. Xie, S.-K. Liu, A. L. Ottova and H. T. Tien , *Anal. Lett.*, (1995) 28,443
22. A. N. Sun, H.-Y Xu, Z.-K. Chen, L. Cui and X.-L. Hai, Mat'l Sci.. Eng. C: 2 (1995) 159-163

23. Wang, E.; Liu, Y. Q.; Dong, S. J.; Ting, JCS, *Faraday Trans.* 1990, *86*, 2243
24. B. Lippert, Cisplatin – Chemistry and Biochemistry of a Leading Anticancer Drug, Wiley-VCH, 1999, pp 576
25. D. Mandler and I. Turyan, Electroanalysis, 8 (1996) 207
26. D. P. Nikolelis,. U. J. Krull, A. L. Ottova and H. T. Tien, *in* Handbook of Chemical and Biological Sensors (*see* R. F. Taylor and J. S. Schultz, above)
27. B. Ivanov (ed.) Thin Liquid Films: Fundamentals and Applications, Dekker, Inc., NY, 1988. p. 927
28. H. Gerischer, *Topics in Applied Physics*, 31 (1979) 115
29. J. O'M. Bockris and F. B. Diniz, J. Electrochem. Soc., 135 (1988) 1947
30. J. Sabo, R. Murgasova A. L. Ottova and H. T. Tien, Thin Solid Films, 1998
31. P. Bianco and J Haladjian, Electrochim. Acta, 39 (1994)
32. K. T. Kinnear and H. G. Monbouquette, Langmuir, 9 (1993) 2255
33. S. M. Zakeeruddin, M. Gratzel and D. M. Fraser, Biosen. Bioelect. 11 (1996) 305
34. Z. P. Yang, I. Engquist, J.-M. Kauffmann, B. Liedberg, Langmuir, 12 (1996) 1704
35. W. Schulmann, S.-P. Heyn and H. E. Gaub, Adv. Materials, 3 (1991) 388
36. E.-L. Florin and H. E. Gaub, Biophys. J. 64 (1993) 375
40. P. Krysinki, H. T. Tien and A. Ottova, Biotechnology Progress, in press (1999)
41. B. W. Koenig, S. Krueger, W. J. Orts, C. F. Majkrzak, N. F. Berk, J. V. Silverton and K. Gawrisch, Langmuir, 12 (1996) 1343
42. N. Murakami, S. S. Singh, V. P. S. Chauhan, M. Elzinga, Biochem. 34 (1995) 60
43. L. Dei, E. Ferroni and G. Sarti, Colloids Surf. B: Biointerfaces 4 (1995) 433
44. N. Garg and D. Madamwar, Appl. Biochem. Biotech., 53 (1995) 183
45. Jun Feng; Yun Xiang Ci, Chun Yang Zhang, Angelica L. Ottova^{+}* and H. T. Tien, Electrochem. Commun. 1 (1999) 145-147
46. C. Bruckner-Lea, Petelenz, D.; J. Janata, *J. Mikrochem. Acta* 1990, *1*, 169.
47. Th. Schalkhammer, E. Mann-Buxhaum, I. Moser, G. Hawa, G. Urban and F. Pittner, in Immobilised Macromolecules: Applications and Potentials (U. B. Sleytr, P. Messner, D. Pum and M. Sara, eds.) Springer-Verlag, London, Heidelberg and NY, 1993. Chapter 9
48. P.-G. Yu and D. Zhou, Analyt. Chim. Acta 300 (1995) 91
49. Z.-J. Liu, B.-H. Liu, M. Zhang, J.-L. Kong and J.-Q. Deng, Anal. Chim. Acat, 392 (1999)135-141
50. M. Ikematsu, M. Iseki, Y. Sugiyama, and A. Mizukami, J. Electrochem. 403 (1996) 61
51. H. Nakanishi, Prog. Surf. Sci., 49 (1995) 197
52. A. Izquierdo and M. D. Luque de Castro, Electroanalysis, 7 (1995) 505
53. Kotowski, J.; Janas, T.; Tien, H. T. *J. Electroanal. Chem.* 1988, *253*, 283; *ibid* 1988, *19*, 405
54. W. M. Albers, G. W. Canters and J. Reedijk, Tetrahedron, 51 (1995) 3895
55. T. Hianik, J. Dlugopolsky, M. Gyeppessova, H. T. Tien, and A. Ottova-Leitmannova, Bioelectrochem. Bioenerg. 39 (1996) 299.
56. L. G. Wang, Y.-H. Li and H. T. Tien, Bioelectrochem. Bioenerg. 36 (1995) 145

57. M. Eray, S. Numan, S. Dogan, S. R. Reiken, H. Sutisna, B. J. Van Wie, A. R. Koch, D. F. Moffett, M. Silber, and W. C. Davis, BioSystem 35 (1995) 183
58. D. Xiao, J. Li and R.-Q. Yu, Chemical Sensors, 2 (1994) 100
59. Yu-Feng. Zhang, Xin-Pu Hou Gang Wu, Rong-Chang Li, Xiu-Wen Qiao. H.T. Tien and A. Ottova, Electrochem. Commun. 1 (1999) 238-241
60. H. Yamaguchi and H. Nakanishi, Biochim. Biophys. Acta, 1148 (1993) 179
61. A. Lamrabte, J. M. Janot, E. Bienvenue, G. Miquel and P. Seta, Bioelectrochem. Bioenerg. 27 (1992) 449
62. Z.-C. Bi, Y.Y. Qian, J.-P. Huang, Z.-J. Xiao and J.-Y. Yu, J. Photochem. Photobiol. A: Chem. 77 (1994) 37
63. L. S. Miller, A. L. Rhoden, N. Byrre, J. Heptinsty and D. J. Walaton, Mat'l Sci. Eng. C: 3 (1995) 187
64. M. Sanger and H. Sigrist, Sens. Actu-A, 51 (1995) 83
65. Y.-J. Xiao, X.-X. Gao, G.-Y. Xie and Y. Zhang, Bioelectrochem. Bioenerg. 39 (1996) 125
66. R. V. Benssason, J.-L. Garaud, S. Leach, G. Miquel and P. Seta, Chem. Phys. Lett. 210 (1993) 141; E. Bienvenue, M. Dellinger, J. Phys. Chem., 98 (1994) 3386
67. R. M. Williams, J. M. Zwier and J. W. V. Cerhoeven, J. Am Chem Soc. 117 (1995) 4093
68. Y. Amao and N. Kumazawa. Nucl. Acids Symp. S. 29 (1993) 149
69. D. Seebach, A. Brunner, H. M. Burger, R. N. Reusch and L. L. Bramble, Helv. Chim. Acta 79 (1996) 507
70. Sherratt, A.F.C., (ed.), Int'l J.Ambient Energy, 7, Ambient Press Ltd., Lancaster, UK, 1986, pp.3-30.
71. Seta, P. and Bienvenue, E., Images Chimie, Suppl. CNRS, 65, 1985.
72. P.-A. Ohlsson, T. Tjarnhage, E. Herbai, S. Lofas and G. Puu, Bioelectrochem. Bioenerg. 38 (1995) 137
73. Tien, H.T., Nature, 219, 272, 1968; ___ and Verma, S.P., Nature, 227, 1232, 1970.
74. Bolton, J.R. and Hall, D.O., Ann. R. Energ., 4, p.353, 1979
75. Porter, G. and Archer, M.D., Interdisc. Sci. Rev., 1, p.119, 1976
76. Chapoy, L.L., Munck, D.K.,Biddle, D., Mol. Cryst. Liq. Cryst., 105, 353, 1985.
77. Tien, H.T.,Z. Salamon, J. Kutnik, P. Krysinski, J. Kotowski, D. Ledermann and T. Janas, J. of Molecular Electronics, Vol. 4 S1-S30, 1988
78. Murthy, A.S.N. and Reddy, K.S., Proc. Ind. Acad. Sci., 93, p.433, 1984
79. Meier, H., Organic Semiconductors, Verlag Chemie, Weimheim, 1974, p.440.
80. Salamon, Z. and Tien, H.T., Liquid Cryst., 3, p.169, 1988; Mol. Cryst. Liq. Cryst., 154, p.195, 1988; Photochem. Photobiol., 58, p.281, 1988.
81. Zhao, X.K., Baral, S., Rolandi, R., and Fendler, J.H., JACS., 110, p.1012, 1988.
82. Harima, Y. and Yamshita, K., J. Electrochem. Soc., 186, p.313, 1985
82. Mountz, J. and Tien, H.T., Solar Energy, 21, p.291, 1978.

http://www.msu.edu/user/ottova/membrane.biophysics.html

This Page Intentionally Left Blank

Index